

ORBIT DETERMINATION AND PREDICTION PROCESSES
FOR LOW ALTITUDE SATELLITES

by

Andrew Joseph Green

A.S., Mohawk Valley Community College
(1970)

B.S., United States Military Academy
(1974)

M.S., Massachusetts Institute of Technology
(1977)

SUBMITTED IN PARTIAL FULFILLMENT
OF THE REQUIREMENT FOR
DEGREE OF
DOCTOR OF PHILOSOPHY

at the
Massachusetts Institute of Technology

DECEMBER 1979

(i.e. February, 1980)

©1979 by The Charles Stark Draper Laboratory, Inc.

Signature of Author _____
Department of Aeronautics and Astronautics
December 1979

Approved by _____
Chairman of Thesis Committee

Approved by _____
Thesis Advisor

Approved by _____
Thesis Advisor

Approved by _____
Thesis Advisor

Accepted by _____
Chairman, Departmental Graduate Committee

ARCHIVES
MASSACHUSETTS INSTITUTE
OF TECHNOLOGY

DEC 31 1979

LIBRARIES

ORBIT DETERMINATION AND PREDICTION
PROCESSES FOR LOW ALTITUDE SATELLITES

by

Andrew Joseph Green

Submitted to the Department of Aeronautics and
Astronautics on 10 December 1979 in partial fulfillment
of the requirements for the Degree of Doctor of Philosophy.

ABSTRACT

This thesis combines the semianalytical satellite theory with current estimation procedures such that orbit determination and prediction processes for low altitude satellites are improved. A general formulation for the first order short periodic variations due to any type of perturbation, conservative or non-conservative, is presented. The short periodic formulation is given in terms of a Fourier series in the mean-mean longitude and permits both analytical and numerical implementation. Based upon the first order short periodic formulation, the averaged equations of motion are rigorously extended to second order for both single and multiple perturbing forces. This formalism is applied to the satellite orbit perturbed by both oblateness and atmospheric drag. The resulting second order drag theory includes a complete treatment of the oblateness/drag coupling that retains the flexibility of the numerical averaging approach, that is, an arbitrarily complex density model may be included. A semianalytical satellite theory for the partial derivatives of perturbed motion is presented. The semianalytical partial derivatives are composed of averaged partial derivatives and short periodic partial derivatives. The semianalytical satellite theory is combined with a batch filter (least squares differential correction algorithm) such that the epoch mean elements and various parameters within the drag formulation can be determined. The solve-for parameters in the drag formulation include the drag coefficient and parameters within an Adaptive Modified Harris-Priester density model. An algorithmic structure for coupling the semianalytical satellite theory with the Kalman filter is also presented. Numerical results for several test cases are presented. It is found that the semianalytical satellite theory can be used to accurately determine and predict satellite ephemerides.

Thesis Supervisor: Walter M. Hollister
Title: Associate Professor of Aeronautics and Astronautics

Thesis Supervisor: John P. Vinti
Title: Lecturer of Aeronautics and Astronautics

Thesis Supervisor: Richard H. Battin
Title: Adjunct Professor of Aeronautics and Astronautics
Associate Department Head, C. S. Draper Laboratory

Thesis Supervisor: Paul J. Cefola
Title: Section Manager, C. S. Draper Laboratory

ACKNOWLEDGEMENT

The author would like to thank the U.S. Army and the Fannie and John Hertz Foundation for the opportunity to do this research. He would also like to thank Professors Battin, Hollister and Vinti of the M.I.T. Aeronautics and Astronautics Department for their helpful comments and encouragement during this investigation. Profound appreciation goes to Dr. P. J. Cefola of the Charles Stark Draper Laboratory whose help and support made this research possible. The author is also indebted to Wayne D. McClain for excellent advice and guidance. Thanks are extended to L. W. Early (CSDL), R. Proulx (CSDL), M. Slutsky (CSDL), A. Bobick (MIT/CSDL), D. Brand (Aerospace), M. Blum (Aerospace) and Maj. J. Bailey (SAMSO) for their helpful discussions, suggestions and support throughout this research effort. Appreciation is also extended to William Manlove (CSDL), Robert Duffy (CSDL) and John Sinkiewicz (formerly CSDL) for their help and advice.

Special thanks go to Captain Jeffrey S. Shaver (USAF) and Sean K. Collins, friends and colleagues, without whose help and encouragement this research would not have been accomplished.

Praise goes to Ms. Karen Smith of CSDL for her professional help, skill and advice in the preparation and editing of this document.

Finally, the author would also like to express his appreciation for the support, encouragement and understanding given to him by his wife, Theresa, and his two children, Christopher and Andrea.

Partial support for this research was provided by the United States Air Force Space Division (formerly SAMSO) under Contract Number F04701-79-C-0062 and by the Advanced Orbit Determination Task in the Charles Stark Draper Laboratory Internal Research and Development program for fiscal year 1979.

TABLE OF CONTENTS

<u>Chapter No.</u>		<u>Page No.</u>
1	INTRODUCTION	
	1.1 Background	8
	1.2 Problem Description	12
	1.3 Prior Work	17
	1.4 Research Objectives	37
2	SEMIANALYTICAL SATELLITE THEORY FOR THE PREDICTION OF PERTURBED MOTION	40
	2.1 Mathematical Preliminaries	43
	2.1.1 The Equinoctial System	43
	2.1.2 A Review of the Semianalytical Satellite Theory	54
	2.2 A First Order Short Periodic Theory	65
	2.2.1 A Time-Independent Formulation	65
	2.2.2 A Weak Time-Dependent Formulation	85
	2.3 A Second Order Drag Theory in the Averaged Equations of Motion	109
	2.4 Numerical Results	123
	2.4.1 Software Overview	124
	2.4.2 Initial Conditions	132
	2.4.3 Low Altitude Circular Test Case	135
	2.4.4 Low Altitude Eccentric Test Case	147

TABLE OF CONTENTS

(cont.)

<u>Chapter No.</u>		<u>Page No.</u>
	2.4.5 Medium Altitude Circular Test Case	150
3	ORBIT DETERMINATION WITH A SEMIANALYTICAL BATCH FILTER	211
	3.1 A Semianalytical Batch Filter	212
	3.2 A Semianalytical Satellite Theory for the Partial Derivatives of Perturbed Motion	228
	3.2.1 A General Formulation for the Semianalytical Partial Derivatives	229
	3.2.2 Determination of the Semi- analytical Partial Deriva- tives by Finite-Differencing of Slowly Varying Quantities	242
	3.3 Numerical Results of the Semianaly- tical Batch Filter	252
	3.3.1 Software Overview	253
	3.3.2 Test Philosophy	258
	3.3.3 Test Case One	259
	3.3.4 Test Case Two	266
	3.3.5 Test Case Three	283
4	SEMIANALYTICAL SATELLITE THEORY AND THE KALMAN FILTER	312
	4.1 Review of the Kalman Filter	313

TABLE OF CONTENTS

(cont.)

<u>Chapter No.</u>		<u>Page No.</u>
	4.2 The Semianalytical Linearized Kalman Filter	332
5	CONCLUSIONS AND FUTURE WORK	355
	5.1 Conclusions	356
	5.2 Future Work	363
 <u>Appendices</u>		
A	VARIATION OF PARAMETERS EQUATIONS OF MOTION	368
B	FINITE-DIFFERENCING	383
C	THE ADAPTIVE MODIFIED HARRIS-PRIESTER ATMOSPHERE	387
D	DRAG- J_2 ANALYTICAL EXPRESSIONS	389
E	CORRECTIONS TO ZEIS' J_2^2 SHORT PERIODIC EXPRESSIONS	403
F	SOFTWARE IMPLEMENTATION	405
G	MEASUREMENT EQUATIONS AND PARTIAL DERIVATIVES	501
 <u>References</u>		 511

Chapter 1

INTRODUCTION

1.1 Background

The Space Age is entering an era in which satellites will be utilized increasingly by the civilian and military sectors. The civilian sector will utilize satellites for both scientific and commercial endeavors, while in the military sector, satellites will become an integral part of the national defense. In order to meet the needs of both sectors, the number and quality of space systems will steadily increase. Space surveillance and the determination of accurate ephemerides are essential for the success of individual space missions and for national security.

Satellite ephemerides are determined by an orbit determination (OD) system. In space surveillance applications, the OD system must be capable of accurately and efficiently generating the ephemerides of a large number of satellites. A high percentage of these satellites are in the near-Earth environment due to the desirability and necessity of satellite missions within this regime. Low altitude satellites are predominantly perturbed by the non-sphericity of the Earth's gravitational field and by atmospheric drag. Failure to accurately account for these perturbations on near-Earth satellites can

significantly degrade the orbit determination and prediction process.

OD systems in operation today utilize special perturbation satellite theories (SP theories) or general perturbation satellite theories (GP theories) for orbit generation. SP theories involve numerical integration of the equations of motion expressed either in Cowell, Encke or Variation of Parameter (VOP) format. SP theories allow flexibility in considering the number and type of disturbing forces while maintaining the desired accuracy. The major disadvantage with SP theories is that they are usually computationally expensive. GP theories permit analytical solutions to the equations of motion that are usually based upon canonical transformation theory. Existing GP theories usually employ restricted force models and therefore are not as accurate as SP theories. GP theories are generally computationally less costly than SP theories.

Drag perturbed satellites are frequently handled with SP theories in operational OD systems because of the inability of analytical methods to accurately handle this perturbation. SP theories will permit an accurate handling of the drag perturbation but will significantly increase the computational costs. An additional advantage of SP theories is that upper atmosphere density models can be changed very easily as new models are determined or old models updated. GP theories do

exist which can handle atmospheric drag. However, they are based upon restrictive density models that can vary significantly from the true density of the upper atmosphere. In order to change density models in a GP theory, an almost complete reformulation of the analytical solution commonly is required.

All OD systems use tracking data (usually from ground based radars) in the orbit determination and prediction process. This is done by use of a batch filter (least squares differential correction algorithm) or a sequential filter (Kalman filter). The batch filter takes all the tracking data over a certain observation span and determines the best estimate of the epoch conditions. The sequential filter determines the best estimate of the current conditions from the tracking data by processing the observations recursively. Knowing the best estimate for either the epoch conditions (batch filter) or the current conditions (sequential filter), the orbit generator can then be used to predict the satellite ephemeris. Some of the variables that can be solved for in the estimation process are the state vectors (position and velocity or an orbital element set), force model parameters, tracking station locations, measurement bias, time bias, etc. The state vector usually solved for in current OD systems is the position and velocity of the spacecraft with respect to an inertial Cartesian coordinate frame (the estimation process is coupled with a SP theory). In the drag perturbed case, the only drag parameter

that is usually solved for in operational OD systems is a multiplicative factor in the drag force, i.e., the drag coefficient or ballistic coefficient. Due to the many modeling errors associated with the drag formulation, filtering (batch or sequential) becomes a very important part of any OD system designed for near-Earth satellites.

Operating procedures for the major OD systems are basically similar. Certain throughput and accuracy requirements must be met. In order to meet these requirements, certain trade-offs are made between accuracy and computer run time. This is typically done by assigning priorities to the various satellites whose ephemerides must be updated. A precision SP theory would be used on satellites with the highest priorities. Then, depending upon the assigned priority, varying degrees of a SP or GP theory would be used upon the other satellites such that all requirements are met. This is especially true for a space computation center which must keep track of very large numbers of space objects.

It is noted that a major portion of any OD system is the satellite theory used for orbit generation. The orbit generator is used in both the estimation and prediction process. An orbit generator, which accurately and efficiently handles all perturbations, is essential to the performance of an OD system.

1.2 Problem Description

Because of the need for space surveillance and accurate ephemeris generation on an ever-increasing number of satellites, it becomes necessary to enhance the throughput requirements of present-day OD systems while maintaining equivalent or even increased accuracy requirements. In order to meet these future requirements, changes will have to be made to the computer hardware and/or orbit generators of current OD systems. Advances in computer hardware may eventually allow OD systems to employ precision SP methods to all satellites and still allow the computer run times to be dramatically decreased (Ref. 1). However, there are many system difficulties and large software costs associated with implementing major computer hardware changes (for example, see Ref. 2). It therefore appears that developing improved orbit generators, which are compatible with current computer hardware and system constraints, is a viable means of improving the performance of current OD systems. Because of the large number of near-Earth satellites and the importance placed upon these satellites, the improved OD system must be able to accurately and efficiently generate the ephemerides of low altitude satellites.

A satellite theory which has the potential to be an improved orbit generator is the semianalytical satellite theory as described in References 3 through 15. Semianalytical satellite theory is based upon the generalized method of averaging

which basically separates the short periodic motion from the long periodic and secular motion. Canonical perturbation theory, which is used in most GP theories, is a specific case of the generalized method of averaging (Ref. 16). Semianalytical satellite theory makes a transformation from osculating element space to mean element space. The transformation equations involve short periodic functions associated with each disturbing force. The mean orbital element rates contain only long periodic and secular motion. Therefore, a much larger numerical integration time step can be used on the mean equations of motion (typically 1 day) than can be used with the osculating equations of motion. The basic procedure for a semianalytical satellite theory is to transform to mean element space, numerically integrate the equations of motion for the mean elements and then transform back to osculating element space. Semianalytical satellite theory has the potential of greatly increasing the speed of current OD systems while retaining accuracy equivalent to SP methods.

This research is therefore concerned with examining semianalytical satellite theory and combining it with current estimation procedures in order to improve orbit determination and prediction processes for low altitude satellites.

The development of a complete semianalytical OD system can be broken into two phases. The first phase involves making

enhancements to the semianalytical satellite theory such that it can accurately and efficiently handle all perturbations. The second phase of the development is the coupling of the semianalytical satellite theory with current estimation procedures.

This study is basically concerned with low altitude satellites. As previously indicated, the major perturbations experienced by a near-Earth satellite are the non-sphericity of the Earth's gravitational field and atmospheric drag. If semianalytical satellite theory is to be applicable for low altitude satellites, it must be able to handle these perturbations. The effects of the non-sphericity of the Earth's gravitational field (conservative force) has been considered successfully in previous investigations (see Section 1.3). Therefore, the present investigation is mainly interested in making enhancements to the semianalytical satellite theory such that atmospheric drag can be handled accurately and efficiently.

Drag is modeled by the following formula

$$\underline{D} = - B \rho(\underline{r}, t) \underline{V}_{rel} \underline{V}_{rel} \quad (1-1)$$

where

$$\underline{D} = \text{perturbing acceleration due to drag}$$

- $B = \frac{C_D A}{2m} \equiv$ ballistic coefficient
 C_D = drag coefficient
 A = projected area of the satellite
 m = mass of the satellite
 $\rho(\underline{r}, t)$ = density as a function of position and time
 \underline{V}_{rel} = relative velocity vector = $\underline{V} - \underline{V}_a$
 \underline{V} = true (inertial) velocity of the satellite
 \underline{V}_a = velocity of the atmosphere

The ballistic coefficient, velocity profile of the upper atmosphere and the density of the upper atmosphere are potential sources of errors in the drag formulation for OD systems (Ref. 17).

The determination of the ballistic coefficient entails knowing the projected area and drag coefficient of the satellite. Both of these parameters vary as the attitude and geometry of the satellite vary. The drag coefficient also varies somewhat with altitude. The drag coefficient usually has to be determined experimentally. Since it is impossible to reproduce the upper atmospheric conditions in a wind tunnel, the determination of C_D is not very accurate. C_D is usually taken to be between 1.9 and 2.5 (Ref. 17). It must therefore be concluded that the ballistic coefficient is an averaged value

that can be a serious source of error in trying to accurately predict the orbits of drag perturbed satellites.

The velocity profile of the upper atmosphere is generally modeled as if the upper atmosphere rotates with an angular rate equal to Earth rate. Various studies have shown that the actual upper atmosphere approximately rotates with the Earth and has both east-west and north-south winds (Ref. 17). King-Hele has shown that these winds have daily and seasonal variations (Ref. 18). It appears that modeling the velocity profile of the upper atmosphere as a rigid rotation with the Earth is a feasible real-world model but that modeling errors are still present.

The density of the upper atmosphere has a dynamic behavior that appears to be caused by variations in the Sun's behavior (see Section 1.3). The upper atmospheric density can change erratically and in an unpredictable manner, particularly during geomagnetic storms. Density models are a major source of modeling errors in any OD system.

It becomes apparent from the above discussion that the drag formulation has inherent uncertainties associated with it. Therefore, in order to improve orbit determination and prediction processes for low altitude satellites, estimation of drag and/or density parameters appears necessary. This is called adaptive estimation.

1.3 Prior Work

Previous investigations of the motion of artificial satellites, that are applicable to this research, fall into the following categories: semianalytical satellite theory, density modeling, drag theories and adaptive estimation. Each area is reviewed in this section.

Semianalytical Satellite Theory

In Reference 19, Uphoff suggested a numerical averaging theory. The approach taken by Uphoff was to determine the mean (averaged) element rates by numerically averaging all perturbations (gravitational, drag, etc.) over one revolution of the satellite. Uphoff included tesseral terms of the Earth's gravitational field in the mean element rates. This introduced frequency components in the mean element rates that restricted the numerical integration stepsize. For a large enough tesseral gravitational field, a numerical averaging satellite theory could be more costly than a SP theory. Lutsky and Uphoff (Ref. 20) extended the numerical averaging theory of Uphoff to include short periodic variations. The approach of Reference 20 is to assume a Fourier series expansion in "mean true anomaly" for the derivatives of the osculating elements with respect to the "mean true anomaly." The coefficients in this Fourier expansion are then constructed via numerical

quadratures. Reference 20 gives numerical results for the gravitational, luni-solar and atmospheric drag perturbations.

Cefola, Long and Holloway (Ref. 10) introduced the basic concept of the current semianalytical satellite theory, i.e., analytical averaging for conservative perturbations and numerical averaging for non-conservative perturbations. Reference 12 recommended that tesseral non-resonance terms be considered as short periodic variations. This removed the restricting frequency components from the mean element rates and therefore allowed large numerical integration time steps. Equinoctial elements (Ref. 15) were used in the above semianalytical developments because of the nonsingular nature of this element set (see Section 2.1). References 11 and 13 expressed the gravitational potential (central body and third body) in terms of equinoctial elements. This allows for the direct analytical determination of the partial derivatives of the potential with respect to the orbital elements in the Lagrangian VOP equations (see Appendix A). These results are necessary in order to obtain analytical expressions for the mean element rates due to these conservative perturbations. The analytical expressions are written in terms of mathematical special functions (Jacobi polynomials and Hansen coefficients) so that recursions are available. The resulting computer code employs these recursions; thus the semianalytical theory has the same flexibility as SP theories. Kaula (Ref. 21) obtained similar expressions

for the gravitational potential in terms of Keplerian elements. References 9 and 12 give some numerical results of the semi-analytical orbit generator without the short periodic variations on the output grid.

The theoretical foundation of the semianalytical satellite theory and how it is derived from the generalized method of averaging was presented by McClain (Refs. 3 and 4). McClain also developed a general functional formulation of the short periodic functions due to any type of perturbation, conservative or non-conservative. For the non-conservative forces, McClain's functional formulation becomes very difficult to implement.

Cefola and McClain (Ref. 5) developed an analytical formulation for the first order short periodic variations due to central body gravitational and lunar-solar point mass effects. The short periodic functions for the zonal terms of the central body gravitational field were expressed in terms of the mean true longitude and were closed form in the eccentricity. The tesseral m -daily terms were expressed in terms of the Greenwich hour angle and were closed form in the eccentricity. The short periodic variations for the tesseral terms were expressed in terms of the mean-mean longitude and truncation on powers of the eccentricity was necessary. Lunar-solar short periodic variations were derived in terms of the mean

eccentric longitude and were closed form in the eccentricity. The lunar-solar short periodic functions were derived using a time-independent assumption, i.e., the third body was held fixed over the analytical averaging integral. As with the analytical expressions for the mean element rates, the short periodic analytical expressions are written in terms of mathematical special functions which have recursive relations available.

Zeis (Refs. 6 and 7) developed a computer program in the MACSYMA language (Ref. 22) whose goal was to construct automatically the corresponding explicit formulas for the mean element rates and short periodic functions. Zeis also developed a methodology for constructing the J_2^2 averaged equations of motion and short periodic functions. Zeis' expressions were good for only direct orbits (see Section 2.1.1) and were truncated at zeroth order in the eccentricity. Two of Zeis' J_2^2 short periodic expressions were later found to be incorrect and the correct versions are given in Appendix E.

Density Modeling

In order to accurately predict the ephemeris of a drag perturbed satellite, it is necessary to accurately model the density of the upper atmosphere (90 km to 1200 km). The density of the upper atmosphere has many variations. A brief summary of these variations, based upon References 23 through

26, is given in this section followed by a discussion of some of the density models that are used in orbit generators.

The upper atmosphere has an oblate shape due to the oblateness of the earth. This should not be surprising but must be considered for accurate density determination.

Another major variation in the upper atmospheric density is the diurnal variation. Radiation from the Sun is maximum at the sub-solar point (local noon). This causes atmospheric heating which results in an increase in the density. This increase in density causes a bulge in the density distribution which is called the diurnal bulge. The bulge follows the path of the Sun but lags the sub-solar point by approximately 30 degrees (2 P.M. local time) because of the rotation of the Earth and transients within the atmosphere. The minimum value of density occurs at approximately 4 A.M. local time. The diurnal effect also has seasonal variations because the bulge is alternately located in the northern and southern hemispheres (ecliptic and equatorial planes are not aligned).

The density of the upper atmosphere also exhibits a 27 day variation which is caused by the 27 day cycle of the Sun's extreme ultraviolet radiation. The decimetric flux from the Sun varies in the same manner as the extreme ultraviolet radiation and therefore serves as an indication of this variation.

The decimetric flux is measured by Earth observatories and given the symbol $F_{10.7}$ (10^{-22} watts m^{-2} Hz^{-1}).

The upper atmospheric density also has a semiannual variation. The cause of this variation has not been determined precisely but it is believed to be caused by solar and/or interstellar corpuscular emissions. Maximum density occurs around the first week in April and October and minimum density occurs during January and July.

The density of the upper atmosphere shows a definite increase during periods of geomagnetic storms. These storms are erratic and usually cannot be predicted. K_p is the geomagnetic index and is a reliable indication of the changes in the density of the upper atmosphere due to geomagnetic storms. The changes in density lag behind changes in the geomagnetic index by about 6 hours. It is also noted that after a strong geomagnetic storm, the density falls to a lower value than it was prior to the storm.

The solar wind has a 11 year cycle and this is paralleled by a corresponding 11 year variation in the density of the upper atmosphere. It has been found that the smoothed monthly mean of the decimetric flux ($F_{10.7}$) is correlated with the long term 11 year solar cycle. $\bar{F}_{10.7}$ denotes the monthly mean $F_{10.7}$.

The helium concentration in the upper atmosphere greatly affects the density. A seasonal increase in the concentration of helium above the winter pole has also been observed. The mechanism of the seasonal migration of helium has not yet been fully explained but empirical equations have been developed that adequately describe the density variations associated with this phenomenon.

Another constituent of the upper atmosphere that can significantly affect the density is the amount of neutral hydrogen. The concentration of neutral hydrogen in the upper atmosphere depends upon its production and escape rates. It has been found that the amount of hydrogen in the upper atmosphere is proportional to the exospheric temperature. This fact has allowed empirical equations to be developed that adequately predict the hydrogen concentration in the upper atmosphere.

Density waves in the upper atmosphere have been observed aboard various instrumented satellites. These waves are usually observed at the higher latitudes and generally propagate from north to south in the northern hemisphere or vice versa in the southern hemisphere. It is believed that these waves are the mechanism by which energy deposited in the auroral zones is conveyed to lower latitudes. The effects of these waves on the density are usually neglected in the orbit determination problem.

From the above discussion it becomes clear that the upper atmospheric density has a dynamic nature. Most, if not all, of the density variations are caused by variations in the Sun's behavior. Better prediction of the Sun's behavior ($F_{10.7}$, $\bar{F}_{10.7}$, and K_p) should improve prediction of the density of the upper atmosphere. This appears to be the approach that some of the Russian scientists are taking (Refs. 27-29).

Density models for the upper atmosphere have been and will be an area of intense investigation. A few density models that are applicable to this investigation will be briefly discussed in this section. Reference 17 gives an excellent discussion of the various density models and the interested reader is directed there for further information.

A density model which is static and does not take into account any of the upper atmospheric variations discussed above is the exponential model. The model is written as

$$\rho = \rho_0 \exp \left[\frac{r_0 - r}{H} \right] \quad (1-2)$$

where

- ρ = density at radius r
- ρ_0 = reference density at reference radius

r_0 = reference radius

H = scale height

The scale height is a function of the altitude but is generally taken as a constant. The exponential density model is used in many GP drag theories due to its simple analytical form. Variations in $F_{10.7}$, $\bar{F}_{10.7}$ and K_p can be partially reflected by changes in ρ_0 , r_0 and H . These changes can become unwieldy and are usually not adequate because the diurnal and oblateness effects are not modeled.

Another static density model is the power law density model. This is represented as

$$\rho = \rho_0 \left[\frac{r_0 - s}{r - s} \right]^\tau \quad (1-3)$$

where ρ_0 , τ and s are constants depending upon the reference radius, r_0 . Lane (Ref. 30) introduced this model for use in his analytical drag development. Again some of the variations in the upper atmosphere can be partially reflected by changes in r_0 , ρ_0 and s . As in the exponential density model, these changes are usually not adequate.

Cook and King-Hele (Ref. 31) have extended the exponential density model to account for the diurnal effect of the upper atmosphere. Chen (Ref. 32) modified the model of Cook

and King-Hele such that the oblateness effects were also included. This model, which will be called the diurnal-oblate exponential density model, can be written as

$$\rho = \rho_0 \exp \left[\frac{h_0 - h}{H} \right] (1 + F \cos \psi) \quad (1-4)$$

where

- ρ = density at point in question
- ρ_0 = density at reference point
- h = height of point in question above the oblate Earth
- h_0 = height of reference point above the oblate Earth
- F = diurnal factor of the atmosphere
- H = scale height of the atmosphere
- ψ = angle between satellite's position and diurnal bulge

Obviously the maximum density (ρ_{\max}) occurs at $\psi = 0^\circ$ and the minimum density (ρ_{\min}) occurs at $\psi = 180^\circ$. Therefore, the ratio of ρ_{\max} to ρ_{\min} for a given altitude, h , can be written as (Ref. 32)

$$f \equiv \frac{\rho_{\max}}{\rho_{\min}} = \frac{1 + F}{1 - F} \quad (1-5)$$

which implies that

$$F = \frac{f - 1}{f + 1} \quad (1-6)$$

If the determination of ρ_{\max} , ρ_{\min} , ρ_0 and H depend upon the solar activity ($F_{10.7}$, $\bar{F}_{10.7}$, and K_p), then the diurnal-oblite exponential density model attempts to account for most of the upper atmospheric variations.

Fominov (Ref. 33) suggested a density model which has the following general form

$$\rho = f(t) [\rho_1 + \rho_\phi + \rho_\psi] \quad (1-7)$$

where

- $f(t)$ = function that reflects the time variations of the density, i.e., $F_{10.7}$, $\bar{F}_{10.7}$, K_p
- ρ_1 = density of a spherically symmetric atmosphere
- ρ_ϕ = factor which represents the density dependence upon latitude
- ρ_ψ = factor which represents the density dependence upon the Sun's position

ρ_ϕ and ρ_ψ are expressed in terms of Legendre polynomials. This model is interesting because it uses spherical harmonics much in the same manner that they are used in expressions for the Earth's gravitational field.

The Jacchia 1971 density model (Ref. 34) is generally considered the "state of the art" in density predictions. In the Jacchia 1971 model the altitude and exospheric temperature are calculated first. Jacchia's model for the exospheric temperature represents most of the variations in the upper atmosphere. Knowing the exospheric temperature and altitude, a series of tables allows the determination of the density. Next, some density corrections are determined and added to the density obtained from the tables. Roberts (Ref. 35) modified Jacchia's density model such that the density tables were not necessary. This density model is called the Analytical Jacchia-Roberts density model and is discussed in detail in Reference 17.

Elyasberg (Ref. 36) introduced a density model which is generally called the U.S.S.R. model. This model was used on the U.S. - U.S.S.R. Apollo-Soyuz mission. The general form of the model is

$$\rho = \rho_h K_1 K_2 K_3 K_4 \quad (1-8)$$

where

- ρ_h = night-time vertical profile of density
- K_1 = factor representing solar radiation density variations ($F_{10.7}$ and $F'_{10.7}$)

- K_2 = factor representing diurnal variations
- K_3 = factor representing semiannual variation
- K_4 = factor representing geomagnetic density variations

Reference 17 gives an excellent discussion of this model. Mueller (Ref. 37) has suggested some modifications to the U.S.S.R. model that apparently improve its performance.

The mass spectrometer and incoherent scatter (MSIS) density model is a recently developed model that appears promising (Ref. 38). Using measurements of the densities of the upper atmospheric constituents (made from mass spectrometers on near-Earth satellites) and neutral temperature measurements inferred from incoherent scatter measurements (made from various ground stations), a model for the densities of the upper atmospheric constituents (N_2 , O, He, Ar, H) is developed. Like the Jacchia model, the MSIS model is based upon an exospheric temperature profile. The exospheric temperature and other quantities are represented by expansions in terms of spherical harmonics. The coefficients of these expansions are determined from the data measurements.

The Modified Harris-Priester density model is the density model used in this research (see Appendix C). The Modified Harris-Priester density model consists of a set of 10

tables each associated with a different smoothed decimetric flux ($\bar{F}_{10.7}$). The range of $\bar{F}_{10.7}$ is from 65 to 275. Each table contains the diurnal maximum and minimum densities at various altitudes from 100 km to 1000 km. The density is then determined by an exponential interpolation algorithm (see Appendix C). The Modified Harris-Priester density model is derived from the Harris-Priester density model and this relationship is described in Reference 17. The Modified Harris-Priester atmosphere (also the Harris-Priester atmosphere) is symmetric with respect to the diurnal bulge. This is not actually the case and an Asymmetric Modified Harris-Priester density model is presented in Reference 17. The Analytical Jacchia-Roberts, MSIS and U.S.S.R. density models account for the asymmetric nature of the diurnal variation. While the Modified Harris-Priester density model was employed in this research primarily for computer software reasons, it is a sufficiently realistic model. In addition, the analysis presented in this work is general with respect to the density model.

Drag Theories

Much research has been done on the motion of drag perturbed satellites. These investigations can generally be classified as analytical or numerical averaging drag theories. Drag theories which consider oblateness and drag perturbations separately and add their effects (i.e., assume superposition

is valid) are called first order drag theories. Those drag theories which consider the effects of oblateness/drag coupling are called second order drag theories. Since the oblateness and drag perturbations are sufficiently large for a low altitude satellite, the coupling between oblateness and drag does exist and must be considered for accurate orbit prediction.

A series of papers by King-Hele, Cook and Walker (Refs. 31 and 39 through 43) studied the effects of atmospheric drag on the semimajor axis, eccentricity and argument of perigee. This work was basically done in order to determine the lifetimes of drag perturbed satellites. Initially the density model was an exponential model but it was subsequently improved until it took into account diurnal effects and the scale height dependence upon altitude. A rotating atmosphere was also assumed. This analysis can be classified as a first order analytical drag theory (J_2 perturbations were not considered). Santora (Ref. 44) basically extended the work of King-Hele, Cook and Walker to include diurnal and Earth oblateness effects such that orbits with small eccentricities ($e = 0$ to 0.01) could be better handled.

A first order analytical drag theory was introduced by Zee (Ref. 45) which basically added the effects of J_2 and drag perturbations. Zee assumed a non-rotating atmosphere with an exponential density. Zee's results were good only for small eccentricity.

Another first order drag theory of interest was developed by Fominov (Ref. 33). Fominov used the density model as given in Equation (1-7) which results in a drag theory with a recursive nature. This can be very desirable from a computational point of view.

A first order drag theory derived via computerized symbolic algebra (FORMAC) was presented by Barry and Rowe (Ref. 46). The Jacchia 1970 density model was approximated by a Fourier series in the true anomaly of the satellite. A rotating atmosphere was assumed.

Reference 47 is a recent first order drag theory. This work suggests a formulation which is applicable to both the drag perturbed satellite and reentry vehicle. A rotating atmosphere with an exponential density was assumed.

Brouwer and Hori (Ref. 48) introduced a second order analytical drag theory based upon canonical perturbation theory. The method of Brouwer and Hori was an extension of Brouwer's earlier work (Ref. 49) and as such was in terms of Delaunay variables. The drag theory of Brouwer and Hori assumed a non-rotating atmosphere with an exponential density model. In order to get an analytical solution, Brouwer and Hori expanded the exponential density function in terms of a series of the

eccentricity to fifth power. For satellites with a low perigee height, the series approximation was not sufficient. Lane (Ref. 50) introduced the power law density model such that the equations of motion could be integrated analytically without the power series expansion in eccentricity. This gave improved performance for satellites with a low perigee height. Lane also assumed a non-rotating atmosphere. Reference 51 extended the work of Lane by assuming a quadratic scale height (Lane's power law density model is representative of a linear scale height variation).

At the same time that Brouwer introduced his satellite theory, Vinti introduced an alternative satellite theory (Ref. 52). Sherrill (Ref. 53) extended Vinti's satellite theory to include drag perturbations. Sherrill assumed a non-rotating oblate spheroidal density with exponential height variations. Sherrill's approach was similar to the approach of Brouwer and Hori and is also a second order analytical drag theory. Watson, Mistretta and Bonavito (Ref. 54) also extended Vinti's theory to account for drag perturbations. The approach of Reference 54 was to use an iteration scheme to correct the Vinti theory until the drag perturbations were accounted for.

Scheifele, Mueller and Stark (Ref. 55) introduced a second order analytical drag theory which was based upon the

previous work of Scheifele (Ref. 56). Reference 55 (also Ref. 56) used non-singular Poincare-Similar elements. The analysis was done in extended phase space with true anomaly as the independent variable. The density model used took into account the oblateness and diurnal effects.

Chen (Ref. 32) suggested a second order drag theory which was based upon the diurnal-oblate exponential density model. A rotating atmosphere was assumed. Chen used Keplerian orbital elements and his solutions were derived by the method of two-variable asymptotic expansions.

Many of the analytical drag theories (King-Hele, Zee, Brouwer-Hori, Lane, Sherrill, etc.) were completed by the late 1960's. These analytical drag theories were very complicated for relatively simple density models. At about this same time, new and more complicated density models were being developed. These facts made numerical averaging drag theories attractive because of the capability to allow complete drag models and to permit different density models to be inserted with relative ease.

A numerical averaging satellite theory is similar to a semianalytical satellite theory except that mean element rates and short periodic variations are all determined numerically. The mean element rates of a first order numerical averaging

drag theory are determined by simply performing a numerical quadrature on the drag disturbing force over a revolution of the satellite. A first order drag theory is usually not sufficient for low altitude satellites because it neglects the coupling of oblateness and drag perturbations.

A second order numerical averaging drag theory was suggested by Pimm (Ref. 57) and Reference 58. The approach proposed in References 57 and 58 was to apply Izsak's J_2 short periodic radial correction (Ref. 59) in the density calculation at each of the abscissas of the quadrature algorithm. This is a good approximation to the effects of oblateness/drag coupling (see Section 2.4.3). Lutsky and Uphoff (Ref. 20) suggested the use of Izsak's J_2 short periodic velocity corrections as well as the height corrections in the density calculation at each quadrature point. This improves the approximation of the oblateness/drag coupling but still does not include all of it.

Another second order numerical averaging drag theory was developed by Liu (Refs. 60 and 61) in terms of Keplerian elements. Liu also used a modified form of Izsak's J_2 short periodic height correction in the density determination. Liu assumed further that drag perturbations affected only the mean element rates for the semimajor axis and eccentricity.

Adaptive Estimation

As stated previously, the drag formulation has many uncertainties associated with it. It appears that adaptive estimation of the drag model may improve orbit determination and prediction processes for low altitude satellites. Adaptive estimation can generally be classified as either adaptive parameter estimation or adaptive noise estimation. Adaptive parameter estimation is the process of trying to improve the force model by solving for uncertain constants within the formulation. Adaptive noise estimation is where characteristics about the noise (system or observational) in the formulation are solved for. This research will be concerned with only adaptive parameter estimation.

A previous investigation that is directly applicable to this investigation was done by Dowd in Reference 17. Dowd used adaptive parameter estimation with an Extended Kalman Filter and showed improved performance in the orbit determination and prediction process. Dowd used a SP theory (Cowell) with Cartesian position and velocity as his state. An Asymmetric Modified Harris-Priester atmosphere was developed and used. Dowd found that adaptive parameter estimation of the density model was a viable means of improving the estimation and prediction of drag perturbed satellites.

Other investigations into adaptive estimation of the drag perturbed satellite problem are given in References 62 through 66. These investigations, like Dowd's work, used sequential filters. Adaptive estimation (parameter and noise) of the drag formulation was done. Reference 17 gives a good overview of these previous investigations.

1.4 Research Objectives

The objective of this research is to combine semianalytical satellite theory with current estimation procedures such that orbit determination and prediction processes for low altitude satellites are improved.

From Section 1.3 it is seen that much of the theoretical foundation already exists for the semianalytical orbit generator. This is especially true for conservative forces for which analytical expressions exist for both the mean element rates and short periodic variations. For non-conservative forces the semianalytical satellite theory uses numerical averaging techniques to obtain the mean element rates to first order. To obtain an approximation to the second order drag effects, Izsak's J_2 short periodic height corrections can be applied to the density calculation at each of the quadrature points. Enhancements that need to be made to the semianalytical satellite theory such that drag perturbed satellites can be better handled are:

1. a short periodic development that adequately handles drag perturbations
2. a more complete second order numerical averaging drag theory.

These developments are presented in Chapter 2. The short periodic development presented is applicable to all perturbations. For conservative forces, the development of Chapter 2 permits analytical expressions.

As previously indicated, the drag formulation has many inherent uncertainties associated with it. This is especially true in the density model. It is therefore necessary to couple the semianalytical satellite theory with current estimation procedures. These current estimation procedures should also be capable of adaptive estimation. A semianalytical batch filter with numerical results is presented in Chapter 3. A development of the semianalytical partial derivatives of perturbed motion is included in Chapter 3. In Chapter 4, the theoretical formulation of a Semianalytical Linearized Kalman Filter is presented.

This development (except the Semianalytical Linearized Kalman Filter) has been implemented into the Research and Development version of the Goddard Trajectory and Determination System (GTDS-RD) at the Charles Stark Draper Laboratory in

Cambridge, Massachusetts. Further details about the implementation are given in Appendix F.

Chapter 2

SEMIANALYTICAL SATELLITE THEORY FOR THE PREDICTION OF PERTURBED MOTION

Semianalytical satellite theory offers significant advantage for precision orbital computations. In comparison with the integration of osculating equations of motion by numerical methods (SP theories), the semianalytical satellite theory gives much greater computational speed while retaining equivalent accuracy. In comparison with conventional GP theories, the semianalytical satellite theory makes it possible to include more complete physical models and to simplify the computations that must be done at each output point.

A semianalytical satellite theory makes a transformation from osculating element space to mean element space. The mean elements are obtained by removing the short periodic motion from the osculating elements by applying the generalized method of averaging. Since the short periodic motion has been removed, the averaged equations of motion allow a much larger numerical integration time step. A semianalytical satellite theory is composed of an Averaged Orbit Generator (AOG) and a Short Periodic Generator (SPG). The AOG integrates the averaged equations of motion and determines the mean elements on the integration grid. The SPG determines the short periodic variations on the output grid. Because of the slowly varying

nature of the mean elements, an interpolator can be used to obtain the mean elements at the output times.

As was previously indicated, the semianalytical orbit generator (AOG and SPG) must be capable of accurately and efficiently handling all types of perturbations, conservative or non-conservative. This research is especially concerned with improving the performance of the semianalytical orbit generator in the presence of atmospheric drag.

This chapter presents a short periodic development and a second order drag theory. The short periodic development includes time-independent and weak time-dependent formulations that are applicable to conservative and non-conservative disturbing forces. For conservative perturbations, analytical expressions are possible. The second order drag theory is a complete treatment of all second order drag effects including the oblateness/drag coupling. The second order drag theory is modular with respect to the atmospheric density model. In this case, modularity means that alternate density models may be inserted with the same ease that occurs in first order numerical averaging drag theories.

In Section 2.1 some mathematical preliminaries are presented. First, the equinoctial system and the transformation from the observational coordinate frame to the inertial coor-

dinate frame are discussed. The basic concepts of the generalized method of averaging and how it applies to the semianalytical satellite theory are presented next. The difference between a time-independent and time-dependent formulation is also discussed.

A first order short periodic theory is discussed in Section 2.2. Time-independent and weak time-dependent formulations are presented. A time-independent formulation assumes that the physical problem has only the satellite's phase angle or that the second phase angle is independent of the satellite's phase angle. Perturbations which generally can be expressed in terms of a single phase angle are zonal terms of the gravitational field, atmospheric drag and solar radiation pressure. Due to the presence of a second phase angle when considering tesseral terms of the gravitational field (Greenwich hour angle) or third body perturbations (mean longitude of the third body), it becomes necessary to introduce a time-dependent short periodic formulation. If the angular rate of the second phase angle is very small in comparison with the satellite's mean motion, it is possible to use a weak time-dependent formulation which is presented in this section. The formulations presented in Section 2.2 are expressed in terms of a Fourier series representation in the mean-mean longitude.

A complete second order drag theory for the semianalytical orbit generator is developed in Section 2.3. For low altitude satellites, the oblateness/drag coupling terms in the AOG can be very important. Having a representation of the first order short periodic variations for J_2 and drag effects allows a rigorous treatment of the secular and long periodic oblateness/drag coupling terms.

Numerical results are presented in Section 2.4. The problem of initial conditions is also discussed in this section. A low altitude circular test case and a low altitude eccentric test case are used to demonstrate the time-independent short periodic formulation in the SPG and the second order drag theory in the AOG. A medium altitude circular test case is used to demonstrate the weak time-dependent formulation.

2.1 Mathematical Preliminaries

2.1.1 The Equinoctial System

The equinoctial elements are defined as follows (Ref. 3):

$$\begin{aligned} a &= a \\ h &= e \sin(\omega + I\Omega) \\ k &= e \cos(\omega + I\Omega) \end{aligned} \tag{2-1}$$

$$\begin{aligned}
p &= \tan^I(i/2) \sin \Omega \\
q &= \tan^I(i/2) \cos \Omega \\
\lambda &= M + \omega + I\Omega
\end{aligned}
\tag{2-1}$$

where a , e , i , Ω , ω , and M are the classical Keplerian element set and where I is the retrograde factor. The retrograde factor has to be $+1$ when $i = 0^\circ$ and -1 when $i = 180^\circ$ in order to avoid a singularity in the Variation of Parameter equations. When i is any value between 0° and 180° , either set of equinoctial elements can be used, but due to mathematical difficulties the switch over should occur prior to getting very close to the limiting values. Since i seldom equals 180° , the direct equinoctial element set ($I = +1$) is generally used.

The equinoctial reference frame is shown in Figure 2-1. The equinoctial coordinate frame can be obtained from the Earth centered inertial frame (mean of 1950) by the following rotations: a rotation of Ω° about the inertial z direction, a rotation of i° about the new x axis followed by a rotation of $-I\Omega^\circ$ about the new z axis. The unit vectors in the equinoctial coordinate frame are \hat{f} , \hat{g} and \hat{w} . The \hat{f} and \hat{g} vectors are in the orbital plane. The \hat{w} vector is normal to the orbital plane.

The transformation from the inertial frame to the equinoctial frame, based upon the concept of the osculating ellipse, can be expressed as

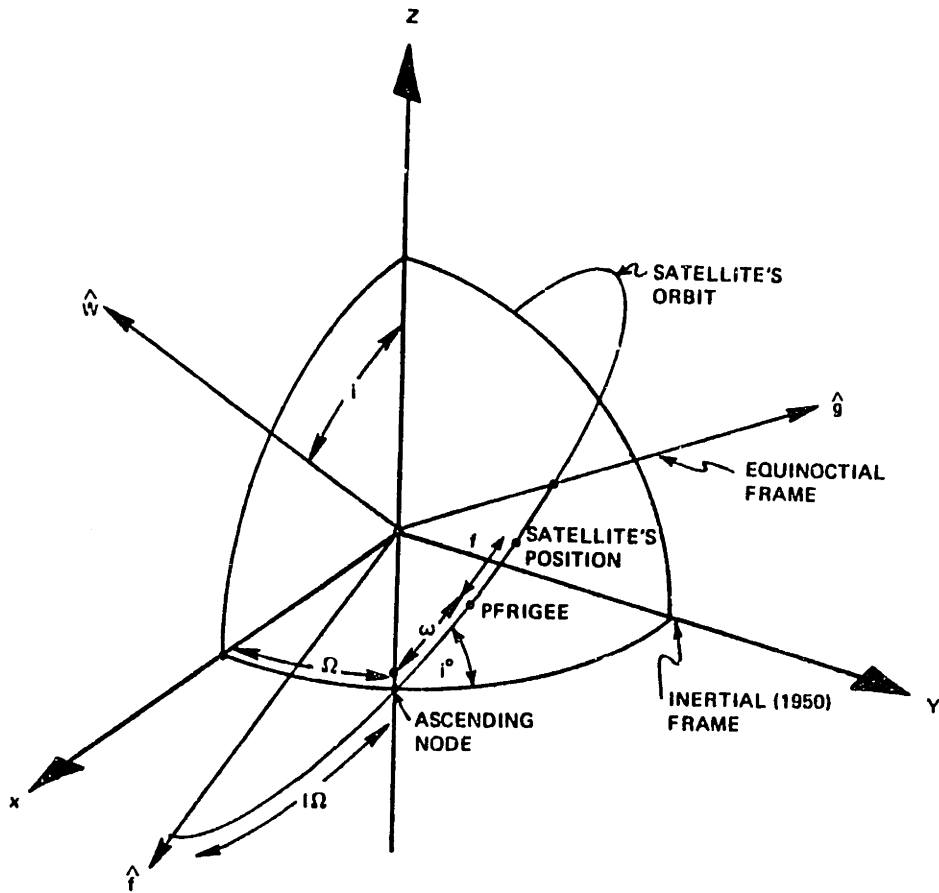


Figure 2-1. Equinoctial Coordinate Frame

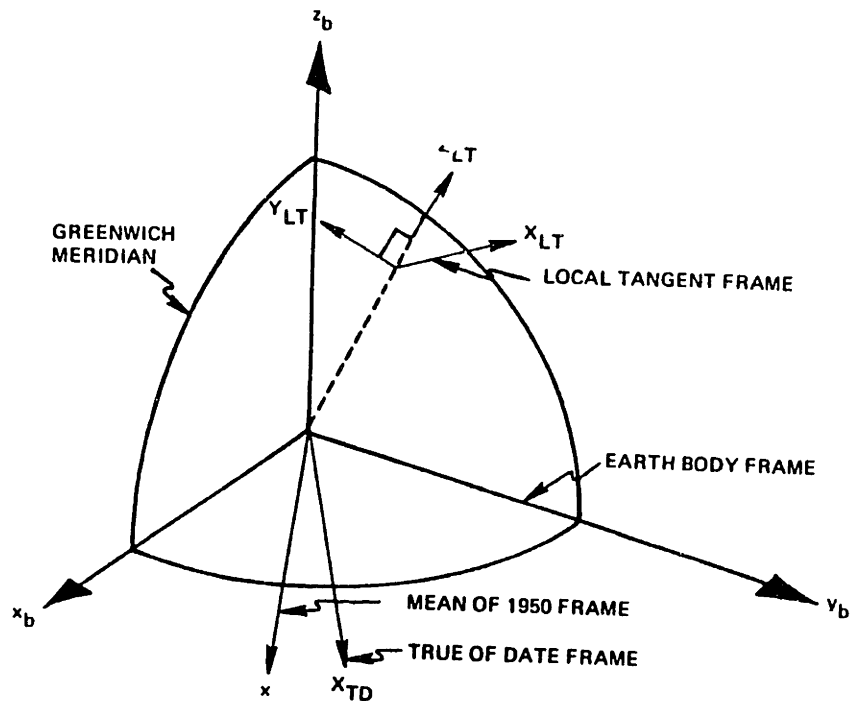


Figure 2-2. Coordinate Frames

$$\begin{aligned}\underline{r}_{eq} &= D \underline{R} \\ \dot{\underline{r}}_{eq} &= D \dot{\underline{R}}\end{aligned}\tag{2-2}$$

where

$$\begin{aligned}\underline{r}_{eq}, \dot{\underline{r}}_{eq} &\equiv \text{position and velocity in the equinoctial frame} \\ \underline{R}, \dot{\underline{R}} &\equiv \text{position and velocity in the inertial frame} \\ D &\equiv \text{rotation matrix}\end{aligned}$$

The rotation matrix can be expressed in terms of Keplerian or equinoctial elements as (Ref. 3)

$$D = \begin{bmatrix} \cos^2\Omega + I \sin^2\Omega \cos i & \cos \Omega \sin \Omega(1-I \cos i) & -I \sin \Omega \sin i \\ I \cos \Omega \sin \Omega(1-I \cos i) & I(\sin^2\Omega + I \cos^2\Omega \cos i) & \cos \Omega \sin i \\ \sin \Omega \sin i & -\cos \Omega \sin i & \cos i \end{bmatrix}\tag{2-3a}$$

or

$$D = \frac{1}{1 + p^2 + q^2} \begin{bmatrix} 1 - p^2 + q^2 & 2pq & -2pI \\ 2pqI & (1 + p^2 - q^2)I & 2q \\ 2p & -2q & (1 - p^2 - q^2)I \end{bmatrix}\tag{2-3b}$$

The mean, eccentric, and true longitudes in the equinoctial reference system are defined respectively as

$$\lambda = M + \omega + I\Omega \quad (2-4a)$$

$$F = E + \omega + I\Omega \quad (2-4b)$$

$$L = f + \omega + I\Omega \quad (2-4c)$$

where M, E and f are respectively the mean, eccentric and true anomalies associated with the Keplerian element set.

The radius in a Keplerian ellipse is expressed as

$$r = \frac{a(1 - e^2)}{1 + e \cos f}$$

It can be shown that

$$e \cos f = k \cos L + h \sin L$$

and

$$e^2 = h^2 + k^2$$

Therefore

$$r = \frac{a(1 - h^2 - k^2)}{1 + k \cos L + h \sin L} \quad (2-5)$$

In a similar fashion it can be shown that

$$r = a(1 - k \cos F - h \sin F) \quad (2-6)$$

From Kepler's second law and Equation (2-4c) the following two-body relation results

$$\frac{dL}{dt} = \frac{na^2\sqrt{1-h^2-k^2}}{r^2} \quad (2-7)$$

Equating the derivatives of Equations (2-5) and (2-6) and rearranging yields another two-body relation

$$\frac{dF}{dt} = \frac{na}{r} \quad (2-8)$$

Position and velocity in the equinoctial frame can be expressed as

$$\underline{r}_{eq} = \begin{bmatrix} X_1 \\ Y_1 \\ 0 \end{bmatrix} \quad \dot{\underline{r}}_{eq} = \begin{bmatrix} \dot{X}_1 \\ \dot{Y}_1 \\ 0 \end{bmatrix} \quad (2-9a)$$

where

$$X_1 = r \cos L \quad (2-9b)$$

$$Y_1 = r \sin L \quad (2-9c)$$

$$\dot{X}_1 = \frac{-na(h + \sin L)}{\sqrt{1-h^2-k^2}} \quad (2-9d)$$

$$\dot{Y}_1 = \frac{na(k + \cos L)}{\sqrt{1-h^2-k^2}} \quad (2-9e)$$

By use of the two-body relations that relate true anomaly to eccentric anomaly, it can be shown that

$$\cos L = \frac{a}{r} [(1 - h^2\beta)\cos F + hk\beta \sin F - k] \quad (2-10a)$$

$$\sin L = \frac{a}{r} [(1 - k^2\beta)\sin F + hk\beta \cos F - h] \quad (2-10b)$$

where

$$\beta = \frac{1}{1 + \sqrt{1 - h^2 - k^2}} \quad (2-10c)$$

It follows from Equations (2-9) and (2-10) that

$$X_1 = a[(1 - h^2\beta)\cos F + hk\beta \sin F - k] \quad (2-11a)$$

$$Y_1 = a[(1 - k^2\beta)\sin F + hk\beta \cos F - h] \quad (2-11b)$$

$$\dot{X}_1 = \frac{na^2}{r} [hk\beta \cos F - (1 - h^2\beta)\sin F] \quad (2-11c)$$

$$\dot{Y}_1 = \frac{na^2}{r} [(1 - k^2\beta)\cos F - hk\beta \sin F] \quad (2-11d)$$

Kepler's equation is given as

$$M = E - e \sin E$$

Adding $\omega + I\Omega$ to each side yields

$$\lambda = F - e \sin[F - (\omega + I\Omega)]$$

Expanding the above Equation and using Equation (2-1) yields Kepler's equation in equinoctial elements

$$\lambda = F - k \sin F + h \cos F \quad (2-12)$$

Since the overall goal of this research is to combine the semianalytical satellite theory with estimation procedures, it is necessary to develop the transformation from the local tangent frame (frame in which the measurement/observations are usually expressed) to the equinoctial frame (frame in which the semianalytical satellite theory is developed). The coordinate frames of interest are the mean of 1950, true of date, Earth body fixed and local tangent coordinate frames. The mean of 1950 frame is an inertial frame whose x-y plane is in the mean 1950 equatorial plane with the x axis along the 1950 node of the mean equatorial and ecliptic planes (mean implies that nutations are neglected). The true of date frame is an inertial frame whose x-y axis is in the true equatorial plane with the x axis along the node of the true equatorial and ecliptic planes (true means that nutations are considered and that the frame is with respect to a certain specified date). The Earth body frame is a coordinate frame whose x-y axis is in the equatorial plane with the x axis along the Greenwich meridian. The local tangent frame has its origin at the observation sight on the

surface of the Earth with its x axis pointing east, y axis pointing north and z axis up. These coordinate frames are shown in Figure 2-2.

The transformation of position and velocity in the mean of 1950 coordinate frame to the Earth body coordinate frame can be expressed as (Ref. 67)

$$\begin{aligned}\underline{r}_b &= B(t) C \underline{R} \\ \dot{\underline{r}}_b &= \dot{B}(t) C \underline{R} + B(t) C \dot{\underline{R}}\end{aligned}\quad (2-13)$$

where

$\underline{r}_b, \dot{\underline{r}}_b \equiv$ position and velocity with respect to the Earth body frame

$\underline{R}, \dot{\underline{R}} \equiv$ position and velocity with respect to the mean of 1950 inertial frame

$B(t) \equiv$ rotation matrix from true of date to Earth body coordinate frame. It is time dependent due to the rotation of the Earth.

$C \equiv$ rotation matrix from mean of 1950 to true of date coordinate frame

The transformation of position and velocity in the Earth body coordinate frame to the local tangent frame can be expressed as (Ref. 67)

$$\begin{aligned}\underline{r}_{LT} &= M_{LT}[\underline{r}_b - \underline{r}_s] \\ \dot{\underline{r}}_{LT} &= M_{LT}[\dot{\underline{r}}_b]\end{aligned}\tag{2-14}$$

where

$\underline{r}_{LT}, \dot{\underline{r}}_{LT} \equiv$ position and velocity with respect to the local tangent frame

$\underline{r}_s \equiv$ Measurement/observation station location with respect to the Earth body frame

$M_{LT} \equiv$ rotation matrix from Earth body to local tangent frame

Combining Equation (2-13) and (2-14) yields

$$\begin{aligned}\underline{r}_{LT} &= M_{LT}[B(t) C \underline{R} - \underline{r}_s] \\ \dot{\underline{r}}_{LT} &= M_{LT}[\dot{B}(t) C \underline{R} + B(t) C \dot{\underline{R}}]\end{aligned}\tag{2-15}$$

Inverting Equation (2-15) and realizing that the inverse of an orthogonal matrix equals the transpose

$$\begin{aligned}\underline{R} &= C^T B^T [M_{LT}^T \underline{r}_{LT} + \underline{r}_s] \\ \dot{\underline{R}} &= C^T B^T [M_{LT}^T \dot{\underline{r}}_{LT} - \dot{B} B^T (M_{LT}^T \underline{r}_{LT} + \underline{r}_s)]\end{aligned}\tag{2-16}$$

Substitution of Equation (2-16) into Equation (2-2) gives the transformation between the local tangent coordinate frame and the equinoctial frame.

$$\begin{aligned}\underline{r}_{eq} &= DC^T B^T [M_{LT}^T \underline{r}_{LT} + \underline{r}_s] \\ \dot{\underline{r}}_{eq} &= DC^T B^T [M_{LT}^T \dot{\underline{r}}_{LT} - \dot{B} B^T (M_{LT}^T \underline{r}_{LT} + \underline{r}_s)]\end{aligned}\tag{2-17}$$

Inverting Equation (2-17) yields

$$\begin{aligned}\underline{r}_{LT} &= M_{LT} [BCD^T \underline{r}_{eq} - \underline{r}_s] \\ \dot{\underline{r}}_{LT} &= M_{LT} [BCD^T \dot{\underline{r}}_{eq} + \dot{BCD}^T \underline{r}_{eq}]\end{aligned}\tag{2-18}$$

Equations (2-17) and (2-18) allow transformation between the local tangent frame and the equinoctial frame and vice versa. The rotation matrices used are defined in Reference 67.

It is usually sufficient to work in the inertial true of date coordinate frame. If this is the case, the additional transformation from the true of date coordinate frame to the mean of 1950 coordinate frame is not necessary. The above expressions will still apply in this case except that the C matrix has to be replaced with the Identity matrix.

2.1.2 A Review of the Semianalytical Satellite Theory

The Variation of Parameter (VOP) equations of motion, for a single disturbing force, can be expressed in either Gaussian or Lagrangian form (see Appendix A). Either form can be expressed functionally in terms of osculating equinoctial variables as

$$\begin{aligned}\dot{a}_i &= \frac{da_i}{dt} = \varepsilon F_i(\underline{a}, \lambda) \quad (i = 1, 2, 3, 4, 5) \\ \dot{\lambda} &= \frac{d\lambda}{dt} = n + \varepsilon F_6(\underline{a}, \lambda)\end{aligned}\tag{2-19}$$

where

\underline{a} = vector of the five slowly varying osculating equinoctial elements, $\underline{a}^T = [a, h, k, p, q] = [a_1, a_2, a_3, a_4, a_5]$

λ = osculating mean longitude of the satellite (fast variable)

n = mean motion = $\mu^{1/2} a_1^{-3/2}$

ε = small parameters (i.e., J_2 , J_3 , Ballistic coefficient, etc.)

The presence of the small parameter is basic to the method of averaging (Ref. 3). The formulation of Equation (2-19) does not include a second phase angle such as the Greenwich hour angle (θ) or the mean longitude of a third body. Therefore,

Equation (2-19) implicitly assumes that λ is independent of any other phase angle associated with the physical problem. This is called a time-independent formulation (Ref. 4). References 4, 68 and 69 address the problem of multiple phase angles in the VOP formulation.

In the method of averaging, a transformation is made from osculating element space to mean element space. The quantities \bar{a}_i and $\bar{\lambda}$ are called the mean elements. The transformation to second order in the small parameter is assumed to be of the form

$$a_i = \bar{a}_i + \epsilon \eta_{i,1}(\bar{a}, \bar{\lambda}) + \epsilon^2 \eta_{i,2}(\bar{a}, \bar{\lambda})$$

$$(i = 1, 2, 3, 4, 5, 6) \quad (2-20)$$

where a_6 equals λ . Equation (2-20) is called the near-identity transformation because it contains powers of the small parameter. The trigonometric components of the short periodic functions will contain only satellite dependent frequencies since it was these frequencies that were removed in order to obtain the mean elements. Assuming that the five slowly varying mean elements are constant over one satellite revolution, it is reasonable to require that the short periodic variations be periodic over 2π in $\bar{\lambda}$ and have zero mean value

$$\int_0^{2\pi} \eta_{i,j}(\bar{a}, \bar{\lambda}) d\bar{\lambda} = 0 \quad (2-21)$$

$$\begin{aligned} (i &= 1, 2, 3, 4, 5, 6) \\ (j &= 1, 2) \end{aligned}$$

It is also assumed that the equations of motion for the mean elements can be written to second order in the small parameter as

$$\begin{aligned} \dot{\bar{a}}_i &= \frac{d\bar{a}_i}{dt} = \epsilon A_{i,1}(\bar{a}) + \epsilon^2 A_{i,2}(\bar{a}) \\ (i &= 1, 2, 3, 4, 5) \end{aligned} \quad (2-22)$$

$$\dot{\bar{\lambda}} = \frac{d\bar{\lambda}}{dt} = \bar{n} + \epsilon A_{6,1}(\bar{a}) + \epsilon^2 A_{6,2}(\bar{a})$$

where the functions $A_{i,j}(\bar{a})$ depend only on the five slowly varying mean elements and where the mean motion, \bar{n} , equals $\mu^{1/2} (\bar{a}_1)^{-3/2}$. The fact that the right hand side of Equation (2-22) contains only the slowly varying mean elements allows the numerical integration time step to be greatly increased over a Special Perturbation technique. This is equivalent to saying that the mean elements contain only the secular and long periodic motion.

Substitution of the near-identity transformation into the right hand side of Equation (2-19) and expanding in a Taylor series about the mean elements yields the following to second order in the small parameter

$$\begin{aligned} \dot{a}_i &= \bar{n} \delta_{i6} + \epsilon [F_i(\bar{a}, \bar{\lambda}) - \frac{3\bar{n} \delta_{i6}}{2\bar{a}_1} \eta_{1,1}(\bar{a}, \bar{\lambda})] \\ &+ \epsilon^2 \left[\sum_{k=1}^6 \eta_{k,1}(\bar{a}, \bar{\lambda}) \frac{\partial F_i(\bar{a}, \bar{\lambda})}{\partial \bar{a}_k} + \frac{15\bar{n} \delta_{i6}}{8\bar{a}_1^2} \eta_{1,1}^2(\bar{a}, \bar{\lambda}) \right. \\ &\quad \left. - \frac{3\bar{n} \delta_{i6}}{2\bar{a}_1} \eta_{1,2}(\bar{a}, \bar{\lambda}) \right] \end{aligned}$$

(i = 1, 2, 3, 4, 5, 6)

(2-23)

where δ_{ij} is the Kroenecker Delta function which is defined as

$$\delta_{ij} = \begin{cases} 0 & \text{if } i \neq j \\ 1 & \text{if } i = j \end{cases} \quad (2-24)$$

Equation (2-23) is very useful in subsequent constructions because it expresses the osculating element rates in terms of the mean elements.

Taking the time derivative of Equation (2-20) and using Equation (2-22) results in

$$\begin{aligned} \dot{a}_i &= \bar{n} \delta_{i6} + \epsilon \left[A_{i,1}(\bar{a}) + \bar{n} \frac{\partial \eta_{i,1}(\bar{a}, \bar{\lambda})}{\partial \bar{\lambda}} \right] \\ &+ \epsilon^2 \left[A_{i,2}(\bar{a}) + \bar{n} \frac{\partial \eta_{i,2}(\bar{a}, \bar{\lambda})}{\partial \bar{\lambda}} \right. \\ &\quad \left. + \sum_{k=1}^6 A_{k,1}(\bar{a}) \frac{\partial \eta_{i,1}(\bar{a}, \bar{\lambda})}{\partial \bar{a}_k} \right] \end{aligned}$$

(i = 1, 2, 3, 4, 5, 6) (2-25)

which is an alternate expression for the osculating element rates expressed in terms of the mean elements.

Equating equal powers of the small parameter in Equations (2-23) and (2-25), that is, matching the alternate approximations for the osculating element rates, results in the following expressions

$$A_{i,1}(\bar{a}) + \bar{n} \frac{\partial \eta_{i,1}(\bar{a}, \bar{\lambda})}{\partial \bar{\lambda}} = F_i(\bar{a}, \bar{\lambda}) - \frac{3\bar{n} \delta_{i6}}{2\bar{a}_1} \eta_{1,1}(\bar{a}, \bar{\lambda}) \quad (2-26)$$

$$\begin{aligned} A_{i,2}(\bar{a}) + \bar{n} \frac{\partial \eta_{i,2}(\bar{a}, \bar{\lambda})}{\partial \bar{\lambda}} + \sum_{k=1}^6 A_{k,1}(\bar{a}) \frac{\partial \eta_{i,1}(\bar{a}, \bar{\lambda})}{\partial \bar{a}_k} \\ = \sum_{k=1}^6 \eta_{k,1}(\bar{a}, \bar{\lambda}) \frac{\partial F_i(\bar{a}, \bar{\lambda})}{\partial \bar{a}_k} + \frac{15\bar{n} \delta_{i6}}{8\bar{a}_1^2} \eta_{1,1}^2(\bar{a}, \bar{\lambda}) \\ - \frac{3\bar{n} \delta_{i6}}{2\bar{a}_1} \eta_{1,2}(\bar{a}, \bar{\lambda}) \end{aligned} \quad (2-27)$$

The first and second order mean element rates are obtained by averaging the above equations with respect to the mean-mean longitude. Assuming that the slowly varying mean elements are constant over one orbit of the satellite and that the yet-to-be determined short periodic functions are "well-behaved" and 2π periodic [see Equation (2-21)], it follows

that the first and second order mean element rates are given by

$$A_{i,1}(\bar{a}) = \frac{1}{2\pi} \int_0^{2\pi} F_i(\bar{a}, \bar{\lambda}) d\bar{\lambda}$$

$$(i = 1, 2, 3, 4, 5, 6) \quad (2-28)$$

$$A_{i,2}(\bar{a}) = \frac{1}{2\pi} \int_0^{2\pi} \left\{ \sum_{k=1}^6 \left[\eta_{k,1}(\bar{a}, \bar{\lambda}) \frac{\partial F_i(\bar{a}, \bar{\lambda})}{\partial \bar{a}_k} \right] + \frac{15\bar{n}}{8\bar{a}_1^2} \delta_{i6} \eta_{1,1}^2(\bar{a}, \bar{\lambda}) \right\} d\bar{\lambda}$$

$$(2-29)$$

It is interesting to note that the second order mean element rates require the first order short periodic functions. For conservative disturbing forces (central and third body gravitational effects), the mean element rates can usually be obtained in analytical form. For non-conservative disturbing forces (drag and solar radiation pressure) a numerical approach usually has to be used. The real difficulty is associated with expressing the equations of motion for non-conservative perturbations in terms of orbital elements. The empirical nature of many realistic atmospheric density models is noted.

Knowing $A_{i,1}(\bar{a})$ and $A_{i,2}(\bar{a})$, Equations (2-26) and (2-27) represent a partial differential equation for the first and second order short periodic functions. Equations (2-26) and (2-27) can therefore be solved to within an arbitrary function of the five slowly varying mean elements. The requirement that the short periodic functions be 2π periodic with respect to the satellite frequency necessitates that this arbitrary function be zero. Equations (2-26), (2-27) and (2-29) also indicate the coupling of the mean fast variable ($\bar{\lambda}$) with the mean semimajor axis (\bar{a}_1) that occurs in the short periodic functions and in the second and higher order mean element rates.

From Equations (2-26) and (2-21), it is seen that the first order short periodic variation can be expressed as

$$\eta_{i,1}(\bar{a}, \bar{\lambda}) = \frac{1}{n} \int \left\{ F_i(\bar{a}, \bar{\lambda}) - A_{i,1}(\bar{a}) - \left(\frac{3\bar{n}}{2\dot{a}_1} \delta_{i6} \right) \eta_{1,1}(\bar{a}, \bar{\lambda}) \right\} d\bar{\lambda} \quad (2-30)$$

References 5 and 6 use Equation (2-30) to obtain analytical expressions for the short periodics due to gravitational effects. When non-conservative disturbing forces are considered, Equation (2-30) usually becomes very difficult to solve.

The development of a semianalytical satellite theory based upon the generalized method of averaging proceeds in a very systematic manner. The Nth order mean element rates, $A_{1,N}(\bar{a})$, depend upon the N-1 previously determined short periodic functions. Using McClain's short periodic formulation (Ref. 3), the Nth order short periodic functions will depend upon the N previously determined mean element rates and the N-1 previously determined short periodic functions.

When more than one disturbing force is considered, the coupling between the various perturbations must be considered. Again, the generalized method of averaging permits a systematic approach to the development of a semianalytical satellite theory. To first order in the small parameters, the averaged equations of motion and the short periodic functions are obtained by summing, respectively, the first order averaged equations of motion and the first order short periodic functions for each separate perturbation (Ref. 3). For higher order terms, mixed (coupled) terms appear in both the averaged equations of motion and the short periodic functions. These higher order mixed terms will depend upon previously determined mean element rates and short periodic functions. For example, the averaged equations of motion to second order in all the small parameters require all the first order short periodic functions. A detailed development of the semianaly-

tical satellite theory for multiple disturbing forces is given in Chapter 3 of Reference 3.

In applying the generalized method of averaging to the problem of an additional phase angle (ϕ) in the disturbing function $[\epsilon F_j(\bar{a}, \bar{\lambda}, \phi)]$, it is necessary to carefully consider the relationship between the two phase angles ($\bar{\lambda}$ and ϕ). If the phase angle ϕ can be considered independent of $\bar{\lambda}$, which is equivalent to being independent of time, the time-independent formulation, as given above, is valid. In other words, a time-independent formulation requires that the phase angles be independent of each other. Therefore the averaging operations, as given in Equations (2-21), (2-28) and (2-29), are performed holding ϕ constant. If ϕ and $\bar{\lambda}$ cannot be considered independent of each other, a time-dependent formulation must be used. A time-dependent formulation must therefore take into account the relationship between ϕ and $\bar{\lambda}$ when the generalized method of averaging is applied.

An example of the difference between a time-independent and a time-dependent formulation, consider the case of a low altitude satellite perturbed by the Sun. In this case, the two phase angles would be the mean-mean longitude of the satellite ($\bar{\lambda}$) and the mean longitude of the Sun (λ'). It is interesting to note that changes in the Sun's position over a revolution of a low altitude satellite will cause variations

in the solar point mass effects, the atmospheric drag and the solar radiation pressure. Variations in the solar point mass effects and solar radiation pressure will be caused directly by changes in the Sun's position. The variation in the drag perturbation will be caused by the changes in the density that results from the Sun's motion. These variations will naturally be very small. The two-body equation of motion for λ' is

$$\dot{\lambda}' = n' \quad (2-31)$$

where n' is the mean motion of the Sun's apparent motion about the Earth which will be assumed to be constant. Equation (2-31) has a solution of the following form

$$\lambda' = n'(t - t_0) + \lambda'_0 \quad (2-32)$$

where t_0 and λ'_0 are the initial conditions. Similarly the two-body solution for $\bar{\lambda}$ can be written as

$$\bar{\lambda} = \bar{n}(t - t_0) + \bar{\lambda}_0 \quad (2-33)$$

where $\bar{\lambda}_0$ is the initial value of $\bar{\lambda}$ at time t_0 . Solving for $(t - t_0)$ in both Equations (2-32) and (2-33), equating the results and rearranging yields

$$\lambda' = \frac{n'}{\bar{n}} (\bar{\lambda} - \bar{\lambda}_0) + \lambda'_0 \quad (2-34a)$$

This can be written in terms of the period of the Sun (P') and the period of the satellite (P) as

$$\lambda' = \frac{P}{P'} (\bar{\lambda} - \bar{\lambda}_0) + \lambda'_0 \quad (2-34b)$$

Equations (2-34a) and (2-34b) show the two-body relationship between $\bar{\lambda}$ and λ' . For a low altitude satellite with a period of 1.5 hours, the ratio $\frac{P}{P'}$ is small, i.e., approximately 0.00017. It is reasonable to assume that λ' is independent of time ($\dot{\lambda}' \sim 0$) over a revolution of $\bar{\lambda}$ and therefore apply the time-independent formulation. Physically this assumption is equivalent to holding the Sun's position fixed over the averaging operation. It is also noted that in the generalized method of averaging, the five slowly varying mean elements (\bar{a}) are also assumed to be constant over the averaging operation.

As the altitude of the satellite is increased or if the third body becomes the moon, the factor $\frac{P}{P'}$ increases. At some point, the assumption of holding λ' constant over a revolution of the satellite is no longer valid. At this point a time-dependent formulation is needed.

In order to be complete in this section, the two-body relation between $\bar{\lambda}$ and the Greenwich hour angle (θ) is presented. Assuming the angular rate of the Earth to be constant

and equal to ω_e , the two-body relation between θ and $\bar{\lambda}$ is derived in a similar manner to the derivation of Equation (2-34a). The result is

$$\theta = \frac{\omega_e}{n} (\bar{\lambda} - \bar{\lambda}_0) + \theta_0 \quad (2-35)$$

Equations (2-34a) and (2-35) are useful in deciding what type of formulation to use.

2.2 A First Order Short Periodic Theory

A first order short periodic theory based upon a Fourier series analysis is presented in this section. A time-independent formulation and a weak time-dependent formulation are developed. These formulations are applicable to perturbations due to zonal terms of the gravitation potential, third body point mass effects for low and medium altitude satellites, atmospheric drag and solar radiation pressure. The short periodic development presented allows a numerical implementation for all applicable perturbations and an analytical implementation for conservative perturbations.

2.2.1 A Time-Independent Formulation

First order short periodic functions could be obtained from the McClain formulation as given in Equation (2-30). As noted previously, this formulation usually becomes very

difficult for non-conservative forces such as drag and solar radiation pressure. This section develops another method of obtaining the short periodic functions which is based upon a Fourier series analysis.

Assume that the osculating element rates can be expressed in a Fourier series in the mean fast variable. Since the VOP equations of motion, $F_i(\underline{a}, \lambda)$, are of bounded variations over one revolution of the satellite, the assumed Fourier series will converge to \dot{a}_i (Ref. 70). This assumption is expressed as follows to first order in the small parameter

$$\dot{a}_i = X_{i0} + \epsilon \sum_{\sigma=1}^{\infty} [X_{i\sigma} \cos(\sigma\bar{\lambda}) + Z_{i\sigma} \sin(\sigma\bar{\lambda})]$$

(i = 1, 2, 3, 4, 5, 6) (2-36a)

where

$$X_{i0} = \frac{1}{2\pi} \int_0^{2\pi} \dot{a}_i d\bar{\lambda} \tag{2-36b}$$

$$\epsilon X_{i\sigma} = \frac{1}{\pi} \int_0^{2\pi} \dot{a}_i \cos(\sigma\bar{\lambda}) d\bar{\lambda} \tag{2-36c}$$

$$\epsilon Z_{i\sigma} = \frac{1}{\pi} \int_0^{2\pi} \dot{a}_i \sin(\sigma\bar{\lambda}) d\bar{\lambda} \tag{2-36d}$$

Substitution of Equation (2-23), taken only to first order in the small parameter, into Equation (2-36b) yields

$$X_{i0} = \frac{1}{2\pi} \int_0^{2\pi} \left[\bar{n} \delta_{i6} + \epsilon F_i(\bar{a}, \bar{\lambda}) - \left(\frac{3\bar{n} \delta_{i6}}{2 \bar{a}_1} \right) \epsilon n_{1,1}(\bar{a}, \bar{\lambda}) \right] d\bar{\lambda}$$

where δ_{i6} is the Kroenecker Delta function as defined in Equation (2-24). Assuming that the five slowly varying mean elements are constant over one revolution of the satellite and applying Equation (2-21) results in

$$X_{i0} = \bar{n} \delta_{i6} + \frac{1}{2\pi} \int_0^{2\pi} \epsilon F_i(\bar{a}, \bar{\lambda}) d\bar{\lambda} \quad (2-37)$$

From Equations (2-22) and (2-28), it is seen that X_{i0} is the mean element rate, i.e.,

$$X_{i0} = \dot{\bar{a}}_i \quad (2-38)$$

Equation (2-36a) can therefore be written as

$$\dot{\bar{a}}_i = \dot{\bar{a}}_i + \epsilon \sum_{\sigma=1}^{\infty} [X_{i\sigma} \cos(\sigma\bar{\lambda}) + Z_{i\sigma} \sin(\sigma\bar{\lambda})] \quad (2-39)$$

Likewise, Equation (2-25) can be rewritten to first order as

$$\dot{\bar{a}}_i = \dot{\bar{a}}_i + \epsilon \left[\frac{\partial \eta_{i,1}(\bar{\underline{a}}, \bar{\lambda})}{\partial \bar{\lambda}} \right] \bar{n} \quad (2-40)$$

Equating Equations (2-39) and (2-40) and cancelling the mean element rates yields the following partial differential equations for the short periodic functions

$$\bar{n} \left[\frac{\partial \epsilon \eta_{i,1}(\bar{\underline{a}}, \bar{\lambda})}{\partial \bar{\lambda}} \right] = \sum_{\sigma=1}^{\infty} [\epsilon X_{i\sigma} \cos(\sigma \bar{\lambda}) + \epsilon Z_{i\sigma} \sin(\sigma \bar{\lambda})] \quad (i = 1, 2, 3, 4, 5, 6) \quad (2-41)$$

Integrating Equation (2-41) with respect to $\bar{\lambda}$ results in

$$\begin{aligned} \epsilon \eta_{i,1}(\bar{\underline{a}}, \bar{\lambda}) = & \sum_{\sigma=1}^{\infty} \left[\frac{\epsilon X_{i\sigma}}{\sigma \bar{n}} \sin(\sigma \bar{\lambda}) \right. \\ & \left. - \frac{\epsilon Z_{i\sigma}}{\sigma \bar{n}} \cos(\sigma \bar{\lambda}) \right] + E_i(\bar{\underline{a}}) \end{aligned}$$

where $E_i(\bar{\underline{a}})$ is an arbitrary function of the five slowly varying elements. Applying the requirement that the short periodic variations be 2π periodic and have zero mean value, as given in Equation (2-21), results in $E_i(\bar{\underline{a}})$ being equal to zero. Therefore

$$\epsilon \eta_{i,1}(\bar{\underline{a}}, \bar{\lambda}) = \sum_{\sigma=1}^{\infty} \left[\frac{\epsilon X_{i\sigma}}{\sigma \bar{n}} \sin(\sigma \bar{\lambda}) - \frac{\epsilon Z_{i\sigma}}{\sigma \bar{n}} \cos(\sigma \bar{\lambda}) \right] \quad (2-42)$$

For convenience the following definitions are made

$$\begin{aligned}\epsilon C_{i\sigma} &\equiv \frac{\epsilon X_{i\sigma}}{\sigma \bar{n}} \\ \epsilon D_{i\sigma} &\equiv \frac{\epsilon Z_{i\sigma}}{\sigma \bar{n}}\end{aligned}\tag{2-43}$$

From Equations (2-23), (2-36), and (2-43), the coefficients $\epsilon C_{i\sigma}$ and $\epsilon D_{i\sigma}$ can be written as

$$\begin{aligned}\epsilon C_{i\sigma} &= \frac{1}{\sigma \bar{n} \pi} \int_0^{2\pi} \epsilon F_i(\bar{a}, \bar{\lambda}) \cos(\sigma \bar{\lambda}) d\bar{\lambda} \\ &+ \frac{\delta_{i6}}{\sigma \pi} \int_0^{2\pi} \cos(\sigma \bar{\lambda}) d\bar{\lambda} \\ &- \frac{3 \delta_{i6}}{2 \sigma \bar{a}_1 \pi} \int_0^{2\pi} \epsilon \eta_{1,1}(\bar{a}, \bar{\lambda}) \cos(\sigma \bar{\lambda}) d\bar{\lambda} \\ \epsilon D_{i\sigma} &= \frac{1}{\sigma \bar{n} \pi} \int_0^{2\pi} \epsilon F_i(\bar{a}, \bar{\lambda}) \sin(\sigma \bar{\lambda}) d\bar{\lambda} \\ &+ \frac{\delta_{i6}}{\sigma \pi} \int_0^{2\pi} \sin(\sigma \bar{\lambda}) d\bar{\lambda} \\ &- \frac{3 \delta_{i6}}{2 \sigma \bar{a}_1 \pi} \int_0^{2\pi} \epsilon \eta_{1,1}(\bar{a}, \bar{\lambda}) \sin(\sigma \bar{\lambda}) d\bar{\lambda}\end{aligned}$$

Noting that

$$\frac{1}{\pi} \int_0^{2\pi} \epsilon \eta_{1,1}(\bar{a}, \bar{\lambda}) \cos(\sigma \bar{\lambda}) d\bar{\lambda} = -\epsilon D_{1\sigma}$$

$$\frac{1}{\pi} \int_0^{2\pi} \epsilon \eta_{1,1}(\underline{\bar{a}}, \bar{\lambda}) \sin(\sigma \bar{\lambda}) d\bar{\lambda} = \epsilon C_{1\sigma}$$

results in the following expression for the short periodic coefficients

$$\begin{aligned} \epsilon C_{i\sigma} &= \frac{1}{\sigma n \pi} \int_0^{2\pi} \epsilon F_i(\underline{\bar{a}}, \bar{\lambda}) \cos(\sigma \bar{\lambda}) d\bar{\lambda} \\ &+ \left(\frac{3 \epsilon D_{1\sigma}}{2 \sigma \bar{a}_1} \right) \delta_{i6} \end{aligned} \tag{2-44}$$

$$\begin{aligned} \epsilon D_{i\sigma} &= \frac{1}{\sigma n \pi} \int_0^{2\pi} \epsilon F_i(\underline{\bar{a}}, \bar{\lambda}) \sin(\sigma \bar{\lambda}) d\bar{\lambda} \\ &- \left(\frac{3 \epsilon C_{1\sigma}}{2 \sigma \bar{a}_1} \right) \delta_{i6} \end{aligned}$$

where i goes from 1 to 6 and δ_{i6} is the Kroenecker Delta function [Equation (2-24)]. The short periodic functions can therefore be written as

$$\epsilon \eta_{i,1}(\underline{\bar{a}}, \bar{\lambda}) = \sum_{\sigma=1}^{\infty} [\epsilon C_{i\sigma} \sin(\sigma \bar{\lambda}) - \epsilon D_{i\sigma} \cos(\sigma \bar{\lambda})] \tag{2-45}$$

Equations (2-44) and (2-45) represent the first order short periodic variation. This is summarized in Table 2-1.

As was stated earlier, Equations (2-44) and (2-45) were derived assuming that λ is independent of any other phase angle. Such an assumption results in a time-independent formulation. A time-independent formulation basically assumes that the Earth or third body is not rotating or moving during the averaging interval. It turns out that this formulation is applicable to zonal terms of the gravitational potential, drag, solar-radiation pressure and third-body effects for low altitude satellites. For high precision orbit generation, tesseral terms of the gravitational potential and third body effects for medium and high altitude satellites are not amenable to the above formulation due to the presence of a second phase angle which cannot be considered constant over the averaging interval.

From Equation (2-44) it can be seen that the short periodic coefficients, $\varepsilon C_{i\sigma}$ and $\varepsilon D_{i\sigma}$, are functions of the five slowly varying mean elements. The short periodic coefficients are therefore slowly varying. This should make it possible to evaluate the coefficients at only a few points during a specified time span and then interpolate in order to determine the coefficients at any time within the time span. At the present time it appears that the short periodic coefficients need only be evaluated on the integration grid of the mean elements. Since the integration grid of the mean elements is on the order of one day, the computational cost

Table 2-1

FIRST ORDER SHORT PERIODIC FUNCTIONS

$$\epsilon \eta_{i,1}(\bar{a}, \bar{\lambda}) = \sum_{\sigma=1}^{\infty} [\epsilon C_{i\sigma} \sin(\sigma\bar{\lambda}) - \epsilon D_{i\sigma} \cos(\sigma\bar{\lambda})]$$

$$\epsilon C_{i\sigma} = \frac{1}{\sigma n \pi} \int_0^{2\pi} \epsilon F_i(\bar{a}, \bar{\lambda}) \cos(\sigma\bar{\lambda}) d\bar{\lambda} + \left(\frac{3 \epsilon D_{1\sigma}}{2 \sigma \bar{a}_1} \right) \delta_{i6}$$

$$\epsilon D_{i\sigma} = \frac{1}{\sigma n \pi} \int_0^{2\pi} \epsilon F_i(\bar{a}, \bar{\lambda}) \sin(\sigma\bar{\lambda}) d\bar{\lambda} - \left(\frac{3 \epsilon C_{1\sigma}}{2 \sigma \bar{a}_1} \right) \delta_{i6}$$

$$i = 1, 2, 3, 4, 5, 6$$

associated with the determination of the short periodic functions should be moderate.

For a numerical averaging satellite theory, the computation of the short periodic coefficients will be determined by a quadrature algorithm. The major portion of the integrand of Equation (2-44), $F_i(\bar{a}, \bar{\lambda})$, will have already been calculated at the abscissas of the quadrature algorithm in the determination of the functions $A_{i,1}(\bar{a})$. By saving the integrand of Equation (2-28) at the abscissas of the quadrature algorithm, multiplying by $\sin(\sigma\bar{\lambda})$ or $\cos(\sigma\bar{\lambda})$, and then applying the same

quadrature algorithm, the evaluation of the short periodic coefficients can be obtained at minimum costs. Lutsky and Uphoff (Ref. 20) have stated that the use of recursion relations for $\sin(\sigma\bar{\lambda})$ and $\cos(\sigma\bar{\lambda})$ will also reduce the computer costs. Multiplication of $\epsilon F_i(\bar{a}, \bar{\lambda})$ by $\sin(\sigma\bar{\lambda})$ may introduce frequency components that could require a higher order quadrature algorithm. In other words, the number of coefficients and quadrature order must be considered jointly.

Another interesting fact about the formulation of the short periodics as given in Table 2-1 is the coupling between the fast variable and the semimajor axis. The coupling is through the short periodic coefficient ($C_{6\sigma}$ and $D_{6\sigma}$) and is rather easy to implement. It appears that Reference 20 neglected this term. This is also the term that Kaula described as a second order short periodic term in the mean anomaly [see Equation (3.115) in Ref. 21]. Neglecting this term significantly degrades the accuracy of the semianalytical orbit generator.

When the disturbing force is derivable from a potential, analytical expressions are usually possible for the short periodic coefficients. The Lagrangian VOP equations of motion can be written as

$$\epsilon F_i(\underline{a}, \lambda) = - \sum_{\ell=1}^6 (a_i, a_\ell) \frac{\partial R}{\partial a_\ell}$$

(i = 1, 2, 3, 4, 5, 6) (2-46)

where

$$(a_i, a_\ell) = \text{Poisson brackets}$$

$$R = R(\underline{a}, \lambda) = \text{disturbing potential}$$

With the use of Leibnitz's rule and the properties of Poisson brackets, Equation (2-28) can be written as

$$\epsilon A_{i,1}(\bar{\underline{a}}) = - \sum_{\ell=1}^5 (\bar{a}_i, \bar{a}_\ell) \frac{\partial \bar{R}}{\partial \bar{a}_\ell}$$

(i = 1, 2, 3, 4, 5, 6) (2-47)

where

$$\bar{R} = \frac{1}{2\pi} \int_0^{2\pi} R(\bar{\underline{a}}, \bar{\lambda}) d\bar{\lambda}$$

(2-48)

Substitution of Equation (2-46) into Equation (2-44) results in the following expressions for the short periodic coefficients

$$\begin{aligned}
\epsilon C_{i\sigma} &= \frac{1}{\sigma n \pi} \int_0^{2\pi} \left\{ - \sum_{\ell=1}^5 (\bar{a}_i, \bar{a}_\ell) \frac{\partial}{\partial \bar{a}_\ell} [R(\bar{a}, \bar{\lambda}) \cos(\sigma \bar{\lambda})] \right. \\
&\quad \left. - (\bar{a}_i, \bar{\lambda}) \left[\frac{\partial R(\bar{a}, \bar{\lambda})}{\partial \bar{\lambda}} \cos(\sigma \bar{\lambda}) \right] \right\} d\bar{\lambda} \\
&\quad + \left(\frac{3 \epsilon D_{1\sigma}}{2 \sigma \bar{a}_1} \right) \delta_{i6} \tag{2-49}
\end{aligned}$$

$$\begin{aligned}
\epsilon D_{i\sigma} &= \frac{1}{\sigma n \pi} \int_0^{2\pi} \left\{ - \sum_{\ell=1}^5 (\bar{a}_i, \bar{a}_\ell)' \frac{\partial}{\partial \bar{a}_\ell} [R(\bar{a}, \bar{\lambda}) \sin(\sigma \bar{\lambda})] \right. \\
&\quad \left. - (\bar{a}_i, \bar{\lambda}) \left[\frac{\partial R(\bar{a}, \bar{\lambda})}{\partial \bar{\lambda}} \sin(\sigma \bar{\lambda}) \right] \right\} d\bar{\lambda} \\
&\quad - \left(\frac{3 \epsilon C_{1\sigma}}{2 \sigma \bar{a}_1} \right) \delta_{i6}
\end{aligned}$$

Note that

$$\begin{aligned}
\left[\frac{\partial R(\bar{a}, \bar{\lambda})}{\partial \bar{\lambda}} \right] \cos(\sigma \bar{\lambda}) &= \frac{\partial [R(\bar{a}, \bar{\lambda}) \cos(\sigma \bar{\lambda})]}{\partial \bar{\lambda}} \\
&\quad + \sigma R(\bar{a}, \bar{\lambda}) \sin(\sigma \bar{\lambda}) \tag{2-50}
\end{aligned}$$

$$\begin{aligned}
\left[\frac{\partial R(\bar{a}, \bar{\lambda})}{\partial \bar{\lambda}} \right] \sin(\sigma \bar{\lambda}) &= \frac{\partial [R(\bar{a}, \bar{\lambda}) \sin(\sigma \bar{\lambda})]}{\partial \bar{\lambda}} \\
&\quad - \sigma R(\bar{a}, \bar{\lambda}) \cos(\sigma \bar{\lambda})
\end{aligned}$$

Substitution of Equation (2-50) into Equation (2-49) and applying Leibnitz's rule and the properties of Poisson Brackets, the short periodic coefficients can be written as

$$\begin{aligned} \epsilon C_{i\sigma} &= \frac{-1}{\sigma \bar{n}} \sum_{\ell=1}^5 (\bar{a}_i, \bar{a}_\ell) \frac{\overline{\partial [R \cos(\sigma \bar{\lambda})]}}{\partial \bar{a}_\ell} \\ &- \frac{(\bar{a}_i, \bar{\lambda})}{\bar{n}} \overline{[R \sin(\sigma \bar{\lambda})]} + \left(\frac{3 \epsilon D_{1\sigma}}{2 \sigma \bar{a}_1} \right) \delta_{i6} \end{aligned} \quad (2-51)$$

$$\begin{aligned} \epsilon D_{i\sigma} &= \frac{-1}{\sigma \bar{n}} \sum_{\ell=1}^5 (\bar{a}_i, \bar{a}_\ell) \frac{\overline{\partial [R \sin(\sigma \bar{\lambda})]}}{\partial \bar{a}_\ell} \\ &+ \frac{(\bar{a}_i, \bar{\lambda})}{\bar{n}} \overline{[R \cos(\sigma \bar{\lambda})]} - \left(\frac{3 \epsilon C_{1\sigma}}{2 \sigma \bar{a}_1} \right) \delta_{i6} \end{aligned}$$

where

$$\overline{[R \cos(\sigma \bar{\lambda})]} = \frac{1}{\pi} \int_0^{2\pi} K(\bar{a}, \bar{\lambda}) \cos(\sigma \bar{\lambda}) d\bar{\lambda} \quad (2-52)$$

$$\overline{[R \sin(\sigma \bar{\lambda})]} = \frac{1}{\pi} \int_0^{2\pi} R(\bar{a}, \bar{\lambda}) \sin(\sigma \bar{\lambda}) d\bar{\lambda}$$

The disturbing potential due to the non-sphericity of the Earth's gravitational field and third body point mass effects are given in terms of a complex disturbing potential (Refs. 3, 4, 11, 13 and 68). Functionally this can be expressed as

$$R(\underline{a}, \bar{\lambda}) = \text{Real}\{U^*(\underline{a}, \bar{\lambda})\} \quad (2-53)$$

where $U^*(\underline{a}, \bar{\lambda})$ is the complex disturbing potential. Substitution of Equation (2-53) into (2-52) and interchanging the order of the operations yields

$$\overline{[R \cos(\sigma\bar{\lambda})]} = \text{Real} \left\{ \frac{1}{\pi} \int_0^{2\pi} U^*(\underline{a}, \bar{\lambda}) \cos(\sigma\bar{\lambda}) d\bar{\lambda} \right\} \quad (2-54)$$

$$\overline{[R \sin(\sigma\bar{\lambda})]} = \text{Real} \left\{ \frac{1}{\pi} \int_0^{2\pi} U^*(\underline{a}, \bar{\lambda}) \sin(\sigma\bar{\lambda}) d\bar{\lambda} \right\}$$

It is noted that

$$\cos(\sigma\bar{\lambda}) = \frac{\exp(j\sigma\bar{\lambda}) + \exp(-j\sigma\bar{\lambda})}{2}$$

$$\sin(\sigma\bar{\lambda}) = \frac{\exp(j\sigma\bar{\lambda}) - \exp(-j\sigma\bar{\lambda})}{2j}$$

$$\text{Real}\{-jx\} = \text{Im}\{x\}$$

where

$$\exp(j\phi) = \cos(\phi) + j \sin(\phi)$$

$$\text{Real}\{x\} \equiv \text{Real part of } x$$

$$\text{Im}\{x\} \equiv \text{Imaginary part of } x$$

Applying the above expressions to Equation (2-54) gives the following

$$\begin{aligned} \overline{[R \cos(\sigma\bar{\lambda})]} &= \text{Real} \left\{ \frac{1}{2\pi} \int_0^{2\pi} [U^*(\underline{a}, \bar{\lambda}) \exp(j\sigma\bar{\lambda}) \right. \\ &\quad \left. + U^*(\underline{a}, \bar{\lambda}) \exp(-j\sigma\bar{\lambda})] d\bar{\lambda} \right\} \end{aligned} \quad (2-55)$$

$$\begin{aligned} \overline{[R \sin(\sigma\bar{\lambda})]} &= \text{Im} \left\{ \frac{1}{2\pi} \int_0^{2\pi} [U^*(\underline{a}, \bar{\lambda}) \exp(j\sigma\bar{\lambda}) \right. \\ &\quad \left. - U^*(\underline{a}, \bar{\lambda}) \exp(-j\sigma\bar{\lambda})] d\bar{\lambda} \right\} \end{aligned}$$

A short periodic coefficient generator, S_x , is defined as follows

$$S_x = \frac{1}{2\pi} \int_0^{2\pi} U^*(\underline{a}, \bar{\lambda}) \exp(jx\bar{\lambda}) d\bar{\lambda} \quad (2-56)$$

With the use of the short periodic coefficient generator, Equation (2-55) can be rewritten as

$$\begin{aligned} \overline{[R \cos(\sigma\bar{\lambda})]} &= \text{Real} \{S_\sigma + S_{-\sigma}\} \\ \overline{[R \sin(\sigma\bar{\lambda})]} &= \text{Im} \{S_\sigma - S_{-\sigma}\} \end{aligned} \quad (2-57)$$

The analytical form of the short periodic coefficients due to a conservative disturbing force is summarized in Table

2-2. Naturally the analytical short periodic coefficients are also functions of the five slowly varying mean elements. Therefore, as discussed before, it should be possible to evaluate the analytical short periodic coefficients only on the integration grid and use an interpolator to obtain the coefficients at the required output times. The coupling of the fast variable with the semimajor axis is still present.

Analytical expressions for the short periodic coefficient generator, S_x , can usually be obtained. In this section S_x will be obtained for zonal terms of the gravitational field and for third body effects.

Zonal Terms

The complex disturbing potential for the non-sphericity of the Earth's gravitational field can be expressed in terms of equinoctial variables as (Refs. 3, 4, 11 and 13)

$$U^*(\underline{a}, \lambda, \theta) = \sum_{n=2}^{\infty} \sum_{m=0}^n U_{nm}^*(\underline{a}, \lambda, \theta) \quad (2-58a)$$

where $U_{nm}^*(\underline{a}, \lambda, \theta)$ is the disturbing potential due to a spherical harmonic pair of the gravitational field. $U_{nm}^*(\underline{a}, \lambda, \theta)$ is given as

Table 2-2

Analytical Short Periodic Coefficients
for Conservative Disturbing Forces

$$\begin{aligned} \varepsilon C_{i\sigma} &= \frac{-1}{\sigma \bar{n}} \sum_{\ell=1}^5 (\bar{a}_i, \bar{a}_\ell) \frac{\overline{\partial [R \cos(\sigma \bar{\lambda})]}}{\partial \bar{a}_\ell} - \frac{(\bar{a}_i, \bar{\lambda})}{\bar{n}} \overline{[R \sin(\sigma \bar{\lambda})]} \\ &+ \left(\frac{3 \varepsilon D_{1\sigma}}{2 \sigma \bar{a}_1} \right) \delta_{i6} \end{aligned}$$

$$\begin{aligned} \varepsilon D_{i\sigma} &= \frac{-1}{\sigma \bar{n}} \sum_{\ell=1}^5 (\bar{a}_i, \bar{a}_\ell) \frac{\overline{\partial [R \sin(\sigma \bar{\lambda})]}}{\partial \bar{a}_\ell} + \frac{(\bar{a}_i, \bar{\lambda})}{\bar{n}} \overline{[R \cos(\sigma \bar{\lambda})]} \\ &- \left(\frac{3 \varepsilon C_{1\sigma}}{2 \sigma \bar{a}_1} \right) \delta_{i6} \end{aligned}$$

$(\bar{a}_i, \bar{a}_\ell)$ = Poisson Bracket

$\overline{[R \cos(\sigma \bar{\lambda})]}$ = Real $\{S_\sigma + S_{-\sigma}\}$

$\overline{[R \sin(\sigma \bar{\lambda})]}$ = Im $\{S_\sigma - S_{-\sigma}\}$

$$S_x = \frac{1}{2\pi} \int_0^{2\pi} U^*(\bar{a}, \bar{\lambda}) \exp(jx\bar{\lambda}) d\bar{\lambda}$$

$R = R(\underline{a}, \lambda)$ = disturbing potential = Real $\{U^*(\underline{a}, \lambda)\}$

$$U_{nm}^* (\underline{a}, \lambda, \theta) = \left(\frac{\mu}{a} \right) \left(\frac{R_e}{a} \right)^n C_{nm}^* \sum_{s=-n}^n V_{n,s}^m S_{2n}^{(m,s)}(p,q) \cdot \sum_{\tau=-\infty}^{\infty} Y_{\tau}^{-n-1,s}(h,k) \exp[j(\tau\lambda - m\theta)]$$

(2-58b)

where

- μ = Earth's gravitational constant
- R_e = Earth's equatorial radius
- C_{nm}^* = $C'_{nm} - jS'_{nm}$ = complex spherical pair, i.e., $C'_{n0} = -J_n$
- θ = Greenwich hour angle
- $V_{n,s}^m$ = coefficient which is not a function of the orbital elements
- $S_{2n}^{(m,s)}(p,q)$ = functions introduced by the rotation from the equatorial frame to the orbital frame
- $Y_{\tau}^{-n-1,s}(h,k)$ = Modified Hansen coefficients introduced when the potential is expressed in terms of the mean longitude

The disturbing potential due to an arbitrary zonal term ($m = 0$) does not depend upon θ and is therefore written as

$$\begin{aligned}
U_{no}^*(\underline{a}, \lambda) &= - \sum_{s=-n}^n \sum_{\tau=-\infty}^{\infty} \left(\frac{\mu}{a}\right) \left(\frac{R_e}{a}\right)^n J_n V_{n,s}^0 \cdot \\
&\cdot S_{2n}^{(0,s)}(p,q) Y_{\tau}^{-n-1,s}(h,k) \exp(j\tau\lambda)
\end{aligned}
\tag{2-59}$$

Substituting Equation (2-59) into Equation (2-56) allows the determination of the short periodic coefficient generator due to an arbitrary zonal term. This can be written as

$$\begin{aligned}
S_x &= - \sum_{s=-n}^n \sum_{\tau=-\infty}^{\infty} \left(\frac{\mu}{a}\right) \left(\frac{R_e}{a}\right)^n J_n V_{n,s}^0 S_{2n}^{(0,s)}(\bar{p}, \bar{q}) \cdot \\
&\cdot Y_{\tau}^{-n-1,s}(\bar{h}, \bar{k}) \left\{ \frac{1}{2\pi} \int_0^{2\pi} \exp[j(\tau\bar{\lambda} + x\bar{\lambda})] d\bar{\lambda} \right\}
\end{aligned}$$

The integral in the above expression will vanish for all values of τ and x except when $\tau = -x$. Therefore, the short periodic coefficient generator due to an arbitrary zonal term is the following

$$\begin{aligned}
S_x &= - \sum_{s=-n}^n \left(\frac{\mu}{a}\right) \left(\frac{R_e}{a}\right)^n J_n V_{n,s}^0 S_{2n}^{(0,s)}(\bar{p}, \bar{q}) \cdot \\
&\cdot Y_{-x}^{-n-1,s}(\bar{h}, \bar{k})
\end{aligned}
\tag{2-60}$$

It is noted that for a small eccentricity (e), the modified Hansen coefficient, $Y_{-x}^{-n-1,s}(\bar{h},\bar{k})$, is proportional to $e^{|s+x|}$. This should therefore allow a mechanism for determining the number of coefficients (σ_{\max}) required in the short periodic functions.

Third Body Effects

The complex disturbing potential for third body point mass effects can be expressed in terms of equinoctial variables as (Refs. 4, 11 and 68)

$$\begin{aligned}
 U^*(\underline{a},\lambda) &= \frac{\mu'}{a^r} \sum_{n=2}^{\infty} \left(\frac{a}{a^r}\right)^n \sum_{m=0}^n K_m V_{n,m} \sum_{r=-n}^n V_{n,r}^m \cdot \\
 &\cdot S_{2n}^{(m,r)}(\alpha,\beta,\gamma) \sum_{s=-\infty}^{\infty} \sum_{\tau=-\infty}^{\infty} Y_s^{-n-1,r}(h',k') \cdot \\
 &\cdot Y_{\tau}^{n,-m}(h,k) \exp[j(\tau\lambda + s\lambda')] \quad (2-61)
 \end{aligned}$$

where

μ' = third body gravitational constant

\underline{a}',λ' = third body equinoctial orbital elements

α,β,γ = direction cosines of third body orbital frame with respect to satellite orbital frame

$K_m, V_{n,m}, V_{n,r}^m$ = coefficients which are not functions of the orbital element

$S_{2n}^{(m,r)}(\alpha, \beta, \gamma)$ = functions introduced by the rotation between the third body frame and the satellite frame

$Y_s^{n-1,r}(h', k'), Y_\tau^{n,-n}(h, k)$ = Modified Hansen coefficients

References 4, 11 and 68 explain the third body potential in much more detail.

Substitution of the above potential into Equation (2-56) yields the following short periodic coefficient generator for third body effects

$$S_x = \frac{\mu'}{a^{\tau'}} \sum_{n=2}^{\infty} \left(\frac{\bar{a}}{a^{\tau'}} \right)^n \sum_{m=0}^n K_m V_{n,m} \sum_{r=-n}^n V_{n,r}^m S_{2n}^{(m,r)}(\alpha, \beta, \gamma) \cdot \sum_{s=-\infty}^{\infty} Y_s^{-n-1,r}(h', k') Y_{-x}^{n,-m}(\bar{h}, \bar{k}) \exp(js\lambda')$$

(2-62)

It should be noted that Equation (2-62) was derived assuming a time-independent formulation. In other words, the third body was held fixed during the averaging operation. For

medium and high altitude satellites this assumption can introduce significant errors. Section 2.2.2 will address this problem.

Again it is noted that for small eccentricities, the modified Hansen coefficients can be used as a means of determining the maximum number of short periodic coefficient required.

2.2.2 A Weak Time-Dependent Formulation*

When the disturbing function has more than one rapidly varying quantity, it may be necessary to apply a time-dependent formulation. In a time-dependent formulation the interaction of the different fast variables is taken into account. If the time rate of change of the additional fast variable is small in comparison with the satellite's mean motion [see Equations (2-34) and (2-35)], it is possible to develop a weak time-dependent formulation which takes advantage of the previously developed time-independent formulation. A weak time-dependent formulation is applicable to third body perturbations on medium altitude satellites. Tesseral terms of the Earth's gravitational field and third body perturbations on high altitude satellites probably cannot employ this

* This concept originated in discussions with P.J. Cefola, W.D. McClain and L.W. Early of the CSDL in August 1979.

development because the time rate of change of the additional phase angle (Greenwich hour angle or mean longitude of the third body) would be too large in comparison to the satellite's mean motion.

The osculating VOP equations of motion can be written in functional form as

$$\begin{aligned} \dot{a}_i &= n \delta_{i6} + \varepsilon F_i(\underline{a}, \lambda, \phi) \\ &(i = 1, 2, 3, 4, 5, 6) \end{aligned} \quad (2-63)$$

where ϕ is the second phase angle* (or fast variable) associated with the VOP formulation. The near-identity transformation is assumed to be

$$\begin{aligned} a_i &= \bar{a}_i + \varepsilon \eta_{i,1}(\bar{a}, \bar{\lambda}, \phi) \\ &(i = 1, 2, 3, 4, 5, 6) \end{aligned} \quad (2-64)$$

where $\varepsilon \eta_{i,1}(\bar{a}, \bar{\lambda}, \phi)$ is the short periodic function which will naturally depend upon both phase angles. The assumed form of the first order averaged equations of motion are

$$\dot{\bar{a}}_i = \bar{n} \delta_{i6} + \varepsilon A_{i,1}(\bar{a}, \phi) \quad (2-65)$$

* In this development ϕ will be referred to as a phase angle but could also represent a fast variable.

where $\epsilon A_{i,1}(\bar{a}, \phi)$ are the mean element rates which will depend upon the five slowly varying mean element rates and also the phase angle ϕ . The mean element rates will not contain the satellite frequency.

Substitution of Equation (2-64) into the right hand side of Equation (2-63) and expanding in a Taylor series about the mean elements yields the following to first order

$$\dot{a}_i = \bar{n} \delta_{i6} + \epsilon \left[F_i(\bar{a}, \bar{\lambda}, \phi) - \left(\frac{3\bar{n} \delta_{i6}}{2\bar{a}_1} \right) \eta_{i,1}(\bar{a}, \bar{\lambda}, \phi) \right] \quad (2-66)$$

An alternate expression for the osculating element rates can be obtained by taking the time derivative of Equation (2-64) and substituting Equation (2-65). This results in

$$\dot{a}_i = \bar{n} \delta_{i6} + \epsilon \left\{ A_{i,1}(\bar{a}, \phi) + \bar{n} \left[\frac{\partial \eta_{i,1}(\bar{a}, \bar{\lambda}, \phi)}{\partial \bar{\lambda}} \right] + \dot{\phi} \left[\frac{\partial \eta_{i,1}(\bar{a}, \bar{\lambda}, \phi)}{\partial \phi} \right] \right\} \quad (2-67)$$

Equating equal powers of the small parameter in Equation (2-66) and (2-67) results in

$$\begin{aligned} \varepsilon F_i(\bar{a}, \bar{\lambda}, \phi) - \left(\frac{3 \bar{n} \delta_{i6}}{2 \bar{a}_1} \right) \varepsilon \eta_{i,1}(\bar{a}, \bar{\lambda}, \phi) &= \varepsilon A'_{i,1}(\bar{a}, \phi) \\ &+ \bar{n} \left[\frac{\partial \varepsilon \eta_{i,1}(\bar{a}, \bar{\lambda}, \phi)}{\partial \bar{\lambda}} \right] + \phi \left[\frac{\partial \varepsilon \eta_{i,1}(\bar{a}, \bar{\lambda}, \phi)}{\partial \phi} \right] \end{aligned}$$

(2-68)

The mean element rates can be obtained from Equation (2-68) by applying the weak time-dependent assumption.

In this development the weak time-dependent assumption will specifically mean that ϕ can be approximated by ϕ_0 over the averaging interval of $\bar{\lambda}$ (ϕ_0 is the value of ϕ at the midpoint of the averaging interval). In other words, ϕ and the five slowly varying mean elements (\bar{a}) are assumed constant over the averaging interval. In addition, it will also be assumed that the short periodic functions are 2π periodic with zero mean when the weak time-dependent assumption is applied. This is represented as

$$\int_{\bar{\lambda}_0 - \pi}^{\bar{\lambda}_0 + \pi} \varepsilon \eta_{i,1}(\bar{a}, \bar{\lambda}, \phi_0) d\bar{\lambda} = 0 \quad (2-69)$$

where ϕ_0 is the value of ϕ when $\bar{\lambda}$ equals $\bar{\lambda}_0$.

Averaging Equation (2-68) with respect to $\bar{\lambda}$ yields

$$\begin{aligned} & \frac{1}{2\pi} \int_0^{2\pi} \epsilon F_i(\bar{a}, \bar{\lambda}, \phi) d\bar{\lambda} - \frac{1}{2\pi} \int_0^{2\pi} \left\{ \left(\frac{3\bar{n} \delta_{i6}}{2\bar{a}_1} \right) \epsilon \eta_{1,1}(\bar{a}, \bar{\lambda}, \phi) \right\} d\bar{\lambda} \\ &= \frac{1}{2\pi} \int_0^{2\pi} \epsilon A_{i,1}(\bar{a}, \phi) d\bar{\lambda} + \frac{1}{2\pi} \int_0^{2\pi} \left\{ \bar{n} \left[\frac{\partial \epsilon \eta_{i,1}(\bar{a}, \bar{\lambda}, \phi)}{\partial \bar{\lambda}} \right] \right. \\ & \quad \left. + \phi \left[\frac{\partial \epsilon \eta_{i,1}(\bar{a}, \bar{\lambda}, \phi)}{\partial \phi} \right] \right\} d\bar{\lambda} \end{aligned}$$

To first order in the small parameter, this can be written as

$$\begin{aligned} & \frac{1}{2\pi} \int_0^{2\pi} \epsilon F_i(\bar{a}, \bar{\lambda}, \phi) d\bar{\lambda} - \frac{1}{2\pi} \int_0^{2\pi} \left\{ \left(\frac{3\bar{n} \delta_{i6}}{2\bar{a}_1} \right) \epsilon \eta_{1,1}(\bar{a}, \bar{\lambda}, \phi) \right\} d\bar{\lambda} \\ &= \frac{1}{2\pi} \int_0^{2\pi} \epsilon A_{i,1}(\bar{a}, \phi) d\bar{\lambda} \\ & \quad + \frac{1}{2\pi} \int_0^{2\pi} \left\{ \frac{d[\epsilon \eta_{i,1}(\bar{a}, \bar{\lambda}, \phi)]}{dt} \right\} d\bar{\lambda} \end{aligned}$$

Since the yet to be determined $\epsilon \eta_{i,1}(\bar{a}, \bar{\lambda}, \phi)$ is assumed to be a "well behaved" function, the order of the integration and differentiation can be interchanged in the above expression- This results in

$$\begin{aligned}
& \frac{1}{2\pi} \int_0^{2\pi} \epsilon F_i(\underline{\bar{a}}, \bar{\lambda}, \phi) d\bar{\lambda} - \frac{1}{2\pi} \int_0^{2\pi} \left\{ \left(\frac{3\bar{n} \delta_{i6}}{2\bar{a}_1} \right) \epsilon \eta_{1,1}(\underline{\bar{a}}, \bar{\lambda}, \phi) \right\} d\bar{\lambda} \\
& = \frac{1}{2\pi} \int_0^{2\pi} \epsilon A_{i,1}(\underline{\bar{a}}, \phi) d\bar{\lambda} \\
& + \frac{d}{dt} \left\{ \frac{1}{2\pi} \int_0^{2\pi} \epsilon \eta_{i,1}(\underline{\bar{a}}, \bar{\lambda}, \phi) d\bar{\lambda} \right\}
\end{aligned}$$

Invoking the weak time-dependent assumption to the above expression results in

$$\begin{aligned}
& \frac{1}{2\pi} \int_{\bar{\lambda}_0 - \pi}^{\bar{\lambda}_0 + \pi} \epsilon F_i(\underline{\bar{a}}, \bar{\lambda}, \phi_0) d\bar{\lambda} - \left(\frac{3\bar{n} \delta_{i6}}{2\bar{a}_1} \right) \left\{ \frac{1}{2\pi} \int_{\bar{\lambda}_0 - \pi}^{\bar{\lambda}_0 + \pi} \epsilon \eta_{1,1}(\underline{\bar{a}}, \bar{\lambda}, \phi_0) d\bar{\lambda} \right\} \\
& = \epsilon A_{i,1}(\underline{\bar{a}}, \phi_0) + \frac{d}{dt} \left\{ \frac{1}{2\pi} \int_{\bar{\lambda}_0 - \pi}^{\bar{\lambda}_0 + \pi} \epsilon \eta_{i,1}(\underline{\bar{a}}, \bar{\lambda}, \phi_0) d\bar{\lambda} \right\}
\end{aligned}$$

Applying Equation (2-69) it is seen that

$$\epsilon A_{i,1}(\underline{\bar{a}}, \phi) = \frac{1}{2\pi} \int_{\bar{\lambda}_0 - \pi}^{\bar{\lambda}_0 + \pi} \epsilon F_i(\underline{\bar{a}}, \bar{\lambda}, \phi_0) d\bar{\lambda} \tag{2-70}$$

It is noted that the weak time-dependent mean element rates are the same as would be obtained with a time-independent formulation. The difference between a time-independent formulation and a weak time-dependent formulation occurs only (to

first order) in the short periodic functions. This is due to the fact that in the weak time-dependent formulation, $\dot{\phi}$, does not equal zero [see Equation (2-68)].

As in the time-independent formulation, it is assumed that the osculating element rates can be expressed in a Fourier series in $\bar{\lambda}$. It is further assumed that the coefficients of the Fourier series depend upon the five slowly varying mean elements and ϕ . This is expressed as

$$\begin{aligned} \dot{a}_i &= X_{i0}(\bar{a}, \phi) + \epsilon \sum_{\sigma=1}^{\infty} [X_{i\sigma}(\bar{a}, \phi) \cos(\sigma\bar{\lambda}) \\ &\quad + Z_{i\sigma}(\bar{a}, \phi) \sin(\sigma\bar{\lambda})] \\ (i = 1, 2, 3, 4, 5, 6) &\qquad\qquad\qquad (2-71a) \end{aligned}$$

where

$$X_{i0}(\bar{a}, \phi) = \frac{1}{2\pi} \int_0^{2\pi} \dot{a}_i d\bar{\lambda} \qquad (2-71b)$$

$$\epsilon X_{i\sigma}(\bar{a}, \phi) = \frac{1}{\pi} \int_0^{2\pi} \dot{a}_i \cos(\sigma\bar{\lambda}) d\bar{\lambda} \qquad (2-71c)$$

$$\epsilon Z_{i\sigma}(\bar{a}, \phi) = \frac{1}{\pi} \int_0^{2\pi} \dot{a}_i \sin(\sigma\bar{\lambda}) d\bar{\lambda} \qquad (2-71d)$$

Substitution of Equation (2-66) into Equation (2-71b) and using the weak time-dependent assumption, it is seen that

$$X_{i0}(\bar{a}, \phi) = \bar{n} \delta_{i6} + \epsilon A_{i,1}(\bar{a}, \phi) \quad (2-72a)$$

where $\epsilon A_{i,1}(\bar{a}, \phi)$ is defined in Equation (2-70). From Equation (2-65) it is seen that

$$X_{i0}(\bar{a}, \phi) = \dot{\bar{a}}_i \quad (2-72b)$$

Equating Equations (2-67) and (2-71a) and cancelling like terms yields the following partial differential equations for the short periodic functions

$$\begin{aligned} \bar{n} \left[\frac{\partial \epsilon \eta_{i,1}(\bar{a}, \bar{\lambda}, \phi)}{\partial \bar{\lambda}} \right] + \dot{\phi} \left[\frac{\partial \epsilon \eta_{i,1}(\bar{a}, \bar{\lambda}, \phi)}{\partial \phi} \right] \\ = \sum_{\sigma=1}^{\infty} [X_{i\sigma}(\bar{a}, \phi) \cos(\sigma \bar{\lambda}) \\ + Z_{i\sigma}(\bar{a}, \phi) \sin(\sigma \bar{\lambda})] \quad (2-73) \end{aligned}$$

The weak time-dependent short periodic functions are assumed to be of the following form

$$\begin{aligned} \epsilon \eta_{i,1}(\bar{a}, \bar{\lambda}, \phi) = \sum_{\sigma=1}^{\infty} [\epsilon U_{i\sigma}(\bar{a}, \phi) \sin(\sigma \bar{\lambda}) \\ - \epsilon V_{i\sigma}(\bar{a}, \phi) \cos(\sigma \bar{\lambda})] \quad (2-74) \end{aligned}$$

where $\epsilon U_{i\sigma}(\bar{a}, \phi)$ and $\epsilon V_{i\sigma}(\bar{a}, \phi)$ are functions to be determined. The assumed form of the Equation (2-74) is not unreasonable since it was shown that the time-independent short periodic functions are of a similar form (see Table 2-1).

Substitution of the assumed form of $\epsilon \eta_{i,1}(\bar{a}, \bar{\lambda}, \phi)$ into the left hand side of Equation (2-73) and rearranging yields

$$\begin{aligned}
 & \sum_{\sigma=1}^{\infty} \left\{ \left[\sigma \bar{n} \epsilon U_{i\sigma}(\bar{a}, \phi) - \dot{\phi} \left[\frac{\partial \epsilon V_{i\sigma}(\bar{a}, \phi)}{\partial \phi} \right] \right] \cos(\sigma \bar{\lambda}) \right. \\
 & \quad \left. + \left[\sigma \bar{n} \epsilon V_{i\sigma}(\bar{a}, \phi) + \dot{\phi} \left[\frac{\partial \epsilon U_{i\sigma}(\bar{a}, \phi)}{\partial \phi} \right] \right] \sin(\sigma \bar{\lambda}) \right\} \\
 & = \sum_{\sigma=1}^{\infty} [\epsilon X_{i\sigma}(\bar{a}, \phi) \cos(\sigma \bar{\lambda}) \\
 & \quad + \epsilon Z_{i\sigma}(\bar{a}, \phi) \sin(\sigma \bar{\lambda})] \tag{2-75}
 \end{aligned}$$

Since the above expression must be true for all values of $\bar{\lambda}$, the following must be true

$$\sigma \bar{n} \epsilon U_{i\sigma}(\bar{a}, \phi) - \dot{\phi} \left[\frac{\partial \epsilon V_{i\sigma}(\bar{a}, \phi)}{\partial \phi} \right] = \epsilon X_{i\sigma}(\bar{a}, \phi)$$

$$\sigma \bar{n} \epsilon V_{i\sigma}(\bar{a}, \phi) + \dot{\phi} \left[\frac{\partial \epsilon U_{i\sigma}(\bar{a}, \phi)}{\partial \phi} \right] = \epsilon Z_{i\sigma}(\bar{a}, \phi)$$

This can be rewritten as

$$\epsilon U_{i\sigma}(\bar{a}, \phi) = \frac{\epsilon X_{i\sigma}(\bar{a}, \phi)}{\sigma \bar{n}} + \left(\frac{\dot{\phi}}{\sigma \bar{n}} \right) \left[\frac{\partial \epsilon V_{i\sigma}(\bar{a}, \phi)}{\partial \phi} \right] \quad (2-76)$$

$$\epsilon V_{i\sigma}(\bar{a}, \phi) = \frac{\epsilon Z_{i\sigma}(\bar{a}, \phi)}{\sigma \bar{n}} - \left(\frac{\dot{\phi}}{\sigma \bar{n}} \right) \left[\frac{\partial \epsilon U_{i\sigma}(\bar{a}, \phi)}{\partial \phi} \right]$$

Equation (2-76) is a set of coupled partial differential equations for the time-dependent short periodic coefficients, $\epsilon U_{i\sigma}(\bar{a}, \phi)$ and $\epsilon V_{i\sigma}(\bar{a}, \phi)$. By substituting the expressions for $\epsilon U_{i\sigma}(\bar{a}, \phi)$ and $\epsilon V_{i\sigma}(\bar{a}, \phi)$ respectively into the right-hand side of Equation (2-76) it is seen that

$$\begin{aligned} \epsilon U_{i\sigma}(\bar{a}, \phi) &= \frac{\epsilon X_{i\sigma}(\bar{a}, \phi)}{\sigma \bar{n}} + \left(\frac{\dot{\phi}}{\sigma \bar{n}} \right) \left[\frac{\partial \left[\frac{\epsilon Z_{i\sigma}(\bar{a}, \phi)}{\sigma \bar{n}} \right]}{\partial \phi} \right] \\ &- \left(\frac{\dot{\phi}}{\sigma \bar{n}} \right)^2 \left[\frac{\partial^2 \left[\frac{\epsilon X_{i\sigma}(\bar{a}, \phi)}{\sigma \bar{n}} \right]}{\partial \phi^2} \right] + \dots \end{aligned} \quad (2-77)$$

$$\begin{aligned} \epsilon V_{i\sigma}(\bar{a}, \phi) &= \frac{\epsilon Z_{i\sigma}(\bar{a}, \phi)}{\sigma \bar{n}} - \left(\frac{\dot{\phi}}{\sigma \bar{n}} \right) \left[\frac{\partial \left[\frac{\epsilon X_{i\sigma}(\bar{a}, \phi)}{\sigma \bar{n}} \right]}{\partial \phi} \right] \\ &+ \left(\frac{\dot{\phi}}{\sigma \bar{n}} \right)^2 \left[\frac{\partial^2 \left[\frac{\epsilon Z_{i\sigma}(\bar{a}, \phi)}{\sigma \bar{n}} \right]}{\partial \phi^2} \right] - \dots \end{aligned}$$

Equation (2-77) shows that the time-dependent short periodic coefficients are represented by an alternating sign series. For a weak time-dependency, $\dot{\phi}$ will be much smaller than \bar{n} which implies that the $\left(\frac{\dot{\phi}}{\sigma\bar{n}}\right)^k$ terms tend rapidly towards zero as k becomes large.

The functions $\epsilon X_{i\sigma}(\bar{a}, \phi)$ and $\epsilon Z_{i\sigma}(\bar{a}, \phi)$ are obtained by substitution of Equation (2-66) into Equations (2-71c) and (2-71d) and applying the weak time-dependent assumption.

Noting that

$$\frac{1}{\pi} \int_{\lambda_0}^{\lambda_0 + \pi} \epsilon \eta_{1,1}(\bar{a}, \bar{\lambda}, \phi_0) \cos(\sigma\bar{\lambda}) d\bar{\lambda} = -\epsilon V_{1\sigma}(\bar{a}, \phi_0)$$

$$\frac{1}{\pi} \int_{\lambda_0}^{\lambda_0 + \pi} \epsilon \eta_{1,1}(\bar{a}, \bar{\lambda}, \phi_0) \sin(\sigma\bar{\lambda}) d\bar{\lambda} = \epsilon U_{1\sigma}(\bar{a}, \phi_0)$$

results in the following

$$\begin{aligned} \frac{\epsilon X_{i\sigma}(\bar{a}, \phi)}{\sigma\bar{n}} &= \frac{1}{\sigma\bar{n}\pi} \int_{\lambda_0}^{\lambda_0 + \pi} \epsilon F_i(\bar{a}, \bar{\lambda}, \phi_0) \cos(\sigma\bar{\lambda}) d\bar{\lambda} \\ &+ \left(\frac{3 \delta_{i6}}{2 \sigma \bar{a}_1} \right) \epsilon V_{1\sigma}(\bar{a}, \phi_0) \end{aligned}$$

(2-78)

$$\begin{aligned} \frac{\epsilon Z_{i\sigma}(\bar{a}, \phi)}{\sigma \bar{n}} &= \frac{1}{\sigma \bar{n} \pi} \int_{\bar{\lambda}_0 - \pi}^{\bar{\lambda}_0 + \pi} \epsilon F_i(\bar{a}, \bar{\lambda}, \phi_0) \sin(\sigma \bar{\lambda}) d\bar{\lambda} \\ &- \left(\frac{3 \delta_{i6}}{2 \sigma \bar{a}_1} \right) \epsilon U_{1\sigma}(\bar{a}, \phi_0) \end{aligned} \quad (2-78)$$

Substitution of Equation (2-77) into Equation (2-78) results in

$$\begin{aligned} \frac{\epsilon X_{i\sigma}(\bar{a}, \phi)}{\sigma \bar{n}} &= \frac{1}{\sigma \bar{n} \pi} \int_{\bar{\lambda}_0 - \pi}^{\bar{\lambda}_0 + \pi} \epsilon F_i(\bar{a}, \bar{\lambda}, \phi_0) \cos(\sigma \bar{\lambda}) d\bar{\lambda} \\ &+ \left(\frac{3 \delta_{i6}}{2 \sigma \bar{a}_1} \right) \left\{ \frac{\epsilon Z_{1\sigma}(\bar{a}, \phi_0)}{\sigma \bar{n}} \right. \\ &- \left. \left(\frac{\dot{\phi}}{\sigma \bar{n}} \right) \left[\frac{\partial \left[\frac{\epsilon X_{1\sigma}(\bar{a}, \phi)}{\sigma \bar{n}} \right]}{\partial \phi} \right]_{\phi_0} + \dots \right\} \end{aligned} \quad (2-79)$$

$$\begin{aligned} \frac{\epsilon Z_{i\sigma}(\bar{a}, \phi)}{\sigma \bar{n}} &= \frac{1}{\sigma \bar{n} \pi} \int_{\bar{\lambda}_0 - \pi}^{\bar{\lambda}_0 + \pi} \epsilon F_i(\bar{a}, \bar{\lambda}, \phi_0) \cos(\sigma \bar{\lambda}) d\bar{\lambda} \\ &- \left(\frac{3 \delta_{i6}}{2 \sigma \bar{a}_1} \right) \left\{ \frac{\epsilon X_{1\sigma}(\bar{a}, \phi_0)}{\sigma \bar{n}} \right. \\ &+ \left. \left(\frac{\dot{\phi}}{\sigma \bar{n}} \right) \left[\frac{\partial \left[\frac{\epsilon Z_{1\sigma}(\bar{a}, \phi)}{\sigma \bar{n}} \right]}{\partial \phi} \right]_{\phi_0} - \dots \right\} \end{aligned}$$

For convenience the following definitions are made

$$\begin{aligned} \epsilon C_{i\sigma} &= \frac{1}{\sigma \bar{n} \pi} \int_{\bar{\lambda}_0 - \pi}^{\bar{\lambda}_0 + \pi} \epsilon F_i(\bar{a}, \bar{\lambda}, \phi_0) \cos(\sigma \bar{\lambda}) d\bar{\lambda} \\ &+ \left(\frac{3 \delta_{i6}}{2 \sigma \bar{a}_1} \right) \epsilon D_{1\sigma} \end{aligned} \quad (2-80)$$

$$\begin{aligned} \epsilon D_{i\sigma} &= \frac{1}{\sigma \bar{n} \pi} \int_{\bar{\lambda}_0 - \pi}^{\bar{\lambda}_0 + \pi} \epsilon F_i(\bar{a}, \bar{\lambda}, \phi_0) \sin(\sigma \bar{\lambda}) d\bar{\lambda} \\ &- \left(\frac{3 \delta_{i6}}{2 \sigma \bar{a}_1} \right) \epsilon C_{1\sigma} \end{aligned}$$

Substitution of Equation (2-80) into Equation (2-79)

and rearranging results in

$$\begin{aligned} \frac{\epsilon X_{i\sigma}(\bar{a}, \phi)}{\sigma \bar{n}} &= \epsilon C_{i\sigma} - \left(\frac{3 \delta_{i6}}{2 \sigma \bar{a}_1} \right) \left\{ \left(\frac{\dot{\phi}}{\sigma \bar{n}} \right) \left[\frac{\partial \epsilon C_{1\sigma}}{\partial \phi} \right]_{\phi_0} \right. \\ &- \left. \left(\frac{\dot{\phi}}{\sigma \bar{n}} \right)^2 \left[\frac{\partial^2 \epsilon D_{1\sigma}}{\partial \phi^2} \right]_{\phi_0} + \dots \right\} \end{aligned} \quad (2-81)$$

$$\begin{aligned} \frac{\epsilon Z_{i\sigma}(\bar{a}, \phi)}{\sigma \bar{n}} &= \epsilon D_{i\sigma} - \left(\frac{3 \delta_{i6}}{2 \sigma \bar{a}_1} \right) \left\{ \left(\frac{\dot{\phi}}{\sigma \bar{n}} \right) \left[\frac{\partial \epsilon D_{1\sigma}}{\partial \phi} \right]_{\phi_0} \right. \\ &- \left. \left(\frac{\dot{\phi}}{\sigma \bar{n}} \right)^2 \left[\frac{\partial^2 \epsilon C_{1\sigma}}{\partial \phi^2} \right]_{\phi_0} + \dots \right\} \end{aligned}$$

The time-dependent short periodic coefficients are obtained by substitution of Equation (2-81) into Equation (2-77), viz.

$$\begin{aligned}
 \epsilon U_{i\sigma}(\bar{a}, \phi) &= \epsilon C_{i\sigma} + \left(\frac{\dot{\phi}}{\sigma \bar{n}} \right) \left[\frac{\partial \epsilon D_{i\sigma}}{\partial \phi} \right] \\
 &- \left(\frac{\dot{\phi}}{\sigma \bar{n}} \right)^2 \left[\frac{\partial^2 \epsilon C_{i\sigma}}{\partial \phi^2} \right] + \dots \\
 &.. \left(\frac{3 \delta_{i6}}{2 \sigma \bar{a}_1} \right) \left\{ \left(\frac{\dot{\phi}}{\sigma \bar{n}} \right) \left[\frac{\partial \epsilon C_{1\sigma}}{\partial \phi} \right] + \dots \right\} \quad (2-82)
 \end{aligned}$$

$$\begin{aligned}
 \epsilon V_{i\sigma}(\bar{a}, \phi) &= \epsilon D_{i\sigma} - \left(\frac{\dot{\phi}}{\sigma \bar{n}} \right) \left[\frac{\partial \epsilon C_{i\sigma}}{\partial \phi} \right] \\
 &+ \left(\frac{\dot{\phi}}{\sigma \bar{n}} \right)^2 \left[\frac{\partial^2 \epsilon D_{i\sigma}}{\partial \phi^2} \right] - \dots \\
 &- \left(\frac{3 \delta_{i6}}{2 \sigma \bar{a}_1} \right) \left\{ \left(\frac{\dot{\phi}}{\sigma \bar{n}} \right) \left[\frac{\partial \epsilon D_{1\sigma}}{\partial \phi} \right] + \dots \right\}
 \end{aligned}$$

Equation (2-82) is an expression for the weak time-dependent short periodic coefficients. The weak time-dependent short periodic functions are given in Equation (2-74). The coupling between the fast variable and the semimajor axis in Equation (2-82) was taken only to first power in $\left(\frac{\dot{\phi}}{\sigma \bar{n}} \right)$. Using the chain rule, Equation (2-82) can be rewritten as

$$\begin{aligned}
\epsilon U_{i\sigma}(\bar{a}, \phi) &= \epsilon C_{i\sigma} + \left(\frac{1}{\sigma \bar{n}}\right) \left[\frac{\partial \epsilon D_{i\sigma}}{\partial t} \right] \\
&- \left(\frac{1}{\sigma \bar{n}}\right)^2 \left[\frac{\partial^2 \epsilon C_{i\sigma}}{\partial t^2} \right] + \dots \\
&- \left(\frac{3 \delta_{i6}}{2 \sigma \bar{a}_1}\right) \left\{ \left(\frac{1}{\sigma \bar{n}}\right) \left[\frac{\partial \epsilon C_{1\sigma}}{\partial t} \right] + \dots \right\} \quad (2-83)
\end{aligned}$$

$$\begin{aligned}
\epsilon V_{i\sigma}(\bar{a}, \phi) &= \epsilon D_{i\sigma} - \left(\frac{1}{\sigma \bar{n}}\right) \left[\frac{\partial \epsilon C_{i\sigma}}{\partial t} \right] \\
&+ \left(\frac{1}{\sigma \bar{n}}\right)^2 \left[\frac{\partial^2 \epsilon D_{i\sigma}}{\partial t^2} \right] - \dots \\
&- \left(\frac{3 \delta_{i6}}{2 \sigma \bar{a}_1}\right) \left\{ \left(\frac{1}{\sigma \bar{n}}\right) \left[\frac{\partial \epsilon D_{1\sigma}}{\partial t} \right] + \dots \right\}
\end{aligned}$$

The weak time-dependent short periodic formulation is summarized in Table 2-3. The weak time-dependent formulation in Table 2-3 is interesting in that it uses the previously defined time-independent short periodic coefficients ($\epsilon C_{i\sigma}$, $\epsilon D_{i\sigma}$) to define the weak time-dependent short periodic coefficients [$\epsilon U_{i\sigma}(\bar{a}, \phi)$, $\epsilon V_{i\sigma}(\bar{a}, \phi)$]. The formulation as given in Table 2-3 also indicates that there is an additional coupling between the fast variable and the semimajor axis beyond the time-independent coupling as given in Equations (2-44) and (2-80).

Table 2-3

Weak Time-Dependent Short Periodic Functions

$$\epsilon \eta_{i,1}(\bar{a}, \bar{\lambda}, \phi) = \sum_{\sigma=1}^{\infty} [\epsilon U_{i\sigma}(\bar{a}, \phi) \sin(\sigma \bar{\lambda}) - \epsilon V_{i\sigma}(\bar{a}, \phi) \cos(\sigma \bar{\lambda})]$$

$$\begin{aligned} \epsilon U_{i\sigma}(\bar{a}, \phi) &= \epsilon C_{i\sigma} + \left(\frac{\dot{\phi}}{\sigma \bar{n}} \right) \left[\frac{\partial \epsilon D_{i\sigma}}{\partial \phi} \right] - \left(\frac{\dot{\phi}}{\sigma \bar{n}} \right)^2 \left[\frac{\partial^2 \epsilon C_{i\sigma}}{\partial \phi^2} \right] + \dots \\ &- \left(\frac{3 \delta_{i6}}{2 \sigma \bar{a}_1} \right) \left\{ \left(\frac{\dot{\phi}}{\sigma \bar{n}} \right) \left[\frac{\partial \epsilon C_{1\sigma}}{\partial \phi} \right] + \dots \right\} \end{aligned}$$

$$\begin{aligned} &= \epsilon C_{i\sigma} + \left(\frac{1}{\sigma \bar{n}} \right) \left[\frac{\partial \epsilon D_{i\sigma}}{\partial t} \right] - \left(\frac{1}{\sigma \bar{n}} \right)^2 \left[\frac{\partial^2 \epsilon C_{i\sigma}}{\partial t^2} \right] + \dots \\ &- \left(\frac{3 \delta_{i6}}{2 \sigma \bar{a}_1} \right) \left\{ \left(\frac{1}{\sigma \bar{n}} \right) \left[\frac{\partial \epsilon C_{1\sigma}}{\partial t} \right] + \dots \right\} \end{aligned}$$

$$\begin{aligned} \epsilon V_{i\sigma}(\bar{a}, \phi) &= \epsilon D_{i\sigma} - \left(\frac{\dot{\phi}}{\sigma \bar{n}} \right) \left[\frac{\partial \epsilon C_{i\sigma}}{\partial \phi} \right] + \left(\frac{\dot{\phi}}{\sigma \bar{n}} \right)^2 \left[\frac{\partial^2 \epsilon D_{i\sigma}}{\partial \phi^2} \right] + \dots \\ &- \left(\frac{3 \delta_{i6}}{2 \sigma \bar{a}_1} \right) \left\{ \left(\frac{\dot{\phi}}{\sigma \bar{n}} \right) \left[\frac{\partial \epsilon D_{1\sigma}}{\partial \phi} \right] + \dots \right\} \end{aligned}$$

$$\begin{aligned} &= \epsilon D_{i\sigma} - \left(\frac{1}{\sigma \bar{n}} \right) \left[\frac{\partial \epsilon C_{i\sigma}}{\partial t} \right] + \left(\frac{1}{\sigma \bar{n}} \right)^2 \left[\frac{\partial^2 \epsilon D_{i\sigma}}{\partial t^2} \right] + \dots \\ &- \left(\frac{3 \delta_{i6}}{2 \sigma \bar{a}_1} \right) \left\{ \left(\frac{1}{\sigma \bar{n}} \right) \left[\frac{\partial \epsilon D_{1\sigma}}{\partial t} \right] + \dots \right\} \end{aligned}$$

Table 2-3

Weak Time-Dependent Short Periodic Functions
(cont.)

$$\epsilon C_{i\sigma} = \frac{1}{\sigma n \pi} \int_{\bar{\lambda}_0 - \pi}^{\bar{\lambda}_0 + \pi} \epsilon F_i(\bar{a}, \bar{\lambda}, \phi_0) \cos(\sigma \bar{\lambda}) d\bar{\lambda} + \left(\frac{3 \delta_{i6}}{2 \sigma \bar{a}_1} \right) \epsilon D_{1\sigma}$$

$$\epsilon D_{i\sigma} = \frac{1}{\sigma n \pi} \int_{\bar{\lambda}_0 - \pi}^{\bar{\lambda}_0 + \pi} \epsilon F_i(\bar{a}, \bar{\lambda}, \phi_0) \sin(\sigma \bar{\lambda}) d\bar{\lambda} - \left(\frac{3 \delta_{i6}}{2 \sigma \bar{a}_1} \right) \epsilon C_{1\sigma}$$

The weak time-dependent short periodic coefficients will be a function of the five slowly varying mean elements and the phase angle ϕ . Since the weak time-dependent assumption requires that ϕ also be slowly varying, the time-dependent short periodic coefficients should be slowly varying. Therefore, as with the time-independent short periodic coefficients, it should be possible to determine the time-dependent short periodic coefficients on the averaged integration grid and interpolate to obtain them at the output time. Numerical results presented in Section 2.4 verify this point.

One of the requirements of the weak time-dependent assumption was that the short periodic functions be 2π periodic with zero mean when ϕ is held constant over the averaging interval [see Equation (2-69)]. This is equivalent to requiring that the short periodic functions do not contain m -daily or s -monthly/yearly frequencies [$(m\theta)$ or $(s\lambda')$ frequencies that appear in the disturbing potentials for tesserals or third body, see Equations (2-58b) or (2-61)]. Therefore, the m -daily or s -monthly/yearly frequencies must be in the mean element rates. In the case of tesseral perturbations this can require the stepsize of the AOG to be considerably less than one day. It is basically for this reason that the weak time-dependent formulation is not applicable to tesseral perturbations. In the case of third body perturbations on a medium

altitude satellite, the AOG should adequately determine the major s-monthly/yearly effects with a one to two day numerical integration time step. In this investigation a medium altitude satellite will refer to satellites with periods not greater than one day.

For a weak time-dependency, the term $\left(\frac{\dot{\phi}}{\sigma\bar{n}}\right)^2$ should be very small and the second derivative of the short periodic coefficients with respect to ϕ should also be small. It should therefore be possible to neglect $\left(\frac{\dot{\phi}}{\sigma\bar{n}}\right)^2$ terms in the expressions for $\epsilon U_{i\sigma}(\bar{a}, \phi)$ and $\epsilon V_{i\sigma}(\bar{a}, \phi)$. This results in

$$\begin{aligned} \epsilon U_{i\sigma}(\bar{a}, \phi) &= \epsilon C_{i\sigma} + \left(\frac{\dot{\phi}}{\sigma\bar{n}}\right) \left[\frac{\partial \epsilon D_{i\sigma}}{\partial \phi} \right] \\ &- \left(\frac{3 \delta_{i6}}{2 \sigma \bar{a}_1} \right) \left(\frac{\dot{\phi}}{\sigma\bar{n}} \right) \left[\frac{\partial \epsilon C_{1\sigma}}{\partial \phi} \right] \end{aligned}$$

(2-84a)

$$\begin{aligned} \epsilon V_{i\sigma}(\bar{a}, \phi) &= \epsilon D_{i\sigma} - \left(\frac{\dot{\phi}}{\sigma\bar{n}}\right) \left[\frac{\partial \epsilon C_{i\sigma}}{\partial \phi} \right] \\ &- \left(\frac{3 \delta_{i6}}{2 \sigma \bar{a}_1} \right) \left(\frac{\dot{\phi}}{\sigma\bar{n}} \right) \left[\frac{\partial \epsilon D_{1\sigma}}{\partial \phi} \right] \end{aligned}$$

or equivalently

$$\begin{aligned} \epsilon U_{i\sigma}(\bar{a}, \phi) &= \epsilon C_{i\sigma} + \left(\frac{1}{\sigma \bar{n}} \right) \left[\frac{\partial \epsilon D_{i\sigma}}{\partial t} \right] \\ &- \left(\frac{3 \delta_{i6}}{2 \sigma \bar{a}_1} \right) \left(\frac{1}{\sigma \bar{n}} \right) \left[\frac{\partial \epsilon C_{1\sigma}}{\partial t} \right] \end{aligned}$$

(2-84b)

$$\begin{aligned} \epsilon V_{i\sigma}(\bar{a}, \phi) &= \epsilon D_{i\sigma} - \left(\frac{1}{\sigma \bar{n}} \right) \left[\frac{\partial \epsilon C_{i\sigma}}{\partial t} \right] \\ &- \left(\frac{3 \delta_{i6}}{2 \sigma \bar{a}_1} \right) \left(\frac{1}{\sigma \bar{n}} \right) \left[\frac{\partial \epsilon D_{1\sigma}}{\partial t} \right] \end{aligned}$$

The determination of the time-dependent short periodic coefficients requires the calculation of the time-independent short periodic coefficients and the various partial derivative of these coefficients with respect to time or ϕ . The calculation of $\epsilon C_{i\sigma}$ and $\epsilon D_{i\sigma}$ would be done as previously described in Section 2.2.1 (numerical quadrature or analytically). The determination of the various partial derivatives of $\epsilon C_{i\sigma}$ and $\epsilon D_{i\sigma}$ with respect to ϕ or t can be done numerically or analytically.

A numerical method of determining the time derivatives of $\epsilon C_{i\sigma}$ and $\epsilon D_{i\sigma}$ is to use a finite-differencing technique (see Appendix B). Functionally this can be written as

$$\left[\frac{\partial \epsilon C_{i\sigma}}{\partial t} \right] \sim \frac{\epsilon C_{i\sigma}(t_0 + \Delta t) - \epsilon C_{i\sigma}(t_0)}{\Delta t}$$

(2-85)

$$\left[\frac{\partial \epsilon D_{i\sigma}}{\partial t} \right] \sim \frac{\epsilon D_{i\sigma}(t_0 + \Delta t) - \epsilon D_{i\sigma}(t_0)}{\Delta t}$$

The advantage of the finite-differencing technique is that much of the same software that is used to calculate $\epsilon C_{i\sigma}$ and $\epsilon D_{i\sigma}$ can be used to obtain their time derivatives. Once the time derivatives of $\epsilon C_{i\sigma}$ and $\epsilon D_{i\sigma}$ are known, Equation (2-84b) can be used to determine the time-dependent short periodic coefficients.

Another numerical method that can be used to obtain the partial derivatives of $\epsilon C_{i\sigma}$ and $\epsilon D_{i\sigma}$ with respect to ϕ is the quadrature approach. Taking the k th partial derivative of Equation (2-80) results in

$$\left[\frac{\partial^k \epsilon C_{i\sigma}}{\partial \phi^k} \right] = \frac{1}{\sigma n \pi} \int_{\bar{\lambda}_0 - \pi}^{\bar{\lambda}_0 + \pi} \left[\frac{\partial^k \epsilon F_i(\bar{a}, \bar{\lambda}, \phi)}{\partial \phi^k} \right]_{\phi_0} \cos(\sigma \bar{\lambda}) d\bar{\lambda} \\ + \left(\frac{3 \delta_{i6}}{2 \sigma \bar{a}_1} \right) \left[\frac{\partial^k \epsilon D_{1\sigma}}{\partial \phi^k} \right]$$

(2-86)

$$\left[\frac{\partial^k \epsilon_{D_{i\sigma}}}{\partial \phi^k} \right] = \frac{1}{\sigma \bar{n} \pi} \int_{\bar{\lambda}_0 - \pi}^{\bar{\lambda}_0 + \pi} \left[\frac{\partial^k \epsilon_{F_i}(\bar{a}, \bar{\lambda}, \phi)}{\partial \phi^k} \right]_{\phi_0} \sin(\sigma \bar{\lambda}) d\bar{\lambda} - \left(\frac{3 \delta_{i6}}{2 \sigma \bar{a}_1} \right) \left[\frac{\partial^k \epsilon_{C_{1\sigma}}}{\partial \phi^k} \right] \quad (2-86)$$

A quadrature algorithm would then be applied to Equation (2-86) in order to determine the partial derivatives of $\epsilon_{C_{i\sigma}}$ and $\epsilon_{D_{i\sigma}}$ with respect to ϕ . Equations (2-82) or (2-84a) could then be used to obtain the time-dependent short periodic coefficients.

For conservative disturbing forces, an analytical approach is usually possible for determining the partial derivatives of $\epsilon_{C_{i\sigma}}$ and $\epsilon_{D_{i\sigma}}$ with respect to ϕ . Taking the k th partial derivatives of Equation (2-51) and realizing that the Poisson Brackets do not depend upon ϕ and that the order of differentiation can be interchanged, the following expression results

$$\left[\frac{\partial^k \epsilon_{C_{i\sigma}}}{\partial \phi^k} \right] = \frac{-1}{\sigma \bar{n}} \sum_{\ell=1}^5 (\bar{a}_i, \bar{a}_\ell) \frac{\partial [R^{(k)} \cos(\sigma \bar{\lambda})]}{\partial \bar{a}_\ell} - \frac{(\bar{a}_i, \bar{\lambda})}{\bar{n}} [R^{(k)} \sin(\sigma \bar{\lambda})] + \left(\frac{3 \delta_{i6}}{2 \sigma \bar{a}_1} \right) \left[\frac{\partial^k \epsilon_{D_{1\sigma}}}{\partial \phi^k} \right] \quad (2-87)$$

$$\begin{aligned} \left[\frac{\partial^k \epsilon_{D_{i\sigma}}}{\partial \phi^k} \right] &= \frac{-1}{\sigma \bar{n}} \sum_{\ell=1}^5 (\bar{a}_i, \bar{a}_\ell) \frac{\overline{\partial [R^{(k)} \sin(\sigma \bar{\lambda})]}}{\partial \bar{a}_\ell} \\ &+ \frac{(\bar{a}_i, \bar{\lambda})}{\bar{n}} \overline{[R^{(k)} \cos(\sigma \bar{\lambda})]} - \left(\frac{3 \delta_{i6}}{2 \sigma \bar{a}_1} \right) \left[\frac{\partial^k \epsilon_{C_{1\sigma}}}{\partial \phi^k} \right] \end{aligned} \quad (2-87)$$

where from Equation (2-52) it is seen that

$$\overline{[R^{(k)} \cos(\sigma \bar{\lambda})]} = \frac{1}{\pi} \int_0^{2\pi} \left[\frac{\partial^k R(\bar{a}, \bar{\lambda}, \phi)}{\partial \phi^k} \right] \cos(\sigma \bar{\lambda}) d\bar{\lambda} \quad (2-88)$$

$$\overline{[R^{(k)} \sin(\sigma \bar{\lambda})]} = \frac{1}{\pi} \int_0^{2\pi} \left[\frac{\partial^k R(\bar{a}, \bar{\lambda}, \phi)}{\partial \phi^k} \right] \sin(\sigma \bar{\lambda}) d\bar{\lambda}$$

When a complex potential, as given in Equation (2-53), is considered, it can be shown that [see the derivation of Equation (2-57)]

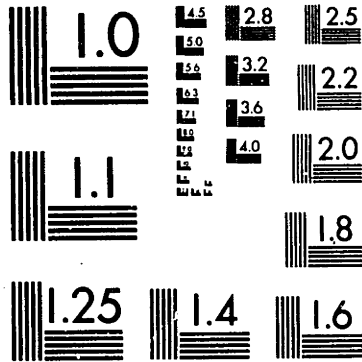
$$\overline{[R^{(k)} \cos(\sigma \bar{\lambda})]} = \text{Real} \{ S_\sigma^{(k)} + S_{-\sigma}^{(k)} \} \quad (2-89)$$

$$\overline{[R^{(k)} \sin(\sigma \bar{\lambda})]} = \text{Im} \{ S_\sigma^{(k)} - S_{-\sigma}^{(k)} \}$$

where

$$S_x^{(k)} = \frac{1}{2\pi} \int_{\bar{\lambda}_0 - \pi}^{\bar{\lambda}_0 + \pi} \left[\frac{\partial^k U^*(\bar{a}, \bar{\lambda}, \phi)}{\partial \phi^k} \right]_{\phi_0} \exp(jx\bar{\lambda}) d\bar{\lambda} \quad (2-90)$$

Table 2-4 summarizes these results.



MICROCOPY RESOLUTION TEST CHART
NATIONAL BUREAU OF STANDARDS-1963-A

20X

NOTICE THIS MATERIAL MAY BE PROTECTED BY
COPYRIGHT LAW (TITLE 17 U.S. CODE)

Table 2-4

Analytical Partial Derivatives of the Short Periodic
Coefficients for Conservative Disturbing Forces

$$\left[\frac{\partial^k \epsilon_{C_{i\sigma}}}{\partial \phi^k} \right] = \frac{-1}{\sigma \bar{n}} \sum_{\ell=1}^5 (\bar{a}_i, \bar{a}_\ell) \frac{\partial \overline{[R^{(k)} \cos(\sigma \bar{\lambda})]}}{\partial \bar{a}_\ell} - \frac{(\bar{a}_i, \bar{\lambda})}{\bar{n}} \overline{[R^{(k)} \sin(\sigma \bar{\lambda})]}$$

$$+ \left(\frac{3 \delta_{i6}}{2 \sigma \bar{a}_1} \right) \left[\frac{\partial^k \epsilon_{D_{1\sigma}}}{\partial \phi^k} \right]$$

$$\left[\frac{\partial^k \epsilon_{D_{i\sigma}}}{\partial \phi^k} \right] = \frac{-1}{\sigma \bar{n}} \sum_{\ell=1}^5 (\bar{a}_i, \bar{a}_\ell) \frac{\partial \overline{[R^{(k)} \sin(\sigma \bar{\lambda})]}}{\partial \bar{a}_\ell} + \frac{(\bar{a}_i, \bar{\lambda})}{\bar{n}} \overline{[R^{(k)} \cos(\sigma \bar{\lambda})]}$$

$$- \left(\frac{3 \delta_{i6}}{2 \sigma \bar{a}_1} \right) \left[\frac{\partial^k \epsilon_{C_{1\sigma}}}{\partial \phi^k} \right]$$

$$\overline{[R^{(k)} \cos(\sigma \bar{\lambda})]} = \text{Real}\{S_\sigma^{(k)} + S_{-\sigma}^{(k)}\}$$

$$\overline{[R^{(k)} \sin(\sigma \bar{\lambda})]} = \text{Im}\{S_\sigma^{(k)} - S_{-\sigma}^{(k)}\}$$

$$S_x^{(k)} = \frac{1}{2\pi} \int_{\bar{\lambda}_0 - \pi}^{\bar{\lambda}_0 + \pi} \frac{\partial^k U^*(\bar{a}, \bar{\lambda}, \phi)}{\partial \phi^k} \exp(jx\bar{\lambda}) d\bar{\lambda}$$

$$R = R(\underline{a}, \lambda, \phi) = \text{disturbing potential} = \text{Real}\{U^*(\underline{a}, \lambda, \phi)\}$$

For third body effects, the complex disturbing potential was given in Equation (2-61). The additional phase angle in this case is the mean longitude of the third body (λ'). Taking the k th derivative of the complex potential with respect to ϕ and substituting into Equation (2-90) results in

$$\begin{aligned}
 S_x^{(k)} = & \frac{\mu'}{a^r} \sum_{n=2}^{\infty} \left(\frac{\bar{a}}{a^r} \right)^n \sum_{m=0}^n K_m V_{n,m} \sum_{r=-n}^n V_{n,r}^m S_{2n}^{(m,r)}(\alpha, \beta, \gamma) \cdot \\
 & \cdot \sum_{s=-\infty}^{\infty} Y_s^{-n-1,r} (h', k') Y_{-x}^{n,-m} (\bar{h}, \bar{k}) (js)^x \cdot \\
 & \cdot \exp(js\lambda'_o) \tag{2-91}
 \end{aligned}$$

Equations (2-62) and (2-91) along with Tables 2-2, 2-3 and 2-4 will yield complete analytical expressions for the third body weak time-dependent short periodic coefficients.

2.3 A Second Order Drag Theory in the Averaged Equations of Motion

A semianalytical satellite theory to first order in the small parameter (the AOG and SPG) may not be sufficient for highly accurate ephemeris generation. This is especially true for low altitude satellites in which the second order long periodic and secular motion caused by oblateness and drag effects may be significant. Since the artificial satellite

problem is a non-linear dynamical system, the coupling between oblateness and drag must also be considered in the second order effects (Refs. 48 and 50).

This section extends the AOG to second order in the small parameters when two perturbing forces are considered. The general functional form of a second order AOG for two perturbations is developed first. Next, the oblateness/drag coupling is formulated in a general form. The general form of the second order AOG is simplified by use of the first order short periodic variations as given in Table 2-1. Finally, algorithmic considerations for the oblateness/drag coupling are discussed.

A Second Order AOG

The osculating VOP equations of motion for two perturbing forces can be expressed functionally as

$$\dot{a}_i = n \delta_{i6} + \epsilon F_i(\underline{a}, \lambda) + \nu G_i(\underline{a}, \lambda) \quad (2-92)$$

where ϵ and ν are the small parameters.

As was stated previously, the second order averaged equations of motion require the first order short periodic functions [see Equation (2-29)]. The transformation equations

from mean element space to osculating element space can therefore be written as

$$\underline{a}_i = \bar{a}_i + \epsilon \eta_{i,1}(\bar{a}, \bar{\lambda}) + \nu \psi_{i,1}(\bar{a}, \bar{\lambda}) \quad (2-93)$$

where $\epsilon \eta_{i,1}(\bar{a}, \bar{\lambda})$ are the first order short periodic functions due to one perturbation (oblateness) and where $\nu \psi_{i,1}(\bar{a}, \bar{\lambda})$ are the first order short periodic functions due to the other perturbation (drag).

The mean element rates are assumed to be a function of the five slowly varying mean elements and must include the mixed or coupling terms that result due to multiple perturbations. To second order in both small parameters, this can be written as (Ref. 3)

$$\begin{aligned} \dot{\underline{a}}_i &= \bar{n} \delta_{i6} + \epsilon B_{i,1,0}(\bar{a}) + \nu B_{i,0,1}(\bar{a}) \\ &+ \epsilon \nu B_{i,1,1}(\bar{a}) + \epsilon^2 B_{i,2,0}(\bar{a}) + \nu^2 B_{i,0,2}(\bar{a}) \end{aligned} \quad (2-94)$$

The coupling term is $\epsilon \nu B_{i,1,1}(\bar{a})$.

The functions $B_{i,j,k}(\bar{a})$ are determined in an analogous manner to the determination of the functions $A_{i,j}(\bar{a})$ [see

Equations (2-28) and (2-29)]. First, expressions for the osculating element rates in terms of the functions $B_{i,j,k}(\bar{a})$ and the first order short periodic functions are obtained by taking the time derivative of Equation (2-93) and substituting Equation (2-94). Next, alternative expressions for the osculating element rates are obtained in terms of the first order short periodic functions and the VOP disturbing functions, [$\epsilon F_i(\bar{a}, \bar{\lambda})$ and $\nu G_i(\bar{a}, \bar{\lambda})$] by substituting the near-identity transformation into the right hand side of the osculating VOP equations of motion [Equation (2-92)] and expanding in a Taylor series. Equating equal powers of the small parameters in these two expressions for the osculating element rates yields expressions for the functions $B_{i,j,k}(\bar{a})$. Averaging these expressions with respect to the mean-mean longitude over one revolution and assuming that the five slowly varying mean elements are constant over the averaging interval, the component functions of the mean element rates to second order in the small parameters are

$$B_{i,1,0}(\bar{a}) = \frac{1}{2\pi} \int_0^{2\pi} F_i(\bar{a}, \bar{\lambda}) d\bar{\lambda} \quad (2-95a)$$

$$B_{i,0,1}(\bar{a}) = \frac{1}{2\pi} \int_0^{2\pi} G_i(\bar{a}, \bar{\lambda}) d\bar{\lambda} \quad (2-95b)$$

$$\begin{aligned}
B_{i,1,1}(\bar{a}) &= \frac{1}{2\pi} \int_0^{2\pi} \left[\sum_{\ell=1}^6 \left\{ \eta_{\ell,1}(\bar{a}, \bar{\lambda}) \left[\frac{\partial G_i(\bar{a}, \bar{\lambda})}{\partial \bar{a}_\ell} \right] \right. \right. \\
&+ \left. \left. \psi_{\ell,1}(\bar{a}, \bar{\lambda}) \left[\frac{\partial F_i(\bar{a}, \bar{\lambda})}{\partial \bar{a}_\ell} \right] \right\} \right. \\
&+ \left. \frac{15 \bar{n} \delta_{i6}}{4 \bar{a}_1^2} \eta_{1,1}(\bar{a}, \bar{\lambda}) \psi_{1,1}(\bar{a}, \bar{\lambda}) \right] d\bar{\lambda}
\end{aligned} \tag{2-95c}$$

$$\begin{aligned}
B_{i,2,0}(\bar{a}) &= \frac{1}{2\pi} \int_0^{2\pi} \left\{ \sum_{\ell=1}^6 \eta_{\ell,1}(\bar{a}, \bar{\lambda}) \left[\frac{\partial F_i(\bar{a}, \bar{\lambda})}{\partial \bar{a}_\ell} \right] \right. \\
&+ \left. \frac{15 \bar{n} \delta_{i6}}{8 \bar{a}_1^2} \eta_{1,1}^2(\bar{a}, \bar{\lambda}) \right\} d\bar{\lambda}
\end{aligned} \tag{2-95d}$$

$$\begin{aligned}
B_{i,0,2}(\bar{a}) &= \frac{1}{2\pi} \int_0^{2\pi} \left\{ \sum_{\ell=1}^6 \psi_{\ell,1}(\bar{a}, \bar{\lambda}) \left[\frac{\partial G_i(\bar{a}, \bar{\lambda})}{\partial \bar{a}_\ell} \right] \right. \\
&+ \left. \frac{15 \bar{n} \delta_{i6}}{8 \bar{a}_1^2} \psi_{1,1}^2(\bar{a}, \bar{\lambda}) \right\} d\bar{\lambda}
\end{aligned} \tag{2-95e}$$

Comparing the above expressions with Equations (2-28) and (2-29) it is seen that the second order effects of multiple perturbations cannot be considered separately. The coupling term, $\epsilon \nu B_{i,1,1}(\bar{a})$, can be a major part of the mean element rates. Although this section has considered only two perturbations,

the extension to an arbitrary number of perturbing forces is straightforward but very tedious.

Oblateness/Drag Coupling

For the case of oblateness/drag coupling, the mixed term, $\epsilon \nu B_{i,1,1}(\bar{\mathbf{a}})$, includes both the J_2 -drag and drag- J_2 coupling. The J_2 -drag coupling is the effect of the first order J_2 short periodic variations [$\epsilon \eta_{i,1}(\bar{\mathbf{a}}, \bar{\lambda})$] on the drag equations of motion [$\nu G_i(\bar{\mathbf{a}}, \bar{\lambda})$]. Similarly, the drag- J_2 coupling is the effect of the first order drag short periodic variations [$\nu \psi_i(\bar{\mathbf{a}}, \bar{\lambda})$] on the J_2 equations of motion [$\epsilon F_i(\bar{\mathbf{a}}, \bar{\lambda})$]. Functionally this can be written as

$$B_{i,1,1}(\bar{\mathbf{a}}) = B_{i,J_2DR}(\bar{\mathbf{a}}) + B_{i,DRJ_2}(\bar{\mathbf{a}}) \quad (2-96)$$

where $B_{i,J_2DR}(\bar{\mathbf{a}})$ represents the J_2 -drag coupling and $B_{i,DRJ_2}(\bar{\mathbf{a}})$ represents the drag- J_2 coupling. From Equation (2-95c) it is seen that

$$B_{i,J_2DR}(\bar{\mathbf{a}}) = \frac{1}{2\pi} \int_0^{2\pi} \left\{ \sum_{\ell=1}^6 \eta_{\ell,1}(\bar{\mathbf{a}}, \bar{\lambda}) \left[\frac{\partial G_i(\bar{\mathbf{a}}, \bar{\lambda})}{\partial \bar{a}_\ell} \right] + \frac{15 \bar{n} \delta_{i6}}{8 \bar{a}_1^2} \eta_{1,1}(\bar{\mathbf{a}}, \bar{\lambda}) \psi_{1,1}(\bar{\mathbf{a}}, \bar{\lambda}) \right\} d\bar{\lambda} \quad (2-97a)$$

$$\begin{aligned}
B_{i,DRJ_2}(\bar{a}) &= \frac{1}{2\pi} \int_0^{2\pi} \left\{ \sum_{\ell=1}^6 \psi_{\ell,1}(\bar{a}, \bar{\lambda}) \left[\frac{\partial F_i(\bar{a}, \bar{\lambda})}{\partial \bar{a}_\ell} \right] \right. \\
&\quad \left. + \frac{15 \bar{n} \delta_{i6}}{8 \bar{a}_1^2} \psi_{1,1}(\bar{a}, \bar{\lambda}) \eta_{1,1}(\bar{a}, \bar{\lambda}) \right\} d\bar{\lambda}
\end{aligned}
\tag{2-97b}$$

By using the first order short periodic formulation as given in Table 2-1, the above expressions can be simplified. From Table 2-1 the J_2 short periodic variations are expressed as

$$\varepsilon \eta_{i,1}(\bar{a}, \bar{\lambda}) = \varepsilon \sum_{\sigma=1}^{\infty} [C_{i\sigma} \sin(\sigma\bar{\lambda}) - D_{i\sigma} \cos(\sigma\bar{\lambda})]
\tag{2-98}$$

and the drag short periodic variations are expressed as

$$\nu \psi_{i,1}(\bar{a}, \bar{\lambda}) = \nu \sum_{k=1}^{\infty} [G_{ik} \sin(k\bar{\lambda}) - H_{ik} \cos(k\bar{\lambda})]
\tag{2-99}$$

From the orthogonality of sines and cosines, it is a simple matter to show that

$$\frac{1}{\pi} \int_0^{2\pi} \eta_{1,1}^2(\bar{a}, \bar{\lambda}) d\bar{\lambda} = \sum_{\sigma=1}^{\infty} [C_{1\sigma}^2 + D_{1\sigma}^2]
\tag{2-100a}$$

$$\frac{1}{\pi} \int_0^{2\pi} \psi_{1,1}^2(\bar{a}, \bar{\lambda}) d\bar{\lambda} = \sum_{\sigma=1}^{\infty} [G_{1\sigma}^2 + H_{1\sigma}^2]
\tag{2-100b}$$

$$\frac{1}{\pi} \int_0^{2\pi} \eta_{1,1}(\bar{a}, \bar{\lambda}) \psi_{1,1}(\bar{a}, \bar{\lambda}) d\bar{\lambda} = \sum_{\sigma=1}^{\infty} [C_{1\sigma} G_{1\sigma} + D_{1\sigma} H_{1\sigma}] \quad (2-100c)$$

Therefore, from Equations (2-95) through (2-100), it is seen that the J_2 -drag and drag- J_2 coupling can be written as

$$\begin{aligned} B_{i, J_2 DR}(\bar{a}) &= \frac{1}{2\pi} \int_0^{2\pi} \sum_{\ell=1}^6 \eta_{\ell,1}(\bar{a}, \bar{\lambda}) \left[\frac{\partial G_i(\bar{a}, \bar{\lambda})}{\partial \bar{a}_\ell} \right] d\bar{\lambda} \\ &+ \left(\frac{15 \bar{n} \delta_{i6}}{16 \bar{a}_1^2} \right) \sum_{\sigma=1}^{\infty} [C_{1\sigma} G_{1\sigma} + D_{1\sigma} H_{1\sigma}] \end{aligned} \quad (2-101a)$$

$$\begin{aligned} B_{i, DR J_2}(\bar{a}) &= \frac{1}{2\pi} \int_0^{2\pi} \sum_{\ell=1}^6 \psi_{\ell,1}(\bar{a}, \bar{\lambda}) \left[\frac{\partial F_i(\bar{a}, \bar{\lambda})}{\partial \bar{a}_\ell} \right] d\bar{\lambda} \\ &+ \left(\frac{15 \bar{n} \delta_{i6}}{16 \bar{a}_1^2} \right) \sum_{\sigma=1}^{\infty} [C_{1\sigma} G_{1\sigma} + D_{1\sigma} H_{1\sigma}] \end{aligned} \quad (2-101b)$$

In a similar manner it can be shown that the second order effects for J_2 and drag are

$$\begin{aligned} B_{i, 2, 0}(\bar{a}) &= \frac{1}{2\pi} \int_0^{2\pi} \sum_{\ell=1}^6 \eta_{\ell,1}(\bar{a}, \bar{\lambda}) \left[\frac{\partial F_i(\bar{a}, \bar{\lambda})}{\partial \bar{a}_\ell} \right] d\bar{\lambda} \\ &+ \left(\frac{15 \bar{n} \delta_{i6}}{16 \bar{a}_1^2} \right) \sum_{\sigma=1}^{\infty} [C_{1\sigma}^2 + D_{1\sigma}^2] \end{aligned} \quad (2-102)$$

$$\begin{aligned}
B_{i,0,2}(\bar{a}) &= \frac{1}{2\pi} \int_0^{2\pi} \sum_{\ell=1}^6 \psi_{\ell,1}(\bar{a}, \bar{\lambda}) \left[\frac{\partial G_i(\bar{a}, \bar{\lambda})}{\partial \bar{a}_\ell} \right] d\bar{\lambda} \\
&+ \left(\frac{15 \bar{n} \delta_{i6}}{16 \bar{a}_1^2} \right) \sum_{\sigma=1}^{\infty} [G_{1\sigma}^2 + H_{1\sigma}^2]
\end{aligned} \tag{2-103}$$

It is possible to obtain a functionally simplified form of the AOG as given in Equations (2-101) through (2-103).

Define the following terms

$$\begin{aligned}
a_i' &\equiv \bar{a}_i + \epsilon \eta_{i,1}(\bar{a}, \bar{\lambda}) + \nu \psi_{i,1}(\bar{a}, \bar{\lambda}) \\
&(i = 1, 2, 3, 4, 5, 6)
\end{aligned} \tag{2-104}$$

By use of Taylor's theorem it is seen that to second order in both small parameters

$$\begin{aligned}
\epsilon F_i(\underline{a}', \lambda') &= \epsilon F_i(\bar{a}, \bar{\lambda}) \\
&+ \nu \epsilon \sum_{\ell=1}^6 \psi_{\ell,1}(\bar{a}, \bar{\lambda}) \left[\frac{\partial F_i(\bar{a}, \bar{\lambda})}{\partial \bar{a}_\ell} \right] \\
&+ \epsilon^2 \sum_{\ell=1}^6 \eta_{\ell,1}(\bar{a}, \bar{\lambda}) \left[\frac{\partial F_i(\bar{a}, \bar{\lambda})}{\partial \bar{a}_\ell} \right]
\end{aligned} \tag{2-105a}$$

$$\begin{aligned}
v G_i(\underline{a}', \lambda') &= v G_i(\underline{\bar{a}}, \bar{\lambda}) \\
&+ \epsilon v \sum_{\ell=1}^6 \eta_{\ell,1}(\underline{\bar{a}}, \bar{\lambda}) \left[\frac{\partial G_i(\underline{\bar{a}}, \bar{\lambda})}{\partial \bar{a}_\ell} \right] \\
&+ v^2 \sum_{\ell=1}^6 \psi_{\ell,1}(\underline{\bar{a}}, \bar{\lambda}) \left[\frac{\partial G_i(\underline{\bar{a}}, \bar{\lambda})}{\partial \bar{a}_\ell} \right]
\end{aligned} \tag{2-105b}$$

Comparing the above expressions with the integrands in Equations (2-95a), (2-95b), (2-101), (2-102) and (2-103), it is seen that the complete second order mean element rates can be written as

$$\begin{aligned}
\dot{\bar{a}}_i &= \bar{n} \delta_{i6} + \frac{1}{2\pi} \int_0^{2\pi} [\epsilon F_i(\underline{a}', \lambda') + v G_i(\underline{a}', \lambda')] d\bar{\lambda} \\
&+ \left(\frac{15 \bar{n} \delta_{i6}}{16 \bar{a}_1^2} \right) \sum_{\sigma=1}^{\infty} [\epsilon^2 (C_{1\sigma}^2 + D_{1\sigma}^2) \\
&+ 2 \epsilon v (C_{1\sigma} G_{1\sigma} + D_{1\sigma} H_{1\sigma}) + v^2 (G_{1\sigma}^2 + H_{1\sigma}^2)]
\end{aligned} \tag{2-106}$$

where \underline{a}' and λ' are defined in Equation (2-104).

The complete second order drag effects can be obtained numerically from Equation (2-106). The definite integral in

Equation (2-106) would be solved by a quadrature algorithm in which the elements \underline{a}' and λ' would be determined by Equations (2-104), (2-98) and (2-99). The five slowly varying mean elements (\bar{a}) and the short periodic coefficients ($\epsilon C_{i\sigma}$, $\epsilon D_{i\sigma}$, νG_{ik} , νH_{ik}) can be assumed to be constant over the averaging interval. This assumption would be valid through second order in the small parameter.

In a similar manner the various components of a second order drag theory can be determined. The drag and J_2 -drag effects can be represented by the following

$$\nu B_{i,0,1}(\bar{a}) + \epsilon \nu B_{i,J_2DR}(\bar{a}) = \frac{1}{2\pi} \int_0^{2\pi} \nu G_i(\underline{a}'', \lambda'') d\bar{\lambda} \quad (2-107a)$$

where

$$\begin{aligned} a''_i &= \bar{a}_i + \epsilon \eta_{i,1}(\bar{a}, \bar{\lambda}) \\ (i &= 1, 2, 3, 4, 5, 6) \end{aligned} \quad (2-107b)$$

There is no coupling between the semimajor axis and the fast variable in Equation (2-107a) because only the J_2 short periodic coefficients are computed in Equation (2-107b). The J_2 and drag- J_2 effects are given as

$$\begin{aligned}
& \epsilon B_{i,1,0}(\bar{a}) + \epsilon v B_{i,DRJ_2}(\bar{a}) \\
& = \frac{1}{2\pi} \int_0^{2\pi} \epsilon F_i(\underline{a}''', \lambda''') d\bar{\lambda} \quad (2-108a)
\end{aligned}$$

where

$$\begin{aligned}
a_i''' & = \bar{a}_i + v \psi_{i,1}(\bar{a}, \bar{\lambda}) \\
& (i = 1, 2, 3, 4, 5, 6) \quad (2-108b)
\end{aligned}$$

Again, there is no coupling term in Equation (2-108a) because only drag short periodic coefficients are computed in Equation (2-108b). The drag, J_2 -drag and drag-squared effects are

$$\begin{aligned}
& v B_{i,0,1}(\bar{a}) + \epsilon v B_{i,J_2DR}(\bar{a}) + v^2 B_{i,0,2}(\bar{a}) \\
& = \frac{1}{2\pi} \int_0^{2\pi} v G_i(\underline{a}', \lambda') d\bar{\lambda} \\
& + \left(\frac{15 \bar{n} \delta_{i6}}{16 \bar{a}_1^2} \right) \sum_{\sigma=1}^{\infty} [\epsilon v (C_{1\sigma} G_{1\sigma} + D_{1\sigma} H_{1\sigma}) \\
& + v^2 (G_{1\sigma}^2 + H_{1\sigma}^2)] \quad (2-109)
\end{aligned}$$

where \underline{a}' and λ' is defined in Equation (2-104). Similarly, the J_2 , drag- J_2 and J_2^2 effects are represented as

$$\begin{aligned}
& \epsilon B_{i,1,0}(\bar{a}) + \epsilon \nu B_{i,DRJ_2}(\bar{a}) + \epsilon^2 B_{i,2,0}(\bar{a}) \\
&= \frac{1}{2\pi} \int_0^{2\pi} \epsilon F_i(\underline{a}', \lambda') d\bar{\lambda} \\
&+ \left(\frac{15 \bar{n} \delta_{i6}}{16 \bar{a}_1} \right) \sum_{\sigma=1}^{\infty} [\epsilon \nu (C_{1\sigma} G_{1\sigma} + D_{1\sigma} H_{1\sigma}) \\
&+ \epsilon^2 (C_{1\sigma}^2 + D_{1\sigma}^2)] \tag{2-110}
\end{aligned}$$

Algorithmic Considerations

For a numerical averaging satellite theory, Equation (2-106) will allow the calculation of the complete second order averaged equations of motion. Assuming that the effects of oblateness and drag perturbations are calculated with separate quadratures, the above formulation would require four quadratures each time the integrator requires a function evaluation: two for the determination of the J_2 and drag short periodic coefficients and two for the determination of the J_2 and drag mean element rates as given in Equation (2-106). The implementation of Equations (2-106) through (2-110) into a numerical averaging satellite theory is easy since most of the same software that is used to obtain the first order mean element rates can be used. It should be noted that including the short periodic variations in the integration of Equations (2-106)

through (2-110) may introduce frequency components that would require a higher order quadrature algorithm than a first order theory would need. In other words a complete second order numerical averaging satellite theory is more than twice as computationally costly than a first order numerical averaging satellite theory.

Zeis (Refs. 6 and 7) has developed explicit expressions for the second order mean element rates due to J_2 . Zeis used MACSYMA computer language (Ref. 22) to solve Equation (2-95d) explicitly for $B_{i,2,0}(\bar{a})$. The expressions obtained are for direct orbits and are good to zeroth order in the eccentricity.

Equation (2-101b) and the MACSYMA approach of Zeis has been used in this investigation to obtain analytical expressions for the drag- J_2 coupling in terms of mean elements and drag short periodic coefficients ($G_{i\sigma}$ and $H_{i\sigma}$). The expressions obtained are for direct orbits and are good to zeroth order in the eccentricity. These expressions and the MACSYMA approach used are presented in Appendix D. The drag short periodic coefficients in these expressions have to be determined by a numerical quadrature. In other words, $B_{i,DRJ_2}(\bar{a})$ can be obtained in analytical form based upon numerically determined coefficients. This shows that the semianalytical satellite theory is truly semi-analytical in nature.

Izsak (Ref. 59) has determined analytical expressions for the radial and velocity first order short periodic variations due to J_2 . Long and McClain (Ref. 12) have shown that applying Izsak's height (radial) correction in the determination of the density significantly improves the accuracy of the AOG. Using Izsak's height correction in the density determination can be viewed as an approximation to the J_2 -drag effect, $B_{i,J_2DR}(\bar{a})$. Numerical results will show that this is a very good approximation.

2.4 Numerical Results

This section presents some of the numerical results obtained during the present investigation. These results extend and improve the numerical results presented in References 9 and 12. The present implementation effort has been concerned basically with demonstrating the accuracy of the semianalytical satellite theory. Current development efforts are improving the computational efficiency as well as the accuracy of the semianalytical satellite theory. Some of the goals and approaches of the current development effort will also be indicated in this section.

A review of the software implementation into the Research and Development version of the Goddard Trajectory Determination

System (GTDS-RD) is presented first in this section. Since the results obtained depend upon the choice of initial mean elements, a brief discussion on how the initial conditions are determined is presented. The orbits considered in this section are a low altitude near circular orbit, a low altitude elliptical orbit and a medium altitude circular orbit. Each of these test cases is discussed separately.

2.4.1 Software Overview

The numerical short periodic variations (SPG) and the oblateness/drag coupling capabilities (AOG) have been implemented in a specially modified version of GTDS-RD that operates on an Amdahl 470 V6. The initial software development has been concerned with testing the accuracy of these conceptual developments. Later development efforts will optimize the software with respect to efficiency. The SPG and AOG are each discussed separately.

The Short-Periodic Generator (SPG)

The SPG is called at each point on the output grid of the semianalytical satellite theory.* In the initial software development, the short periodic coefficients also are computed at each point on the output grid. The numerical results

* The call to the SPG occurs in subroutine 'ORBITV' of GTDS-RD just before the call to the output subroutines (see Appendix F).

indicate that the short periodic coefficients can be computed on the averaging integration grid and an interpolator used to determine them at the output times. A development effort presently underway incorporates this option (Ref. 71).

The present SPG determines the short periodic variations by time-independent and weak time-dependent numerical techniques for several types of perturbations. Perturbations are broken into three separate types: conservative, drag and solar radiation pressure (the AOG handles numerical averaging perturbations in the same fashion). Conservative perturbations include central body non-sphericity and third body effects. At the present time, the explicit expressions (good to zeroth order in the eccentricity and for direct orbits) that Zeis (Ref. 6) obtained for J_2^2 short periodic variations have been included in the SPG. The formulas for the Δq and $\Delta \lambda$ due to J_2^2 were rederived via the MACSYMA capability available on the MIT Lab for Computer Science/Artificial Intelligence Group's LISP computer during the present effort. These results differ from the results given in Reference 6. The new results are given in Appendix E. Eventually the SPG will be able to handle all conservative perturbations analytically; in particular, tesseral harmonics of the gravitational potential will be included analytically (Ref. 5).

The SPG is as flexible as the AOG with respect to the handling of perturbations. The SPG is not coupled to the AOG, i.e., a perturbation could be handled one way in the AOG and another way in the SPG. It is also possible to have a different perturbation model in the AOG and SPG. In other words, the AOG could have an 8×0 gravitational field with atmospheric drag and lunar-solar effects and the SPG could have a simple 2×0 field. Although all conservative perturbations are presently considered in one numerical quadrature, it will eventually be possible to handle some conservative perturbations analytically and others numerically if that is desired. Drag and solar radiation pressure will be handled numerically in the present effort. This provides great flexibility with respect to including new density models or complicated spacecraft solar radiation pressure models.

The present SPG allows up to 10 pairs of time-independent short periodic coefficients [the C_{ik} and D_{ik} in Equation (2-44)]. In other words, the short periodic functions are expanded through the $10 \bar{\lambda}$ terms. This upper limit on the number of time-independent short periodic coefficients was imposed because a $10 \bar{\lambda}$ term should be handled at the very minimum with a 48 point numerical quadrature and this was the maximum quadrature order that the present SPG has available. As was stated previously, the number of coefficients and the quadrature order must be considered jointly. It should also

be noted that although the determination of the short periodic variations can conceptually require as much as 120 quadrature operations (20 coefficients for the 6 elements), it is in effect only one numerical quadrature operation since the software can be implemented such that the perturbing accelerations (right hand side of the VOP equations of motion) have to be evaluated only once at each of the abscissas of the quadrature algorithm. The determination of the time-independent short periodic coefficients due to each type of perturbation (conservative, drag and solar-pressure) requires a separate numerical quadrature.

The present SPG also has the capability to include the weak time-dependent corrections to the time-independent short periodic coefficients (see Table 2-3). These corrections are computed by a single-sided finite-differencing technique as given in Equations (2-84b) and (2-85). The weak time-dependent correction is applicable to conservative, drag and solar radiation pressure perturbations.

All quadratures in GTDS-RD (AOG and SPG) use the eccentric longitude, \bar{F} , as the fast variable. Transformation from mean-mean longitude, $\bar{\lambda}$, to mean eccentric longitude, \bar{F} , is accomplished by the following two-body relation

$$d\bar{\lambda} = \begin{pmatrix} \bar{r} \\ \bar{a}_1 \end{pmatrix} d\bar{F} \quad (2-111)$$

The advantages of such a transformation is that Kepler's equation does not need to be solved whenever the accelerations need to be evaluated and there is a generally desirable smoothing of the perturbations around perigee.

The Averaged Orbit Generator (AOG)

The second order oblateness/drag coupling effects have been implemented into GTDS-RD.* The present AOG does J_2 and J_2^2 mean element rates analytically. There are seven (7) options that can be used to handle the coupled oblateness/drag effects. These options are listed below.

1. First order drag effects only. This is done by performing a numerical quadrature on Equation (2-95b).
2. First order drag effects with Izsak's J_2 height correction used in the determination of the density. This option obtains the first order drag effects and an approximation to the J_2 -drag effects $[\epsilon \nu B_{i,J_2DR}(\bar{a})]$. This option is done by performing a numerical quadrature on Equation (2-95b) and adding

* These improvements to the AOG occur in subroutine 'HODRAG' that is called from subroutine 'AVRAGE' of GTDS-RD (see Appendix F).

Izsak's height correction to the radial distance when a density calculation is made at the abscissas of the quadrature algorithm.

3. Drag and J_2 -drag effects. This is done by performing a numerical quadrature on Equation (2-107). This option requires two quadratures: one to obtain the J_2 short periodic coefficients and one to solve Equation (2-107).
4. Drag, J_2 -drag and drag-squared effects. This option is represented by Equation (2-109). This option presently requires three quadratures: two in order to obtain the J_2 and drag short periodic coefficients and one in order to solve Equation (2-109).
5. Drag, J_2 -drag, drag- J_2 and drag-squared effects. Since the J_2 and J_2^2 effects are done analytically, this option is represented as

$$\begin{aligned}
 & vB_{i,0,1}(\bar{a}) + \epsilon vB_{i,J_2DR}(\bar{a}) + \epsilon vB_{i,DRJ_2}(\bar{a}) + v^2 B_{i,0,2}(\bar{a}) = \\
 & \frac{1}{2\pi} \int_0^{2\pi} \{ \epsilon F_i(\underline{a}''', \lambda''') + vG_i(\underline{a}', \lambda') \} d\bar{\lambda} - \frac{1}{2\pi} \int_0^{2\pi} \epsilon F_i(\bar{a}, \bar{\lambda}) d\bar{\lambda} \\
 & + \left(\frac{15 \bar{n} \delta_{i6}}{16 \bar{a}_1^2} \right) \sum_{\sigma=1}^{\infty} [2\epsilon v(C_{1\sigma} G_{1\sigma} + D_{1\sigma} H_{1\sigma}) + v^2 (G_{1\sigma}^2 + H_{1\sigma}^2)]
 \end{aligned}$$

(2-112)

where \underline{a}' and λ' are defined in Equation (2-104) and where \underline{a}'' and λ'' are defined in Equation (2-108b). This option presently requires five quadratures: two in order to obtain the J_2 and drag short periodic coefficients and three in order to solve Equation (2-112). The last quadrature in Equation (2-112) could have been eliminated if J_2 and J_2^2 effects were not done analytically. This option determines the complete mean element rates to second order in both small parameters.

6. Drag, J_2 -drag and drag-squared effects done numerically and drag- J_2 effects done analytically with the expressions obtained in Appendix D. This option is accomplished by adding the analytically determined drag- J_2 rates to the rates obtained from option 4. This option is good for near-circular, direct orbits. The advantage of this option is that it gives a very good approximation of the complete second order oblateness/drag effects with only three numerical quadratures.

7. First order drag effects with Izsak's J_2 height correction and analytical drag- J_2 terms. This option obtains the first order drag effects and approximates the J_2 -drag and drag- J_2 effects (for an

orbit with zero mean eccentricity, the drag- J_2 effects would be exact). The drag-squared effects are neglected in this option. This option requires two numerical quadratures: one in order to determine the drag short periodic coefficients that are used in the drag- J_2 expressions and one that is used to determine the first order drag terms with Izsak's correction (see option 2).

The number of short periodic coefficients that are used in the above options must be considered jointly with the quadrature order of the averaging operation. This is because including short periodic variations in the above averaging operations may introduce frequency components that could necessitate a higher order quadrature algorithm. The maximum quadrature order that is available in the present AOG is a 48-point quadrature. It is also possible to have a different number of short periodic coefficients in the SPG and in the AOG.

The present AOG also has Zeis' explicit expressions for the second order mean element rates due to J_2 programmed (Refs. 6 and 7). It is possible to use either the expressions for J_2^2 that GTDS-RD has or the Zeis expressions for J_2^2 . Zeis'

expressions are for direct orbits* and good to zeroth order in the eccentricity whereas the J_2^2 expressions in GTDS-RD are good for any orbit. As was discussed in References 6 and 7, Zeis' expressions differ from the GTDS-RD expressions for the zero eccentricity case. The numerical results have indicated that for near-circular orbits, Zeis' J_2^2 expressions for the mean element rates give better results than the present GTDS-RD expressions.

One additional comment is appropriate. When the analytical J_2 short periodic expressions are available in GTDS-RD, one numerical quadrature will be eliminated from options 3, 4, 5 and 6.

2.4.2 Initial Conditions

As was stated in the Mathematical Preliminaries section, semianalytical satellite theory employs a transformation from osculating element space to mean element space. Since errors in the initial conditions result in a secularly-growing prediction error, it is very important to obtain accurate initial mean elements. Three methods of obtaining the initial mean elements that were considered in this investigation are: Numerical Osculating to Mean, Precise Conversion of Elements and Epoch Point Conversion.

* Truncated expressions valid for both direct and retrograde cases have recently (August 1979) been programmed into GTDS-RD at CSDL.

The Numerical Osculating to Mean (NOM) method is a present capability of GTDS-RD. The NOM procedure generates a file of the osculating orbital elements over a revolution of the satellite by a Cowell (Special Perturbation) technique. The mean elements are obtained by averaging the osculating elements over one mean period of the satellite, i.e.,

$$\bar{a}_i(t_0) = \frac{1}{\bar{P}} \int_{t_0 - \frac{\bar{P}}{2}}^{t_0 + \frac{\bar{P}}{2}} a_i(t) dt \quad (2-113)$$

where \bar{P} stands for the mean period and t_0 stands for the epoch time. Since the mean period depends solely on the mean semi-major axis, it is necessary to first perform a Newton-Raphson iteration on Equation (2-113) for the mean semimajor axis. Once the mean period is known, the other mean elements can be obtained by a direct application of Equation (2-113).

The Precise Conversion of Elements (PCE) method is also presently in GTDS-RD. The PCE procedure is a differential correction algorithm that can be applied to the semianalytical satellite theory (AOG and SPG) with a Cowell-generated orbit file used as the observational data. The PCE can be performed over any time span. For this research the PCE was generally done over a two hour time span. The PCE requires an accurate SPG such that the observational residuals are small enough to allow convergence. The initial guess of the epoch mean elements for the PCE is obtained by a NOM procedure.

The Epoch Point Conversion (EPC) procedure is a single point conversion method. The algorithm would employ the technique of successive substitution into the near-identity transformation until a specified agreement is reached. This can be represented as

$$\bar{a}_i^{[1]}(t_0) = a_i(t_0) \quad (2-114a)$$

$$\bar{a}_i^{[k+1]}(t_0) = a_i(t_0) - \Delta a_i[\bar{a}^{[k]}(t_0), \bar{\lambda}^{[k]}(t_0)] \quad (2-114b)$$

where $\Delta a_i[\bar{a}^{[k]}(t_0), \bar{\lambda}^{[k]}(t_0)]$ represents all the short periodic variations (J_n , drag, J_2^2 , etc.) and is dependent upon the epoch mean elements determined from the previous (kth) iteration. Equation (2-114a) indicates that the initial guess of the epoch mean elements is the epoch osculating elements. The EPC method is not presently in GTDS-RD. If the initial mean elements are assumed known, it is possible to obtain the initial osculating elements by a direct substitution into the near-identity transformation. Functionally this can be written as

$$a_i(t_0) = \bar{a}_i(t_0) + \Delta a_i[\bar{a}(t_0), \bar{\lambda}(t_0)] \quad (2-115)$$

where $\bar{a}_i(t_0)$ is assumed to be known. This can be thought of as the inverse of the EPC method and will be denoted as (EPC)⁻¹.

The (EPC)⁻¹ procedure is available in the present GTDS-RD and requires only an evaluation of the SPG at the epoch time.

The mean elements obtained by a NOM, a PCE or an EPC method are dependent upon the perturbation model chosen. It is therefore necessary to have a consistent set of initial mean elements with each ephemeris generation. In other words, the orbit generation should use the same perturbation model as the NOM, PCE or EPC used in generating the initial conditions.

2.4.3 Low Altitude Circular Test Case

The Low Altitude Circular Test Case (Table 2-5) serves as a good test of the SPG and the AOG. The orbit has a perigee height of 200 kilometers and never exits the atmosphere. The apogee of the orbit is 333 kilometers. The atmospheric density model used was the Modified Harris-Priester atmospheric model. The life time of this satellite is less than 21 days.

Table 2-5. Osculating Elements and Parameters for the Low Altitude Circular Test Case

a = 6644.586 km	Epoch = 10 hrs. 24 min. 21 Oct. 1974
e = .01	Reference Frame = True of Date
i = 67.98538419°	C _D = 2.0
Ω = 91.99738419°	Area = 1.86 m ²
ω = 200.6741688°	Mass = 677 kg
M = 164.3173126°	Density = Modified Harris-Priester
Period = 1.492785 hrs.	with $\bar{F}_{10.7} = 150 \text{ } 10^{-22}$
	watts m ⁻² Hz ⁻¹

Within this test case, the following issues are investigated:

1. The importance of the coupling of the semimajor axis in the short periodic function for the fast variable.
2. The various AOG options (described previously).
3. The PCE initial condition procedure versus the NOM initial condition procedure.
4. The use of the semianalytical satellite theory, consisting of the AOG and SPG, to produce accurate ephemerides.
5. The slowly varying nature of the short periodic coefficients.

The following conventions are adopted in this section and will also apply to future sections. First, whenever drag is considered in the AOG, one of the seven options, as given in Section 2.4.1, will be specified. The number of short periodic coefficients and quadrature order will be specified by the following notation (# short periodic coefficients/quadrature order). For example, (7/48) indicates that the summation in Table 2-1 goes to seven and that a 48 point Gaussian quadrature is used to determine the coefficients (for a drag option, it also indicates the quadrature order used in determining the

element rates). Finally, unless otherwise indicated, the integrator used in both the AOG and in the Cowell orbit generator is a 12th order Adams-Bashforth Predictor/Adams-Moulton Corrector.

Figures 2-3 and 2-4 show the effects of the coupling between the fast variable and the semimajor axis as given in Equation (2-44). Obviously this coupling term, as given in Equations (2-30) and (2-44), is of major importance. As discussed in previous sections, these are the terms that appear to be neglected in Reference 20. The irregular shape of Figure 2-3 is due to the selection effect of one point every 15 minutes. The major cause of the near-linear increase in the along track error in Figure 2-4 is due to an incorrect initial mean semimajor axis. This point will be discussed subsequently.

In Table 2-6, a 25 hour comparison is made between ephemerides generated by the semianalytical satellite theory with the various drag options and by the Cowell orbit generator. This table should be viewed with a certain amount of caution since the sampling rate is nearly commensurable with the satellite's period. This means that the six points sampled per orbit are nearly the same for every orbit during the 25 hour compare. The result of this fact is that the actual maximum error could be slightly larger. It should also be noted that Table 2-6 does not consider the J_2^2 short periodic effects.

Table 2-6. 25 Hour Orbital Comparison[†]/Semianalytical versus Cowell for the Low Altitude Circular Test Case

Drag* Options	Max Sampled Radial Difference (m)	Max Sampled Cross Track Difference (m)	Max Sampled Along Track Difference (m)	Max Sampled Δr (m)
1	442.65	15.38	18572.41	18577.69
2	8.30	11.02	21.31	22.54
3	8.52	11.02	21.40	22.64
4	8.17	11.02	23.42	24.38
5	8.33	11.15	12.10	15.82
6	8.35	11.16	11.40	15.52
7	8.46	11.18	7.20	15.32

† The sampling rate was once every 15 minutes.

* The drag options used a 48 point quadrature with 4 short periodic coefficients when needed (4/48).

Perturbations:

Cowell: 6x0 gravitational field and drag; 30 second numerical integration time step.

AOG: 1st order analytical expressions for the 6x0 gravitational field, Zeis' expressions for J_2^2 effects and drag options as indicated; 1 day numerical integration time step.

SPG: 6x0 gravitational field (7/48) and drag (7/48), both to 1st order (time-independent).

Initial Conditions: 2 hour PCE with consistent perturbation models. Option 1 used the same initial mean elements as Option 2 (PCE for Option 1 would not converge).

Figures 2-5, 2-6 and 2-7 are the radial, cross track and along track error signatures over the first orbit of drag option 6 in Table 2-6. In Figures 2-5, 2-6 and 2-7, the sampling rate is about one point per minute. From Figure 2-7, it is seen that the sampling rate of Table 2-6 will sample the maximum along track difference. From Figures 2-5 and 2-6 it is seen that a 15 minute sampling rate would yield maximum radial and cross track differences which could be 2 to 5 meters less than the actual maximum differences.

Table 2-6 also seems to indicate some small discrepancies. First of all, option 2 (Izsak's height correction) appears to be better than option 3 (numerical J_2 -drag effects) even though option 2 should be an approximation to option 3. Option 4 (numerical J_2 -drag and drag-squared effects) should give better results than option 3 since it is a more complete model. Similarly, option 6 (numerical J_2 -drag and drag-squared effects with analytical drag- J_2 effects) and option 7 (Izsak's height correction and analytical drag- J_2 effects) are approximations to option 5 (numerical J_2 -drag, drag- J_2 and drag-squared effects), yet they give slightly better results.

It is felt that these discrepancies may be due to any or all of the following reasons: the sampling rate, lack of J_2^2 terms in the AOG, quadrature noise, and possible small instabilities within the integrator. Changing the drag option

changes the perturbation model slightly and this would result in a different error signature over each orbit. The sampling rate used in generating Table 2-6 may be causing some of the observed discrepancies. The use of 4 short periodic coefficients in the second order AOG is in effect a zero eccentricity assumption (Ref. 6). Applying Izsak's J_2 height correction (valid for any eccentricity) into the density calculation may be a better approximation than the implicit zero eccentricity approximation used in options 3, 4 and 5 of Table 2-6. Since most of the discrepancies in options 2 through 8 of Table 2-6 are less than a meter, the possibility of quadrature noise as a source of some of the error must also be considered. For a circular orbit, a 48 point numerical quadrature should be sufficient for 4 short periodic coefficients in the second order AOG. It was found that the 12th order Adams-Bashforth Predictor/Adams-Moulton Corrector integrator had some instabilities associated with it when drag was considered with a Modified Harris-Priester atmosphere. It is felt that these instabilities are caused by the tabular nature of the Modified Harris-Priester density model which has a discontinuous derivative of the density with respect to altitude. Therefore, integrator noise could be causing some or all of the discrepancies noted in Table 2-6.

It is also observed from Table 2-6 that the cross track difference remains approximately 11 meters in options 2 through

7. In options 5, 6 and 7, the cross track error is a major component of the total position error. In Figure 2-6, one can begin to see the secular growth of the cross track error. It is felt that this secular error growth may be due to the lack of J_2^2 e terms in Zeis' explicit expressions (Ref. 6) for the mean element rates due to J_2^2 effects. Since the rotation of the line of nodes is strongly affected by oblateness, the lack of J_2^2 e terms in the AOG may be causing the secular growth of the cross track error (note that the osculating eccentricity of this test case is .01). This fact could also explain why the cross track error remains at 11 meters in Table 2-6 for options 2 through 7.

From Table 2-6 it can be concluded that second order drag effects are very important for low altitude satellites. The major second order drag effect is the J_2 -drag coupling. It also appears that applying Izsak's J_2 height correction to the density calculation (option 2) is an adequate and efficient means of representing the J_2 -drag effect. For high precision low altitude orbit prediction, drag- J_2 is an important effect and must be considered. It is interesting to note that option 7 (Izsak's J_2 height correction and the analytical drag- J_2 expressions) gives very good results. The additional computational cost of option 7 over option 2 is moderate. The small difference between options 3 and 4 seem to indicate that the drag-squared effect can be neglected in this case.

A comparison of Figures 2-4 and 2-7 indicates that the PCE procedure for obtaining initial mean elements is significantly superior to the NOM procedure. This was expected since the PCE used NOM initial conditions as the first guess. From Table 2-7 it is seen that the PCE procedure used in Figure 2-7 increased the initial mean semimajor axis by 5.5 meters over the initial mean semimajor axis obtained by the NOM procedure used in Figure 2-4.

Table 2-7. Comparison of NOM and PCE Initial Mean Equinoctial Elements for Drag Option 6 of Table 2-6

	NOM	PCE
\bar{a} =	6636.3742041 km	6636.3797106 km
\bar{h} =	$-9.81788006 \times 10^{-3}$	$-9.81801561 \times 10^{-3}$
\bar{k} =	$4.00771339 \times 10^{-3}$	$4.00785279 \times 10^{-3}$
\bar{p} =	$6.73729951 \times 10^{-1}$	$6.73730536 \times 10^{-1}$
\bar{q} =	$-2.34672347 \times 10^{-2}$	$-2.34672726 \times 10^{-2}$
$\bar{\lambda}$ =	1.692578400 (rad)	1.69257015 (rad)

Figures 2-8, 2-9 and 2-10 are radial, cross track and along track differences, respectively, between the semianalytical orbit generator and Cowell orbit generator after 23 hours from epoch. Drag option 7 was used in the AOG and Zeis' J_2^2 expressions (with corrections as given in Appendix E) were

used in the SPG. The maximum position error over the time span shown was 12.6 meters. A comparison of this with drag option 7 of Table 2-6 indicates that J_2^2 short periodic variations significantly improve the radial, along track and maximum position errors. The cross track difference is still about 11 meters and is the major source of error.

It is also interesting to note that applying the weak time-dependent corrections to the time-independent drag short periodic coefficients made no noticeable change in Figures 2-8, 2-9 and 2-10, or, for that matter, in the drag short periodic coefficients themselves. This should be expected since the Sun only moves about $\frac{1}{5670}$ th of a degree during a complete revolution of this satellite. It can therefore be concluded that drag perturbations can adequately be handled with a time-independent formulation. This may not be the case if the time variations of $F_{10.7}$, $\bar{F}_{10.7}$ and/or K_p are taken into account in the density model.

A five-day comparison was made between the semianalytical orbit generator and the Cowell orbit generator with the same initial conditions and perturbations as given in Figure 2-8. The maximum position error was 715.5 meters. A similar five-day comparison of the semianalytical and Cowell orbit generator was made with the initial conditions and perturbations as in drag option 6 of Table 2-6. Zeis' expressions for

J_2^2 short periodic effects were also included in the PCE and the comparison. The maximum position error in this case was 460.5 meters. The along track error was the major error in both cases. Obviously drag option 6 is superior to drag option 7. This is not surprising since drag option 6 includes all second order drag effects whereas drag option 7 approximates the J_2 -drag effect and neglects drag-squared effects.

Figures 2-11 and 2-12 show, respectively, a one orbit comparison of the osculating semimajor axis and eccentricity as generated by the semianalytical theory and a Cowell orbit generator. The plus (+) will overwrite the star (*) whenever the two orbit generators are the same. The discretizing of data in the plot routine is the cause for the few apparent differences between the semianalytical satellite theory and the Cowell orbit generator that is seen in Figures 2-11 and 2-12. The semianalytical satellite theory, as presented in this paper, can generate ephemerides with precision approaching that of a Cowell orbit generator.

Figure 2-13 shows the effect of a drag perturbation only on the semimajor axis for the Low Altitude Circular Test Case. Perigee for this orbit occurs at about 49 minutes after epoch. Even though this orbit has an eccentricity of .01 and an apogee height of 333 kilometers, the major effect of drag still occurs close to perigee.

Figures 2-14, 2-15 and 2-16 are time histories of the mean semimajor axis, mean h and mean k respectively, over a 10 day time span. Figures 2-14, 2-15 and 2-16 also show that the mean elements contain only the secular and long periodic motion. The advantage of numerical integration in mean element space over numerical integration in osculating element space is vividly seen by comparing Figures 2-14, 2-15 and 2-16 to Figures 2-11 and 2-12 (note the different time scales).

The first order zonal (J_2 through J_8) short periodic variations for the semimajor axis, h and k , are shown in Figures 2-17, 2-18 and 2-19, respectively. Figure 2-17 indicates that the first order semimajor axis short periodic variation for this test case can be an 8 kilometer effect.

The first order drag short periodic variation for the semimajor axis, h , k and λ are shown respectively in Figures 2-20, 2-21, 2-22 and 2-23. Perigee passage for this orbit occurs at approximately 49 minutes. Figure 2-20 shows that the drag short periodic variation for the semimajor axis can be a 35 meter effect for this test case. As the perigee height is lowered, this effect will become much larger. Drag short periodic variations must be considered for low altitude, high accuracy, orbit generation.

Figures 2-24 through 2-33 show some of the zonal and drag short periodic coefficients over a 10 day time span for the Low Altitude Circular Test Case. The slowly varying nature of these coefficients is evident. Obviously the time-independent short periodic coefficients do not need to be determined at every output time. The time-independent short periodic coefficients can be determined on the integration grid of the semianalytical satellite theory (typically 1 day) and an interpolator used to obtain them efficiently at the output times. Even for the most rapidly varying short periodic coefficients as given in Figures 2-25 and 2-31, this procedure will be possible. It is interesting to note that the more rapidly varying short periodic coefficients are one to two orders of magnitude less than the dominant short periodic coefficients for that element and perturbation (Figures 2-24 and 2-30).

Figures 2-14 through 2-16 and 2-24 through 2-33 also suggest that the formulation of the osculating elements as given by Equation (2-98) may be an efficient means of representing and storing ephemerides. The mean elements and short periodic coefficients can both be interpolated over long time spans. This may be advantageous for spacecraft on-board computation since the on-board computer would only need a relatively low order interpolator.

The above figures also indicate that estimation procedures in the mean element space may have distinct advantages over current estimation procedures in the osculating element space. The near linear nature of the mean elements indicates that the linearization assumptions used in a batch and sequential estimation process will be better satisfied.

2.4.4 Low Altitude Eccentric Test Case

The Low Altitude Eccentric Test Case (Table 2-8) is a demanding test of the semianalytical satellite theory. The orbit has a perigee height of 115 kilometers and an apogee height of 4100 kilometers. The satellite is therefore entering and exiting the atmosphere. The drag effect is concentrated in a very narrow region around perigee.

Table 2-8. Osculating Elements and Parameters for the Low Altitude Eccentric Test Case

a = 8520.320139 km	Epoch = 10 hrs. 24 mins. 26
e = .237768825	Feb. 74
i = 68.06458843°	Reference Frame = True of Date
Ω = 91.56426845°	C_D = 2.0
ω = 93.81101481°	Area = 1.86 m ²
Period = 2.174163268 hrs.	Mass = 677 kg
	Density = Modified Harris-Priester density model with $\bar{F}_{10.7} = 150$ (10 ⁻²² watts m ⁻² Hz ⁻¹)

Table 2-9 gives the initial condition procedure and perturbations used in this test case. It was found that drag option 7 gave the best results. This was expected because for larger eccentricities, the required number of short periodic coefficients in the second order AOG for drag options 3 through 6 introduce frequency components that bring the 48-point numerical quadrature into question.

Table 2-9. Initial Conditions and Perturbations
for the Low Altitude Eccentric Test Case

Perturbations

Cowell: 4x0 gravitational field and drag: 10 second numerical integration time step.

AOG: 1st order analytical expression for the 4x0 gravitational field. Zeis expressions for J_2^2 effects and drag option 7 (4/48): 1 day numerical integration time step.

SPG: 6x0 gravitational field (8/48) and drag (10/48) both to first order (time-independent)

Initial Conditions: 2 hour PCE

$$\begin{aligned} \bar{a} &= 8514.8171053 \\ \bar{e} &= .23791153768 \\ \bar{i} &= 68.056536888^\circ \\ \bar{\Omega} &= 91.553565358^\circ \\ \bar{\omega} &= 93.860226464^\circ \\ \bar{M} &= 275.28693265^\circ \end{aligned}$$

Figures 2-34 through 2-36 are the radial, cross track and along track difference over the first orbit of the Low Altitude Eccentric Test Case. The maximum position difference is 211 meters. One cause for the error between the semi-analytical satellite theory and Cowell is probably the small eccentricity assumptions made in both the AOG and SPG.

Figures 2-37 through 2-41 are comparisons of the osculating Keplerian elements, a , e , i , Ω , and ω , as obtained by the semianalytical satellite theory and the Cowell orbit generator. Perigee and apogee passage occur respectively at 30 minutes and 96 minutes into the orbit. The osculating elements produced by the semianalytical theory track the 'true' Cowell elements very closely.

Figure 2-42 shows the effects of only the drag perturbation on the Low Altitude Eccentric Test Case. This figure shows that the drag effect occurs around perigee only. This figure also shows that modeling the short periodic variations by a Fourier series can lead to Gibb's phenomenon when the perturbation is discontinuous and concentrated in one area. Gibb's phenomenon can be reduced by increasing the number of time-independent short periodic coefficients and the quadrature order. Another solution to the Gibb's phenomenon is to reformulate the short periodic variations in another geometric variable such that the perturbation effect is smoothed around

perigee. Figure 2-42 also indicates that the semianalytical satellite theory is slightly biased after perigee passage. This is probably due to the fact that the semianalytical satellite theory did not properly model the drag perturbation around perigee. Increasing the quadrature order and number of short periodic coefficients will probably reduce this bias.

2.4.5 Medium Altitude Circular Test Case

The Medium Altitude Circular Test Case (Table 2-10) serves as a good test of the weak time-dependent formulation. The orbit is near circular and has a mean period of 12 hours. This test case is representative of a Global Positioning Satellite (GPS).

Table 2-10. Initial Mean Elements and Parameters for the Medium Altitude Circular Test Case

\bar{a}	= 26559.5 km	Epoch	= 0.0 hrs., 0.0 mins., 1 July 1979
\bar{e}	= .001	Reference Frame	= True of Date
\bar{i}	= 63.0°	Reflectivity Constant	= 1.5
$\bar{\Omega}$	= 0°	Area	= 9.091 m ²
$\bar{\omega}$	= 0°	Mass	= 454.217 kg
\bar{M}	= 0°		
$\overline{\text{Period}}$	= 12 hours		

A comparison of Figures 2-43 and 2-44 shows the importance of the weak time-dependent formulation. In Figure 2-43 it is seen that the mean along track error (compared to Cowell) is about 32 meters in 24 hours when a time-independent formulation is used. When a weak time-dependent formulation is used (Figure 2-44), the mean along track error is reduced to about one meter in 24 hours. It is felt that the remaining error in Figure 2-44 is due to the single-sided finite-differencing technique used to approximate the time derivatives of the short periodic coefficients [see Equation (2-85) or Appendix B] and/or the neglect of $\left(\frac{\dot{\phi}}{\omega n}\right)^2$ terms in Equation (2-83). The perturbing time increment used in the finite differencing technique was five minutes for the lunar-solar point mass effects (about .01% of the Lunar period) and one hour for solar radiation pressure effects (about .01% of the apparent Solar period). Table 2-11 gives a comparison of the [EPC]⁻¹ initialization procedure for both the time-independent and weak time-dependent formulation. As can be seen from Table 2-11, the weak time-dependent formulation increased the initial osculating semimajor axis by 1.32 meters over the time-independent formulation. Figures 2-45 and 2-46 are the radial and cross track differences corresponding to Figure 2-44.

Table 2-11. Initial Osculating Elements
from an [EPC]⁻¹ Procedure

Time-independent formulation
with perturbations as given
in Figure 2-43

a = 26561.56435 km
e = .0010482547
i = 63.00112426°
Ω = 359.9999661°
ω = 359.8607354°
M = .1390436311

Weak time-dependent formu-
lation with perturbations
as given in Figure 2-44

a = 26561.56557 km
e = .0010484201
i = 63.00112407°
Ω = 359.9999657°
ω = 359.8560915°
M = 0.1436848842°

It was also noted that neglect of the weak time-dependent formulation for solar radiation pressure effects made minor changes in the above results. This indicates that the time-independent formulation for the lunar-solar point mass effects is the major source of error in Figure 2-43. It therefore appears that lunar-solar point mass effects on medium altitude satellites cannot be adequately handled with a time-independent formulation for high precision semianalytical orbit generation. The weak time-dependent formulation is a means of obtaining accurate ephemeris for medium altitude satellites.

Figures 2-47, 2-48 and 2-49 are comparisons of the osculating semimajor axis, eccentricity and inclination respectively over the first orbit of the satellite. The (+) denotes the semianalytical orbit generator and the (*) denotes

the Cowell orbit generator. The (+) will overwrite the (*) when the values for the element coincide to within the discretization of the plot. Obviously, the semianalytical satellite theory can generate precision ephemerides.

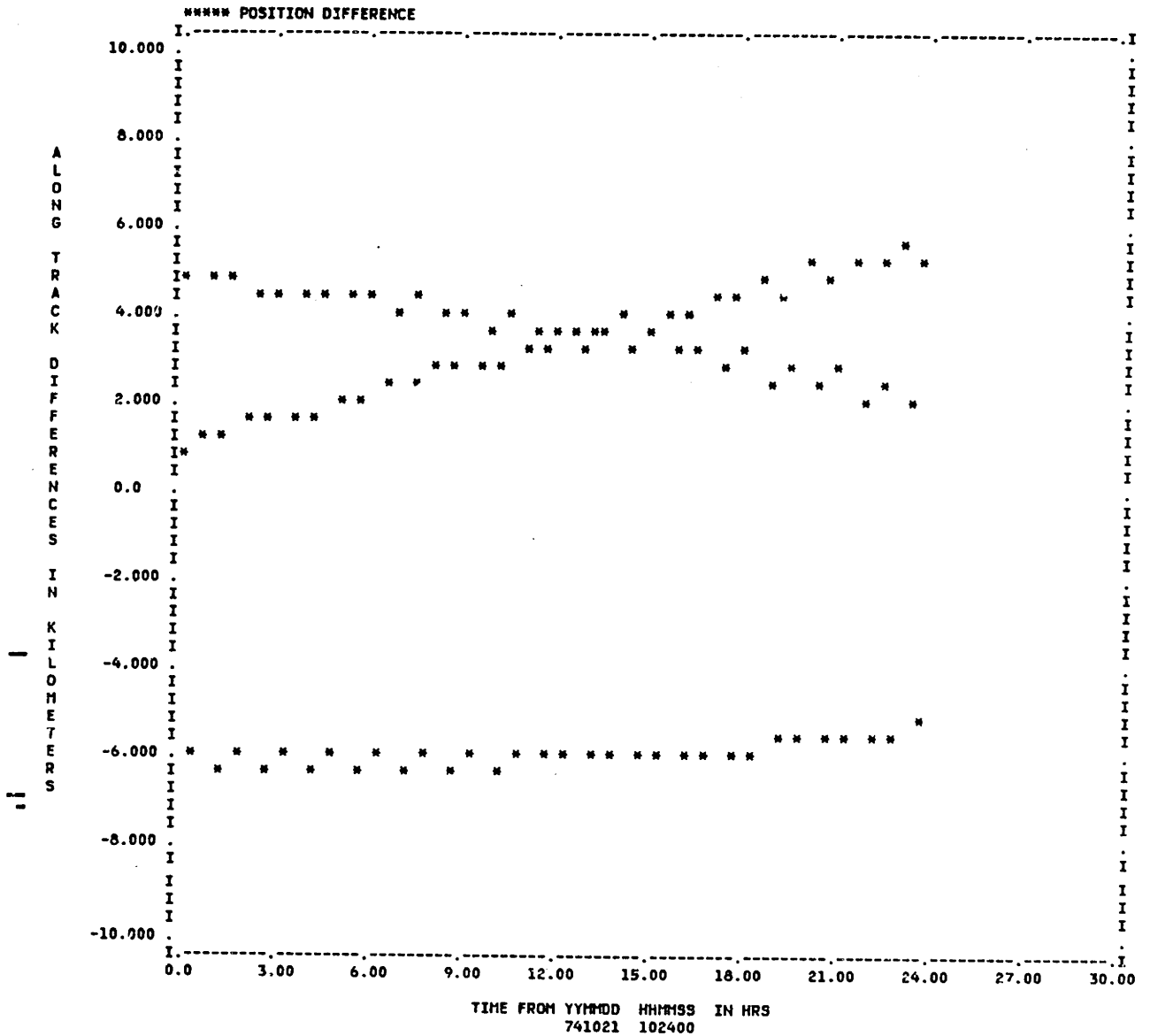
Figure 2-50 is a plot of the first order short periodic variation due to solar radiation pressure for the Medium Altitude Test Case. The solar radiation pressure short periodic variation is a 10 meter effect for this test case.

A one orbit plot of the first order lunar semimajor axis short periodic variation is presented in Figure 2-51. Only lunar perturbations were considered in both the AOG and SPG. The numerical weak time-dependent short periodic formulation was used. As can be seen from Figure 2-51, the lunar short periodic variation on a medium altitude satellite is a 150 meter effect. The lunar short periodic variation must be considered for accurate orbit generation on medium and high altitude satellites.

Figures 2-52 through 2-58 show some of the lunar weak time-dependent short periodic coefficients over a 12 day time span. The weak time-dependent short periodic coefficients show more of a time variation than the time-independent short periodic coefficients (see Section 2.4.3). Evaluation of the weak time-dependent coefficients on the integration grid and

use of an interpolator to obtain them at the output times, still appears to be possible. A higher order interpolator algorithm may be needed for the weak time-dependent short periodic coefficients than for the time-independent short periodic coefficients. It is also noted that the more rapidly varying weak time-dependent short periodic coefficients are one to two orders of magnitude less than the dominant coefficients (Figures 2-53 and 2-54).

Figure 2-3. Along Track Difference/Semianalytical* minus Cowell for the Low Altitude Circular Test Case



* The coupling terms in the fast variable short periodic coefficients were not included.

Perturbations

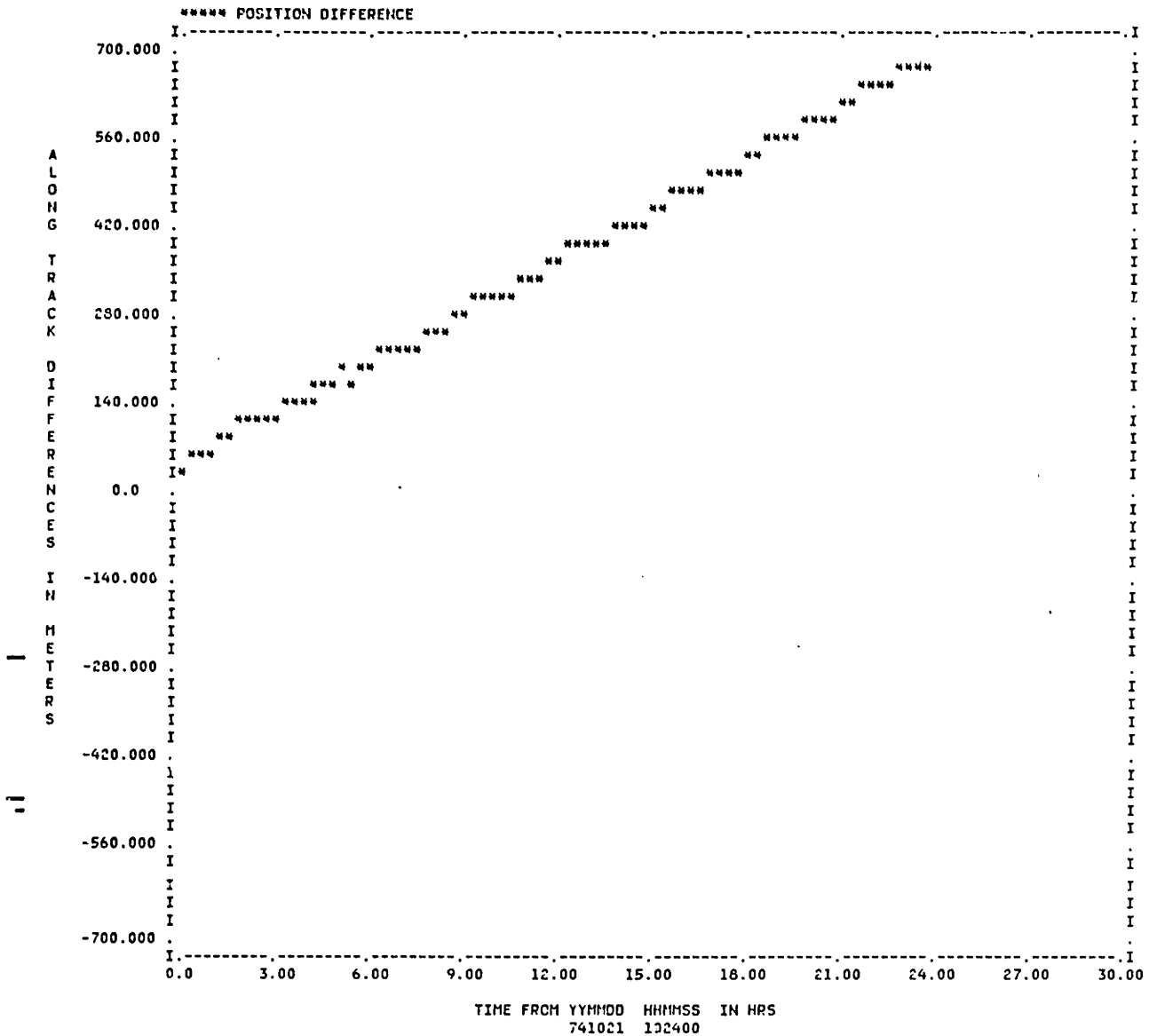
COWELL: 6x0 gravitational field and drag: 30 sec time step

AOG: 1st order analytical expressions for the 6x0 gravitational field, Zeis' expressions for J_2^2 effects and option 6 for drag (4/48): 1 day numerical integration time step

SPG: 6x0 gravitational field (7/48) and drag (7/48), both to 1st order (time-independent)

Initial Conditions: NOM

Figure 2-4. Along Track Difference/Semianalytical* minus Cowell for the Low Altitude Circular Test Case



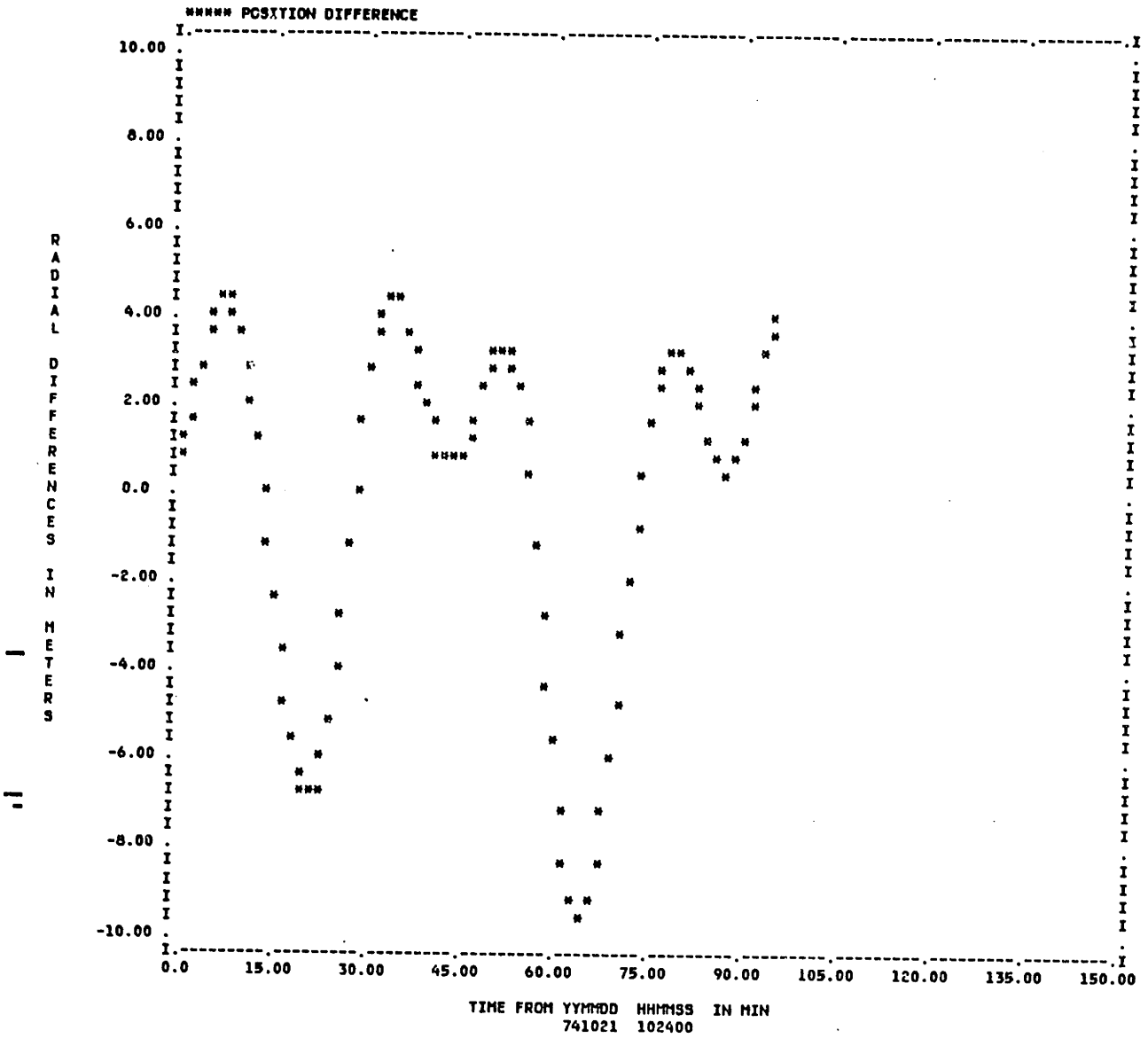
* The coupling terms in the fast variable short periodic coefficients were included.

Perturbations

- COWELL: 6x0 gravitational field and drag: 30 sec numerical integration time step
- AOG: 1st order analytical expressions for the 6x0 gravitational field, Zeis' expressions for J_2 effects and option 6 for drag (4/48): 1 day numerical integration time step
- SPG: 5x0 gravitational field (7/48) and drag (7/48), both to 1st order (time-independent)

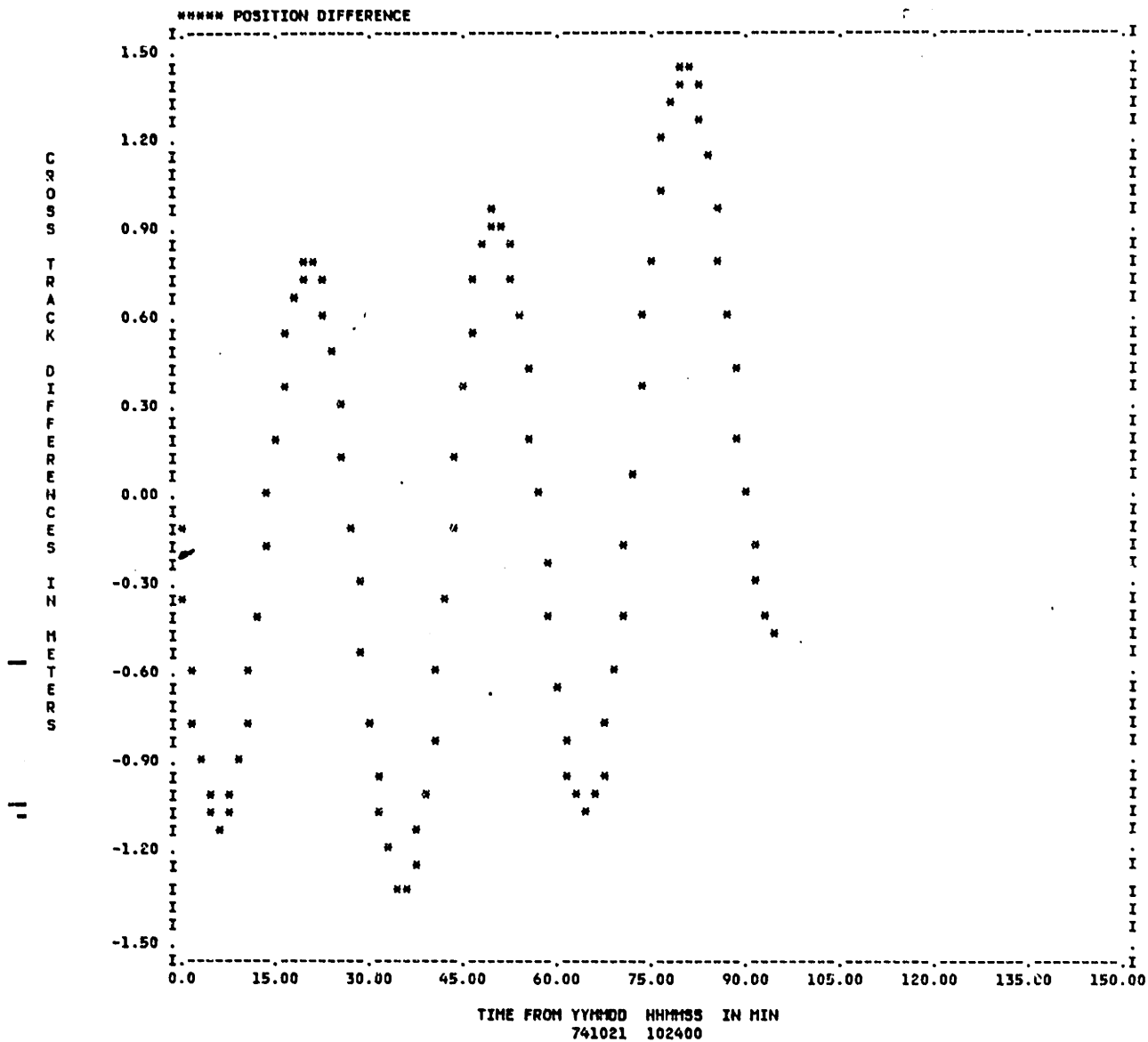
Initial Conditions: NOM

Figure 2-5. Radial Difference/Semianalytical minus Cowell for the Low Altitude Circular Test Case



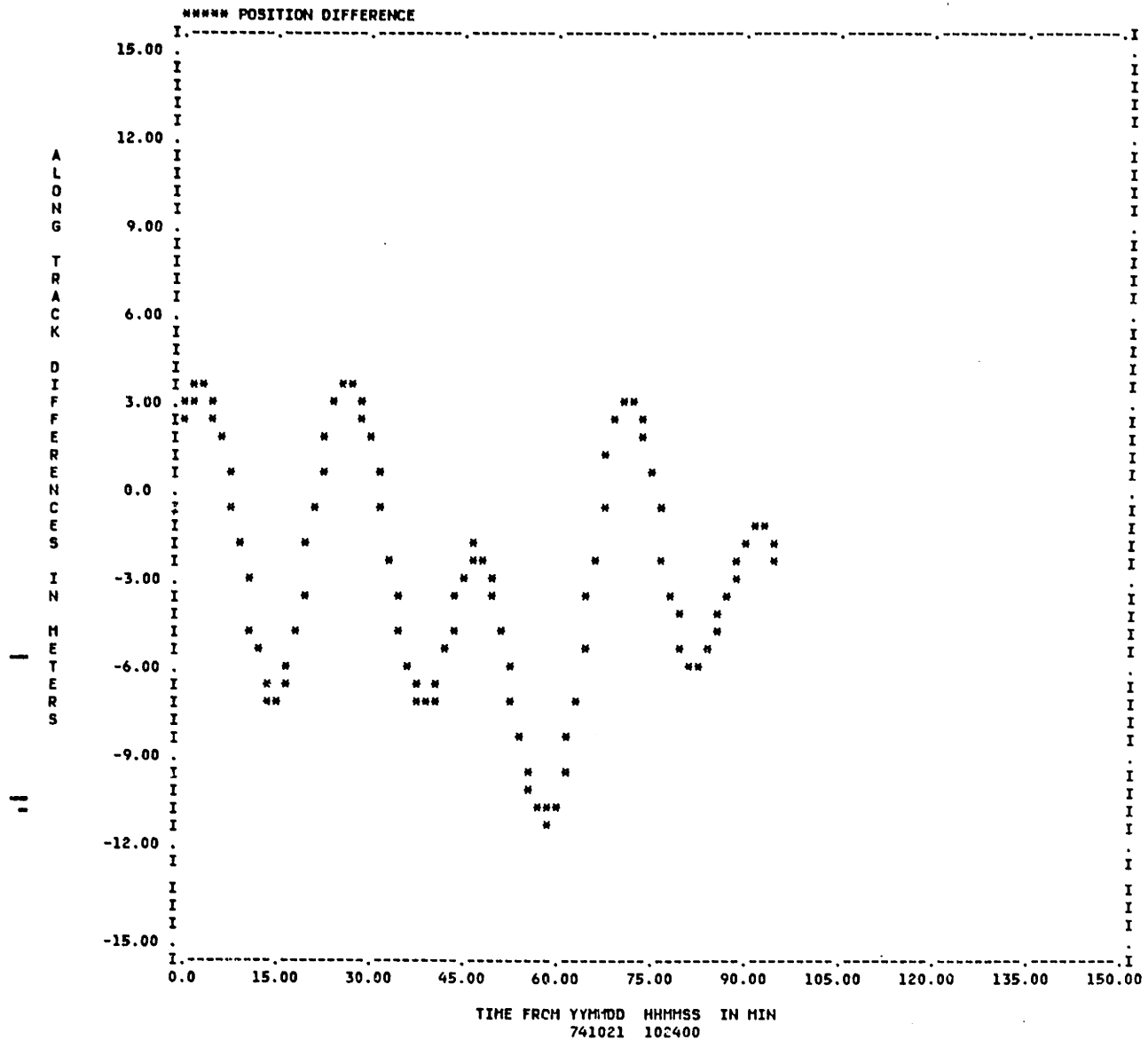
Same initial conditions and perturbations as in drag option 6 of Table 2-6.

Figure 2-6. Cross Track Difference/Semianalytical minus Cowell for the Low Altitude Circular Test Case



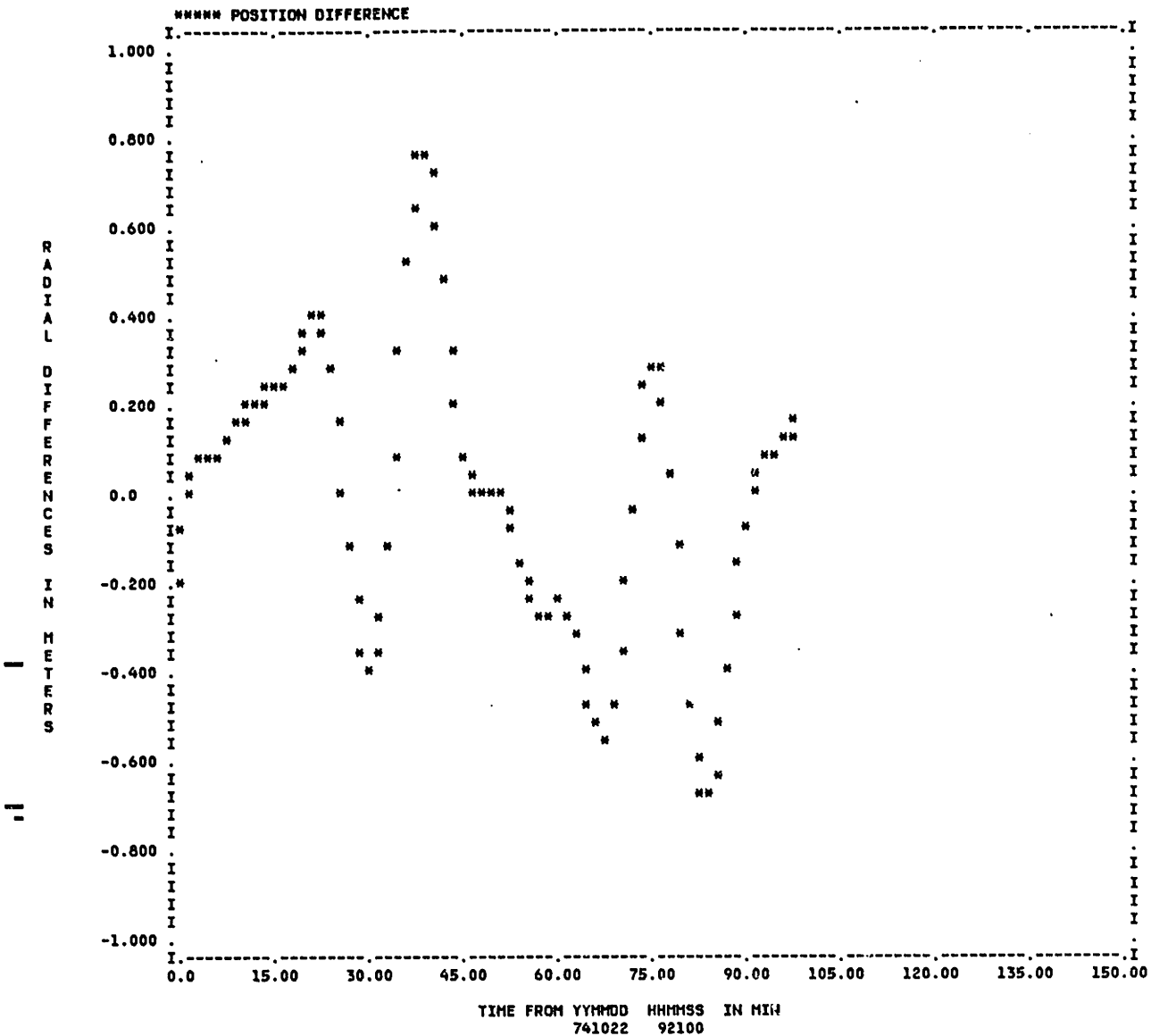
Same initial conditions and perturbations as in drag option 6 of Table 2-6.

Figure 2-7. Along Track Difference/Semianalytical minus Cowell for the Low Altitude Circular Test Case



Same initial conditions and perturbations as in drag option 6 of Table 2-6.

Figure 2-8. Radial Difference after 23 hours from Epoch/Semianalytical minus Cowell for the Low Altitude Circular Test Case



Perturbations

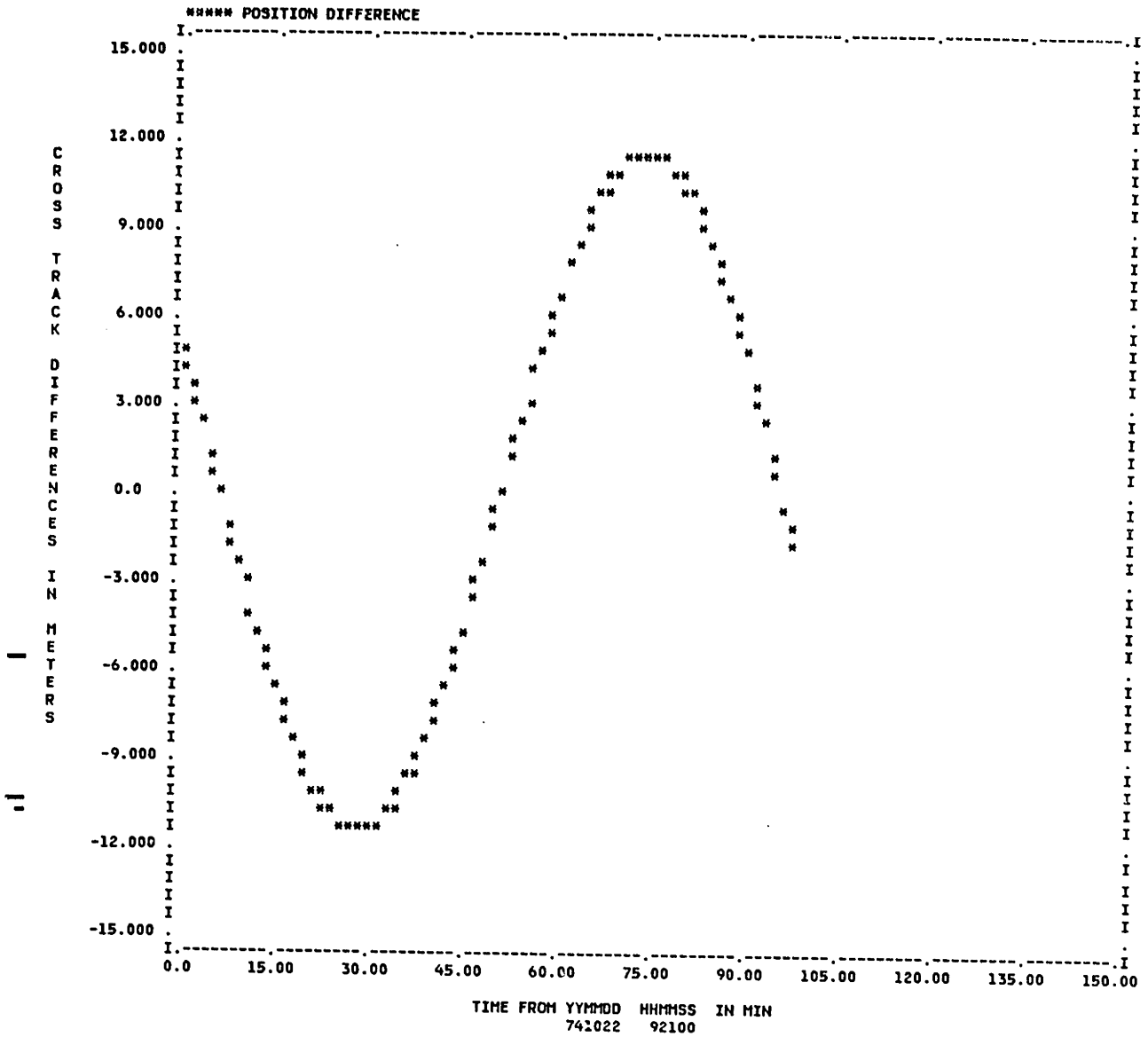
Cowell: 6x0 gravitational field and drag: 30 sec numerical integration time step.

AOG: 1st order analytical expressions for the 6x0 gravitational field, Zeis' expressions for J_2^2 effects and option 7 for drag (48 pt quadrature order); 1 day numerical integration time step.

SPG: 6x0 gravitational field (7/48) and drag (7/48) both to first order (time-independent), Zeis' expressions for J_2^2 effects.

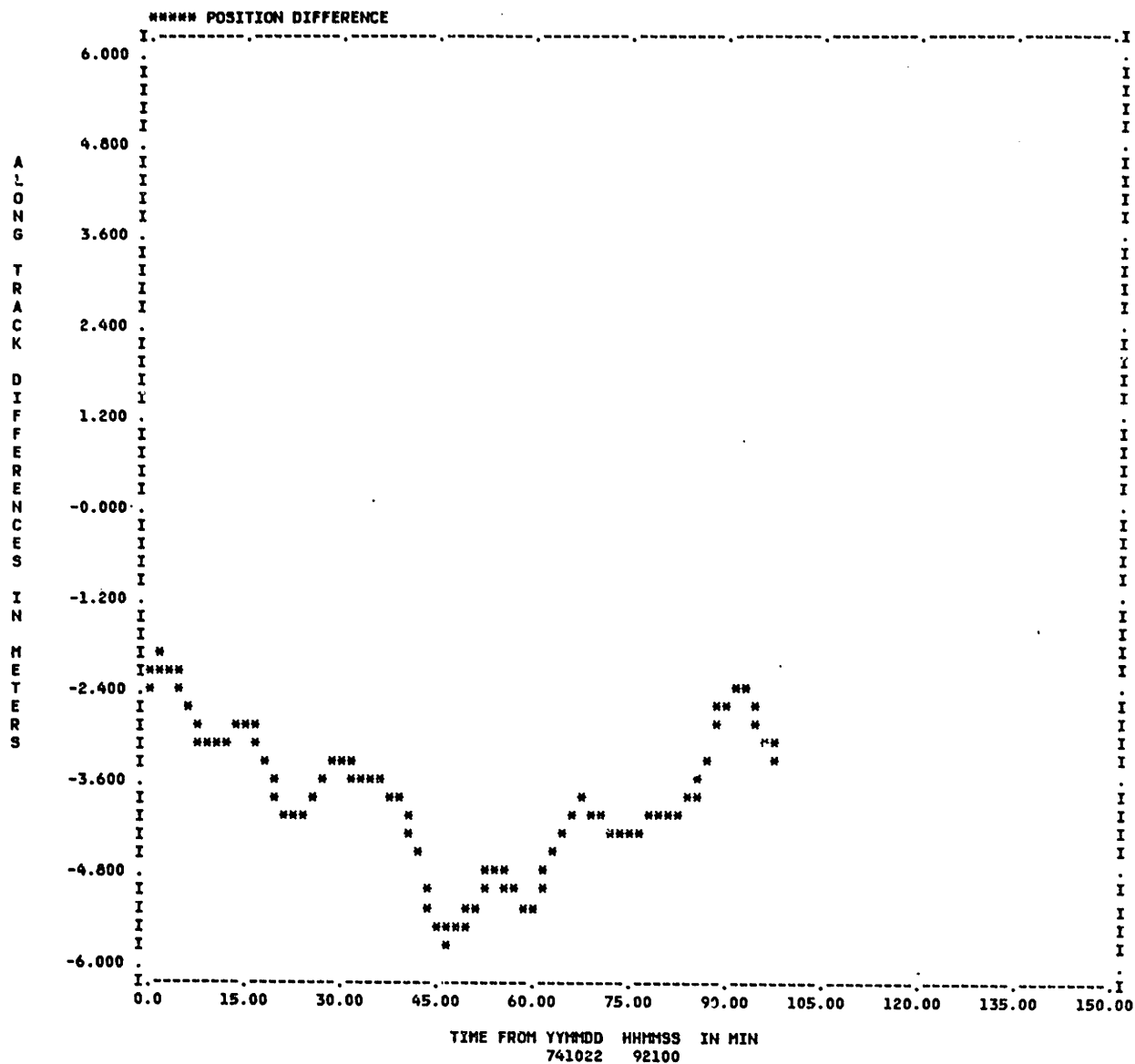
Initial Conditions: 2 hour PCE

Figure 2-9. Cross Track Difference after 23 Hours from Epoch/Semianalytical minus Cowell for the Low Altitude Circular Test Case



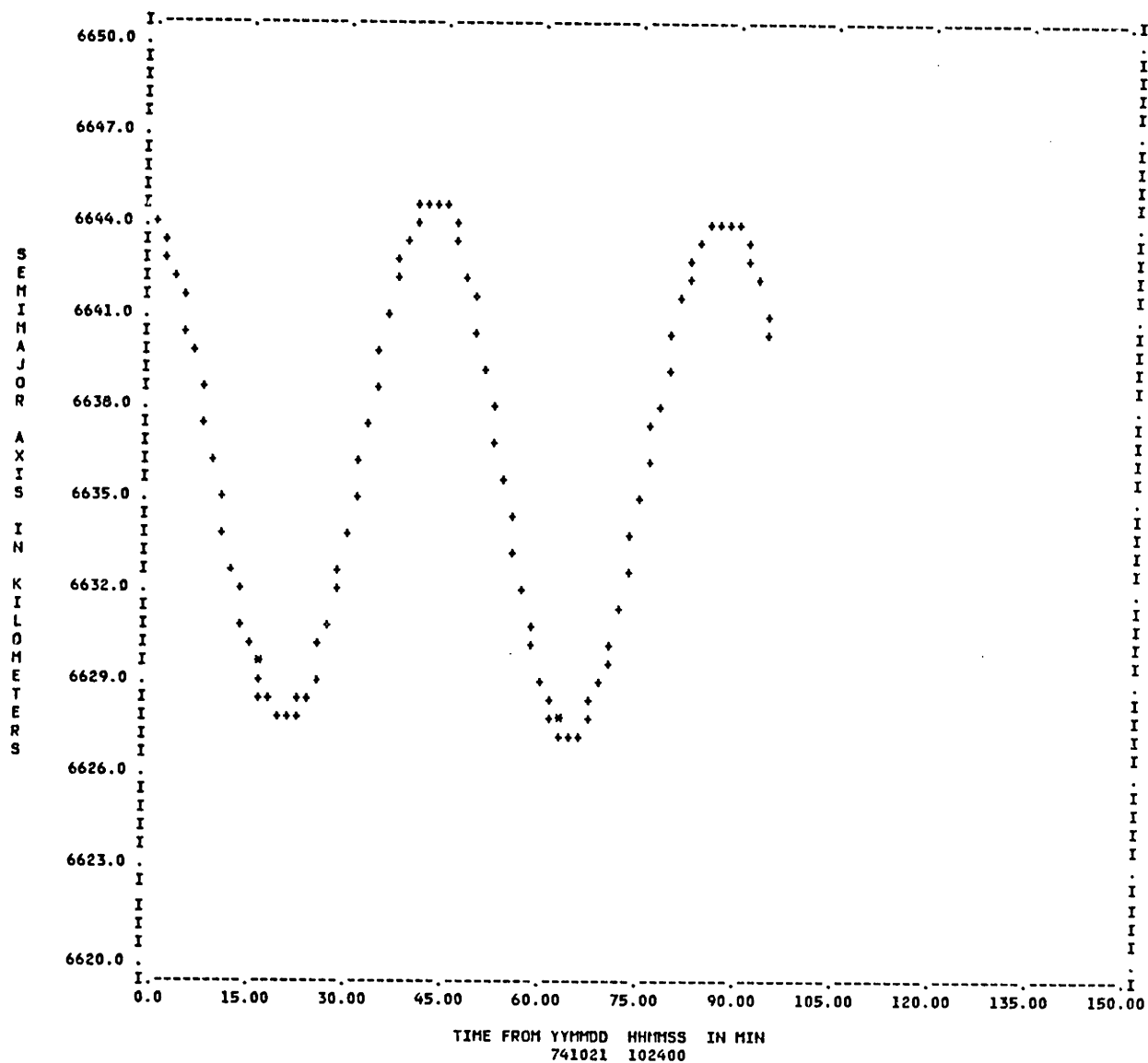
Same initial conditions and perturbations as in Figure 2-8.

Figure 2-10. Along Track Difference after 23 Hours from Epoch/Semianalytical minus Cowell for the Low Altitude Circular Test Case



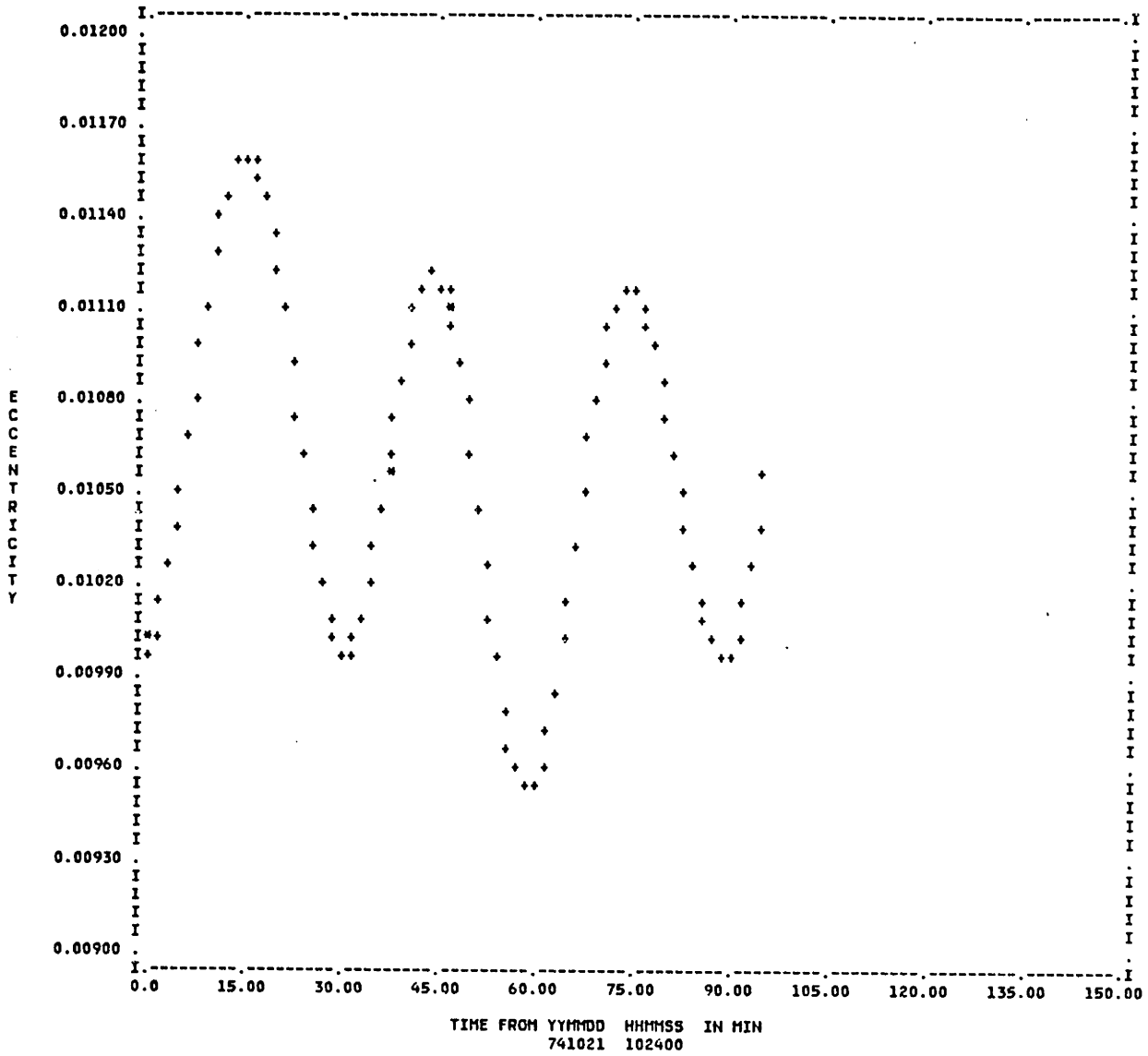
Same initial conditions and perturbations as in Figure 2-8.

Figure 2-11. Osculating Semimajor Axis Comparison/Semianalytical versus Cowell
for the Low Altitude Circular Test Case



Same initial conditions and perturbations as in drag option 6 of Table 2-6.

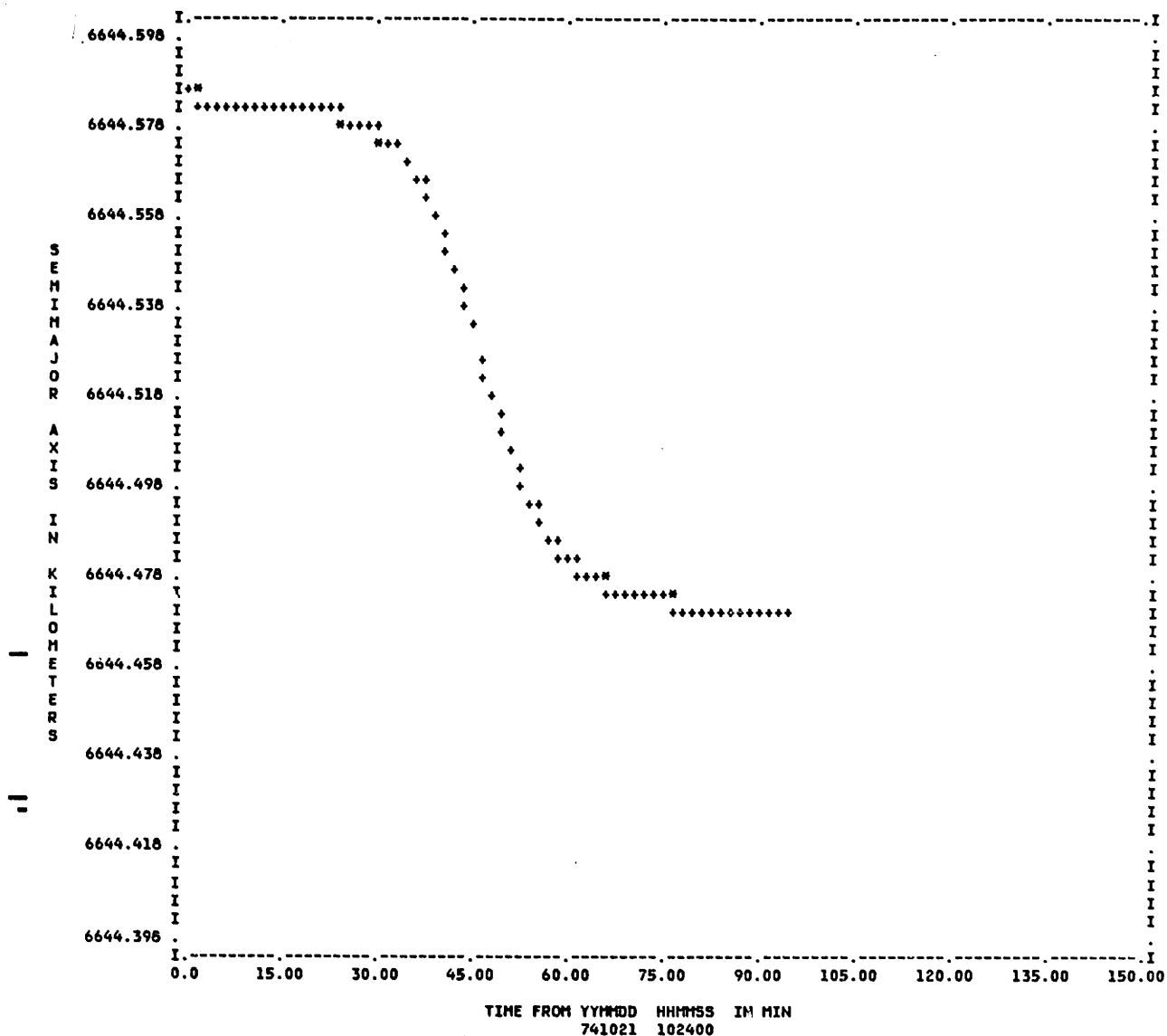
Figure 2-12. Osculating Eccentricity Comparison/Semianalytical versus Cowell
for the Low Altitude Circular Test Case



***** ELEMENTS FROM ORB1 FILE ON UNIT 24, DATA RECORDS START AT 741021 102400: Cowell
 ++++++ ELEMENTS FROM ORB1 FILE ON UNIT 81, DATA RECORDS START AT 741021 102400: AOG & SPG

Same initial conditions and perturbations as in drag option 6 of Table 2-6.

Figure 2-13. Osculating Semimajor Axis Comparison/Semianalytical versus Cowell for the Low Altitude Circular Test Case



***** ELEMENTS FROM ORB1 FILE ON UNIT 24, DATA RECORDS START AT 741021 102400: Cowell
 ++++++ ELEMENTS FROM ORB1 FILE ON UNIT 81, DATA RECORDS START AT 741021 102400: AOG & SPG

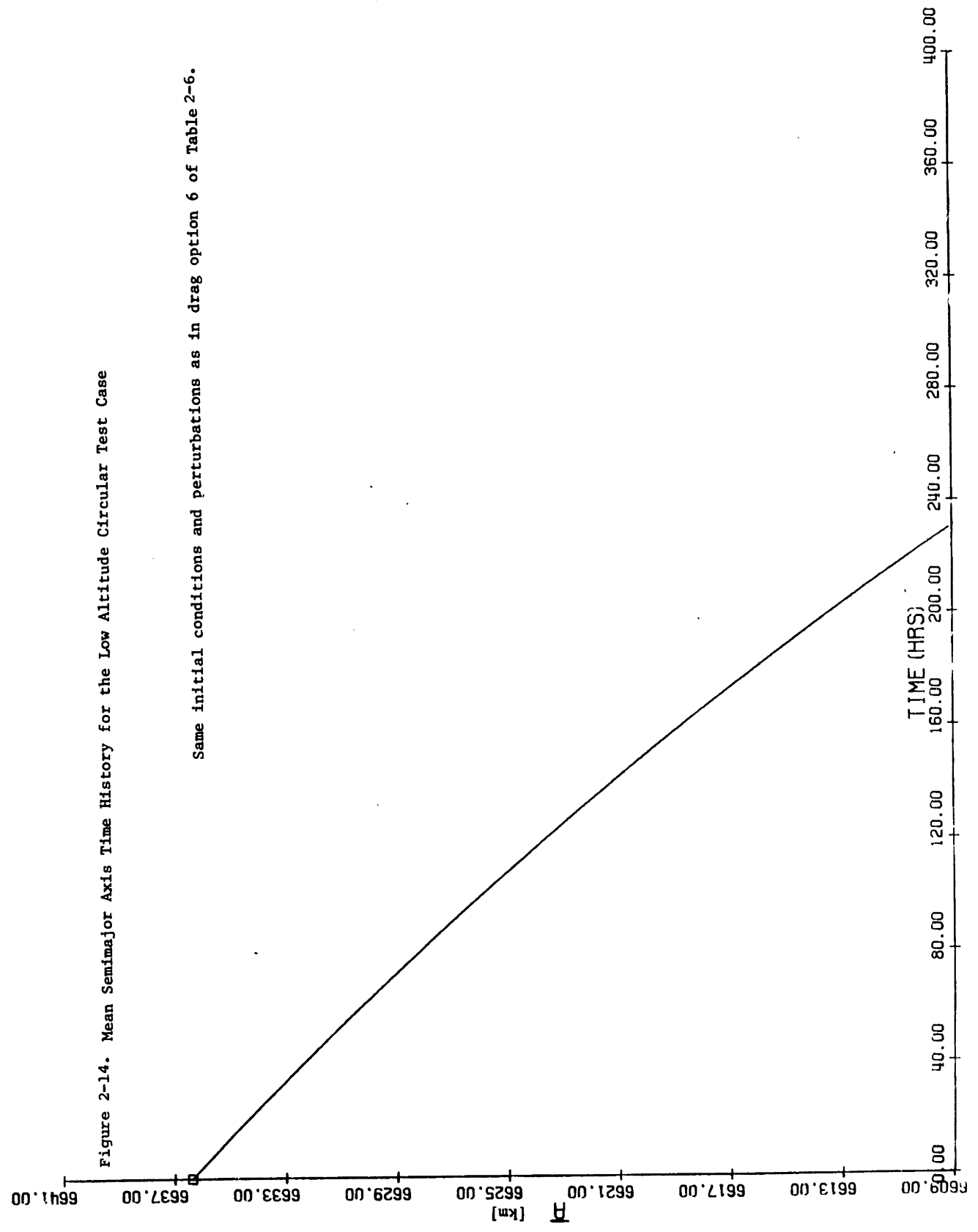
Perturbations

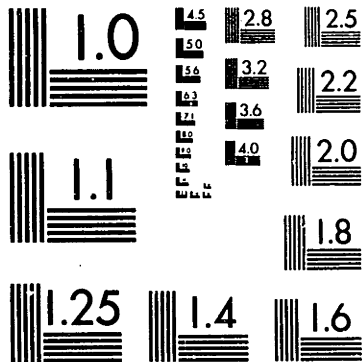
- Cowell: drag only (30 sec numerical integration time step)
- AOG: drag only, option 1 (48 pt quadrature)
1 day numerical integration time step
- SPG: 1st order drag only (10/48), time-independent formulation

Initial Conditions: NOM

Figure 2-14. Mean Semimajor Axis Time History for the Low Altitude Circular Test Case

Same initial conditions and perturbations as in drag option 6 of Table 2-6.





MICROCOPY RESOLUTION TEST CHART
NATIONAL BUREAU OF STANDARDS-1963-A

20X

NOTICE THIS MATERIAL MAY BE PROTECTED BY
COPYRIGHT LAW (TITLE 17 U.S. CODE)

Figure 2-15. \bar{h} Time History for the Low Altitude Circular Test Case

Same initial conditions and perturbations as in drag option 6 of Table 2-6.

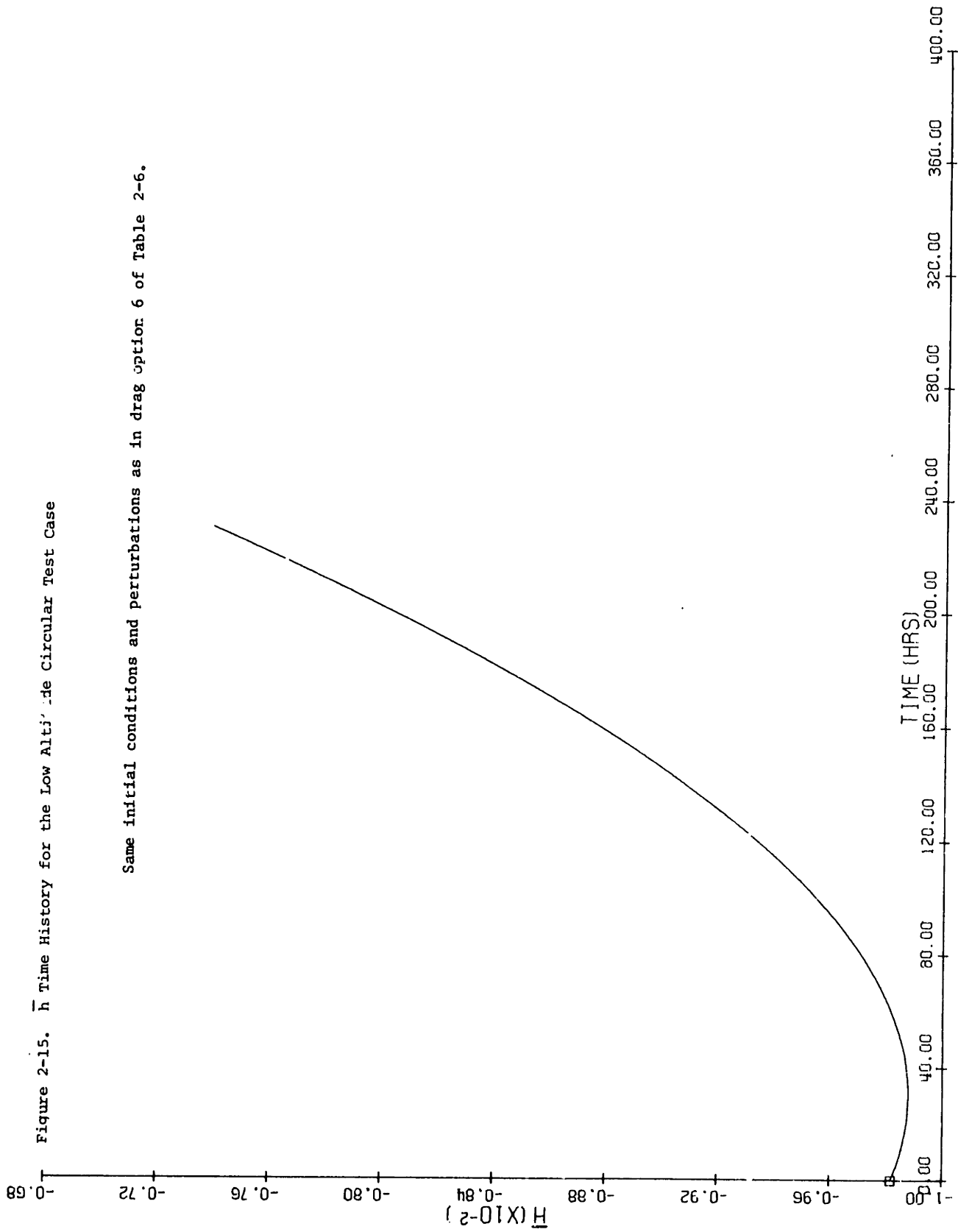


Figure 2-16. \bar{k} Time History for the Low Altitude Circular Test Case

Same initial conditions and perturbations as in diag option 6 of Table 2-6.

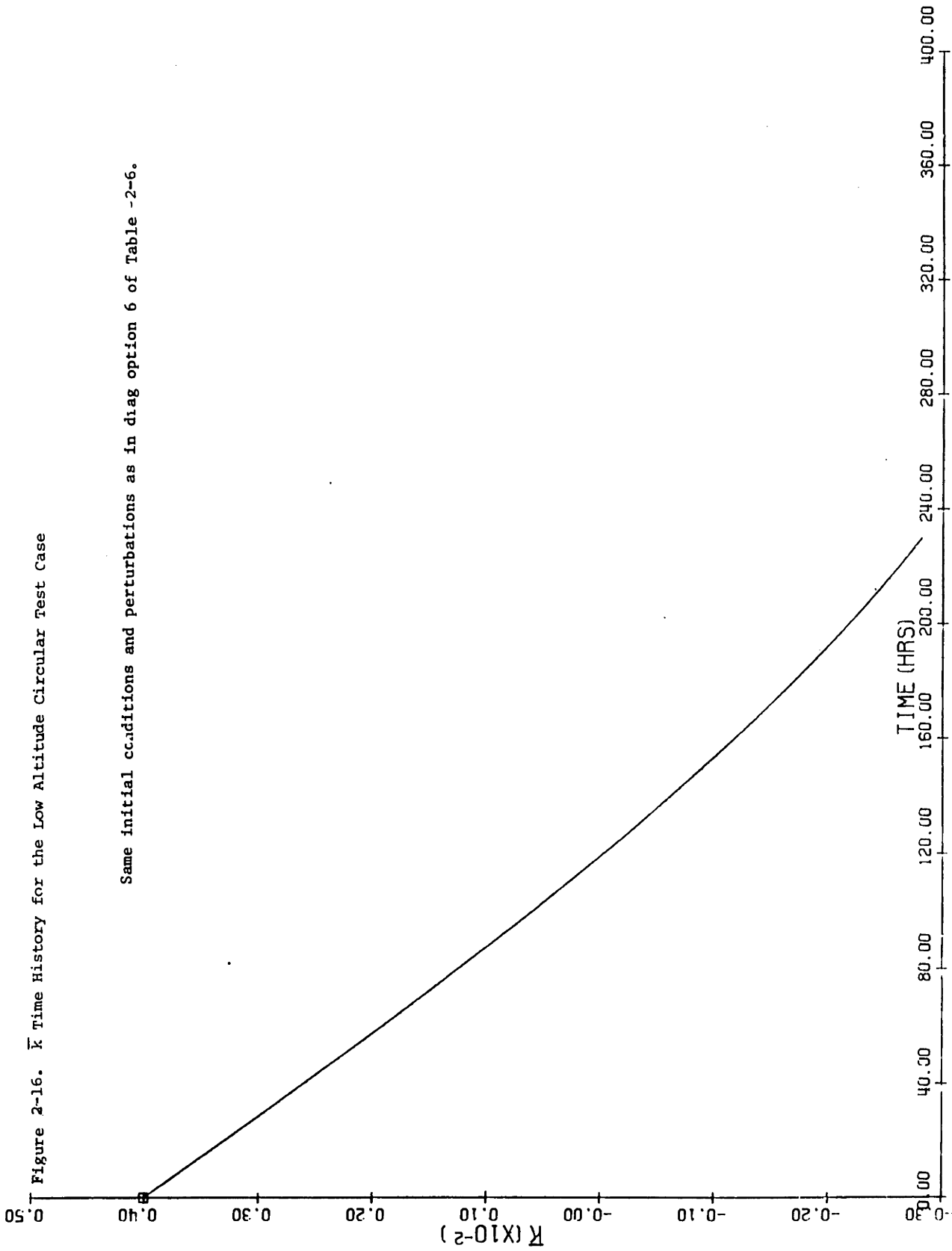
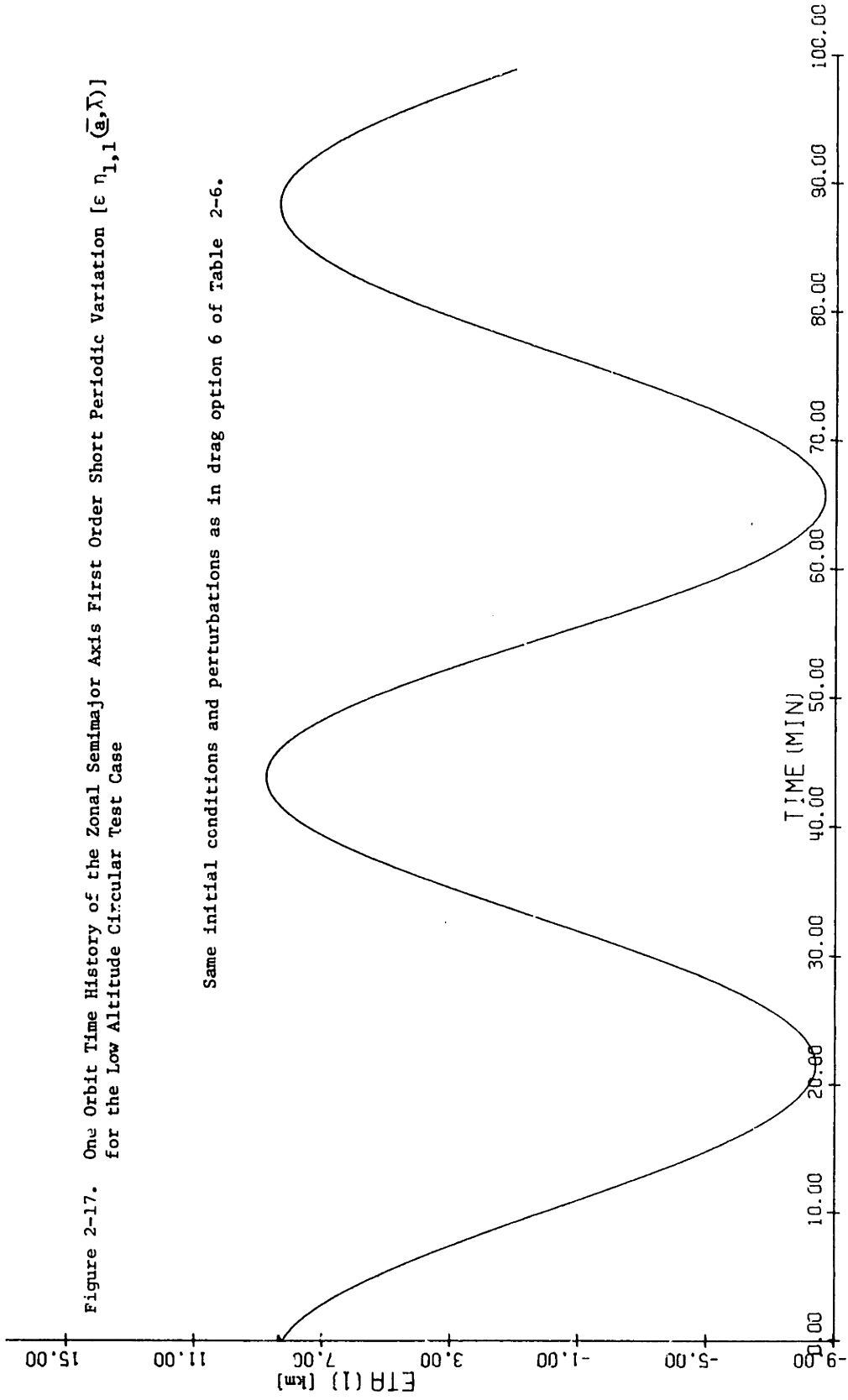
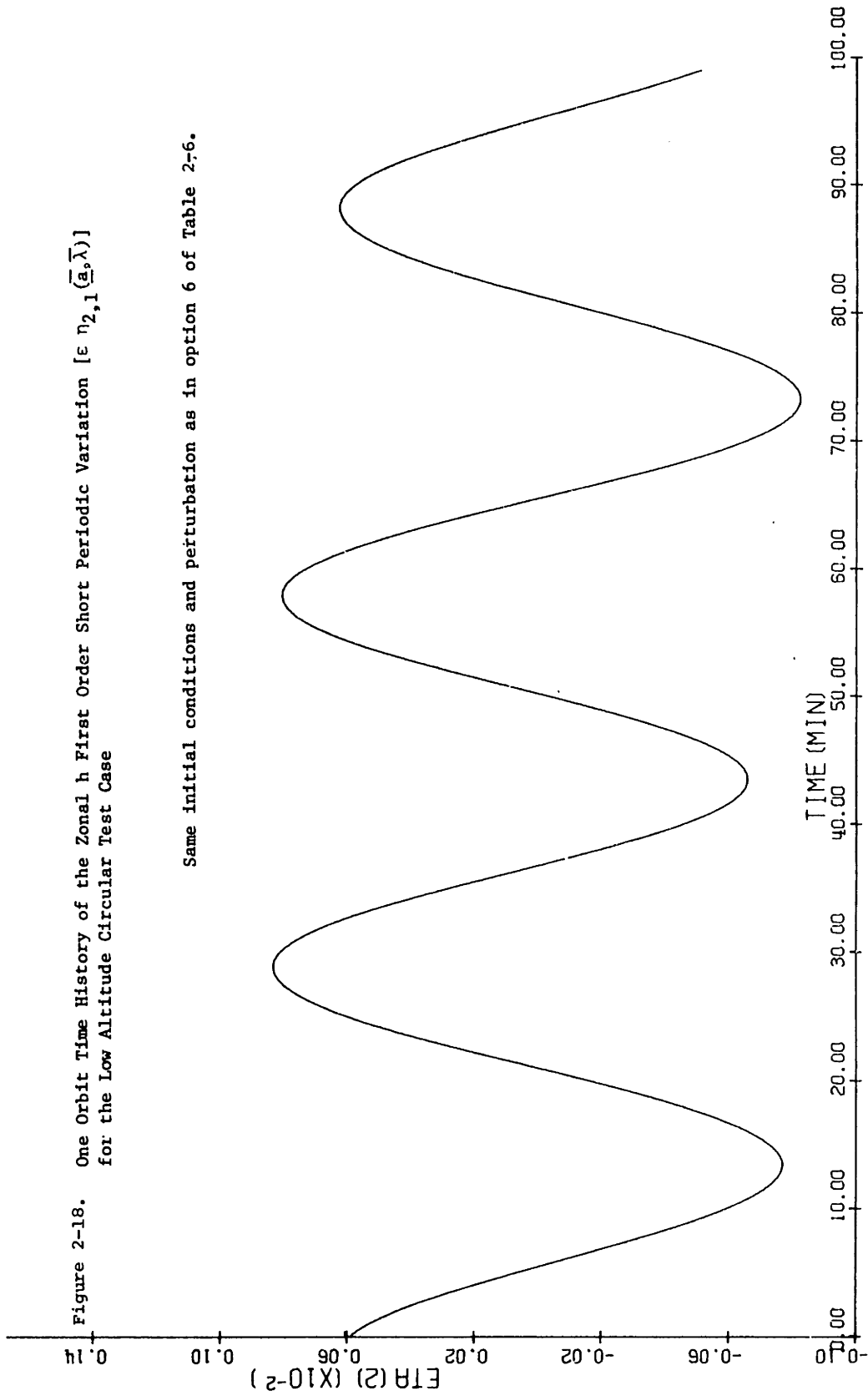


Figure 2-17. One Orbit Time History of the Zonal Semimajor Axis First Order Short Periodic Variation $[\epsilon \eta_{1,1}(\bar{a}, \bar{\lambda})]$ for the Low Altitude Circular Test Case



Same initial conditions and perturbations as in drag option 6 of Table 2-6.

Figure 2-18. One Orbit Time History of the Zonal h First Order Short Periodic Variation $[\varepsilon n_{2,1}(\bar{a}, \bar{\lambda})]$ for the Low Altitude Circular Test Case



Same initial conditions and perturbation as in option 6 of Table 2-6.

Figure 2-19. One Orbit Time History of the Zonal k First Order Short Periodic Variation $[\epsilon \eta_{3,1}(\bar{a}, \bar{\lambda})]$ for the Low Altitude Circular Test Case

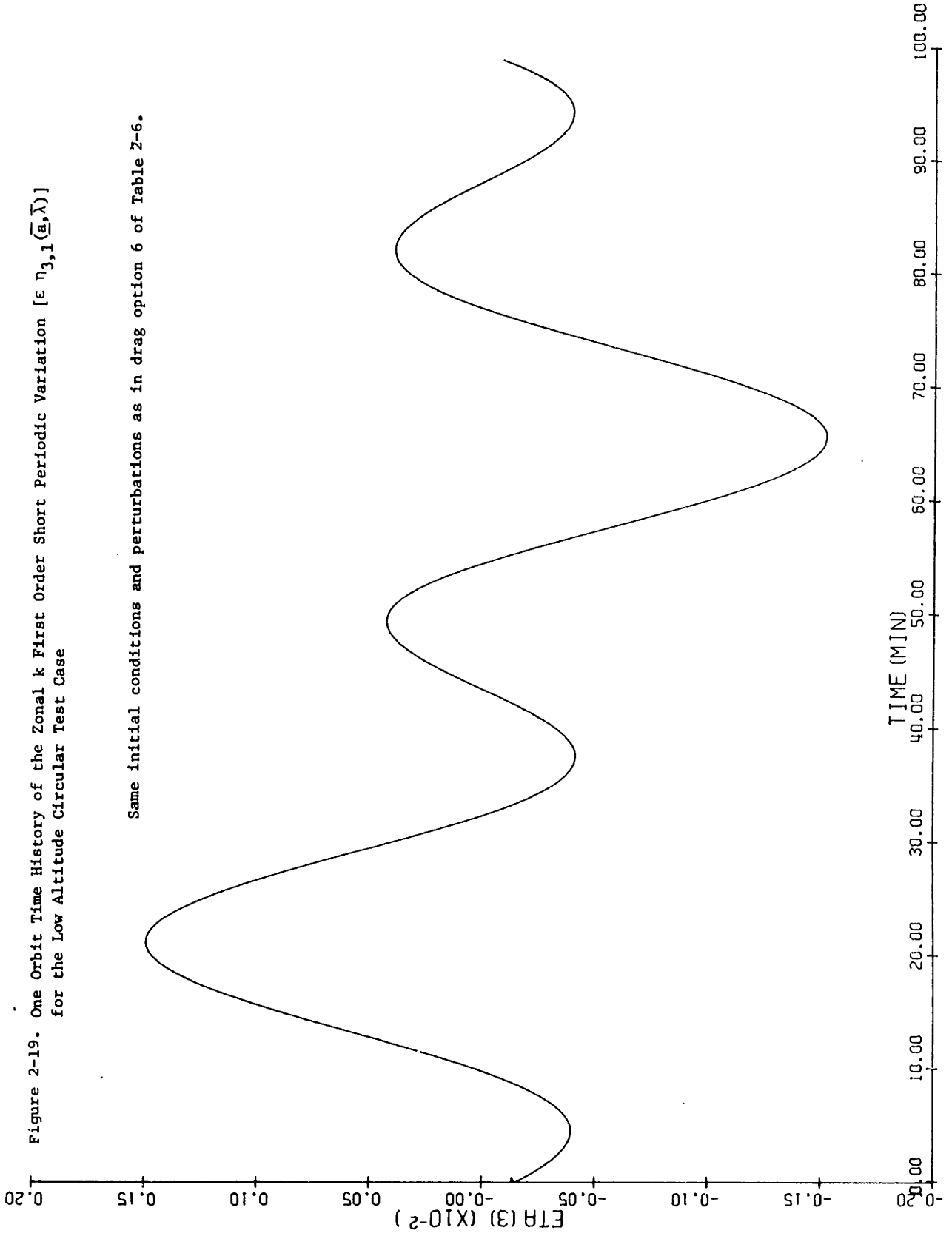
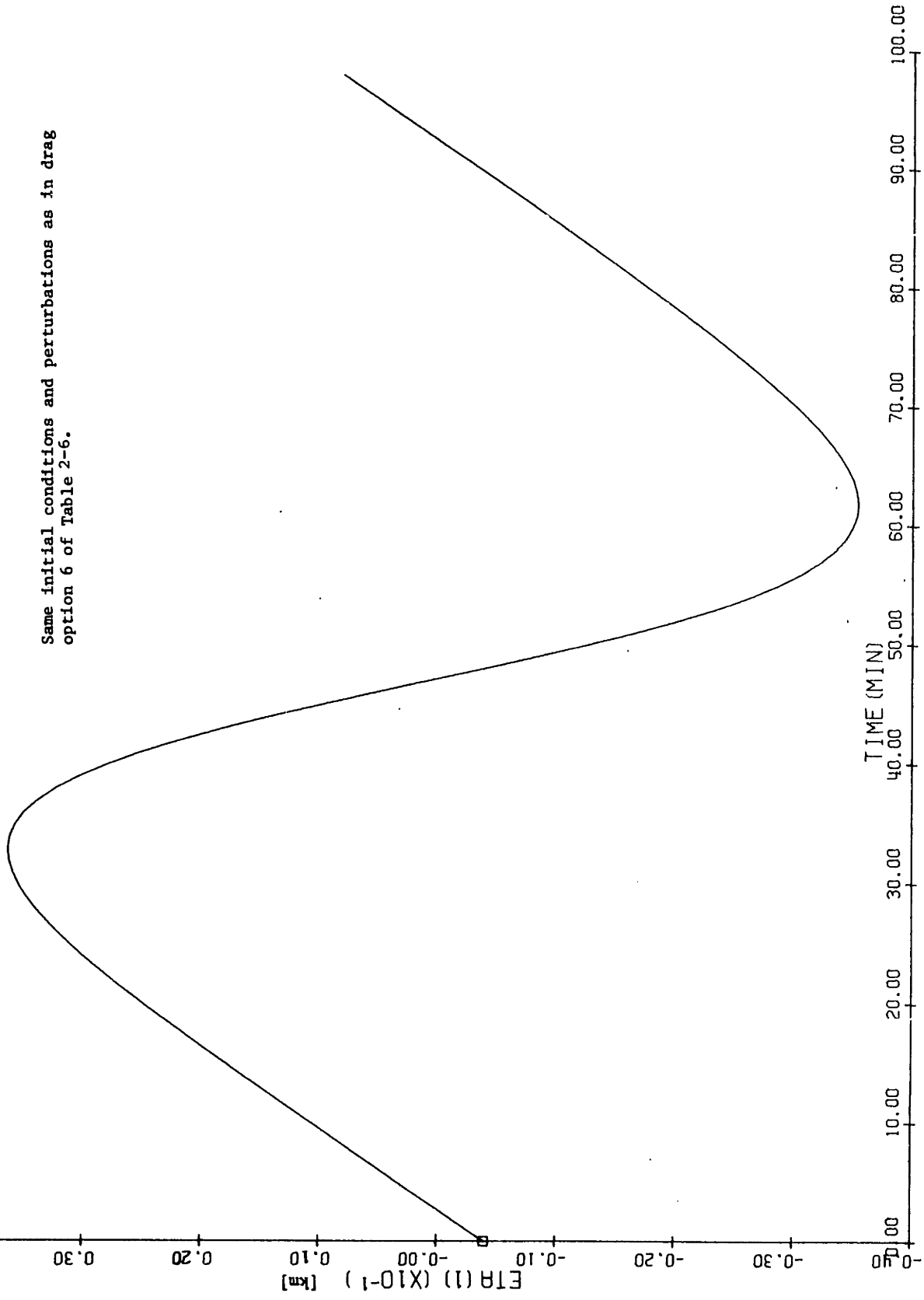


Figure 2-20. One Orbit Time History of the Drag Semimajor Axis First Order Short Periodic Variation
 $[\nu \psi_{1,1}(\underline{a}, \lambda)]$ for the Low Altitude Circular Test Case



Same initial conditions and perturbations as in drag option 6 of Table 2-6.

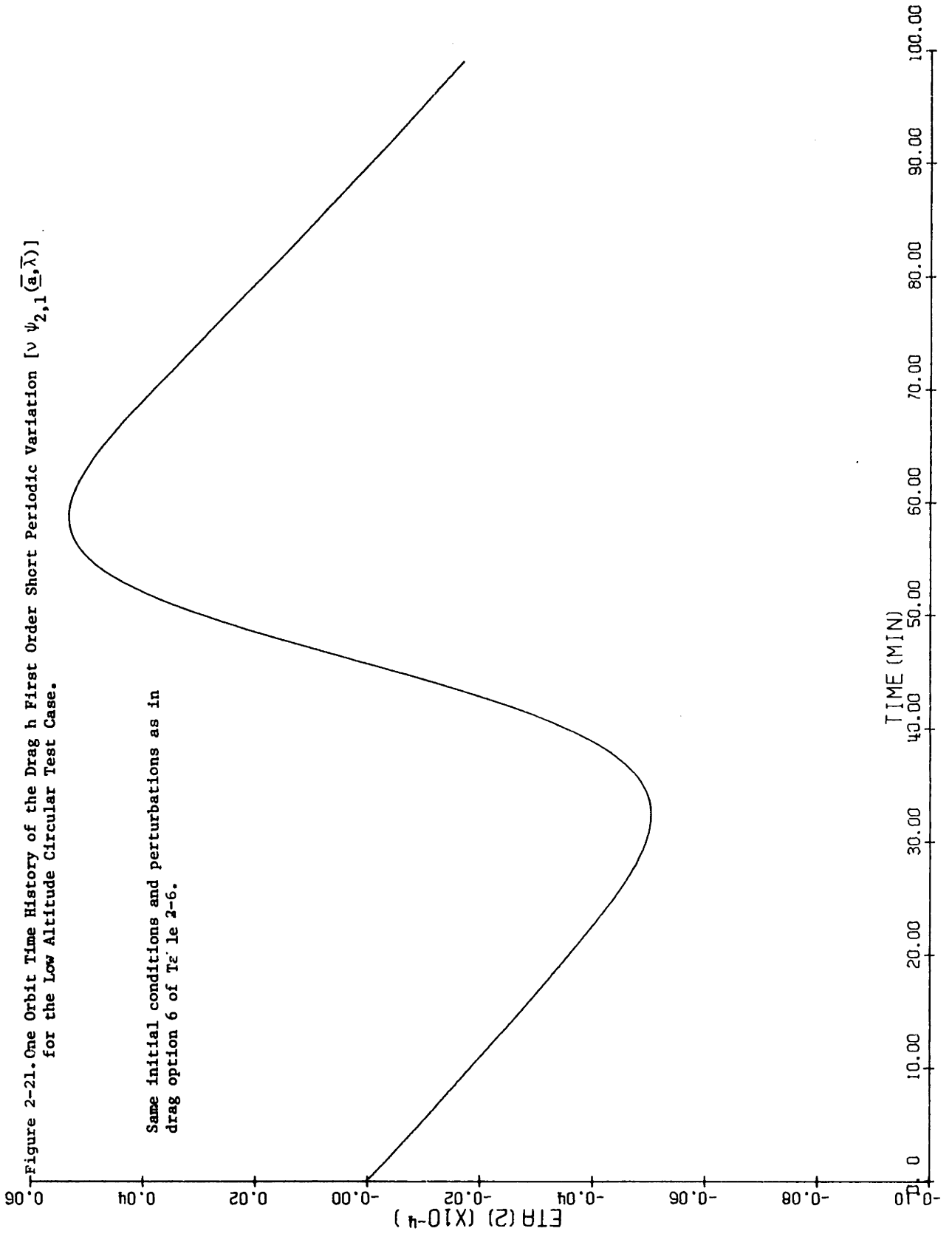


Figure 2-22. One Orbit Time History of the Drag k First Order Short Periodic Variation [$\nu \psi_{3,1}(\bar{a}, \bar{\lambda})$] for the Low Altitude Circular Test Case

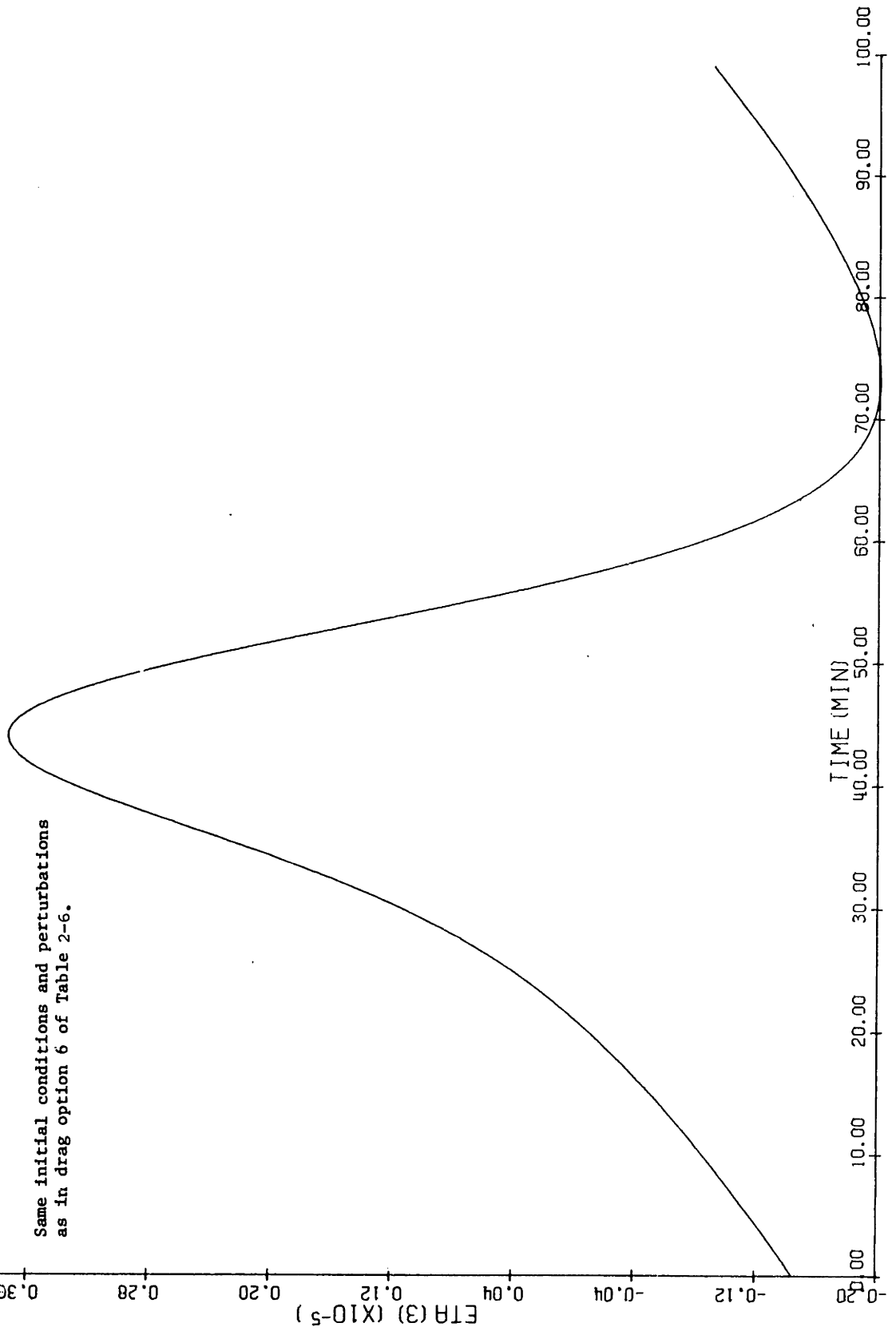


Figure 2-23. One Orbit Time History of the Drag λ First Order Short Periodic Variation $[\nu \psi_{6,1}(\bar{a}, \lambda)]$ for the Low Altitude Circular Test Case

Same initial conditions and perturbations as in drag option 6 of Table 2-6.

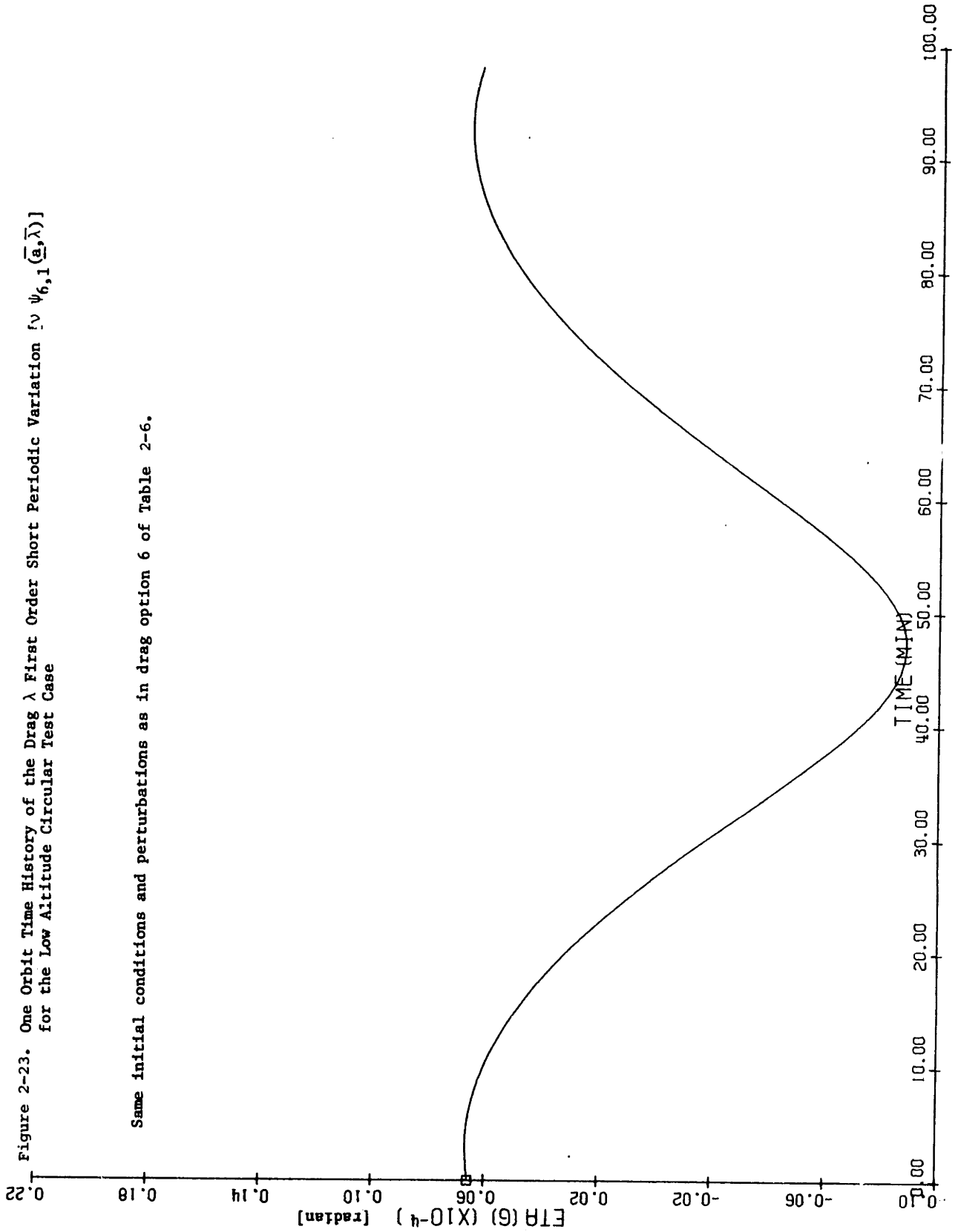


Figure 2-24. Time History of the Zonal Semimajor Axis Short Periodic Coefficients* for the Low Altitude Circular Test Case

* The $2\bar{\lambda}$ coefficients, $C_{1,2}$ and $D_{1,2}$, as in Table 2-1.

Same initial conditions and perturbations as in drag option 6 of Table 2-6.

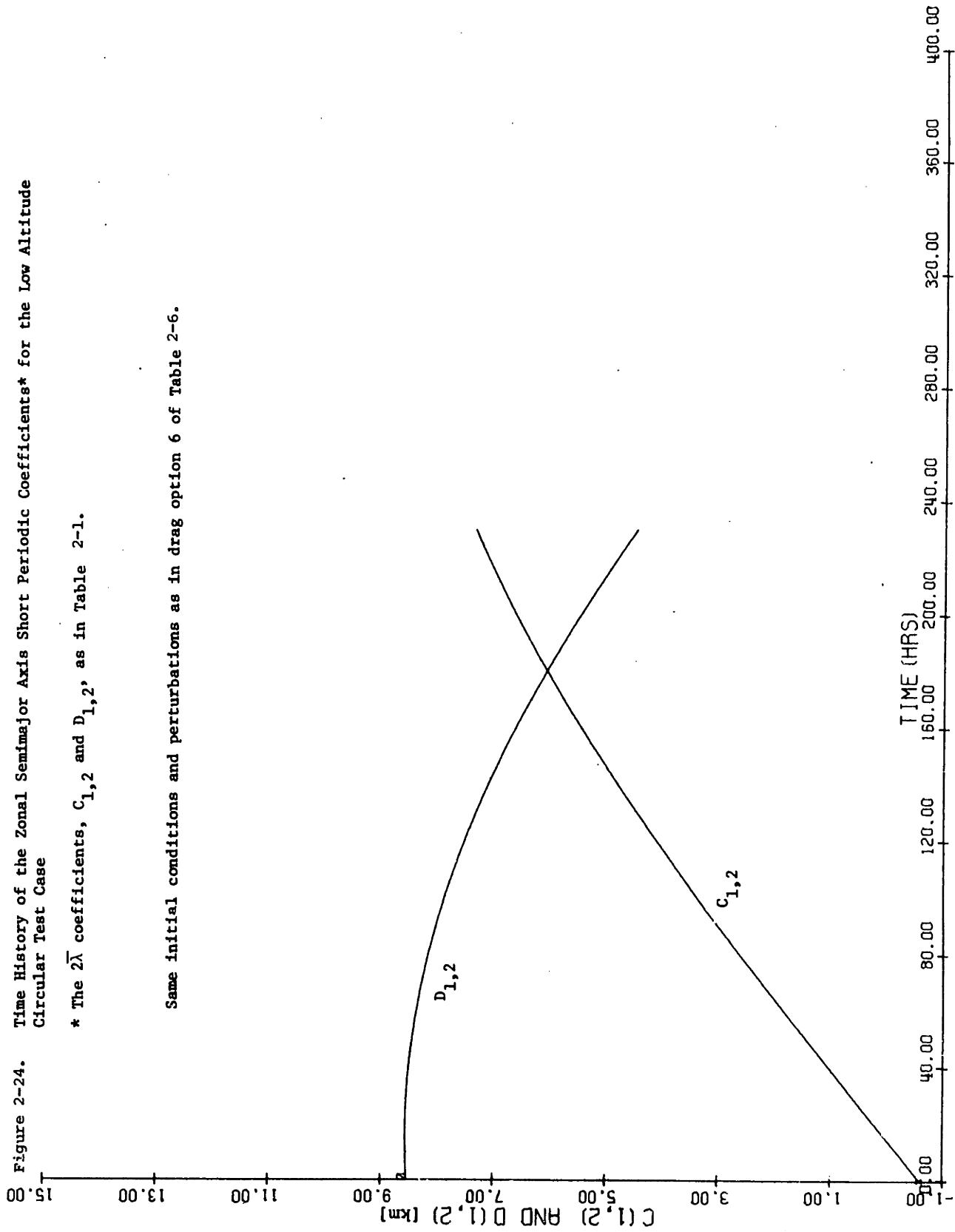


Figure 2-25. Time History of the Zonal Semimajor Axis Short Periodic Coefficients* for the Low Altitude Circular Test Case

* The $3\bar{\lambda}$ coefficients, $C_{1,3}$ and $D_{1,3}$, as in Table 2-1.
 Same initial conditions and perturbations as in drag option 6 of Table 2-6.

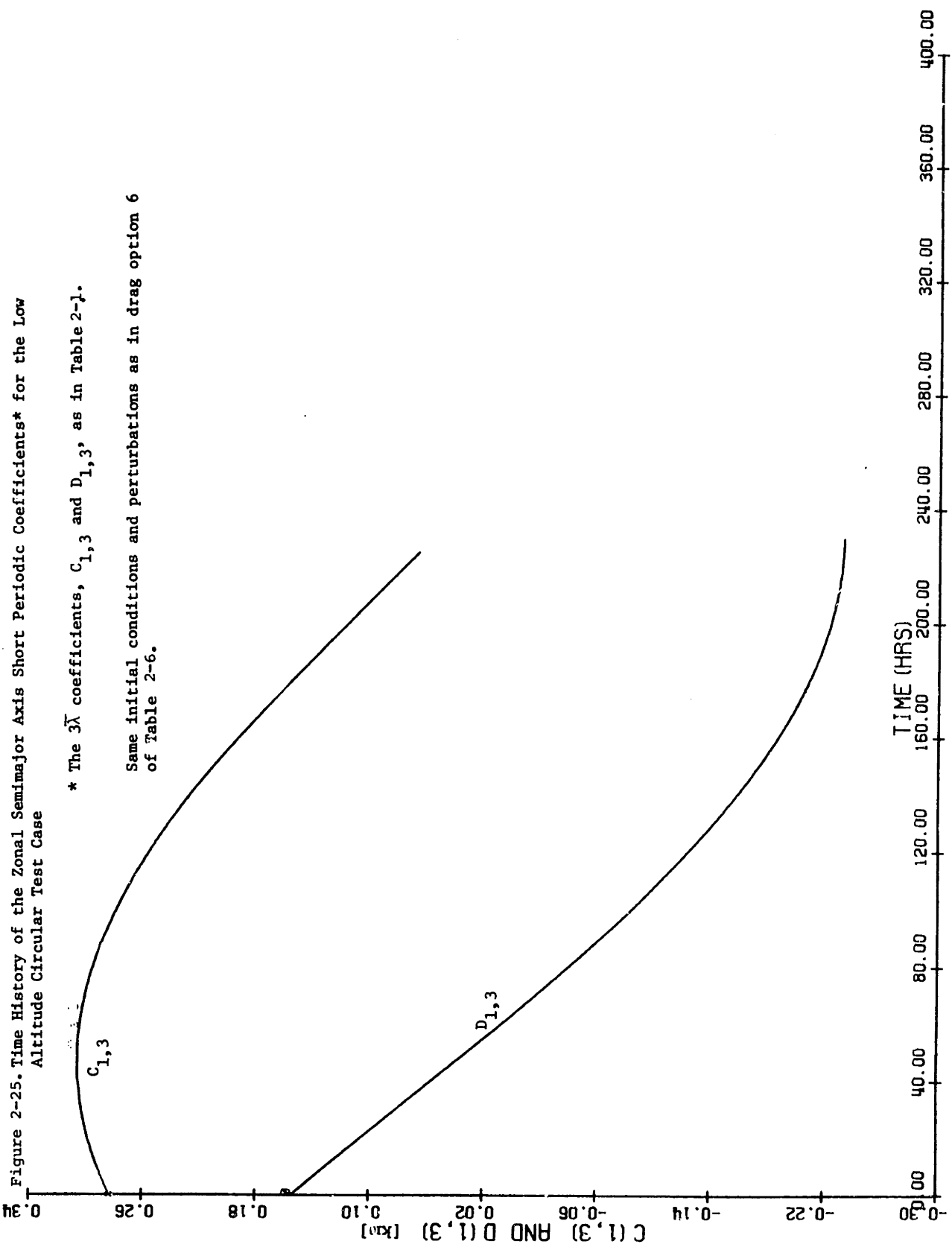


Figure 2-26. Time History of the Zonal h Short Periodic Coefficients* for the Low Altitude Circular Test Case

* The $2\bar{\lambda}$ coefficients, $C_{2,2}$ and $D_{2,2}$, as in Table 2-1.

Same initial conditions and perturbations as in drag option 6 of Table 2-6.

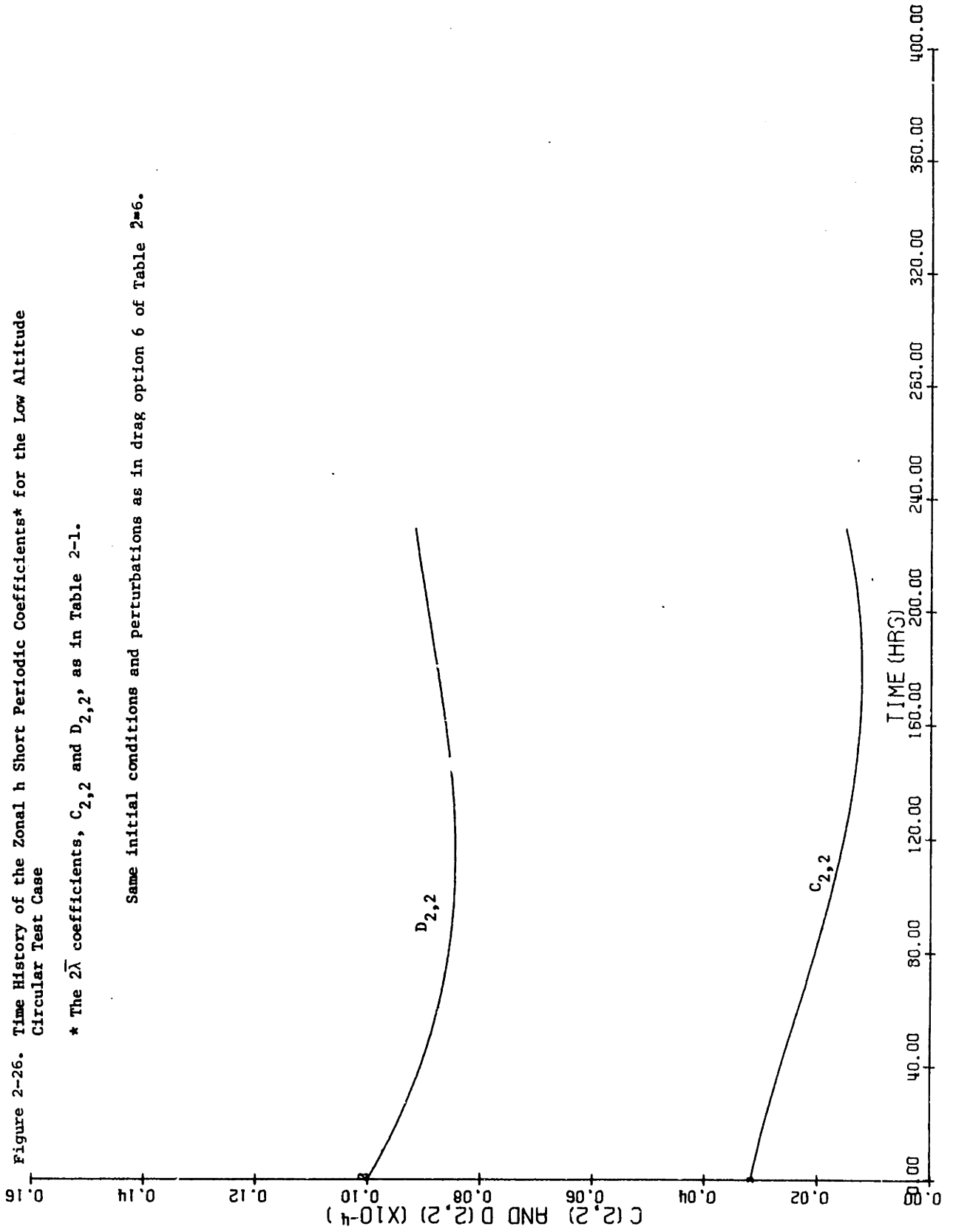


Figure 2-27. Time History of the Zonal h Short Periodic Coefficients* for the Low Altitude Circular Test Case

* The $3\bar{\lambda}$ coefficients, $C_{2,3}$ and $D_{2,3}$, as in Table 2-1.

Same initial conditions and perturbations as in drag portion 6 of Table 2-6.

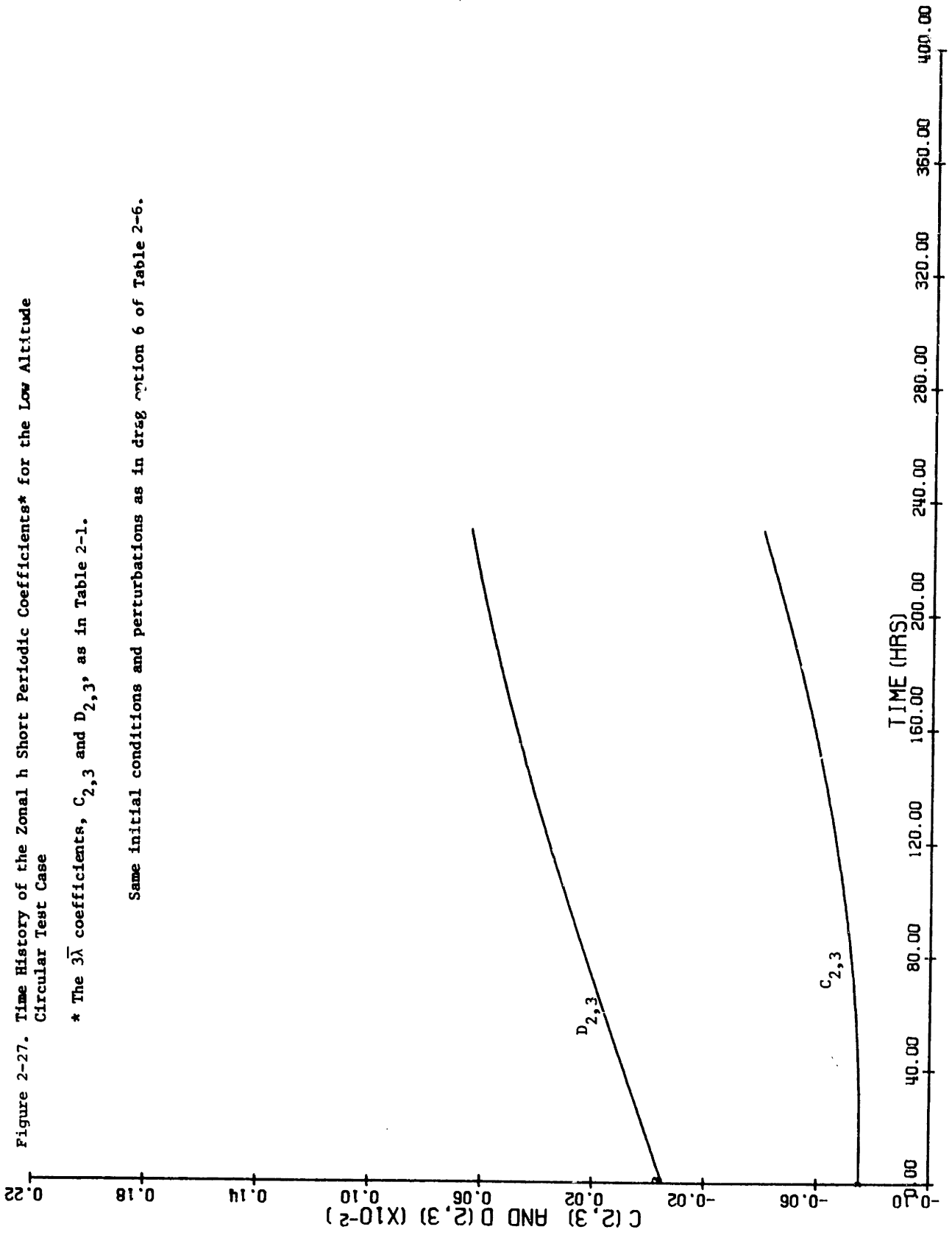


Figure 2-28. Time History of the Zonal k Short Periodic Coefficients* for the Low Altitude Circular Test Case

* The $\bar{1}\lambda$ coefficient, $C_{3,1}$ and $D_{3,1}$, as in Table 2-1.

Same initial conditions and perturbations as in drag option 6 of Table 2-6.

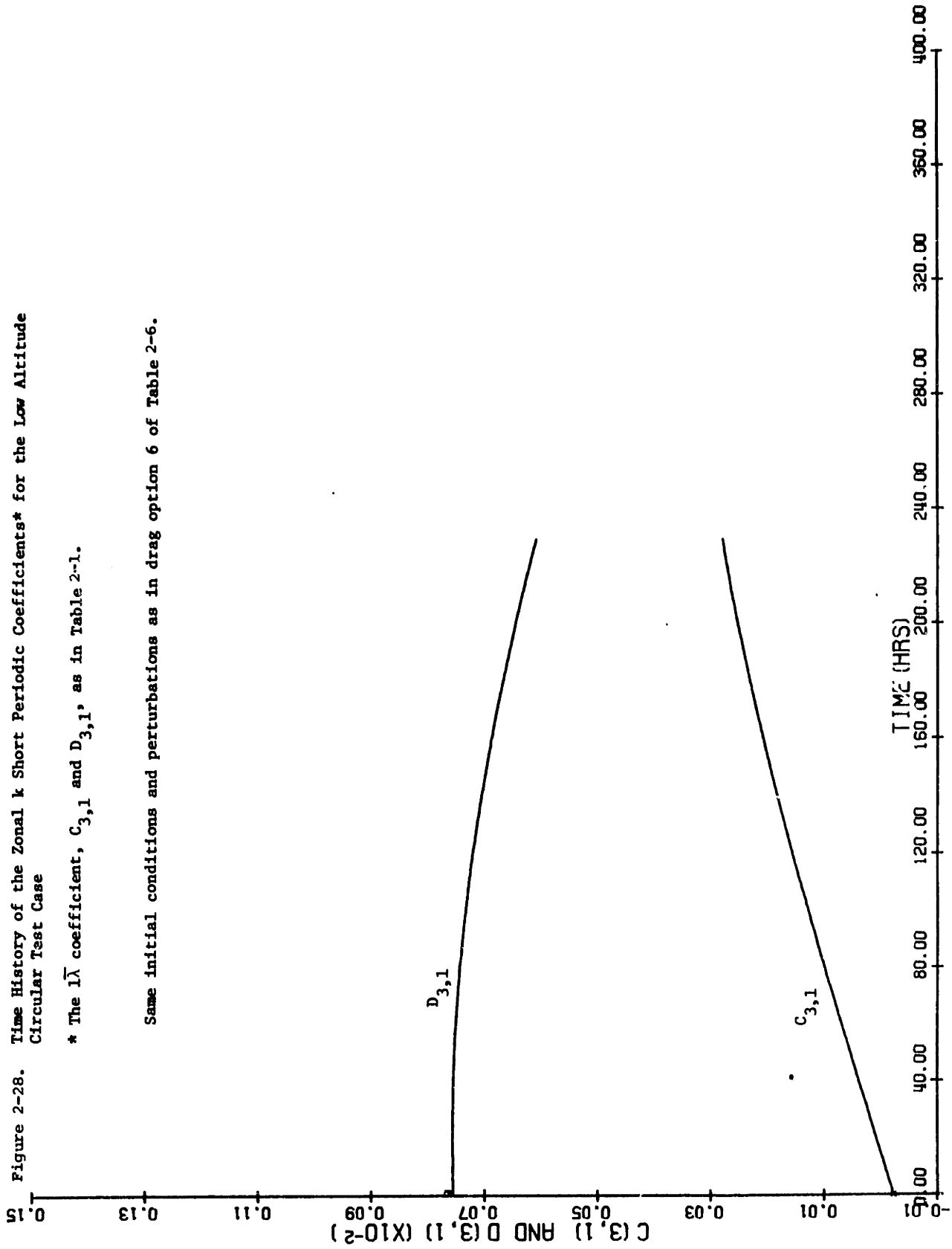


Figure 2-29. Time History of the Zonal λ Short Periodic Coefficients* for the Low Altitude Circular Test Case

* The $2\bar{\lambda}$ coefficients, $C_{6,2}$ and $D_{6,2}$, as in Table 2-1.

Same initial conditions and perturbations as in drag option 6 of Table 2-6.

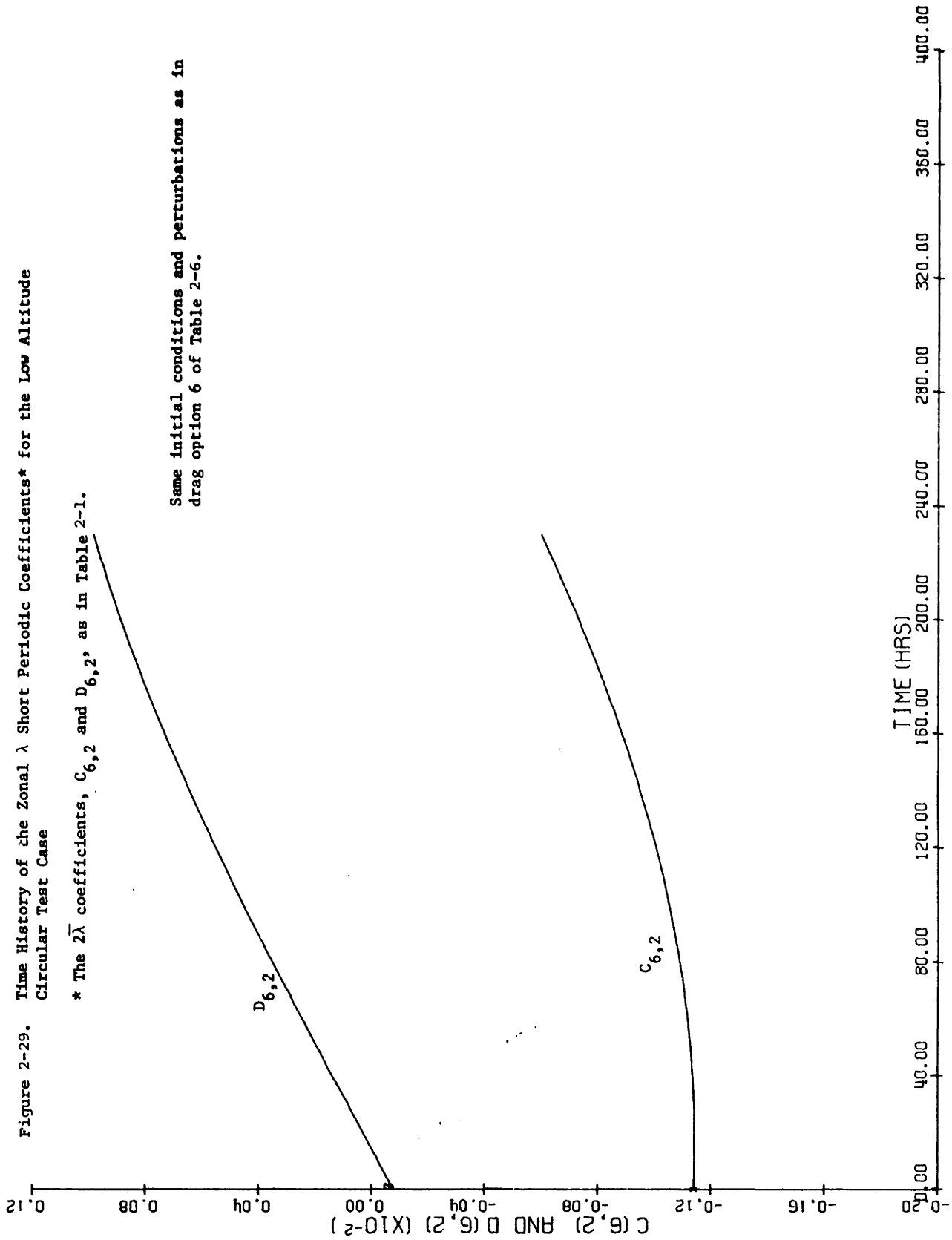


Figure 2-30. Time History of the Drag Semimajor Axis Short Periodic Coefficients* for the Low Altitude Circular Test Case

* The $\bar{I}\lambda$ coefficients, $C_{1,1}$ and $D_{1,1}$, as in Table 2-1.

Same initial conditions and perturbations as in drag option 6 of Table 2-6.

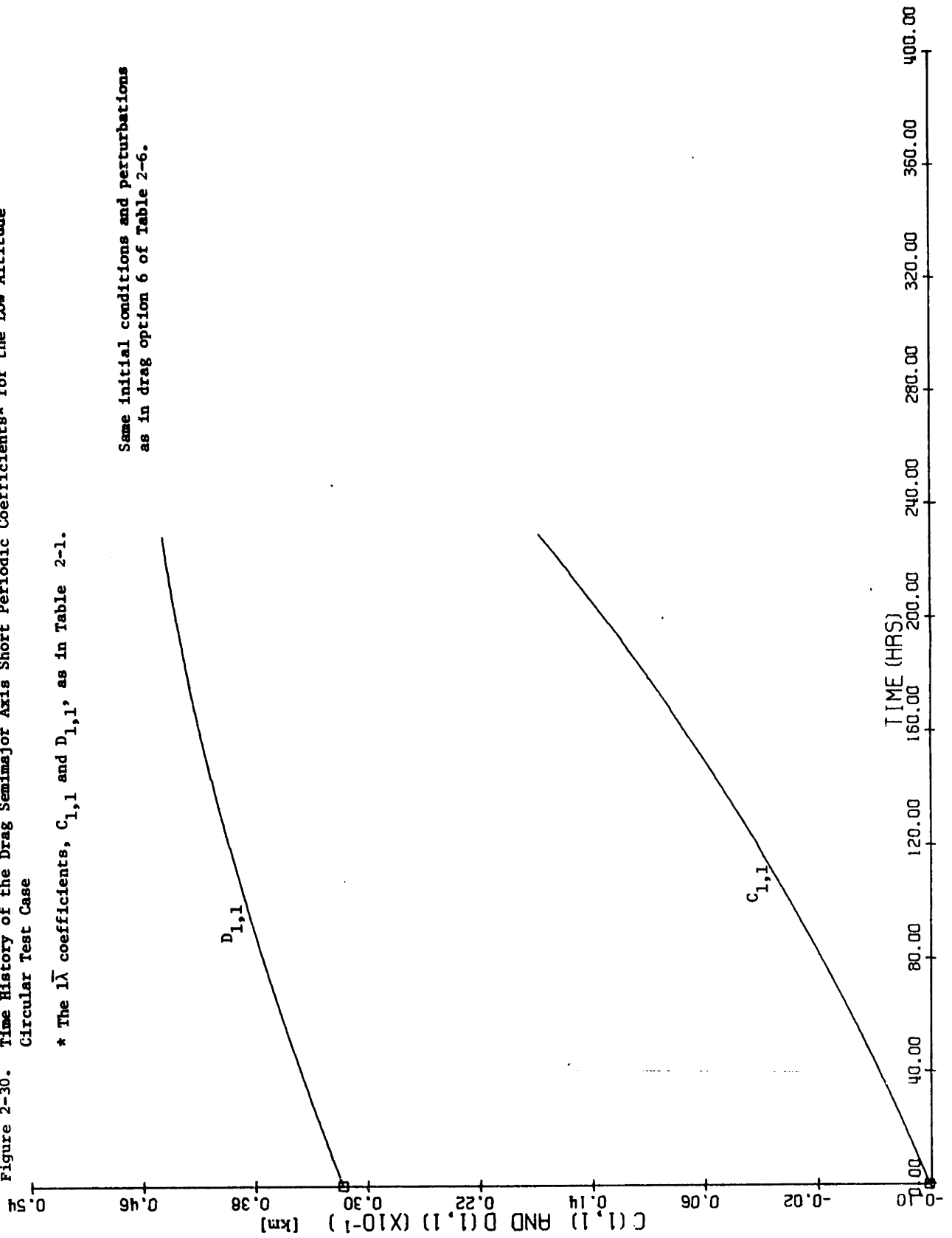


Figure 2-31. Time History of the Drag Semimajor Axis Short Periodic Coefficients* for the Low Altitude Circular Test Case

* The $4\bar{\lambda}$ coefficients, $C_{1,4}$ and $D_{1,4}$, as in Table 2-1.

Same initial conditions and perturbations as in drag option 6 of Table 2-6.

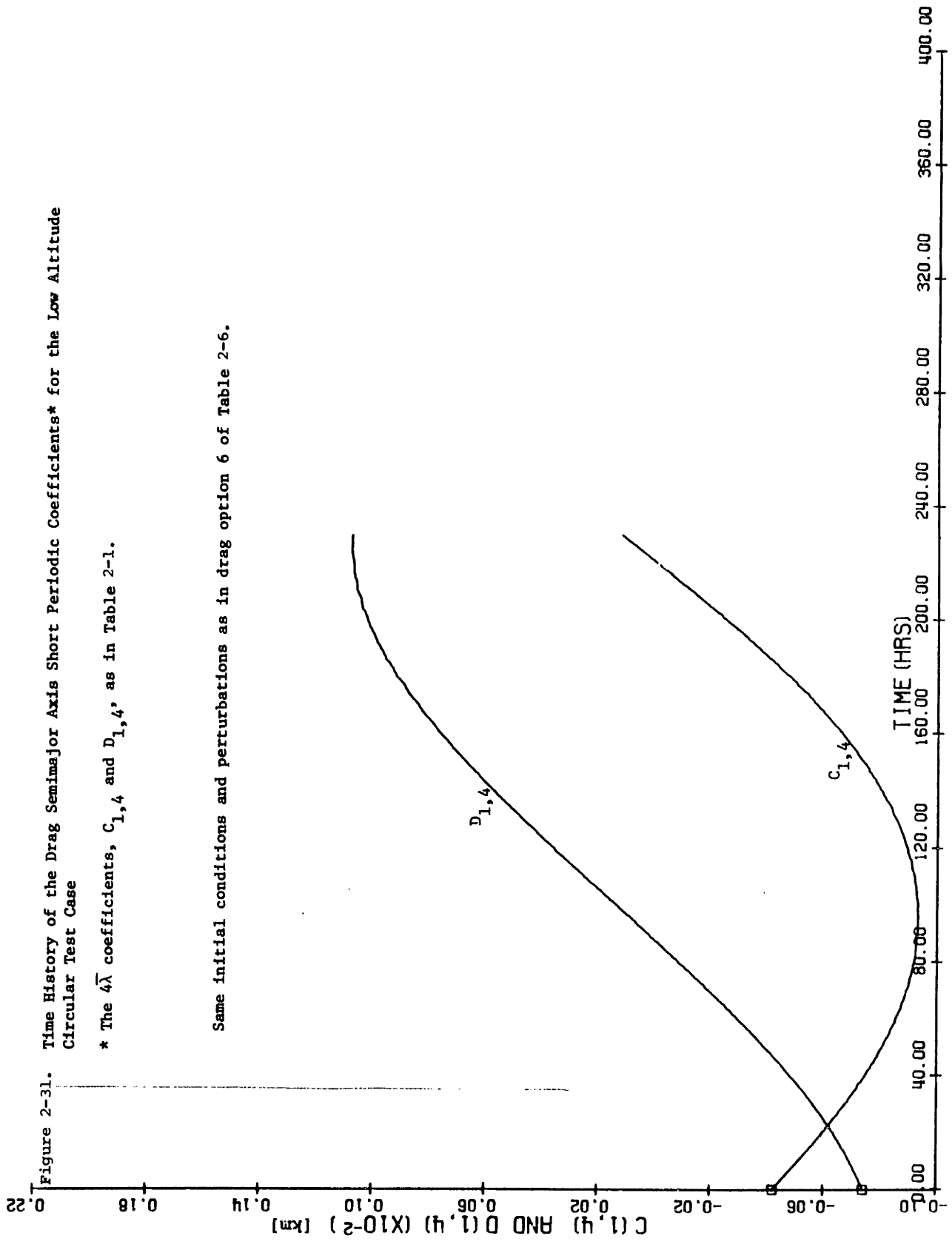


Figure 2-32. Time History of the Drag h Short Periodic Coefficients* for the Low Altitude Circular Test Case

* The $1\bar{\lambda}$ coefficients, $C_{2,1}$ and $D_{2,1}$, as in Table 2-1.

Same initial conditions and perturbations as in drag option 6 of Table 2-6.

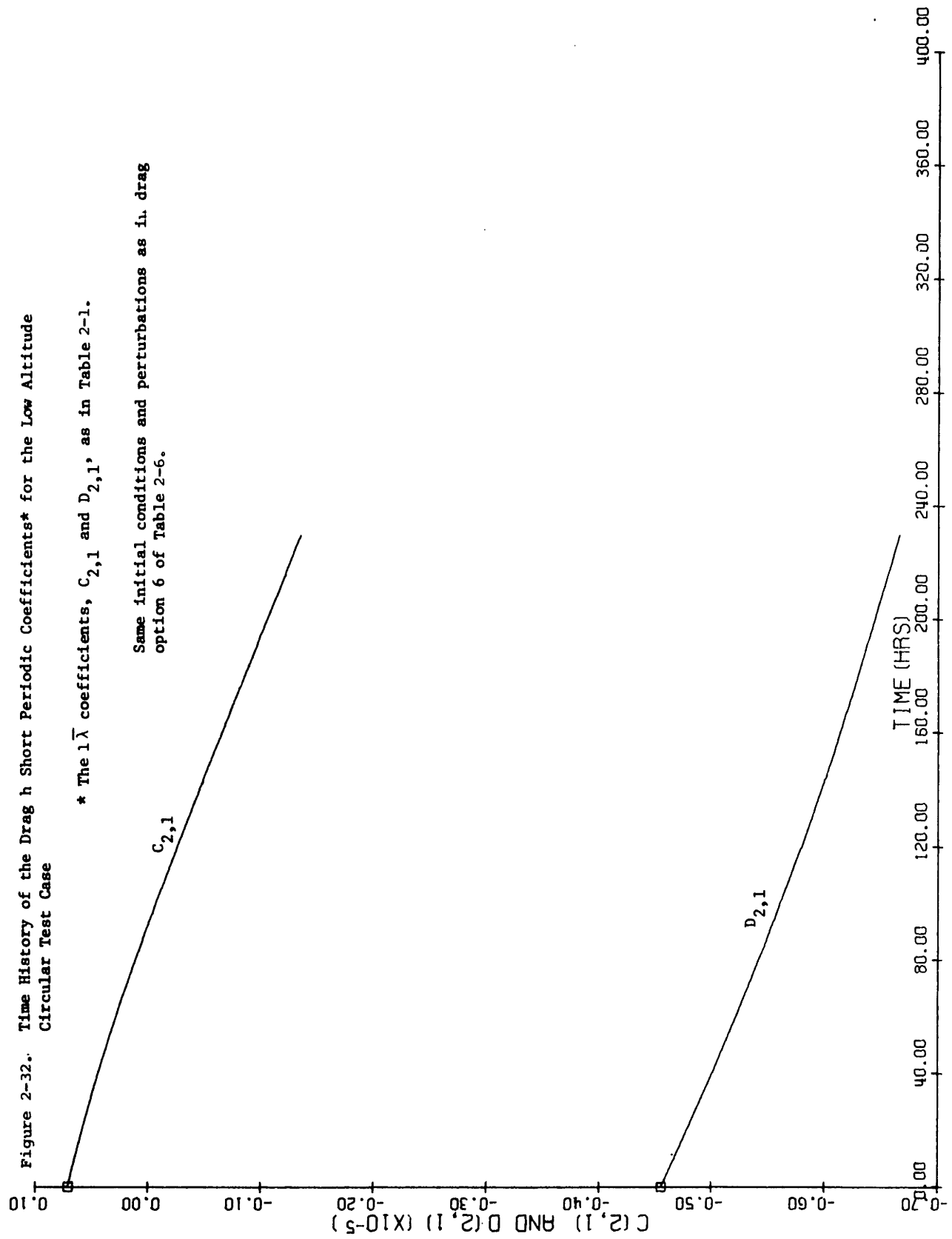


Figure 2-33. Time History of the Drag λ Short Periodic Coefficients* for the Low Altitude Circular Test Case

* The $\bar{\lambda}$ coefficients, $C_{6,1}$ and $D_{6,1}$, as in Table 2-1.

Same initial conditions and perturbations as in drag option 6 of Table 2-6.

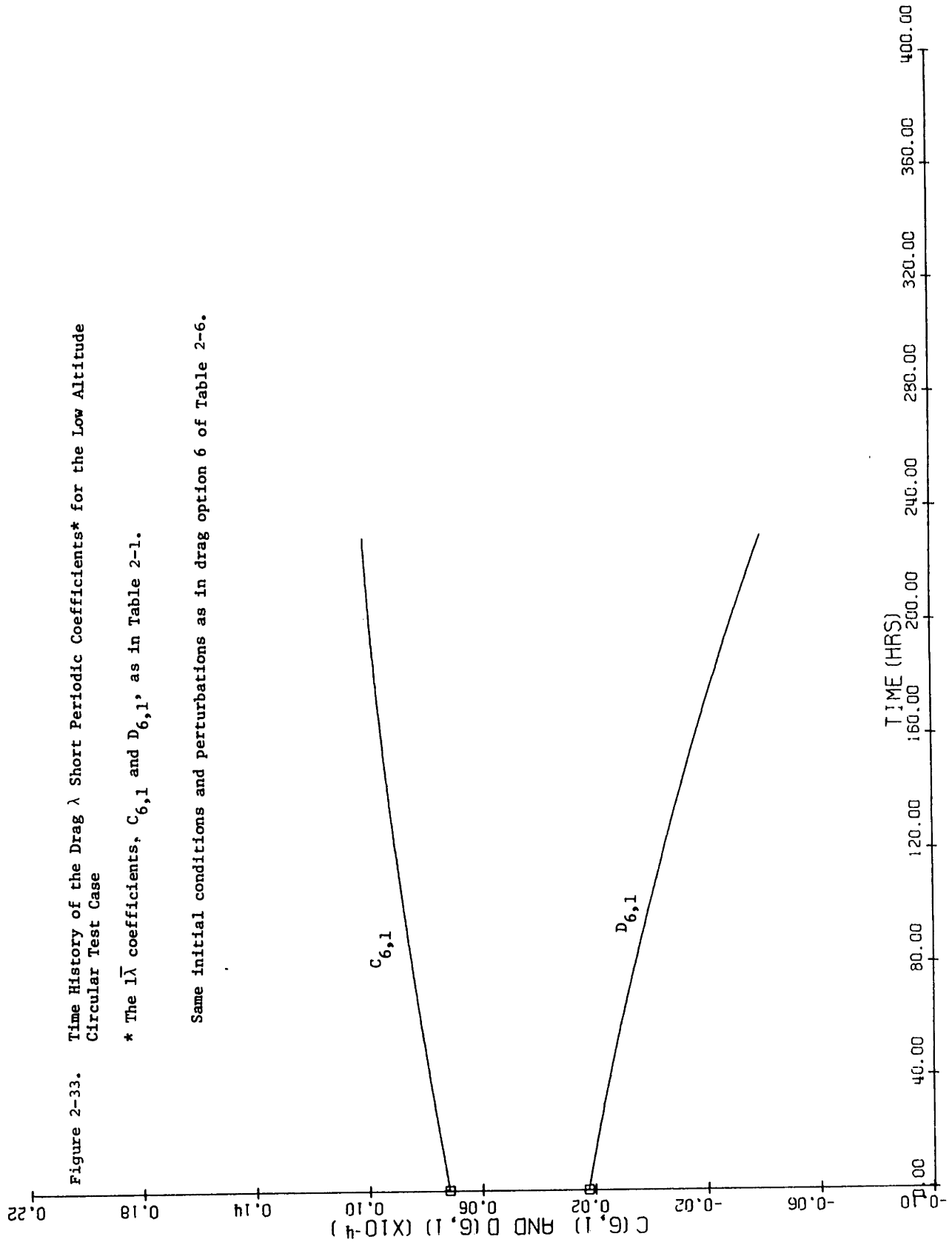
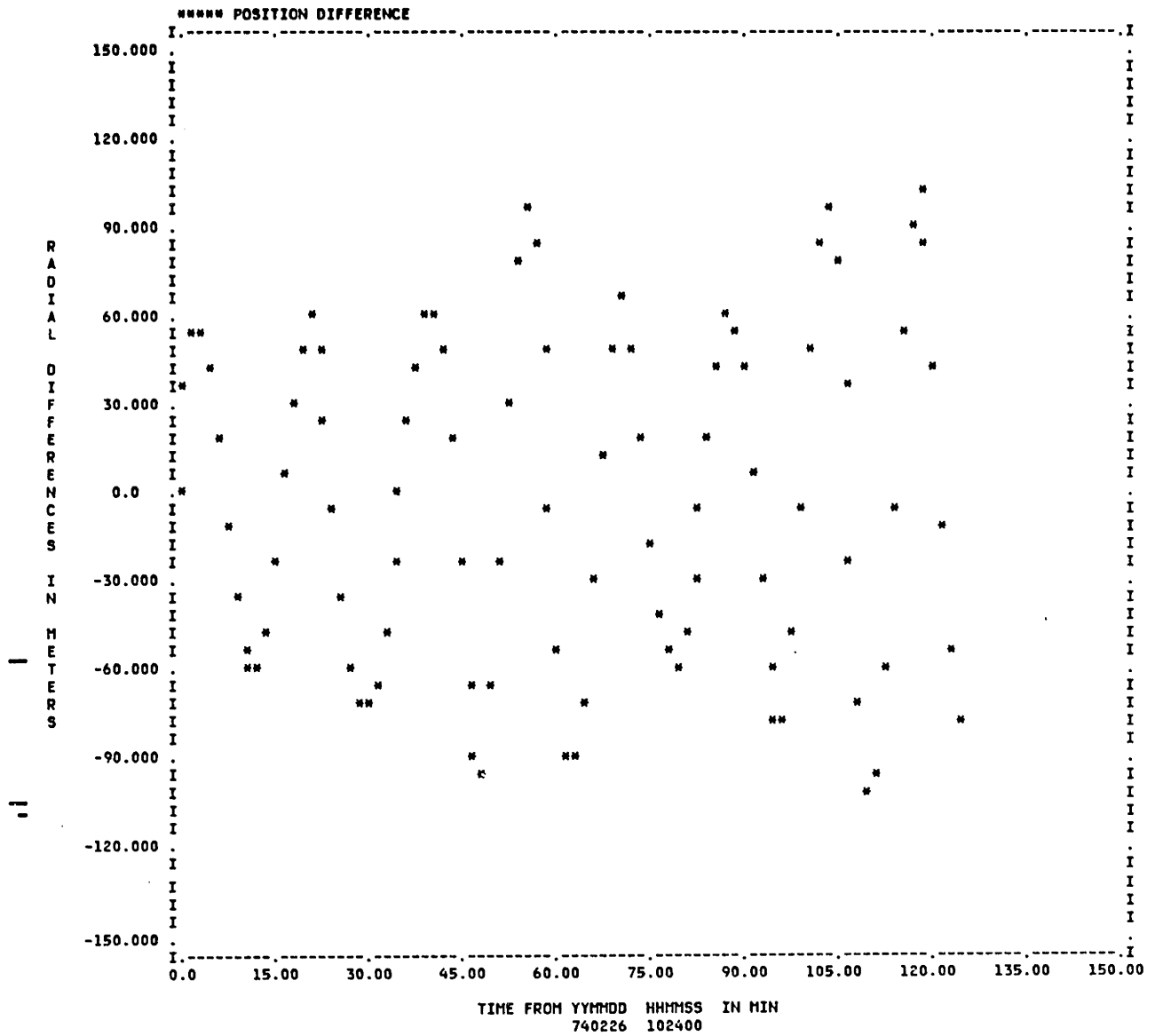
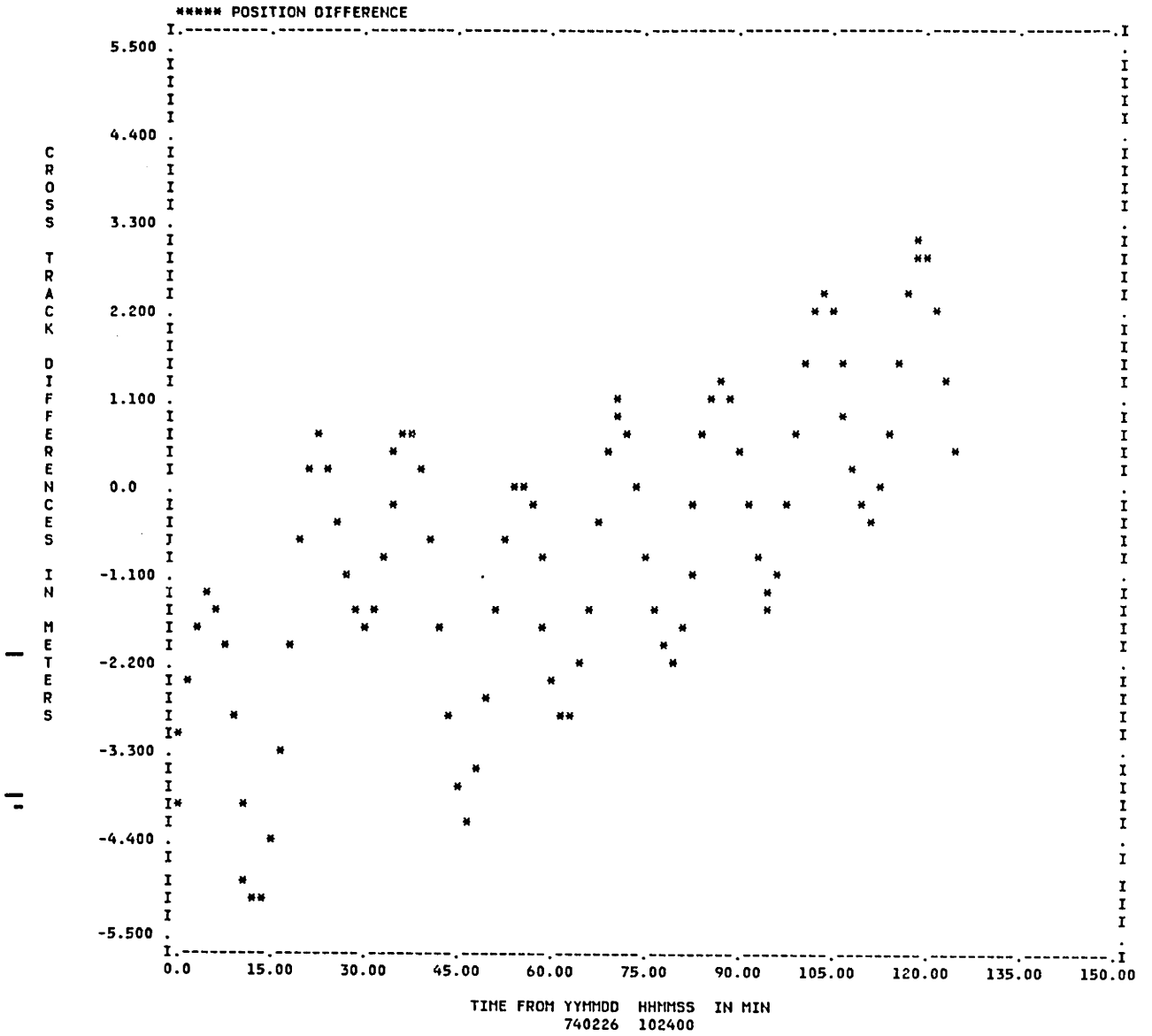


Figure 2-34. Radial Difference/Semianalytical minus Cowell for the Low Altitude Eccentric Test Case



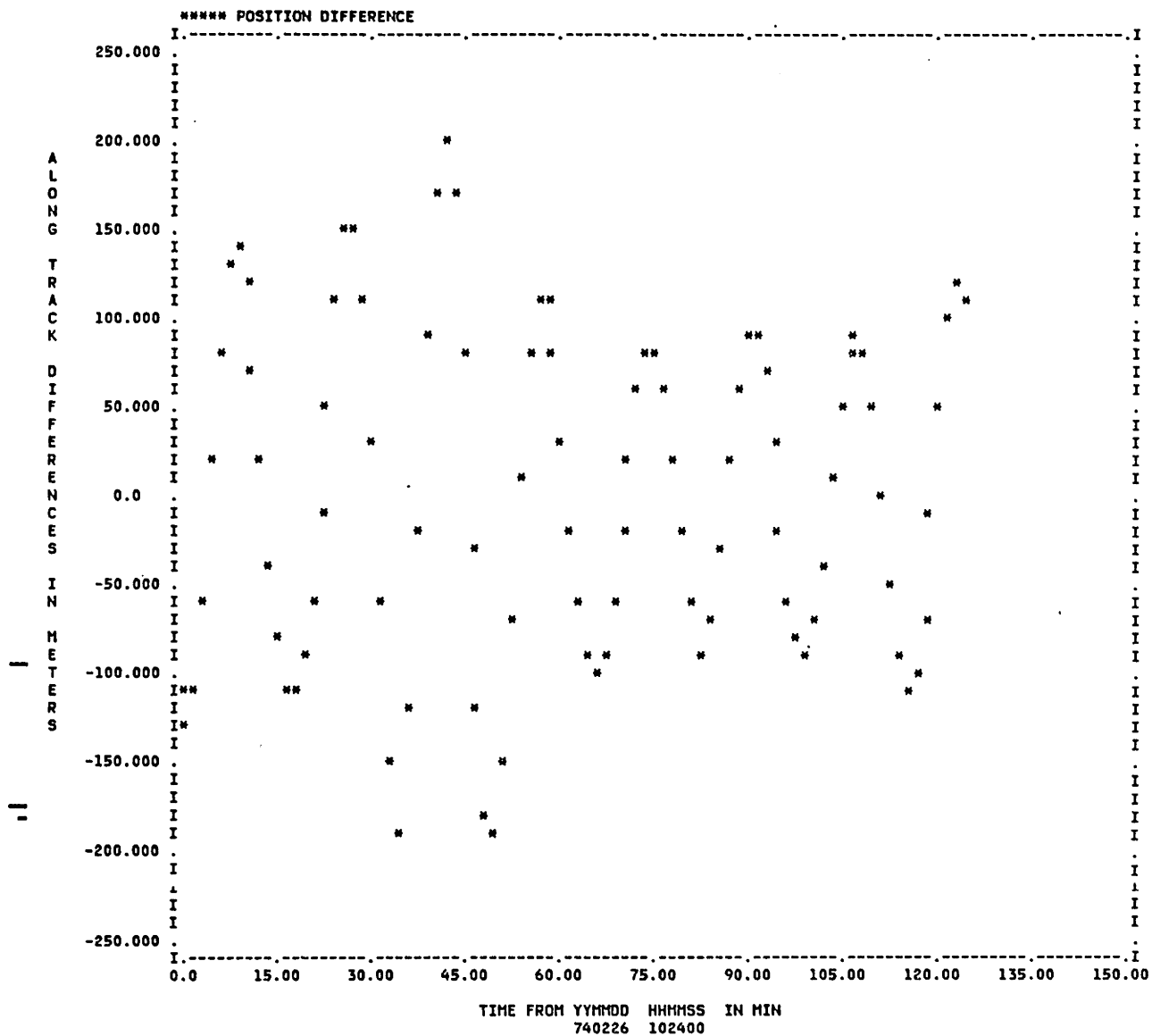
Initial conditions and perturbations as in Table 2-9.

Figure 2-35. Cross Track Difference/Semianalytical minus Cowell for the Low Altitude Eccentric Test Case



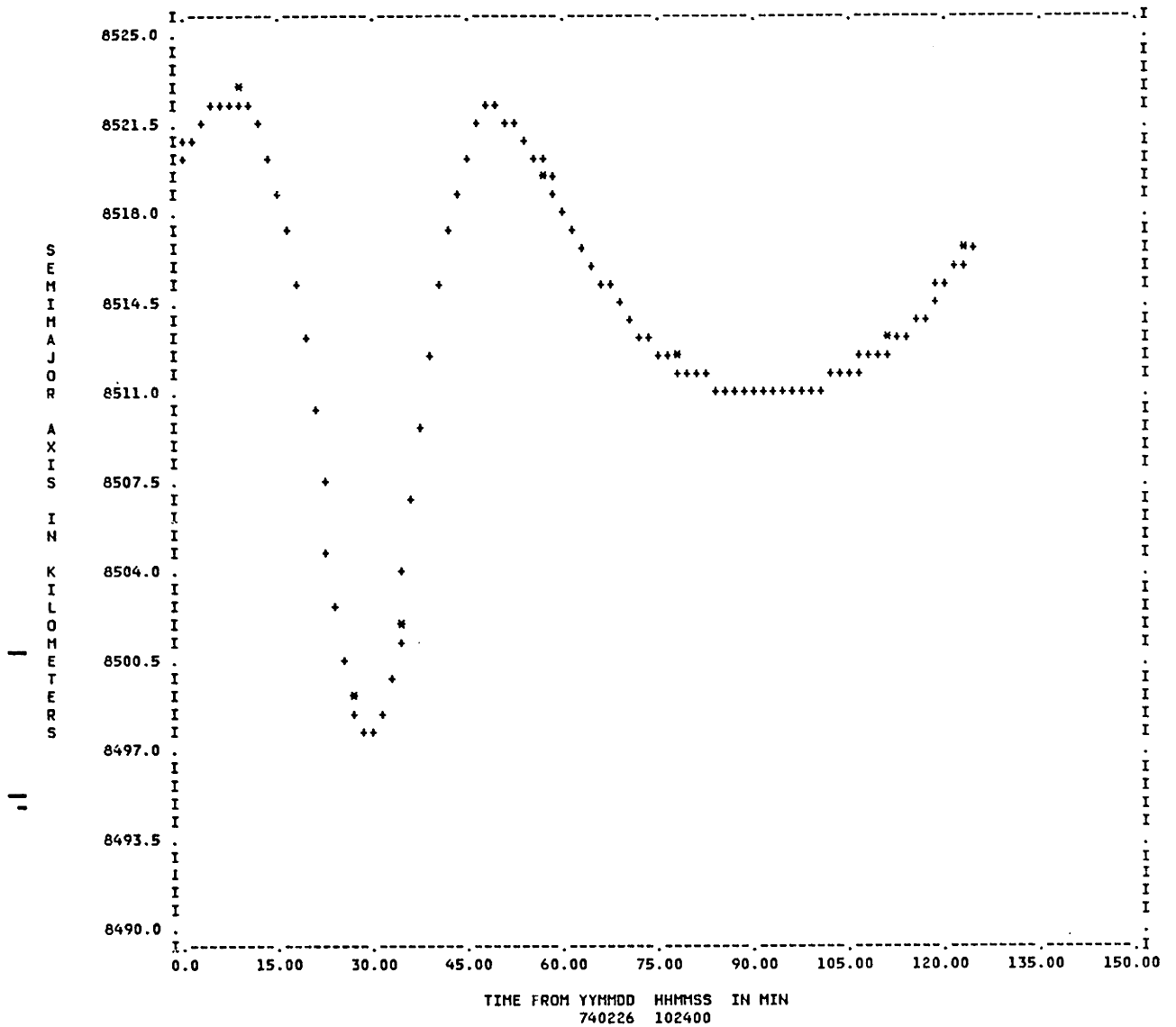
Initial conditions and perturbations as in Table 2-9.

Figure 2-36. Along Track Difference/Semianalytical minus Cowell for the Low Altitude Eccentric Test Case



Initial conditions and perturbations as in Table 2-9.

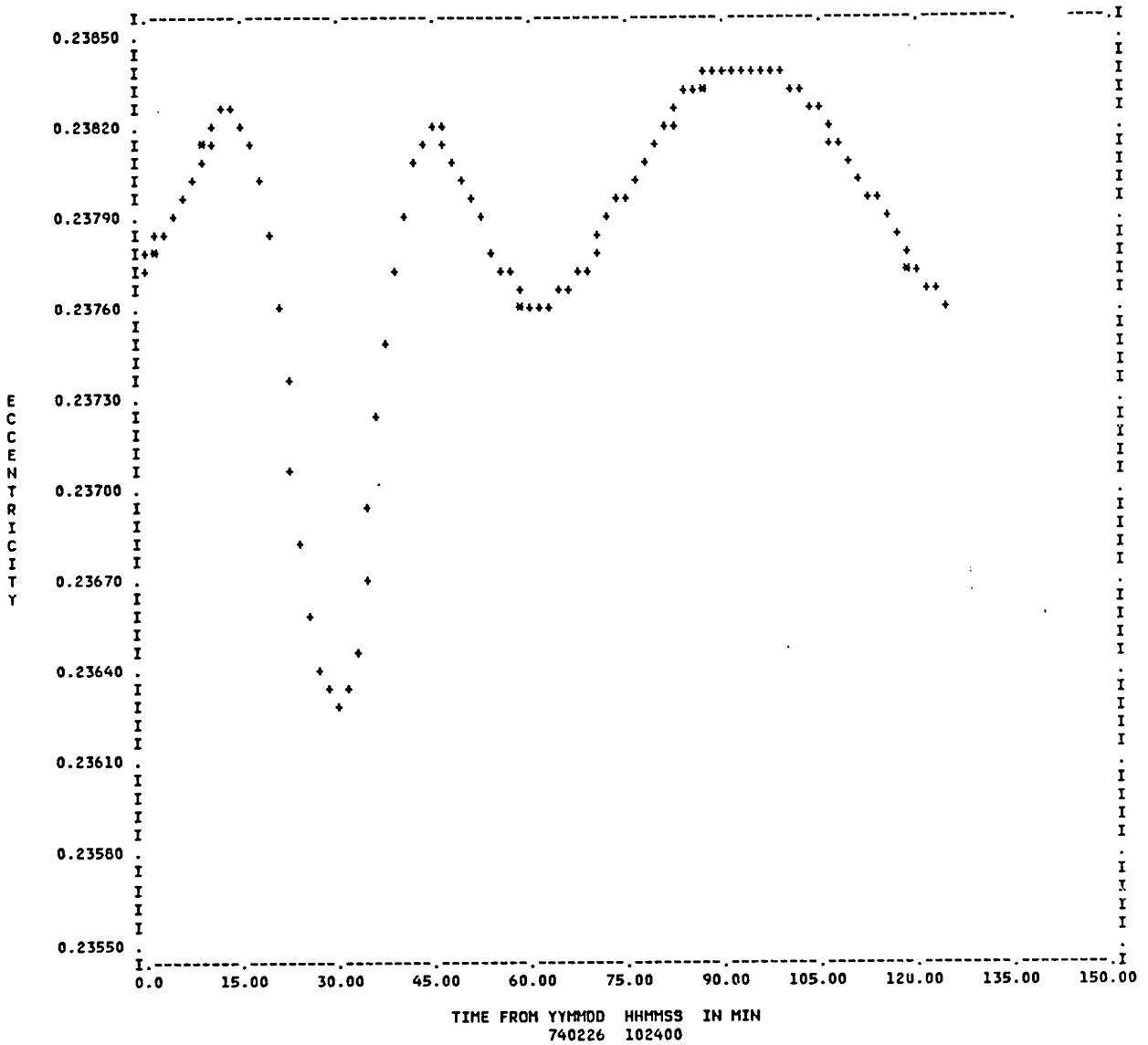
Figure 2-37. Osculating Semimajor Axis Comparison/Semianalytical versus Cowell for the Low Altitude Eccentric Test Case



***** ELEMENTS FROM ORB1 FILE ON UNIT 24, DATA RECORDS START AT 740226 102400 : Cowell
 ++++++ ELEMENTS FROM ORB1 FILE ON UNIT 81, DATA RECORDS START AT 740226 102400 : AOG and SPG

Initial conditions and perturbations as in Table 2-9.

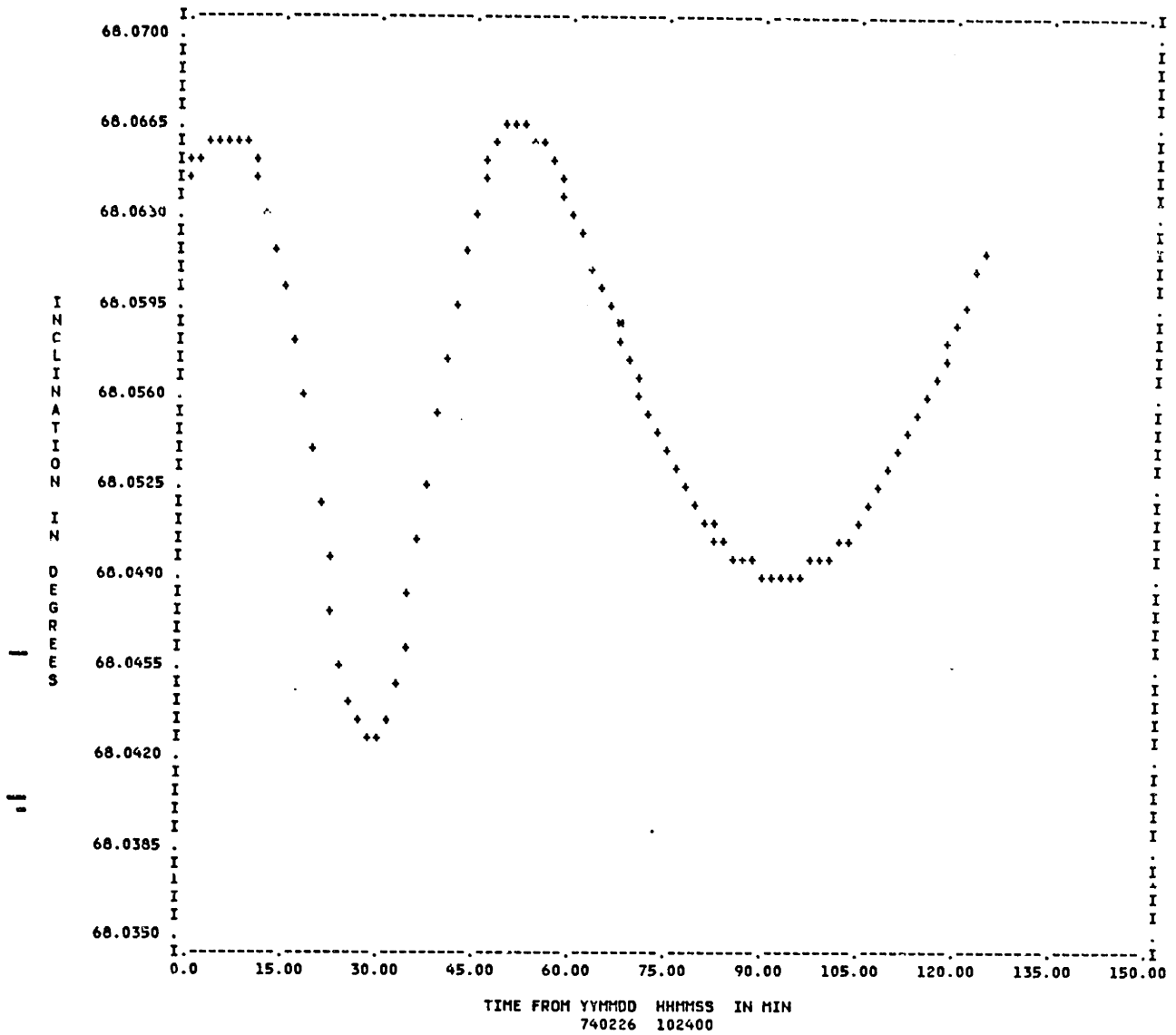
Figure 2-38. Osculating Eccentricity Comparison/Semianalytical versus Cowell for the Low Altitude Eccentric Test Case



***** ELEMENTS FROM ORB1 FILE ON UNIT 24, DATA RECORDS START AT 740226 102400: Cowell
 ++++++ ELEMENTS FROM ORB1 FILE ON UNIT 81, DATA RECORDS START AT 740226 102400: AOG and SPG

Initial conditions and perturbations as in Table 2-9.

Figure 2-39. Osculating Inclination Comparison/Semianalytical versus Cowell for the Low Altitude Eccentric Test Case

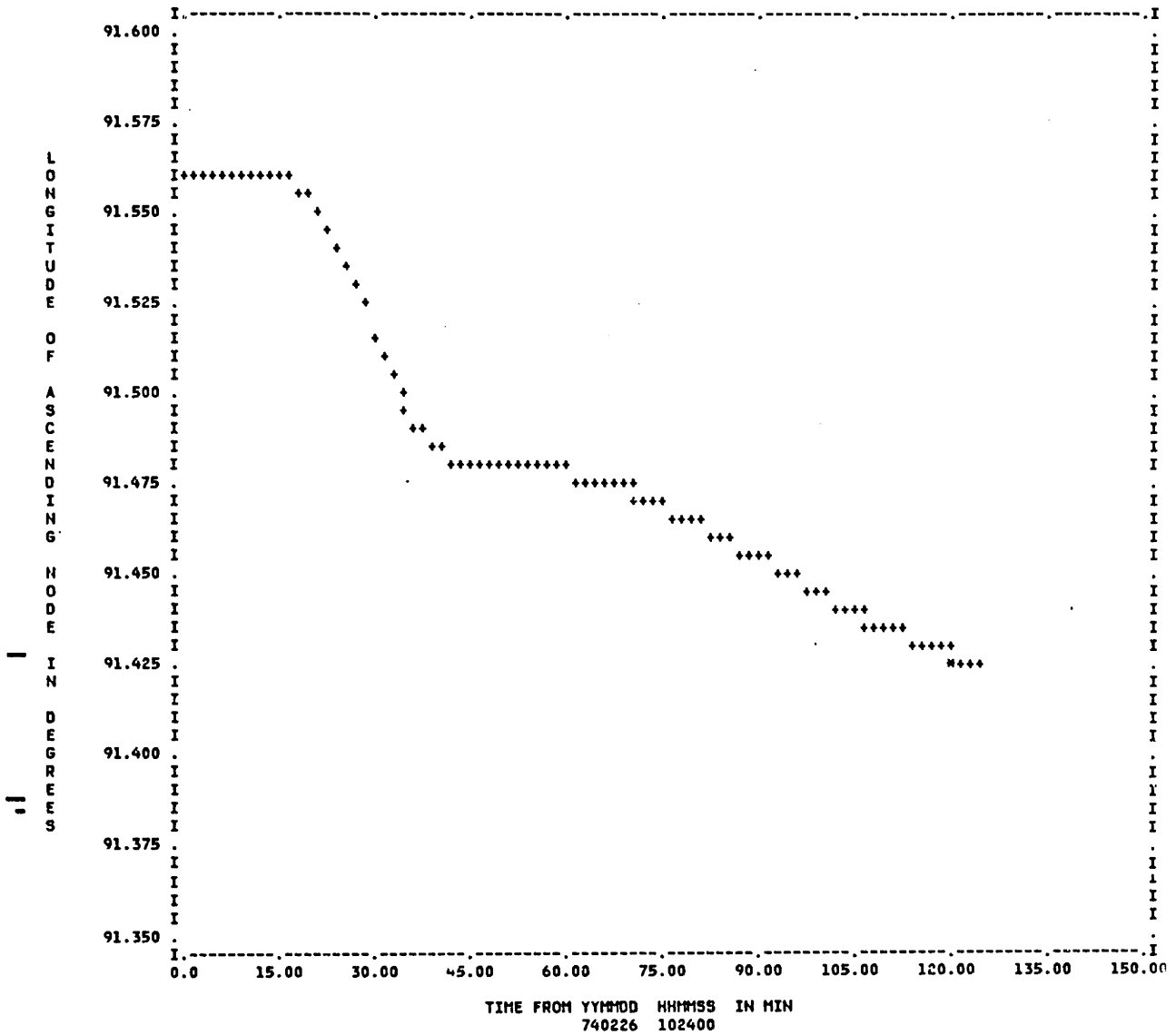


***** ELEMENTS FROM ORB1 FILE ON UNIT 24, DATA RECORDS START AT 740226 102400 : Cowell

+++++ ELEMENTS FROM ORB1 FILE ON UNIT 81, DATA RECORDS START AT 740226 102400 : AOG and SPG

Initial conditions and perturbations as in Table 2-9.

Figure 2-40. Osculating Ω Comparison/Semianalytical versus Cowell for the Low Altitude Eccentric Test Case

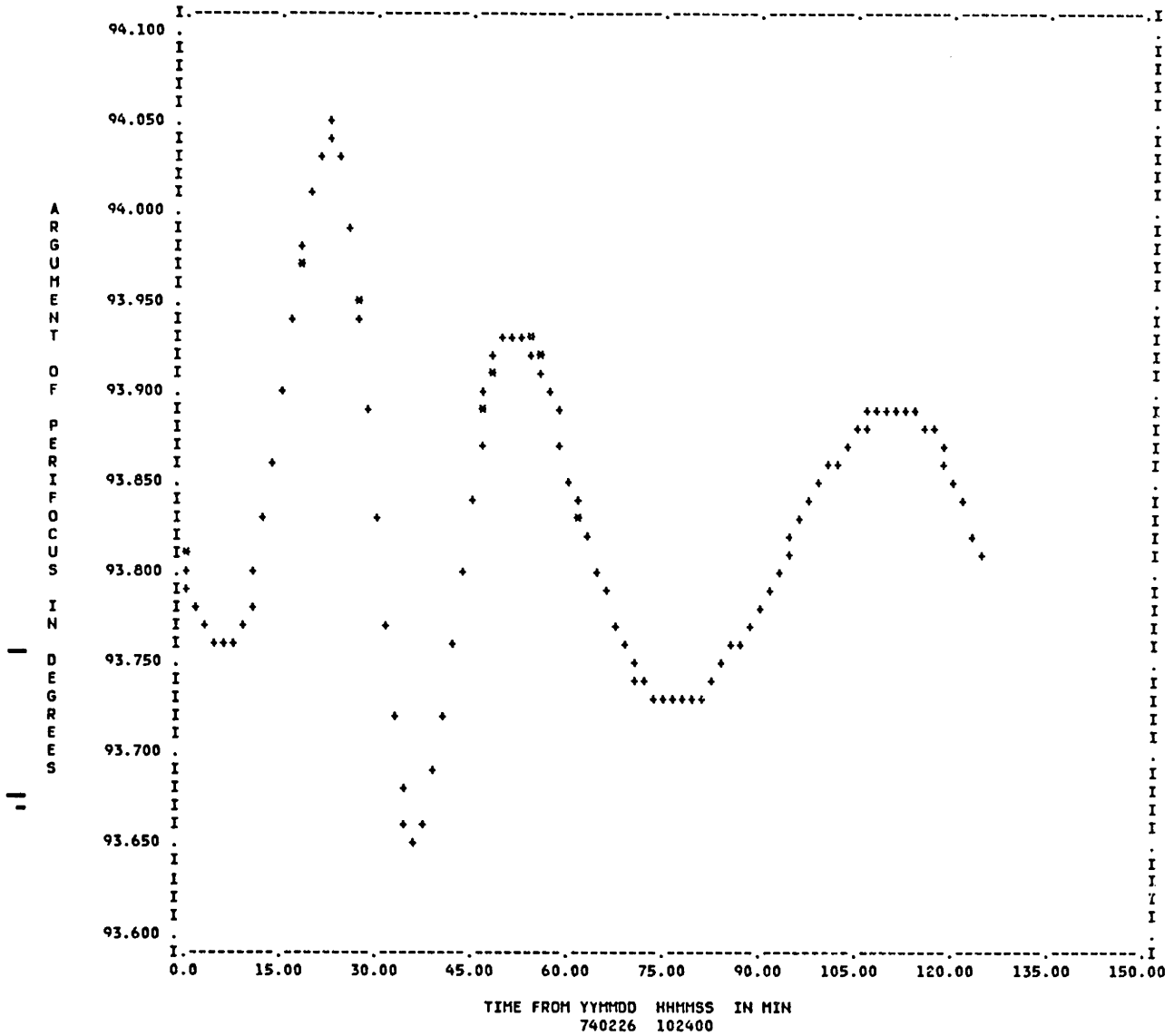


***** ELEMENTS FROM ORB1 FILE ON UNIT 24, DATA RECORDS START AT 740226 102400: Cowell

+++++ ELEMENTS FROM ORB1 FILE ON UNIT 81, DATA RECORDS START AT 740226 102400: AOG and SPG

Initial conditions and perturbations as in Table 2-9.

Figure 2-41. Osculating ω Comparison/Semianalytical versus Cowell for the Low Altitude Eccentric Test Case

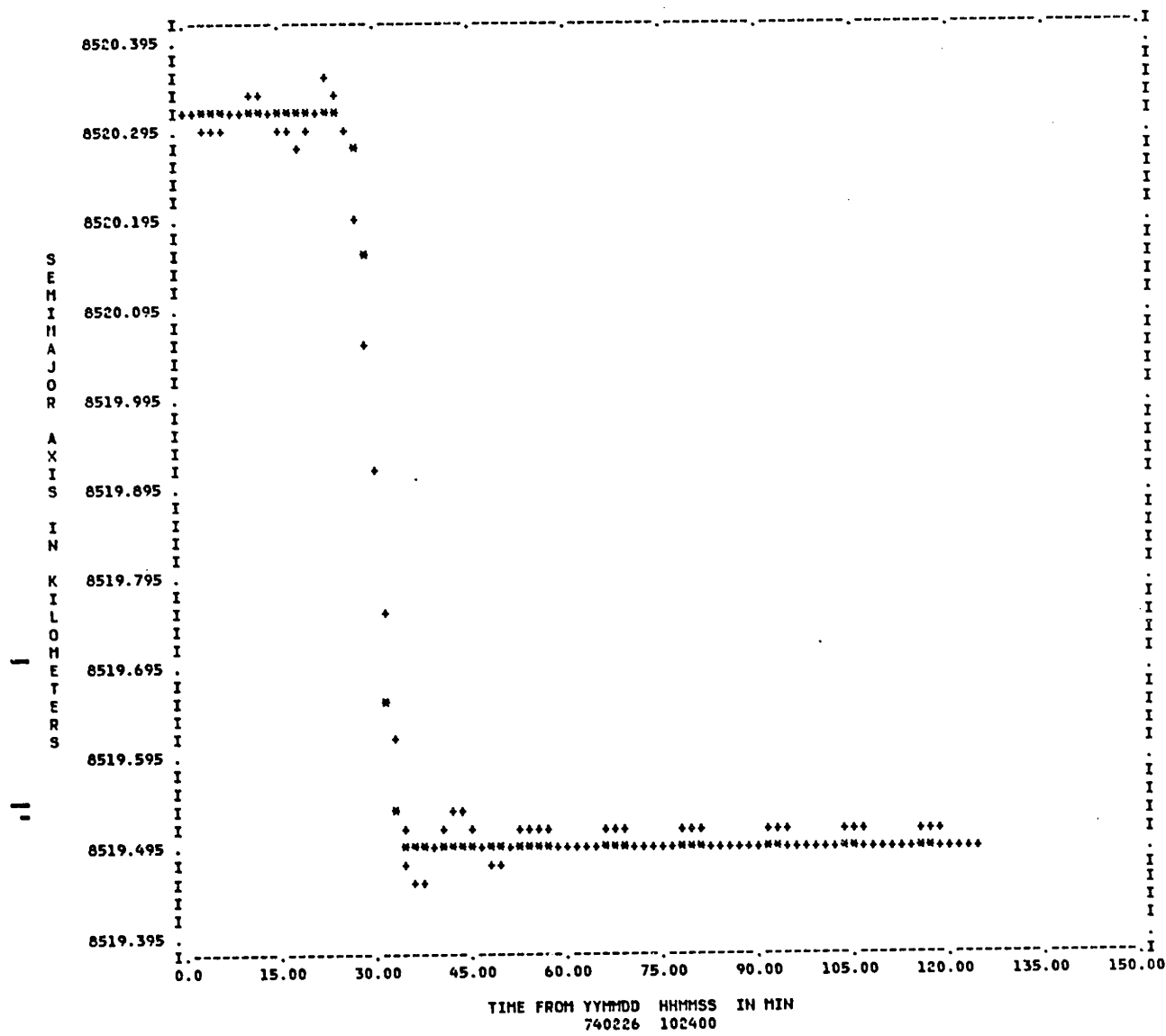


***** ELEMENTS FROM ORB1 FILE ON UNIT 24, DATA RECORDS START AT 740226 102400 : Cowell

+++++ ELEMENTS FROM ORB1 FILE ON UNIT 81, DATA RECORDS START AT 740226 102400 : AOG and SPG

Initial conditions and perturbations as in Table 2-9.

Figure 2-42. Osculating Semimajor Axis Comparison/Semianalytical versus Cowell for the Low Altitude Eccentric Test Case



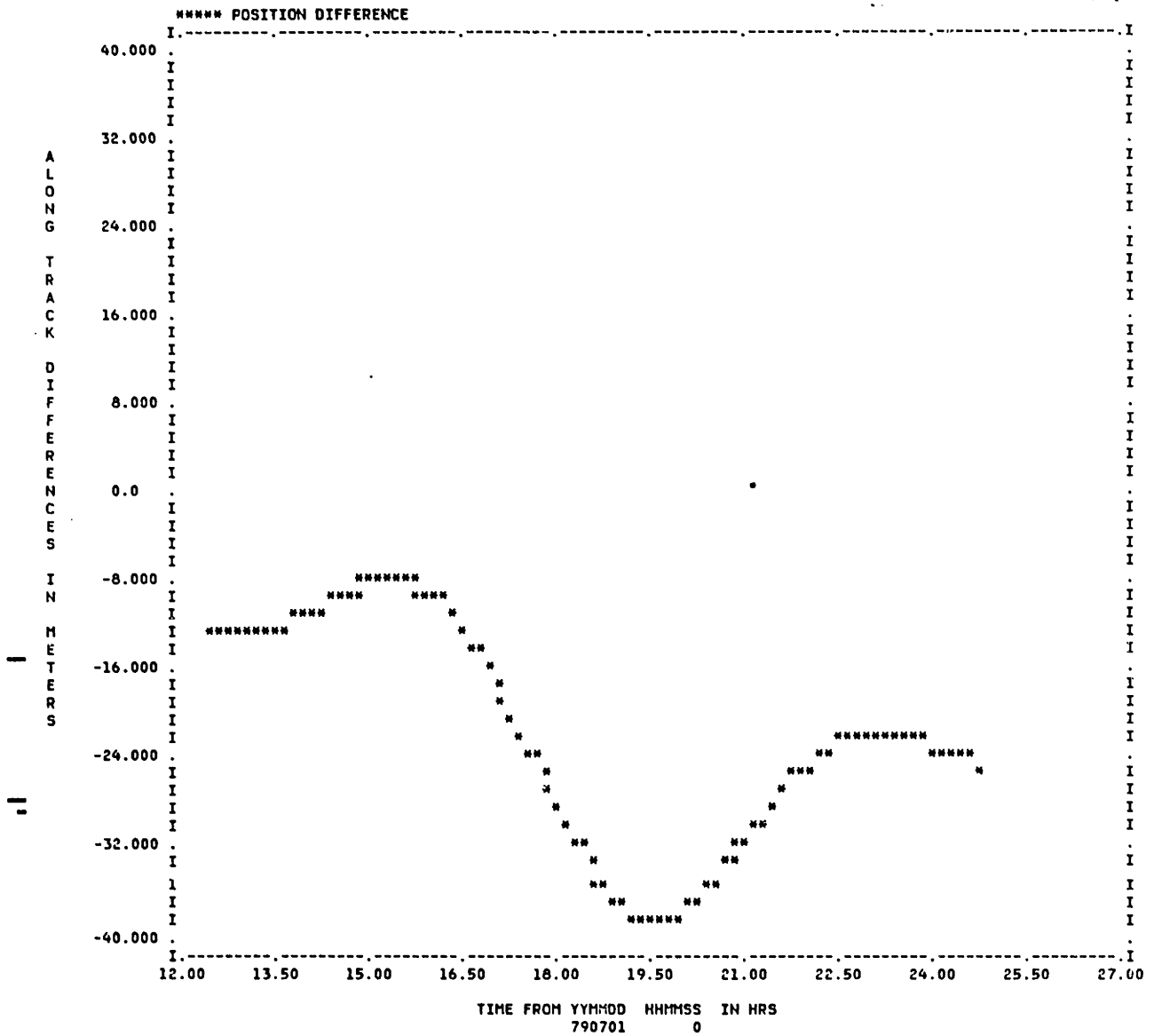
***** ELEMENTS FROM ORB1 FILE ON UNIT 24, DATA RECORDS START AT 740226 102400 : Cowell
 ++++++ ELEMENTS FROM ORB1 FILE ON UNIT 81, DATA RECORDS START AT 740226 102400 : AOG and SPG

Perturbations

- Cowell: drag only (10 sec numerical integration time step)
- AOG: drag only, option 1 (48 pt quadrature)
1 day numerical integration time step
- SPG: 1st order drag only (10/48), time-independent formulation

Initial conditions: NOM

Figure 2-43. Along Track Difference after 12 hours from Epoch/Semianalytical* minus Cowell for the Medium Altitude Circular Test Case



* Weak Time-Dependent corrections were not used.

Perturbations:

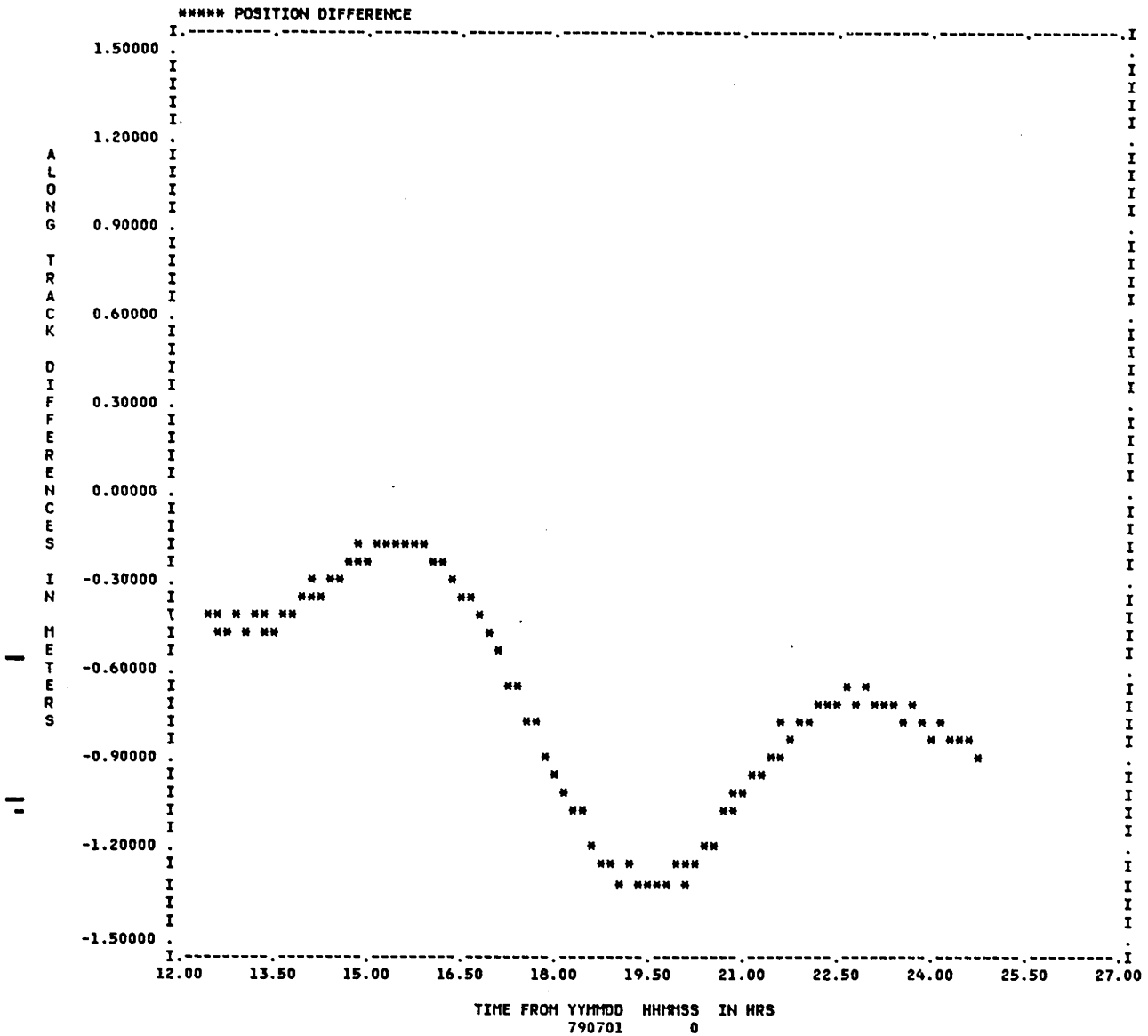
Cowell: 6x0 gravitational field, lunar-solar, solar radiation pressure: 300 sec integration time step

AOG: 1st order analytical expressions for 6x0 gravitational field and lunar-solar point mass effects, Zeis' J_2^2 expressions, numerical solar radiation pressure effects (48 pt quadrature): 1 day integration time steps

SPG: 1st order time-independent model for 6x0 gravitational field (7/48), lunar-solar effects (7/48), solar radiation pressure effects (4/48), Zeis' J_2^2 expressions.

Initial Conditions: $[EPC]^{-1}$ (see Table 2-11)

Figure 2-44. Along Track Difference after 12 hours from Epoch/Semianalytical minus Cowell for the Medium Altitude Circular Test Case

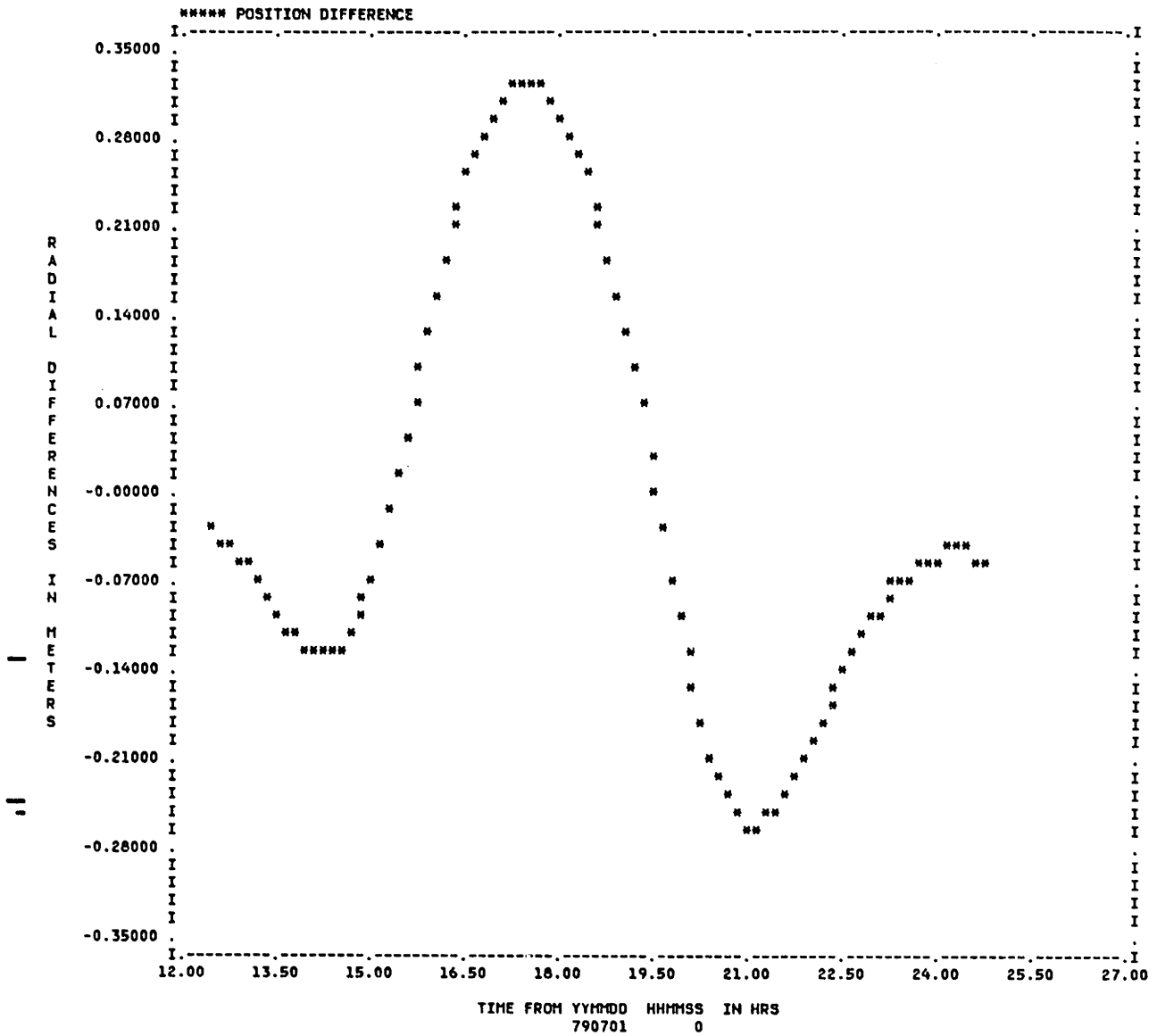


Perturbations:

- Cowell: 6x0 gravitational field, lunar-solar, solar radiation pressure: 300 sec. integration time step
- AOG: 1st order analytical expressions for 6x0 gravitational field and lunar-solar point mass effects, Zeis' J_2^2 expressions, numerical solar radiation pressure effects (48 pt quadrature order): 1 day integration time step
- SPG: 1st order weak time-dependent model for 6x0 gravitational field (7/48), lunar-solar effects (7/48), solar radiation pressure effects (4/48), Zeis' J_2^2 expressions.

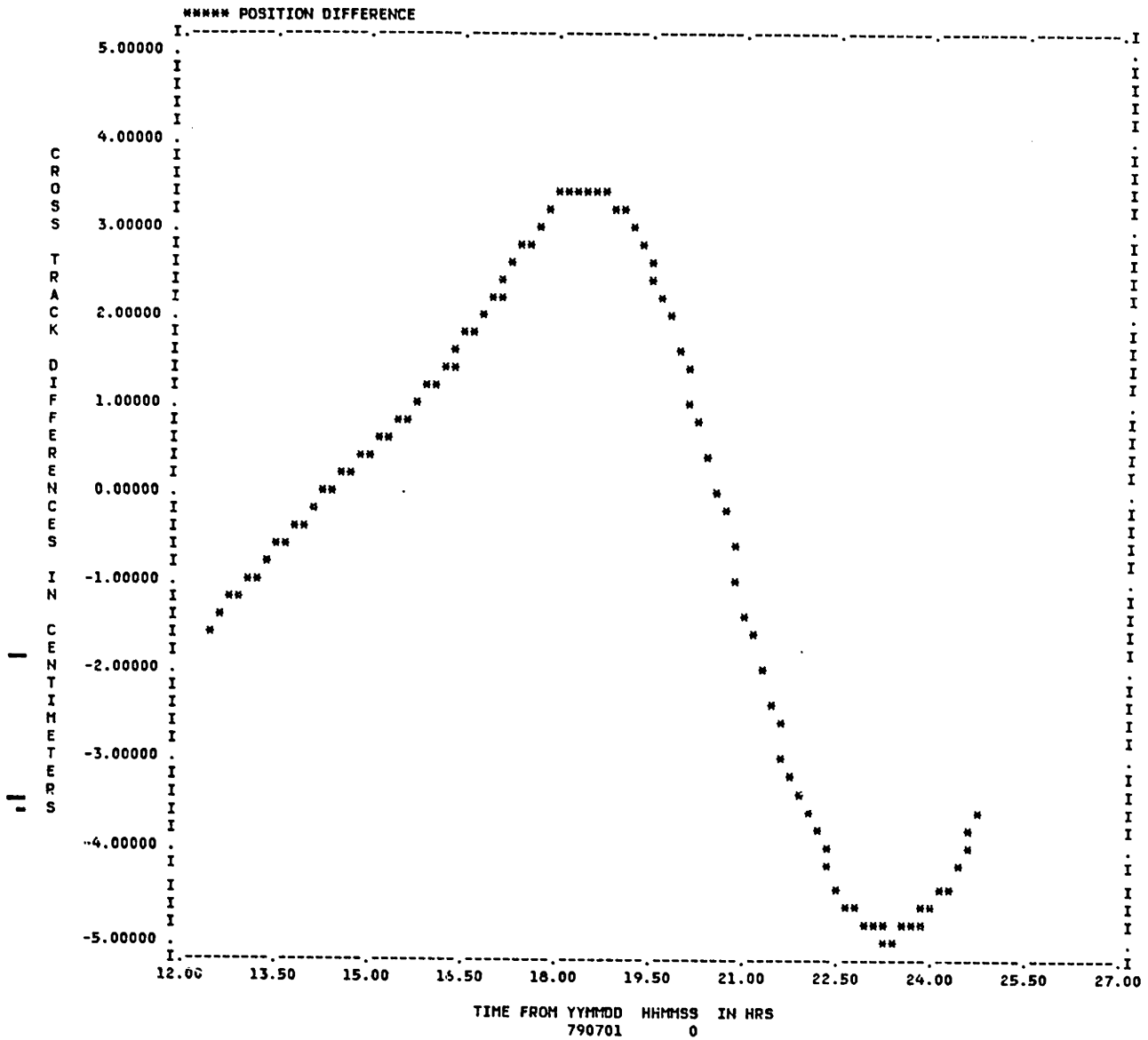
Initial Conditions: $[EPC]^{-1}$ (see Table 2-11)

Figure 2-45. Radial Difference after 12 hours from Epoch/Semianalytical minus Cowell for the Medium Altitude Circular Test Case



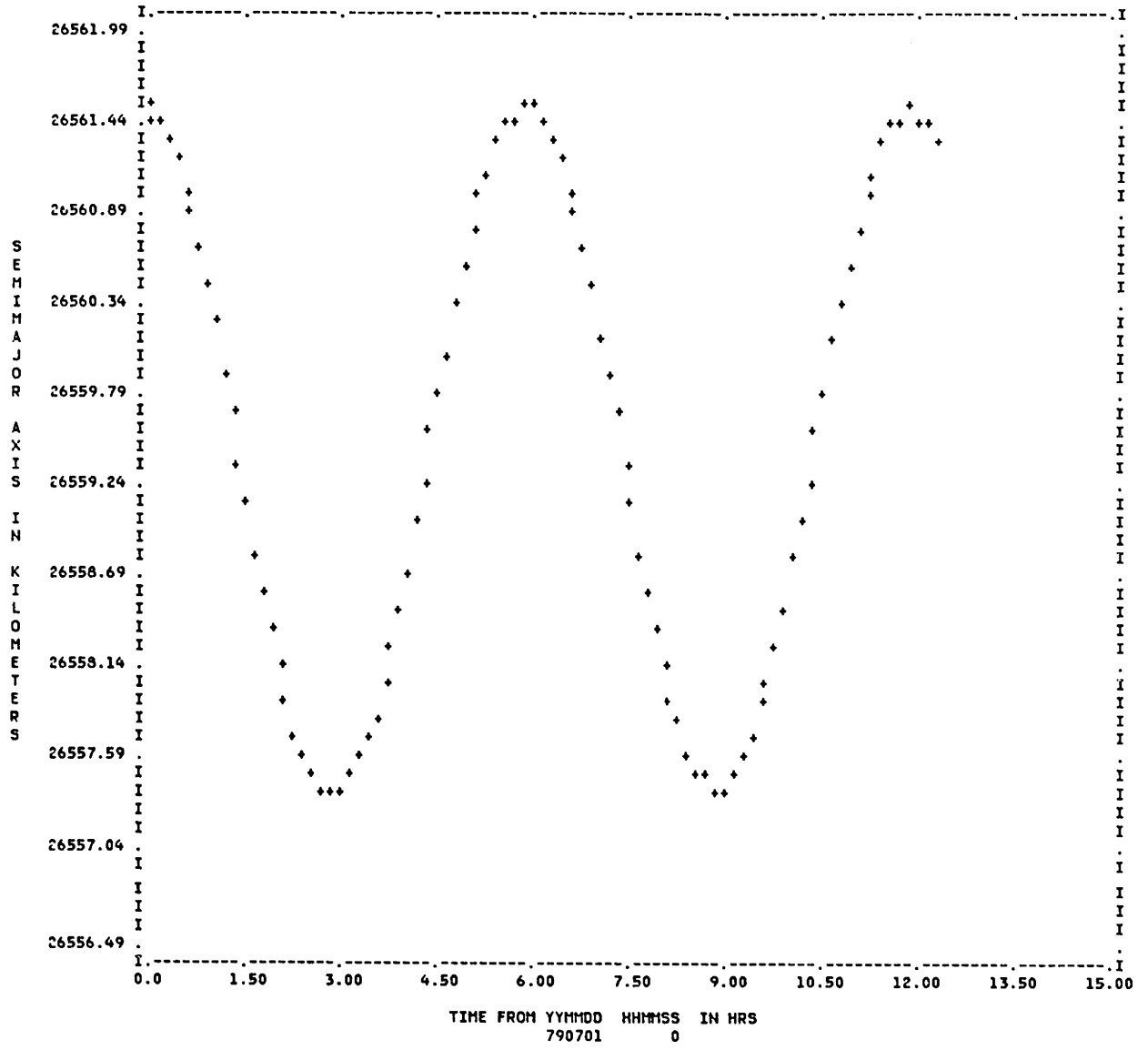
Initial conditions and perturbations as in Figure 2-44.

Figure 2-46. Cross Track Difference after 12 hours from Epoch/Semianalytical minus Cowell for the Medium Altitude Circular Test Case



Initial conditions and perturbations as in Figure 2-44.

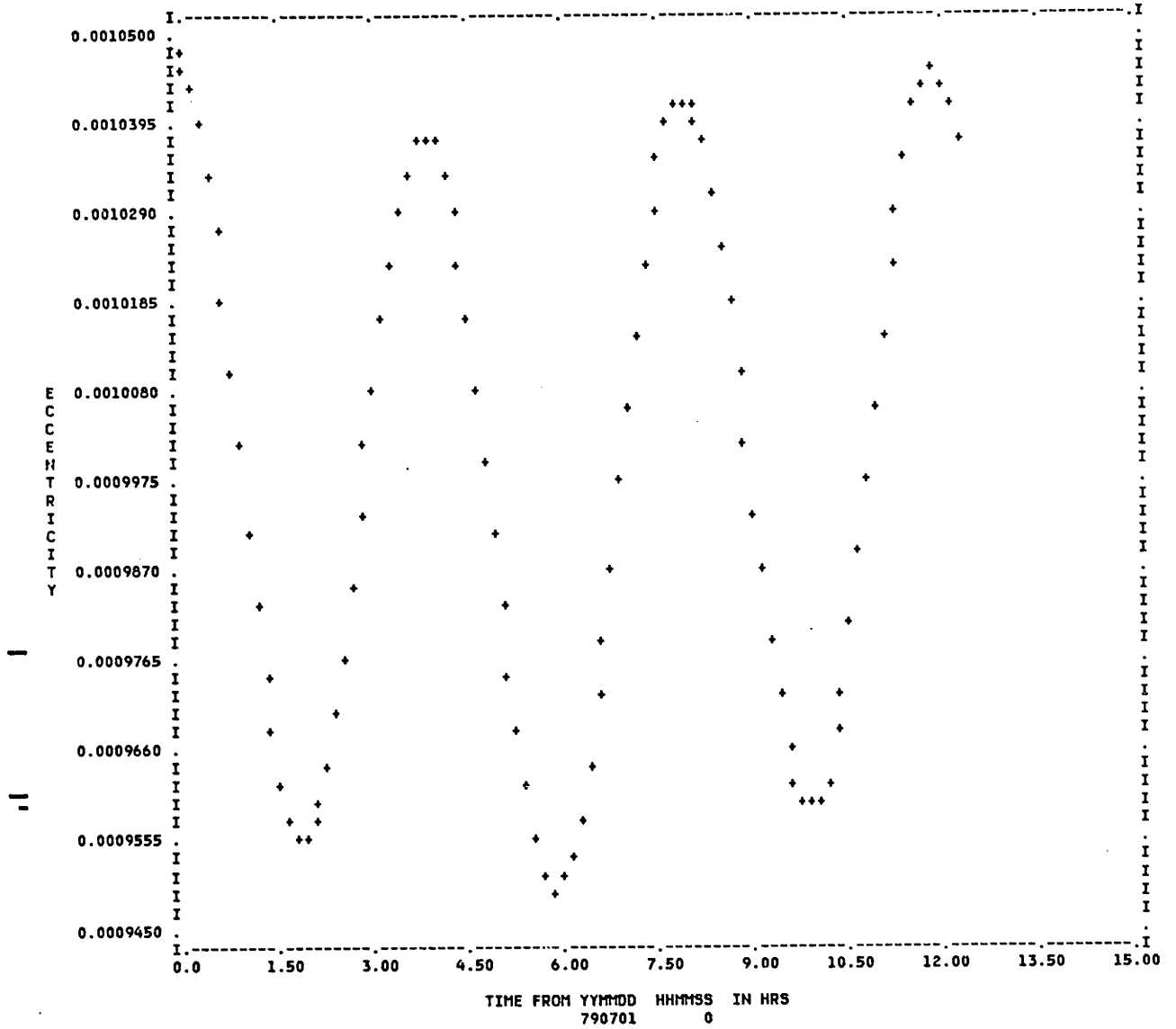
Figure 2-47. Osculating Semimajor Axis Comparison/Semianalytical versus Cowell for the Medium Altitude Circular Test Case.



***** ELEMENTS FROM ORB1 FILE ON UNIT 24, DATA RECORDS START AT 790701 0 : Cowell
 ++++++ ELEMENTS FROM ORB1 FILE ON UNIT 81, DATA RECORDS START AT 790701 0 : AOG and SPG

Same initial conditions and perturbations as in Figure 2-44.

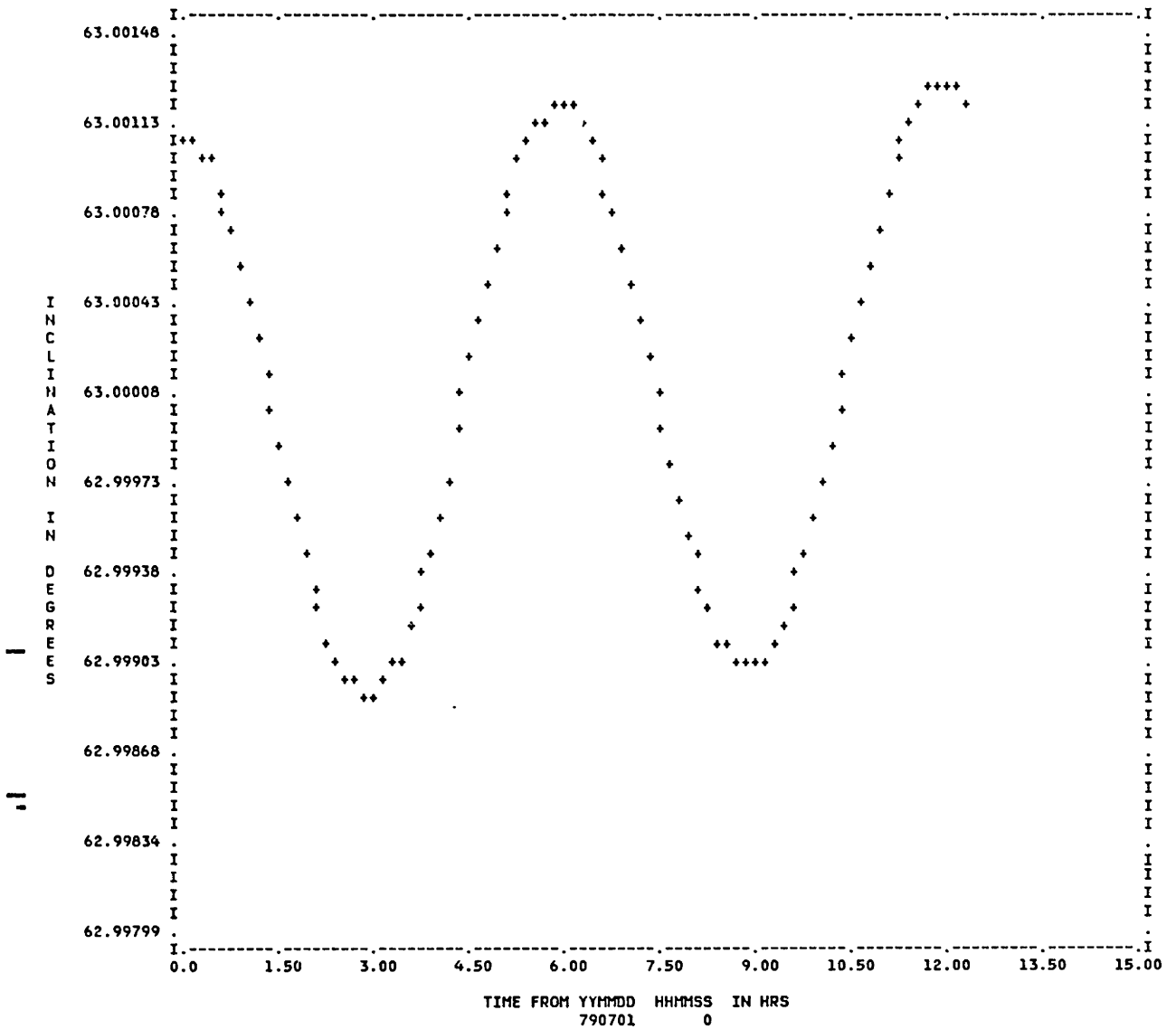
Figure 2-48. Osculating Eccentricity Comparison/Semianalytical versus Cowell
for the Medium Altitude Circular Test Case



***** ELEMENTS FROM ORB1 FILE ON UNIT 24, DATA RECORDS START AT 790701 0 : Cowell
 ++++++ ELEMENTS FROM ORB1 FILE ON UNIT 81, DATA RECORDS START AT 790701 0 : AOG and SPG

Same initial conditions and perturbations as in Figure 2-44.

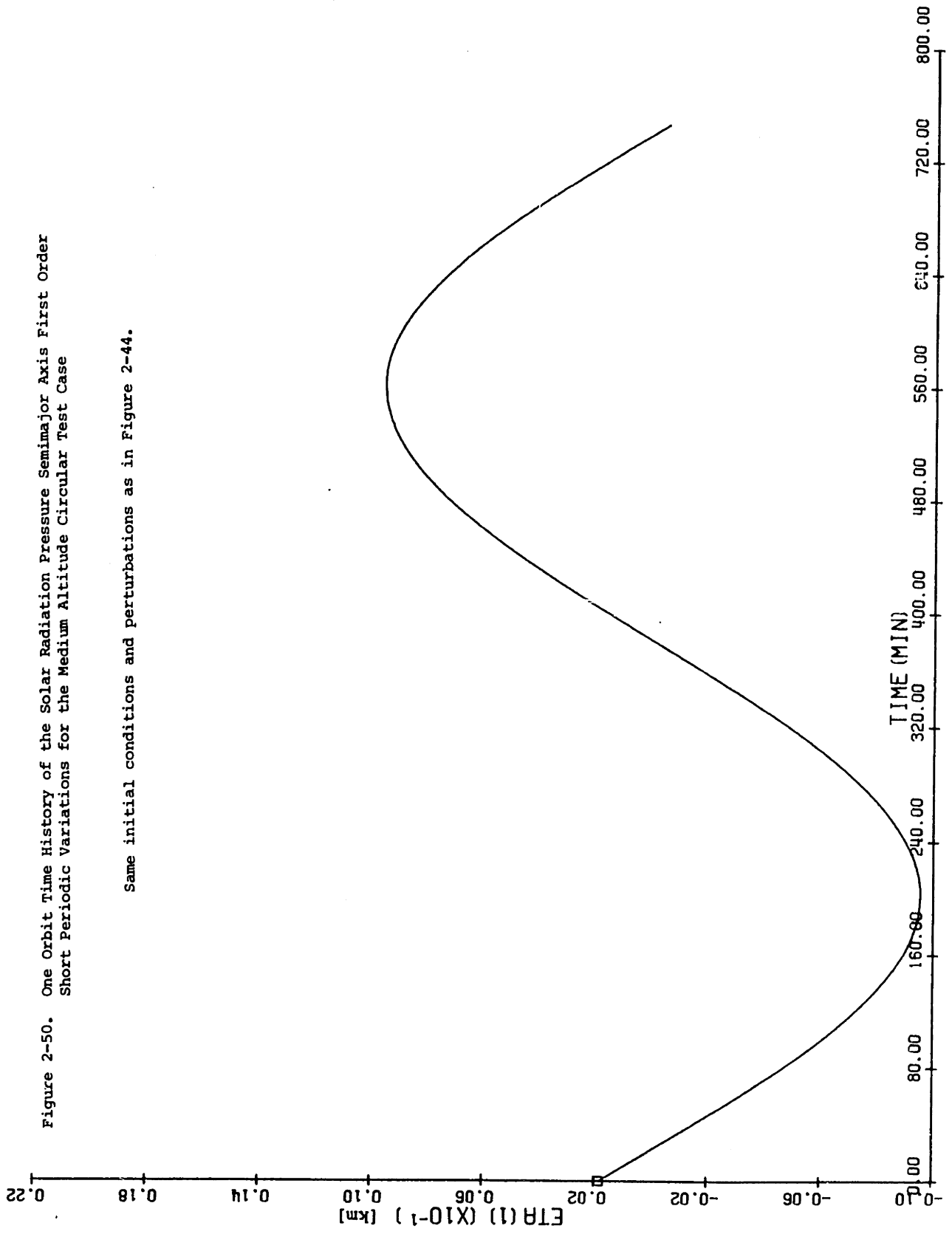
Figure 2-49. Osculating Inclination Comparison/Semianalytical versus Cowell
for the Medium Altitude Circular Test Case



***** ELEMENTS FROM ORB1 FILE ON UNIT 24, DATA RECORDS START AT 790701 0 : Cowell
+++++ ELEMENTS FROM ORB1 FILE ON UNIT 81, DATA RECORDS START AT 790701 0 : AOG and SPG

Same initial conditions and perturbations as in Figure 2-44.

Figure 2-50. One Orbit Time History of the Solar Radiation Pressure Semimajor Axis First Order Short Periodic Variations for the Medium Altitude Circular Test Case



Same initial conditions and perturbations as in Figure 2-44.

Figure 2-51. One Orbit Time History of the Lunar Semimajor Axis First Order Short Periodic Variations for the Medium Altitude Circular Test Case

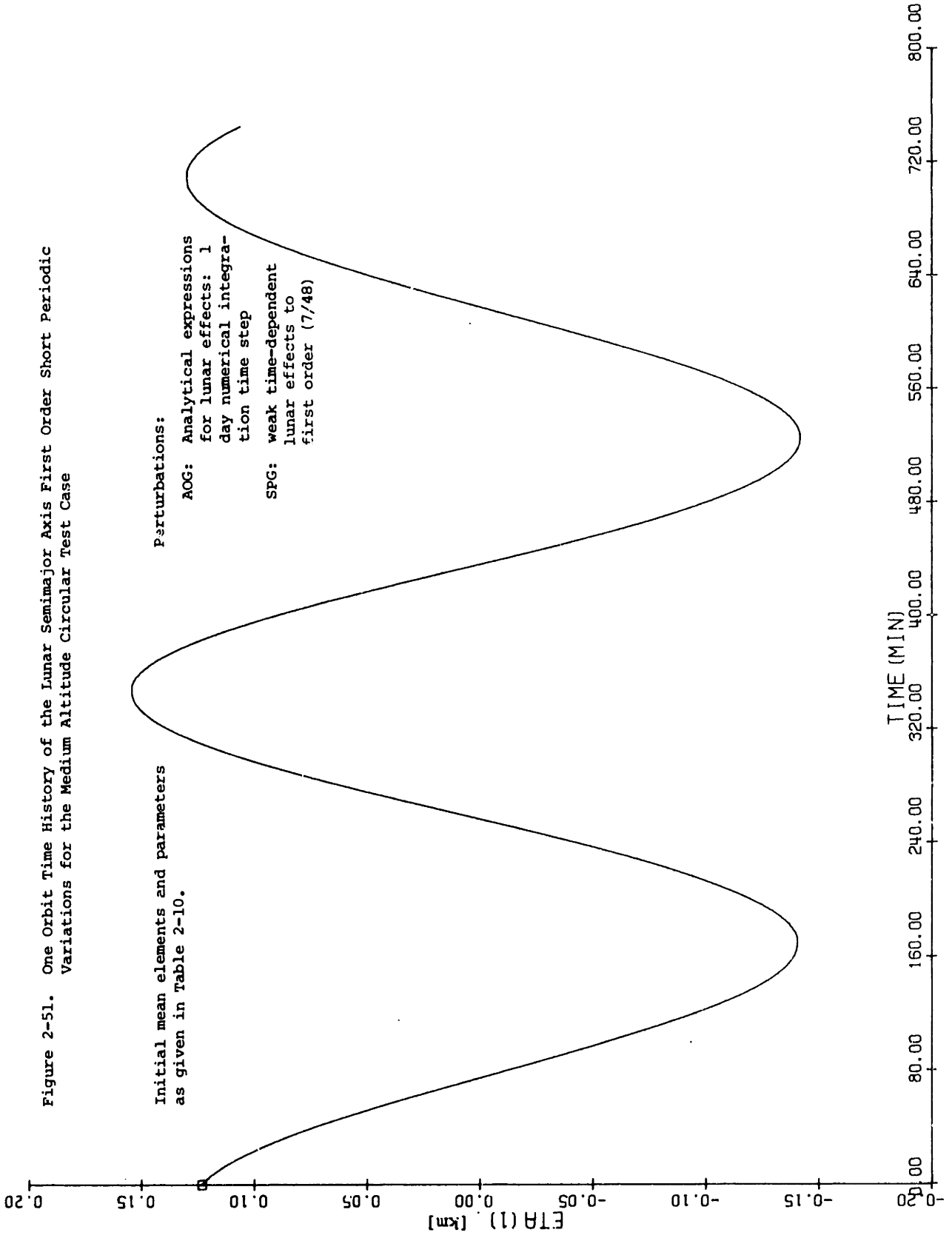


Figure 2-52. Time History of the Lunar Semimajor Axis Weak Time-Dependent Short Periodic Coefficients* for the Medium Altitude Circular Test Case.

* The $\bar{\lambda}$ coefficients as given in Table 2-3.

Same initial conditions and perturbations as in Figure 2-51.

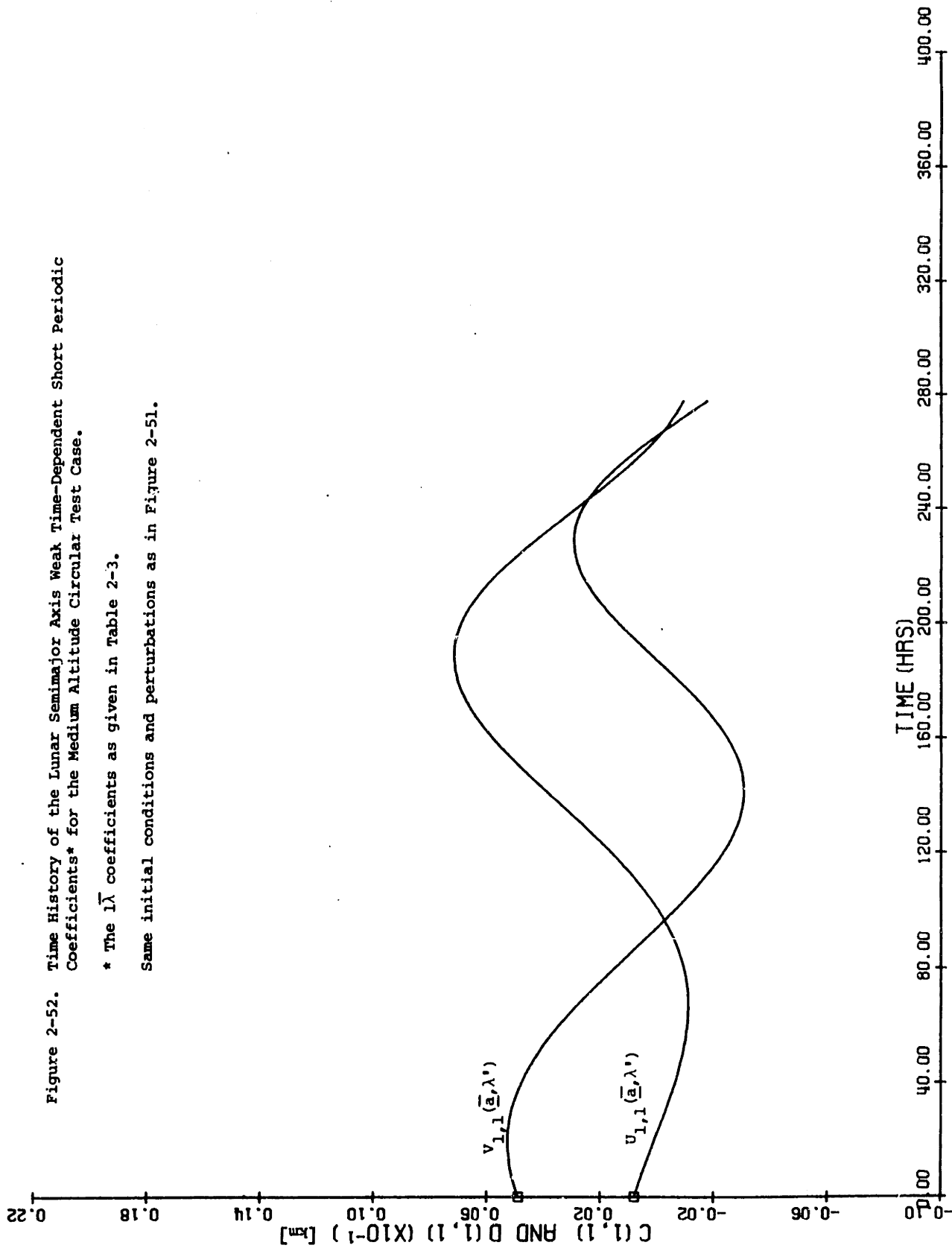


Figure 2-53. Time History of the Lunar Semimajor Axis Weak Time-Dependent Short Periodic Coefficients* for the Medium Altitude Circular Test Case

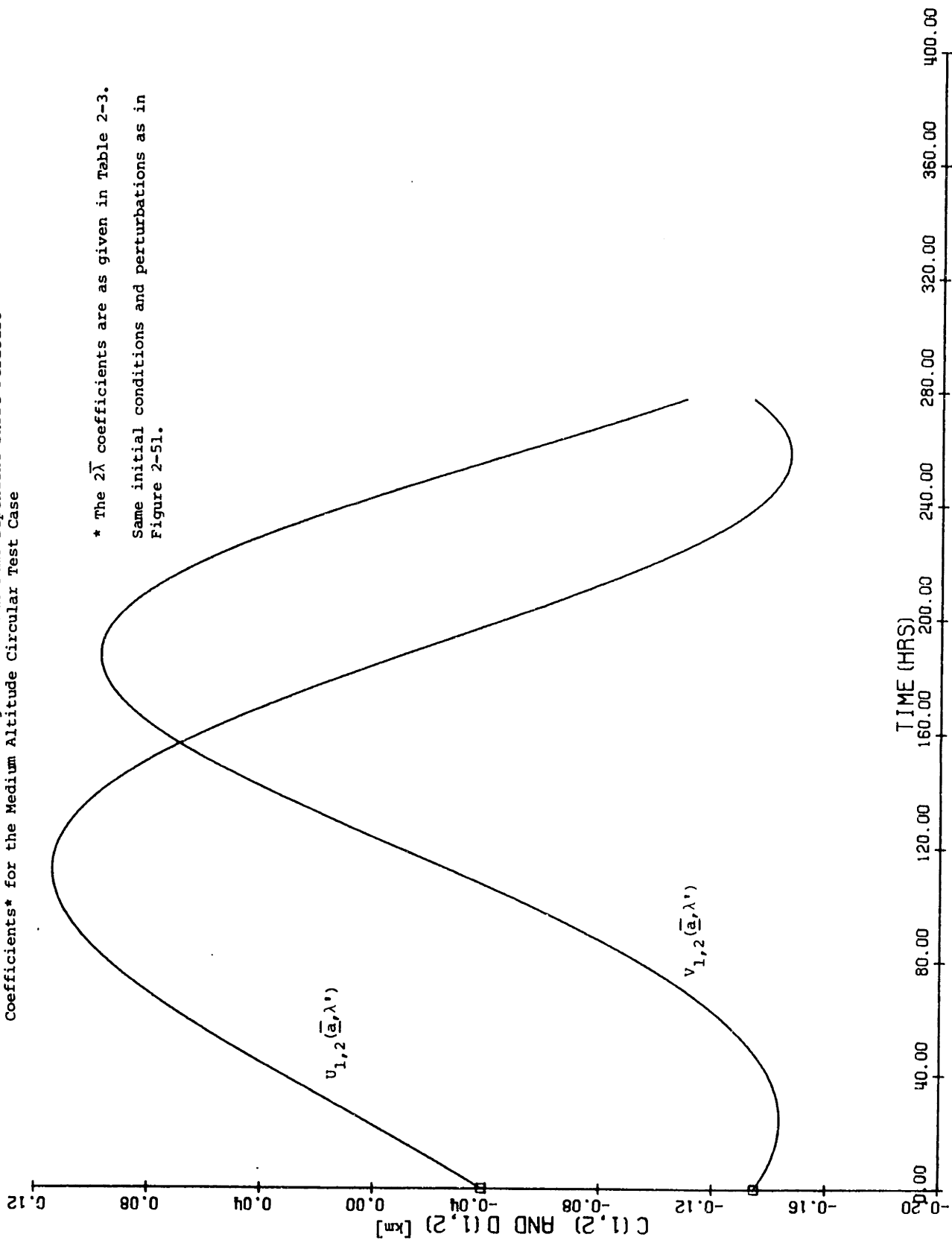
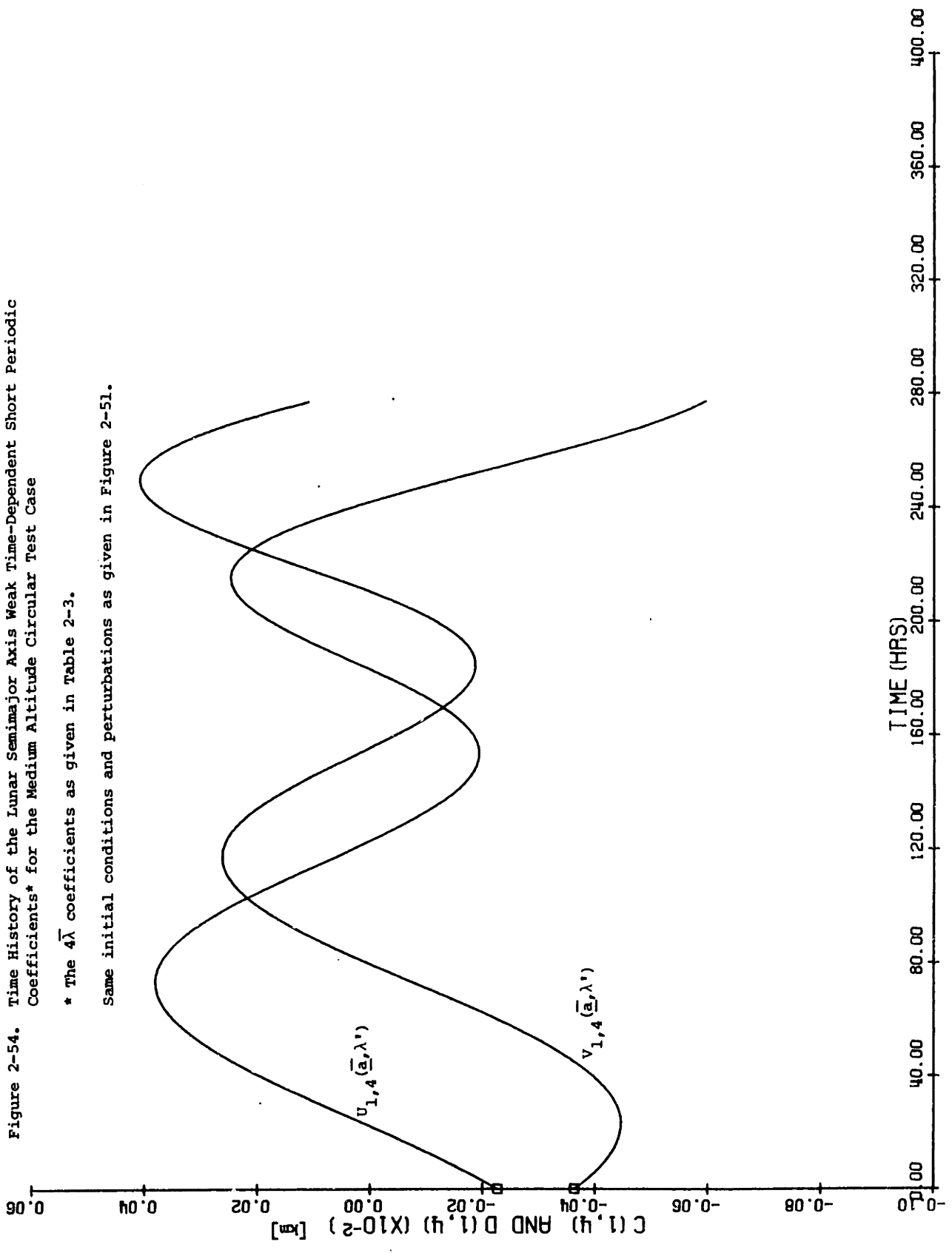


Figure 2-54. Time History of the Lunar Semimajor Axis Weak Time-Dependent Short Periodic Coefficients* for the Medium Altitude Circular Test Case

* The $4\bar{\lambda}$ coefficients as given in Table 2-3.

Same initial conditions and perturbations as given in Figure 2-51.



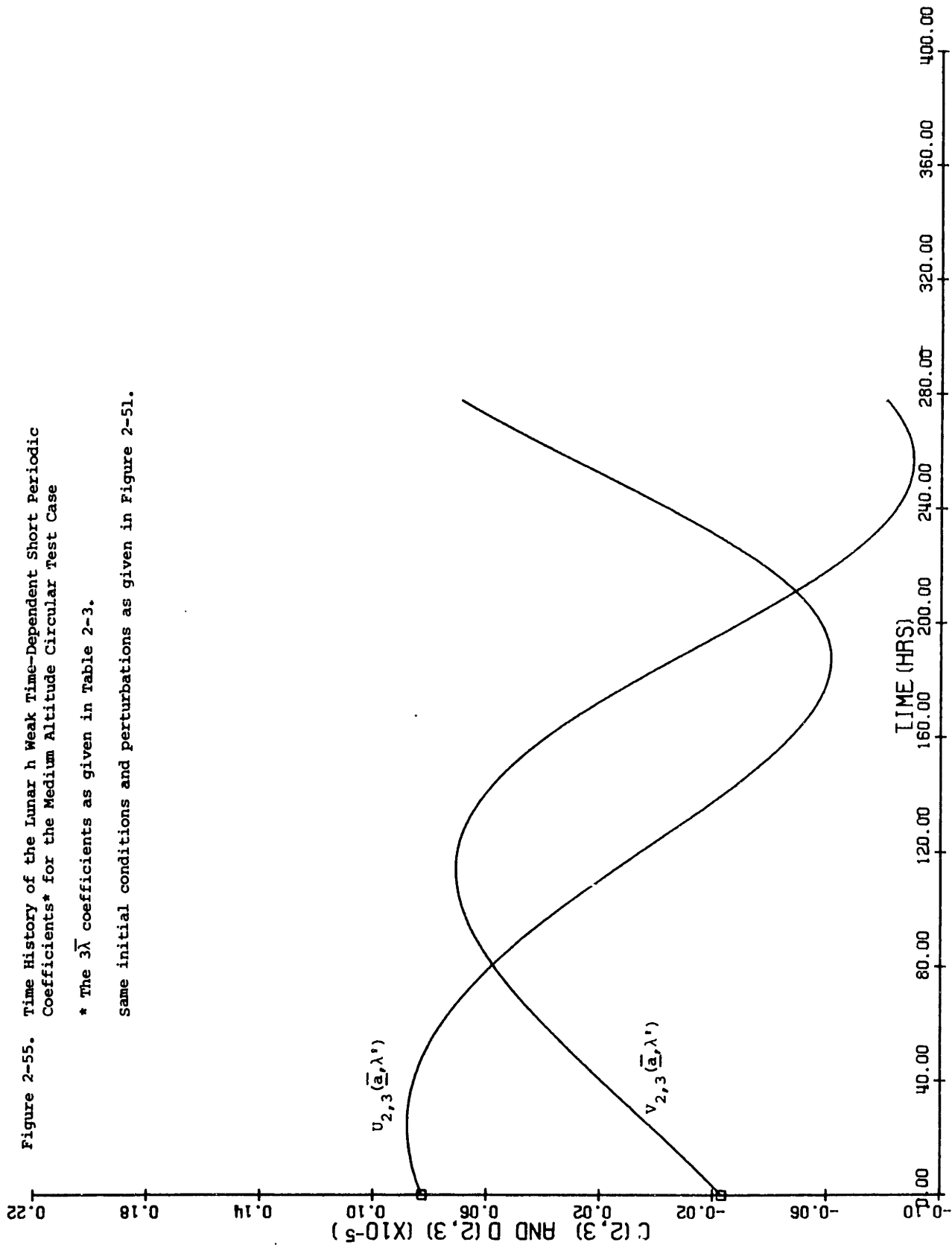


Figure 2-55. Time History of the Lunar h Weak Time-Dependent Short Periodic Coefficients* for the Medium Altitude Circular Test Case
 * The $3\bar{\lambda}$ coefficients as given in Table 2-3.
 Same initial conditions and perturbations as given in Figure 2-51.

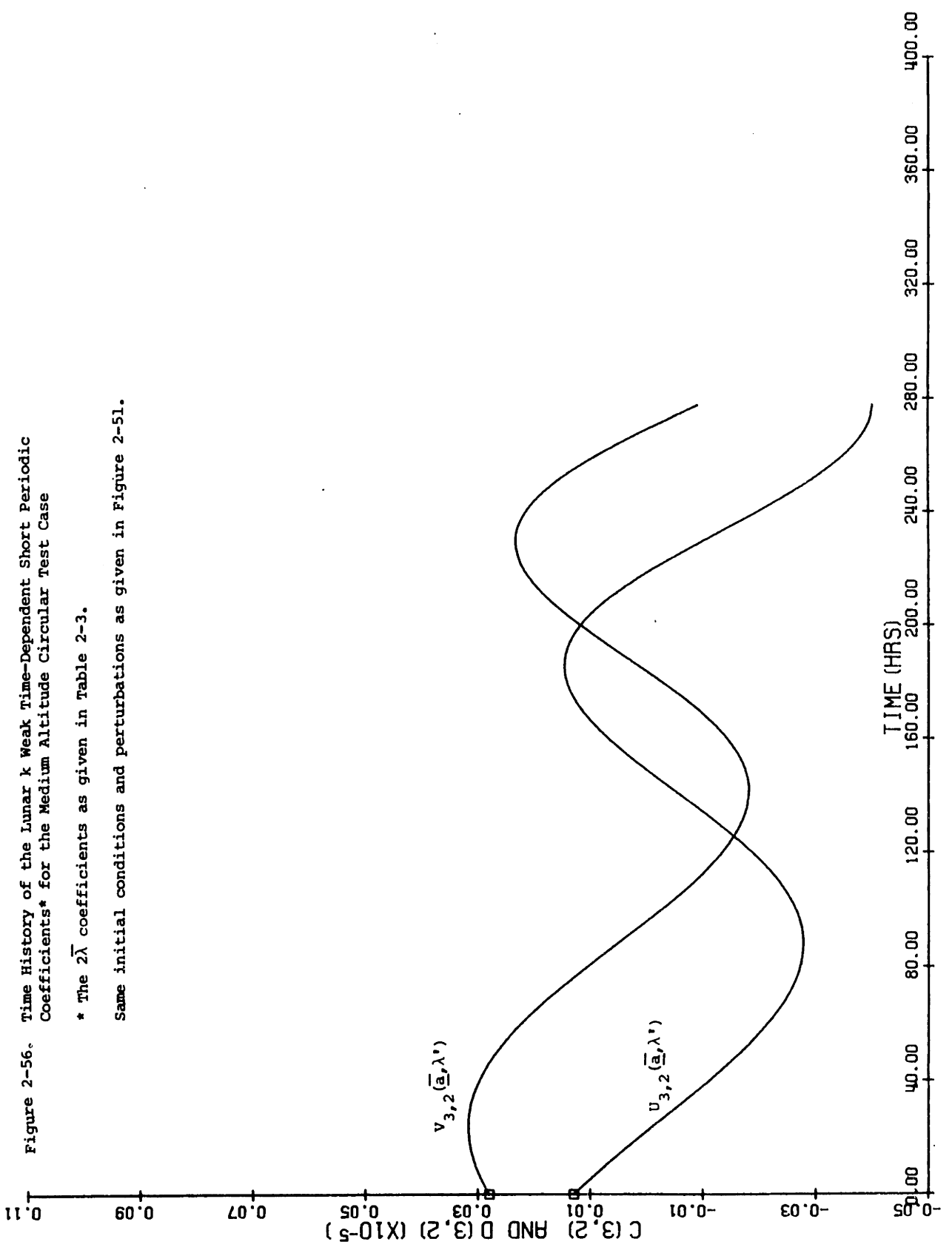


Figure 2-56. Time History of the Lunar k Weak Time-Dependent Short Periodic Coefficients* for the Medium Altitude Circular Test Case

* The $2\bar{\lambda}$ coefficients as given in Table 2-3.

Same initial conditions and perturbations as given in Figure 2-51.

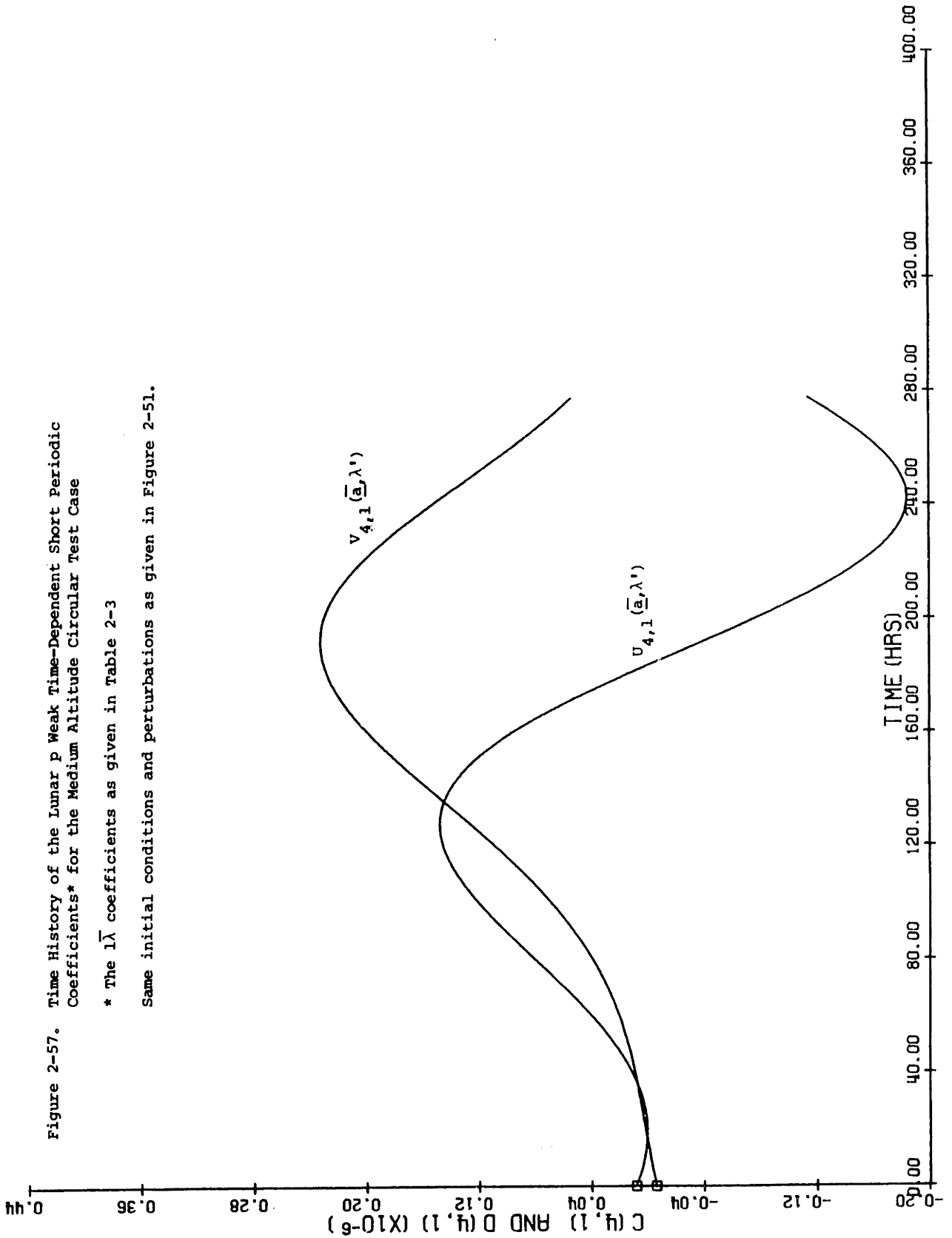
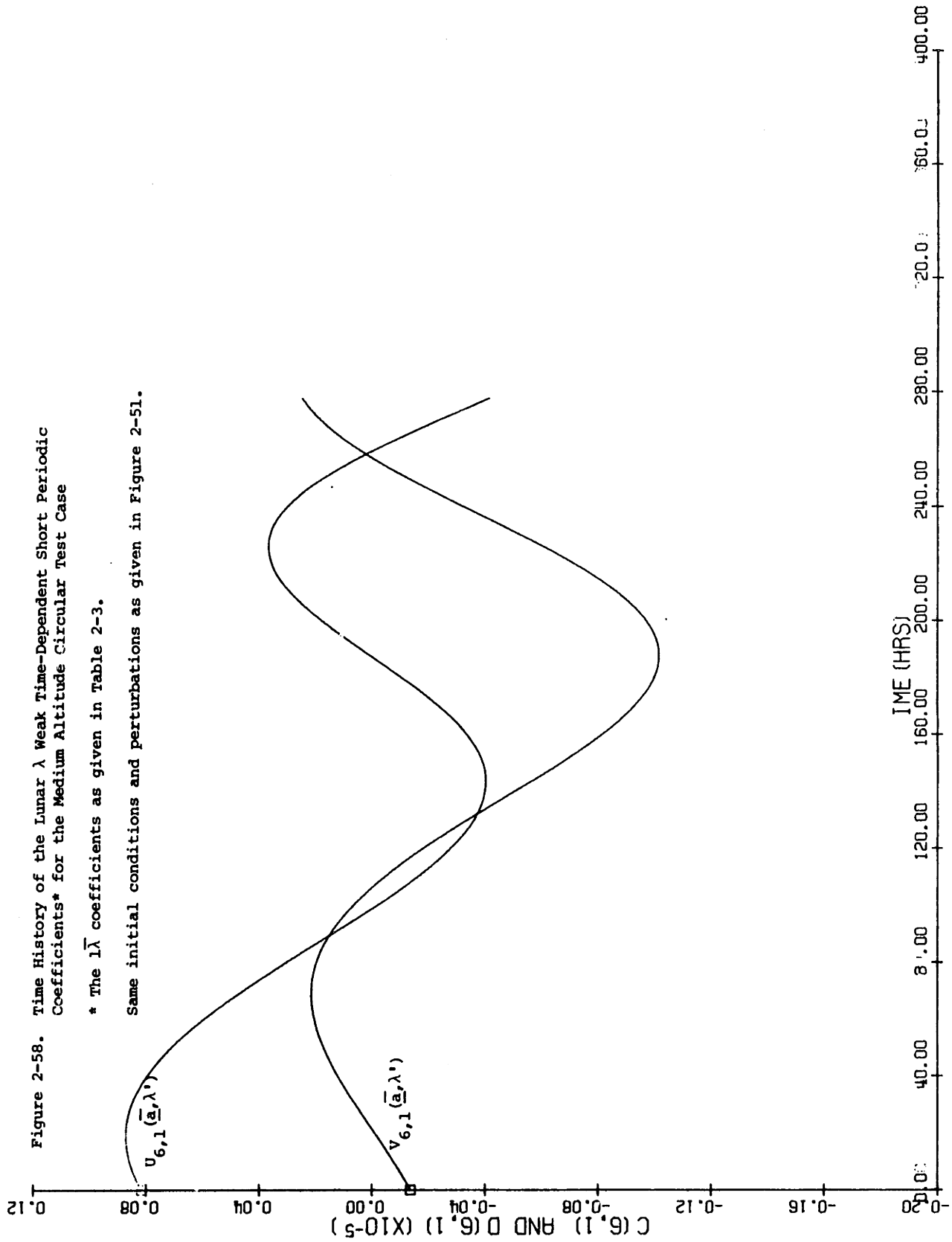


Figure 2-57. Time History of the Lunar p Weak Time-Dependent Short Periodic Coefficients* for the Medium Altitude Circular Test Case

* The $\bar{\lambda}$ coefficients as given in Table 2-3

Same initial conditions and perturbations as given in Figure 2-51.



CHAPTER 3

ORBIT DETERMINATION WITH A SEMIANALYTICAL BATCH FILTER

If it were possible to model the disturbing forces experienced by an artificial satellite exactly, there would be no need to use observation data for the purpose of improving the estimate of the satellite's state. Obviously this is not the case and estimation procedures become a very important part of an OD system. This is especially true for near-Earth satellites due to the presence of atmospheric drag and the uncertainties associated with this perturbation.

An estimation procedure which is used extensively by most OD systems is the batch filter. The batch filter is a least squares differential correction algorithm which takes all the tracking data over an observation span and determines the best estimate of the satellite's state at a reference time (usually epoch). An adaptive batch filter solves for uncertain parameters within the force model in addition to the satellite's state (position and velocity or an orbital element set). A major portion of the batch filter, or for that matter any estimation process, is the satellite theory used for orbit generation. The previous chapter demonstrated that the semianalytical satellite theory is a viable orbit generator. The coupling of the semianalytical satellite theory with an adaptive batch filter may significantly increase the performance of OD systems.

It is the purpose of this chapter to present an adaptive semianalytical batch filter. Drag perturbed satellites are of primary concern in this chapter. A means of adaptively estimating modeled parameters within an atmospheric density model is presented. Observational data is simulated and is processed by the semianalytical batch filter.

This chapter is divided into three sections. Section 3.1 presents the basic algorithmic structure of the semianalytical batch filter. The semianalytical partial derivatives of perturbed motion, which are required for a semianalytical batch filter, are developed in Section 3.2. Numerical results of the adaptive semianalytical batch filter are presented in Section 3.3.

3.1 A Semianalytical Batch Filter

This section develops the basic functional formulation of the semianalytical batch filter. In this research the term batch filter will imply a weighted least squares estimator. First a brief heuristic review of the weighted least squares algorithm is presented. Next the weighted least squares algorithm is formulated in terms of the semianalytical satellite theory.

A Review of the Batch Filter

Assume that the system dynamics can be expressed as

$$\dot{\underline{x}}(t) = \underline{f}[\underline{x}(t)] + \underline{w}(t) \quad (3-1)$$

where $\underline{x}(t)$ is the actual or true state vector of the system and $\underline{w}(t)$ is the modeling/system noise. The best estimate of the actual state will be denoted as $\hat{\underline{x}}(t)$. Associated with $\hat{\underline{x}}(t)$ is the covariance matrix $P(t)$. The covariance matrix is defined as

$$P(t) = E\{[\hat{\underline{x}}(t) - \underline{x}(t)][\hat{\underline{x}}(t) - \underline{x}(t)]^T\} \quad (3-2)$$

where $E\{ \}$ denotes the expected or mean value of the quantity within the brackets (see Ref. 72). It is noted that

$$\text{Trace}[P(t)] = E\{[\hat{\underline{x}}(t) - \underline{x}(t)]^T[\hat{\underline{x}}(t) - \underline{x}(t)]\} \quad (3-3)$$

where $\text{Trace}[P(t)]$ denotes the operation of adding together the terms on the main diagonal of $P(t)$. It can be seen from Equation (3-3) that as the $\text{Trace}[P(t)]$ decreases, the magnitude of the expected error between $\hat{\underline{x}}(t)$ and $\underline{x}(t)$ decreases. Therefore, the covariance matrix can be thought of as an indicator of the confidence in $\hat{\underline{x}}(t)$.

Obviously, the state can be propagated forward (or backward) in time by the following differential equation

$$\dot{\hat{\underline{x}}}(t) = \underline{f}[\hat{\underline{x}}(t)] \quad (3-4a)$$

with the initial conditions

$$\hat{\underline{x}}(t_0) = \tilde{\underline{x}}_0 \quad (3-4b)$$

$$P(t_0) = P_0 \quad (3-4c)$$

The symbol \sim denotes that this is an a priori estimate of $\underline{x}(t_0)$. P_0 is the covariance matrix (confidence) associated with $\tilde{\underline{x}}_0$. From Equation (3-4a) it is seen that $\hat{\underline{x}}(t)$ will depend upon $\hat{\underline{x}}(t_0)$. In other words, given a set of initial conditions, a unique system trajectory, $\hat{\underline{x}}(t)$, is defined through Equation (3-4a).

In this development the solve-for parameters for the least squares estimate (batch filter) will be $\hat{\underline{x}}(t_0)$. The notation $\hat{\underline{x}}(t_0^-)$ will denote the value of $\hat{\underline{x}}(t_0)$ prior to the estimation process. Similarly, $\hat{\underline{x}}(t_0^+)$ will indicate the value of $\hat{\underline{x}}(t_0)$ after the estimation process. The notation $\hat{\underline{x}}(t^+)$ or $\hat{\underline{x}}(t^-)$ will denote the estimated system trajectory [analytical or numerical solution to Equation (3-4a)] associated with the initial conditions $\hat{\underline{x}}(t_0^+)$ or $\hat{\underline{x}}(t_0^-)$ respectively.

Defining \underline{O}_a to be a vector of all the actual observations and $\underline{O}_c[\underline{x}(t)]$ as the model of the observations (the computed observations), it is seen that

$$\underline{O}_a = \underline{O}_c[\underline{x}(t)] + \underline{v}(t) \quad (3-5)$$

where $\underline{v}(t)$ is the noise associated with the observation process. The measurement noise is assumed to have a normal distribution with zero mean and a covariance of R . Naturally, the computed observations will depend upon the actual system trajectory, $\underline{x}(t)$.

It is desired that after the weighted least squares estimation process, the following be true

$$\hat{\underline{x}}(t+) = \underline{x}(t) \quad (3-6)$$

Equation (3-6) indicates that the estimation process is required to yield an updated system trajectory which is equal to the actual (true) system trajectory. Let $\delta\underline{b}$ denote the observation residual vector prior to the estimation process and $\hat{\underline{x}}(t_0)$ denotes the resulting update for the solve-for vector. Mathematically these quantities can be expressed as

$$\delta\underline{b} \equiv \underline{O}_a - \underline{O}_c[\hat{\underline{x}}(t-)] \quad (3-7)$$

$$\hat{\underline{x}}(t_0) \equiv \hat{\underline{x}}(t_0+) - \hat{\underline{x}}(t_0-) \quad (3-8)$$

Expanding Equation (3-5) in a Taylor series about $\hat{\underline{x}}(t_0^-)$ and noting that $\hat{\underline{x}}(t_-)$ is the system trajectory corresponding to $\hat{\underline{x}}(t_0^-)$, the following expression results

$$\underline{O}_a = \underline{O}_c [\hat{\underline{x}}(t_-)] + F \delta \hat{\underline{x}}(t_0) + \underline{E} \quad (3-9a)$$

where \underline{E} is the error vector associated with such a formulation and where

$$F = \left[\frac{\partial \underline{O}_c [\underline{x}(t)]}{\partial \underline{x}(t_0)} \right]_{\hat{\underline{x}}(t_0^-)} \quad (3-9b)$$

Equation (3-9a) can be written as

$$\delta \underline{b} = F \delta \hat{\underline{x}}(t_0) + \underline{E} \quad (3-10)$$

The basic concept of a weighted least squares estimation procedure is to pick $\delta \hat{\underline{x}}(t_0)$ such that the weighted square of \underline{E} is minimized. The cost function for such a concept can be expressed as

$$J = \underline{E}^T W \underline{E} \quad (3-11)$$

where W is the weighting matrix. The weighting matrix is usually taken to be the inverse of the covariance of the measurement/observation noise vector (Ref. 67). Assuming the

measurements to be uncorrelated and the errors to have a zero mean value, the weighting matrix can be expressed as

$$W = R^{-1} = \begin{bmatrix} \sigma_{m1}^{-2} & & 0 \\ & \sigma_{m2}^{-2} & \\ 0 & & \ddots \\ & & & \sigma_{mp}^{-2} \end{bmatrix} \quad (3-12)$$

where σ_{mi} is the standard deviation of the i th measurement.

Substitution of Equation (3-10) into Equation (3-11) results in

$$J = [\delta \underline{b} - F \hat{\delta \underline{x}}(t_0)]^T W [\delta \underline{b} - F \hat{\delta \underline{x}}(t_0)]$$

which reduces to

$$J = \delta \underline{b}^T W \delta \underline{b} - 2 \delta \underline{b}^T W F \hat{\delta \underline{x}}(t_0) + \hat{\delta \underline{x}}^T(t_0) F^T W F \hat{\delta \underline{x}}(t_0) \quad (3-13)$$

As was previously indicated, the weighted least squares estimator determines $\hat{\delta \underline{x}}(t_0)$ such that Equation (3-13) is minimized.

Setting $\frac{\partial J}{\partial [\delta \underline{x}(t_0)]}$ equal to zero results in

$$0 = -2 \delta \underline{b}^T W F + 2 \hat{\delta \underline{x}}^T(t_0) F^T W F \quad (3-14)$$

which implies that

$$\hat{\underline{x}}(t_0) = (F^T WF)^{-1} F^T W \delta \underline{b} \quad (3-15)$$

Taking $\frac{\partial^2 J}{\partial [\delta \underline{x}(t_0)]^2}$ results in $2F^T WF$ which is positive definite and therefore Equation (3-15) is the value of $\hat{\underline{x}}(t_0)$ which minimizes J (Ref. 72).

Equation (3-15) is the classical weighted least squares estimator. The residual, $\delta \underline{b}$, and the matrix F are computed* and substituted into Equation (3-15) in order to determine $\hat{\underline{x}}(t_0)$. The updated estimate of the epoch conditions, $\hat{\underline{x}}(t_0+)$, is determined from Equation (3-8). Knowing $\hat{\underline{x}}(t_0+)$, the system trajectory, $\hat{\underline{x}}(t+)$, can be obtained by solving Equation (3-4a).

Due to linearization errors and other errors associated with the formulation, the classical weighted least squares estimator usually has to iterate on Equation (3-15) until the minimum is reached to within a specified tolerance. Letting k denote the iteration number it is easily shown that

$$\hat{\underline{x}}_{-k}(t_0) = (F^T WF)^{-1} F^T W \delta \underline{b}_{-k} \quad (3-16a)$$

$$\delta \underline{b}_{-k} = \underline{0}_a - \underline{0}_c [\hat{\underline{x}}_{-k}(t-)] \quad (3-16b)$$

* The actual algorithmic structure is explained in Chapter 8 of Reference 67.

$$F = \left[\frac{\partial O_c[\underline{x}(t)]}{\partial \underline{x}(t_0)} \right]_{\hat{\underline{x}}_k(t_0^-)} \quad (3-16c)$$

$$\dot{\hat{\underline{x}}}(t) = f[\hat{\underline{x}}(t)] \text{ with } \hat{\underline{x}}(t_0) = \hat{\underline{x}}_k(t_0) \quad (3-16d)$$

where

$$\hat{\underline{x}}_k(t_0^+) = \hat{\underline{x}}_k(t_0^-) + \delta \hat{\underline{x}}_k(t_0) \quad (3-16e)$$

The above development did not take into account any information about the a priori knowledge of the initial conditions. For example, if a component of the initial state is known exactly, the batch filter should be constrained such that it does not adjust that component during the update. As the confidence in the a priori initial conditions, $\tilde{\underline{x}}_0$, decreases, the estimation process should have less constraints in choosing the update. This information can be conveyed to the batch filter by adding a term to the cost function in Equation (3-13) which takes into account the value of $\hat{\underline{x}}(t_0)$ to within the limits of its uncertainty (Ref. 67). The new cost function, on the k th iteration, can be written as

$$J = \delta \underline{b}_{-k}^T W \delta \underline{b}_{-k} - 2 \delta \underline{b}_{-k}^T W F \delta \hat{\underline{x}}_k(t_0) + \delta \hat{\underline{x}}_k^T(t_0) F^T W F \delta \hat{\underline{x}}_k(t_0) \\ + [\hat{\underline{x}}_k(t_0^+) - \hat{\underline{x}}_0]^T P_0^{-1} [\hat{\underline{x}}(t_0^+) - \tilde{\underline{x}}_0] \quad (3-17)$$

By defining $\delta \hat{\underline{x}}_k(t_0^-)$ as follows

$$\delta \hat{\underline{x}}_k(t_0^-) = \hat{\underline{x}}_0 - \hat{\underline{x}}_k(t_0^-) \quad (3-18)$$

it is seen that

$$[\hat{\underline{x}}(t_0^+) - \hat{\underline{x}}_0] = \delta \hat{\underline{x}}_k(t_0) - \delta \hat{\underline{x}}_k(t_0^-) \quad (3-19)$$

From Equation (3-18) it is noted that on the first iteration, $\delta \hat{\underline{x}}_1(t_0^-) = 0$ since $\hat{\underline{x}}_1(t_0^-) = \hat{\underline{x}}_0$. Substitution of Equation (3-19) into Equation (3-17) and expanding yields

$$\begin{aligned} J = & \delta \underline{b}_k^T W \delta \underline{b}_k - 2 \delta \underline{b}_k^T W F \delta \hat{\underline{x}}_k(t_0) \\ & + \delta \hat{\underline{x}}^T(t_0) F^T W F^T \delta \hat{\underline{x}}(t_0) + \delta \hat{\underline{x}}_k^T(t_0) P_0^{-1} \delta \hat{\underline{x}}_k^T(t_0) \\ & - 2 \delta \hat{\underline{x}}_k^T(t_0) P_0^{-1} \delta \hat{\underline{x}}_k(t_0) + \delta \hat{\underline{x}}_k(t_0^-) P_0^{-1} \delta \hat{\underline{x}}_k(t_0^-) \end{aligned} \quad (3-20)$$

Taking $\frac{\partial J}{\partial [\delta \hat{\underline{x}}_k(t_0)]}$, setting equal to zero and rearranging yields (Ref. 67)

$$\delta \hat{\underline{x}}_k(t_0) = (F^T W F + P_0^{-1})^{-1} [F^T W \delta \underline{b}_k + P_0^{-1} \delta \hat{\underline{x}}_k(t_0^-)] \quad (3-21)$$

Equation (3-21) is the batch filter used in GTDS-RD (Refs. 67 and 73). This is summarized in Table 3-1.

The covariance matrix associated with the converged estimate of the initial conditions is the gain matrix in Equation (3-21). This is expressed as

$$P_c(t_0) = (F^T W F + P_0^{-1})^{-1} \quad (3-22)$$

where $P_c(t_0)$ indicates that this is for the converged solution. Reference 67 gives a detailed derivation of Equation (3-22).

Semianalytical Satellite Theory and the Batch Filter

The solve-for vector in the adaptive semianalytical batch filter is defined as

$$\underline{x}(t_0) = \begin{bmatrix} \bar{a}^*(t_0) \\ \underline{c} \end{bmatrix} = \begin{bmatrix} \bar{a}^*_0 \\ \underline{c} \end{bmatrix} \quad (3-23)$$

where

$$\bar{a}^*_0 = \begin{bmatrix} \bar{a}_0 \\ \bar{\lambda}_0 \end{bmatrix} \quad (3-24a)$$

$$\bar{a}_0 = [\bar{a}_0, \bar{h}_0, \bar{k}_0, \bar{p}_0, \bar{q}_0]^T \quad (3-24b)$$

Table 3-1
The Batch Filter

$$\hat{\underline{x}}_k(t_0) = [F^T W F + P_0^{-1}]^{-1} [F^T W \delta \underline{b}_k + P_0^{-1} \delta \underline{\tilde{x}}_k(t_0^-)]$$

$$\delta \underline{x}_k(t_0) = \hat{\underline{x}}_k(t_0^+) - \hat{\underline{x}}_k(t_0^-)$$

$$\delta \underline{\tilde{x}}_k(t_0) = \underline{\tilde{x}}_0 - \hat{\underline{x}}_k(t_0^-)$$

$$\delta \underline{b}_k = \underline{O}_a - \underline{O}_c [\hat{\underline{x}}_k(t_0^-)]$$

$$F = \left[\frac{\partial \underline{O}_c [\underline{x}(t)]}{\partial \underline{x}(t_0)} \right]_{\hat{\underline{x}}_k(t_0^-)}$$

$$\dot{\hat{\underline{x}}}(t) = f[\hat{\underline{x}}(t)] \text{ with } \hat{\underline{x}}(t_0) = \hat{\underline{x}}_k(t_0)$$

$\hat{\underline{x}}_k(t_0^-) \equiv$ best estimate of the initial state prior to kth iteration of the batch filter

$\hat{\underline{x}}_k(t_0^+) \equiv$ best estimate of the initial state after the kth iteration of the batch filter

$\underline{\tilde{x}}_0 \equiv$ a priori initial state

$P_0 \equiv$ a priori covariance matrix associated with $\underline{\tilde{x}}_0$

$\underline{O}_a =$ actual observations

$\underline{O}_c [\hat{\underline{x}}_k(t_0^-)] =$ computed observations on kth iteration of the batch filter

and where \underline{c} represents the modeled solve-for parameters. Obviously $\underline{\bar{a}}_0^*$ denotes the epoch conditions for the six mean equinoctial elements as given in Chapter 2. The modeled parameters considered in this research deal only with the drag formulation. The drag solve-for parameters include C_D [see Equation (1-1)] or the a_1 through a_5 parameters in the Adaptive Modified Harris-Priester density model (see Appendix C). The actual estimation options are described in Section 3.3.

From Table 3-1 it is seen that in order to couple the semianalytical satellite theory with the batch filter, the observational residual vector, $\delta\underline{b}_k$, and the F matrix must be determined. In other words, the adaptive semianalytical batch filter is the algorithm presented in Table 3-1 with the solve-for vector defined in Equation (3-23) and the observation residual vector and F matrix computed in terms of the semianalytical satellite theory.

The computation of the observation residual vector, $\delta\underline{b}_k$, in terms of the semianalytical satellite theory is rather simple and straightforward. Given the best estimate for the epoch mean elements, the AOG, as described in Chapter 2, is used to determine the mean elements throughout the observation span. Again it is noted that the AOG uses the large numerical integration time step associated with the semianaly-

tical satellite theory (typically 1 day). The mean elements are determined at the observation times by use of an interpolator. Next the short periodic variations at the observation times are computed by use of the SPG as described in Chapter 2. It is noted that the concept of determining the short periodic coefficients on the integration grid and interpolating to obtain them at the output/observation times should greatly reduce the computational costs of the SPG. Given the mean elements and short periodic functions at an observation time, the precision osculating equinoctial elements can then be determined by use of the near-identity transformation. Knowing the osculating equinoctial elements, the position and velocity in the local tangent coordinate frame (frame the observations are determined in) can be obtained [see Equations (2-9) and (2-18)]. Given the observation model, the computed observation is then determined (see Ref. 67 or Appendix G). The observation residual vector can be obtained by subtracting the computed observations from the actual observations. For example, suppose a radar tracking station determined a range observation at time t [denote the actual observation as $\rho_a(t_i)$]. Also suppose that this range observation is modeled as

$$\rho_c(t_i) = \sqrt{\underline{r}_{LT}^T(t_i) \cdot \underline{r}_{LT}(t_i)} \quad (3-25)$$

Obviously Equation (3-25) assumes a perfect measurement and does not take into account signal propagation characteristics,

biases, atmospheric refraction or any other effects (see Chapter 7 of Ref. 67). After determining $\underline{r}_{LT}(t_i)$ from Equation (2-18), $\rho_c(t_i)$ can be determined from Equation (3-25). The residual observation at time t_i is therefore given as

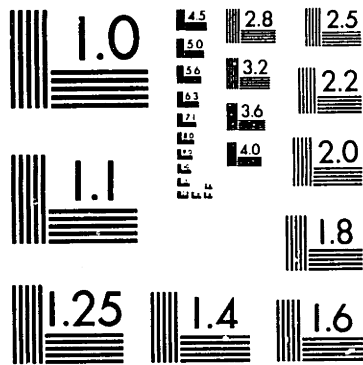
$$\delta b(t_i) = \rho_a(t_i) - \rho_c(t_i) \quad (3-26)$$

The F matrix is the partial derivative of the observations with respect to the solve-for parameters. Since the observation models are usually defined in terms of the local tangent coordinate frame, the F matrix can be written as

$$F = \left[\begin{array}{c} \frac{\partial O}{\partial \underline{c}} [\underline{r}_{LT}, \dot{\underline{r}}_{LT}] \\ \partial \underline{x}(t_o) \end{array} \right]_{\hat{\underline{x}}(t_o)} \quad (3-27)$$

By use of the chain rule of differentiation and assuming that there are p measurements and ℓ solve-for parameters, it is seen that

$$F_{p \times \ell} = \left\{ \left[\begin{array}{c} \frac{\partial O}{\partial \underline{c}} [\underline{r}_{LT}, \dot{\underline{r}}_{LT}] \\ \partial \underline{r}_{LT}(t) \end{array} \right] \left| \left[\begin{array}{c} \frac{\partial O}{\partial \underline{c}} [\underline{r}_{LT}, \dot{\underline{r}}_{LT}] \\ \partial \dot{\underline{r}}_{LT}(t) \end{array} \right] \right\}_{p \times 6} \cdot \left\{ \left[\begin{array}{c} \frac{\partial \underline{r}_{LT}(t)}{\partial \underline{R}(t)} \right] \left| \left[\begin{array}{c} \frac{\partial \underline{r}_{LT}(t)}{\partial \dot{\underline{R}}(t)} \end{array} \right] \right\}_{6 \times 6} \cdot \left\{ \left[\begin{array}{c} \frac{\partial \underline{R}(t)}{\partial \underline{a}^*(t)} \\ \frac{\partial \dot{\underline{R}}(t)}{\partial \underline{a}^*(t)} \end{array} \right] \right\}_{6 \times 6} \cdot \left\{ \left[\begin{array}{c} \frac{\partial \underline{a}^*(t)}{\partial \underline{x}(t_o)} \end{array} \right] \right\}_{6 \times \ell} \right\}_{\hat{\underline{x}}(t_o)} \quad (3-28)$$



MICROCOPY RESOLUTION TEST CHART
NATIONAL BUREAU OF STANDARDS-1963-A

20X

NOTICE THIS MATERIAL MAY BE PROTECTED BY
COPYRIGHT LAW (TITLE 17 U.S. CODE.)

where

- $\underline{r}_{LT}, \dot{\underline{r}}_{LT}$ \equiv position and velocity vector with respect to the local tangent frame
 $\underline{R}(t), \dot{\underline{R}}(t)$ \equiv position and velocity vector with respect to an inertial reference frame [mean of 1950 or true of date]
 $\underline{a}^*(t)$ \equiv osculating equinoctial elements

The first matrix in Equation (3-28) is the partial derivatives of the observations with respect to the position and velocity vectors in the local tangent coordinate frame. For example, if the perfect range measurement model of Equation (3-25) is assumed, the following would be true

$$\left\{ \frac{\partial O_C [\underline{r}_{LT}, \dot{\underline{r}}_{LT}]}{\partial \underline{r}_{LT}(t)} \right\} = \frac{\underline{r}_{LT}^T(t)}{\rho_C(t)} \quad (3-29a)$$

$$\left\{ \frac{\partial O_C [\underline{r}_{LT}, \dot{\underline{r}}_{LT}]}{\partial \dot{\underline{r}}_{LT}(t)} \right\} = 0 \quad (3-29b)$$

Reference 67 gives a detailed discussion of the above partial derivatives for realistic observation models (see Appendix G also) and this is presently implemented into GTDS-RD.

The second matrix in Equation (3-28) can be obtained from the transformation equations between the local tangent frame and the inertial frame (see Section 2.1.1). Assuming

that the inertial coordinate frame is the mean of 1950 coordinate frame, the following can be obtained from Equation (2-15)

$$\left\{ \frac{\partial \underline{r}_{LT}(t)}{\partial \underline{R}(t)} \right\} = M_{LT} B(t) C \quad (3-30a)$$

$$\left\{ \frac{\partial \underline{r}_{LT}(t)}{\partial \dot{\underline{R}}(t)} \right\} = 0 \quad (3-30b)$$

$$\left\{ \frac{\partial \dot{\underline{r}}_{LT}(t)}{\partial \underline{R}(t)} \right\} = M_{LT} \dot{B}(t) C \quad (3-30c)$$

$$\left\{ \frac{\partial \dot{\underline{r}}_{LT}(t)}{\partial \dot{\underline{R}}(t)} \right\} = M_{LT} B(t) C \quad (3-30d)$$

where M_{LT} , $B(t)$ and C are coordinate transformations described in Section 2.1.1 and Reference 67. If the true of date coordinate frame is used as the inertial frame, the above expressions will still apply as long as the C matrix is replaced with the identity matrix.

The third matrix in Equation (3-28) can be obtained directly from the two-body relations between the inertial position and velocity and the equinoctial orbital elements [see Equations (2-2) and (2-9)]. Reference 74 gives a complete list of these derivatives.

The last matrix in Equation (3-28) is defined as

$$G = \left[\left\{ \frac{\partial \underline{a}^*(t)}{\partial \underline{a}_0} \right\} \middle| \left\{ \frac{\partial \underline{a}^*(t)}{\partial \underline{c}} \right\} \right] \quad (3-31)$$

The elements of the G matrix are the partial derivatives of perturbed motion. This is discussed in detail in the next section.

3.2 A Semianalytical Satellite Theory for the Partial Derivatives of Perturbed Motion

This section develops the semianalytical partial derivatives of perturbed motion. These partial derivatives are essential to the development and implementation of the semianalytical batch filter. A general formulation for the semianalytical partial derivatives is presented. The generation of the semianalytical partial derivatives is done by an Averaged Partial Generator (APG) and a Short Periodic Partial Generator (SPPG). The APG integrates a matrix differential equation for the mean semianalytical partial derivatives. The APG uses the large numerical integration time step associated with the semianalytical satellite theory. The SPPG determines, on the output/observation grid, the short periodic portion of the semianalytical partial derivatives. Many of the advantages that result from using the AOG and SPG in orbit generation are also applicable to the use of the APG and SPPG in partial derivative generation.

3.2.1 A General Formulation for the Semianalytical Partial Derivatives

The averaged equations of motion will be assumed to be of the following vector form

$$\dot{\underline{a}}^* = \bar{n} \underline{e}_6 + \epsilon \underline{A}_1(\bar{\underline{a}}) \quad (3-32)$$

where

$$\begin{aligned} \bar{\underline{a}}^* &= [\bar{a}, \bar{h}, \bar{k}, \bar{p}, \bar{q}, \bar{\lambda}]^T \\ \bar{n} &= \text{mean-mean motion} \\ \underline{e}_6 &= [0, 0, 0, 0, 0, 1]^T \\ \epsilon \underline{A}_1(\bar{\underline{a}}) &= [\epsilon A_{1,1}(\bar{\underline{a}}), \epsilon A_{2,1}(\bar{\underline{a}}), \epsilon A_{3,1}(\bar{\underline{a}}), \epsilon A_{4,1}(\bar{\underline{a}}), \\ &\quad \epsilon A_{5,1}(\bar{\underline{a}}), \epsilon A_{6,1}(\bar{\underline{a}})]^T \end{aligned}$$

The vector form of the near-identity transformation is assumed to be

$$\underline{a}^* = \bar{\underline{a}}^* + \epsilon \underline{\eta}_1(\bar{\underline{a}}^*) \quad (3-33)$$

where

$$\epsilon \underline{\eta}_1(\bar{\underline{a}}) = \sum_{\sigma=1}^{\infty} [\epsilon \underline{C}_{-\sigma} \sin(\sigma \bar{\lambda}) - \epsilon \underline{D}_{-\sigma} \cos(\sigma \bar{\lambda})] \quad (3-34)$$

and where

$$\underline{\epsilon C}_{-\sigma} = [\epsilon C_{1\sigma}, \epsilon C_{2\sigma}, \epsilon C_{3\sigma}, \epsilon C_{4\sigma}, \epsilon C_{5\sigma}, \epsilon C_{6\sigma}]^T \quad (3-35)$$

$$\underline{\epsilon D}_{-\sigma} = [\epsilon D_{1\sigma}, \epsilon D_{2\sigma}, \epsilon D_{3\sigma}, \epsilon D_{4\sigma}, \epsilon D_{5\sigma}, \epsilon D_{6\sigma}]^T$$

Although the development in this chapter will only consider the case of a single time-independent disturbing force to first order in the small parameter in both the AOG and SPG, the extension to a more general case is straightforward.

Equation (3-31) can be written as

$$G = [G_2^0 \mid G_2^1] \quad (3-36)$$

where

$$G_2^0 = \begin{bmatrix} \frac{\partial \underline{a}^*(t)}{\partial \underline{\bar{a}}^*(t)} \\ \frac{\partial \bar{a}^*(t)}{\partial \underline{\bar{a}}^*(t)} \end{bmatrix} \quad (3-37a)$$

and

$$G_2^1 = \begin{bmatrix} \frac{\partial \underline{a}^*(t)}{\partial \underline{\bar{a}}^*(t)} \\ \frac{\partial \bar{a}^*(t)}{\partial \underline{\bar{a}}^*(t)} \end{bmatrix} \begin{bmatrix} \frac{\partial \bar{a}^*(t)}{\partial \underline{c}} \\ \frac{\partial \underline{a}^*(t)}{\partial \underline{c}} \end{bmatrix} + \begin{bmatrix} \frac{\partial \underline{a}^*(t)}{\partial \underline{c}} \\ \frac{\partial \bar{a}^*(t)}{\partial \underline{c}} \end{bmatrix}_{\text{explicit}} \quad (3-37b)$$

Equation (3-37b) indicates that the osculating elements have both an implicit and an explicit dependence upon the modeled parameters. The implicit dependence results because a change in the modeled parameters change the trajectory of the mean elements. The explicit dependence is due to the fact that the near-identity transformation is dependent upon the force model. Since the near-identity transformation does not explicitly depend upon the initial mean elements, Equation (3-37a) shows only an implicit dependence.

Substitution of Equations (3-37a) and (3-37b) into Equation (3-36) results in the following after some rearranging

$$G = \begin{bmatrix} \frac{\partial \underline{a}^*(t)}{\partial \underline{a}^*(t)} \end{bmatrix} \cdot \left[\begin{array}{c} \left\{ \frac{\partial \underline{a}^*(t)}{\partial \underline{a}^*(t)} \right\} \\ \left\{ \frac{\partial \underline{a}^*(t)}{\partial \underline{c}} \right\} \end{array} \right] + \left[\begin{array}{c} \left\{ 0 \right\} \\ \left\{ \frac{\partial \underline{a}^*(t)}{\partial \underline{c}} \right\} \text{ explicit} \end{array} \right] \quad (3-38)$$

From Equation (3-33) it is seen that

$$\begin{bmatrix} \frac{\partial \underline{a}^*(t)}{\partial \underline{a}^*(t)} \end{bmatrix} = \left[\mathbf{I} + \left\{ \frac{\partial \epsilon \underline{\eta}_1(\underline{a}^*)}{\partial \underline{a}^*(t)} \right\} \right] \quad (3-39)$$

and

$$\left[\frac{\partial \underline{a}^*(t)}{\partial \underline{c}} \right]_{\text{explicit}} = \left[\frac{\partial \epsilon \eta_1(\underline{a}^*)}{\partial \underline{c}} \right] \quad (3-40)$$

Equation (3-38) can therefore be written as

$$G = [I + B_1][B_2 \mid B_3] + [0 \mid B_4] \quad (3-41)$$

where

$$B_2 = \left[\frac{\partial \underline{a}^*(t)}{\partial \underline{a}_o^*} \right]_{6 \times 6} \quad (3-42)$$

$$B_3 = \left[\frac{\partial \underline{a}^*(t)}{\partial \underline{c}} \right]_{6 \times (\ell-6)} \quad (3-43)$$

$$B_1 = \left[\frac{\partial \epsilon \eta_1(\underline{a}^*)}{\partial \underline{a}^*(t)} \right]_{6 \times 6} \quad (3-44)$$

$$B_4 = \left[\frac{\partial \epsilon \eta_1(\underline{a}^*)}{\partial \underline{c}} \right]_{6 \times (\ell-6)} \quad (3-45)$$

The matrices B_1 and B_4 represent the short periodic portion of the semianalytical partial derivatives and will be called the Short Periodic Partial Generator (SPPG). The B_2 and B_3 matrices are the partial derivatives of the mean elements with respect to the solve-for parameters and will be called the

Averaged Partial Generator (APG). The similarities between the APG/SPPG and the AOG/SPG are evident.

The differential equations for the APG can be obtained from the averaged equations of motion. Taking the partial derivatives of Equation (3-32) with respect to the solve-for vector, it is seen that

$$\left[\frac{\partial \dot{\bar{a}}^*(t)}{\partial \bar{a}_o^*} \right] = \left[\frac{\partial \{ \bar{n} \underline{e}_6 + \epsilon \underline{A}_1(\bar{a}) \}}{\partial \bar{a}^*(t)} \right] \left[\frac{\partial \bar{a}^*(t)}{\partial \bar{a}_o^*} \right] \quad (3-46a)$$

$$\begin{aligned} \left[\frac{\partial \dot{\bar{a}}^*(t)}{\partial \underline{c}} \right] &= \left[\frac{\partial \{ \bar{n} \underline{e}_6 + \epsilon \underline{A}_1(\bar{a}) \}}{\partial \bar{a}^*(t)} \right] \left[\frac{\partial \bar{a}^*(t)}{\partial \underline{c}} \right] \\ &+ \left[\frac{\partial \{ \bar{n} \underline{e}_6 + \epsilon \underline{A}_1(\bar{a}) \}}{\partial \underline{c}} \right] \text{explicit} \end{aligned} \quad (3-46b)$$

Equation (3-46b) indicates that the partial derivatives of the mean element rates with respect to the modeled parameters have both an implicit and explicit dependence. Assuming that the mean elements are "well-behaved," it is possible to interchange the order of differentiation on the left hand side of Equations (3-46a) and (3-46b). This results in

$$\frac{d}{dt} \left[\frac{\partial \bar{a}^*(t)}{\partial \bar{a}_o^*} \right] = \left[\frac{\partial [\dot{\bar{a}}^*]}{\partial \bar{a}^*(t)} \right] \left[\frac{\partial \bar{a}^*(t)}{\partial \bar{a}_o^*} \right] \quad (3-47a)$$

$$\frac{d}{dt} \left[\frac{\partial \bar{a}^*(t)}{\partial \underline{c}} \right] = \left[\frac{\partial [\dot{\bar{a}}^*]}{\partial \bar{a}^*(t)} \right] \left[\frac{\partial \bar{a}^*(t)}{\partial \underline{c}} \right] + \left[\frac{\partial [\dot{\bar{a}}^*]}{\partial \underline{c}} \right]$$

(3-47b)

where it is understood that $[\dot{\bar{a}}^*]$ stands for the right hand side of the averaged equations of motion. It is also noted

that at the epoch time, $\left[\frac{\partial \bar{a}^*(t_0)}{\partial \bar{a}^*_0} \right]$ is equal to the identity

matrix and $\left[\frac{\partial \bar{a}^*(t_0)}{\partial \underline{c}} \right]$ is equal to the null matrix. This last

fact is true because a change in the modeled parameters at epoch will not affect the value of the mean elements at epoch. Therefore the APG can be expressed as

$$\dot{B}_2 = A B_2 \quad \text{with } B_2|_{t_0} = I \quad (3-48)$$

and

$$\dot{B}_3 = A B_3 + D \quad \text{with } B_3|_{t_0} = 0 \quad (3-49)$$

where

$$A = \left[\frac{\partial [\dot{\bar{a}}^*]}{\partial \bar{a}^*(t)} \right]_{6 \times 6} \quad (3-50)$$

and

$$D = \left[\begin{array}{c} \frac{\partial [\dot{\underline{a}}^*]}{\partial \underline{c}} \end{array} \right]_{6 \times (\ell-6)} \quad (3-51)$$

Since the mean element rates do not contain the fast variable ($\bar{\lambda}$), the sixth column of the A matrix will contain all zeroes. The A and D matrices are functions of only the five slowly varying mean elements and therefore the integration of the APG can be done with the same numerical integration time step associated with the AOG (1 day). The determination of the B_2 and B_3 matrices at the output/observation times can be done with an interpolator.

The SPPG (B_1 and B_4 matrices) can be obtained by a direct application of Equations (3-44) and (3-45). If the short periodic functions are expressed in terms of a Fourier series representation [see Equations (3-34) and (3-35)] and if it is noted that the short periodic coefficients ($\epsilon C_{-\sigma}$ and $\epsilon D_{-\sigma}$) are functions of the five slowly varying elements only, it is seen that the B_1 and B_4 matrices can be written

$$B_1 = \left\{ \left[\sum_{\sigma=1}^{\infty} \left\{ M_{\sigma} [\sin(\sigma\bar{\lambda})] - N_{\sigma} [\cos(\sigma\bar{\lambda})] \right\} \right]_{6 \times 5} \left\{ \left[\sum_{\sigma=1}^{\infty} \left\{ \begin{array}{l} \epsilon C_{-\sigma} \cos(\sigma\bar{\lambda}) \\ + \epsilon D_{-\sigma} \sin(\sigma\bar{\lambda}) \end{array} \right\} \right]_{6 \times 1} \right\} \right\} \quad (3-52)$$

$$B_4 = \left\{ \sum_{\sigma=1}^{\infty} \left[K_{\sigma} [\sin(\sigma\bar{\lambda})] - L_{\sigma} [\cos(\sigma\bar{\lambda})] \right] \right\}_{6 \times (\ell-6)} \quad (3-53)$$

where

$$M_{\sigma} = \begin{bmatrix} \partial & \varepsilon C_{\sigma} \\ \partial & \bar{a}(t) \end{bmatrix}_{6 \times 5} \quad (3-54a)$$

$$N_{\sigma} = \begin{bmatrix} \partial & \varepsilon D_{\sigma} \\ \partial & \bar{a}(t) \end{bmatrix}_{6 \times 5} \quad (3-54b)$$

$$K_{\sigma} = \begin{bmatrix} \partial & \varepsilon C_{\sigma} \\ \partial \underline{c} \end{bmatrix}_{6 \times (\ell-6)} \quad (3-54c)$$

$$L_{\sigma} = \begin{bmatrix} \partial & \varepsilon D_{\sigma} \\ \partial \underline{c} \end{bmatrix}_{6 \times (\ell-6)} \quad (3-54d)$$

and where $[\sin(\sigma\bar{\lambda})]$ and $[\cos(\sigma\bar{\lambda})]$ are square matrices $[5 \times 5$ or $(\ell-6) \times (\ell-6)]$ with $\sin(\sigma\bar{\lambda})$ or $\cos(\sigma\bar{\lambda})$, respectively, for each of the main diagonal elements and zero for all the off-diagonal elements. The M_{σ} , N_{σ} , K_{σ} and L_{σ} matrices are functions of only the five slowly varying mean elements (\bar{a}). It should therefore be possible to determine these matrices on the large integration grid and interpolate to obtain them at the output/

observation times. This should greatly reduce the computational costs associated with the SPPG.

The APG and SPPG are summarized in Table 3-2. An obvious advantage of the semianalytical partial derivatives is that the APG and SPPG can be considered independent of each other. In other words, the force models of the APG and SPPG could be completely different. It would even be possible to completely neglect the SPPG.

The A , D , B_1 and B_4 matrices must be determined in order to obtain the semianalytical partial derivatives of perturbed motion. These matrices can be obtained by analytical, quadrature or finite-differencing approaches.

Analytical expressions for the A , D , B_1 and B_4 matrices are obtained by taking the indicated partial derivatives of the analytical expressions for the mean element rates and short periodic functions. For example, the A and B_1 matrices, corresponding to J_2 effects, could be obtained by taking the required partial derivatives of Zeis' or Kaniecki's expressions for the J_2 mean element rates or short periodic functions* (Refs. 6 or 69). The M_0 and N_0 matrices could be obtained by taking the indicated partial derivatives of ϵC_{i0} and ϵD_{i0} as

* Recent development efforts at the Draper Laboratory have implemented into GTDS-RD the analytical expressions for the A and B_1 matrices due to J_2 effects.

Table 3-2
Semianalytical Partial Derivative Generator

$$G = \left[\left\{ \frac{\partial \underline{a}^*(t)}{\partial \underline{a}_0} \right\} \middle| \left\{ \frac{\partial \underline{a}^*(t)}{\partial \underline{c}} \right\} \right]$$

$$G = [I + B_1][B_2 \mid B_3] + [0 \mid B_4]$$

THE APG

$$\dot{B}_2 = AB_2 \quad B_2|_{t=t_0} = I$$

$$\dot{B}_3 = AB_3 + D \quad B_3|_{t=t_0} = 0$$

$$A = \left[\frac{\partial [\dot{\underline{a}}^*]}{\partial \underline{a}^*(t)} \right] \quad D = \left[\frac{\partial [\dot{\underline{a}}^*]}{\partial \underline{c}} \right]$$

THE SPPG

$$B_1 = \left[\frac{\partial \epsilon \eta_1(\underline{a}^*)}{\partial \underline{a}^*(t)} \right] \quad B_4 = \left[\frac{\partial \epsilon \eta_1(\underline{a}^*)}{\partial \underline{c}} \right]$$

$$B_1 = \left\{ \left[\sum_{\sigma=1}^{\infty} \{M_{\sigma}[\sin(\sigma\bar{\lambda})] - N_{\sigma}[\cos(\sigma\bar{\lambda})]\} \right] \middle| \left[\sum_{\sigma=1}^{\infty} \{ \epsilon \underline{C}_{\sigma} \cos(\sigma\bar{\lambda}) + \epsilon \underline{D}_{\sigma} \sin(\sigma\bar{\lambda}) \} \right] \right\}$$

$$B_4 = \left\{ \sum_{\sigma=1}^{\infty} \left[K_{\sigma}[\sin(\sigma\bar{\lambda})] - L_{\sigma}[\cos(\sigma\bar{\lambda})] \right] \right\}$$

$$M_{\sigma} = \left[\frac{\partial \epsilon \underline{C}_{\sigma}}{\partial \underline{a}(t)} \right] \quad N_{\sigma} = \left[\frac{\partial \epsilon \underline{D}_{\sigma}}{\partial \underline{a}(t)} \right] \quad K_{\sigma} = \left[\frac{\partial \epsilon \underline{C}_{\sigma}}{\partial \underline{c}} \right] \quad L_{\sigma} = \left[\frac{\partial \epsilon \underline{D}_{\sigma}}{\partial \underline{c}} \right]$$

given in Table 2-2. The analytical approach yields expressions which are generally more accurate and computationally more efficient than the quadrature or finite-differencing approaches.

The required matrices can also be obtained by a quadrature approach. From Equations (2-22) and (2-28) it is seen that

$$\dot{\bar{a}}_i = \bar{n} \delta_{i6} + \frac{1}{2\pi} \int_0^{2\pi} \epsilon F_i(\bar{a}, \bar{\lambda}) d\bar{\lambda} \quad (3-55a)$$

where $\epsilon F_i(\bar{a}, \bar{\lambda})$ is the disturbing function for the i th element, \bar{n} is the mean-mean motion and δ_{i6} is the Kroenecker Delta function defined in Equation (2-24). Define the vector \underline{x} as the state vector at time t , i.e.,

$$\underline{x} = \underline{x}(t) = \begin{bmatrix} \bar{a}^*(t) \\ \underline{c} \end{bmatrix} \quad (3-55b)$$

It is noted that $\underline{x}(t_0)$ is the solve-for vector [see Equation (3-23)]. Taking the required partial derivatives of Equation (3-55a) and interchanging the order of integration and differentiation, it is seen that

$$\begin{aligned} [A \mid D]_{ij} &= \left[\frac{\partial [\dot{\bar{a}}_i]}{\partial x_j} \right] = - \left(\frac{3\bar{n}}{2\bar{a}_1} \right) \delta_{i6} \delta_{1j} \\ &+ \frac{1}{2\pi} \int_0^{2\pi} \left[\frac{\partial \epsilon F_i(\bar{a}, \gamma)}{\partial x_j} \right] d\gamma \end{aligned} \quad (3-56)$$

where γ is used as the dummy variable in the integration operation, x_j represents the j th element of the vector \underline{x} and where $[A \mid D]_{ij}$ represents the element in the i th row and j th column of the 6×6 matrix $[A \mid D]$. The direct application of a quadrature algorithm to Equation (3-56) allows the determination of the A and D matrices. It should be noted that the sixth column of the $[A \mid D]$ matrix will be zero since $\left[\frac{\partial \epsilon F(\bar{a}, \gamma)}{\partial \bar{\lambda}} \right] = 0$.

Similarly, the short periodic coefficient matrices M_σ , N_σ , K_σ and L_σ can be obtained by taking the respective partial derivatives of $\epsilon C_{i\sigma}$ and $\epsilon D_{i\sigma}$ as given in Table 2-1. The resulting expressions can be written as

$$\begin{aligned}
 [M_\sigma \mid 0 \mid K_\sigma]_{ij} &= \left[\frac{\partial \epsilon C_{i\sigma}}{\partial x_j} \right] = \frac{1}{\sigma n \pi} \int_0^{2\pi} \left[\frac{\partial \epsilon F_i(\bar{a}, \gamma)}{\partial x_j} \right] \cos(\sigma \gamma) d\gamma \\
 &+ \left[\frac{3\epsilon C_{i\sigma}}{2\bar{a}_1} - \frac{9\epsilon D_{1\sigma} \delta_{i6}}{4\sigma (\bar{a}_1)^2} \right] \delta_{1j} \\
 &+ \left[\frac{3[N_\sigma \mid 0 \mid L_\sigma]_{1j}}{2\sigma \bar{a}_1} - \frac{3\epsilon D_{1\sigma} \delta_{1j}}{2\sigma (\bar{a}_1)^2} \right] \delta_{i6}
 \end{aligned}$$

(3-57a)

$$\begin{aligned}
[N_{\sigma} \mid 0 \mid L_{\sigma}]_{ij} &= \left[\frac{\partial \epsilon D_{i\sigma}}{\partial x_j} \right] = \frac{1}{\sigma \bar{n} \pi} \int_0^{2\pi} \left[\frac{\partial \epsilon F_i(\bar{a}, \gamma)}{\partial x_j} \right] \sin(\sigma \gamma) d\gamma \\
&+ \left[\frac{3\epsilon D_{i\sigma}}{2\bar{a}_1} - \frac{9\epsilon C_{1\sigma} \delta_{i6}}{4\sigma (\bar{a}_1)^2} \right] \delta_{1j} \\
&- \left[\frac{3[M_{\sigma} \mid 0 \mid K_{\sigma}]_{1j}}{2\sigma \bar{a}_1} - \frac{3\epsilon C_{1\sigma} \delta_{1j}}{2\sigma (\bar{a}_1)^2} \right] \delta_{i6}
\end{aligned}
\tag{3-57b}$$

It is noted that the major portion of Equations (3-56), (3-57a) and (3-57b) is the evaluation of the partial derivative of the

disturbing function, i.e., $\left[\frac{\partial \epsilon F_i(\bar{a}, \gamma)}{\partial x_j} \right]$. By saving the integrand of Equation (3-56) when the A and D matrices are determined and multiplying by $\sin(\sigma \gamma)$ or $\cos(\sigma \gamma)$ and then applying the same quadrature algorithm, the M_{σ} , N_{σ} , K_{σ} and L_{σ} can be obtained at minimum computational costs. Knowing the M_{σ} , N_{σ} , K_{σ} and L_{σ} matrices, the B_1 and B_4 can be obtained by applying Equations (3-52) and (3-53).

A finite-differencing approach for the determination of the A, D, M_{σ} , N_{σ} , K_{σ} and L_{σ} matrices is discussed in the next section.

3.2.2 Determination of the Semianalytical Partial Derivatives by Finite-Differencing of Slowly Varying Quantities

As was previously indicated, the determination of the semianalytical partial derivatives requires the determination of the A , D , M_σ , N_σ , K_σ and L_σ matrices. A finite-differencing approach can be used to obtain these matrices. It is noted that these matrices are functions of the five slowly varying mean elements and therefore are slowly varying themselves.

An obvious advantage of a finite-differencing approach is that the force models and much of the software of the AOG and SPG can be used. This permits minimum software development in implementing the semianalytical partial derivatives. This also makes it possible to easily change the perturbation models that are included in the semianalytical partial derivatives.

In this development, a double-sided finite-differencing approach (see Appendix B) was used to determine the A , D , M_σ , N_σ , K_σ and L_σ matrices. Functionally the finite-differencing approach used can be written as

$$[A \mid D]_{ij} \sim \frac{\dot{a}_i(x_j + \Delta x_j) - \dot{a}_i(x_j - \Delta x_j)}{2\Delta x_j} \quad (3-58a)$$

$$[M_{\sigma} \mid 0 \mid K_{\sigma}]_{ij} \sim \frac{\varepsilon C_{i\sigma}(x_j + \Delta x_j) - \varepsilon C_{i\sigma}(x_j - \Delta x_j)}{2\Delta x_j} \quad (3-58b)$$

$$[M_{\sigma} \mid 0 \mid L_{\sigma}]_{ij} \sim \frac{\varepsilon D_{i\sigma}(x_j + \Delta x_j) - \varepsilon D_{i\sigma}(x_j - \Delta x_j)}{2\Delta x_j} \quad (3-58c)$$

where x_j is the j th element of the vector \underline{x} as defined in Equation (3-55b) and where $[]_{ij}$ denotes the element in the i th row and j th column of the matrix as indicated in $[]$. In this development it was found that good results were obtained when Δx_j was 10^{-5} of x_j , i.e.,

$$\Delta x_j = (10^{-5})x_j \quad (3-59)$$

The A and D matrices were computed at the request times of the integrator in subroutine 'VARDIF' (see Appendix F). The short periodic coefficient matrices, M_{σ} , N_{σ} , K_{σ} and L_{σ} were computed at the output/observation times in subroutine 'VRSPFD' (see Appendix F). The concept of determining the short periodic coefficient matrices on the integration grid and using an interpolator to obtain them at the output/observation times was not explored in this research.

The actual implementation into GTDS-RD uses the initial mean position and mean velocity vectors as the state solve-for vector. Therefore, the actual solve-for vector in GTDS-RD can be written as

$$\underline{x}(t_0) = \begin{bmatrix} \underline{\bar{R}}(t_0) \\ \dot{\underline{\bar{R}}}(t_0) \\ \underline{c} \end{bmatrix} \quad (3-60)$$

where $\underline{\bar{R}}(t_0)$ and $\dot{\underline{\bar{R}}}(t_0)$ are the mean position and velocity vectors associated with the mean elements $\underline{\bar{a}}^*$. The only matrix which is different than previously defined is the B_2 matrix. The B_2 matrix which is implemented into GTDS-RD is defined as follows

$$B_2 = \left[\left\{ \frac{\partial \underline{\bar{a}}^*(t)}{\partial \underline{\bar{R}}(t_0)} \right\} \middle| \left\{ \frac{\partial \underline{\bar{a}}^*(t)}{\partial \dot{\underline{\bar{R}}}(t_0)} \right\} \right]_{6 \times 6} \quad (3-61)$$

where

$$\dot{B}_2 = AB_2 \quad (3-62a)$$

with the initial conditions

$$B_2|_{t_0} = \left[\left\{ \frac{\partial \underline{\bar{a}}^*(t_0)}{\partial \underline{\bar{R}}(t_0)} \right\} \middle| \left\{ \frac{\partial \underline{\bar{a}}^*(t_0)}{\partial \dot{\underline{\bar{R}}}(t_0)} \right\} \right] \quad (3-62b)$$

Equation (3-62b) comes from the two-body relationships between the position and velocity and the equinoctial orbital elements (see Ref. 74 for a listing of these derivatives). The A matrix is as defined in Equation (3-50).

The remainder of this section presents some numerical results of the semianalytical partial derivatives. First the semianalytical partial derivatives are compared to the high precision Cowell partial derivatives. Next some results with changing the perturbation model of the APG and SPPG are presented.

Comparison with Cowell Partial Derivatives

The Cowell partial derivatives are defined as follows

$$Z(t) = \left[\begin{array}{c|c} \left\{ \frac{\partial \underline{R}(t)}{\partial \underline{R}(t_0)} \right\} & \left\{ \frac{\partial \underline{R}(t)}{\partial \dot{\underline{R}}(t_0)} \right\} \\ \hline \left\{ \frac{\partial \dot{\underline{R}}(t)}{\partial \underline{R}(t_0)} \right\} & \left\{ \frac{\partial \dot{\underline{R}}(t)}{\partial \dot{\underline{R}}(t_0)} \right\} \end{array} \right] \quad (3-63)$$

The semianalytical partial derivatives are defined as

$$Y(t) = \left[\begin{array}{c} \left\{ \frac{\partial \underline{R}(t)}{\partial \underline{a}^*(t)} \right\} \\ \hline \left\{ \frac{\partial \dot{\underline{R}}(t)}{\partial \underline{a}^*(t)} \right\} \end{array} \right] G \quad (3-64a)$$

where the G matrix is defined in Equation (3-41) with the B_2 matrix as given in Equation (3-61). This can be rewritten as

$$Y(t) = \left[\begin{array}{c|c} \left\{ \frac{\partial \underline{R}(t)}{\partial \underline{R}(t_0)} \right\} & \left\{ \frac{\partial \underline{R}(t)}{\partial \dot{\underline{R}}(t_0)} \right\} \\ \hline \left\{ \frac{\partial \dot{\underline{R}}(t)}{\partial \underline{R}(t_0)} \right\} & \left\{ \frac{\partial \dot{\underline{R}}(t)}{\partial \dot{\underline{R}}(t_0)} \right\} \end{array} \right] \quad (3-64b)$$

The Cowell partial derivatives and the semianalytical partial derivatives can be compared at time t by use of the following relation

$$Z(t) = Y(t) [Y(t_0)]^{-1} \quad (3-65)$$

This can be rewritten as

$$Z(t) Y(t_0) = Y(t) \quad (3-66)$$

Equation (3-66) allows a comparison of the semianalytical partial derivatives to the Cowell partial derivatives. A matrix multiplication of the Cowell partial derivatives at time t and the epoch semianalytical partial derivatives should yield the semianalytical partial derivatives at time t.

The above comparison was done for a low altitude satellite (similar to the Low Altitude Circular Test Case of Section 2.4.3) with the initial conditions and parameters as given in Table 3-3. The perturbation models used in the partial derivative test are given in Table 3-4. In the SPG the notation (7/48) indicates that 7 short periodic coefficients were used with a 48 point numerical quadrature. Likewise, in the SPPG the notation (5/48) indicates that 5 short periodic coefficient matrices were used in the determination of the B_1 matrix [see Equation (3-52)] and a 48 point quadrature algorithm was used in the determination of the short periodic coefficients. The comparison was done at a time of 2 days into the orbit generation. The computer printout of the partial derivatives in GTDS-RD shows only four (4) significant digits. The above comparison [Equation (3-66)] agreed to the four significant digits shown. Comparisons at other times between 1 and 2 days gave similar results. Some discrepancies were noted in a few of the elements in the 4th significant digit. These discrepancies were probably due to round-off errors.

It is felt that the above tests verify the theoretical developments of Section 3.2.1 and the finite-differencing approach presented in this section.

Table 3-3
Initial Conditions and Parameters for the
Partial Derivative Test

Initial Conditions: [EPC]⁻¹

<u>Mean Elements</u>	<u>Osculating Elements</u>
\bar{a} = 6644.586 km	a = 6652.796017 km
\bar{e} = .01	e = .009397030651
\bar{i} = 67.98538419°	i = 67.99983930°
$\bar{\Omega}$ = 91.99738418°	Ω = 91.99985809°
$\bar{\omega}$ = 200.6741688°	ω = 201.1973744°
\bar{M} = 164.3173126°	M = 163.8032616°

Parameters:

Epoch	= 10 hrs. 24 min. 21 Oct 1974
Reference Frame	= True of Date
C_D	= 2.0
Area	= 1.86 m ²
Mass	= 677 kg
Density	= Modified Harris-Priester with $\bar{F}_{10.7} = 150 \cdot 10^{-22}$ watts m ⁻² Hz ⁻¹

Table 3-4

Perturbation Models for the Partial Derivative Test

Cowell: 6x0 gravitational field and drag effects with a 30 second integration time step for both the equations of motion and the variational equations (partial derivatives).

Semianalytical:

AOG and APG

6x0 gravitational field (analytical), Zeis' J_2^2 expressions, drag option: 7 (4/48): 1 day numerical integration time step.

SPG

6x0 gravitational field and drag to first order with a time-independent formulation (7/48), Zeis' corrected analytical J_2^2 expressions

SPPG

6x0 gravitational field and drag to first order with time-independent formulation (5/48)

Initial Conditions: $[EPC]^{-1}$, see Table 3-3

Comparison with Different Perturbation Models

A comparison of the semianalytical partial derivatives obtained with different perturbation models is presented in Table 3-5. The low altitude test case of Table 3-3 was used. All comparisons were made to the semianalytical partial derivatives obtained with the perturbations as given in Table 3-4. The comparisons in Table 3-5 were done at 2 days from epoch. It is noted that at this time the baseline partial derivatives were shown to equal the Cowell partial derivatives to at least 4 significant digits.

The number of significant digits indicates that all the partial derivatives agreed to the baseline partial derivatives for that many significant digits. For example, two (2) significant digits in Table 3-5 indicates that all the partial derivatives had the first two digits agreeing with the baseline. Some of the elements may agree to more than 2 significant digits but all had at least two significant digits. The notation 2^- indicates that some of partial derivatives (one to three) did not agree to two significant digits. Table 3-5 should be viewed as a very coarse measurement of the effects of different perturbations on the semianalytical partial derivatives. It is also noted again that the computer printout showed only four significant digits and that round-off in the fourth digit could be causing some of the apparent agreements or disagreements.

Table 3-5

Comparison* of the Semianalytical Partial Derivatives
with Different Perturbations

Run #	Perturbation Model**		# Significant Digits at 2 days from Epoch
	APG [†]	SPPG ^{††}	
A	J_2	---	2
B	J_2	J_2	3 ⁻
C	J_2 and drag option 1	---	2
D	J_2 and drag option 2	---	3
E	J_2 and drag option 2	J_2	4 ⁻
F	J_2 , J_2^2 and drag option 2	J_2	4 ⁻
G	J_2 - J_6 , J_2^2 and drag option 2	---	3
H	J_2 - J_6 , J_2^2 and drag option 2	J_2 - J_6	4

* The baseline was the semianalytical partial derivatives obtained with the initial conditions, parameters and perturbations of Tables 3-3 and 3-4.

** Initial conditions and parameters as given in Table 3-3. The AOG and SPG had perturbations as given in Table 3-4.

† Analytical expressions were used for the element rates due to the gravitational field, drag options (see Section 2.4.1) used a 48 point numerical quadrature.

†† First order time-independent formulation, (5/48).

From Table 3-5 it can be concluded that drag perturbations do not need to be included in the SPPG (at least for the case considered). It also appears that for precision semi-analytical partial derivatives, J_2 effects need to be considered in the SPPG*. For the case considered, the APG must include at least J_2 effects and drag effects with Izsak's height correction (see Section 2.4.1). It is interesting to note that the batch filter results presented in the next section used perturbation models equivalent to Run G of Table 3-5. The analytical partial derivatives that are currently in GTDS-RD were also determined for this test case and only one (1) significant digit of agreement with the baseline of Table 3-5 was obtained.

3.3 Numerical Results of the Semianalytical Batch Filter

This section presents some of the numerical results obtained with the semianalytical batch filter. It is felt that the results presented in this section demonstrate the semi-analytical batch filter and the concept of adaptive parameter estimation of the drag formulation for low altitude satellites. Again it should be noted that this research was primarily concerned with demonstrating the accuracy and feasibility of the semianalytical batch filter. Development efforts now in progress are concerned with improving the computational efficiency as well as the accuracy of the semianalytical batch filter.

* Recent development efforts at the CSDL have included analytical expressions for the B_1 matrix.

An overview of the software used in the current investigation is presented first in this section. Next, the test philosophy used is explained. Three separate test cases are presented and discussed.

3.3.1 Software Overview

The semianalytical batch filter, as described in Sections 3.1 and 3.2, has been implemented into a specially modified version of GTDS-RD that operates on an Amdahl 470 V6 computer at the Charles Stark Draper Laboratory in Cambridge, MA. A detailed description of the software used to implement the semianalytical batch filter is presented in Appendix F.

The batch filter of GTDS-RD is given in Table 3-1. The solve-for vector for the semianalytical batch filter is the initial mean position vector, the initial mean velocity vector and a vector of modeled parameters [see Equation (3-60)]. The semianalytical partial derivatives, as described in Section 3.2, were coupled to the batch filter of Table 3-1. The coordinate transformations, observation models and partial derivatives of the observation models that are presently in GTDS-RD were not modified [see Equation (3-28) and Appendix G].

A Cowell batch filter will refer to a batch filter which uses a Cowell orbit generator (SP theory). The term

states will refer to the initial conditions (the first six elements of the solve-for vector) of the equations of motion. For a Cowell batch filter the states are the initial osculating position and velocity vectors. For a semianalytical batch filter the states are the initial mean position and velocity vectors. It should be noted that the orbital elements (osculating or mean) corresponding to the initial state can be obtained by the two-body relations (see Section 2.1.1). The results presented in this section are usually expressed in terms of the osculating and/or mean orbital elements.

The Cowell batch filter in GTDS-RD currently has two estimation options for the drag formulation (see Table 3-6). The first option is to solve for the states only. In other words, no modeled parameters are solved for in this option. The second option is to solve for the states and the variation in the drag coefficient (ρ_1). The drag coefficient is written as (Ref. 67)

$$C_D = C_{D0}(1 + \rho_1) \quad (3-67)$$

The a priori guess of ρ_1 is usually taken as zero.

The semianalytical batch filter, when the Adaptive Modified Harris-Priester density model (see Appendix C) is used, has 6 estimation options. These options are listed in Table 3-6.

It should be noted that setting the adaptive parameters in the Adaptive Modified Harris-Priester density model to the following

$$\begin{aligned} a_1 &= a_2 = 1.0 \\ a_3 &= 6.0 \\ a_4 &= a_5 = 0.0 \end{aligned} \tag{3-68}$$

yields the standard Modified Harris-Priester atmosphere of GTDS-RD. Equation (3-68) is usually the a priori guess for the adaptive parameters in the Adaptive Modified Harris-Priester atmosphere.

The semianalytical batch filter and Cowell batch filter allow the inclusion of an a priori covariance matrix associated with the a priori solve-for vector (see Table 3-1 and/or Section 3.1). The a priori covariance matrix (P_0) is assumed diagonal with the diagonal elements equal to the respective variance ($\sigma_{x_i}^2$) of the a priori solve-for parameters. If the variances of the a priori solve-for parameters are not given, the P_0 matrix is neglected in the implementation of Table 3-1. It is also possible to include some of the a priori variances and neglect others. For example, if in the states and C_D estimation option, only the variance of the a priori value of C_D is included, the P_0^{-1} matrix of Table 3-1 would be written as

$$P_0^{-1} = \left\{ \begin{array}{c|c} [0]_{6 \times 6} & 0 \\ \hline 0 & \frac{1}{\sigma_{C_D}^2} \end{array} \right\} \quad (3-69)$$

It will be assumed in the remainder of this chapter that if the variance of an a priori solve-for parameter is not given, its respective element on the main diagonal of P_0^{-1} will be zero. Likewise, if the variance of an a priori solve-for parameter is given, its corresponding element on the main diagonal of P_0^{-1} will be $\frac{1}{\sigma_{x_i}^2}$.

The convergence criteria in GTDS-RD is based on iterative reduction of the square root of the mean square of the observation residuals (Ref. 67). This is expressed as

$$\text{RMS} = \left\{ \frac{1}{p} [\delta \underline{b}_{-k}^T W \delta \underline{b}_{-k} + \delta \underline{\tilde{x}}_k(t_0^-) P_0^{-1} \delta \underline{x}_k(t_0^-)] \right\}^{1/2} \quad (3-70)$$

where $\delta \underline{b}_{-k}$, P_0 , W and $\delta \underline{\tilde{x}}_k(t_0^-)$ are defined in Table 3-1 and where p is the number of observations. The predicted RMS is computed by the following formula (Ref. 67)

$$\text{RMSP} = \left\{ \frac{1}{p} \left[[\delta \underline{b}_{-k} - F \hat{\delta \underline{x}}_k(t_0)]^T W [\delta \underline{b}_{-k} - F \hat{\delta \underline{x}}_k(t_0)]^T + [\hat{\delta \underline{x}}_k(t_0) - \delta \underline{\tilde{x}}_k(t_0^-)]^T P_0^{-1} [\hat{\delta \underline{x}}_k(t_0) - \delta \underline{\tilde{x}}_k(t_0^-)] \right] \right\}^{1/2} \quad (3-71)$$

where F and $\hat{\delta x}_k(t_0)$ are defined in Table 3-1. If the value of the RMS [Equation (3-70)] decreases during two consecutive iterations, the solution is converging. The batch filter is considered converged when the following is true (Ref. 67)

$$\left| \frac{\text{RMSB} - \text{RMSP}}{\text{RMSB}} \right| < \zeta \quad (3-72)$$

where

RMSB \equiv the smallest RMS achieved

ζ \equiv tolerance criteria

Table 3-6
Estimation Options

<u>Cowell Batch Filter</u>	<u>Semianalytical Batch Filter*</u>
1. States only ($\underline{R}_0, \dot{\underline{R}}_0$)	1. States only ($\bar{\underline{R}}_0, \dot{\bar{\underline{R}}}_0$)
2. States and ρ_1 [$C_D = C_{D0}(1 + \rho_1)$]	2. States and C_D
	3. States, a_1, a_2, a_3, a_4 and a_5
	4. States, a_1, a_2 and a_3
	5. States, a_1 and a_2
	6. States, C_D and a_4

* see Adaptive Modified Harris-Priester density model in Appendix C.

GTDS-RD contains a Data Simulation (Datasim) Program which computes simulated observations for a given set of tracking stations and observation intervals (Ref. 73). The Datasim Program requires a satellite ephemeris. The simulated observations are based upon the observation models in GTDS-RD (see Ref. 67 or Appendix G) and are computed at a specified frequency. Random and bias errors can be included in the observations. No modifications were made to the Datasim Program of GTDS-RD in this research.

3.3.2 Test Philosophy

The test philosophy used in this research is presented in Table 3-7. The truth ephemeris is generated with the Cowell orbit generator. The density model used in the truth ephemeris is generally the Analytical Jacchia Roberts density (the first test case used the Modified Harris-Priester atmosphere).

Table 3-7

Orbit Determination Test Philosophy

1. Generate truth ephemeris
2. Simulate observations using the truth ephemeris in the Datasim Program.
3. Process the observations with operational force models in the Batch Filter.
4. Predict the orbit using the operational force models and solve-for vector obtained from the Batch Filter.
5. Compare the predicted ephemeris to the truth ephemeris.

An observation net is assumed and the Datasim Program of GTDS-RD is used to generate simulated observations over an assumed observation time. The simulated observations are processed in a semianalytical or Cowell batch filter to give the solve-for vector associated with the various estimation options. The batch filter uses force models which are generally different than the force models used to generate the truth ephemeris. For the cases considered in this research, the density models were different. A predicted ephemeris, corresponding to the solve-for vector, is then determined by using the same orbit generator and force models that were associated with the solve-for vector in the data processing step. The predicted ephemeris is then compared to the truth ephemeris.

3.3.3 Test Case One

This test case was used to demonstrate that the implementation of the semianalytical batch filter was correct and that modeling errors could be sensed by the filter.

Tables 3-8 and 3-9 give the truth ephemeris and data simulation for Test Case One. It is noted that the truth ephemeris used the standard form of the Modified Harris-Priester density model.

Table 3-8
Truth Ephemeris for Test Case One

Initial Osculating Elements and Parameters

a = 6644.586 km	Epoch	= 1024 hrs. 21 Oct 1974
e = .01	Reference Frame	= True of Date
i = 67.98538419°	C_D	= 2.0
Ω = 91.99738418°	Area	= 1.86 m ²
ω = 200.6741688°	Mass	= 677 kg
M = 164.3173126°		

Perturbations

6x0 gravitational field with drag. The Modified Harris-Priester Atmosphere was used ($a_1 = a_2 = 1$, $a_3 = 6$, $a_4 = a_5 = 0$). $\bar{F}_{10.7}$ was $150 \cdot 10^{-22}$ watts m⁻² Hz⁻¹

Orbit Generator

Cowell orbit generator with a 30 second numerical integration time step was used (12th order Adams-Bashforth Predictor/Adams-Moulton Corrector integrator).

Table 3-9
Data Simulation for Test Case One

Tracking Stations: Net A (see Table 3-10)

Observation Type: VHF range (ρ) and range rate ($\dot{\rho}$)

$$\sigma_{\rho} = 5 \text{ meters} \quad \sigma_{\dot{\rho}} = .55 \text{ cm/sec}$$

Observations: Generated every 60 seconds while in sight (15° minimum elevation). Maximum time of observation interval per satellite pass is 300 seconds. No random noise included.

Observation Span: From Epoch to 1000 hrs 22 Oct. 1974

Truth Ephemeris: see Table 3-8

Table 3-10
Tracking Net A

Station Name	Symbol	Latitude (deg.)	Longitude (deg.)	Height (m.)
Canberra	CANV	-35.5833900	148.9777300	1149
Carnarvon	CARV	-24.9066444	113.7253249	8
Guam	UAMV	13.3104666	144.7374610	76
Dodaira	DODV	36.0055300	139.1919900	879
Kokee	KOKV	22.1261200	200.3348900	1123
Fairbanks	FAIV	64.9719499	212.486686	340
Goldstone	GOLV	35.3415110	243.1261749	920
Guaymas	GUAV	27.9629777	249.2787249	-28
Rosman	OSSV	35.1960110	277.1238332	818
Merritt Is.	MERV	28.5080944	279.3064194	-45
Grand Bahama	GRAV	26.6326638	281.7621972	-46
Santiago	SANV	-33.1497000	289.3315700	710
Ascension	ASCV	- 7.9553600	345.6724400	555
Winkfield	WINV	51.4462200	359.3022000	90
Greece	GREV	38.0789900	23.9327800	490
Shiraz	SHIV	29.6371600	52.5197900	1564
Nainital	NAIV	29.3592500	79.4575200	1856
Addis Ababa	ADDV	8.7474200	38.9591600	1901
Johannesburg	JOHV	-25.8838300	27.7072800	1541
Tananarive	TANV	-19.0110800	47.4247200	1367

Geodetic Coordinates, taken from Table 5.1 of Reference 17

Semianalytical Batch Filter - States and C_D as the Solve-for Vector

A semianalytical batch filter with states and C_D as the solve-for vector was used to process the simulated observations (see Table 3-9). The perturbation model of the semianalytical batch filter is given in Table 3-11. Table 3-12 gives the a priori and final values of the solve-for vector. It is noted that the only difference between the perturbation model that generated the truth ephemeris and the perturbation model used in the semianalytical batch filter is that the a priori C_D in the batch filter is about 15% larger.

From Table 3-12 it is seen that the semianalytical batch filter converged (7 iterations) to a value of C_D that varies from the true C_D by less than 0.0035%. A comparison of the final solve-for vector in Table 3-12 to the initial PCE elements of the Low Altitude Circular Test Case of Section 2.4.3 (see Table 2-7), reveals that the initial mean semi-major axis differs by about 2 centimeters (note that drag option 6 was used in generating Table 2-7).

Semianalytical Batch Filter - States, a_1 and a_2 as the Solve-for Vector

A semianalytical batch filter with states, a_1 and a_2 as the solve-for vector was also used to process the simulated

Table 3-11
 Perturbation Model for the
 Semianalytical Batch Filter*

AOG**:

First order analytical expressions for the 6x0 gravitational field, Zeis' expressions for the J_2^2 effects, drag option 7 (4/48) for drag effects: .5 day numerical integration time step

SPG:

6x0 gravitational field (7/48) and drag (7/48) both to first order (time-independent), Zeis' J_2^2 expressions

APG**:

Analytical expressions for the mean element rates due to 6x0 gravitational field, drag option 2 for the drag element rates (48 pt quadrature)

SPPG: neglected

* An Adaptive Modified Harris-Priester Density model was used,

Test Case One: $\bar{F}_{10.7} = 150 \cdot 10^{-22} \text{ watts m}^{-2} \text{ Hz}^{-1}$

Test Cases Two and Three: $\bar{F}_{10.7} = 75 \cdot 10^{-22} \text{ watts m}^{-2} \text{ Hz}^{-1}$

** A 4th order Runge-Kutta integrator was used (see Ref. 75)

Table 3-12

Results of the Semianalytical Batch Filter
with States and C_D as the Solve-For Vector

<u>A Priori*</u>	<u>Final**</u>
$\bar{a} = 6636.45790974 \text{ km}$	$\bar{a} = 6636.37973177 \text{ km}$
$\bar{e} = .010600946793$	$\bar{e} = .010604560838$
$\bar{i} = 67.9708552769^\circ$	$\bar{i} = 67.9709267987^\circ$
$\bar{\Omega} = 91.9949096046^\circ$	$\bar{\Omega} = 91.9949014161^\circ$
$\bar{\omega} = 200.213582516^\circ$	$\bar{\omega} = 200.210968206^\circ$
$\bar{M} = 164.768801765^\circ$	$\bar{M} = 164.771253150^\circ$
$C_D = 2.30, \sigma_{C_D}^2 = .333$	$C_D = 2.00006917685$

* Initial state elements (\bar{a}_0^*) were obtained by a NOM procedure applied to the initial osculating elements of Table 3-8 with $a_1 = a_2 = 1, a_3 = 6, a_4 = a_5 = 0$ and $C_D = 2.3$.

** Took 7 iterations to converge

observations of Table 3-9. The perturbation model of the filter is given in Table 3-11. Table 3-13 gives the a priori and final values of the solve-for vector. Different a priori values for a_1 and a_2 are the only differences between the perturbation models of the semianalytical batch filter and the truth ephemeris.

From Table 3-13 it is seen that the semianalytical batch filter required 15 iterations to converge. The converged values of a_1 and a_2 were within .4% of the true values of a_1 and a_2 . A comparison of the final solve-for vector in Table 3-13 to the PCE elements of Table 2-7 shows that the semimajor axis differs by about 3.5 millimeters.

It is felt that the above tests demonstrate that the adaptive semianalytical batch filter is sensitive to and can correct for modeling errors in the drag formulation. The above tests give confidence that the software implementation into GTDS-RD is correct.

3.3.4 Test Case Two

This test case is basically the test case presented by Dowd in Reference 17. The truth ephemeris, observation net and observations are similar. Dowd used an Extended Kalman filter (coupled to an SP orbit generator) and adaptively estimated parameters in an Asymmetric Modified Harris Priester density

Table 3-13

Results of the Semianalytical Batch Filter
with States, a_1 and a_2 as the Solve-For Vector

<u>A Priori*</u>	<u>Final**</u>
$\bar{a} = 6636.458 \text{ km}$	$\bar{a} = 6636.37971418$
$\bar{e} = .01060095$	$\bar{e} = .010604645740$
$\bar{i} = 67.97086^\circ$	$\bar{i} = 67.9709289907^\circ$
$\bar{\Omega} = 91.99491^\circ$	$\bar{\Omega} = 91.9949029114^\circ$
$\bar{\omega} = 200.2137^\circ$	$\bar{\omega} = 200.210673276^\circ$
$\bar{M} = 164.7687^\circ$	$\bar{M} = 164.771556441^\circ$
$a_1 = 1.20, \sigma_{a_1}^2 = .1$	$a_1 = .99526846$
$a_2 = 1.10, \sigma_{a_2}^2 = .1$	$a_2 = 1.00335613$

* Initial states elements (\bar{a}_0^*) were obtained by a NOM procedure applied to initial osculating elements of Table 3-8 with $a_1 = 1.2$, $a_2 = 1.1$, $a_3 = 6.0$, $a_4 = a_5 = 0.0$ and $C_D = 2.0$.

** Took 15 iterations to converge.

model which basically correspond to the a_1 , a_2 and a_3 parameters of the Adaptive Modified Harris-Priester atmosphere (see Appendix C).

Table 3-14 gives the inputs for the truth ephemeris for Test Case Two. This test case has an initial perigee height of about 300 km and an initial apogee height of about 309 km. It is noted that the density model used to generate the truth ephemeris was the Analytical Jacchia-Roberts density model. The simulation of the observational data is explained in Table 3-15 and the GTDS station pass report is given in Table 3-16. The simulated observations did not include random noise and were generated at a rate of one set of observations (range and range rate) every 10 seconds while in the field of view of the tracking station. The maximum time that a tracking station was allowed to observe the satellite during a single pass was 5 minutes. A total of 331 range observations and 331 range-rate observations were generated.

Cowell Batch Filter - States Only as the Solve-For Vector

A Cowell batch filter with states only as the solve-for vector was used to process the simulated data. The perturbation model and a priori values used in the Cowell Batch filter are given in Tables 3-17 and 3-18. The results of the Cowell batch filter are presented in Table 3-19. The filter took

Table 3-14
Truth Ephemeris for Test Case Two

Initial Osculating Elements and Parameters

a = 6682.47355 km	Epoch	= 2 hrs. 47.93 min. 16 Dec. 1973
e = .000646254	Reference Frame	= True of Date
i = 67.991163°	C_D	= 2.0
Ω = 254.26°	Area	= 1.86 m ²
ω = 0°	Mass	= 677 kg
M = 0°		

Perturbations

6x0 gravitational field with drag. The Analytical Jacchia-Roberts density model was used.

Orbit Generator

Cowell with a 30 second numerical integration time step

Table 3-15
Data Simulation for Test Case Two

Tracking Station: Net A (see Table 3-10)

Observation Type: VHF range (ρ) and range rate ($\dot{\rho}$)

$$\sigma_{\rho} = 5 \text{ meters} \quad \sigma_{\dot{\rho}} = .55 \text{ cm/sec}$$

Observations: Generated every 10 seconds while in sight (15° minimum elevation). Maximum time of observation interval per satellite pass is 300 seconds. No random noise included.

Observation Span: From Epoch to 1630 hrs 16 Dec 1973

Truth Ephemeris: See Table 3-14

Table 3-16. Station Pass Report for Test Case Two

REV NUM	0	1	2	3	4	5	6	7
START	1731216/731216/731216/731216/731216/731216/731216/731216/731216	246091/410/51/54231/71957/71957/65034/100310/115147/1132231	731216/731216/731216/731216/731216/731216/731216/731216/731216	54231/410/51/54231/71957/71957/65034/100310/115147/1132231	731216/731216/731216/731216/731216/731216/731216/731216/731216	45110/731216/731216/731216/731216/731216/731216/731216/731216	45110/731216/731216/731216/731216/731216/731216/731216/731216	45110/731216/731216/731216/731216/731216/731216/731216/731216
CI AOS								
AI								
LI								
VI								
ELMAX								
AOSL								
CI AOS								
AI								
LI								
VI								
ELMAX								
AOSL								
CI AOS								
AI								
LI								
VI								
ELMAX								
AOSL								
CI AOS								
AI								
LI								
VI								
ELMAX								
AOSL								
CI AOS								
AI								
LI								
VI								
ELMAX								
AOSL								
CI AOS								
AI								
LI								
VI								
ELMAX								
AOSL								
CI AOS								
AI								
LI								
VI								
ELMAX								
AOSL								
CI AOS								
AI								
LI								
VI								
ELMAX								
AOSL								

AOS = Acquisition of Signal
 LOS = Loss of Signal
 ELMAX = Maximum Elevation Angle this Pass
 AOSL = Local Time of AOS

Table 3-17

Perturbation Model for the Cowell
Orbit Generator/Batch Filter

6x0 gravitational field with drag. A Modified Harris-Priester Atmosphere was used with $\bar{F}_{10.7} = 75 \cdot 10^{-22}$ watts m^{-2} Hz^{-1} . The Cowell orbit generator used a 12th order Adams-Bashforth Predictor/Adams-Moulton Corrector integrator with a 30 second numerical integration time step.

Table 3-18
A Priori Values for Test Case Two

<u>Semianalytical Batch Filter*</u>	<u>Cowell Batch Filter**</u>
$\bar{a} = 6674.04345478$	$a = 6682.47355 \text{ km}$
$\bar{e} = .000016055664$	$e = .000646254$
$\bar{i} = 67.9763516649^\circ$	$i = 67.991163^\circ$
$\bar{\Omega} = 254.260152633^\circ$	$\Omega = 254.26^\circ$
$\bar{\omega} = 359.449849018^\circ$	$\omega = 0.0^\circ$
$\bar{M} = .549789997042^\circ$	$M = 0.0^\circ$
$C_D = 2.0, \sigma_{C_D}^2 = .333$	$C_{DO} = 2.0$
$a_1 = a_2 = 1.0, \sigma_{a_1}^2 = \sigma_{a_2}^2 = .1$	$\rho_1 = 0.0$
$a_3 = 6.0, \sigma_{a_3}^2 = 10^{-4}$	
$a_4 = a_5 = 0.0, \sigma_{a_4}^2 = \sigma_{a_5}^2 = 10^{-12}$	

$C_D = C_{DO}(1+\rho_1)$

* Initial state elements were obtained by a NOM procedure applied to initial osculating elements of Table 3-14 with $a_1 = a_2 = 1, a_3 = 6, a_4 = a_5 = 0$ and $C_D = 2.0$.

** Cowell batch filter could not use the Adaptive Modified Harris-Priester Atmosphere.

Table 3-19

Final* Results of the Cowell Batch Filter with
States Only as the Solve-For Vector

$$a = 6682.463898 \text{ km}$$

$$e = .0006465268$$

$$i = 67.99106851^\circ$$

$$\Omega = 254.2604117^\circ$$

$$\omega = .1711699991^\circ$$

$$M = 359.8277233^\circ$$

* Took 3 iterations to converge, RMS = 73.96.

3 iterations to converge. This is not surprising since the a priori guess of the state (Table 3-18) was the actual initial state of the truth ephemeris (Table 3-14). A comparison of Tables 3-19 and 3-18 reveals that the Cowell batch filter decreased the semimajor axis by about 10 meters from the a priori starting value.

A predicted ephemeris corresponding to the solve-for vector of Table 3-19 was generated and compared to the truth ephemeris over a 72 hour time span from epoch. The along track error was dominant and is shown in Figure 3-1.

Semianalytical Batch Filter - States Only as the Solve-For Vector

The results of a semianalytical batch filter with states only as the solve-for vector are shown in Table 3-20. The semianalytical batch filter used the perturbation model of Table 3-11 and the a priori solve-for vector of Table 3-18. The along

Table 3-20

Final* Results of the Semianalytical Batch Filter
with States Only as the Solve-For Vector

\bar{a} = 6673.954887 km
 \bar{e} = .0000149613
 \bar{I} = 67.97686382°
 $\bar{\Omega}$ = 254.2604506°
 $\bar{\omega}$ = 21.28302544°
 \bar{M} = 338.7155903°

* Values came from the 13th iteration. The batch filter was converging but had not converged to a final value, RMS = 34.02.

track difference between the predicted ephemeris corresponding to the solve-for vector of Table 3-20 and the truth ephemeris is presented in Figure 3-2. The semianalytical orbit generator used to obtain the predicted ephemeris is given in Table 3-21.

Table 3-21

Perturbation Model of the Semianalytical Orbit Generator Used in Generating the Predicted Ephemerides

AOG: First order analytical expressions for the 6x0 gravitational field, Zeis' expressions for the J_2^2 effects, drag* option 7 (4/48): 1 day numerical integration time step.

SPG: 6x0 gravitational field (7/48) and drag* (7/48), both to first order (time-independent), Zeis' J_2^2 expressions.

Integrator: For Test Case Two - 6th order Runge-Kutta
For Test Case Three - 12th order Adams-Bashforth Predictor/Adams-Moulton Corrector

* An Adaptive Modified Harris-Priester Atmosphere with the respective adaptive parameters and with $\bar{F}_{10.7} = 75 \cdot 10^{-22}$ watts m^{-2} Hz $^{-1}$.

Comparison of Figures 3-2 and 3-1 shows that the semianalytical batch filter yields similar results to the Cowell batch filter.

Cowell Batch Filter - States and ρ_1 as the Solve-For Vector

Table 3-22 shows the final results of processing the simulated data of Test Case Two with a Cowell batch filter which solves for the variation in C_D (ρ_1) in addition to the initial states. Tables 3-17 and 3-18 give the perturbations and a priori values of the adaptive Cowell batch filter. Figure 3-3 shows the along track error between the predicted ephemeris associated with the solve-for vector of Table 3-22 and the truth ephemeris of Test Case Two. A comparison of Figures 3-1 and 3-3 indicates that solving for states and C_D (or ρ_1) gives better prediction results over the 72 hours predict span than solving for states only.

Table 3-22

Final* Results of the Cowell Batch Filter
with States and ρ_1 as the Solve-For Vector

a = 6682.474163 km	ω = .0054429055°
e = .0006465726	M = 359.9945420°
i = 67.99115226°	ρ_1 = .2335674365
Ω = 254.2599985°	

* Values came from the 15th iteration. The batch filter was converging but had not converged to a final value, RMS = .8966.

Semianalytical Batch Filter - States and C_D as the Solve-For Vector

A semianalytical batch filter with states and C_D as the solve-for vector was also used to process the simulated data of Test Case Two. Tables 3-11 and 3-18 give the perturbation model and the a priori solve-for vector used in the batch filter. Table 3-23 gives the final results of the semianalytical batch filter for this test case. The final RMS value in Table 3-23 is slightly larger than the RMS in Table 3-22 [see Equation (3-70) for the definition of the RMS]. The larger value of the RMS in Table 3-23 could be due partly to the fact that the a priori value of C_D had a variance of .333 and therefore P_0^{-1} was not zero in Equation (3-70). It is also interesting to note that the value of C_D in Table 3-23 varies by less than .025% from the final value of C_D obtained with the Cowell batch filter.

Table 3-23

Final* Results of the Semianalytical Batch Filter
with States and C_D as the Solve-For Vector

\bar{a}	=	6673.966073 km	$\bar{\omega}$	=	356.8969264°
\bar{e}	=	.0000128192	\bar{M}	=	3.102968644°
\bar{I}	=	67.97637954°	C_D	=	2.466603290
$\bar{\Omega}$	=	254.2601548°			

* Values came from the 15th iteration. The batch filter was converging but had not converged to a final value, RMS = 1.331.

Figure 3-4 shows the along track difference between the predicted ephemeris corresponding to Table 3-23. A comparison of Figures 3-3 and 3-4 shows that the semianalytical batch filter gives results very similar to the Cowell Batch filter.

Semianalytical Batch Filter - States, a_1 and a_2 as the Solve-For Vector

Table 3-24 gives the final results of the semianalytical batch filter with states, a_1 and a_2 as the solve-for vector. The perturbation model and a priori values are given in Tables 3-11 and 3-18. The final value for the epoch mean semimajor axis is about .5 meters more than the epoch mean semimajor axis as given in Table 3-23. It is also noted that the RMS value is considerably less than any of the previously obtained RMS values [see Equation (3-70) for definition of RMS].

Table 3-24

Final* Results of the Semianalytical Batch Filter
with States, a_1 and a_2 as the Solve-For Vector

\bar{a} = 6673.966564 km	$\bar{\omega}$ = 356.7534244°
\bar{e} = .0000122015	\bar{M} = 3.246535807°
\bar{i} = 67.97638780°	a_1 = 1.453672222
$\bar{\Omega}$ = 254.2601561°	a_2 = .9847238034

* Values came from the 14th iteration. The batch filter was converging but had not converged to a final value, RMS = .5882.

Figure 3-5 gives the along track difference between the predicted ephemeris associated with this estimation option and the truth ephemeris of this test case. Comparing Figures 3-2 and 3-5 indicates that the states plus a_1 and a_2 estimation option gives better results than a states only estimation option. Comparing Figures 3-4 and 3-5 indicates that for this test case the states plus C_D estimation option is superior to the states plus a_1 and a_2 estimation option over the prediction span.

Summary for Test Case Two

Table 3-25 gives a 72 hour comparison between the predicted ephemerides of this test case and the truth ephemeris. This table has to be viewed with a certain amount of caution since the sampling rate of once per 45 minutes is approximately equal to one half the orbital period.

Table 3-25 shows that for states only and states plus C_D as the solve-for parameters, the semianalytical and Cowell batch filters give nearly equivalent results for the orbit prediction problem. Table 3-25 also indicates that over the three day predict span, the states plus C_D estimation option gave the best results. This demonstrates that adaptive estimation of the drag formulation does significantly improve the orbit determination and prediction processes for low altitude satellites.

Table 3-25 also indicates that the states plus a_1 and a_2 estimation option in the semianalytical batch filter is not as good as the states plus C_D estimation option over the two day predict span. Comparing the final RMS values of the batch filter in Tables 3-19, 3-20, 3-22, 3-23 and 3-24 indicates that the states plus a_1 and a_2 may be slightly superior to the other estimation options over the observation span. This point will be examined in Test Case Three.

The other semianalytical estimation options as given in Table 3-6 were also used to process the simulated data of this test case. It was found that the semianalytical batch filter with these estimation options (states plus a_1 , a_2 and a_3 , states plus a_1 , a_2 , a_3 , a_4 and a_5 and states plus C_D and a_4) would not converge unless the variances on a_3 , a_4 and a_5 were set to the values given in Table 3-18. This is basically "telling" the batch filter that a_3 , a_4 and a_5 are known extremely well. The parameters a_3 , a_4 and a_5 of the Adaptive Modified Harris-Priester density model are, for all practical purposes, unobservable to the semianalytical batch filter. The states, a_1 , a_2 and a_3 estimation option (using $\sigma_{a_3}^2 = 10^{-4}$) gives results that are nearly equivalent to the results of the states plus a_1 and a_2 estimation option. Likewise, the states, C_D and a_4 estimation option (using $\sigma_{a_4}^2 = 10^{-12}$) resulted in a predicted ephemeris which was not as good as the predicted ephemeris of the states and C_D estimation option.

Table 3-25
 72 Hour Comparison of the Predicted Ephemerides
 with the Truth Ephemeris of Test Case Two

Batch Filter	Solve-For Vector	Maximum Sampled* Position Error (km)				Sampled* Position RMS (km)			
		Radial	Cross Track	Along Track	$ \Delta r $	Radial	Cross Track	Along Track	$ \Delta r $
Cowell	states only	.1343	.0445	18.31	18.31	.0581	.0267	7.696	7.696
Cowell	states and ρ_1	.0273	.0025	4.334	4.334	.0136	.0018	2.079	2.079
Semianalytical	states only	.1598	.0916	17.98	17.98	.0628	.0749	7.519	7.52
Semianalytical	states and C_D	.0275	.0290	4.363	4.363	.0137	.0135	2.090	2.090
Semianalytical	states, a_1 and a_2	.0290	.0300	6.397	6.397	.0163	.0141	2.935	2.935

* Sampling rate was one point every 45 minutes.

3.3.5 Test Case Three

This test case is representative of a real-world operational OD system. The inputs for the truth ephemeris used in this test case are presented in Table 3-26. Note that the perigee height (200 km) is approximately 100 km lower than for the test case of Section 3.3.4. As can be seen, the truth ephemeris is the Low Altitude Test Case presented in Section 2.4.3 with an Analytical Jacchia-Roberts atmosphere. The simulation of the observational data is explained in Tables 3-27 and 3-28. The simulated data did include random noise corresponding to the standard deviation of the measurements as given in Table 3-27. A unified S-band tracking net was used. A total of 51 range observations, 30 range rate observations and 60 gimbal angle observations (27 X_{30} , 27 Y_{30} , 3 X_{85} and 3 Y_{30} measurements, see Appendix G or Ref. 67) were generated.

Cowell Batch Filter - States Only as the Solve-For Vector

A Cowell batch filter with states only as the solve-for vector was used to process the simulated data of Test Case Three. The perturbation model used in the batch filter is given in Table 3-17. The a priori values of the solve-for parameters are given in Table 3-30. The results of the Cowell batch filter are given in Table 3-31. Figures 3-6 and 3-7 give 12 hour and 72 hour comparisons, respectively, of the along track difference between the predicted ephemeris corresponding to the solve-for vector of Table 3-31 and the truth ephemeris of this test case.

Table 3-26
Truth Ephemeris for Test Case Three

Initial Osculating Elements and Parameters

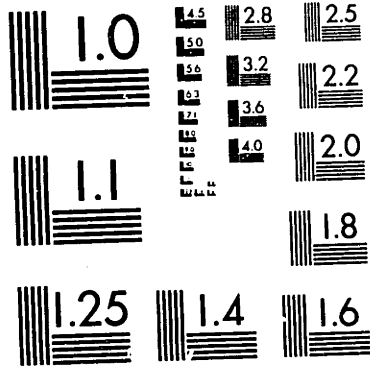
a = 6644.586 km Epoch = 10 hrs. 24 min. 21 Oct. 74
e = .01 Reference Frame = True of Date
i = 67.98538419° C_D = 2.0
Ω = 91.99738418° Area = 1.86 m²
ω = 200.6741688° Mass = 677 kg
M = 164.3173126°

Perturbations

6x0 gravitational field with drag. The Analytical Jacchia-Roberts density model was used.

Orbit Generator

Cowell with a 30 second numerical integration time step.



MICROCOPY RESOLUTION TEST CHART
NATIONAL BUREAU OF STANDARDS-1963-A

20X

NOTICE THIS MATERIAL MAY BE PROTECTED BY
COPYRIGHT LAW (TITLE 17 U.S. CODE.)

Table 3-27
Data Simulation for Test Case Three

Tracking Stations: Net B (see Table 3-29)

Observation Type: Unified S-band range (ρ), range rate ($\dot{\rho}$) and gimbal angles (X_{30} , Y_{30} , X_{85} or Y_{85})

$$\sigma_{\rho} = 15 \text{ meters}, \quad \sigma_{\dot{\rho}} = 2 \text{ cm/sec}$$

$$\sigma_{X_{30}} = \sigma_{X_{85}} = \sigma_{Y_{30}} = \sigma_{Y_{85}} = 3506.5017 \text{ sec-arc}$$

Observations: Generated every 60 seconds while in sight (20° minimum elevation). Maximum time of observation interval per satellite pass is 300 seconds. Random noise corresponding to observation type was included.

Observation Span: From Epoch to 0600 hrs 22 Oct. 1974

Truth Ephemeris: see Table 3-26

Table 3-28. Station Pass Report for Test Case Three

REV	MMN	0	1	2	3	4	5	6	7	8	9	10	11	12	13
START		741021	741021	741021	741021	741021	741021	741021	741021	741021	741021	741022	741022	741022	741022
		102252	115242	132233	145223	162213	175204	192154	205144	222135	235125	121151	251051	420561	550461

A	AOS					741021							741022		
C						170600							41300		
H	LOS					741021							741022		
S						171200							42000		
W	ELMAX					35							22		
	AOSL					741022							741023		
						160844							31542		

A	AOS								741021						741022
C									214200						70500
H	LOS								741021						741022
S									214700						71300
W	ELMAX								42						24
	AOSL								741022						741023
									165920						22220

E	AOS	741021													
L		103000													
C	LOS	741021													
S		103500													
W	ELMAX	0													
	AOSL	741022													
		61122													

E	AOS	741021	741021				741021								
L		103000	120300				182200								
C	LOS	741021	741021				741021								
S		103300	120800				182400								
W	ELMAX	57	0				0								
	AOSL	741022	741022				741022								
		52238	65538				121438								

G	AOS		741021	741021											
L			115800	132900											
C	LOS		741021	741021											
S			120300	133700											
W	ELMAX		0	24											
	AOSL		741022	741022											
			41030	54130											

G	AOS					741021									
L						175100									
C	LOS					741021									
S						175600									
W	ELMAX					0									
	AOSL					741022									
						32957									

H	AOS				741021	741021									
L					145300	162700									
C	LOS				741021	741021									
S					150100	163200									
W	ELMAX				24	0									
	AOSL				741022	741022									
					41420	54820									

H	AOS			741021	741021										
L				135200	152300										
C	LOS			741021	741021										
S				135700	153000										
W	ELMAX			0	23										
	AOSL			741022	741022										
				133520	150620										

H	AOS	741021								741021					
L		103000								195500					
C	LOS	741021								741021					
S		103500								200000					
W	ELMAX	55								0					
	AOSL	741022								741022					
		50714								143214					

C	ACS				741021										
R					160700										
S	LOS				741021										
S					161400										
W	ELMAX				0										
	ACS				741022										
					20250										

U	ACS				741021	741021	741021	741021	741021						
L					150600	163600	180700	193900	211200						
C	LOS				741021	741021	741021	741021	741021						
S					151100	164300	181500	194700	211900						
W	ELMAX				0	28	56	35	51						
	AOSL				741022	741022	741022	741022	741022						
					51557	64557	81657	96857	112157						

AOS = ACQUISITION OF SIGNAL
LOS = LOSS OF SIGNAL

ELMAX = MAXIMUM ELEVATION ANGLE THIS PASS
AOSL = LOCAL TIME OF AOS

Table 3-29
Tracking Net B

Station Name	Symbol	Latitude (deg.)	Longitude (deg.)	Height (m)
Ascension	ACN3W	- 7.954825	345.672936	528.0
Santiago	AGO3W	-33.150994	289.333633	706.18
Bermuda	BDA3W	32.3503	295.342206	34.0
Greenbelt	ETC3W	38.998567	283.157286	- 1.0
Goldstone	GDS3W	35.342205	243.126545	912.71
Guam	GWM3W	13.310625	144.736814	116.0
Kauai	HAW3W	22.126239	200.334842	1139.0
Madrid	MAD8W	40.455464	355.831553	808.0
Merritt Is.	MIL3W	28.50875	279.306625	-55.0
Orroral	ORR3W	-35.627969	148.957039	929.0
Fairbanks	ULA3W	64.972	212.487053	338.51

Geodetic Coordinates, taken from GTDS-RD User's Guide
(Ref. 73)

Table 3-30

A Priori Values for Test Case Three

<u>Semianalytical Batch Filter*</u>	<u>Cowell Batch Filter**</u>
$\bar{a} = 6636.45593986 \text{ km}$	$a = 6644.586 \text{ km}$
$\bar{e} = .010600675342$	$e = .01$
$\bar{i} = 67.9708551529^\circ$	$i = 67.98538419^\circ$
$\bar{\Omega} = 91.9949093860^\circ$	$\Omega = 91.99738418^\circ$
$\bar{\omega} = 200.209177391^\circ$	$\omega = 200.6741688^\circ$
$\bar{M} = 164.773135897^\circ$	$M = 164.3173126^\circ$
$C_D = 2.0, \sigma_{C_D}^2 = .333$	$C_{DO} = 2.0$
$a_1 = a_2 = 1.0, \sigma_{a_1}^2 = \sigma_{a_2}^2 = .1$	$\rho_1 = 0.0$
$a_3 = 6.0, \sigma_{a_3}^2 = 10^{-4}$	$C_D = C_{DO}(1+\rho_1)$
$a_4 = a_5 = 0.0, \sigma_{a_4}^2 = \sigma_{a_5}^2 = 10^{-12}$	

* Initial state elements were obtained by a NOM procedure applied to the initial osculating elements of Table 3-26.

** Cowell batch filter could not use the Adaptive Modified Harris-Priester Atmosphere

Table 3-31

Final* Results of the Cowell Batch Filter
with States Only as the Solve-For Vector

a = 6644.37884315 km
e = .010294090436
i = 67.9743471306°
 Ω = 91.9960440160°
 ω = 201.305628665°
M = 163.656474108

* took 12 iterations to converge, RMS = 59.87

Semianalytical Batch Filter - States Only as the Solve-For Vector

The results of processing the observational data of Test Case Three with a semianalytical batch filter with states only as the solve-for vector are shown in Table 3-32. The semianalytical batch filter used the perturbation model of Table 3-11 and the a priori solve-for vector of Table 3-30. Figures 3-8 and 3-9 show the along track difference between the predicted ephemeris corresponding to the solve-for vector of Table 3-32 and the truth ephemeris of this test case over a 12 hour and a 72 hour time span. It is noted that the semianalytical batch filter with the states only estimation option gives results equivalent to the Cowell batch filter with the same estimation option.

Table 3-32

Final* Results of the Semianalytical Batch Filter
with States Only as the Solve-For Vector

$$\bar{a} = 6636.17653458 \text{ km}$$

$$\bar{e} = .010897761885$$

$$\bar{i} = 67.9598842035^\circ$$

$$\bar{\Omega} = 91.9936086178^\circ$$

$$\bar{\omega} = 200.816521950^\circ$$

$$\bar{M} = 164.136382471^\circ$$

* Took 12 iterations to converge, RMS = 59.89

Cowell Batch Filter - States and ρ_1 as the Solve-For Vector

Using the perturbation models of Table 3-17 and the a priori values of Table 3-30, a Cowell batch filter with states and ρ_1 as the solve-for vector gave the final results of Table 3-33. The along track error between the predicted ephemeris associated with Table 3-33 and the truth ephemeris is shown in Figures 3-10 and 3-11 for 12 and 72 hour comparisons, respectively. It is interesting to note that, as in Test Case Two, the states plus C_D (or ρ_1) estimation option gives significantly better 72 hour prediction results than the states only estimation option. The states plus C_D estimation option also significantly improves the prediction error during the observation span (Figure 3-10).

Table 3-33

Final* Results of the Cowell Batch Filter
with States and ρ_1 as the Solve-For Vector

a = 6644.56026507 km
 e = .009996692517
 i = 67.9863983353°
 Ω = 91.9971347242°
 ω = 200.664730933°
 M = 164.326691616°
 ρ_1 = .269831999344

* Took 13 iterations to converge, RMS = 3.412

Semianalytical Batch Filter - States and C_D as the Solve-For Vector

Table 3-34 gives the final results of processing the observational data of Test Case Three with a semianalytical batch filter with states and C_D as the solve-for parameters. The perturbation models and a priori values used are given in Tables 3-11 and 3-30. Figures 3-12 and 3-13 are plots of the along track difference between the predicted ephemeris with the initial conditions of Table 3-34 and the truth ephemeris of this test case. As expected, the semianalytical batch filter with states plus C_D as the estimation option is equivalent to the Cowell batch filter with states and ρ_1 (C_D) as the solve-for vector.

Table 3-34

Final* Results of the Semianalytical Batch Filter
with States and C_D as the Solve-For Vector

$$\bar{a} = 6636.35295242 \text{ km}$$

$$\bar{e} = .010601078192$$

$$\bar{i} = 67.9720308217^\circ$$

$$\bar{\Omega} = 91.9946124323^\circ$$

$$\bar{\omega} = 200.200474381^\circ$$

$$\bar{M} = 164.781700625^\circ$$

$$C_D = 2.54063409983$$

* Took 13 iterations to converge, RMS = 3.317

Semianalytical Batch Filter - States, a_1 and a_2 as the Solve-
for Vector

The semianalytical batch filter with states, a_1 and a_2 as the solve-for vector was also used to process the simulated data of Test Case Three. The perturbation model and a priori values used are given in Tables 3-11 and 3-30. Table 3-35 gives the final results of the semianalytical batch filter with states plus a_1 and a_2 as the solve-for parameters. Figures 3-14 and 3-15 are plots of the along track difference between the predicted ephemeris corresponding to Table 3-35 and the truth ephemeris of this test case for 12 and 72 hour comparisons, respectively. Figures 3-12 and 3-14 indicate that the

Table 3-35

Final* Results of the Semianalytical Batch Filter
with States, a_1 and a_2 as the Solve-For Vector

$$\bar{a} = 6636.35451813 \text{ km}$$

$$\bar{e} = .010595641200$$

$$\bar{i} = 67.9716923016^\circ$$

$$\bar{\Omega} = 91.9945682623^\circ$$

$$\bar{\omega} = 200.239053854^\circ$$

$$\bar{M} = 164.742323444^\circ$$

$$a_1 = 1.54777983011$$

$$a_2 = 1.12096690690$$

* Took 13 iterations to converge, RMS = 3.102

states plus a_1 and a_2 estimation option gives slightly better results over the observation span than the states plus C_D estimation option. Over the prediction span the states plus a_1 and a_2 estimation option is not as good as the states plus C_D estimation option.

Summary for Test Case Three

Tables 3-36 and 3-37 give a 12 hour and a 72 hour comparison, respectively, between the predicted ephemerides of this test case and the truth ephemeris. Table 3-36 represents the observation span (from Table 3-28 it is seen that the

Table 3-36
 12 Hour Comparison of the Predicted Ephemerides
 with the Truth Ephemeris of Test Case Three

Batch Filter	Solve-For Vector	Maximum Sampled* Position Error (km)				Sampled* Position RMS (km)			
		Radial	Cross Track	Along Track	$ \Delta r $	Radial	Cross Track	Along Track	$ \Delta r $
Cowell	states only	2.264	1.295	8.347	8.422	1.509	.9081	4.119	4.480
Cowell	states and ρ_1	.0502	.1209	.3760	.3811	.0231	.0845	.1967	.2153
Semianalytical	states only	2.268	1.296	8.358	8.433	1.511	.9074	4.125	4.486
Semianalytical	states and C_D	.0503	.1348	.3733	.3809	.0231	.0928	.1948	.2170
Semianalytical	states, a_1 and a_2	.0914	.0999	.3344	.3472	.0458	.0676	.1646	.1837

* Sampling rate was one point every 8 minutes

Table 3-37
 72 Hour Comparison of the Predicted Ephemerides
 with the Truth Ephemeris of Test Case Three

Batch Filter	Solve-For Vector	Maximum Sampled* Position Error (km)				Sampled Position RMS (km)			
		Radial	Cross Track	Along Track	$ \Delta \underline{r} $	Radial	Cross Track	Along Track	$ \Delta \underline{r} $
Cowell	states only	6.509	.9775	167.9	168.1	2.729	.5183	68.22	68.28
Cowell	states and ρ_1	.1511	.0954	16.60	16.60	.0755	.0684	8.910	8.910
Semianalytical	states only	6.523	1.012	168.2	168.4	2.783	.5370	68.34	68.40
Semianalytical	states and C_D	.1523	.0719	16.55	16.55	.0758	.0609	8.878	8.878
Semianalytical	states, a_1 and a_2	.2628	.528	23.64	23.65	.1049	.0488	11.40	11.40

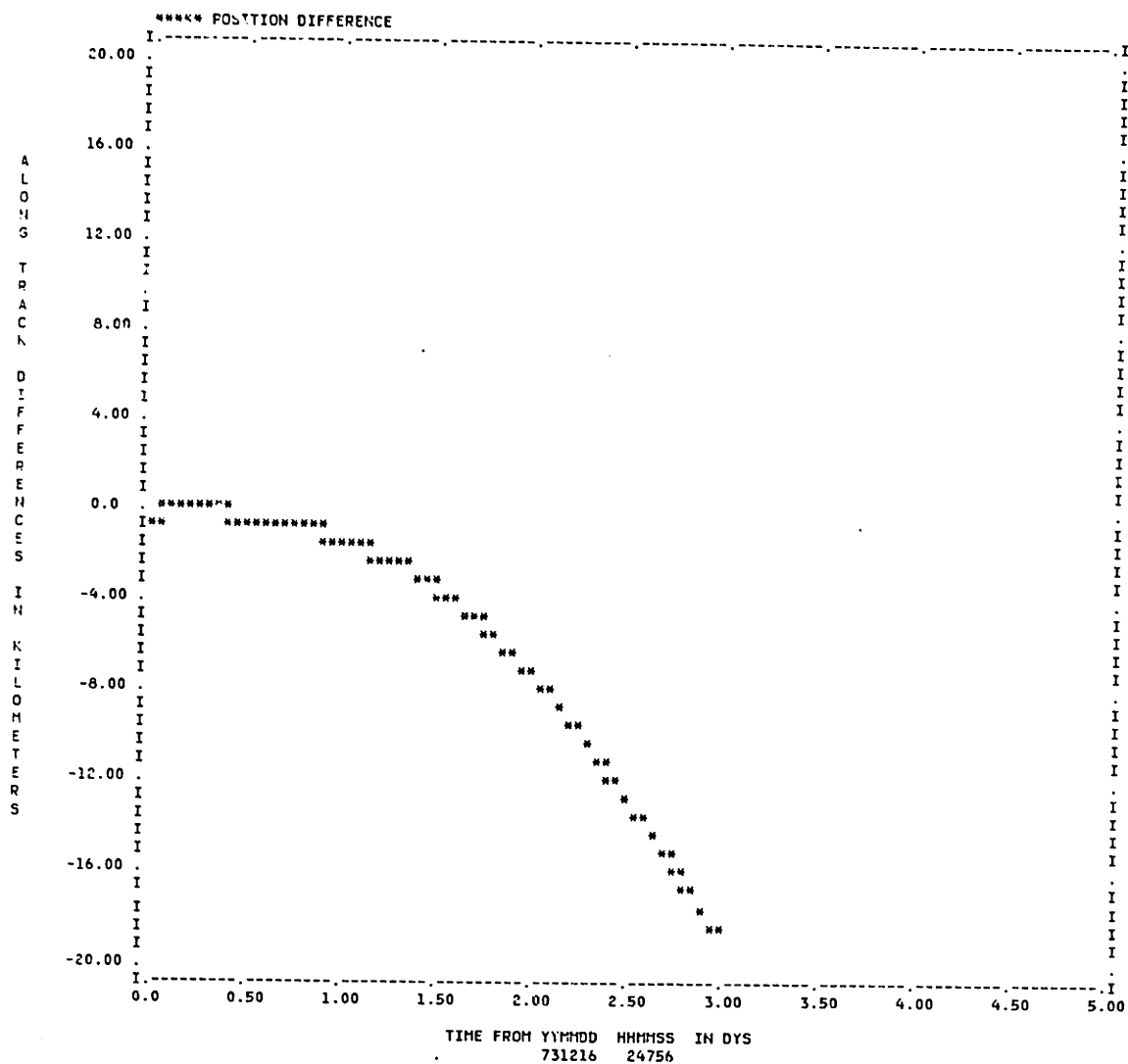
* Sampling rate was one point every 45 minutes.

effective observation span is 10.5 hours). Table 3-37 represents the prediction span. The sampling rate in Table 3-36 is one point every 8 minutes whereas the sampling rate in Table 3-37 is one point every 45 minutes.

From Tables 3-36 and 3-37 it is seen that for the states only and the states plus C_D (or ρ_1) estimation options, the semianalytical batch filter yields results that are equivalent to the Cowell batch filter. From Table 3-36 it is seen that over the observation span the states plus a_1 and a_2 estimation option gives results which are about 30 meters (total position error) better than the states plus C_D estimator option. Over the prediction span, the states plus C_D estimation option gives the best results.

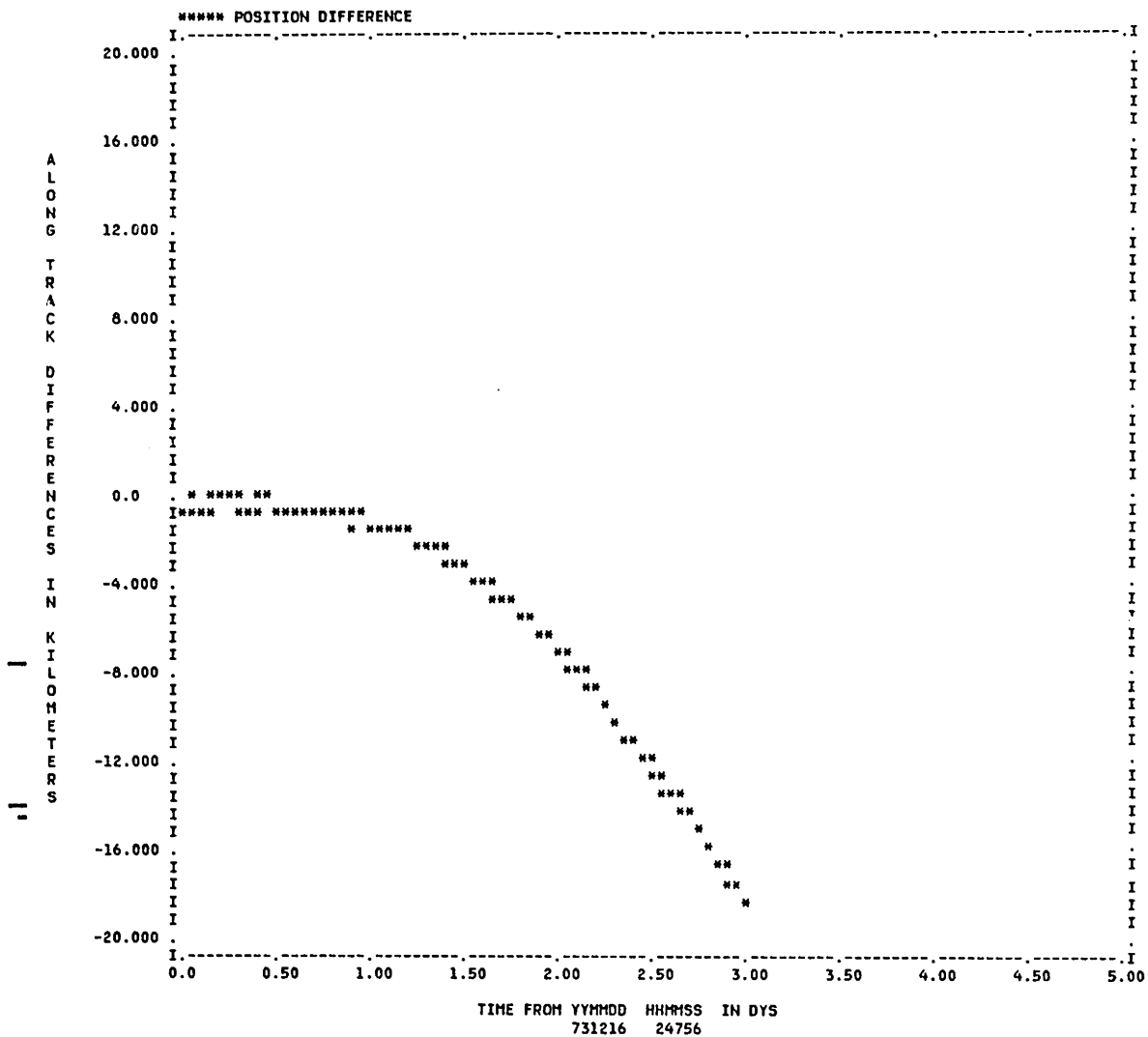
As was done in Test Case Two, the other estimation options, as given in Table 3-6, were used to process the simulated observational data of this test case. The semianalytical batch filter would not converge unless the variances on a_3 , a_4 and a_5 were set to the values given in Table 3-30. It was also found that the results obtained with these estimation options were not as good as the states plus a_1 and a_2 estimation option and/or states plus C_D estimation option.

Figure 3-1. Along Track Difference/Cowell* minus the Truth
Ephemeris of Test Case Two



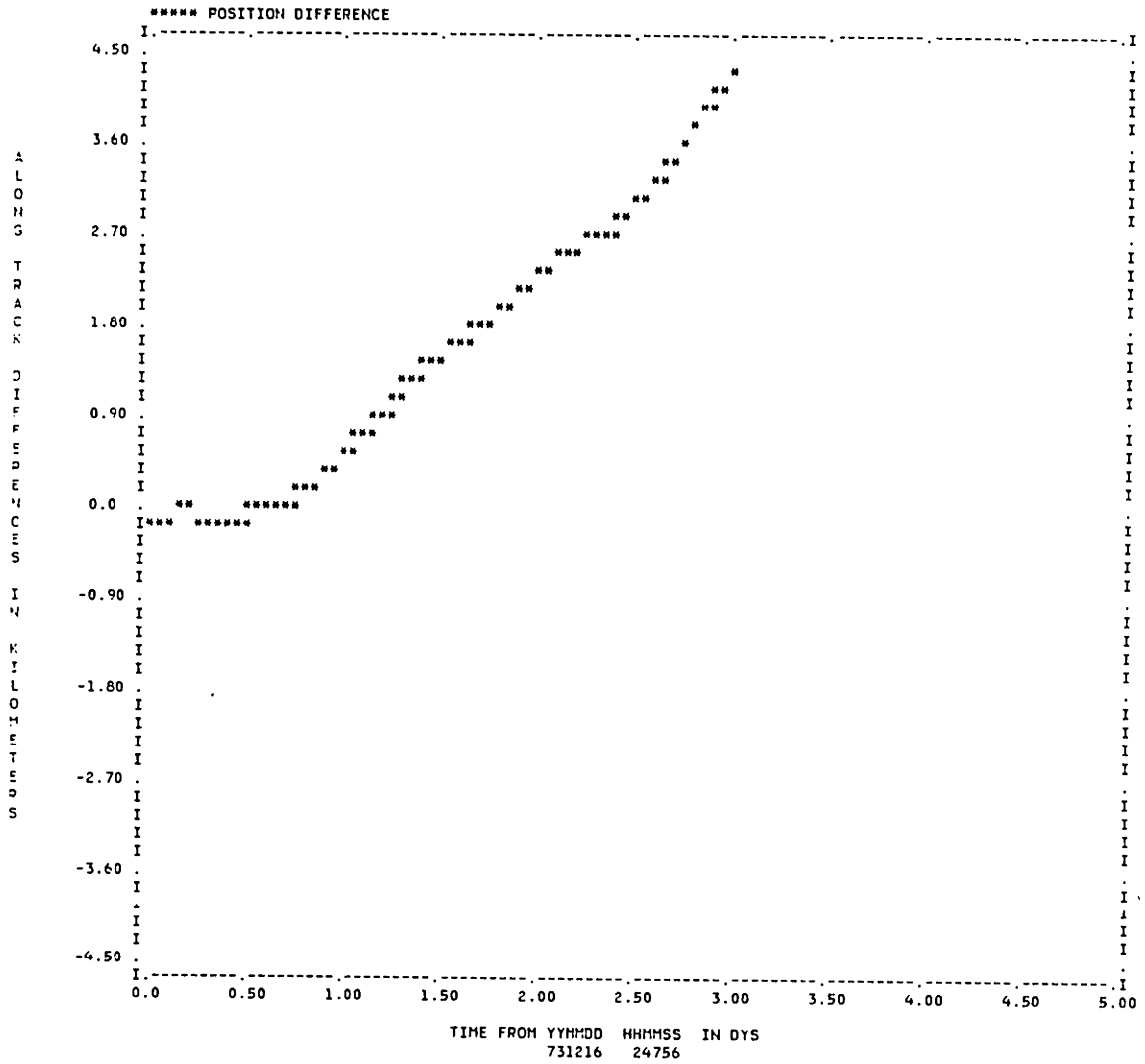
* Initial conditions from the Cowell batch filter with states only as solve-for vector (see Table 3-19). The perturbation model for the Cowell orbit generator is given in Table 3-17.

Figure 3-2. Along Track Difference/Semianalytical* minus the Truth Ephemeris of Test Case Two



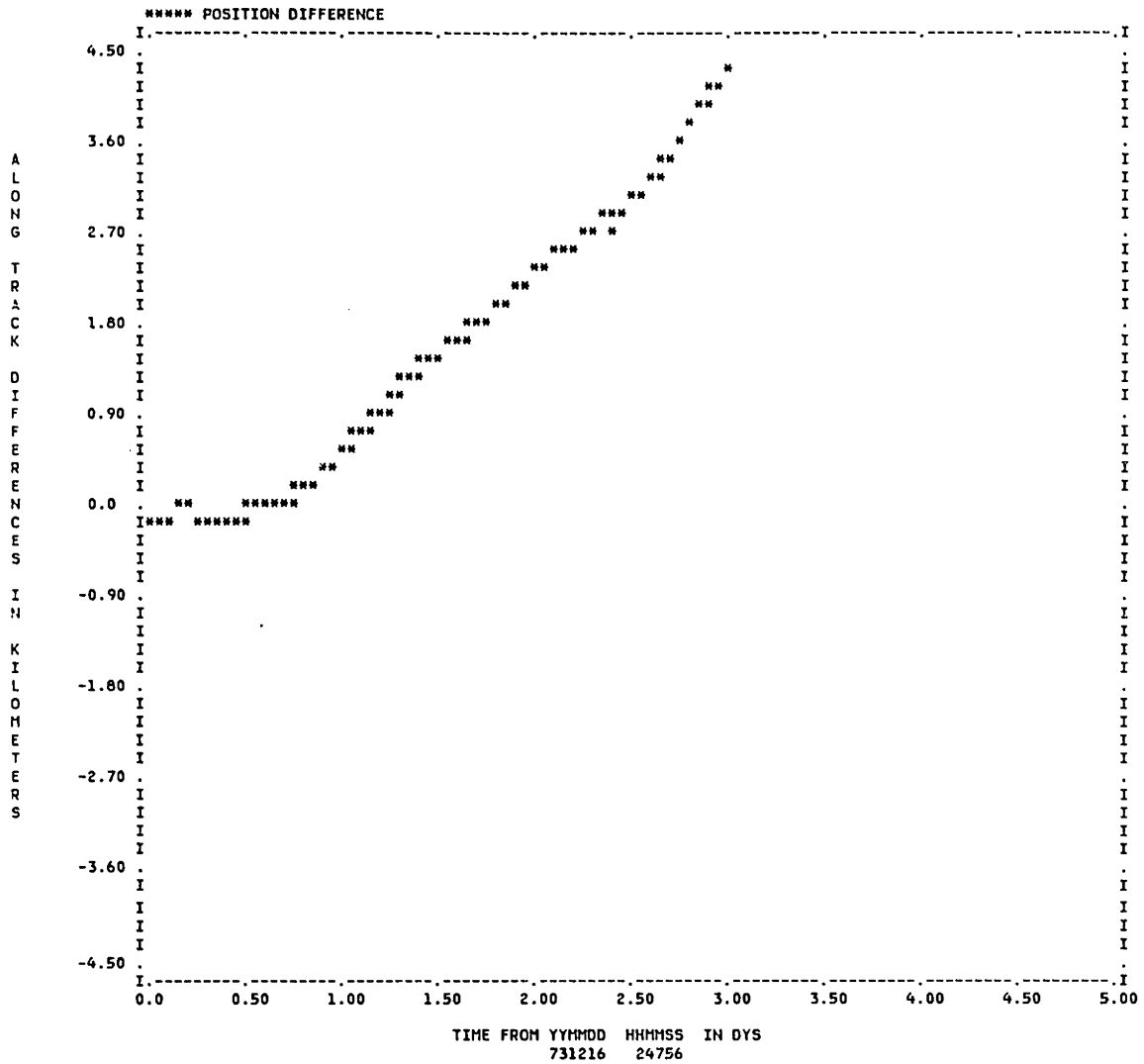
* Initial conditions from the semianalytical batch filter with states only as solve-for vector (see Table 3-20). The perturbation model for the semianalytical orbit generator is given in Table 3-21.

Figure 3-3. Along Track Difference/Cowell* minus the Truth
Ephemeris of Test Case Two



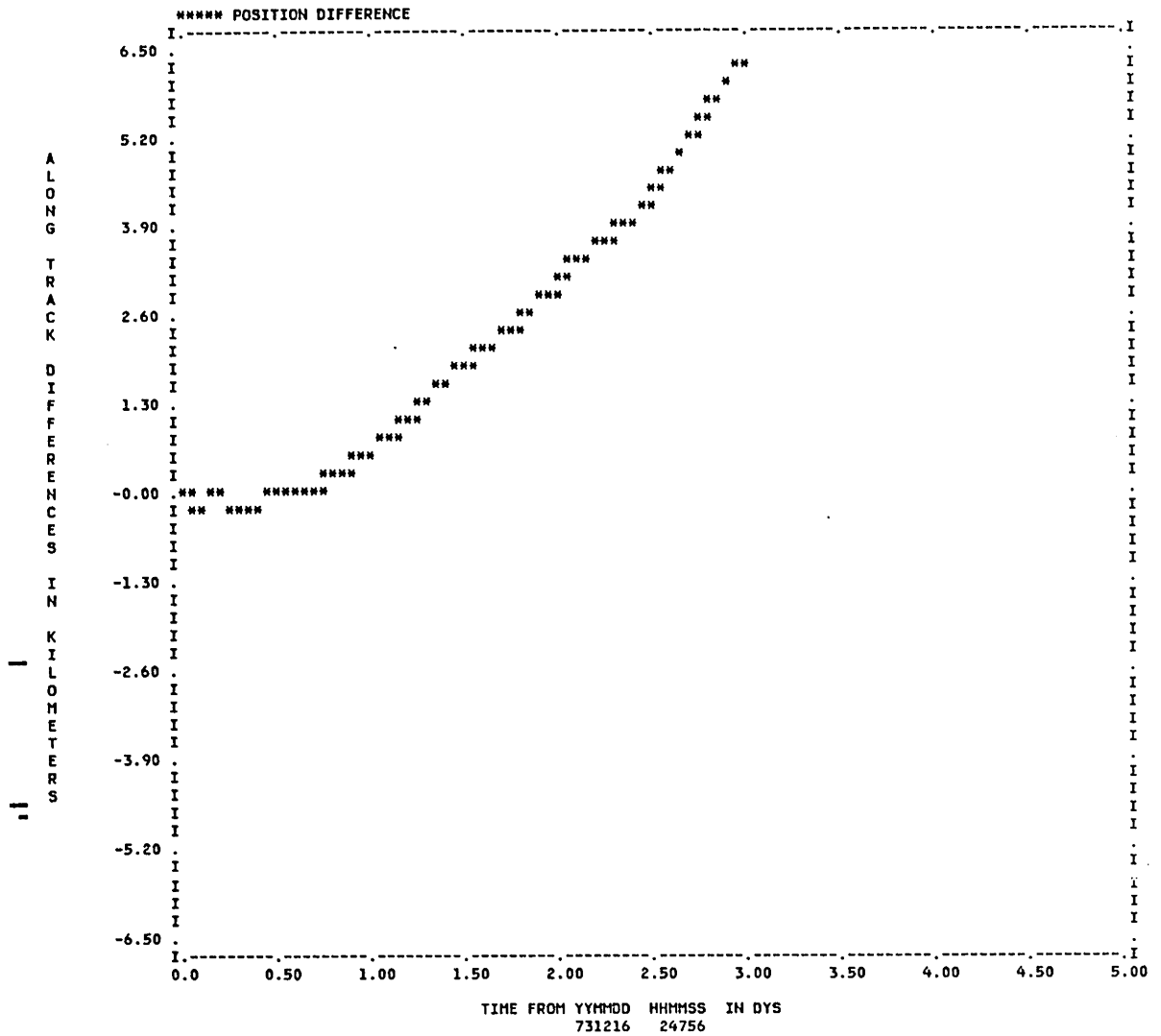
* Initial conditions from the Cowell batch filter with states and ρ_1 as solve-for vector (see Table 3-22). The perturbation model for the Cowell orbit generator is given in Table 3-17.

Figure 3-4. Along Track Difference/Semianalytical* minus the Truth Ephemeris of Test Case Two



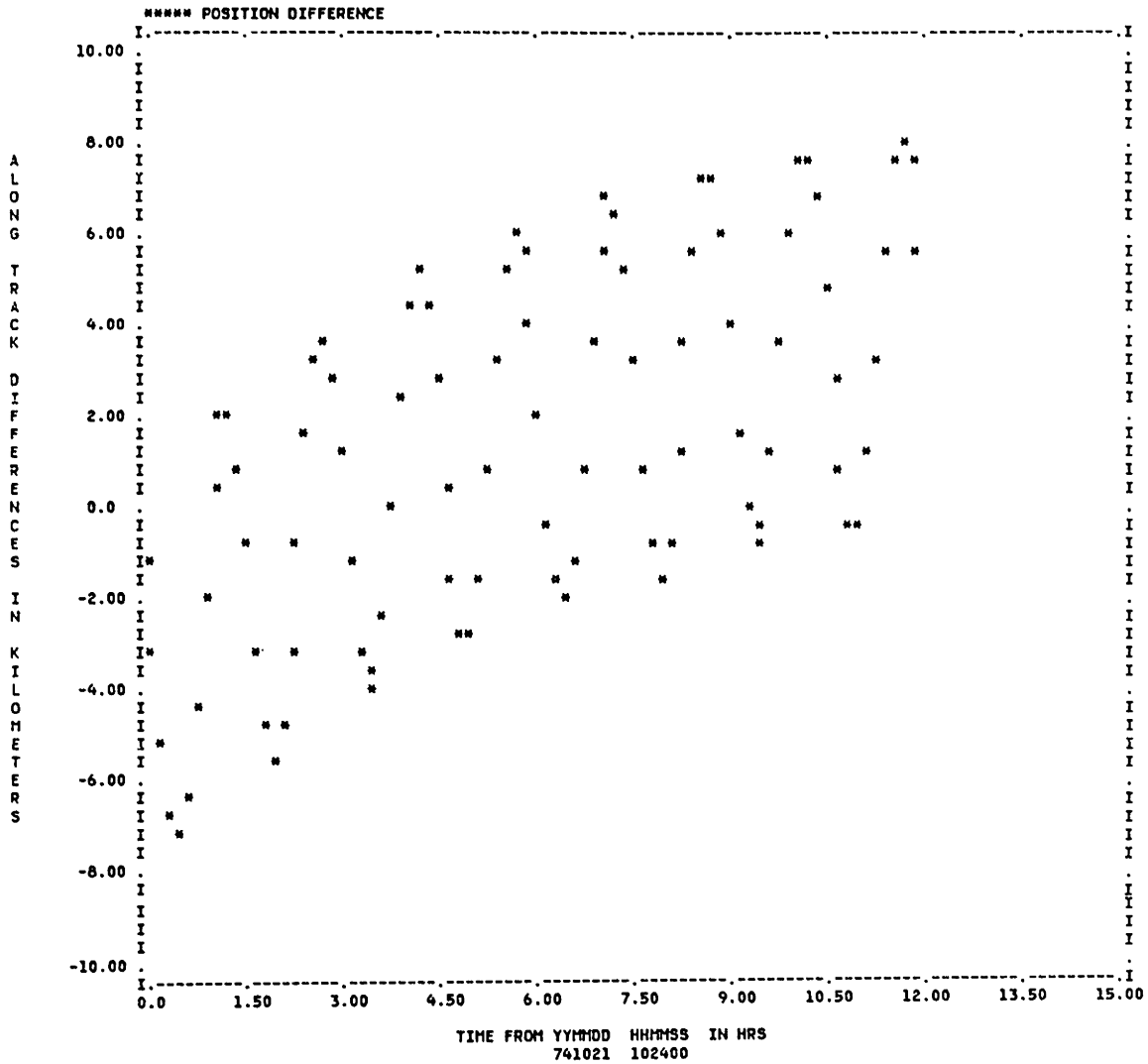
* Initial conditions from the semianalytical batch filter with states and C_D as solve-for vector (see Table 3-23). The perturbation model for the semianalytical orbit generator is given in Table 3-21.

Figure 3-5. Along Track Difference/Semianalytical* minus the Truth Ephemeris of Test Case Two



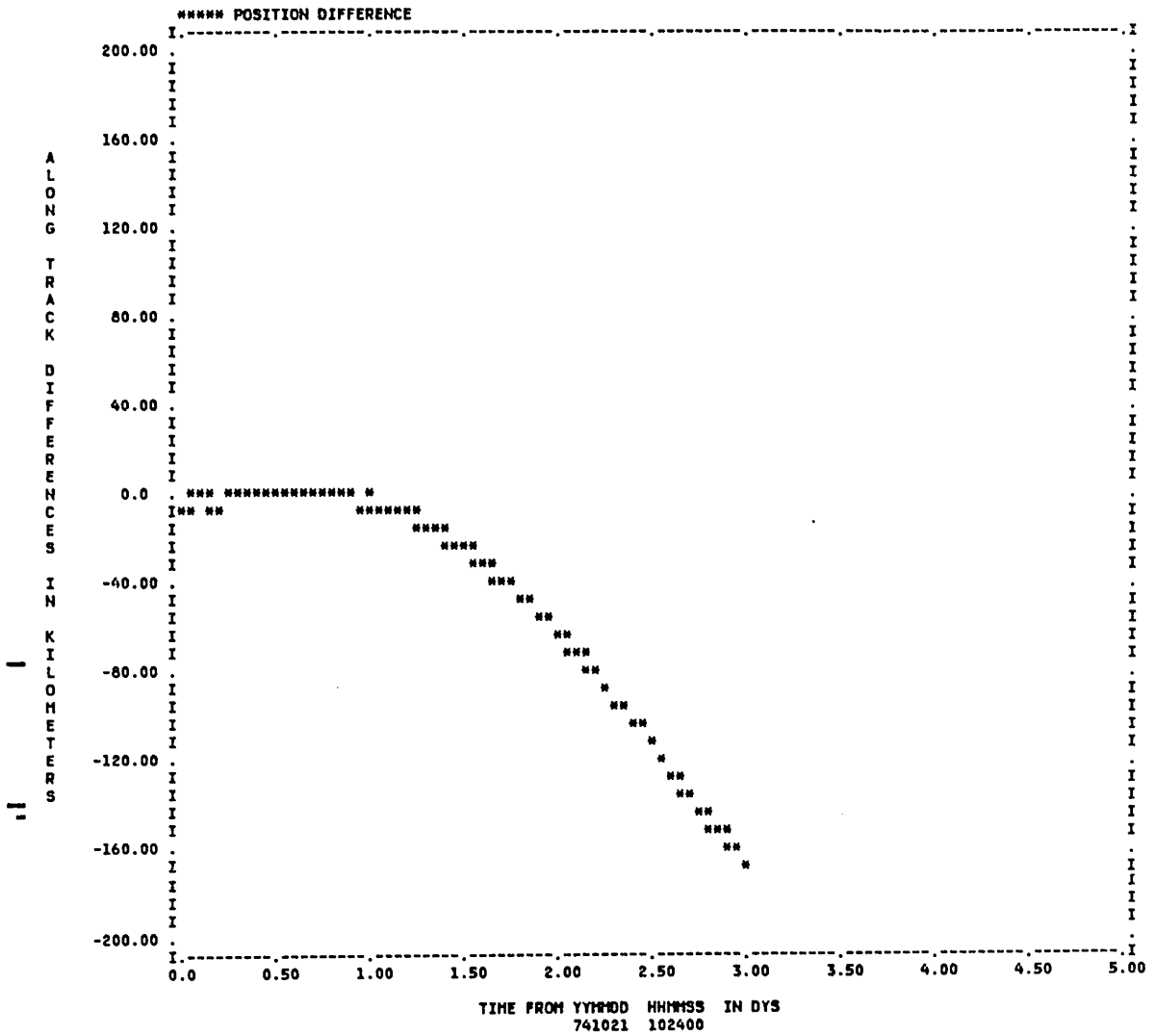
* Initial conditions from the semianalytical batch filter with states, a_1 and a_2 as solve-for vector (see Table 3-24). The perturbation model for the semianalytical orbit generator is given in Table 3-21.

Figure 3-6. Along Track Difference over 12 Hours/Cowell* minus the Truth Ephemeris of Test Case Three



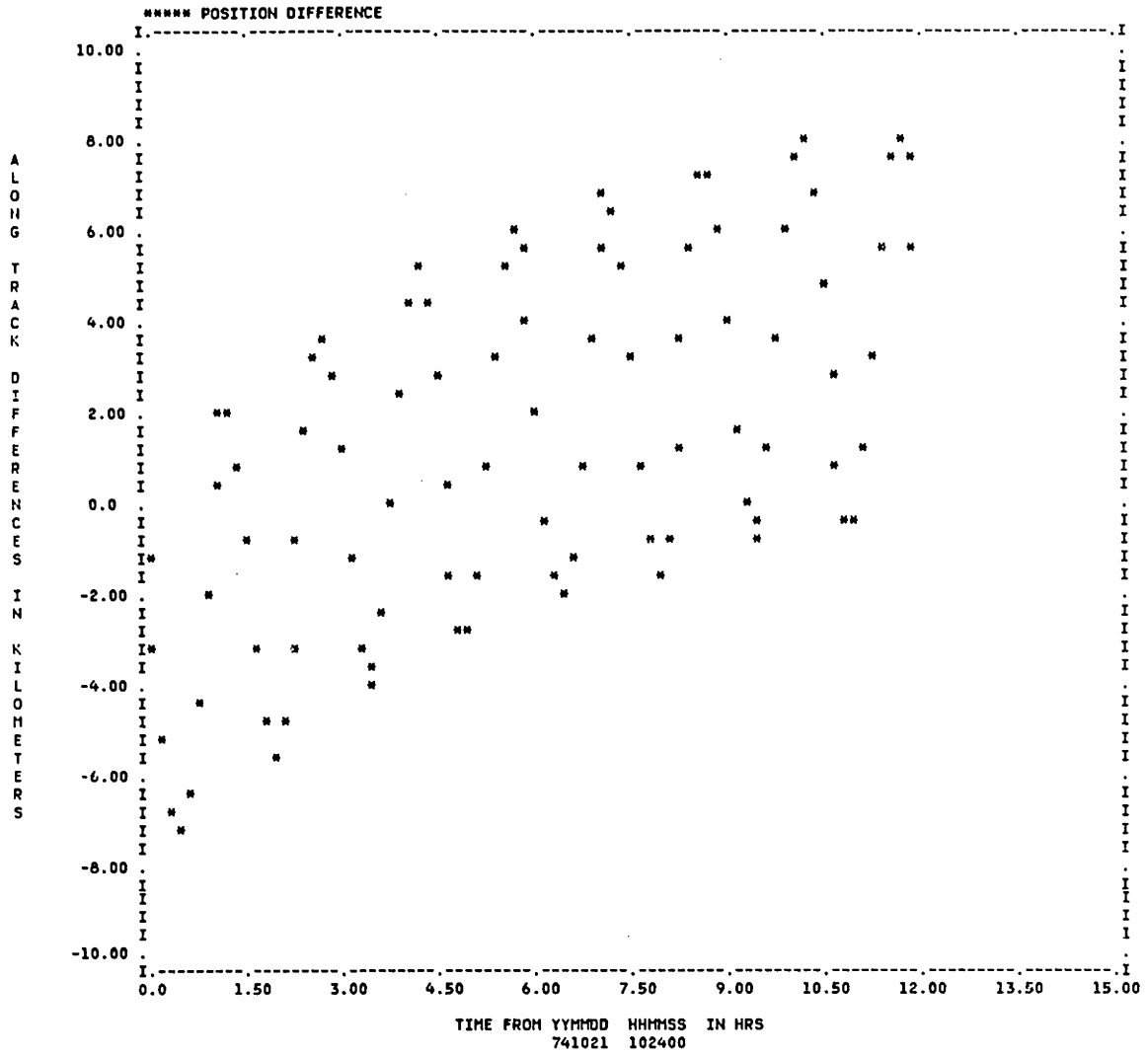
* Initial conditions from the Cowell batch filter with states only as the solve-for vector (see Table 3-31). The perturbation model for the Cowell orbit generator is given in Table 3-17.

Figure 3-7. Along Track Difference over 72 Hours/Cowell* minus the Truth Ephemeris of Test Case Three



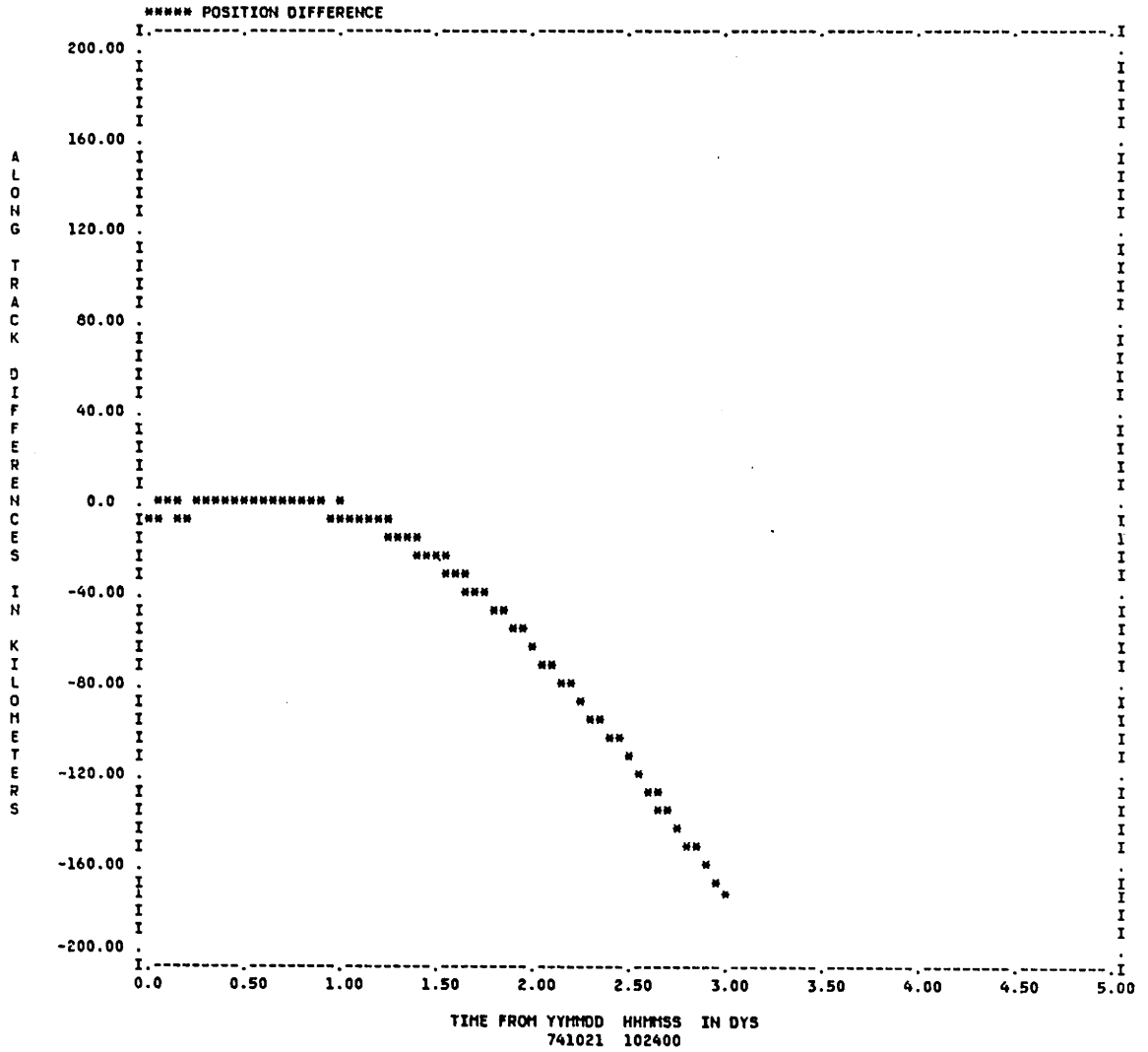
* Initial conditions from the Cowell batch filter with states only as the solve-for vector (see Table 3-31). The perturbation model for the Cowell orbit generator is given in Table 3-17.

Figure 3-8. Along Track Difference over 12 Hours/Semianalytical* minus the Truth Ephemeris of Test Case Three



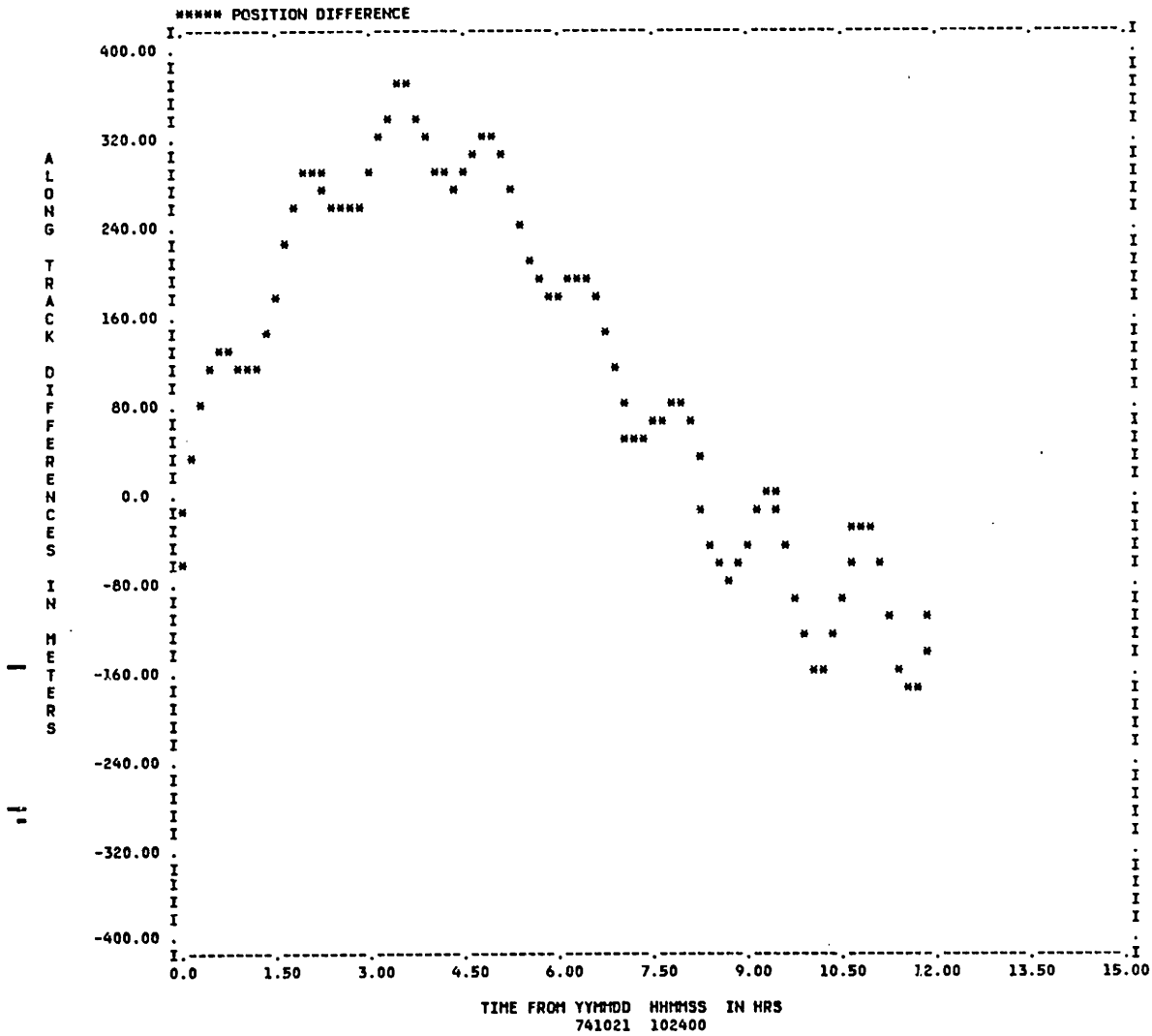
* Initial conditions from the semianalytical batch filter with states only as the solve-for vector (see Table 3-32). The perturbation model for the semianalytical orbit generator is given in Table 3-21.

Figure 3-9. Along Track Difference over 72 Hours/Semianalytical* minus the Truth Ephemeris of Test Case Three



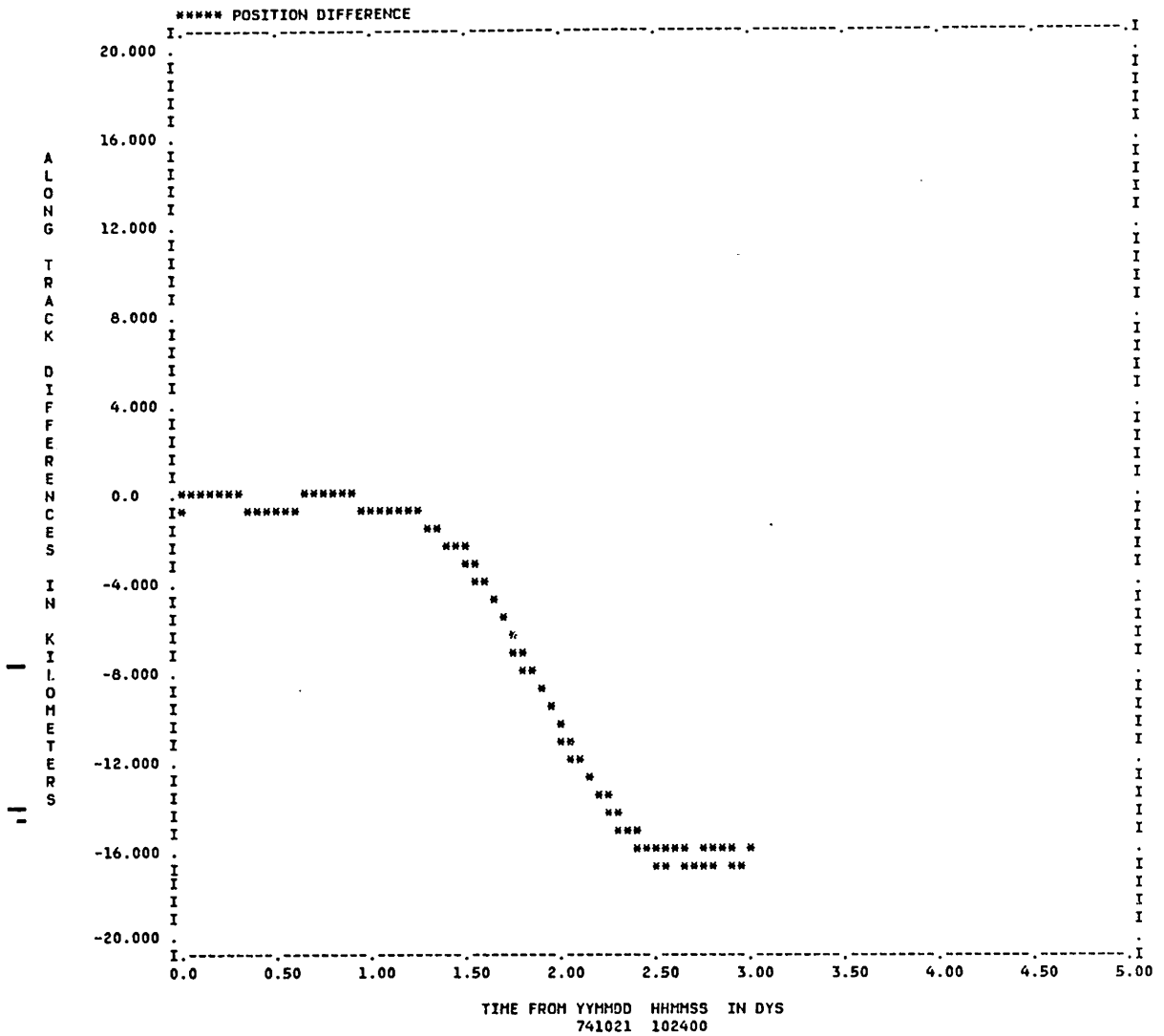
* Initial conditions from the semianalytical batch filter with states only as the solve-for vector (see Table 3-32). The perturbation model for the semianalytical orbit generator is given in Table 3-21.

Figure 3-10. Along Track Difference over 12 Hours/Cowell* minus the Truth Ephemeris of Test Case Three



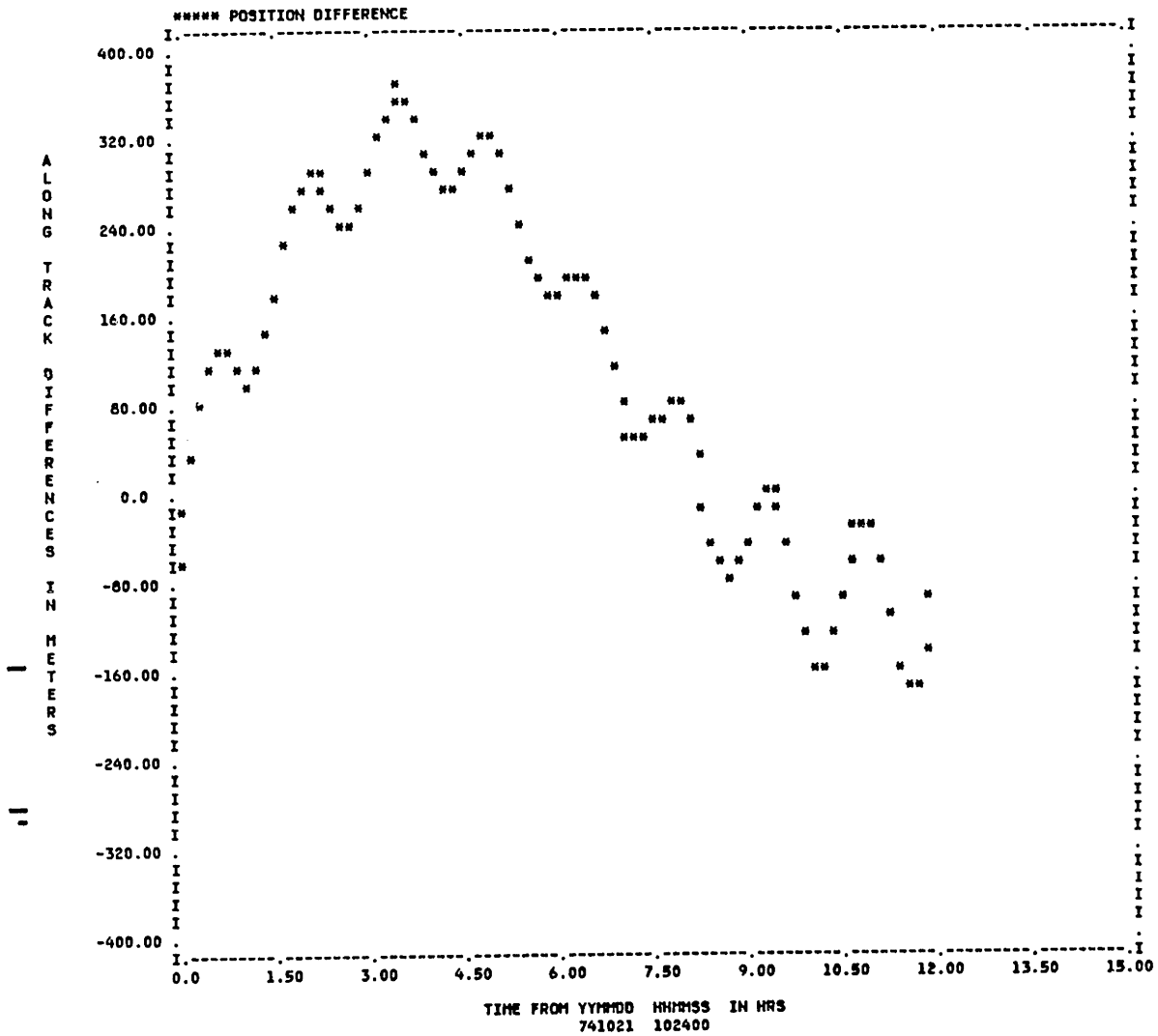
* Initial conditions from the Cowell batch filter with states and ρ_1 as the solve-for vector (see Table 3-33). The perturbation model for the Cowell orbit generator is given in Table 3-17.

Figure 3-11. Along Track Difference over 72 Hours/Cowell* minus the Truth Ephemeris of Test Case Three



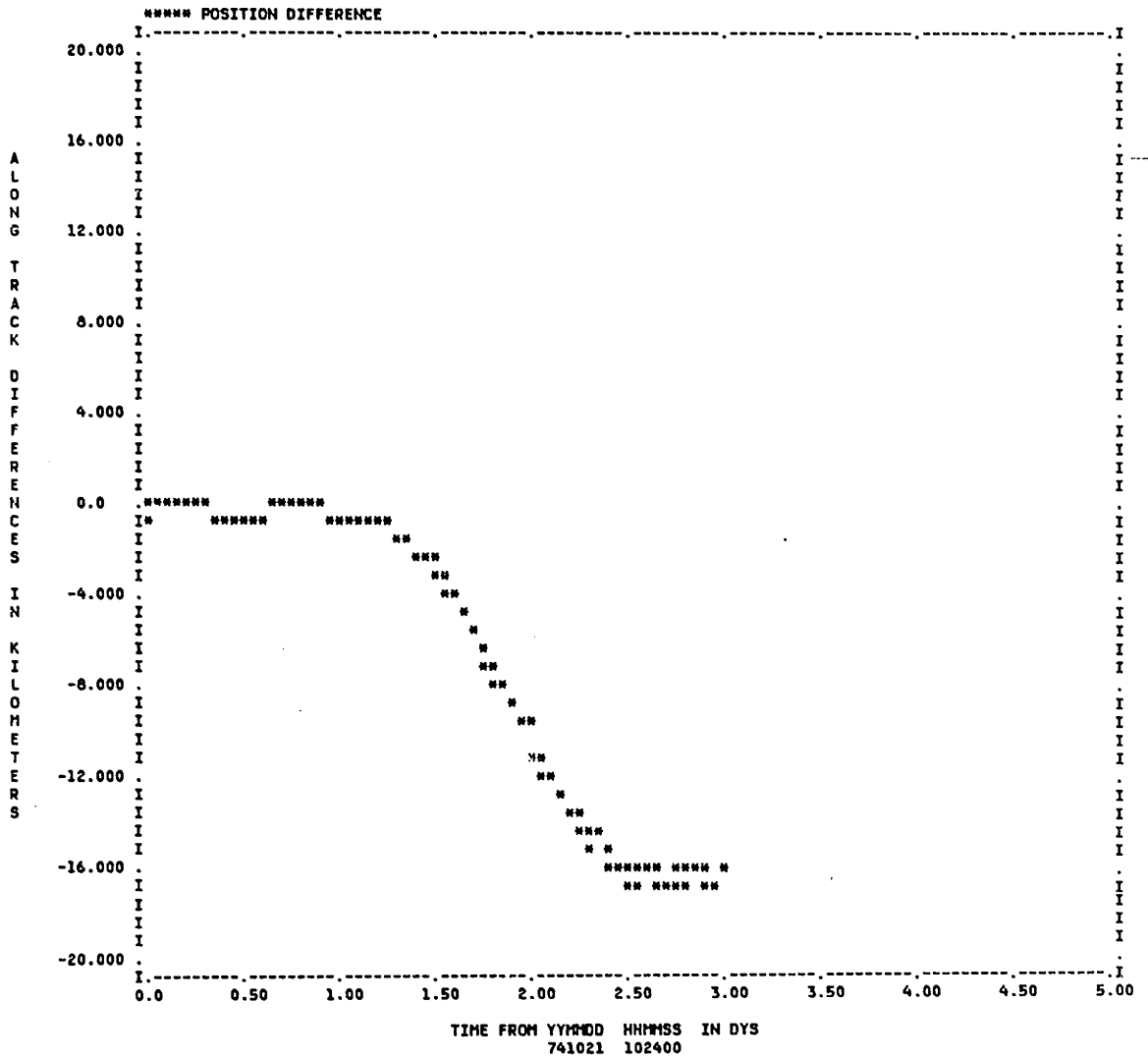
* Initial conditions from the Cowell batch filter with states and ρ_1 as the solve-for vector (see Table 3-33). The perturbation model for the Cowell orbit generator is given in Table 3-17.

Figure 3-12. Along Track Difference over 12 Hours/Semianalytical* minus the Truth Ephemeris of Test Case Three



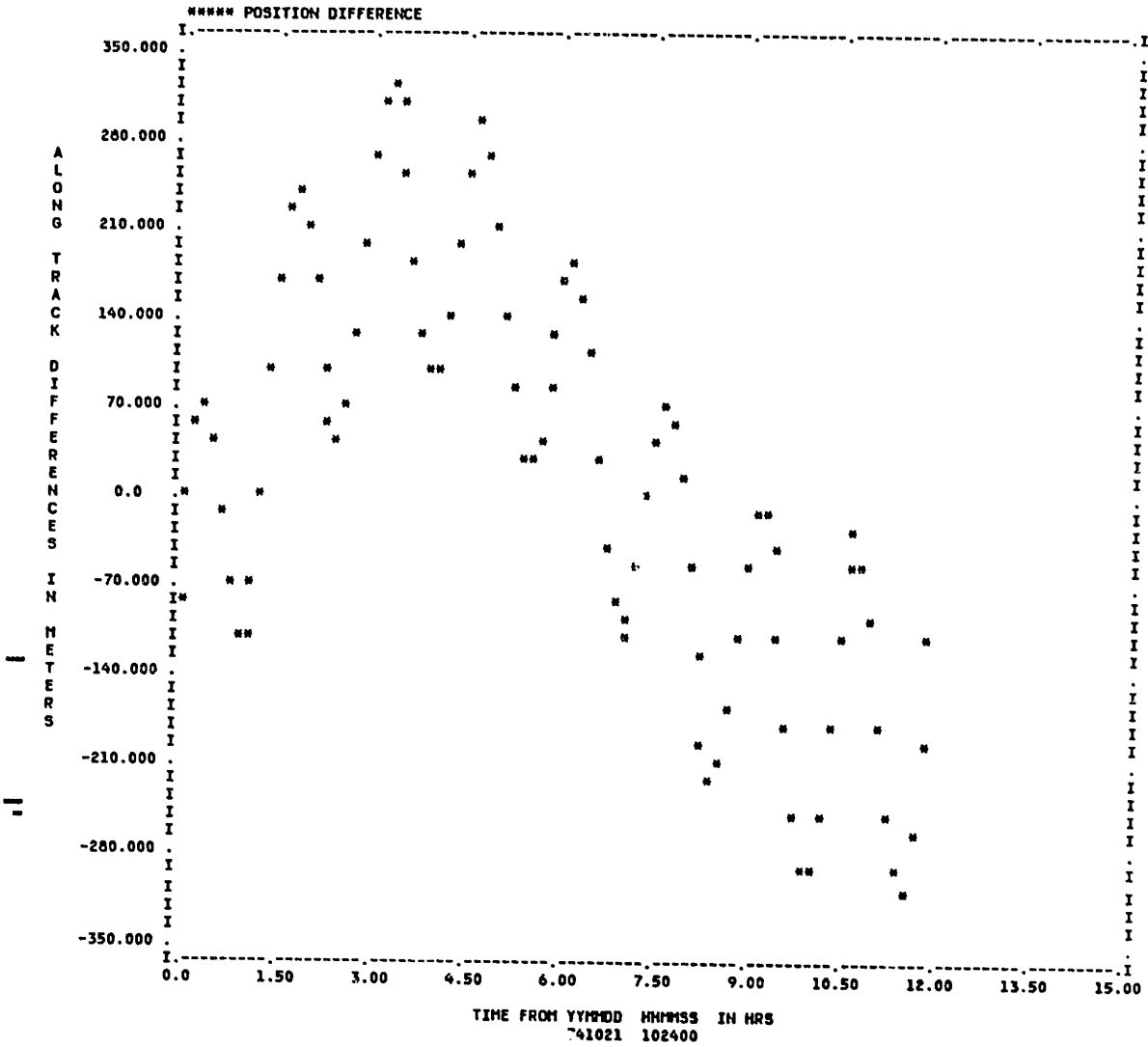
* Initial conditions from the semianalytical batch filter with states and C_D as the solve-for vector (see Table 3-34). The perturbation model for the semianalytical orbit generator is given in Table 3-21.

Figure 3-13. Along Track Difference over 72 Hours/Semianalytical* minus the Truth Ephemeris of Test Case Three



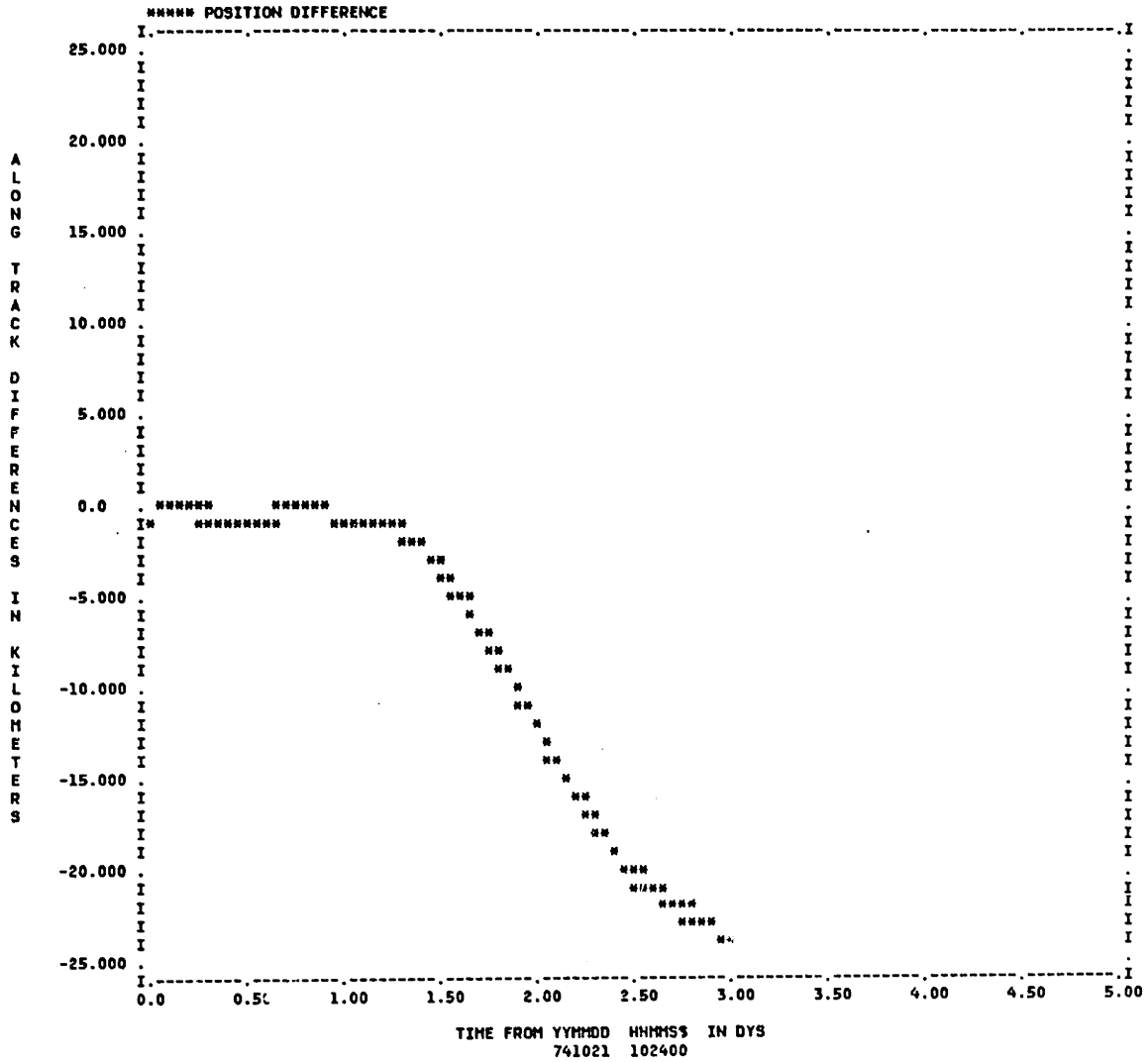
* Initial conditions from the semianalytical batch filter with states and C^D as the solve-for vector (see Table 3-34). The perturbation model for the semianalytical orbit generator is given in Table 3-21.

Figure 3-14. Along Track Difference over 12 Hours/Semianalytical* minus the Truth Ephemeris of Test Case Three



* Initial conditions from the semianalytical batch filter with states, a_1 and a_2 as the solve-for vector (see Table 3-35). The perturbation model for the semianalytical orbit generator is given in Table 3-21.

Figure 3-15. Along Track Difference over 72 Hours/Semianalytical* minus the Truth Ephemeris of Test Case Three



* Initial conditions from the semianalytical batch filter with states, a_1 and a_2 as the solve-for vector (see Table 3-35). The perturbation model for the semianalytical orbit generator is given in Table 3-21.

Chapter 4

SEMIANALYTICAL SATELLITE THEORY AND THE KALMAN FILTER

The previous chapter demonstrated that the semianalytical satellite theory can be coupled with a batch filter. A batch filter uses all the measurements over an observation span to determine the best estimate of the epoch (or any reference time) conditions. It sometimes becomes desirable to use an estimation procedure which processes the observations sequentially and computes the current estimate of a satellite's state. This is especially true for a space surveillance system which is required to operate in a real-time environment.

A sequential filter is an estimation procedure which does not need to use past measurements for the computation of the current estimate. For a linear system the optimal sequential filter is the Kalman filter (Ref. 72). The processing of observational data by a Kalman filter is done presently in only a few operational OD systems due to real-time requirements and/or the sequential nature of this estimation procedure. If the semianalytical satellite theory is to be applicable to all aspects of an OD system, it is necessary to couple the semianalytical satellite theory with the Kalman filter. Combining the semianalytical satellite theory with the Kalman filter may improve the accuracy and efficiency of current OD systems.

This chapter will present the algorithmic structure for coupling the semianalytical satellite theory with the Kalman filter. First a brief, heuristic review of the Kalman filter is presented. A Semianalytical Linearized Kalman filter is developed and discussed next.

4.1 Review of the Kalman Filter

Since this research is concerned with using the Kalman filter with an orbit determination process, it will be assumed that the system dynamics are continuous and that the observational data is received in a discrete fashion. In this section, the Kalman filter for a linear system with discrete measurements will be discussed first. Next the Linearized Kalman filter and Extended Kalman filter will be briefly reviewed.

For a linear system, the system dynamics are assumed to be of the form

$$\dot{\underline{x}} = A\underline{x} + \underline{\omega}(t) \quad (4-1a)$$

where \underline{x} is the actual state, $\underline{\omega}(t)$ is the noise vector and A is the system matrix. The noise vector is assumed to have a normal distribution with zero mean and a covariance of $Q(t)$. This is represented as

$$\underline{\omega}(t) \sim N(0, Q(t)) \quad (4-1b)$$

The measurement model is assumed to be of the form

$$\underline{O}_a(t_k) = H_k \underline{x}_k + \underline{v}_k \quad (4-2a)$$

$$\underline{v}_k \sim N(0, R_k) \quad (4-2b)$$

The basic concept of a Kalman filter is that given an a priori estimate of the state at t_k , $\hat{\underline{x}}(t_k^-)$, an updated estimate, $\hat{\underline{x}}(t_k^+)$, can be obtained based only on $\hat{\underline{x}}(t_k^-)$ and $\underline{O}_a(t_k)$. This can be written as

$$\hat{\underline{x}}(t_k^+) = K'_k \hat{\underline{x}}(t_k^-) + K_k \underline{O}_a(t_k) \quad (4-3)$$

where K'_k and K_k are time-varying weighting matrices that must be determined. In order to determine K'_k and K_k , the following conditions are placed upon the filter

$$E[\delta \hat{\underline{x}}(t_k^+)] = 0 \quad (4-4a)$$

$$\text{minimize } E[\delta \hat{\underline{x}}^T(t_k^+) \delta \hat{\underline{x}}(t_k^+)] \quad (4-4b)$$

where

$$\delta \hat{\underline{x}}(t_k^+) = \hat{\underline{x}}(t_k^+) - \underline{x}(t_k) \quad (4-5)$$

and where $\hat{\underline{x}}(t_k+)$ is the updated estimate, $\underline{x}(t_k)$ is the actual state and $E[d]$ denotes the expected or mean value of d . Equation (4-4a) implies that the expected value of $\hat{\underline{x}}(t_k+)$ equals the expected value of $\underline{x}(t_k)$. Equation (4-4b) implies that the filter will give an estimate that makes the length of the error vector, $\hat{\underline{x}}(t_k+) - \underline{x}(t_k)$, minimum. The covariance matrix of $\hat{\underline{x}}(t_k)$ is defined as

$$P \equiv E[\delta \hat{\underline{x}}(t_k) \delta \hat{\underline{x}}^T(t_k)] \quad (4-6)$$

It is noted that P is a symmetric matrix and that the trace of P is called the variance of $\hat{\underline{x}}(t_k)$. It is also noted that

$$\text{Trace}(P) = E[\delta \hat{\underline{x}}^T(t_k) \delta \hat{\underline{x}}(t_k)] \quad (4-7)$$

It becomes obvious that the desired Kalman filter [Equations (4-3), (4-4a) and (4-4b)] is unbiased and minimum variance.

From Equation (4-5) it is seen that

$$\begin{aligned} \hat{\underline{x}}(t_k+) &= \delta \hat{\underline{x}}(t_k+) + \underline{x}(t_k) \\ \hat{\underline{x}}(t_k-) &= \delta \hat{\underline{x}}(t_k-) + \underline{x}(t_k) \end{aligned} \quad (4-8)$$

Substitution of Equation (4-8) into Equation (4-3) yields after some rearranging

$$\begin{aligned}\hat{\delta \underline{x}}(t_k+) &= [K'_k + K_k H_k - I] \underline{x}(t_k) \\ &+ K'_k \hat{\delta \underline{x}}(t_k-) + K_k \underline{v}_k\end{aligned}$$

Taking the expectation of the above expression and noting that

$$E[\hat{\delta \underline{x}}(t_k+)] = E[\hat{\delta \underline{x}}(t_k-)] = E[\underline{v}_k] = 0$$

yields

$$0 = [K'_k + K_k H_k - I] E[\underline{x}(t_k)]$$

Since $E[\underline{x}(t_k)]$ does not necessarily equal zero, it follows that

$$K'_k = I - K_k H_k \quad (4-9)$$

Equation (4-5) can be rewritten as

$$\hat{\delta \underline{x}}(t_k+) = [I - K_k H_k] \hat{\delta \underline{x}}(t_k-) + K_k [H_k \hat{\underline{x}}(t_k+) + \underline{v}_k]$$

which reduces to

$$\hat{\delta \underline{x}}(t_k+) = [I - K_k H_k] \hat{\delta \underline{x}}(t_k-) + K_k \underline{v}_k \quad (4-10)$$

From Equations (4-6) and (4-10) it follows that

$$\begin{aligned}
P(t_k+) &= (I - K_k H_k) E[\hat{\delta x}(t_k-) \hat{\delta x}^T(t_k-)] (I - K_k H_k)^T \\
&+ K_k E[v_k v_k^T] K_k^T + (I - K_k H_k) E[\hat{\delta x}(t_k-) v_k^T] K_k^T \\
&+ K_k E[v_k \hat{\delta x}^T(t_k-)] (I - K_k H_k)^T
\end{aligned}$$

Assuming that the measurement errors are uncorrelated with $\hat{\delta x}(t_k-)$ and that $E[v_k v_k^T] = R_k$, the above expression reduces to

$$\begin{aligned}
P(t_k+) &= (I - K_k H_k) P(t_k-) (I - K_k H_k)^T \\
&+ K_k R_k K_k^T
\end{aligned} \tag{4-11a}$$

which yields

$$\begin{aligned}
P(t_k+) &= P(t_k-) - K_k H_k P(t_k-) - P(t_k-) H_k^T K_k^T \\
&+ K_k H_k P(t_k-) H_k^T K_k^T + K_k R_k K_k^T
\end{aligned} \tag{4-11b}$$

It can be seen from Equations (4-4b) and (4-7) that the second filter criterion can be expressed as minimizing the trace of $P(t_k+)$. The following relations with regard to the operation of the trace of a matrix are noted

$$\text{Trace}[A+B] = \text{Trace}[A] + \text{Trace}[B] \tag{4-12a}$$

$$\text{Trace}[A^T] = \text{Trace}[A] \tag{4-12b}$$

$$\frac{\partial [\text{Trace}(ABA^T)]}{\partial A} = 2AB \quad (B \text{ is symmetric}) \quad (4-12c)$$

$$\frac{\partial [\text{Trace}(BA^T)]}{\partial A} = B \quad (4-12d)$$

Applying the filter conditions as given in Equation (4-4b) results in

$$\frac{\partial \{\text{Trace}[P(t_k+)]\}}{\partial K_k} = 0 \quad (4-13)$$

By use of Equations (4-11b) and (4-12), it is seen that

$$K_k = P(t_k^-)H_k^T [H_k P(t_k^-)H_k^T + R_k]^{-1} \quad (4-14)$$

Substitution of Equation (4-14) into Equation (4-11) gives the updated covariance matrix as

$$P(t_k+) = [I - K_k H_k] P(t_k^-) \quad (4-15)$$

The general form of the Kalman filter is obtained by substituting Equation (4-9) into Equation (4-3). This results in

$$\hat{\underline{x}}(t_k+) = \hat{\underline{x}}(t_k^-) + K_k [O_a(t_k) - H_k \hat{\underline{x}}(t_k^-)] \quad (4-16)$$

The next problem that must be solved is the propagation of the updated state and covariance matrix to the next observation

time. Taking the expectation of each side of Equation (4-1a) and noting that $E[\dot{\underline{x}}] = \frac{d}{dt} [E[\underline{x}]] = \dot{\underline{x}}$ and that $E[\underline{\omega}(t)] = 0$, it is seen that

$$\dot{\underline{\hat{x}}} = \underline{\hat{A}} \underline{\hat{x}} \quad (4-17)$$

Equation (4-17) can be used to propagate the state forward by a numerical integration technique. Equation (4-17) can also be solved by use of the state transition matrix, i.e.,

$$\underline{\hat{x}}(t) = \Phi(t, t_0) \underline{\hat{x}}(t_0) \quad (4-18a)$$

where

$$\dot{\Phi}(t, t_0) = \underline{\hat{A}} \Phi(t, t_0) \quad (4-18b)$$

$$\Phi(t_0, t_0) = \underline{I} \quad (4-18c)$$

It is noted that the state transition matrix has the following important characteristics (Ref. 72)

$$\Phi(t_2, t_0) = \Phi(t_2, t_1) \Phi(t_1, t_0) \quad (4-18d)$$

$$\Phi^{-1}(t_k, t_0) = \Phi(t_0, t_k) \quad (4-18e)$$

$$\Phi(t, t) = \underline{I} \quad (4-18f)$$

The error covariance matrix is written as [Equation (4-6)]

$$P(t) = E[\hat{\delta \underline{x}}(t) \hat{\delta \underline{x}}^T(t)] \quad (4-19)$$

From Equation (4-5) it is seen that

$$\hat{\delta \underline{x}}(t) = \hat{\underline{x}}(t) - \underline{x}(t)$$

Therefore

$$\dot{\hat{\delta \underline{x}}}(t) = \dot{\hat{\underline{x}}}(t) - \dot{\underline{x}}(t)$$

and

$$\dot{\hat{\underline{x}}} = A \hat{\underline{x}} + \underline{\omega}(t) \quad (4-20)$$

Taking the derivative of Equation (4-19), noting that $\frac{d}{dt} = E[a] = E[\frac{da}{dt}]$ and using Equation (4-20), the following expression results

$$\begin{aligned} \dot{P}(t) &= E[A \hat{\delta \underline{x}} \hat{\delta \underline{x}}^T] + E[\underline{\omega}(t) \hat{\delta \underline{x}}^T] \\ &\quad + E[\hat{\delta \underline{x}} \hat{\delta \underline{x}}^T A^T] + E[\hat{\delta \underline{x}} \underline{\omega}^T(t)] \\ \dot{P}(t) &= A P(t) + P(t) A^T + E[\underline{\omega}(t) \hat{\delta \underline{x}}^T] \\ &\quad + E[\hat{\delta \underline{x}} \underline{\omega}^T(t)] \end{aligned} \quad (4-21)$$

Equation (4-20) can be solved by the variation of constant formula (Ref. 72)

$$\hat{\underline{x}}(t) = \Phi(t, t_0) \hat{\underline{x}}(t_0) + \int_{t_0}^t \Phi(t, \tau) \underline{\omega}(\tau) d\tau \quad (4-22)$$

Post-multiplying Equation (4-22) by $\underline{\omega}^T(t)$ and taking the expectation of the resulting expression yields the following

$$\begin{aligned} E[\hat{\underline{x}}(t) \underline{\omega}^T(t)] &= \Phi(t, t_0) E[\hat{\underline{x}}(t_0) \underline{\omega}^T(t)] \\ &+ \int_{t_0}^t \Phi(t, \tau) E[\underline{\omega}(\tau) \underline{\omega}^T(t)] d\tau \end{aligned}$$

Assuming that the system noise and initial state deviation, $\hat{\underline{x}}(t_0)$, are independent implies that

$$E[\hat{\underline{x}}(t) \underline{\omega}^T(t)] = \int_{t_0}^t \Phi(t, \tau) Q(\tau) \delta(t-\tau) d\tau$$

where $\delta(t-\tau)$ is the Dirac-Delta function. Noting that (Ref. 72)

$$\int_a^b f(x) \delta(b-x) dx = \frac{1}{2} f(b) \quad (4-23)$$

results in

$$E[\hat{\underline{x}}(t) \underline{\omega}^T(t)] = \frac{1}{2} \Phi(t, t) Q(t) = \frac{1}{2} Q(t) \quad (4-24a)$$

In a similar manner it can be shown that

$$E[\underline{\omega}(t) \hat{\delta \underline{x}}^T(t)] = \frac{1}{2} Q(t) \quad (4-24b)$$

Therefore Equation (4-21) becomes

$$\dot{P}(t) = AP(t) + P(t)A^T + Q(t) \quad (4-25)$$

The error covariance matrix can be propagated by a numerical integration of Equation (4-25). The homogeneous solution of Equation (4-25) is

$$P(t) = \Phi(t, t_0) P(t_0) \Phi^T(t, t_0) \quad (4-26)$$

where $\Phi(t, t_0)$ is defined in Equations (4-18b) through (4-18f). Equation (4-26) can be shown to be correct by taking the time derivative and reducing this to the homogeneous part of Equation (4-25), i.e.,

$$\begin{aligned} \dot{P}(t) &= \dot{\Phi}(t, t_0) P(t_0) \Phi^T(t, t_0) \\ &\quad + \Phi(t, t_0) P(t_0) \dot{\Phi}^T(t, t_0) \\ \dot{P}(t) &= A \Phi(t, t_0) P(t_0) \Phi^T(t, t_0) \\ &\quad + \Phi(t, t_0) P(t_0) \Phi^T(t, t_0) A^T \\ \dot{P}(t) &= A P(t) + P(t) A^T \end{aligned}$$

By use of the variation of constants formula it can be shown that the solution to Equation (4-25) is (Ref. 72)

$$\begin{aligned}
 P(t) &= \Phi(t, t_0) P(t_0) \Phi^T(t, t_0) \\
 &+ \int_{t_0}^t \Phi(t, \tau) Q(\tau) \Phi^T(t, \tau) d\tau
 \end{aligned}
 \tag{4-27}$$

A summary of the Kalman filter for a linear system is given in Table 4-1 (Ref. 72). The Kalman filter as given in Table 4-1 must be modified for non-linear systems. Two such modifications are the Extended Kalman filter (EKF) and the Linearized Kalman filter (LKF).

The Linearized Kalman filter results when the system dynamics and measurement models are linearized about a nominal trajectory, $\underline{x}_N(t)$. The nominal trajectory can be obtained from a reduced dynamic model or from a numerical integration of the equations of motion. The system model can be expressed functionally as

$$\dot{\underline{x}} = f(\underline{x}, t) + \underline{\omega}(t)
 \tag{4-28}$$

The estimated dynamics are assumed to be

$$\dot{\hat{\underline{x}}} = \underline{f}(\hat{\underline{x}}, t)
 \tag{4-29}$$

Table 4-1
Kalman Filter for a Linear System
with Discrete Measurements

System Model:	$\dot{\underline{x}}(t) = A\underline{x}(t) + \underline{\omega}(t)$	$\underline{\omega}(t) \sim N(0, Q(t))$
Measurement Model:	$\underline{O}_a(t_k) = H_k \underline{x}(t_k) + \underline{v}_k$	$\underline{v}_k \sim N(0, R_k)$
Initial Conditions:	$\underline{x}(0) \sim N(\hat{\underline{x}}_0, P_0)$	
Assumptions:	$E[\underline{v}_k \delta \hat{\underline{x}}^T(t_k^-)] = 0$	$\delta \hat{\underline{x}}(t_k) = \hat{\underline{x}}(t_k) - \underline{x}(t_k)$
	$E[\underline{\omega}(t) \delta \hat{\underline{x}}^T(t_0)] = 0$	$E[\underline{\omega}(t) \underline{v}_k^T] = 0$
State Estimate	$\dot{\hat{\underline{x}}} = A\hat{\underline{x}}$	
Propagation:	$\hat{\underline{x}}(t) = \Phi(t, t_0) \hat{\underline{x}}(t_0)$	
Error Covariance	$\dot{P}(t) = AP(t) + P(t)A^T + Q(t)$	
Propagation:	$P(t) = \Phi(t, t_0) P(t_0) \Phi^T(t, t_0) + \int_{t_0}^t \Phi(t, \tau) Q(\tau) \Phi^T(t, \tau) d\tau$	
State Estimate		
Update:	$\hat{\underline{x}}(t_k^+) = \hat{\underline{x}}(t_k^-) + K_k [\underline{O}_a(t_k) - H_k \hat{\underline{x}}(t_k^-)]$	
Error Covariance		
Update:	$P(t_k^+) = [I - K_k H_k] P(t_k^-)$	
Gain Matrix:	$K_k = P(t_k^-) H_k^T [H_k P(t_k^-) H_k^T + R_k]^{-1}$	
State Transition	$\dot{\Phi}(t, t_0) = A \Phi(t, t_0)$	
Matrix:	$\Phi(t_0, t_0) = I$	

Now linearizing about the nominal trajectory yields

$$\begin{aligned} \dot{\underline{\hat{x}}} &= \underline{f}(\underline{x}_N, t) + \left[\frac{\partial \underline{f}}{\partial \underline{x}} \right]_{\underline{x}_N} (\underline{\hat{x}} - \underline{x}_N) \\ &+ O[(\underline{\hat{x}} - \underline{x}_N)^2] \end{aligned} \quad (4-30)$$

The following quantities are defined

$$F \equiv \left[\frac{\partial \underline{f}(\underline{x}, t)}{\partial \underline{x}} \right]_{\underline{x}_N} \quad (4-31a)$$

$$\Delta \underline{\hat{x}} = \underline{\hat{x}} - \underline{x}_N \quad (4-31b)$$

Equation (4-30) can therefore be written to first order in $\Delta \underline{\hat{x}}$ as

$$\dot{\Delta \underline{\hat{x}}} = F \Delta \underline{\hat{x}} \quad (4-32)$$

The actual measurement model can be expressed as

$$\underline{O}_a(t_k) = \underline{h}_k[\underline{x}(t_k)] + \underline{v}_k \quad (4-33a)$$

The best estimate of the measurement model is

$$\underline{O}_c(t_k) = \underline{h}_k[\underline{\hat{x}}(t_k)] \quad (4-33b)$$

where $\underline{O}_c(t_k)$ represents the computed observations. Linearizing about the nominal trajectory yields

$$\underline{z}(t_k) = H_k \Delta \hat{\underline{x}} \quad (4-34a)$$

where

$$H_k \equiv \left[\frac{\partial h_k[\underline{x}(t_k)]}{\partial \underline{x}} \right]_{\underline{x}_N} \quad (4-34b)$$

$$\underline{z}(t_k) \equiv \underline{O}_a(t_k) - h_k[\underline{x}_N(t_k)] \quad (4-34c)$$

Equations (4-32) and (4-34a) are in linear form so the Kalman filter as given in Table 4-1 applies. A summary of the Linearized Kalman filter is given in Table 4-2 (Ref. 72). The main advantage of the LKF is that once the nominal trajectory has been obtained, the error covariance matrix and Kalman gain matrix are defined (assuming that the observation model is known for each observation point in advance). This means that $P(t)$ and K_k can be obtained off-line, i.e., prior to when the actual estimation process is required. A major disadvantage of the LKF is that over long observation spans, the nominal trajectory can vary greatly from the actual trajectory causing erroneous estimates.

Table 4-2
 Linearized Kalman Filter for a Non-Linear
 System with Discrete Measurements

System Model: $\dot{\underline{x}}(t) = \underline{f}[\underline{x}(t), t] + \underline{\omega}(t) \quad \underline{\omega}(t) \sim N(0, Q(t))$

Measurement model: $\underline{O}_a(t_k) = \underline{h}_k[\underline{x}(t_k)] + \underline{v}_k \quad \underline{v}_k \sim N(0, R_k)$

Initial Conditions: $\underline{x}(0) \sim N(\hat{\underline{x}}_0, P_0)$

Assumptions: $E[\underline{\omega}(t) \underline{v}_k^T] = 0, E[\underline{v}_k (\Delta \hat{\underline{x}}(t_k^-) - \Delta \underline{x}(t_k^-))^T] = 0$

$$E[\underline{\omega}(t) (\Delta \hat{\underline{x}}(t_0) - \Delta \underline{x}(t_0))^T] = 0,$$

$$\Delta \hat{\underline{x}}(t) \equiv \hat{\underline{x}}(t) - \underline{x}_N(t)$$

State Estimate $\dot{\Delta \underline{x}} = F \Delta \underline{x}, \Delta \hat{\underline{x}}(t) = \Phi(t, t_0) \Delta \hat{\underline{x}}(t_0)$

Propagation: $\dot{\underline{x}} = \underline{f}(\underline{x}_N, t) + F[\hat{\underline{x}}(t) - \underline{x}_N(t)]$

Error Covariance $P(t) = \Phi(t, t_0) P(t_0) \Phi^T(t, t_0)$

Propagation: $+ \int_{t_0}^t \Phi(t, \tau) Q(\tau) \Phi^T(t, \tau) d\tau$

$$\dot{P}(t) = F P(t) + P(t) F^T + Q(t)$$

State Estimate $\Delta \hat{\underline{x}}(t_k+) = \Delta \hat{\underline{x}}(t_k-) + K_k [O_a(t_k) - h_k[\hat{\underline{x}}(t_k-)]]$

Update: $\hat{\underline{x}}(t_k+) = \hat{\underline{x}}(t_k-) + K_k [O_a(t_k) - h_k[\hat{\underline{x}}(t_k-)]]$

$$h_k[\hat{\underline{x}}(t_k-)] = h_k[\underline{x}_N(t_k)] + H_k \Delta \hat{\underline{x}}(t_k-)$$

Table 4-2

(cont.)

Error Covariance $P(t_k+) = [I - K_k H_k] P(t_k-)$

Update:

Gain Matrix: $K_k = P(t_k-) H_k^T [H_k P(t_k-) H_k^T + R_k]^{-1}$

Matrix Definitions:

$$F = \left[\frac{\partial \underline{f}[\underline{x}(t), t]}{\partial \underline{x}} \right]_{\underline{x}_N(t)}$$

$$H_k = \left[\frac{\partial \underline{h}_k[\underline{x}(t)]}{\partial \underline{x}} \right]_{\underline{x}_N(t)}$$

State Transition

Matrix:

$$\dot{\Phi}(t, t_0) = F \Phi(t, t_0)$$

$$\Phi(t_0, t_0) = I$$

Nominal

Trajectory:

$$\dot{\underline{x}}_N(t) = \underline{f}[\underline{x}_N(t), t], \quad \underline{x}_N(t_0) = \hat{\underline{x}}_0$$

The Extended Kalman filter develops a nominal trajectory between observations based upon the best estimate of the state at the last observation time. Linearization about the nominal trajectory is done only for the propagation of the error covariance matrix and in the determination of the Kalman gain matrix. The propagation of the state is done by a numerical/analytical integration of Equation (4-29) with the updated value of the state at the last observation time as the initial condition. This usually results in the nominal trajectory being closer to the actual state and therefore reduces the linearization errors associated with the LKF. A summary of the EKF is shown in Table 4-3. A major disadvantage of the EKF is that the state and error covariance matrix must be integrated (usually numerically) between observation times with new initial conditions after each observation. An advantage of the EKF is that since the nominal trajectory is being improved, longer observation spans are usually possible.

It is also possible to iterate in order to improve the state estimate. Using the best estimate of state at the end of the observation span, the state is integrated back to the epoch conditions and then the estimation process is continued over the observation span until the sum of the residuals is minimum.

Table 4-3
 Extended Kalman Filter for a Non-Linear
 System with Discrete Measurements

System Model: $\dot{\underline{x}}(t) = \underline{f}[\underline{x}(t), t] + \underline{\omega}(t) \quad \underline{\omega}(t) \sim N(0, Q(t))$

Measurement Model: $\underline{O}_a(t_k) = \underline{h}_k[\underline{x}(t_k)] + \underline{v}_k \quad \underline{v}_k \sim N(0, R_k)$

Initial Conditions: $\underline{x}(0) \sim N(\hat{\underline{x}}_0, P_0)$

Assumptions: $E[\underline{\omega}(t) \underline{v}_k^T] = 0, E[\underline{v}_k (\Delta \hat{\underline{x}}(t_k^-) - \Delta \underline{x}(t_k^-))^T] = 0$

$$E[\underline{\omega}(t) (\Delta \hat{\underline{x}}(t_0) - \Delta \underline{x}(t_0))^T] = 0$$

$$\Delta \hat{\underline{x}}(t) \equiv \hat{\underline{x}}(t) - \underline{x}_N(t)$$

State Estimate $\dot{\hat{\underline{x}}} = \underline{f}[\hat{\underline{x}}(t), t]$

Propagation:

Error Covariance $\dot{P}(t) = F P(t) + P(t) F^T + Q(t)$

Propagation:

State Estimate $\hat{\underline{x}}(t_k+) = \hat{\underline{x}}(t_k-) + K_k [\underline{O}_a(t_k) - \underline{h}_k[\hat{\underline{x}}(t_k-)]]$

Update:

Error Covariance $P(t_k+) = [I - K_k H_k] P(t_k-)$

Update:

Gain Matrix: $K_k = P(t_k-) H_k^T [H_k P(t_k-) H_k^T + R_k]^{-1}$

Table 4-3
(cont.)

Matrix Definitions:

$$F = \left[\frac{\partial \underline{f}[\underline{x}(t), t]}{\partial \underline{x}} \right]_{\underline{x}_N(t)}$$

$$H_k = \left[\frac{\partial h_k[\underline{x}(t)]}{\partial \underline{x}} \right]_{\underline{x}_N(t_k)}$$

Nominal Trajectory:

$$\dot{\underline{x}}_N(t) = \underline{f}[\underline{x}_N(t), t], \quad \underline{x}_N(t_k) = \hat{\underline{x}}(t_k^+)$$

$$t_k \leq t \leq t_{k+1}$$

A problem with both the LKF and the EKF is that filter divergence can develop (erroneous estimates). Filter divergence generally occurs due to modeling errors. Because of the linearization of the system model, the error covariance matrix tends to decrease as time increases. As the error covariance matrix decreases, the filter believes it is following the actual trajectory and therefore disregards new measurements. Because of the modeling errors the actual and estimated trajectories diverge. It should also be noted that computational procedures (round-off errors) can also cause filter divergence.

4.2 The Semianalytical Linearized Kalman Filter

In this section the semianalytical satellite theory is coupled to the Linearized Kalman filter. It is felt that the coupling of these two concepts may increase the computational speed and accuracy of current OD systems. The computational speed will be increased due to the computational efficiency of the semianalytical orbit generator. Accuracy improvements may result because the linearization assumptions used in the LKF may be better satisfied due to the near-linear behavior of the mean elements over an integration step (typically one day). This development will be called a Semianalytical Linearized Kalman Filter (SLKF).

The system vector, $\underline{x}(t)$, is defined as

$$\underline{x}(t) = \begin{bmatrix} \bar{a}^* \\ \bar{c} \end{bmatrix} \quad (4-35a)$$

where

$$\underline{\bar{a}}^* = \begin{bmatrix} \underline{\bar{a}} \\ \underline{\bar{\lambda}} \end{bmatrix} \quad (4-35b)$$

with

$$\underline{\bar{a}} = [\underline{\bar{a}}, \underline{\bar{h}}, \underline{\bar{k}}, \underline{\bar{p}}, \underline{\bar{q}}]^T \quad (4-35c)$$

and where \underline{c} represents the modeled solve-for parameters. The system dynamics can be represented as

$$\dot{\underline{x}}(t) = \begin{bmatrix} \underline{\bar{n}} \underline{e}_6 + \epsilon \underline{A}_1(\underline{\bar{a}}) \\ \hline 0 \end{bmatrix} + \underline{\omega} \quad (4-36a)$$

where $\underline{\omega}$ is the system noise associated with the formulation and where $\underline{\bar{n}}$, \underline{e}_6 and $\underline{A}_1(\underline{\bar{a}})$ were previously defined in Equation (3-32). The system noise is assumed to have a normal distribution with zero mean and a covariance of $Q(t)$. This is represented as

$$\underline{\omega} \sim N(0, Q(t)) \quad (4-36b)$$

The vector form of the near-identity transformation is assumed to be of the following form

$$\underline{a}^* = \underline{\bar{a}}^* + \epsilon \underline{n}_1(\underline{\bar{a}}^*) \quad (4-37)$$

where

$$\varepsilon \underline{\eta}_1(\bar{\underline{a}}^*) = \sum_{\sigma=1}^{\infty} [\varepsilon \underline{C}_{\sigma} \sin(\sigma \bar{\lambda}) - \varepsilon \underline{D}_{\sigma} \cos(\sigma \bar{\lambda})] \quad (4-38)$$

and where $\varepsilon \underline{C}_{\sigma}$ and $\varepsilon \underline{D}_{\sigma}$ are defined in Equation (3-35). It is noted that this development will only consider a single time-independent disturbing force to first order in the small parameter in both the AOG and SPG. The extension to a more general case is straightforward.

A nominal trajectory for the system vector, \underline{x} , is formed over the integration grid. The system vector is composed of the six mean elements and the modeled parameters, \underline{c} . The AOG (see Chapter 2) is used to generate a nominal trajectory for $\bar{\underline{a}}^*$ over an integration step of the semianalytical satellite theory (typically 1 day). The modeled parameters are assumed constant over the integration step for the nominal trajectory. The nominal trajectory is denoted as \underline{x}_n which can be written as

$$\underline{x}_n = \begin{bmatrix} \bar{\underline{a}}^*_n \\ \underline{c} \end{bmatrix} \quad (4-39)$$

As was discussed in Chapter 2, an interpolator is used to determine the mean elements, $\bar{\underline{a}}^*_n$, at points off the integration grid.

From Table 4-2 it is seen that the linearized system matrix can be represented as

$$F = \left[\frac{\partial [\dot{\underline{x}}(t)]}{\partial \underline{x}(t)} \right]_{\underline{x}_n} \quad (4-40a)$$

which can be written as

$$F = \left[\begin{array}{c|c} \left[\frac{\partial [\dot{\underline{a}}^*]}{\partial \underline{a}^*} \right] & \left[\frac{\partial [\dot{\underline{a}}^*]}{\partial \underline{c}} \right] \\ \hline 0 & 0 \end{array} \right]_{\underline{x}_n} \quad (4-40b)$$

where it is understood that $[\dot{\underline{a}}^*]$ stands for the right hand side of the averaged equations of motion. From Equations (3-50) and (3-51) it is seen that the F matrix is composed of the A and D matrices of the semianalytical partial derivatives (see Table 3-2). Equation (4-40b) can therefore be written as

$$F = \left[\begin{array}{c|c} A & D \\ \hline 0 & 0 \end{array} \right] \quad (4-41)$$

where the A and D matrix are defined in Section 3.2.1. The determination of the A and D matrices can be done as discussed in Sections 3.2.1 and 3.2.2. Much of the software that is used to compute the A and D matrices in the semianalytical batch filter can be used to calculate the F matrix. It is noted that the

F matrix is a function of the slowly varying mean elements. It should therefore be possible to evaluate the F matrix on the integration grid and use an interpolator in order to obtain the F matrix on the output/observation grid. This should greatly reduce the computational costs associated with the determination of the F matrix.

The state transition matrix is expressed as

$$\dot{\phi}(t, t_0) = F \phi(t, t_0) \quad (4-42a)$$

with

$$\phi(t_0, t_0) = I \quad (4-42b)$$

Since the F matrix is a function of only the five slowly varying mean elements, the state transition matrix can be integrated with the large numerical integration time step associated with the semianalytical satellite theory. It should be noted that because of the interpolator for the F matrix, the integration algorithm will not require a full re-evaluation of the F matrix. In other words, at the request points of the integration algorithm for the state transition matrix, the interpolator for the F matrix can be used. In this development such an integration scheme will be called an integrator-interpolator algorithm. It is therefore expected that using an integrator-interpolator

algorithm with a large numerical integration time step should allow the determination of the state transition matrix at minimum computational cost. Due to the slowly varying nature of the state transition matrix, an interpolation algorithm can also be used to determine the state transition matrix at the output/observation times. By using Equation (4-18d) and the interpolator for the state transition matrix over the integration grid, the state transition matrix between observations can be obtained. For example, the state transition matrix between observations at t_k and t_{k+1} can be expressed as

$$\Phi(t_{k+1}, t_k) = \Phi(t_{k+1}, t_0) \Phi^{-1}(t_k, t_0) \quad (4-43)$$

where $\Phi(t_{k+1}, t_0)$ and $\Phi(t_k, t_0)$ can be determined directly from the interpolator for the state transition matrix.

The observation model is assumed to be of the form

$$\underline{O}_a(t_k) = \underline{h}_k(\underline{r}_{LT}, \dot{\underline{r}}_{LT}) + \underline{v}_k \quad (4-44a)$$

where \underline{v}_k is the noise vector associated with the measurement at t_k and where \underline{r}_{LT} and $\dot{\underline{r}}_{LT}$ are the position and velocity vector in the local tangent frame (see Section 2.1.1). The noise is assumed to have a normal distribution with a zero mean and a covariance of R_k . This is denoted as

$$\underline{v}_k \sim N(0, R_k) \quad (4-44b)$$

Obviously the computed observations would be expressed as

$$\underline{o}_c(t_k) = \underline{h}_k(\hat{\underline{r}}_{LT}, \dot{\hat{\underline{r}}}_{LT}) \quad (4-45)$$

From Table 4-2 it is seen that the linearized measurement matrix can be written as follows

$$H_k = \left\{ \left[\frac{\partial [O_c(t_k)]}{\partial \underline{\bar{a}}^*} \right]_{p \times 6} \mid \left[\frac{\partial [O_c(t_k)]}{\partial \underline{c}} \right]_{p \times (\ell-6)} \right\}_{\underline{x}_n} \quad (4-46)$$

where p is the number of observations at t_k and ℓ is the number of solve-for parameters. With the use of Equation (4-45) it is seen that

$$H_k = \left\{ \left[\frac{\partial \underline{h}_k(\underline{r}_{LT}, \dot{\underline{r}}_{LT})}{\partial \underline{a}^*} \right] \left[\left\{ \frac{\partial \underline{a}^*}{\partial \underline{\bar{a}}^*} \right\} \mid \left\{ \frac{\partial \underline{a}^*}{\partial \underline{c}} \right\} \right] \right\}_{\underline{x}_n} \quad (4-47)$$

where \underline{a}^* represents the six osculating orbital elements. By taking the partial derivatives of the near-identity transformation with respect to $\underline{\bar{a}}^*$ and \underline{c} , it is seen that Equation (4-47) can be written as

$$H_k = \left[\frac{\partial h_k(\underline{r}_{LT}, \dot{\underline{r}}_{LT})}{\partial \underline{a}^*} \right] \left[I + B_1 \mid B_4 \right] \quad (4-48)$$

where the B_1 and B_4 matrices are defined in Equation (3-44) and (3-45) [see Table 3-2 also]. When the short periodic functions are assumed to be of the form given in Table 2-1 [or Equation (4-38)], the B_1 and B_4 matrices are given in Equations (3-52) and (3-53). From Equations (3-28) and (3-30), it can be shown that

$$H_k = \left[\left\{ \frac{\partial h_k(\underline{r}_{LT}, \dot{\underline{r}}_{LT})}{\partial \underline{r}_{LT}} \right\} \mid \left\{ \frac{\partial h_k(\underline{r}_{LT}, \dot{\underline{r}}_{LT})}{\partial \dot{\underline{r}}_{LT}} \right\} \right] \cdot \left[\begin{array}{c|c} M_{LT}B(t)C & 0 \\ \hline M_{LT}\dot{B}(t)C & M_{LT}B(t)C \end{array} \right] \cdot \left[\begin{array}{c} \left\{ \frac{\partial \underline{R}}{\partial \underline{a}^*} \right\} \\ \hline \left\{ \frac{\partial \dot{\underline{R}}}{\partial \underline{a}^*} \right\} \end{array} \right] \cdot [I + B_1 \mid B_4] \quad (4-49)$$

where \underline{r}_{LT} , $\dot{\underline{r}}_{LT}$, \underline{R} , $\dot{\underline{R}}$, \underline{a}^* , M_{LT} , $B(t)$ and C are defined in Section 2.1.1. Sections 3.1 and 3.2 explain the determination of each of the matrices in Equation (4-49). Again it is noted that much of the same software used in the semianalytical batch filter can be used in the SLKF.

Linearization about the nominal trajectory yields the following for the variation of the system vector from the nominal trajectory (see Section 4.1)

$$\dot{\Delta \underline{\hat{x}}}(t) = F \Delta \underline{\hat{x}}(t) \quad (4-50)$$

where

$$\Delta \underline{\hat{x}}(t) = \underline{\hat{x}}(t) - \underline{x}_N \quad (4-51)$$

The initial condition for Equation (4-50) is zero at the beginning of the integration step [$\Delta \underline{\hat{x}}(t_0) = 0$] and equal to $\Delta \underline{\hat{x}}(t_k+)$ after the processing of the observations at t_k [see the state estimate update algorithm in Table 4-2]. The propagation of the system variation vector, $\Delta \underline{\hat{x}}(t)$, can be done by the use of an integrator-interpolator algorithm applied to Equation (4-50). Equivalently, the state transition matrix could be used to propagate $\Delta \underline{\hat{x}}(t)$ between observations. For example, between t_k and t_{k+1} , the system variation vector would be propagated by

$$\Delta \underline{\hat{x}}(t_{k+1}-) = \Phi(t_{k+1}, t_k) \Delta \underline{\hat{x}}(t_k+) \quad (4-52)$$

where $\Phi(t_{k+1}, t_k)$ is given in Equation (4-43).

In order to process the observations at t_k , it is necessary to add the short periodic variations to $\bar{\underline{a}}_N$ such that the nominal osculating orbital elements can be determined. As was demonstrated in Chapter 2, the short periodic coefficients are slowly varying and can be determined on the integration grid and an interpolator can be used to determine them at the output/observation times. The nominal values of the short periodic coefficients will be denoted as $[\underline{\epsilon C}]_n$ and $[\underline{\epsilon D}]_n$. Obviously, as the estimate of the system vector varies from the nominal trajectory, the estimate of the short periodic coefficients also varies from their nominal values. One way of obtaining the updated short periodic coefficients is to re-evaluate the short periodic coefficients (analytically or numerically) using the updated value of the system vector, $\hat{\underline{x}}(t_k)$. This could be computationally expensive if done many times. Another way of obtaining the updated short periodic coefficients is by performing a linearization about the nominal trajectory. To first order in $\hat{\Delta \underline{x}}(t)$ it is seen that

$$\hat{\underline{\epsilon C}}_{-\sigma} = [\underline{\epsilon C}]_n + \left[\frac{\partial \underline{\epsilon C}_{-\sigma}}{\partial \underline{x}} \right]_{\underline{x}_N} \hat{\Delta \underline{x}}(t) \quad (4-53)$$

$$\hat{\underline{\epsilon D}}_{-\sigma} = [\underline{\epsilon D}]_n + \left[\frac{\partial \underline{\epsilon D}_{-\sigma}}{\partial \underline{x}} \right]_{\underline{x}_N} \hat{\Delta \underline{x}}(t)$$

where $\hat{\epsilon}_{\underline{C}_\sigma}$ and $\hat{\epsilon}_{\underline{D}_\sigma}$ represent the updated short periodic coefficients. From Table 3-2 and/or Equation (3-57) it is seen that the change in the short periodic coefficients can be expressed as

$$\Delta \epsilon_{\underline{C}_\sigma} = [M_\sigma \mid 0 \mid K_\sigma]_{6 \times \ell} \hat{\Delta \underline{x}}(t) \quad (4-54a)$$

$$\Delta \epsilon_{\underline{D}_\sigma} = [N_\sigma \mid 0 \mid L_\sigma]_{6 \times \ell} \hat{\Delta \underline{x}}(t)$$

where

$$M_\sigma = \left\{ \begin{bmatrix} \frac{\partial \epsilon_{\underline{C}_\sigma}}{\partial \underline{a}} \end{bmatrix}_{6 \times 5} \right\}_{\underline{x}_n} \quad (4-54b)$$

$$N_\sigma = \left\{ \begin{bmatrix} \frac{\partial \epsilon_{\underline{D}_\sigma}}{\partial \underline{a}} \end{bmatrix}_{6 \times 5} \right\}_{\underline{x}_n} \quad (4-54c)$$

$$K_\sigma = \left\{ \begin{bmatrix} \frac{\partial \epsilon_{\underline{C}_\sigma}}{\partial \underline{c}} \end{bmatrix}_{6 \times (\ell-6)} \right\}_{\underline{x}_n} \quad (4-54d)$$

$$L_\sigma = \left\{ \begin{bmatrix} \frac{\partial \epsilon_{\underline{D}_\sigma}}{\partial \underline{c}} \end{bmatrix}_{6 \times (\ell-6)} \right\}_{\underline{x}_n} \quad (4-54e)$$

and where ℓ is the total number of solve-for parameters (including the six orbital elements). From Equation (4-53) it is seen that the updated short periodic coefficients can be expressed as

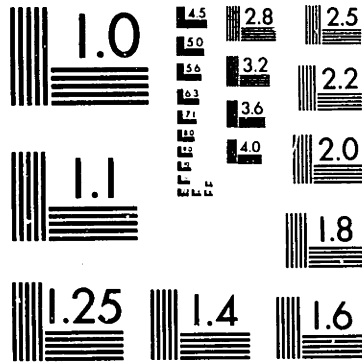
$$\begin{aligned}\hat{\varepsilon}_{\underline{C}}^{\sigma} &= [\varepsilon_{\underline{C}}^{\sigma}]_n + \Delta \varepsilon_{\underline{C}}^{\sigma} \\ \hat{\varepsilon}_{\underline{D}}^{\sigma} &= [\varepsilon_{\underline{D}}^{\sigma}]_n + \Delta \varepsilon_{\underline{D}}^{\sigma}\end{aligned}\tag{4-55}$$

Since the B_1 and B_4 matrices, and therefore the M_{σ} , N_{σ} , K_{σ} and L_{σ} matrices [see Equations (3-52) and (3-53)], have to be determined in the computation of the linearized observation matrix, (H_k) , the use of Equations (4-54) and (4-55) to update the short periodic coefficients may be advantageous. The determination of the A , D , M_{σ} , N_{σ} , K_{σ} and L_{σ} matrices was described in Section 3.2. The use of the quadrature approach as given in Equations (3-56) and (3-57) is interesting in that it allows the calculation of these matrices with minimum evaluations of the partial derivatives of the disturbing functions.

The calculation of the nominal osculating elements at the observation times is determined by the following

$$\underline{a}^*_{n} = \bar{\underline{a}}^*_{n} + \sum_{\sigma=1}^{\infty} \{ [\varepsilon_{\underline{C}}^{\sigma}]_n \sin(\sigma\bar{\lambda}) - [\varepsilon_{\underline{D}}^{\sigma}]_n \cos(\sigma\bar{\lambda}) \}\tag{4-56}$$

The updated osculating elements can be written as



MICROCOPY RESOLUTION TEST CHART
NATIONAL BUREAU OF STANDARDS-1963-A

20X

NOTICE THIS MATERIAL MAY BE PROTECTED BY
COPYRIGHT LAW (TITLE 17 U.S. CODE)

$$\begin{aligned} \hat{\underline{a}}^* &= \hat{\underline{a}}^*_N + \Delta \underline{a}^*(t) + \sum_{\sigma=1}^{\infty} \{ [[\underline{\varepsilon}_{C_{-\sigma}}]_n + \Delta \underline{\varepsilon}_{C_{-\sigma}}] \sin(\sigma \bar{\lambda}) \\ &\quad - [[\underline{\varepsilon}_{D_{-\sigma}}]_n + \Delta \underline{\varepsilon}_{D_{-\sigma}}] \cos(\sigma \bar{\lambda}) \} \end{aligned} \quad (4-57)$$

The computed observations and linearized measurement matrix are calculated using the nominal values of the orbital elements (see Table 4-2). Linearization errors associated with the measurement model may be reduced if the updated osculating orbital elements [Equation (4-57)] are used instead of the nominal osculating elements in the calculation of $\underline{h}_{-k}(\underline{r}_{-LT}, \dot{\underline{r}}_{-LT})$ and H_k .

From Table 4-2 it is seen that the differential equation for the error covariance matrix can be written as

$$\dot{P}(t) = F P(t) + P(t) F^T + Q(t) \quad (4-58)$$

where F is the linearized system matrix and $Q(t)$ is the covariance matrix associated with the system noise. The initial conditions for Equation (4-58) is the a priori value of the error covariance matrix at t_0 [$P(t_0)$] and equal to $P(t_k^+)$ after the estimation update at t_k [see the error covariance update in Table 4-2]. It is assumed that the system noise is slowly varying in the same manner as the mean elements, i.e., $Q(t)$

contains only secular and long periodic terms. This should not be a bad assumption since the mean elements and modeled parameters contain only secular and long periodic terms. Modeling errors in the short periodic variations will result in transformation errors and will generally not affect the system dynamics (at least to first order). This means that $Q(t)$ should not contain short periodic terms.

Since the F matrix is slowly varying and can be obtained by an interpolator, and since $Q(t)$ is assumed to be slowly varying, the error covariance matrix can be propagated between observations by using an integrator-interpolator algorithm applied to Equation (4-58) with the large numerical integration time step. The state transition matrix can also be used to propagate $P(t)$. Between t_k and t_{k+1} , the error covariance matrix would be propagated by the following (see Table 4-2)

$$\begin{aligned}
 P(t_{k+1}^-) &= \Phi(t_{k+1}, t_k) P(t_k^+) \Phi^T(t_{k+1}, t_k) \\
 &+ \int_{t_k}^{t_{k+1}} \Phi(t_{k+1}, \tau) Q(\tau) \Phi^T(t_{k+1}, \tau) d\tau
 \end{aligned}
 \tag{4-59}$$

The matrix $\Lambda(t, t_0)$ is defined as follows

$$\Lambda(t, t_0) \equiv \int_{t_0}^t \Phi(t, \tau) Q(\tau) \Phi^T(t, \tau) d\tau
 \tag{4-60}$$

Using Equation (4-60), it is seen that Equation (4-59) can be written as

$$P(t_{k+1}^-) = \Phi(t_{k+1}, t_k) P(t_k^+) \Phi^T(t_{k+1}, t_k) + \Lambda(t_{k+1}, t_k) \quad (4-61)$$

$P(t_k^-)$ comes from the error covariance update (see Table 4-2) and $\Phi(t_{k+1}, t_k)$ is determined in Equation (4-43). The matrix $\Lambda(t_{k+1}, t_k)$ could be obtained by an integrator-interpolator algorithm applied between each observation. For many observations this could be computationally expensive. It is possible to determine $\Lambda(t_{k+1}, t_k)$ in what may be a more efficient manner.

Since the state transition matrix and $Q(t)$ are slowly varying matrices, $\Lambda(t, t_0)$ can be determined with an integrator-interpolator algorithm over the entire integration grid. The large numerical integration time step associated with the semi-analytical satellite theory can be used in determining $\Lambda(t, t_0)$. An interpolator can be used to determine $\Lambda(t, t_0)$ at the output/observation times. It is also known that

$$\int_{t_0}^{t_{k+1}} \Phi(t_{k+1}, \tau) Q(\tau) \Phi^T(t_{k+1}, \tau) d\tau = \int_{t_k}^{t_{k+1}} \Phi(t_{k+1}, \tau) Q(\tau) \Phi^T(t_{k+1}, \tau) d\tau + \int_{t_0}^{t_k} \Phi(t_{k+1}, \tau) Q(\tau) \Phi^T(t_{k+1}, \tau) d\tau$$

From Equation (4-60) it is seen that the above expression can be written as

$$\begin{aligned} \Lambda(t_{k+1}, t_0) &= \Lambda(t_{k+1}, t_k) \\ &+ \int_{t_0}^{t_k} \Phi(t_{k+1}, \tau) Q(\tau) \Phi^T(t_{k+1}, \tau) d\tau \end{aligned} \quad (4-62)$$

From Equation (4-18d) it is seen that

$$\Phi(t_{k+1}, \tau) = \Phi(t_{k+1}, t_k) \Phi(t_k, \tau) \quad (4-63)$$

Substitution of Equation (4-63) into Equation (4-62) and using the definition of $\Lambda(t_k, t_0)$ [see Equation (4-60)] it is seen that

$$\begin{aligned} \Lambda(t_{k+1}, t_0) &= \Lambda(t_{k+1}, t_k) \\ &+ \Phi(t_{k+1}, t_k) \Lambda(t_k, t_0) \Phi^T(t_{k+1}, t_k) \end{aligned}$$

which can be written as

$$\begin{aligned} \Lambda(t_{k+1}, t_k) &= \Lambda(t_{k+1}, t_0) \\ &- \Phi(t_{k+1}, t_k) \Lambda(t_k, t_0) \Phi^T(t_{k+1}, t_k) \end{aligned} \quad (4-64)$$

Equation (4-64) is useful in that it allows the calculation of $\Lambda(t_{k+1}, t_k)$ in terms of readily obtainable quantities. $\Lambda(t_{k+1}, t_0)$ and $\Lambda(t_k, t_0)$ are obtained from the interpolator for $\Lambda(t, t_0)$ over the integration grid. $\Phi(t_{k+1}, t_k)$ is given in Equation (4-43). Therefore, with the use of Equations (4-61) and (4-64), the error covariance matrix can be propagated between observations.

Iterations on the integration grid are possible with the SLKF. After processing all the observational data over the integration grid of the semianalytical satellite theory, the system vector is integrated backwards to the beginning of the integration step and the estimation process is repeated. The iteration procedure would be continued until the sum of the residuals is minimum and/or no longer changes to within a specified amount. It should also be noted that the SLKF also allows iterations over the entire observation span (global iteration).

The SLKF also permits rectification on the integration grid. After all observational data is processed within an integration grid of the semianalytical satellite theory (to include integration grid iterations), a new nominal trajectory is formed for the next integration grid based upon the best estimate of the system vector at the end of the last integration grid. In other words, the best estimate of $\hat{\underline{x}}(t_f)$ and $P(t_f)$ at the end of an integration grid (t_f), is used as the initial conditions

for the nominal trajectory for the next integration grid. The short periodic coefficients, linearized system matrix, state transition matrix, linearized measurement matrix, $\Lambda(t, t_0)$ and short periodic coefficient matrices are all re-initialized and determined based upon the new nominal trajectory. This should greatly reduce the linearization errors and allow the SLKF to process long observation spans without experiencing filter divergence.

The SLKF is best explained by giving the sequence of events which would be followed in processing observational data. The following is a suggested sequence of events for the SLKF when the state transition matrix is used in the propagation of $\hat{\Delta \underline{x}}(t)$ and $P(t)$ and when the short periodic functions are formulated as given in Equation (4-38).

Integration Grid Calculations

1. Form the nominal trajectory for $\bar{\underline{a}}^*$ over an integration time step (modeled parameters are assumed constant).
 - a. Integrate the mean equations of motion (AOG) with the best estimate of the mean elements and modeled parameters at the beginning of the integration grid.
 - b. Form an interpolator for $\bar{\underline{a}}^*_n$ over the integration grid.

2. Determine the short periodic coefficients on the integration grid and form the interpolators for them over the integration grid.

3. Determine the F matrix and short periodic coefficient matrices (M_{σ} , N_{σ} , K_{σ} and L_{σ}) on the integration grid and form the interpolators for them over the integration grid. Note that for those perturbations that the quadrature approach is used, these matrices can be determined jointly [see Equations (3-56) and (3-57)].

4. Determine the state transition matrix on the integration grid.
 - a. Use integrator-interpolator on Equation (4-42) with the large integration time step.
 - b. Form interpolator over the integration grid.

5. Determine $\Lambda(t, t_0)$ on the integration grid.
 - a. Use integrator-interpolator on Equation (4-60) with the large integration time step.
 - b. Form interpolator over the integration grid.

Observation Processing at t_{k+1}

6. Determine by the use of the interpolators, $\bar{\underline{a}}_N^*$, $[\underline{\varepsilon C}]_n$, $[\underline{\varepsilon D}]_n$, M_σ , N_σ , K_σ and L_σ at the observation time, t_{k+1} .
7. Calculate \underline{a}_n^* [see Equation (4-56)].
8. Determine $\Phi(t_{k+1}, t_k)$ and $\Lambda(t_{k+1}, t_k)$ [see Equations (4-43) and (4-64)].
9. Determine the system variation vector at the observation time, $\hat{\Delta \underline{x}}(t_{k+1}^-)$ [see Equation (4-52)].
10. Determine the error covariance matrix at the observation time, $P(t_{k+1}^-)$ [see Equation (4-61)].
11. Determine the computed observation, $\underline{O}_C(t_{k+1}^-)$, the linearized measurement matrix, H_{k+1} , and the Kalman gain matrix, K_{k+1} [see Equations (4-45), (4-49) and (4-14)].
12. Update the system vector, $\hat{\Delta \underline{x}}(t_{k+1}^+)$ [see Table 4-2].
13. Update the error covariance matrix, $P(t_{k+1}^+)$ [see Table 4-2].

14. Determine updated short periodic coefficients if output and/or updated osculating orbital elements are required [see Equation (4-57)].
15. Move to next observation time and repeat steps 6 through 14.
16. After the last observation in the integration grid is processed, propagate the best estimate of the system vector and error covariance matrix to the end of the integration step (t_f).
17. If integration grid iteration is done, integrate the system vector back to the start time and repeat steps 1 through 16 until the sum of the residuals is minimized (or acceptable).

Rectification at the End of the Integration Step (t_f)

18. Determine $\hat{\underline{x}}(t_f^-)$ and set this equal to $\underline{x}_N(t_0)$.
19. Determine $P(t_f^-)$ and set this equal to $P(t_0)$.
20. Set $\phi(t_f, t_f) = \phi(t_0, t_0) = I$.

21. The short periodic coefficients at t_f are calculated using $\hat{\underline{x}}(t_f^-)$ and set equal to $[\epsilon \underline{C}_\sigma(t_o)]_n$ and $[\epsilon \underline{D}_\sigma(t_o)]_n$.
22. Repeat steps 1 through 21 for next integration grid.

The above procedure is continued until the end of the observation span is reached. If a global iteration procedure is used, the best estimate of the system vector at the end of the observation span is integrated back to the epoch time and steps 1 through 22 are repeated. This is continued until the sum of the residuals is minimized (or acceptable).

If the short periodic formulation as given in Equation (4-38) is not used and/or if analytical expressions for the B_1 and B_4 matrices are used, the calculation of the M_σ , N_σ , K_σ and L_σ matrices would not be necessary. The B_1 and B_4 matrices would be calculated at each observation time when the linearized measurement matrix is determined (step 11 in the above procedure). It should also be possible to use reduced perturbation models in the generation of the F , B_1 and B_4 matrices. For example, it may be possible to consider J_2 perturbations only in the F matrix and neglect the B_1 and B_4 matrices.

It is felt that the above development has coupled the semianalytical satellite theory with the Kalman filter. The

performance of current OD systems may be increased with the use of a Semianalytical Linearized Kalman filter.

Chapter 5

CONCLUSIONS AND FUTURE WORK

This research has been concerned with adding new capabilities to the semianalytical satellite theory and combining the theory with current estimation procedures such that orbit determination and prediction processes for low altitude satellites are improved. Enhancements to the semianalytical satellite theory include a short periodic development which is applicable to all types of perturbations (conservative and non-conservative) and a second order drag theory which allows a complete treatment of all second order drag effects. The semianalytical satellite theory has been combined with a batch filter (least squares differential correction algorithm) such that the epoch mean orbital elements and various parameters within the drag formulation can be determined. The semianalytical batch filter necessitated the development and implementation of a semianalytical theory for the partial derivatives of perturbed motion. The solve-for parameters within the drag formulation include the drag coefficient and adaptive parameters within the Adaptive Modified Harris-Priester density model. An algorithmic structure for coupling the semianalytical satellite theory with the Kalman filter has also been developed.

5.1 Conclusions

It is concluded that the semianalytical satellite theory can be used in an orbit determination (OD) system to accurately determine and predict satellite ephemerides. It is further concluded that a semianalytical OD system can accurately and efficiently handle drag perturbed satellites. The accuracy of the semianalytical orbit generator and semianalytical batch filter is comparable to special perturbation techniques, i.e., Cowell orbit generator and Cowell batch filter.

The first order time-independent short periodic formulation, as given in Section 2.2.1, is a valid means of determining the short periodic variations due to zonal terms of the central body gravitational field, third body effects for low altitude satellites, atmospheric drag and solar radiation pressure. The coupling in the short periodic formulation (see Table 2-1) between the semimajor axis and the satellite's fast variable is a major first order effect and must be considered for accurate orbit generation. The time-independent short periodic formulation permits both analytical and numerical implementations. The numerical approach has been implemented into the Research and Development version of the Goddard Trajectory Determination System (GTDS-RD). The numerical approach for drag and solar radiation pressure perturbations allows the consideration of complicated density models and/or spacecraft solar radiation pressure models.

The time-independent short periodic coefficients ($\epsilon C_{i\sigma}$ and $\epsilon D_{i\sigma}$, see Table 2-1) are functions of the five slowly varying mean elements and are therefore slowly varying themselves. This fact makes it possible to determine the short periodic coefficients on the integration grid of the semianalytical satellite theory and use an interpolator to determine them at the output/observation time within the integration grid. This should significantly reduce the computational costs associated with the short periodic generator.

For the low altitude near-circular test case considered in Section 2.4.3, the drag short periodic variation was a 35 meter effect in the semimajor axis and can cause up to a 50 meter effect in the along track error. It is concluded, at least for the test cases examined in this research, that the drag short periodic variation must be considered for precision orbit generation.

The weak time-dependent short periodic formulation, as given in Section 2.2.2, is required in order to achieve high accuracy for third body perturbations on medium altitude satellites (such as GPS). The weak time-dependent short periodic variations are obtained by including corrections to the time-independent short periodic coefficients. Both analytical and numerical methods are possible for the calculation of the weak time-dependent short periodic coefficients. For the test case

considered in Section 2.4.5, it appears that the lunar weak time-dependent short periodic coefficient can also be determined on the integration grid of the semianalytical satellite theory and an interpolator can be used to determine them at the output times.

The dependence of the drag and solar radiation pressure short periodic variations on the solar motion was shown to be very small for the test cases considered. It appears that these perturbations can be considered adequately by a time-independent short periodic formulation.

For the osculating to mean conversion, the Precision Conversion of Elements (PCE) initialization procedure coupled with an accurate Short Periodic Generator (SPG) is superior to the Numerical Osculating to Mean (NOM) initialization procedure (see Sections 2.4.2 and 2.4.3). It also appears that the Epoch Point Conversion (EPC) with an accurate SPG will be an accurate and efficient means of converting initial osculating elements to initial mean elements. It is felt that the EPC procedure will be superior to the NOM procedure.

The generalized method of averaging permits a systematic approach to the second order averaged equations of motion based upon the first order short periodic functions. This is particularly useful in the investigation of the second order effects

of oblateness and drag. This research has shown that the second order oblateness/drag effect can be broken into four parts: J_2 -drag, drag- J_2 , J_2^2 and drag-squared effects. Analytical expressions good to zeroth order in the eccentricity and for direct orbits only have been developed for the drag- J_2 effect. These results are given in Appendix D. The second order oblateness/drag effects, including both numerical averaging and analytical drag- J_2 formulations, have been implemented into GTDS-RD. The implementation into GTDS-RD is completely general with respect to the density model.

This second order treatment of the oblateness/drag effects is comparable, in purpose, to the canonical approaches of Brouwer-Hori (Ref. 48), Lane (Ref. 50), Sherrill (Ref. 53), Willey and Pisacane (Ref. 51), Watson, Mistretta and Bonavito (Ref. 54), and Scheifele, Mueller and Starke (Refs. 55, 76). The present work also extends the treatment of the drag perturbed orbits given by Lutsky and Uphoff (Ref. 20) and Long and McClain (Ref. 12).

For the low altitude near-circular case considered, the J_2 -drag effect is the dominant second order oblateness/drag effect. Izsak's J_2 height (radial) correction, applied to the density calculations, gives a good approximation to the J_2 -drag effect. It has also been shown that the drag- J_2 effect must be considered for high accuracy orbit generation. For a near

circular satellite at a height of 200 kilometers, the drag-squared effect is small and can be neglected over a short arc. The present numerical testing with the Modified Harris-Priester atmosphere demonstrates the capability to include complex density variations with height, oblate atmosphere, diurnal, atmospheric rotation, and $\bar{F}_{10.7}$ variations.

The net result of this research effort is that the semianalytical satellite theory as implemented can generate an ephemeris for the low altitude circular test case of Section 2.4.3 that will vary from a precision Cowell generated ephemeris by less than 15 meters at the end of a one day time span (500 meters at the end of a 5 day time span).

A semianalytical theory for the partial derivatives of perturbed motion has been developed and implemented into GTDS-RD. The semianalytical partial derivatives are composed of an Average Partial Generator (APG) and Short Periodic Partial Generator (SPPG). The APG integrates, with the large numerical integration time step, a matrix differential equation of the mean semianalytical partial derivatives. The SPPG determines the semianalytical partial derivatives of the short periodic variations at the output/observation times. The perturbation models of the APG and SPPG can be different from each other. The semianalytical partial derivatives can be determined by analytical and/or numerical methods. The semianalytical partial

derivatives, as implemented in this research, have been shown to be equivalent to high precision Cowell generated partial derivatives with the same perturbation models.

For the test case considered in Section 3.2.2, it appears that for accurate semianalytical partial derivatives, J_2 effects must be considered in the SPPG and the APG must include at least J_2 effects and drag effects with Izsak's height correction applied to the density calculations (approximation to the J_2 -drag effects). Drag perturbations do not need to be considered in the SPPG.

A semianalytical batch filter has been developed and implemented into GTDS-RD. The semianalytical batch filter can solve for the six mean epoch orbital elements and parameters within the drag formulation. The drag parameters that can be solved for are the coefficient of drag (C_D) and adaptive parameters (a_1 through a_5) within the Adaptive Modified Harris-Priester Atmosphere (see Appendix C). For the same estimation option, the semianalytical batch filter, as implemented in this research, has been shown to be equivalent to a Cowell batch filter.

For the test cases considered in Section 3.3, the states plus C_D estimation option was superior to the states only estimation option over both the observation span and the prediction

span. The states plus a_1 and a_2 estimation option was better than the states plus C_D estimation option over the observation span. Over the prediction span used in Section 3.3, the states plus C_D estimation option gave the best results of all the estimation options considered. The other adaptive density estimation options (see Table 3-6) were not as good as the states plus a_1 and a_2 estimation option for the test cases considered.

It is felt that this research has shown that adaptive estimation of the drag formulation is a means of improving the performance of OD systems designed for near-Earth satellites. Adaptive estimation of the drag coefficient, which is presently used by most operational OD systems, does significantly improve the orbit determination and prediction of low altitude satellites. Adaptive estimation of the density model also appears to be a feasible and viable means of accounting for uncertainties in the drag formulation. Adaptive estimation of different density models and using longer observation spans may show dramatic improvements over the results obtained by this research.

The algorithmic structure for developing the Semianalytical Linearized Kalman filter (SLKF) has been presented. The system equations of motion, short periodic coefficients, linearized system matrix, state transition matrix and covariance matrix are functions of only the five slowly varying mean elements and therefore need only to be evaluated on the large

integration grid of the semianalytical satellite theory. Interpolators can be used to obtain these quantities at the output/observation times within the integration grid. The SLKF demonstrates that the semianalytical satellite theory can be gracefully interfaced with sequential as well as batch estimation procedures.

5.2 Future Work

This research has investigated the concept of developing a complete operational OD system based upon the semianalytical satellite theory. It is felt that this research has demonstrated this concept and has also indicated areas in which future work needs to be done in order to improve the performance of the semianalytical OD system. These areas of future work are discussed below.

Additional work that should be performed in the short periodic generator includes the implementation of analytical short periodic variations of the central body, including m-dailies, and third-body gravitational effects based upon Reference 5. Zeis' J_2^2 short periodic variations should either be extended to a higher order in the eccentricity or be replaced by closed-form expressions. Eventually, the J_2^2 formulation should be extended to the retrograde case. The determination of the short periodic coefficients should be put on the integration grid of the semianalytical satellite theory to improve

computational speed. The analytical short periodic formulation, as given in Reference 5, should be reformulated in terms of short periodic coefficients that are functions of the five slowly varying elements. The short periodic variation may need to be reformulated in terms of another geometric variable or orthogonal function such that the drag short periodic variation associated with a higher eccentricity orbit can be better modeled (see Figure 2-42). Related investigations of the solar radiation pressure shadow function may be helpful in this area. Further testing of the numerical short periodic generator should be performed so that its accuracy can be determined for much lower (more strongly drag perturbed) and much higher orbits (where lunar-solar and solar radiation pressure short-periodic variations are important). It should be noted that some of the above mentioned areas of future work are presently being done in the MIT/CSDL community.

Future work in the average orbit generator should involve improvements and refinements to the present models. Zeis' expressions for the J_2^2 mean element rates should be extended to at least the $J_2^2 e$ terms or be replaced with closed form expressions. The inclusion of closed form analytical J_2 short periodic variations should also improve the accuracy of the higher order AOG. The drag- J_2 analytical expressions should be extended to the retrograde case and also to higher order in the eccentricity.

Most of the improvements of the AOG will involve increasing the accuracy of higher eccentricity orbits.

Future research also needs to be done on the density models used in OD systems. One way of improving density determination is by developing improved density models. Research in this area should continue but due to the unpredictable nature of the upper atmosphere it is expected that this approach will not yield dramatic increases in accuracy for drag perturbed satellites. It appears that adaptive estimation of the density model is a means of improving the accuracy of orbit determination and prediction on near-Earth satellites and should be considered in future research. Adaptive estimation of other than the Adaptive Modified Harris-Priester density model should be attempted. A density model that should readily permit adaptive density estimation is the USSR density model (see Ref. 17 for a good description of this model). Since the major portion of the drag effect occurs around perigee (see Figures 2-13 and 2-42), and since the Sun's position and the location of perigee, with respect to inertial space, changes slowly, it may be advantageous to develop perigee density models. A perigee density model tries to accurately predict the density around perigee but may not be accurate at other points away from perigee. The diurnal-oblate exponential density model [see Equation (1-4)], with the perigee point as the reference point, may be a good perigee density model.

Another aspect that must be considered with density models used in the semianalytical satellite theory is how to handle the discontinuous nature of the $F_{10.7}$, $\bar{F}_{10.7}$ and K_p over the integration time step. One way of handling the discrete nature of these quantities is to fit them with polynomial interpolators over the integration grid of the semianalytical satellite theory. This would require that analytical continuous density models be used.

Additional work also needs to be done in the semianalytical batch filter. The analytical and quadrature approaches for determining the semianalytical partial derivatives need to be implemented. More testing of the semianalytical batch filter also needs to be done. The effects of longer and shorter observation spans, different perturbation models (to include different density models), different observation types and increased measurement errors needs to be examined. The semianalytical batch filter also needs to be tested in different flight regimes such that its accuracy for much lower and much higher orbits can be determined. The semianalytical batch filter should also be tested with real data. The test protocol used in this research was to generate simulated data from a Cowell generated truth orbit and compare the predicted ephemeris to the truth orbit. The actual performance of the semianalytical batch filter should be determined in an operational environment.

The semianalytical satellite theory should be coupled to sequential estimation procedures.* The SLKF appears to be a means of accomplishing this. Extensive testing and evaluation of this concept should be done.

The storing of satellite ephemerides by using the mean elements and the short periodic formulation developed in Chapter 2 should also be examined. It appears that the mean elements and short periodic coefficients can be represented over a one day time span by a low order interpolator. It should therefore be possible to store the ephemeris of a satellite over a long time span with a relatively small amount of data points. For example, suppose that the time, six mean elements and 120 short periodic coefficients (assuming upper limit of summation in Table 2-1 is 10) are stored at one day intervals, a 5th order Lagrangian interpolator could be used to determine the six mean elements and short periodic coefficients at any time within the five day time span. Knowing the mean elements and short periodic coefficients, the six osculating orbital elements can be determined by the use of the near-identity transformation. This may have application to the on-board computation and storage of satellite ephemerides.

* Currently being done in a MIT Masters thesis at the CSDL by 2Lt S. Taylor, ENG, U.S. Army, Hertz Fellow.

Appendix A

VARIATION OF PARAMETERS EQUATIONS OF MOTION

The Lagrangian and Gaussian form of the Variation of Parameters (VOP) equations of motion are presented. The development is brief and taken from References 15, 21, 74, 78, 79 and 80.

Lagrangian VOP Equations of Motion

The Lagrangian form of the VOP equations of motion is applicable only for conservative forces, i.e., forces derivable from a potential. The equation of motion can be written in Cartesian coordinates as

$$\ddot{\underline{x}} = - \underline{\nabla} V \quad (\text{A-1})$$

where \underline{x} is the position vector, $\underline{\nabla}$ is the gradient operation and V is the potential function. This can be written in scalar form as

$$\frac{dx_i}{dt} = \dot{x}_i \quad (\text{A-2})$$

$$\frac{d^2 x_i}{dt^2} = - \frac{\partial V_i}{\partial x_i}$$

$$(i = 1, 2, 3)$$

where x_i are the 3 components of the position vector and \dot{x}_i are the 3 components of the velocity vector. With a set of six osculating orbital elements (a_k) which describe the motion, Equation (A-2) can be written as

$$\sum_{k=1}^6 \frac{\partial \dot{x}_i}{\partial a_k} \dot{a}_k = \ddot{x}_i \quad (A-3a)$$

($i = 1, 2, 3$)

$$\sum_{k=1}^6 \frac{\partial \dot{x}_i}{\partial a_k} \dot{a}_k = - \frac{\partial V}{\partial x_i} \quad (A-3b)$$

Multiplying Equation (A-3a) by $-\frac{\partial \dot{x}_i}{\partial a_\ell}$ and Equation (A-3b) by

$+\frac{\partial \dot{x}_i}{\partial a_\ell}$, then adding both expressions together and summing over

i , yields the following after some rearranging

$$\sum_{k=1}^6 \sum_{i=1}^3 \left[\frac{\partial \dot{x}_i}{\partial a_\ell} \frac{\partial \dot{x}_i}{\partial a_k} - \frac{\partial \dot{x}_i}{\partial a_\ell} \frac{\partial \dot{x}_i}{\partial a_k} \right] \dot{a}_k$$

$$= - \sum_{i=1}^3 \left[\frac{\partial \dot{x}_i}{\partial a_\ell} \dot{x}_i + \frac{\partial V}{\partial x_i} \frac{\partial \dot{x}_i}{\partial a_\ell} \right] \quad (A-4)$$

Define the Lagrange bracket as follows

$$[a_\ell, a_k] \equiv \sum_{i=1}^3 \left[\frac{\partial x_i}{\partial a_\ell} \frac{\partial \dot{x}_i}{\partial a_k} - \frac{\partial \dot{x}_i}{\partial a_\ell} \frac{\partial x_i}{\partial a_k} \right] \quad (\text{A-5})$$

From the definition of the Lagrange bracket it is seen that

$$[a_\ell, a_\ell] = 0 \quad (\text{A-6a})$$

$$[a_\ell, a_k] = -[a_k, a_\ell] \quad (\text{A-6b})$$

It can also be shown that

$$\frac{\partial}{\partial t} [a_\ell, a_k] = 0 \quad (\text{A-6c})$$

The matrix of Lagrange brackets is defined as [LM], viz.

$$[\text{LM}] = \begin{bmatrix} [a_1, a_1] & [a_1, a_2] & \dots & [a_1, a_6] \\ [a_2, a_1] & \cdot & & \vdots \\ \vdots & & \cdot & \vdots \\ [a_6, a_1] & \dots & & [a_6, a_6] \end{bmatrix} \quad (\text{A-7})$$

The matrix of Lagrange brackets can be written as

$$[\text{LM}] = \Gamma^{-T} J \Gamma^{-1} \quad (\text{A-8})$$

where

$$\Gamma = \left\{ \begin{array}{c|c} \left[\frac{\partial \underline{a}^*}{\partial \underline{x}} \right] & \left[\frac{\partial \underline{a}^*}{\partial \dot{\underline{x}}} \right] \\ \hline \left[\frac{\partial \underline{x}}{\partial \underline{a}^*} \right] & \left[\frac{\partial \dot{\underline{x}}}{\partial \underline{a}^*} \right] \end{array} \right\}_{6 \times 6} \quad (\text{A-9})$$

$$J = \left[\begin{array}{c|c} 0 & I \\ \hline -I & 0 \end{array} \right]_{6 \times 6} \quad (\text{A-10})$$

and where \underline{a}^* represents the vector of six orbital elements. It is noted that Γ is the matrizant of the two-body problem and naturally its inverse exists and can be written as

$$\Gamma^{-1} = \left\{ \begin{array}{c|c} \left[\frac{\partial \underline{x}}{\partial \underline{a}^*} \right] & \left[\frac{\partial \dot{\underline{x}}}{\partial \underline{a}^*} \right] \\ \hline \left[\frac{\partial \underline{x}}{\partial \dot{\underline{a}}^*} \right] & \left[\frac{\partial \dot{\underline{x}}}{\partial \dot{\underline{a}}^*} \right] \end{array} \right\}_{6 \times 6} \quad (\text{A-11})$$

It is also noted that

$$J^{-1} = -J \quad (\text{A-12a})$$

and

$$\Gamma^{-T} = [\Gamma^T]^{-1} = [\Gamma^{-1}]^T \quad (\text{A-12b})$$

Substitution of Equation(A-5) into Equation (A-4) yields

$$\sum_{k=1}^6 [a_\ell, a_k] \dot{a}_k = - \sum_{i=1}^3 \left[\frac{\partial \dot{x}_i}{\partial a_\ell} x_i + \frac{\partial V}{\partial x_i} \frac{\partial x_i}{\partial a_\ell} \right] \quad (\text{A-13})$$

It is noted that

$$\sum_{i=1}^3 \left[\frac{\partial \dot{x}_i}{\partial a_\ell} x_i \right] = \frac{\partial}{\partial a_\ell} \left[\sum_{i=1}^3 \left\{ \frac{1}{2} (\dot{x}_i)^2 \right\} \right] = \frac{\partial T}{\partial a_\ell} \quad (\text{A-14})$$

where T is the kinetic energy of the system.

It is also noted that

$$\sum_{i=1}^3 \left[\frac{\partial V}{\partial x_i} \frac{\partial x_i}{\partial a_\ell} \right] = \frac{\partial V}{\partial a_\ell} \quad (\text{A-15})$$

Substitution of Equations (A-14) and (A-15) into Equation (A-13) yields after some rearranging

$$\sum_{k=1}^6 [a_\ell, a_k] \dot{a}_k = \frac{\partial F}{\partial a_\ell} \quad (\text{A-16})$$

where F is the Delaunay function which is equal to the negative of the Hamiltonian of the system. This is expressed as

$$F = -H = -(T + V) \quad (\text{A-17})$$

It is noted that the potential can be written as

$$V = -\frac{\mu}{r} + R \quad (\text{A-18})$$

where $-\frac{\mu}{r}$ is the two-body part of the potential and where R is the disturbing potential. A two-body relation between kinetic energy and potential energy is

$$T - \frac{\mu}{r} = -\frac{\mu}{2a} \quad (\text{A-19})$$

Substitution of Equations (A-18) and (A-19) into Equation (A-17) yields

$$F = \frac{\mu}{2a} - R \quad (\text{A-20})$$

Equation (A-16) can be written in vector form with the use of the matrix of the Lagrange brackets as

$$[\text{LM}]_{\underline{a}^*} \dot{\underline{a}}^* = \left[\frac{\partial F}{\partial \underline{a}^*} \right]^T \quad (\text{A-21})$$

The element rates can therefore be written as

$$\dot{\underline{a}}^* = [\text{LM}]^{-1} \left[\frac{\partial F}{\partial \underline{a}^*} \right]^T \quad (\text{A-22})$$

From Equation (A-8) it is seen that

$$[\text{LM}]^{-1} = -\Gamma J \Gamma^T \quad (\text{A-23})$$

The matrix of Poisson Brackets is defined as

$$[PM] = \Gamma J \Gamma^T \quad (A-24)$$

which denotes the following matrix

$$[PM] = \begin{bmatrix} (a_1, a_1) & (a_1, a_2) & \dots & (a_1, a_6) \\ (a_2, a_1) & \cdot & & \\ \vdots & & \cdot & \\ (a_6, a_1) & \dots & & (a_6, a_6) \end{bmatrix} \quad (A-25)$$

From Equation (A-24) it can be shown that a scalar Poisson bracket is defined as

$$(a_\ell, a_k) = \sum_{i=1}^3 \left[\frac{\partial a_\ell}{\partial x_i} \frac{\partial a_k}{\partial \dot{x}_i} - \frac{\partial a_\ell}{\partial \dot{x}_i} \frac{\partial a_k}{\partial x_i} \right] \quad (A-26)$$

It can be easily shown that the Poisson brackets have the following characteristics

$$(a_\ell, a_\ell) = 0 \quad (A-27a)$$

$$(a_\ell, a_k) = -(a_k, a_\ell) \quad (A-27b)$$

$$\frac{\partial}{\partial t} (a_\ell, a_k) = 0 \quad (A-27c)$$

Obviously, the relation between the matrix of Lagrange brackets and the matrix of Poisson brackets is

$$[\text{LM}]^{-1} = -[\text{PM}] \quad (\text{A-27})$$

Substitution of Equation (A-27) into Equation (A-22) yields

$$\dot{\underline{a}}^* = -[\text{PM}] \left[\frac{\partial F}{\partial \underline{a}^*} \right]^T \quad (\text{A-28})$$

Substitution of Equation (A-20) into Equation (A-28) yields after some rearranging

$$\dot{\underline{a}}^* = -[\text{PM}] \begin{bmatrix} -\frac{\mu}{2(a_1)^2} \\ 0 \\ 0 \\ 0 \\ 0 \\ 0 \end{bmatrix} - [\text{PM}] \left[\frac{\partial R}{\partial \underline{a}^*} \right]^T$$

which can be written as

$$\dot{\underline{a}}^* = \begin{bmatrix} (a_1, a_1) \\ (a_2, a_1) \\ (a_3, a_1) \\ (a_4, a_1) \\ (a_5, a_1) \\ (a_6, a_1) \end{bmatrix} \left[\frac{\mu}{2(a_1)^2} \right] - [\text{PM}] \left[\frac{\partial R}{\partial \underline{a}^*} \right]^T \quad (\text{A-29})$$

It has been shown in the above mentioned references that

$$(a_j, a_1) = 0 \quad \text{for } j = 1, 2, 3, 4, 5 \quad (\text{A-30})$$

$$(a_6, a_1) = \frac{2}{na_1}$$

where n is the mean motion and is equal to $\mu^{1/2} (a_1)^{-3/2}$. Substitution of Equation (A-30) into Equation (A-29) yields the vector form of the Lagrangian VOP equations of motion, viz.

$$\dot{\underline{a}}^* = \underline{e}_6 n - [\text{PM}] \left[\frac{\partial R}{\partial \underline{a}^*} \right]^T \quad (\text{A-31a})$$

where

$$\underline{e}_6 = [0 \ 0 \ 0 \ 0 \ 0 \ 1]^T \quad (\text{A-31b})$$

In scalar form the Lagrangian VOP equations of motion can be written as

$$\dot{a}_i = n \delta_{i6} - \sum_{\ell=1}^6 (a_i, a_\ell) \frac{\partial R}{\partial a_\ell} \quad (\text{A-32})$$

$$(i = 1, 2, 3, 4, 5, 6)$$

where δ_{ij} is the Kroenecker Delta function defined in Equation (2-24) and where R is the disturbing potential.

Gaussian VOP Equations of Motion

The Gaussian form of the VOP equations of motion is applicable for conservative or non-conservative forces. The general form of the equation of motion in Cartesian coordinates can be expressed as

$$\ddot{\underline{r}} + \frac{\mu \underline{r}}{r^3} = \underline{Q} \quad (\text{A-33})$$

where \underline{r} is the position vector in the inertial Cartesian coordinate frame, $\ddot{\underline{r}}$ is the acceleration vector, μ is the gravitational constant and \underline{Q} is the total perturbing acceleration. The unperturbed or two-body problem can be written as

$$\ddot{\underline{x}} + \frac{\mu \underline{x}}{x^3} = 0 \quad (\text{A-34})$$

where \underline{x} denotes unperturbed or two-body position vector. The solution to Equation (A-34) is the two-body solution and is denoted functionally as

$$\underline{x} = \underline{x}(\underline{a}^*) \quad (\text{A-35})$$

where \underline{a}^* denotes the vector of orbital elements which describe the two-body motion. It is noted that the orbital element set is such that the matrizant of the two-body problem (equivalently the Jacobian of the transformation) and its inverse exist. In other words, Γ and Γ^{-1} , as given in Equations (A-9) and (A-11),

exist and are well defined. The two-body velocity vector can be obtained by taking the time derivative of Equation (A-35), i.e.,

$$\dot{\underline{x}} = \begin{bmatrix} \frac{\partial \underline{x}}{\partial \underline{a}^*} \end{bmatrix} \dot{\underline{a}}^* \quad (\text{A-36})$$

In the case of the equinoctial orbital element set it is seen that

$$\underline{a}^* = [a \ h \ k \ p \ q \ \lambda]^T \quad (\text{A-37a})$$

and

$$\dot{\underline{a}}^* = [0 \ 0 \ 0 \ 0 \ 0 \ n]^T \quad (\text{A-37b})$$

where n is the mean motion.

The solution to the perturbed case is assumed to have the following functional form

$$\underline{r} = \underline{x}[\underline{a}^*(t)] \quad (\text{A-38})$$

where $\underline{a}^*(t)$ is the orbital element set that contains both the unperturbed and perturbed motion. This is represented as

$$\underline{a}^*(t) = \underline{a}^* + \underline{a}_p^*(t) \quad (\text{A-39})$$

where \underline{a}^* represents the two-body motion of the orbital element set and $\underline{a}^*_p(t)$ represents the perturbed motion of the orbital element set. Equation (A-38) is requiring that the perturbed position vector and the two-body position vector be the same at each instant of time (the concept of the osculating ellipse). Taking the time derivative of Equation (A-38) yields the following for the perturbed velocity vector

$$\dot{\underline{r}} = \begin{bmatrix} \frac{\partial \underline{x}}{\partial \underline{a}^*} \end{bmatrix} \dot{\underline{a}}^*(t) \quad (\text{A-40})$$

From Equation (A-39) it is seen that

$$\dot{\underline{a}}^*(t) = \dot{\underline{a}}^* + \dot{\underline{a}}^*_p(t) \quad (\text{A-41})$$

With the use of Equations (A-41) and (A-36), Equation (A-40) can be written as

$$\dot{\underline{r}} = \dot{\underline{x}} + \begin{bmatrix} \frac{\partial \underline{x}}{\partial \underline{a}^*} \end{bmatrix} \dot{\underline{a}}^*_p(t) \quad (\text{A-42})$$

The concept of the osculating ellipse requires that the perturbed velocity vector equal the two-body velocity vector at each instant of time. In other words, it is required that

$$\begin{bmatrix} \frac{\partial \underline{x}}{\partial \underline{a}^*} \end{bmatrix} \dot{\underline{a}}^*_p(t) = 0 \quad (\text{A-43})$$

Equation (A-42) can therefore be expressed as

$$\underline{\dot{r}} = \underline{\dot{x}} \quad (\text{A-44})$$

Taking the time derivative of Equation (A-44) yields

$$\underline{\ddot{r}} = \left[\frac{\partial \underline{\dot{x}}}{\partial \underline{a}^*} \right] \underline{\dot{a}}^*(t)$$

which is

$$\underline{\ddot{r}} = \left[\frac{\partial \underline{\dot{x}}}{\partial \underline{a}^*} \right] \underline{\dot{a}}^* + \left[\frac{\partial \underline{\dot{x}}}{\partial \underline{a}^*} \right] \underline{\dot{a}}^*_P(t) \quad (\text{A-45})$$

From Equation (A-36) and Equation (A-37b), it is seen that the two-body velocity vector can be expressed functionally in terms of the vector of orbital elements. In other words

$$\underline{\dot{x}} = \underline{\dot{x}}(\underline{a}^*) \quad (\text{A-46})$$

Taking the time derivative of Equation (A-46) yields

$$\underline{\ddot{x}} = \left[\frac{\partial \underline{\dot{x}}}{\partial \underline{a}^*} \right] \underline{\dot{a}}^* \quad (\text{A-47})$$

With the use of Equations (A-33) and (A-47) it is seen that Equation (A-45) can be rewritten as

$$\underline{Q} - \frac{\mu r}{r^3} = \underline{\ddot{x}} + \begin{bmatrix} \frac{\partial \underline{\dot{x}}}{\partial \underline{a}^*} \end{bmatrix} \dot{\underline{a}}^*_p(t)$$

Using Equation (A-38) it is seen that

$$\underline{Q} = \underline{\ddot{x}} + \frac{\mu x}{x^3} + \begin{bmatrix} \frac{\partial \underline{\dot{x}}}{\partial \underline{a}^*} \end{bmatrix} \dot{\underline{a}}^*_p(t)$$

The two-body equations of motion [Equation (A-34)] requires that

$$\underline{Q} = \begin{bmatrix} \frac{\partial \underline{\dot{x}}}{\partial \underline{a}^*} \end{bmatrix} \dot{\underline{a}}^*_p(t) \quad (\text{A-48})$$

Therefore, the concept of the osculating ellipse requires that Equations (A-43) and (A-48) be satisfied. This can be written as

$$\begin{bmatrix} \begin{bmatrix} \frac{\partial \underline{\dot{x}}}{\partial \underline{a}^*} \end{bmatrix} \\ \begin{bmatrix} \frac{\partial \underline{\dot{x}}}{\partial \underline{a}^*} \end{bmatrix} \end{bmatrix} \dot{\underline{a}}^*_p(t) = \begin{bmatrix} 0 \\ \underline{Q} \end{bmatrix} \quad (\text{A-49})$$

With the use of the two-body matrizant, as given in Equations (A-9) and (A-11), Equation (A-49) is equivalently expressed as

$$\Gamma^{-1} \dot{\underline{a}}^*_p(t) = \begin{bmatrix} 0 \\ \underline{Q} \end{bmatrix} \quad (\text{A-50})$$

Inverting the two-body matrizant in the above expression yields

$$\dot{\underline{a}}^*_p(t) = \Gamma \begin{bmatrix} 0 \\ \underline{Q} \end{bmatrix} \quad (\text{A-51})$$

which reduces to

$$\dot{\underline{a}}^*_p(t) = \begin{bmatrix} \frac{\partial \underline{a}^*}{\partial \dot{\underline{x}}} \end{bmatrix} \cdot \underline{Q} \quad (\text{A-52})$$

Substitution of Equation (A-52) into Equation (A-41) and noting that the two-body element rate is given in Equation (A-37b), yields the vector form of the Gaussian VOP equations of motion, viz.

$$\underline{a}^*(t) = \underline{e}_6 n + \begin{bmatrix} \frac{\partial \underline{a}^*}{\partial \dot{\underline{x}}} \end{bmatrix} \cdot \underline{Q} \quad (\text{A-53})$$

where \underline{e}_6 is defined in Equation (A-31b). In scalar form the Gaussian VOP equations of motion can be written as

$$\dot{a}_i = n \delta_{i6} + \sum_{k=1}^3 \left\{ \begin{bmatrix} \frac{\partial a_i}{\partial \dot{x}_k} \end{bmatrix} Q_k \right\} \quad (\text{A-54})$$

where δ_{i6} is the Kroenecker Delta function defined in Equation (2-24) and where Q_k denotes the kth component of the disturbing acceleration. The matrizant for the two-body problem is given in the above mentioned references.

Appendix B

FINITE-DIFFERENCING

Single-sided and double-sided finite-differencing techniques were used in this research to obtain the partial derivatives of various quantities. In this appendix both techniques will be developed in terms of a scalar function of x , i.e., $f(x)$.

The Double-Sided Finite-Differencing Technique

By use of a Taylor series it is seen that

$$\begin{aligned} f(x_0 + \Delta x) &= f(x_0) + \Delta x \left[\frac{\partial f(x)}{\partial x} \right]_{x=x_0} \\ &+ \frac{(\Delta x)^2}{2} \left[\frac{\partial^2 f(x)}{\partial x^2} \right]_{x=x_0} \\ &+ \frac{(\Delta x)^3}{6} \left[\frac{\partial^3 f(x)}{\partial x^3} \right]_{x=x_0} + \dots \end{aligned} \quad (\text{B-1})$$

It is also seen that

$$\begin{aligned} f(x_0 - \Delta x) &= f(x_0) - \Delta x \left[\frac{\partial f(x)}{\partial x} \right]_{x=x_0} + \frac{(\Delta x)^2}{2} \left[\frac{\partial^2 f(x)}{\partial x^2} \right]_{x=x_0} \\ &- \frac{(\Delta x)^3}{6} \left[\frac{\partial^3 f(x)}{\partial x^3} \right]_{x=x_0} + \dots \end{aligned} \quad (\text{B-2})$$

Subtracting $f(x_0 - \Delta x)$ from $f(x_0 + \Delta x)$ yields

$$\begin{aligned}
 f(x_0 + \Delta x) - f(x_0 - \Delta x) &= 2(\Delta x) \left[\frac{\partial f(x)}{\partial x} \right]_{x=x_0} \\
 &+ \frac{(\Delta x)^3}{6} \left[\frac{\partial^3 f(x)}{\partial x^3} \right]_{x=x_0} + \dots
 \end{aligned}
 \tag{B-3}$$

Obviously the partial derivative of $\left[\frac{\partial f(x)}{\partial x} \right]_{x_0}$ can be approximated as

$$\left[\frac{\partial f(x)}{\partial x} \right]_{x=x_0} \sim \frac{f(x_0 + \Delta x) - f(x_0 - \Delta x)}{2(\Delta x)}
 \tag{B-4}$$

Equation (B-4) is the form of the double-sided finite-differencing technique. There are two sources of error for this approach: neglect of higher order terms and round-off. The error due to the neglect of higher order terms will be less than or equal to the following

$$\text{Error} \leq \left\{ \frac{(\Delta x)^2}{6} \left[\max \left| \frac{\partial^3 f(x)}{\partial x^3} \right| \right] \right\}
 \tag{B-5}$$

where $\max \left| \frac{\partial^3 f(x)}{\partial x^3} \right|$ denotes the maximum of this quantity over the range of interest. Round-off errors are due to the finite word length of the digital computer that this technique is implemented on. Varying the stepsize (Δx) can significantly affect the round-off error. With double precision on the Amdahl 470 V6 (16 digits), it was found that good results were obtained when Δx was 10^{-5} of x , i.e.

$$\Delta x = (10^{-5})x \quad (\text{B-6})$$

With single precision (8 digits), a good stepsize is

$$\Delta x = (10^{-3})x \quad (\text{B-7})$$

The Single-Sided Finite-Differencing Technique

Subtracting $f(x_0)$ from $f(x_0 + \Delta x)$ as given in Equation (B-1) yields

$$\begin{aligned} f(x_0 + \Delta x) - f(x_0) &= \Delta x \left[\frac{\partial f(x)}{\partial x} \right]_{x=x_0} \\ &+ \frac{(\Delta x)^2}{2} \left[\frac{\partial^2 f(x)}{\partial x^2} \right]_{x=x_0} + \dots \end{aligned} \quad (\text{B-8})$$

The single-sided finite-difference approximation is therefore

$$\left[\frac{\partial f(x)}{\partial x} \right]_{x=x_0} \sim \frac{f(x_0 + \Delta x) - f(x_0)}{\Delta x} \quad (\text{B-9})$$

Again it is noted that the errors in this technique are the neglect of higher order terms and round-off. The error due to the neglect of higher order terms will be less than or equal to the following

$$\text{Error} \leq \left\{ \frac{\Delta x}{2} \left[\max \left| \frac{\partial^2 f(x)}{\partial x^2} \right| \right] \right\} \quad (\text{B-10})$$

Again it is noted that the stepsize can significantly affect the round-off error. It was found that a stepsize as given in Equations (B-6) and (B-7) also gave good results for the single-sided finite-difference technique. The single-sided finite-differencing technique is not recommended for the semianalytical partial derivatives of Chapter 3.

Appendix C

THE ADAPTIVE MODIFIED HARRIS-PRIESTER ATMOSPHERE

The Adaptive Modified Harris-Priester Atmosphere is defined as

$$\rho = \exp[a_4 h + a_5/h] \{ a_1 \rho_{\min}(h) + [a_2 \rho_{\max}(h) - a_1 \rho_{\min}(h)] \cos^{a_3}(\psi/2) \} \quad (C-1)$$

where

- ρ = density at point in question
- a_1, a_2, a_3, a_4, a_5 = adaptive density parameters
- h = height above the reference ellipsoid ($h_1 \leq h \leq h_2$)
- ψ = angle between the diurnal bulge and satellite

$$\rho_{\min}(h) = \rho_{\min_1} \exp \left[\frac{h_1 - h}{H_{\min}} \right] \quad (C-2)$$

$$\rho_{\max}(h) = \rho_{\max_1} \exp \left[\frac{h_1 - h}{H_{\max}} \right] \quad (C-3)$$

$$H_{\min} = \frac{h_1 - h_2}{\ln[\rho_{\min_2} / \rho_{\min_1}]} \quad (\text{C-4})$$

$$H_{\max} = \frac{h_1 - h_2}{\ln[\rho_{\max_2} / \rho_{\max_1}]} \quad (\text{C-5})$$

and where h_1 , h_2 , ρ_{\min_1} , ρ_{\min_2} , ρ_{\max_1} and ρ_{\max_2} come from the Modified Harris-Priester density table corresponding to the $\bar{F}_{10.7}$ of interest. It is noted that the standard form of the Modified Harris-Priester density model results when the adaptive density parameters are

$$\begin{aligned} a_1 &= a_2 = 1.0 \\ a_3 &= 6.0 \\ a_4 &= a_5 = 0.0 \end{aligned} \quad (\text{C-6})$$

The Modified Harris-Priester density model is discussed in detail in References 17 and 67.

Appendix D

DRAG-J₂ ANALYTICAL EXPRESSIONS

From Equation (2-101b) it can be seen that the drag-J₂ term of the mean element rates can be written as

$$\begin{aligned} \epsilon v B_{i, DRJ2}(\bar{a}) = & ADRJ2i + \left(\frac{15\bar{n} \delta_{i6}}{16\bar{a}_1^2} \right) \sum_{\sigma=1}^{\infty} [\epsilon C_{1\sigma} v G_{1\sigma} \\ & + \epsilon D_{1\sigma} v H_{1\sigma}] \end{aligned} \quad (D-1)$$

where

$$ADRJ2i = \frac{1}{2\pi} \int_0^{2\pi} \sum_{\ell=1}^6 v \psi_{\ell,1}(\bar{a}, \bar{\lambda}) \left[\frac{\partial \epsilon F_i(\bar{a}, \bar{\lambda})}{\partial \bar{a}_\ell} \right] d\bar{\lambda} \quad (D-2)$$

and where

- $v \psi_{\ell,1}(\bar{a}, \bar{\lambda})$ = drag short periodic variations [see Equation (2-99)]
- $\epsilon F_i(\bar{a}, \bar{\lambda})$ = VOP disturbing function due to J₂ effects
- $\epsilon C_{i\sigma}, \epsilon D_{i\sigma}$ = J₂ short periodic coefficients
- $v G_{i\sigma}, v H_{i\sigma}$ = drag short periodic coefficients

Equation (D-2) was solved using MACSYMA (Ref. 22). MACSYMA is a large computer programming system used for performing symbolic as well as numerical mathematical manipulations. MACSYMA is written in LISP and is being developed by the Matlab Group at the MIT Laboratory for Computer Science. The VOP disturbing function due to J_2 effects, $\epsilon F_i(\bar{a}, \bar{\lambda})$, was obtained by the MACSYMA orbital mechanics package of Zeis as explained in Section 2.4 of Reference 6. Zeis' package is only good for direct orbits. Due to the present limitations of the MACSYMA system hardware, $\epsilon F_i(\bar{a}, \bar{\lambda})$ could only be obtained to first order in powers of the eccentricity. Taking the required partial derivatives of $\epsilon F_i(\bar{a}, \bar{\lambda})$ as indicated in Equation (D-2), made the results obtained for ADRJ2i good only to zeroth order in the eccentricity. Performing the indicated operations of Equation (D-2) on the MACSYMA system gave the analytical drag- J_2 expressions. These expressions are given below. It should be noted that due to the limitations of the present MACSYMA computer system hardware, Equation (D-2) had to be broken into smaller component parts and the final results added together. The following notation was used:

$Cx(i, \sigma), Dx(i, \sigma)$	\equiv	drag short periodic coefficients $v_{G_{i\sigma}}, v_{H_{i\sigma}}$
MU	\equiv	μ = gravitational constant
RE	\equiv	r_e = equatorial radius of the Earth
XN	\equiv	n = mean motion
C	\equiv	$P^2 + Q^2$
A, H, K, P, Q, L	\equiv	equinoctial elements = a, h, k, p, q, λ

ADRJ21:

$$12 J \frac{DX(5, 2)}{2} MU P (4 P^2 - C - 1) RE^2$$

$$A^4 (C + 1)^3 XN$$

$$12 J \frac{CX(5, 2)}{2} MU (4 P^2 - C + 1) Q RE^2$$

$$A^4 (C + 1)^3 XN$$

$$12 J \frac{DX(4, 2)}{2} MU (4 P^2 - C - 1) Q RE^2 \quad + \quad 24 J \frac{CX(6, 2)}{2} MU P Q RE^2$$

$$A^4 (C + 1)^3 XN$$

$$A^4 (C + 1)^2 XN$$

$$63 J \frac{DX(3, 3)}{2} MU P Q RE^2 \quad + \quad 3 J \frac{DX(3, 1)}{2} MU P Q RE^2$$

$$A^4 (C + 1)^2 XN$$

$$A^4 (C + 1)^2 XN$$

$$63 J \frac{CX(2, 3)}{2} MU P Q RE^2 \quad + \quad 3 J \frac{CX(2, 1)}{2} MU P Q RE^2$$

$$A^4 (C + 1)^2 XN$$

$$A^4 (C + 1)^2 XN$$

$$30 \frac{DX(1, 2)}{2} J MU P Q RE^2 \quad + \quad 12 J \frac{CX(4, 2)}{2} MU P (4 P^2 - 3 C - 1) RE^2$$

$$A^5 (C + 1)^2 XN$$

$$A^4 (C + 1)^3 XN$$

$$3 J \frac{CX(3, 1)}{2} MU (2 P^2 + C - 5 C + 1) RE^2$$

$$2 A^4 (C + 1)^2 XN$$

$$3 J \frac{DX(2, 1)}{2} MU (2 P^2 - C + 3 C - 1) RE^2$$

$$2 A^4 (C + 1)^2 XN$$

$$\begin{array}{r}
\frac{12 J \text{ IX}(6, 2) \text{ MU}(2 P^2 - C) \text{ RE}^2}{2} \\
\hline
\frac{4}{2} A (C + 1)^2 \text{ XN}
\end{array}
+
\begin{array}{r}
\frac{63 J \text{ CX}(3, 3) \text{ MU}(2 P^2 - C) \text{ RE}^2}{2} \\
\hline
\frac{4}{2} A (C + 1)^2 \text{ XN}
\end{array}$$

$$\begin{array}{r}
\frac{63 J \text{ IX}(2, 3) \text{ MU}(2 P^2 - C) \text{ RE}^2}{2} \\
\hline
\frac{4}{2} A (C + 1)^2 \text{ XN}
\end{array}
+
\begin{array}{r}
\frac{15 \text{ CX}(1, 2) J \text{ MU}(2 P^2 - C) \text{ RE}^2}{2} \\
\hline
\frac{5}{2} A (C + 1)^2 \text{ XN}
\end{array}$$

i

ADRJ229

$$21 \text{ J } \text{CX}(5, 3) \text{ MU P } (4 \text{ O}^2 - \text{C} - 1) \text{ RE}^2$$

$$2 \text{ A}^5 (\text{C} + 1)^3 \text{ XN}$$

$$3 \text{ J } \text{CX}(5, 1) \text{ MU P } (4 \text{ O}^2 - \text{C} - 1) \text{ RE}^2$$

$$2 \text{ A}^5 (\text{C} + 1)^3 \text{ XN}$$

$$21 \text{ J } \text{DX}(5, 3) \text{ MU } (4 \text{ P}^2 - \text{C} + 1) \text{ O RE}^2$$

$$2 \text{ A}^5 (\text{C} + 1)^3 \text{ XN}$$

$$21 \text{ J } \text{CX}(4, 3) \text{ MU } (4 \text{ P}^2 - \text{C} - 1) \text{ O RE}^2$$

$$2 \text{ A}^5 (\text{C} + 1)^3 \text{ XN}$$

$$3 \text{ J } \text{CX}(4, 1) \text{ MU } (4 \text{ P}^2 - \text{C} - 1) \text{ O RE}^2$$

$$2 \text{ A}^5 (\text{C} + 1)^3 \text{ XN}$$

$$3 \text{ J } \text{DX}(5, 1) \text{ MU } (4 \text{ P}^2 - 7 \text{ C} + 7) \text{ O RE}^2 \quad 63 \text{ J } \text{DX}(6, 3) \text{ MU P O RE}^2$$

$$2 \text{ A}^5 (\text{C} + 1)^3 \text{ XN}$$

$$2 \text{ A}^5 (\text{C} + 1)^2 \text{ XN}$$

$$3 \text{ J } \text{DX}(6, 1) \text{ MU P O RE}^2 \quad 51 \text{ J } \text{CX}(3, 4) \text{ MU P O RE}^2$$

$$2 \text{ A}^5 (\text{C} + 1)^2 \text{ XN}$$

$$5 \text{ A}^5 (\text{C} + 1)^2 \text{ XN}$$

$$\begin{array}{r}
\frac{51 J \text{ DX}(2, 4) \text{ MU P O RE}^2}{2} + \frac{3 J \text{ DX}(2, 2) \text{ MU P O RE}^2}{2} \\
\hline
\frac{5}{A} (C + 1)^2 \text{ XN} + \frac{5}{A} (C + 1)^2 \text{ XN} \\
\\
\frac{147 \text{ CX}(1, 3) J \text{ MU P O RE}^2}{2} - \frac{21 \text{ CX}(1, 1) J \text{ MU P O RE}^2}{2} \\
\hline
\frac{6}{4 A} (C + 1)^2 \text{ XN} + \frac{6}{4 A} (C + 1)^2 \text{ XN} \\
\\
\frac{3 J \text{ CX}(3, 2) (C + 4) \text{ MU P O RE}^2}{2} \\
\hline
\frac{5}{A} (C + 1)^2 \text{ XN} \\
\\
\frac{3 J \text{ DX}(3, 2) \text{ MU} (4 (C + 4) P^2 + C^2 - 20 C + 3) \text{ RE}^2}{2} \\
\hline
\frac{5}{4 A} (C + 1)^2 \text{ XN} \\
\\
\frac{3 J \text{ CX}(2, 2) \text{ MU} (4 P^2 - (C - 3) (3 C - 1)) \text{ RE}^2}{2} \\
\hline
\frac{5}{4 A} (C + 1)^2 \text{ XN} \\
\\
\frac{21 J \text{ DX}(4, 3) \text{ MU P} (4 P^2 - 3 C - 1) \text{ RE}^2}{2} \\
\hline
\frac{5}{2 A} (C + 1)^3 \text{ XN} \\
\\
\frac{3 J \text{ DX}(4, 1) \text{ MU P} (4 P^2 - 9 C + 5) \text{ RE}^2}{2} \\
+ \hline
\frac{5}{2 A} (C + 1)^3 \text{ XN}
\end{array}$$

$$\begin{array}{r}
\frac{3}{2} J_{CX}(6, 1) MU (2 P^2 + C^2 - 5 C + 1) RE^2 \\
\hline
4 A^5 (C + 1)^2 XN \\
\frac{21}{2} DX(1, 1) J MU (2 P^2 + C^2 - 5 C + 1) RE^2 \\
+ \hline
8 A^6 (C + 1)^2 XN \\
\frac{63}{2} J_{CX}(6, 3) MU (2 P^2 - C) RE^2 \quad \frac{51}{2} J_{DX}(3, 4) MU (2 P^2 - C) RE^2 \\
+ \hline
4 A^5 (C + 1)^2 XN \quad \quad \quad 2 A^5 (C + 1)^2 XN \\
\frac{51}{2} J_{CX}(2, 4) MU (2 P^2 - C) RE^2 \quad \frac{147}{2} DX(1, 3) J MU (2 P^2 - C) RE^2 \\
\hline
2 A^5 (C + 1)^2 XN \quad \quad \quad 8 A^6 (C + 1)^2 XN
\end{array}$$

ADR.J23:

$$\begin{array}{r}
 21 \text{ J } \text{DX}(5, 3) \text{ MU P } (4 \text{ O}^2 - \text{C} - 1) \text{ RE}^2 \\
 \hline
 2 \text{ A}^5 (\text{C} + 1)^3 \text{ XN} \\
 \\
 3 \text{ J } \text{DX}(5, 1) \text{ MU P } (4 \text{ O}^2 - \text{C} - 1) \text{ RE}^2 \\
 + \hline
 2 \text{ A}^5 (\text{C} + 1)^3 \text{ XN} \\
 \\
 3 \text{ J } \text{CX}(5, 1) \text{ MU } (4 \text{ P}^2 + 5 \text{ C} - 5) \text{ O RE}^2 \\
 \hline
 2 \text{ A}^5 (\text{C} + 1)^3 \text{ XN} \\
 \\
 21 \text{ J } \text{CX}(5, 3) \text{ MU } (4 \text{ P}^2 - \text{C} + 1) \text{ O RE}^2 \\
 \hline
 2 \text{ A}^5 (\text{C} + 1)^3 \text{ XN} \\
 \\
 21 \text{ J } \text{DX}(4, 3) \text{ MU } (4 \text{ P}^2 - \text{C} - 1) \text{ O RE}^2 \\
 + \hline
 2 \text{ A}^5 (\text{C} + 1)^3 \text{ XN} \\
 \\
 3 \text{ J } \text{DX}(4, 1) \text{ MU } (4 \text{ P}^2 - \text{C} - 1) \text{ O RE}^2 \quad 63 \text{ J } \text{CX}(6, 3) \text{ MU P O RE}^2 \\
 + \hline
 2 \text{ A}^5 (\text{C} + 1)^3 \text{ XN} \quad 2 \text{ A}^5 (\text{C} + 1)^2 \text{ XN} \\
 \\
 3 \text{ J } \text{CX}(6, 1) \text{ MU P O RE}^2 \quad 51 \text{ J } \text{DX}(3, 4) \text{ MU P O RE}^2 \\
 \hline
 2 \text{ A}^5 (\text{C} + 1)^2 \text{ XN} \quad \text{A}^5 (\text{C} + 1)^2 \text{ XN}
 \end{array}$$

$$\begin{array}{r}
\frac{3}{2} J \text{ DX}(3, 2) \text{ MU P } 0 \text{ RE}^2 + \frac{51}{2} J \text{ CX}(2, 4) \text{ MU P } 0 \text{ RE}^2 \\
\hline
\frac{5}{A} (C + 1)^2 \text{ XN} + \frac{5}{A} (C + 1)^2 \text{ XN} \\
\\
\frac{147}{2} \text{ DX}(1, 3) J \text{ MU P } 0 \text{ RE}^2 + \frac{21}{2} \text{ DX}(1, 1) J \text{ MU P } 0 \text{ RE}^2 \\
\hline
\frac{6}{4A} (C + 1)^2 \text{ XN} + \frac{6}{4A} (C + 1)^2 \text{ XN} \\
\\
\frac{3}{2} J \text{ CX}(2, 2) (C + 4) \text{ MU P } 0 \text{ RE}^2 \\
\hline
\frac{5}{A} (C + 1)^2 \text{ XN} \\
\\
\frac{3}{2} J \text{ DX}(2, 2) \text{ MU} (4(C + 4) P^2 - 5C^2 + 4C - 3) \text{ RE}^2 \\
\hline
\frac{5}{4A} (C + 1)^2 \text{ XN} \\
\\
\frac{3}{2} J \text{ CX}(3, 2) \text{ MU} (4P^2 + 3C^2 - 14C + 3) \text{ RE}^2 \\
\hline
\frac{5}{4A} (C + 1)^2 \text{ XN} \\
\\
\frac{3}{2} J \text{ CX}(4, 1) \text{ MU P} (4P^2 + 3C^2 - 7) \text{ RE}^2 \\
\hline
\frac{5}{2A} (C + 1)^3 \text{ XN} \\
\\
\frac{21}{2} J \text{ CX}(4, 3) \text{ MU P} (4P^2 - 3C - 1) \text{ RE}^2 \\
\hline
\frac{5}{2A} (C + 1)^3 \text{ XN}
\end{array}$$

$$\begin{array}{r}
3 J \text{ DX}(6, 1) \text{ MU} (2 P^2 - C^2 + 3 C - 1) \text{ RE}^2 \\
\hline
4 A^5 (C + 1)^2 \text{ XN} \\
21 \text{ CX}(1, 1) \text{ J} \text{ MU} (2 P^2 - C^2 + 3 C - 1) \text{ RE}^2 \\
\hline
8 A^6 (C + 1)^2 \text{ XN} \\
63 J \text{ DX}(6, 3) \text{ MU} (2 P^2 - C) \text{ RE}^2 \quad + \quad 51 J \text{ CX}(3, 4) \text{ MU} (2 P^2 - C) \text{ RE}^2 \\
\hline
4 A^5 (C + 1)^2 \text{ XN} \quad + \quad 2 A^5 (C + 1)^2 \text{ XN} \\
51 J \text{ DX}(2, 4) \text{ MU} (2 P^2 - C) \text{ RE}^2 \quad + \quad 147 \text{ CX}(1, 3) \text{ J} \text{ MU} (2 P^2 - C) \text{ RE}^2 \\
\hline
2 A^5 (C + 1)^2 \text{ XN} \quad + \quad 8 A^6 (C + 1)^2 \text{ XN}
\end{array}$$

ADR J241

$$\begin{array}{r}
 \frac{3 J}{2} DX(5, 2) MU (4 P^2 + C^2 - 1) RE^2 \quad \frac{3 J}{2} CX(5, 2) MU P^2 RE^2 \\
 \hline
 4 A^5 (C + 1)^2 XN \quad A^5 (C + 1)^2 XN \\
 \\
 \frac{3 J}{2} DX(4, 2) MU P^2 RE^2 \quad \frac{3 J}{2} CX(6, 2) (C - 1) MU P^2 RE^2 \\
 + \hline
 A^5 (C + 1)^2 XN \quad 2 A^5 (C + 1)^2 XN \\
 \\
 \frac{21 J}{2} DX(3, 3) (C - 1) MU P^2 RE^2 \quad \frac{21 J}{2} DX(3, 1) (C - 1) MU P^2 RE^2 \\
 + \hline
 8 A^5 (C + 1)^2 XN \quad 8 A^5 (C + 1)^2 XN \\
 \\
 \frac{21 J}{2} CX(2, 3) (C - 1) MU P^2 RE^2 \quad \frac{15 J}{2} CX(2, 1) (C - 1) MU P^2 RE^2 \\
 - \hline
 8 A^5 (C + 1)^2 XN \quad 8 A^5 (C + 1)^2 XN \\
 \\
 \frac{21 J}{2} DX(1, 2) (C - 1) MU P^2 RE^2 \quad \frac{3 J}{2} CX(4, 2) MU (4 P^2 + C^2 - 1) RE^2 \\
 - \hline
 8 A^6 (C + 1)^2 XN \quad 4 A^5 (C + 1)^2 XN \\
 \\
 \frac{3 J}{2} DX(6, 2) (C - 1) MU P^2 RE^2 \quad \frac{21 J}{2} CX(3, 3) (C - 1) MU P^2 RE^2 \\
 + \hline
 2 A^5 (C + 1)^2 XN \quad 8 A^5 (C + 1)^2 XN \\
 \\
 \frac{3 J}{2} CX(3, 1) (C - 1) MU P^2 RE^2 \quad \frac{21 J}{2} DX(2, 3) (C - 1) MU P^2 RE^2 \\
 + \hline
 8 A^5 (C + 1)^2 XN \quad 8 A^5 (C + 1)^2 XN \\
 \\
 \frac{3 J}{2} DX(2, 1) (C - 1) MU P^2 RE^2 \quad \frac{21 J}{2} CX(1, 2) (C - 1) MU P^2 RE^2 \\
 - \hline
 8 A^5 (C + 1)^2 XN \quad 8 A^6 (C + 1)^2 XN
 \end{array}$$

ADP J251

$$\begin{array}{r}
 \frac{3 J}{2} CX(5, 2) MU (4 P^2 + C^2 - 1) RE^2 \quad \frac{3 J}{2} DX(5, 2) MU P O RE^2 \\
 \hline
 4 A^5 (C + 1)^2 XN \quad \quad \quad A^5 (C + 1)^2 XN \\
 + \\
 \frac{3 J}{2} CX(4, 2) MU P O RE^2 \quad \frac{3 J}{2} DX(6, 2) (C - 1) MU O PE^2 \\
 \hline
 A^5 (C + 1)^2 XN \quad \quad \quad 2 A^5 (C + 1) XN \\
 + \\
 \frac{21 J}{2} CX(3, 3) (C - 1) MU O PE^2 \quad \frac{3 J}{2} CX(3, 1) (C - 1) MU O RE^2 \\
 \hline
 8 A^5 (C + 1) XN \quad \quad \quad 8 A^5 (C + 1) XN \\
 + \\
 \frac{21 J}{2} DX(2, 3) (C - 1) MU O PE^2 \quad \frac{3 J}{2} DX(2, 1) (C - 1) MU O RE^2 \\
 \hline
 8 A^5 (C + 1) XN \quad \quad \quad 8 A^5 (C + 1) XN \\
 + \\
 \frac{21 CX(1, 2) J}{2} (C - 1) MU O RE^2 \quad \frac{3 J}{2} DX(4, 2) MU (4 P^2 + C^2 - 1) RE^2 \\
 \hline
 8 A^6 (C + 1) XN \quad \quad \quad 4 A^5 (C + 1)^2 XN \\
 + \\
 \frac{3 J}{2} CX(6, 2) (C - 1) MU P RE^2 \quad \frac{21 J}{2} DX(3, 3) (C - 1) MU P PE^2 \\
 \hline
 2 A^5 (C + 1) XN \quad \quad \quad 8 A^5 (C + 1) XN \\
 + \\
 \frac{15 J}{2} DX(3, 1) (C - 1) MU P RE^2 \quad \frac{21 J}{2} CX(2, 3) (C - 1) MU P RE^2 \\
 \hline
 8 A^5 (C + 1) XN \quad \quad \quad 8 A^5 (C + 1) XN \\
 + \\
 \frac{21 J}{2} CX(2, 1) (C - 1) MU P PE^2 \quad \frac{21 DX(1, 2) J}{2} (C - 1) MU P RE^2 \\
 \hline
 8 A^5 (C + 1) XN \quad \quad \quad 8 A^6 (C + 1) XN
 \end{array}$$

ADRJ263

$$\frac{3 J_2 CX(5, 2) MU P (2 (C - 15) P^2 - (C - 7) (C + 1)) RE^2}{A^5 (C + 1)^3 XN}$$

$$+ \frac{3 J_2 CX(4, 2) MU (2 (C - 15) P^2 - (C - 7) (C + 1)) \emptyset RE^2}{A^5 (C + 1)^3 XN}$$

$$+ \frac{3 J_2 DX(5, 2) MU (2 (C - 15) P^2 + 9 C - 7) \emptyset RE^2}{A^5 (C + 1)^3 XN}$$

$$+ \frac{6 J_2 DX(6, 2) (C - 7) MU P \emptyset RE^2}{A^5 (C + 1)^2 XN} + \frac{21 CX(1, 2) J_2 (C - 7) MU P \emptyset RE^2}{2 A^6 (C + 1)^2 XN}$$

$$- \frac{21 J_2 CX(3, 3) (2 C - 15) MU P \emptyset RE^2}{4 A^5 (C + 1)^2 XN} + \frac{3 J_2 CX(3, 1) (2 C - 15) MU P \emptyset RE^2}{4 A^5 (C + 1)^2 XN}$$

$$- \frac{21 J_2 DX(2, 3) (2 C - 15) MU P \emptyset RE^2}{4 A^5 (C + 1)^2 XN} - \frac{3 J_2 DX(2, 1) (2 C - 15) MU P \emptyset RE^2}{4 A^5 (C + 1)^2 XN}$$

$$+ \frac{3 J_2 CX(2, 1) MU (2 (2 C - 15) P^2 + 23 C^2 - 49 C + 13) RE^2}{8 A^5 (C + 1)^2 XN}$$

$$+ \frac{3 J_2 DX(3, 1) MU (2 (2 C - 15) P^2 - 27 C^2 + 79 C - 13) RE^2}{8 A^5 (C + 1)^2 XN}$$

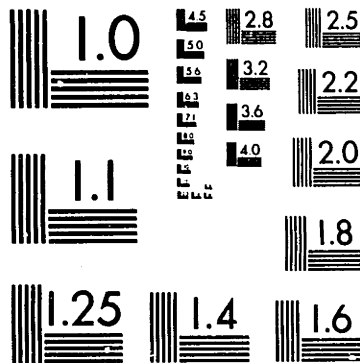
$$\begin{array}{r} 3 J \text{ DX}(4, 2) \text{ MU P } (2 (C - 15) P^2 - 2 C^2 + 21 C + 7) \text{ RE}^2 \\ + \hline 5 \\ A (C + 1)^3 \text{ XN} \end{array}$$

$$\begin{array}{r} 3 J \text{ CX}(6, 2) (C - 7) \text{ MU } (2 P^2 - C) \text{ RE}^2 \\ - \hline 5 \\ A (C + 1)^2 \text{ XN} \end{array}$$

$$\begin{array}{r} 21 \text{ DX}(1, 2) J (C - 7) \text{ MU } (2 P^2 - C) \text{ RE}^2 \\ + \hline 6 \\ 4 A (C + 1)^2 \text{ XN} \end{array}$$

$$\begin{array}{r} 21 J \text{ DX}(3, 3) (2 C - 15) \text{ MU } (2 P^2 - C) \text{ RE}^2 \\ - \hline 5 \\ 3 A (C + 1)^2 \text{ XN} \end{array}$$

$$\begin{array}{r} 21 J \text{ CX}(2, 3) (2 C - 15) \text{ MU } (2 P^2 - C) \text{ RE}^2 \\ + \hline 5 \\ 8 A (C + 1)^2 \text{ XN} \end{array}$$



MICROCOPY RESOLUTION TEST CHART
NATIONAL BUREAU OF STANDARDS-1963-A

20X

NOTICE THIS MATERIAL MAY BE PROTECTED BY
COPYRIGHT LAW (TITLE 17 U.S. CODE)

Appendix E
CORRECTIONS TO ZEIS' J_2^2 SHORT PERIODIC EXPRESSIONS

The second order J_2 short periodic variation for the fifth* (Δq) and the sixth ($\Delta \lambda$) variables as given in Reference 6 were rederived during the present development effort. The results obtained were different than Zeis' expressions. The new expressions obtained are

$$\begin{aligned}
 J22ETA52 = & \frac{-3J_2^2 (\bar{c} - 1) R_e^4}{16a^4 (\bar{c} + 1)^3} \left[\bar{q}(72\bar{p}^2 - 12\bar{c}) \cos(2\bar{\lambda}) \right. \\
 & + \bar{p}(72\bar{p}^2 - 48\bar{c}) \sin(2\bar{\lambda}) + \bar{q}[(12\bar{c} + 20)\bar{p}^2 - 3\bar{c}^2 \\
 & \left. - 5\bar{c}] \cos(4\bar{\lambda}) + \bar{p}[(12\bar{c} + 20)\bar{p}^2 - 9\bar{c}^2 - 15\bar{c}] \sin(4\bar{\lambda}) \right]
 \end{aligned}
 \tag{E-1}$$

and

$$\begin{aligned}
 J22ETA62 = & \frac{3J_2^2 R_e^4}{16a^4 (\bar{c} + 1)^4} \left[16\bar{p} \bar{q}(13\bar{c}^2 - 13\bar{c} + 7) \cos(2\bar{\lambda}) \right. \\
 & - 8(\bar{q}^2 - \bar{p}^2)(13\bar{c}^2 - 13\bar{c} + 7) \sin(2\bar{\lambda}) \\
 & - 4\bar{p} \bar{q}(\bar{q}^2 - \bar{p}^2)(3\bar{c}^2 + 10\bar{c} - 45) \cos(4\bar{\lambda}) \\
 & \left. + (\bar{c}^2 - 8\bar{p}^2 \bar{q}^2)(3\bar{c}^2 + 10\bar{c} - 45) \sin(4\bar{\lambda}) \right]
 \end{aligned}
 \tag{E-2}$$

* J. P. Kaniecki discovered the error in the Δq in August 1979.

where

$\bar{a}, \bar{h}, \bar{k}, \bar{p}, \bar{q}$, and $\bar{\lambda}$ = the mean equinoctial elements

$$\bar{c} = \bar{p}^2 + \bar{q}^2$$

R_e \equiv equatorial radius of Earth

$$\text{J22ETA52} \equiv \epsilon^2 \eta_{5,2}(\bar{a}, \bar{\lambda})$$

$$\text{J22ETA62} \equiv \epsilon^2 \eta_{6,2}(\bar{a}, \bar{\lambda})$$

Appendix F

SOFTWARE IMPLEMENTATION

The short periodic development, second order drag theory, semianalytical partial derivatives and semianalytical batch filter were implemented into GTDS-RD. The new subroutines developed are presented in this appendix. Subroutines 'ORBITV' and 'AVRAGE' which are standard subroutines of GTDS-RD are also presented due to the necessary interfaces that were required in these subroutines.

The necessary switches and flags used in order to exercise different options were set in subroutines 'HWIRE' and 'ESTSET.' Subroutine 'HWIRE' set the necessary switches and flags used in the short periodic development and in the implementation of the second order drag theory. Subroutine 'HWIRE' is called from the GTDS-RD subroutine 'AVRINT.' Subroutine 'ESTSET' sets the necessary switches and flags used in the implementation of the semianalytical partial derivatives and the semianalytical batch filter. Subroutine 'ESTSET' is called from the GTDS-RD subroutine 'INTOGN.' These subroutines and the other new subroutines were linked with the GTDS-RD load module. Eventually these switches and flags will be standard input options and/or initialization procedures in GTDS-RD.

The software implementation of this research can be divided into the following areas: SPG, second order drag effects in the AOG, APG, SPPG and semianalytical batch filter. Each of these areas will be discussed separately followed by a listing of new subroutines in alphabetical order.

SPG

The present SPG is on the output grid. A flow diagram for the SPG is given in Table F-1. The numerical time-independent short periodic formulation was implemented. Weak time-dependent short periodic corrections, using a single-sided finite-differencing technique, were also implemented. Zeis' J_2^2 short periodic expressions (with the corrections as indicated in Appendix E) were implemented by Leo W. Early of CSDL. Present development efforts are implementing the analytical short periodic expressions as given in Reference 5. The implementation of the SPG also required changes in the GTDS-RD subroutines 'ANAVIN' and 'AVRINT.'

Second Order Drag Effects in the AOG

A flow chart for the implementation of the second order drag effects into the AOG is presented in Table F-2. This implementation also required changes in the GTDS-RD subroutines 'ANAVIN,' 'AVRINT,' 'EQINT' and 'EQUNPV.'

Table F-1
Flow Chart for the SPG

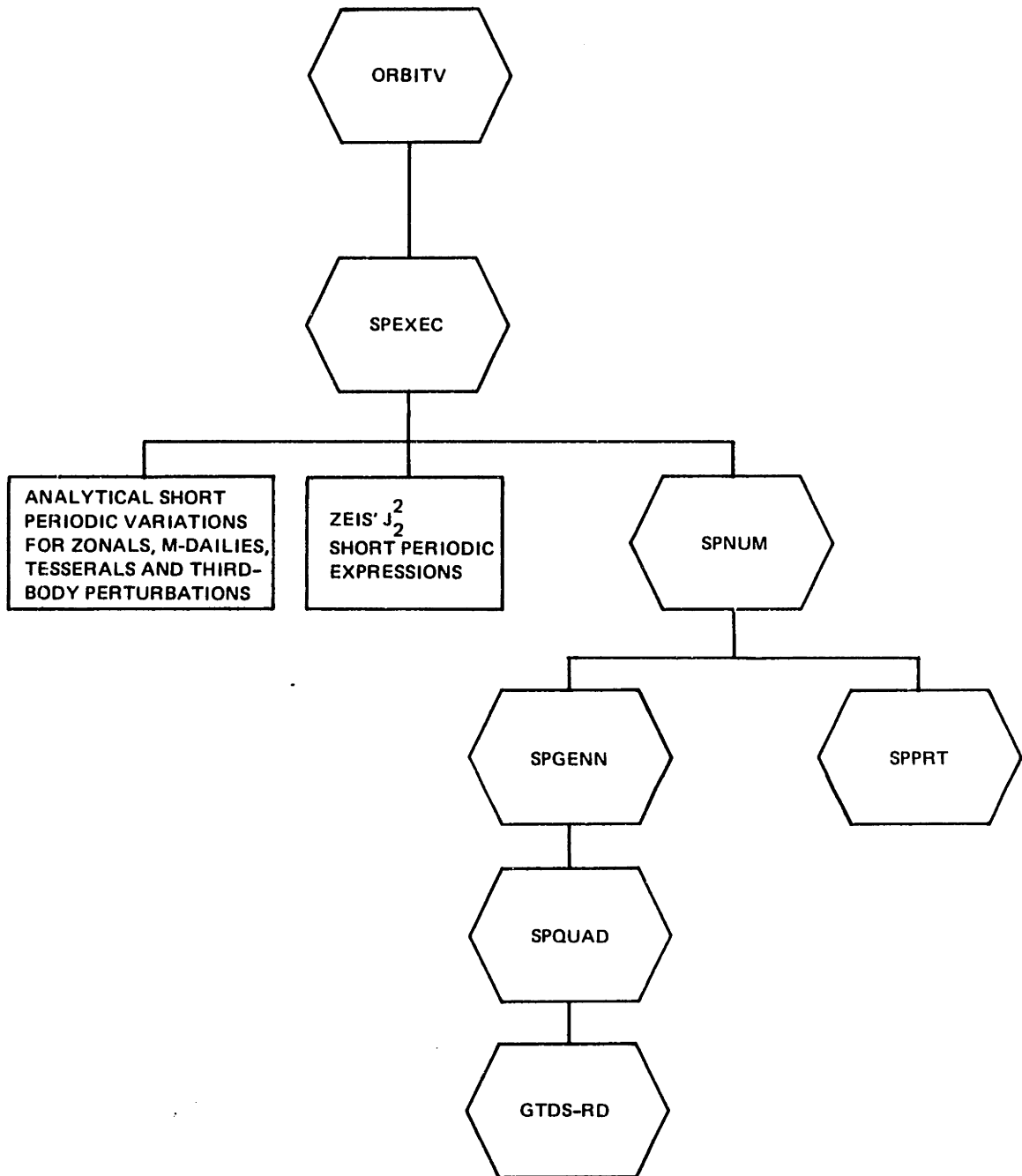
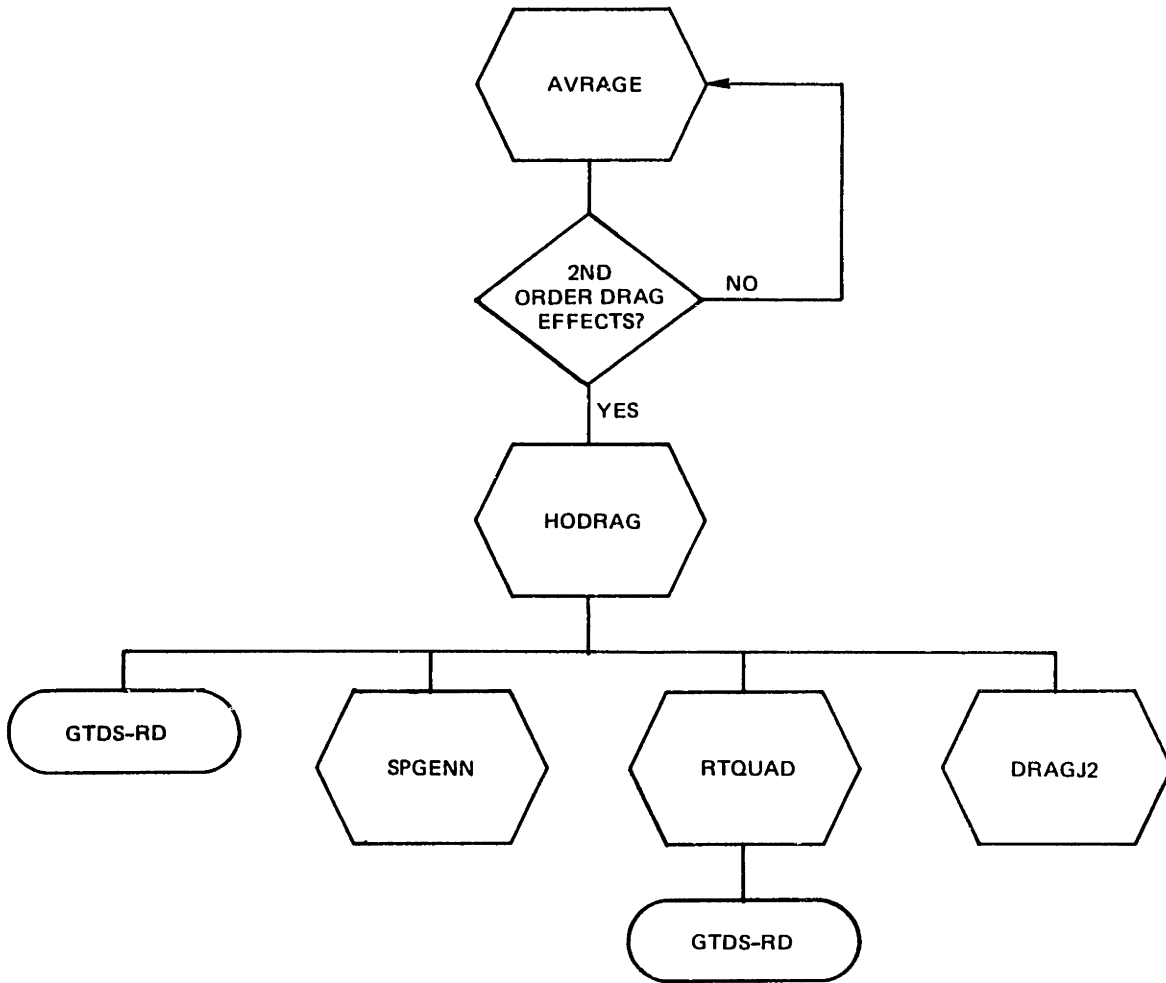


Table F-2

Flow Chart for Second Order Drag Effects in the AOG



APG

The APG is on the integration grid of the semianalytical satellite theory. A flow chart for the APG is presented in Table F-3. The determination of the A and D matrices (see Chapter 3) was done by a double-sided finite-differencing technique. The integration subroutines are 'CSTEPX' and 'RKINTG.' Subroutine 'CSTEPX' is the predictor-corrector integrator of GTDS-RD. Subroutine 'RKINTG' is a Runge-Kutta integrator and was recently implemented into GTDS-RD by A. Bobick of CSDL. The initialization of the APG in the GTDS-RD subroutine 'RESINV' required the use of subroutine 'EPART.' Subroutine 'EPART' was recently implemented into GTDS-RD by R. Proulx of CSDL. Subroutine 'EPART' calculates the matrizant of the two-body problem. Subroutine 'EPART' is also used on the output grid to form the required partial derivatives as given by Equation (3-28). The implementation of the APG also required changes in the GTDS-RD subroutines 'ATMOS,' 'CSTEPX,' 'GVCVL,' 'INTOGR,' 'MULSTP,' 'OUTPAR,' 'RESINV' and 'SOLTAB.' Subroutine 'ATMOS' had to be changed in order to implement the Adaptive Modified Harris-Priester density model.

SPPG

The SPPG is on the output grid. Table F-4 shows the flow chart for the SPPG. A double-sided finite-differencing technique

Table F-3
Flow Chart for the APG

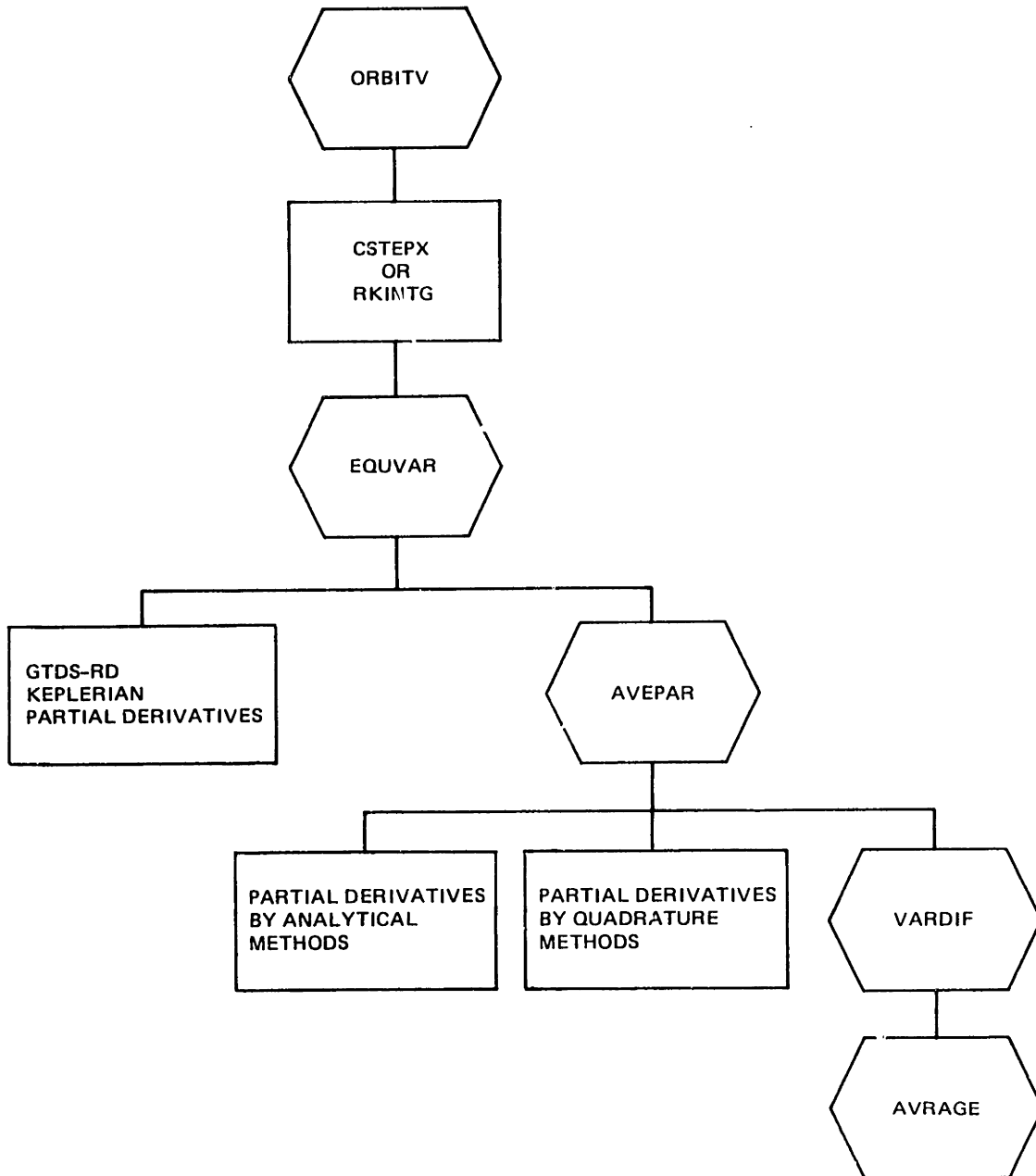
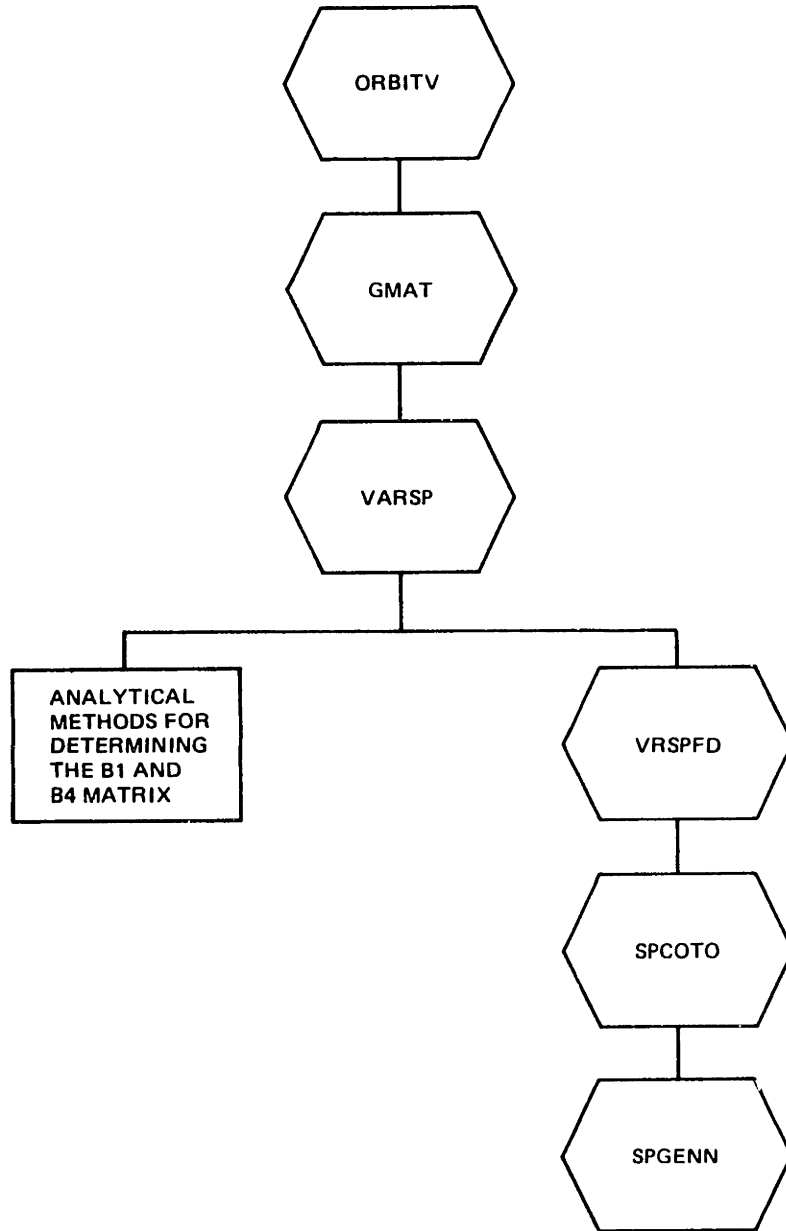


Table F-4
Flow Chart for the SPPG



was used to obtain the M_{σ} , N_{σ} , K_{σ} and L_{σ} matrices. The implementation of the SPPG also required changes in the GTDS-RD subroutine 'INTOGN.'

Semianalytical Batch Filter

The implementation of the semianalytical batch filter required interfacing the semianalytical orbit generator (including the generation of semianalytical partial derivatives) to the batch filter of GTDS-RD. The development of the semianalytical batch filter involved changes in the following GTDS-RD subroutines: 'GVCVL,' 'INTOGN,' 'PSET,' 'RESINV,' and 'SOLTAB.'

```

SUBROUTINE AVEPAR                                00000010
VERSION OF 20 JULY 1979 IMPLEMENTED AT CSDL ON AN AMDAHL 470 V6 00000020
PURPOSE                                           00000030
EXECUTIVE PROGRAM FOR THE DETERMINATION OF THE A AND D MATRIX 00000040
IN THE DIFFERENTIAL EQUATIONS FOR THE PERTURBED PARTIALS.    00000050
PARAMETERS                                         00000060
/ESTFLG/                                           00000070
                                                    00000080
IANAL      I   CONTROL SWITCH FOR ANALYTICAL APPROACH IN THE 00000090
AVERAGED PARTIAL GENERATOR.*                          00000100
IDIFF      I   CONTROL SWITCH FOR FINITE-DIFFERENCING APPROACH 00000110
IN THE AVERAGED PARTIAL GENERATOR.                    00000120
0=APPROACH NOT USED                                   00000130
1=A MATRIX ONLY                                       00000140
2=D MATRIX ONLY                                       00000150
3=BOTH A AND D MATRICES                               00000160
IQDRT     I   CONTROL SWITCH FOR QUADRATURE APPROACH IN THE 00000170
AVERAGED PARTIAL GENERATOR                             00000180
0=APPROACH NOT USED                                   00000190
1=A MATRIX ONLY                                       00000200
2=D MATRIX ONLY                                       00000210
3=BOTH A AND D MATRICES                               00000220
ICBVAR    I   CENTRAL GRAVITATIONAL BODY CONTROL SWITCH FOR 00000230
THE AVERAGED PARTIAL GENERATOR.                       00000240
0=NONE                                                00000250
1=ANALYTICALLY                                       00000260
2=FINITE-DIFFERENCING WITH THE AOG CENTRAL            00000270
BODY FIELD                                             00000280
3=FINITE-DIFFERENCING WITH A NX0 FIELD                00000290
J22VAR    I   J2 SQUARED CONTROL SWITCH IN THE AVERAGED    00000300
PARTIAL GENERATOR.                                    00000310
0=OFF                                                  00000320
1=FINITE-DIFFERENCING                                 00000330
ITBVAR    I   THIRD-BODY CONTROL SWITCH IN THE AVERAGED    00000340
PARTIAL GENERATOR.                                    00000350
0=OFF                                                  00000360
1=FINITE-DIFFERENCING WITH THE AOG THIRD-BODY        00000370
MODEL                                                  00000380
IDRVAR    I   DRAG CONTROL SWITCH IN THE AVERAGED PARTIAL 00000390
GENERATOR.                                             00000400
0=OFF                                                  00000410
1=FINITE-DIFFERENCING                                 00000420
2=QUADRATURE APPROACH                                 00000430
ISRVAR    I   SOLAR RADIATION PRESSURE CONTROL SWITCH IN THE 00000440
AVERAGED PARTIAL GENERATOR.                           00000450
0=OFF                                                  00000460
1=FINITE-DIFFERENCING                                 00000470
2=QUADRATURE APPROACH                                 00000480
NVAR      I   MAXIMUM DEGREE OF THE CENTRAL BODY GRAVITATIONAL 00000490
FIELD TO BE CONSIDERED IN THE AVERAGED PARTIAL      00000500
GENERATOR WHEN ICBVAR=3.                              00000510
LEVAR     I   MAXIMUM POWER OF E IN THE POWER SERIES EXPANSION 00000520

```

C			FOR THE ANALYTICAL HARMONIC POTENTIAL CONSIDERED	00000580
C			IN THE AVERAGED PARTIAL GENERATOR WHEN ICBVAR=3	00000590
C			(AT MOST CAN BE NVAR-2).	00000600
C	KDRFLG	I	CONTROL SWITCH FOR CONSIDERING 2ND ORDER DRAG	00000610
C			EFFECTS IN THE AVERAGED PARTIAL GENERATOR.	00000620
C			0=NO 2ND ORDER DRAG EFFECTS	00000630
C			1=J2-DRAG EFFECTS	00000640
C			2=J2-DRAG AND DRAG-DRAG EFFECTS	00000650
C			3=J2-DRAG, DRAG-J2 AND DRAG-DRAG EFFECTS	00000660
C			DONE NUMERICALLY	00000670
C			4=J2-DRAG AND DRAG-DRAG EFFECTS DONE	00000680
C			NUMERICALLY, DRAG-J2 DONE ANALYTICALLY	00000690
C			5=ISZAK'S J2 HEIGHT CORRECTION AND ANALYTIC	00000700
C			DRAG-J2 EFFECTS	00000710
C			6=ISZAK'S J2 HEIGHT CORRECTION ONLY	00000720
C				00000730
C	/FRC/			00000740
C				00000750
C	NMAX	0	MAXIMUM DEGREE OF THE CENTRAL BODY GRAVITATIONAL	00000760
C			FIELD.	00000770
C	MMAX	0	MAXIMUM ORDER OF THE CENTRAL BODY GRAVITATIONAL	00000780
C			FIELD.	00000790
C				00000800
C	/ANAVIN/			00000810
C				00000820
C	ITESS	0	LOW-ORDER CENTRAL BODY SPHERICAL HARMONIC	00000830
C			AVERAGING OPTION.	00000840
C			0 = NO LOW-ORDER SPHERICAL HARMONICS.	00000850
C			1 = TIME-DEPENDENT NUMERICAL AVERAGING.	00000860
C			2 = TIME-INDEPENDENT NUMERICAL AVERAGING.	00000870
C			3 = ANALYTICAL AVERAGING.	00000880
C	NEND	0	DEGREE OF ANALYTICALLY AVERAGED NONRESONANT	00000890
C			CENTRAL BODY SPHERICAL HARMONIC FIELD.	00000900
C	MEND	0	ORDER OF ANALYTICALLY AVERAGED NONRESONANT	00000910
C			CENTRAL BODY SPHERICAL HARMONIC FIELD.	00000920
C	LEND	0	MAXIMUM POWER OF E IN THE POWER SERIES	00000930
C			EXPANSION FOR THE ANALYTICALLY AVERAGED	00000940
C			NONRESONANT CENTRAL BODY SPHERICAL HARMONIC	00000950
C			POTENTIAL.	00000960
C	NCSRES	0	NUMBER OF ANALYTICALLY AVERAGED RESONANT	00000970
C			CENTRAL BODY SPHERICAL HARMONIC TERMS.	00000980
C	ITHIRD	0	THIRD-BODY AVERAGING OPTION.	00000990
C			POTENTIALS OF THE NONCENTRAL BODIES.	00001000
C	JTWSQ	0	SECOND-ORDER J2 PERTURBATION CONTRL SWITCH.	00001010
C	IDRAG	0	QUADRATURE ORDER CONTROL SWITCH FOR DRAG.	00001020
C	ISOLAR	0	QUADRATURE ORDER CONTROL SWITCH FOR SOLAR	00001030
C			RADIATION PRESSURE.	00001040
C	ICORR	0	CONTROL SWITCH FOR SOLAR RADIATION PRESSURE.*	00001050
C	IDRDR	0	CONTROL SWITCH FOR 2ND ORDER DRAG EFFECTS.	00001060
C				00001070
C	/VARMAT/			00001080
C				00001090
C	AMAT	I	THE A MATRIX.	00001100
C	DMAT	I	THE D MATRIX.	00001110
C				00001120
C	/WORKER/			00001130
C				00001140

```

C      PVOP      0      THE TOTAL A MATRIX.                00001150
C      VELPAR    0      THE TOTAL D MATRIX.                00001160
C      NQ        I      THE NUMBER OF VARIATIONAL EQUATIONS. 00001170
C      NOPARM    I      THE NUMBER OF ORBITAL ELEMENTS.     00001180
C
C      /SWITCH/
C
C      IRESON    0      CENTRAL BODY FIELD CONTROL SWITCH.  00001210
C                        2=NXM FIELD                        00001230
C                        4=NO CENTRAL BODY FIELD            00001240
C
C      REFERENCES
C      "ORBIT DETERMINATION AND PREDICTION PROCESSES FOR LOW 00001260
C      ALTITUDE SATELLITES." BY A.J. GREEN                 00001270
C
C      ANALYSIS
C      ANDREW J. GREEN, CPT, U.S. ARMY                      00001300
C
C      PROGRAMMER
C      ANDREW J. GREEN, CPT, U.S. ARMY                      00001340
C
C      IMPLICIT REAL*8(A-H,O-Z)
C      DIMENSION PVOP(6,6),VELPAR(6,20)
C
C      COMMON/ANAVIN/  ISTESS      ,ITESSE      ,ITRESE      ,ISTHIR      ,00001400
C      1                ITHRAR      ,ITHRE       ,ITESS       ,HEND        ,00001410
C      2                MEND        ,LEND       ,ITRES       ,NRES(10)    ,00001420
C      3                MRES(10)    ,JRES(10)   ,NCSRES      ,LENDRS      ,00001430
C      4                ITHIRD      ,NENDTH(8)  ,MENDTH(8)   ,JTWOSQ      ,00001440
C      5                IQUAD(4)    ,NGUAD(4)   ,JPCS        ,JA          ,00001450
C      6                JB          ,JC         ,JGHA        ,KPOS        ,00001460
C      7                KA          ,KB         ,KC          ,KGHA        ,00001470
C      8                ICORR       ,IFOS       ,IMOON       ,IMEAN       ,00001480
C      9                IGHA        ,ISTRES     ,ITERM       ,ISHAD       ,00001490
C      1               JTMDEP      ,JTMIND     ,JDRAG       ,JSOLAR      ,00001500
C      2               J2SQSP      ,JSFCGB     ,JSPTHR      ,JSPFOS      ,00001510
C      3               JSFA        ,JSFB       ,JSPC        ,JSPGHA      ,00001520
C      4               KSPPOS      ,KSPA       ,KSFB        ,KSPC        ,00001530
C      5               KSPGHA      ,KSPNC(4)   ,KSPPRT(4)  ,NMIXSP      ,00001540
C      6               NMIXSP      ,IDRDR      ,NCHOJ2      ,NCHODR      ,00001550
C
C      COMMON/FRC /  RFRC(1300) ,IFRC(50)
C      EQUIVALENCE (NMAX ,IFRC(3) )
C      1            (NMAX ,IFRC(4) )
C
C      COMMON/WORKER/ DWRK(3264),INWRK(13)
C      EQUIVALENCE (DWRK(2227) ,PVOP(1,1) )
C      1            (DWRK(2263) ,VELPAR(1,1) )
C      2            (INWRK(3) ,NOPARM )
C      3            (INWRK(5) ,NEQ )
C
C      COMMON/ESTFLG/ IANAL      ,IDIFF      ,IQDRT      ,ICBVAR      ,J22VAR      , 00001670
C      1            ITBVAR      ,IDRVAR      ,ISRVAR      ,NVAR        ,LEVAR       , 00001680
C      2            KCRFLG      ,KFAR        ,KSTEF(20) ,KVRFLG      ,KCPSP      , 00001690
C      3            KCSFP      ,KTESFP      ,KDRSFP      ,KRSFP       ,NVARSP     , 00001700
C      4            IVSFC(4) ,KATHOS      ,KPRTB1      ,KPRTB2      ,KPRTB3     , 00001710

```

AVEPAR

AJG1324.GTDS.UPDATE.FORT

```

      5          KPRTB4
C
      COMMON/SWITCH/ IND(225)
      EQUIVALENCE      ( IRESON                      ,IND(38)
C
      COMMON/VARMAT/ AMAT(6,6),DMAT(6,14),BIMAT(6,6),B4MAT(6,14)
C
      INITIALIZE AND SAVE THE VARIOUS SWITCHES.
C
      N=NOPARM+1
      DO 30 I=1,6
      DO 10 J=1,6
      PVOP(I,J)=0.DO
10  CONTINUE
      DO 20 L=1,NEQ
      VELPAR(I,L)=0.DO
20  CONTINUE
30  CONTINUE
C
      KNMAX=NMAX
      KMMAX=MMAX
      KNEND=MEND
      KMEND=MEND
      KLEND=LEND
      KTHIRD=ITHIRD
      KJ2SQ=JTHOSQ
      KDRAG=IDRAG
      KORDR=IDRDR
      KCORR=ICORR
      KSOLAR=ISOLAR
      KTESS=ITESS
      KNCRES=NCSRES
      KRES=IRESON
C
      DETERMINATION OF THE A MATRIX ANALYTICALLY.
C
      IF(IANAL.EQ.1) GO TO 100
      CALL VARANL
C
      ACCUMULATE THE A MATRIX.
C
      DO 50 I=1,6
      DO 40 J=1,6
      PVOP(I,J)=AMAT(I,J)
40  CONTINUE
50  CONTINUE
C
      DETERMINATION OF THE A AND/OR D MATRIX BY FINITE-DIFFERENCING.
C
100 IF(IDIFF.EQ.0) GO TO 200
C
      CENTRAL BODY GRAVITATIONAL EFFECTS.
C
      IF(ICBVAR.LE.1) GO TO 110
      IF(ICBVAR.EQ.2) GO TO 120
      NMAX=NVAR
      MMAX=0

```

```

00001720
00001730
00001740
) 00001750
00001760
00001770
00001780
00001790
00001800
00001810
00001820
00001830
00001840
00001850
00001860
00001870
00001880
00001890
00001900
00001910
00001920
00001930
00001940
00001950
00001960
00001970
00001980
00001990
00002000
00002010
00002020
00002030
00002040
00002050
00002060
00002070
00002080
00002090
00002100
00002110
00002120
00002130
00002140
00002150
00002160
00002170
00002180
00002190
00002200
00002210
00002220
00002230
00002240
00002250
00002260
00002270
00002280

```

	IRESON=2	00002290
	NEND=NVAR	00002300
	MEND=0	00002310
	NCSRES=0	00002320
	LEND=LEVAR	00002330
	IF(NVAR.GE.2)GO TO 120	00002340
110	NMAX=0	00002350
	MMAX=0	00002360
	IRESON=4	00002370
	ITESS=0	00002380
	NCSRES=0	00002390
C		00002400
C	J2 SQUARED EFFECTS.	00002410
C		00002420
120	IF(J22VAR.EQ.1) GO TO 130	00002430
	JTWOSQ=2	00002440
C		00002450
C	THIRD-BODY EFFECTS.	00002460
C		00002470
130	IF(ITBVAR.EQ.1) GO TO 140	00002480
	ITHIRD=0	00002490
C		00002500
C	DRAG EFFECTS.	00002510
C		00002520
140	IF(IDRVAR.EQ.1) GO TO 145	00002530
	IDRAG=0	00002540
	GO TO 150	00002550
145	IDRDR=KDRFLG	00002560
	ICCR=2	00002570
	IF(IDRDR.LT.5)GO TO 150	00002580
	ICCR=1	00002590
	IF(IDRDR.EQ.6) IDRDR=0	00002600
C		00002610
C	SOLAR RADIATION PRESSURE EFFECTS.	00002620
C		00002630
150	IF(ISRVAR.EQ.1) GO TO 160	00002640
	ISOLAR=0	00002650
C		00002660
C	COMPUTE THE MATRICES.	00002670
C		00002680
160	CALL VARDIF	00002690
C		00002700
C	ACCUMULATE THE A AND D MATRICES.	00002710
C		00002720
	DO 190 I=1,6	00002730
	DO 170 J=1,6	00002740
	PVOP(I,J)=PVOP(I,J)+AMAT(I,J)	00002750
170	CONTINUE	00002760
	DO 180 L=N,NEQ	00002770
	II=L-NOPARM	00002780
	VELPAR(I,L)=DMAT(I,II)	00002790
180	CONTINUE	00002800
190	CONTINUE	00002810
C		00002820
C	DETERMINATION OF THE A AND/OR D MATRIX BY A QUADRATURE APPROACH.	00002830
C		00002840
200	IF(IQDRT.EQ.0) GO TO 300	00002850

11

AVEPAR

AJG1324.GTDS.UPDATE.FORT

C		00002860
C	ONLY DRAG AND SOLAR RADIATION PRESSURE ARE DONE.	00002870
C		00002880
	NMAX=0	00002890
	MMAX=0	00002900
	IRESON=4	00002910
	ITESS=0	00002920
	NCSRES=0	00002930
	ITHIRD=0	00002940
	JTWOSQ=2	00002950
C		00002960
C	DRAG EFFECTS.	00002970
C		00002980
	IF(IDRVAR.EQ.2) GO TO 210	00002990
	IDRAG=0	00003000
	GO TO 220	00003010
210	IDRAG=KDRAG	00003020
	IDRDR=KDRFLG	00003030
	ICORR=2	00003040
	IF(IDRDR.LT.5)GO TO 220	00003050
	ICORR=1	00003060
	IF(IDRDR.EQ.6) IDRDR=0	00003070
C		00003080
C	SOLAR RADIATION PRESSURE EFFECTS.	00003090
C		00003100
220	IF(ISRVAR.EQ.2) GO TO 230	00003110
	ISOLAR=0	00003120
	GO TO 240	00003130
230	ISOLAR=KSOLAR	00003140
C		00003150
C	COMPUTE THE MATRICES.	00003160
C		00003170
240	CALL VARQDR	00003180
C		00003190
C	ACCUMULATE THE A AND D MATRICES.	00003200
C		00003210
	DO 270 I=1,6	00003220
	DO 250 J=1,6	00003230
	PVOP(I,J)=PVOP(I,J)+AMAT(I,J)	00003240
250	CONTINUE	00003250
	DO 260 L=N,NEQ	00003260
	II=L-NOPARM	00003270
	VELPAR(I,L)=VELPAR(I,L)+DMAT(I,II)	00003280
260	CONTINUE	00003290
270	CONTINUE	00003300
C		00003310
C	RESTORE THE FLAGS.	00003320
C		00003330
300	NMAX=KNMAX	00003340
	MMAX=KMMAX	00003350
	NEND=KNEND	00003360
	MEND=KMEND	00003370
	LEND=KLEND	00003380
	ITHIRD=KTHIRD	00003390
	JTWOSQ=KJ2SQ	00003400
	IDRAG=KDRAG	00003410
	IDRDR=KDRDR	00003420

11

AVEPAR

AJG1324.GTDS.UPDATE.FORT

ICORR=KCORR
ISOLAR=KSOLAR
ITESS=KTESS
NCSRES=KNCREC
IPESON=KRES

C

RETURN
END

00003430
00003440
00003450
00003460
00003470
00003480
00003490
00003500

***** END OF MEMBER AVEPAR 350 RECORDS *****

AVRAGE

AJG1324.GTDS.UPDATE.FORT

```
C          SUBROUTINE AVRAGE                                00000010
C          VERSION OF 19 MARCH 1979 IMPLEMENTED AT CSDL ON AMDAHL 470 V6 00000020
C          PURPOSE                                          00000030
C          TO CONTROL THE EVALUATION OF THE AVERAGED ELEMENT RATES FOR 00000040
C          THE AVERAGED VOP ORBIT GENERATOR                00000050
C          CALLING SEQUENCE                                  00000060
C          CALL AVRAGE                                     00000070
C          INPUT                                             00000080
C          VIA BLOCK COMMON                                 00000090
C          VARIABLES IN COMMON CONST                       00000100
C          PI      = THE CONSTANT PI                       00000110
C          TWOPI   = TWO TIMES PI                         00000120
C          VARIABLES IN COMMON FRC                        00000130
C          NB      = NUMBER OF CENTRAL AND NON-CENTRAL BODIES 00000140
C          GM      = ARRAY OF GRAVITATIONAL CONSTANTS     00000150
C          ICENT   = CENTRAL BODY INDICATOR              00000160
C          VARIABLES IN COMMON SWITCH                    00000170
C          IND     = ARRAY OF INTEGRATION SWITCHES       00000180
C          VARIABLES IN COMMON WORKER                     00000190
C          VPCLMT  = ORBITAL ELEMENT VECTOR              00000200
C          K       = DERIVATIVE ARRAY INDICATOR OF VALUE AT T=T(K) 00000210
C          NOPARM  = NUMBER OF ORBITAL ELEMENTS          00000220
C          T       = TIME FROM EPOCH IN SECONDS          00000230
C          VARIABLES IN COMMON ANAVIN                    00000240
C          JTWOSQ  = CONTROL SWITCH FOR 2ND ORDER J2 PERTURBATION 00000250
C          ITMDEP  = CONTROL SWITCH FOR NUMERICAL TIME-DEPENDENT 00000260
C                   AVERAGING                            00000270
C          ITMIND  = CONTROL SWITCH FOR NUMERICAL TIME-INDEPENDENT 00000280
C                   AVERAGING                            00000290
C          IDRAG   = CONTROL SWITCH FOR DRAG              00000300
C          ISOLAR  = CONTROL SWITCH FOR SOLAR RADIATION PRESSURE 00000310
C          ITSS    = CONTROL SWITCH FOR LOW-ORDER CENTRAL BODY 00000320
C                   SPHERICAL HARMONIC AVERAGING        00000330
C          ITRES   = CONTROL SWITCH FOR HIGH-ORDER CENTRAL BODY 00000340
C                   SPHERICAL HARMONIC AVERAGING        00000350
C          IORDR   = CONTROL SWITCH FOR 2ND ORDER DRAG EFFECTS 00000360
C          OUTPUT                                          00000370
C          VARIABLES IN COMMON SWITCH                    00000380
C          NBOPT   = ARRAY OF CENTRAL AND NON-CENTRAL BODY INDICATORS 00000390
C          IQUAD   = ARRAY OF QUADRATURE CONTROL SWITCHES 00000400
```

AVRAGE

AJG1324.GTDS.UPDATE.FORT

```

C
C
C      VARIABLES IN COMMON WORKER
C
C      DPARRY = ARRAY OF ELEMENT DERIVATIVES
C      XMEAN  = MEAN MOTION
C      XMEANO = XMEAN AT TZERO
C      TZERO  = TIME OF THE DERIVATIVE EVALUATION
C      SELEMS = VPCLMT AT TZERO
C      XLAMDA = VALUE OF THE MEAN LONGITUDE AT TIME TZERO
C      NPERTB = PERTURBATION INDICATOR
C              = 0 FOR CONTINUOUS PERTURBATIONS
C              = 1 FOR DRAG ONLY
C              = 2 FOR SOLAR RADIATION PRESSURE ONLY
C      NTIME  = COUNTER FOR QUADRATURE INTEGRANDS
C      AVRATE = VECTOR OF INTEGRALS EVALUATED IN VOQUAD
C
C      EXTERNAL REFERENCES
C
C      VOQUAD
C      LIMITE
C
C      REFERENCE
C
C      GTDS SUBROUTINE DESCRIPTION AVRAGE
C
C      METHOD
C      METHOD IS OUTLINED IN REFERENCE
C
C      ANALYSIS
C      ANNE C. LONG, COMPUTER SCIENCES CORPORATION
C
C      PROGRAMMER
C      ANNE C. LONG, COMPUTER SCIENCES CORPORATION
C
C      MODIFICATIONS
C      06/15/74 BY R.PAJERSKI- ADDED NEW ELEMENT SET(KEPLERIAN)
C      01/01/75 BY J. M. MEYER TO MODULARIZE THE AVERAGING PROGRAM
C      1/1/78 BY LEO W. EARLY JR. TO MODULARIZE AVERAGING, ELIM-
C      INATE ERRORS, AND PUT CODE IN STRUCTURED FORM.
C      19/3/79 BY ANDREW J. GREEN, CPT, U.S. ARMY, CSDL, INCLUDED
C      2ND-ORDER DRAG EFFECTS
C      7/30/79 BY A. BOBICK, CSDL, TO COUNT FORCE EVALUATIONS
C
C*****START PROGRAM*****
C
C      IMPLICIT REAL*8(A-H,O-Z)
C      DIMENSION DPARRY(15,10) ,VPCLMT(10) ,AVRATE(10) ,
C      2          GM(11) ,POSVEL(6,8),DUMMY(3)
C      DIMENSION IBODY(9) ,IBODYS(3)
C
C      COMMON/ANAVIN/ ISTESS ,ITESSE ,ITRESE ,ISTHIR ,
C      1              ITHRAR ,ITHRE ,ITESS ,NEND ,
C      2              MEND ,LEND ,ITRES ,NRES(10) ,
C      3              NRES(10) ,JRES(10) ,NCSRES ,LENDRS ,
C      4              ITHIRD ,MENDTH(8) ,MENDTH(8) ,JTWOSQ ,
C      5              IQUAD(4) ,NQUAD(4) ,JPOS ,JA

```

11

AVRAGE

AJG1324.GTDS.UPDATE.FORT

6	JB	,JC	,JGHA	,KPOS	,00001140
7	KA	,KB	,KC	,KGHA	,00001150
8	ICORR	,IFOS	,IMOON	,IMEAN	,00001160
9	IGHA	,ISTRES	,ITERM	,ISHAD	,00001170
1	JTMDEP	,JTMIND	,JDRAG	,JSOLAR	,00001180
2	J2SQSP	,JSFCGB	,JSPTHR	,JSPPOS	,00001190
3	JSPA	,JSFB	,JSFC	,JSFGHA	,00001200
4	KSPPOS	,KSPA	,KSFB	,KSFC	,00001210
5	KSPGHA	,KSFNC(4)	,KSPPRT(4)	,NMAXSP	,00001220
6	MMAXSP	,IDRRD	,HCHOJ2	,NCHCDR	00001230
	EQUIVALENCE	(ITHDEP	,IQUAD(1)		,00001240
2		(ITHIND	,IQUAD(2)		,00001250
3		(IDRAG	,IQUAD(3)		,00001260
4		(ISOLAR	,IQUAD(4)) 00001270
C					00001280
	COMMON/CONST /	RCONST(51)			00001290
	EQUIVALENCE	(THOPI	,RCONST(1)) 00001300
C					00001310
	COMMON/FRC /	RFRC(1300) ,IFRC(50)			00001320
	EQUIVALENCE	(GM(1)	,RFRC(2)		,00001330
2		(POSVEL(1,1)	,RFRC(101)		,00001340
3		(NSODY	,IFRC(7)		,00001350
4		(ISUN	,IFRC(14)) 00001360
C					00001370
	COMMON/SWITCH/	ISWIT(225)			00001380
	EQUIVALENCE	(IVOP	,ISWIT(3)		,00001390
2		(ITHOBD	,ISWIT(6)		,00001400
3		(IPRESCH	,ISWIT(39)		,00001410
4		(IBODY(1)	,ISWIT(201)		,00001420
5		(ICENT	,IBODY(1)) 00001430
C					00001440
	COMMON/TIMER/	TIM(51), NOFC			00001443
C					00001446
	COMMON/WORKER/	RWORK(3264) ,IWORK(13)			00001450
	EQUIVALENCE	(DPARRY(1,1)	,RWORK(7)		,00001460
2		(VPFELMT(1)	,RWORK(2829)		,00001470
3		(AVRATE(1)	,RWORK(3068)		,00001480
4		(XLANDA	,RWORK(2851)		,00001490
5		(XMEAN	,RWORK(2814)		,00001500
6		(T	,RWORK(3215)		,00001510
7		(TZERO	,RWORK(2850)) 00001520
	EQUIVALENCE	(K	,IWORK(2)		,00001530
2		(NOPARM	,IWORK(3)		,00001540
3		(NFERT	,IWORK(9)) 00001550
C					00001560
C		***** START PROGRAM *****			00001561
C					00001562
C		*** INCREMENT NUMBER OF FORCE EVALUATIONS			00001563
C					00001564
	NOFC = NOFC + 1				00001565
C					00001566
	SAVE THE TIME AND FAST VARIABLE.				00001570
C					00001580
	TZERO = T				00001590
C		XLANDA = VPFELMT(NOPARM)			00001600
C					00001610
C		INITIALIZE THE AVERAGED ELEMENT RATES.			00001620

11

AVRAGE

AJG1324.GTDS.UPDATE.FORT

```
C
  DO 100 I=1,NOPARM                                00001630
    DPARRY(K,I) = 0.DO                              00001640
  100 CONTINUE                                     00001650
C                                                  00001660
C COMPUTE THE MEAN MOTION AND TEST FOR TWO-BODY MOTION AND KEPLERIAN AVERAGING. 00001670
C AVERAGING.                                     00001680
C                                                  00001690
C XMEAN = DSQRT(GM(ICENT)/(VPELMT(1)*VPELMT(1)*VPELMT(1))) 00001700
C IF (ITNOBD.EQ.1) GO TO 600                       00001710
C IF (IVOP.NE.12) GO TO 200                        00001720
C                                                  00001730
C COMPUTE AUXILIARY QUANTITIES.                   00001740
C                                                  00001750
C CALL AUXPAR(VPELMT)                             00001760
C                                                  00001770
C COMPUTE THE ELEMENT RATES FOR ANALYTICALLY AVERAGED PERTURBATIONS. 00001780
C                                                  00001790
C CALL ANAVR                                       00001800
C                                                  00001810
C ACCUMULATE THE ELEMENT RATES.                  00001820
C                                                  00001830
C DO 110 I=1,NOPARM                                00001840
  DPARRY(K,I) = AVRATE(I)                          00001850
  110 CONTINUE                                     00001860
C                                                  00001870
C COMPUTE THE ELEMENT RATES DUE TO THE J2 SQUARED 00001880
C PERTURBATION.                                   00001890
C                                                  00001900
C IF (JTWOSQ.NE.1) GO TO 200                      00001910
C CALL J2SQR(AVRATE)                              00001920
C                                                  00001930
C ACCUMULATE THE ELEMENT RATES.                  00001940
C                                                  00001950
C DO 120 I=1,NOPARM                                00001960
  DPARRY(K,I) = DPARRY(K,I) + AVRATE(I)           00001970
  120 CONTINUE                                     00001980
C                                                  00001990
C COMPUTE THE ELEMENT RATES DUE TO NUMERICALLY AVERAGED 00002000
C TIME-DEPENDENT CONTINUOUS PERTURBATIONS.       00002010
C                                                  00002020
C 200 IF (ITMDEP.EQ.0) GO TO 300                  00002030
C                                                  00002040
C SET THE CENTRAL BODY SPHERICAL HARMONIC SWITCH. 00002050
C                                                  00002060
C IRESNS = IRESON                                 00002070
C                                                  00002080
C IF (ITESS.NE.1) GO TO 202                       00002090
C IF (ITRES.NE.1) GO TO 201                       00002100
C IF (IRESON.NE.1) GO TO 201                     00002110
C IRESON = 1                                       00002120
C GO TO 210                                         00002130
C 201 IRESON = 2                                    00002140
C GO TO 210                                         00002150
C                                                  00002160
C 202 IF (ITRES.NE.1) GO TO 203                   00002170
C IF (IRESON.NE.1) GO TO 203                     00002180
C                                                  00002190
```

AVRAGE

AJG1324.GTDS.UPDATE.FORT

```

      IRESON = 3                                00002200
      GO TO 210                                00002210
203   IRESON = 4                                00002220
C                                           00002230
C           COMPUTE THE LIMITS AND VALUE OF THE AVERAGING
C           INTEGRAL.                          00002240
C                                           00002250
C                                           00002260
210   NPERT = 1                                00002270
      CALL LIMITS(FLOW,FHIGH,XLAMDA)           00002280
      CALL VOQUAD(FLOW,FHIGH)                  00002290
C                                           00002300
C           ACCUMULATE THE ELEMENT RATES.      00002310
C                                           00002320
      DO 220 I=1,NOPARM                         00002330
      DPARRY(K,I) = DPARRY(K,I) + AVRATE(I)/TWOPI 00002340
220   CONTINUE                                 00002350
C                                           00002360
C           RESTORE THE CENTRAL BODY HIGH-ORDER RESONANCE SWITCH.00002370
C                                           00002380
      IRESON = IRESNS                          00002390
C                                           00002400
C           RESTORE THE TIME.                  00002410
C                                           00002420
      T = TZERO                                 00002430
C                                           00002440
C           COMPUTE THE ELEMENT RATES DUE TO NUMERICALLY AVERAGED00002450
C           TIME-INDEPENDENT CONTINUOUS PERTURBATIONS. 00002460
C                                           00002470
300   IF (ITMIND.EQ.0) GO TO 400                00002480
C                                           00002490
C           SET THE CENTRAL BODY SPHERICAL HARMONIC SWITCH. 00002500
C                                           00002510
      IRESNS = IRESON                          00002520
C                                           00002530
      IF (ITESS.NE.2) GO TO 301                00002540
      IRESON = 2                                00002550
      GO TO 310                                00002560
301   IRESON = 4                                00002570
C                                           00002580
C           COMPUTE THE POSITIONS OF THE PERTURBING BODIES. 00002590
C                                           00002600
310   CALL EVAL(TZERO,KPOS,KA,KB,KC,KGHA,IBODY,POSVEL) 00002610
C                                           00002620
C           COMPUTE THE LIMITS AND VALUE OF THE AVERAGING
C           INTEGRAL.                          00002630
C                                           00002640
C                                           00002650
      NPERT = 2                                00002660
      IF (ITMDEP.EQ.0) CALL LIMITS(FLOW,FHIGH,XLAMDA) 00002670
      CALL VOQUAD(FLOW,FHIGH)                  00002680
C                                           00002690
C           ACCUMULATE THE ELEMENT RATES.      00002700
C                                           00002710
      DO 320 I=1,NOPARM                         00002720
      DPARRY(K,I) = DPARRY(K,I) + AVRATE(I)/TWOPI 00002730
320   CONTINUE                                 00002740
C                                           00002750
C           RESTORE THE CENTRAL BODY HIGH-ORDER RESONANCE SWITCH.00002760

```

AVRAGE

AJG1324.GTDS.UPDATE.FORT

```
C IRESON = IRESNS 00002770
C 00002780
C COMPUTE THE ELEMENT RATES DUE TO DRAG. 00002790
C 00002800
C 400 IF (IDRAG.EQ.0) GO TO 500 00002810
C 00002820
C COMPUTE THE HIGHER ORDER DRAG EFFECTS 00002830
C 00002840
C 00002850
C IF (IDRDR.EQ.0) GO TO 410 00002860
C CALL HODRAG 00002870
C IF(IDRDR.NE.5)GO TO 500 00002880
C 00002890
C COMPUTE FIRST-ORDER EFFECTS IF NECESSARY. 00002900
C 00002910
C COMPUTE THE LIMITS OF THE AVERAGING INTEGRAL. 00002920
C 00002930
C 410 NPERT = 3 00002940
C CALL LIMITS(FLOW,FHIGH,XLANDA) 00002950
C IF (NPERT.EQ.0) GO TO 500 00002960
C 00002970
C FIND THE POSITION OF THE SUN SO THAT THE DIURNAL 00002980
C BULGE IN THE ATMOSPHERE CAN BE LOCATED. 00002990
C 00003000
C IBDYDYS(2) = IBDYDYS(2) 00003010
C IBDYDYS(3) = IBDYDYS(3) 00003020
C NBDYDYS = NBDYDYS 00003030
C 00003040
C IBDYDYS(2) = 3 00003050
C IBDYDYS(3) = 0 00003060
C NBDYDYS = 2 00003070
C 00003080
C CALL EVAL(TZERO,1,2,2,2,2,IBDYDYS,POSVEL) 00003090
C 00003100
C COMPUTE THE VALUE OF THE AVERAGING INTEGRAL. 00003110
C 00003120
C CALL VOQUAD(FLOW,FHIGH) 00003130
C 00003140
C ACCUMULATE THE ELEMENT RATES. 00003150
C 00003160
C DO 420 I=1,NOPARM 00003170
C DPARRY(K,I) = DPARRY(K,I) + AVRATE(I)/TWOPI 00003180
C 420 CONTINUE 00003190
C 00003200
C RESTORE THE THIRD BODIES. 00003210
C 00003220
C 440 IF (ISOLAR.NE.0) GO TO 510 00003230
C IBDYDYS(2) = IBDYDYS(2) 00003240
C IBDYDYS(3) = IBDYDYS(3) 00003250
C NBDYDYS = NBDYDYS 00003260
C GO TO 600 00003270
C 00003280
C COMPUTE THE ELEMENT RATES DUE TO SOLAR RADIATION 00003290
C PRESSURE. 00003300
C 00003310
C 500 IF (ISOLAR.EQ.0) GO TO 600 00003320
C 00003330
```

AVRAGE

AJG1324.GTOS.UPDATE.FORT

```
C          FIND AND STORE THE POSITION OF THE SUN.          00003340
C
C          IBOBYS(2) = IBODY(2)          00003350
C          IBOBYS(3) = IBODY(3)          00003360
C          NBOBYS = NBOBY                00003370
C
C          IBODY(2) = 3                    00003380
C          IBODY(3) = 0                    00003390
C          NBOBY = 2                      00003400
C
C          CALL EVAL(TZERO,1,2,2,2,2,IBODY,POSVEL)          00003410
C
C          510 ISUNS = ISUN                00003420
C          ISUN = - 1                      00003430
C          CALL PMASS(IBODY,DUMMY,DUMMY,IERR)                00003440
C          ISUN = 1                          00003450
C
C          COMPUTE THE LIMITS AND VALUE OF THE AVERAGING    00003460
C          INTEGRAL.                                         00003470
C
C          NPERT = 4                                         00003480
C          CALL LIMITS(FLOW,FHIGH,XLAMDA)                    00003490
C          CALL VOQUAD(FLOW,FHIGH)                          00003500
C
C          ACCUMULATE THE ELEMENT RATES.                    00003510
C
C          DO 520 I=1,NOPARM                                00003520
C             DPARRY(K,I) = DPARRY(K,I) + AVRATE(I)/TWOPI  00003530
C          520 CONTINUE                                     00003540
C
C          RESTORE THE THIRD BODIES.                        00003550
C
C          IBODY(2) = IBOBYS(2)                          00003560
C          IBODY(3) = IBOBYS(3)                          00003570
C          NBOBY = NBOBYS                                 00003580
C          ISUN = ISUNS                                   00003590
C
C          RESTORE THE FAST VARIABLE AND ACCUMULATE THE TWO- 00003600
C          BODY ELEMENT RATES.                              00003610
C
C          600 VPELMT(NOPARM) = XLAMDA                    00003620
C          DPARRY(K,NOPARM) = DPARRY(K,NOPARM) + XMEAN    00003630
C          RETURN                                           00003640
C
C          END                                             00003650
C
C          END                                             00003660
C
C          END                                             00003670
C
C          END                                             00003680
C
C          END                                             00003690
C
C          END                                             00003700
C
C          END                                             00003710
C
C          END                                             00003720
C
C          END                                             00003730
C
C          END                                             00003740
C
C          END                                             00003750
C
C          END                                             00003760
C
C          END                                             00003770
C
C          END                                             00003780
```

***** END OF MEMBER AVRAGE 367 RECORDS *****


```

SUBROUTINE DRAGJ2                                00000010
C                                                    00000020
C VERSION OF 11 MAY 1979 IMPLEMENTED AT CSDL ON ANDAHL 470 V6 00000030
C                                                    00000040
C PURPOSE                                           00000050
C ANALYTICALLY DETERMINE THE DRAG-J2 COUPLING EFFECT, GOOD TO 00000060
C ZERO ORDER IN THE ECCENTRICITY AND FOR DIRECT ORBITS ONLY. 00000070
C                                                    00000080
C PARAMETERS                                         00000090
C /WORKER/                                           00000100
C                                                    00000110
C A      I  MEAN A                                   00000120
C XH     I  MEAN H                                   00000130
C XK     I  MEAN K                                   00000140
C P      I  MEAN P                                   00000150
C Q      I  MEAN Q                                   00000160
C XL     I  MEAN LAMDA                               00000170
C XN     I  MEAN MEAN MOTION                         00000180
C AVRATE I  ARRAY OF THE MEAN ELEMENT RATES          00000190
C                                                    00000200
C /TRC/                                             00000210
C                                                    00000220
C AB     I  ARRAY OF EQUATORIAL RADIUS FOR THE VARIOUS BODIES 00000230
C GM     I  ARRAY OF THE GRAVITATIONAL CONSTANTS(I.E. MU) 00000240
C CS     I  ARRAY OF THE SPHERICAL HARMONIC COEFFICIENTS 00000250
C                                                    00000260
C REFERENCES                                         00000270
C                                                    00000280
C "ORBIT DETERMINATION AND PREDICTION PROCESSES FOR LOW ALTITUDE 00000290
C SATELLITES." BY ANDREW J. GREEN                   0000300
C                                                    00000310
C ANALYSIS                                           00000320
C ANDREW J. GREEN, CPT, U.S. ARMY, CSDL             00000330
C                                                    00000340
C PROGRAMMER                                         00000350
C ANDREW J. GREEN, CPT, U.S. ARMY, CSDL             00000360
C                                                    00000370
C *****START PROGRAM*****                       00000380
C                                                    00000390
C IMPLICIT REAL*8(A-H,O-Z)                           00000400
C DIMENSION CS(504),AVRATE(10) ,GM(11),AB(11)       00000410
C DIMENSION IBODY(9)                                 00000420
C                                                    00000430
C COMMON/FRC / RFRC(1300) ,IFRC(50)                 00000440
C EQUIVALENCE (GM(1) ,RFRC(2) ) ,00000450
C 1 (AB(1) ,RFRC(24) ) ,00000460
C 2 (CS(1) ,RFRC(355) ) 00000470
C                                                    00000480
C COMMON/SWITCH/ ISWIT(225)                          00000490
C EQUIVALENCE (IBODY(1) ,ISWIT(201) ) ,00000500
C 1 (ICENT ,IEODY(1) ) 00000510
C                                                    00000520
C COMMON/WORKER/ RWORK(3264) ,IWORK(13)             00000530
C EQUIVALENCE (A ,RWORK(2829) ) ,00000540
C 2 (XH ,P:CRK(2830) ) ,00000550

```

DRAGJ2

AJG1324.GTDS.UPDATE.FORT

```

3          (XK          ,RWORK(2831)          ),00000580
4          (P          ,RWORK(2832)          ),00000590
5          (Q          ,RWORK(2833)          ),00000600
6          (XL          ,RWORK(2834)          ),00000610
7          (AVRATE(1)  ,RWORK(3068)         ),00000620
8          (XLAMDA     ,RWORK(2851)         ),00000630
9          (XN          ,RWORK(2814)         ) 00000640
COMMON/SPCOEF/ CX(10,10),DX(10,10) 00000650
C          00000660
C          SET THE COMMON FACTORS. 00000670
C          00000680
P2=P*P      00000690
Q2=Q*Q      00000700
C=P2+Q2     00000710
C2=C*C      00000720
A4=A*A*A*A  00000730
CP1=C+1     00000740
CP12=CP1*CP1 00000750
RE=AB(ICENT) 00000760
FACT42=(-CS(2)*GM(ICENT)*RE*RE)/(A4*CP12*XN) 00000770
FACT43=FACT42/CP1 00000780
FACT52=FACT42/A 00000790
FACT53=FACT52/CP1 00000800
FACT62=FACT52/A 00000810
FACT51=FACT52*CP1 00000820
FACT61=FACT62*CP1 00000830
C          00000840
C          DETERMINE A-DOT. 00000850
C          00000860
ADOT42=FACT42*P*Q*(-24.D0*CX(6,2)-63.D0*DX(3,3)+3.D0*DX(3,1)+
*63.D0*CX(2,3)+3.D0*CX(2,1))+ 00000870
*FACT42*(-3.D0*CX(3,1)*(2.D0*P2+C2-5.D0*C+1.D0)/2.D0+ 00000880
*3.D0*DX(2,1)*(2.D0*P2-C2+3.D0*C-1.D0)/2.D0)+ 00000890
*FACT42*(2.D0*P2-C)*( -12.D0*DX(6,2)+63.D0*CX(3,3)/2.D0+ 00000900
*63.D0*DX(2,3)/2.D0) 00000910
ADOT43=FACT43*(12.D0*DX(5,2)*P*(4.D0*Q2-C-1.D0)- 00000920
*12.D0*CX(5,2)*Q*(4.D0*P2-C+1.D0)+12.D0*DX(4,2)*Q*(4.D0*P2-C- 00000930
*1.D0)-12.D0*CX(4,2)*P*(4.D0*P2-3.D0*C-1.D0)) 00000940
ADOT52=FACT52*(30.D0*DX(1,2)*P*Q-15.D0*CX(1,2)*(2.D0*P2-C)) 00000950
C          00000960
C          00000970
AVRATE(1)=ADOT42+ADOT43+ADOT52 00000980
C          00000990
C          DETERMINE H-DOT 00001000
C          00001010
DOTH52=FACT52*P*Q*(-63.D0*DX(6,3)/2.D0+3.D0*DX(6,1)/2.D0+ 00001020
*51.D0*CX(3,4)+51.D0*DX(2,4)+3.D0*DX(2,2)-3.D0*CX(3,2)*(C+4.D0))- 00001030
*FACT52*(3.D0*DX(3,2)*(4.D0*(C+4.D0)*P2+C2-20.D0*C+3.D0)+ 00001040
*3.D0*CX(2,2)*(4.D0*P2-(C-3.D0)*(3.D0*C-1.D0)))/4.D0+ 00001050
*FACT52*(2.D0*P2-C)*(63.D0*CX(6,3)/4.D0+51.D0*DX(3,4)/2.D0- 00001060
*51.D0*CX(2,4)/2.D0)- 00001070
*FACT52*3.D0*CX(6,1)*(2.D0*P2+C2-5.D0*C+1.D0)/4.D0 00001080
DOTH53=FACT53*(4.D0*Q2-C-1.D0)*P*(-21.D0*CX(5,3)/2.D0+ 00001090
*3.D0*CX(5,1)/2.D0)+ 00001100
*FACT53*(4.D0*P2-C-1.D0)*Q*(-21.D0*CX(4,3)/2.D0+ 00001110
*3.D0*CX(4,1)/2.D0)+ 00001120
*FACT53*(-21.D0*DX(5,3)*(4.D0*P2-C+1.D0)*Q/2.D0+ 00001130
*3.D0*DX(5,1)*(4.D0*P2-7.D0*C+7.D0)*Q/2.D0)+ 00001140

```

DRAGJ2

AJG1324.GTDS.UPDATE.FORT

```

*FACT53*(-21.D0*DX(4,3)*P*(4.D0*P2-3.D0*C-1.D0)+
*3.D0*DX(4,1)*P*(4.D0*P2-9.D0*C+5.D0))/2.D0      00001150
DOTH62=FACT62*P*Q*(-147.D0*CX(1,3)+21.D0*CX(1,1))/4.D0+ 00001160
*FACT62*(21.D0*DX(1,1)*(2.D0*P2+C2-5.D0*C+1.D0)-    00001170
*147.D0*DX(1,3)*(2.D0*P2-C))/8.D0                  00001180

```

C
C
C
C

```

AVRATE(2)=DOTH52+DOTH53+DOTH62      00001190
                                         00001200
                                         00001210
                                         00001220
DETERMINE K-DOT.                    00001230

```

```

DOTK52=FACT52*P*Q*(-63.D0*CX(6,3)/2.D0-3.D0*CX(6,1)/2.D0-
*51.D0*DX(3,4)+51.D0*CX(2,4)+3.D0*DX(3,2)+3.D0*CX(2,2)*(C+4.D0))+
*FACT52*(3.D0*DX(2,2)*(4.D0*(C+4.D0)*P2-5.D0*C2+4.D0*C-3.D0)-
*3.D0*CX(3,2)*(4.D0*P2+3.D0*C2-14.D0*C+3.D0))/4.D0+ 00001250
*FACT52*(2.D0*P2-C)*(-63.D0*DX(6,3)/4.D0+51.D0*CX(3,4)/2.D0+ 00001260
*51.D0*DX(2,4)/2.D0)-
*FACT52*3.D0*DX(6,1)*(2.D0*P2-C2+3.D0*C-1.D0)/4.D0 00001270
DOTK53=FACT53*(4.D0*Q2-C-1.D0)*P*(21.D0*DX(5,3)/2.D0+ 00001280
*3.D0*DX(5,1)/2.D0)+
*FACT53*(4.D0*P2-C-1.D0)*Q*(21.D0*DX(4,3)/2.D0+    00001290
*3.D0*DX(4,1)/2.D0)+
*FACT53*(-21.D0*CX(5,3)*(4.D0*P2-C+1.D0)*Q/2.D0-    00001300
*3.D0*CX(5,1)*(4.D0*P2+5.D0*C-5.D0)*Q/2.D0)-
*FACT53*(21.D0*CX(4,3)*P*(4.D0*P2-3.D0*C-1.D0)+    00001310
*3.D0*CX(4,1)*P*(4.D0*P2+3.D0*C-7.D0))/2.D0
DOTK62=FACT62*P*Q*(147.D0*DX(1,3)+21.D0*DX(1,1))/4.D0- 00001320
*FACT62*(21.D0*CX(1,1)*(2.D0*P2-C2+3.D0*C-1.D0)+ 00001330
*147.D0*CX(1,3)*(2.D0*P2-C))/8.D0                  00001340

```

C
C
C
C

```

AVRATE(3)=DOTK52+DOTK53+DOTK62      00001350
                                         00001360
                                         00001370
                                         00001380
DETERMINE P-DOT.                    00001390

```

```

PDOT51=FACT51*(C-1.D0)*Q*(3.D0*CX(6,2)/2.D0+(21.D0*DX(3,3)-
*21.D0*DX(3,1)-21.D0*CX(2,3)+15.D0*CX(2,1))/8.D0)+ 00001400
*FACT51*(C-1.D0)*P*(3.D0*DX(6,2)/2.D0+(-21.D0*CX(3,3)+3.D0*CX(3,1)-
*21.D0*DX(2,3)-3.D0*DX(2,1))/8.D0)                  00001410
FDOT52=FACT52*(3.D0*DX(5,2)*(4.D0*Q2+C2-1.D0)/4.D0+ 00001420
*3.D0*P*Q*(-CX(5,2)+DX(4,2))-3.D0*CX(4,2)*(4.D0*P2+C2-1.D0)/4.D0) 00001430
PDOT61=FACT61*21.D0*(C-1.D0)*(-Q*DX(1,2)+P*CX(1,2))/8.D0 00001440

```

C
C
C
C

```

AVRATE(4)=PDOT51+PDOT52+PDOT61      00001450
                                         00001460
                                         00001470
                                         00001480
DETERMINE Q-DOT.                    00001490

```

```

QDOT51=FACT51*(C-1.D0)*Q*(-3.D0*DX(6,2)/2.D0+(21.D0*CX(3,3)-
*3.D0*CX(3,1)+21.D0*DX(2,3)+3.D0*DX(2,1))/8.D0)+ 00001500
*FACT51*(C-1.D0)*P*(3.D0*CX(6,2)/2.D0+(21.D0*DX(3,3)+15.D0*DX(3,1)-
*21.D0*CX(2,3)-21.D0*CX(2,1))/8.D0)                  00001510
QDOT52=FACT52*(3.D0*CX(5,2)*(4.D0*Q2+C2-1.D0)/4.D0+ 00001520
*3.D0*P*Q*(DX(5,2)+CX(4,2))+3.D0*DX(4,2)*(4.D0*P2+C2-1.D0)/4.D0) 00001530
QDOT61=FACT61*21.D0*(C-1.D0)*(-Q*CX(1,2)-P*DX(1,2))/8.D0 00001540

```

C
C
C
C

```

AVRATE(5)=QDOT51+QDOT52+QDOT61      00001550
                                         00001560
                                         00001570
                                         00001580
DETERMINE LAMDA-DOT.                00001590

```

```

                                         00001600
                                         00001610
                                         00001620
                                         00001630
                                         00001640
                                         00001650
                                         00001660
                                         00001670
                                         00001680
                                         00001690
                                         00001700
                                         00001710

```

DRAGJ2

AJG1324.GTDS.UPDATE.FORT

C7=C-7.D0	00001720
C15=C-15.D0	00001730
C215=2.D0*C-15.D0	00001740
DOTL52=FACT52*P*Q*(C7*6.D0*DX(6,2)+C215*(-21.D0*CX(3,3)+	00001750
*3.D0*CX(3,1)-21.D0*DX(2,3)-3.D0*DX(2,1))/4.D0)+	00001760
*FACT52*3.D0*CX(2,1)*(2.D0*P2*C215+23.D0*C2-49.D0*C+	00001770
*13.D0)/8.D0+	00001780
*FACT52*3.D0*DX(3,1)*(2.D0*P2*C215-27.D0*C2+79.D0*C-	00001790
*13.D0)/8.D0+	00001800
FACT52(2.D0*P2-C)*(-3.D0*C7*CX(6,2)+21.D0*C215*	00001810
*(-DX(3,3)+CX(2,3))/8.D0)	00001820
DOTL53=FACT53*3.D0*CX(5,2)*P*(2.D0*C15*Q2-C7*CP1)+	00001830
*FACT53*3.D0*CX(4,2)*Q*(2.D0*C15*P2-C7*CP1)+	00001840
*FACT53*3.D0*DX(5,2)*(2.D0*C15*P2+9.D0*C-7.D0)*Q+	00001850
*FACT53*3.D0*DX(4,2)*P*(2.D0*C15*P2-2.D0*C2+21.D0*C+7.D0)	00001860
DOTL62=FACT62*21.D0*C7*(CX(1,2)*P*Q/2.D0+DX(1,2)*(2.D0*P2-C)/4.D0)	00001870
C	00001830
AVRATE(6)=DOTL52+DOTL53+DOTL62	00001890
C	00001900
RETURN	00001910
C	00001920
END	00001930

***** END OF MEMBER DRAGJ2 193 RECORDS *****

EQUVAR

AJG1324.GTDS.UPDATE.FORT

```

SUBROUTINE EQUVAR                                00000010
C                                                  00000020
C  PURPOSE                                       00000030
C                                                  00000040
C    EXECUTIVE PROGRAM FOR THE EVALUATION OF THE RIGHT HAND
C    SIDE OF THE DIFFERENTIAL EQUATION FOR THE PARTIALS. 00000050
C                                                  00000070
C  PARAMETERS                                    00000080
C                                                  00000090
C    /SWITCH/                                    00000100
C                                                  00000110
C    IND(3)  I  VOP INDICATOR.                  00000120
C                                                  00000130
C              8 = OSCULATING KEPLERIAN
C              12 = AVERAGED EQUINOCTIAL        00000140
C                                                  00000150
C  PROGRAMMER                                    00000160
C                                                  00000170
C    ANDREW J. GREEN, CPT, U.S. ARMY, CSDL      00000180
C                                                  00000190
C                                                  00000200
C    IMPLICIT REAL*8(A-H,O-Z)                   00000210
C    COMMON/SWITCH/ IND(225)                   00000220
C                                                  00000230
C    IF(IND(3).EQ.8) GO TO 10                   00000240
C    IF(IND(3).EQ.12) GO TO 20                 00000250
C    GO TO 90                                   00000260
C  10 CALL VARFRC                               00000270
C    CALL VARFRV                               00000280
C    GO TO 100                                 00000290
C  20 CALL AVEPAR                               00000300
C    GO TO 100                                 00000310
C  90 WRITE(6,1000)                            00000320
C  100 RETURN                                  00000330
C  1000 FORMAT(/,'PARTIALS ARE ASKED FOR BUT THE VOP ORBIT TYPE IS WRONG',
C    END                                         00000350

```

***** END OF MEMBER EQUVAR

35 RECORDS *****

ESTSET

AJG1324.GTDS.UPDATE.FORT

```

SUBROUTINE ESTSET                                00000010
C                                                  00000020
C PURPOSE                                        00000030
C                                                  00000040
C   FOR THE INITIAL DESIGN, THIS SUBROUTINE SETS THE VALUES OF THE 00000050
C   SWITCHES USED IN THE AVERAGE PARTIAL GENERATOR AND THE SHORT 00000060
C   PERIODIC PARTIAL GENERATOR.                    00000070
C                                                  00000080
C PROGRAMMER                                     00000090
C   ANDREW J. GREEN, CPT, U.S. ARMY, CSDL          00000100
C                                                  00000110
C IMPLICIT REAL*8(A-H,O-Z)                        00000120
C                                                  00000130
COMMON/ESTFLG/ IANAL   ,IDIFF   ,IQDRT   ,ICBVAR   ,J22VAR   ,
1 ITBVAR   ,IDRVAR   ,ISRVAR   ,NVAR    ,LEVAR   ,
2 KDRFLG   ,KPAR    ,KSTEP(20),KVRFLG ,KCPSP   ,
3 KCBSPP   ,KTBSPP  ,KDRSPP   ,KRSRSP   ,NVARSP   ,
4 IVSPNC(4),KATMOS  ,KPRTB1   ,KPRTB2   ,KPRTB3   ,
5 KPRTB4
C                                                  00000190
COMMON/NEWPAR/ XS(20)   ,APAR(5)   ,APARVR(5),CDRVAR  00000200
C                                                  00000210
COMMON/FRC / RFR(1300) ,IFRC(50)   00000220
EQUIVALENCE (NMAX ,IFRC(3) ) ,00000240
1 (MMAX ,IFRC(4) ) 00000250
C /ESTFLG/                                        00000260
C IANAL CONTROL SWITCH FOR ANALYTICAL APPROACH IN THE 00000290
C AVERAGED PARTIAL GENERATOR.* 00000300
C IDIFF CONTROL SWITCH FOR FINITE-DIFFERENCING APPROACH 00000310
C IN THE AVERAGED PARTIAL GENERATOR. 00000320
C 0=APPROACH NOT USED 00000330
C 1=A MATRIX ONLY 00000340
C 2=D MATRIX ONLY 00000350
C 3=BOTH A AND D MATRICES 00000360
C IQDRT CONTROL SWITCH FOR QUADRATURE APPROACH IN THE 00000370
C AVERAGED PARTIAL GENERATOR 00000380
C 0=APPROACH NOT USED 00000390
C 1=A MATRIX ONLY 00000400
C 2=D MATRIX ONLY 00000410
C 3=BOTH A AND D MATRICES 00000420
C ICBVAR CENTRAL GRAVITATIONAL BODY CONTROL SWITCH FOR 00000430
C THE AVERAGED PARTIAL GENERATOR. 00000440
C 0=NONE 00000450
C 1=ANALYTICALLY 00000460
C 2=FINITE-DIFFERENCING WITH THE AOG CENTRAL 00000470
C BODY FIELD 00000480
C 3=FINITE-DIFFERENCING WITH A NXO FIELD 00000490
C J22VAR J2 SQUARED CONTROL SWITCH IN THE AVERAGED 00000500
C PARTIAL GENERATOR. 00000510
C 0=OFF 00000520
C 1=FINITE-DIFFERENCING 00000530
C ITBVAR THIRD-BODY CONTROL SWITCH IN THE AVERAGED 00000540
C PARTIAL GENERATOR. 00000550
C 0=OFF 00000560
C 1=FINITE-DIFFERENCING WITH THE AOG THIRD-BODY 00000570

```

11

ESTSET

AJG1324.GTDS.UPDATE.FORT

C		MODEL	0000580
C	IDRVAR	DRAG CONTROL SWITCH IN THE AVERAGED PARTIAL GENERATOR.	0000590
C		0=OFF	0000600
C		1=FINITE-DIFFERENCING	0000610
C		2=QUADRATURE APPROACH	0000620
C	ISRVAR	SOLAR RADIATION PRESSURE CONTROL SWITCH IN THE AVERAGED PARTIAL GENERATOR.	0000630
C		0=OFF	0000640
C		1=FINITE-DIFFERENCING	0000650
C		2=QUADRATURE APPROACH	0000660
C	NVAR	MAXIMUM DEGREE OF THE CENTRAL BODY GRAVITATIONAL FIELD TO BE CONSIDERED IN THE AVERAGED PARTIAL GENERATOR WHEN ICBVAR=3.	0000670
C			0000680
C	LEVAR	MAXIMUM POWER OF E IN THE POWER SERIES EXPANSION FOR THE ANALYTICAL HARMONIC POTENTIAL CONSIDERED IN THE AVERAGED PARTIAL GENERATOR WHEN ICBVAR=3 (AT MOST CAN BE NVAR-2).	0000690
C			0000700
C			0000710
C	KDRFLG	CONTROL SWITCH FOR CONSIDERING 2ND ORDER DRAG EFFECTS IN THE AVERAGED PARTIAL GENERATOR.	0000720
C		0=NO 2ND ORDER DRAG EFFECTS	0000730
C		1=J2-DRAG EFFECTS	0000740
C		2=J2-DRAG AND DRAG-DRAG EFFECTS	0000750
C		3=J2-DRAG, DRAG-J2 AND DRAG-DRAG EFFECTS DONE NUMERICALLY	0000760
C		4=J2-DRAG AND DRAG-DRAG EFFECTS DONE NUMERICALLY, DRAG-J2 DONE ANALYTICALLY	0000770
C		5=ISZAK'S J2 HEIGHT CORRECTION AND ANALYTIC DRAG-J2 EFFECTS	0000780
C		6=ISZAK'S J2 HEIGHT CORRECTION ONLY	0000790
C	KPAR	PARAMETER ESTIMATION OPTION.	0000800
C		0=NONE	0000810
C		1=SOLVE FOR CDAG	0000820
C		2=SOLVE FOR THE 5 PARAMETERS, A1 - A5, IN THE ADAPTIVE MODIFIED HARRIS-FRIESTER ATMOSPHERE.	0000830
C		3=SOLVE FOR THE 3 PARAMETERS, A1 - A3, IN THE ADAPTIVE MODIFIED HARRIS-FRIESTER ATMOSPHERE.	0000840
C	KSTEP	ARRAY OF CONTROL SWITCHES FOR THE PERTURBING STEPSIZE.	0000850
C		1=STEPSIZE IS GIVEN IN XS	0000860
C		2=STEPSIZE IS XS*PARAMETER	0000870
C	KVRFLG	CONTROL SWITCH FOR THE SHORT PERIODIC PARTIALS.	0000880
C		0=NONE	0000890
C		1=B1 MATRIX - ANALYTICALLY	0000900
C		2=B1 MATRIX ONLY - FINITE DIFFERENCING	0000910
C		3=B4 MATRIX ONLY - FINITE DIFFERENCING	0000920
C		4=BOTH B1 AND B4 MATRICES - FINITE DIFFERENCING	0000930
C	KCPSP	CONTROL SWITCH FOR CONTINUOUS TIME-INDEPENDENT PERTURBATIONS IN THE SHORT PERIODIC PARTIALS.*	0000940
C			0000950
C	KCBSPP	CONTROL SWITCH FOR CENTRAL BODY PERTURBATIONS IN THE SHORT PERIODIC PARTIALS.*	0000960
C			0000970
C	KTBSPP	CONTROL SWITCH FOR THIRD-BODY PERTURBATIONS IN THE SHORT PERIODIC PARTIALS.*	0000980
C			0000990
C	KDRSPP	CONTROL SWITCH FOR DRAG PERTURBATIONS IN THE SHORT PERIODIC PARTIALS.*	0001000
C			0001010
C			0001020
C			0001030
C	KRSRPP	CONTROL SWITCH FOR SOLAR RADIATION PRESSURE PERTURBATIONS IN THE SHORT PERIODIC PARTIALS.*	0001040
C			0001050
C			0001060
C			0001070
C			0001080
C			0001090
C			0001100
C			0001110
C			0001120
C			0001130
C			0001140

11

11

ESTSET

AJG1324.GTDS.UPDATE.FORT

```

C      NVARSP      MAXIMUM DEGREE OF THE CENTRAL BODY GRAVITATIONAL 00001150
C      FIELD TO BE CONSIDERED IN THE SHORT PERIODIC 00001160
C      GENERATOR. 00001170
C      IVSPNC      ARRAY OF THE NUMBER OF SHORT PERIODIC COEF- 00001180
C      FICIENTS FOR EACH PERTURBATIONS TO BE 00001190
C      CONSIDERED IN THE SHORT PERIODIC PARTIALS. 00001200
C      KATMOS      CONTROL SWITCH FOR THE TYPE OF MODIFIED HARRIS- 00001210
C      PRIESTER ATMOSPHERIC MODEL. 00001220
C      1=STANDARD GTDS 00001230
C      2=FULL ADAPTIVE(KPAR=2) 00001240
C      3=PART ADAPTIVE(KPAR=3) 00001250
C      KPRTB1      CONTROL SWITCH FOR PRINTING THE B1 MATRIX.* 00001260
C      KPRTB2      CONTROL SWITCH FOR PRINTING THE B2 MATRIX.* 00001270
C      KPRTB3      CONTROL SWITCH FOR PRINTING THE B3 MATRIX.* 00001280
C      KPRTB4      CONTROL SWITCH FOR PRINTING THE B4 MATRIX.* 00001290
C      /NEWPAR/ 00001300
C      XS          ARRAY OF STEPSIZES FOR THE SOLVE-FOR-PARAMETERS 00001310
C      USED TO COMPUTE THE PARTIALS WITH FINITE- 00001320
C      DIFFERENCING. 00001330
C      APAR        ARRAY OF DENSITY PARAMETERS USED IN THE ADAPTIVE 00001340
C      HARRIS-PRIESTER ATMOSPHERE. 00001350
C      APARVR      ARRAY OF THE VARIANCE FOR APAR. 00001360
C      CDRVAR      VARIANCE OF THE COEFFICIENT OF DRAG. 00001370
C      * 1=YES    *=NO 00001380
C      ESTSET FLAGS 00001390
C      IANAL = 2 00001400
C      IDIFF = 3 00001410
C      IQDRT = 0 00001420
C      ICBVAR = 2 00001430
C      NVAR = NMAX 00001440
C      LEVAR= NVAR-2 00001450
C      J22VAR = 1 00001460
C      ITBVAR = 0 00001470
C      IDRVAR = 1 00001480
C      ISRVAR = 0 00001490
C      KDRFLG = 6 00001500
C      KPAR = 1 00001510
C      KATMOS = 1 00001520
C      DO 10 I=1,20 00001530
C      KSTEP(I)=2 00001540
C      XS(I) =0.0000100 00001550
C      10 CONTINUE 00001560
C      KVRFLG = 0 00001570
C      KCPSFP = 2 00001580
C      KCDSP = 2 00001590
C      NVARSP = NMAX 00001600
C      00001610
C      00001620
C      00001630
C      00001640
C      00001650
C      00001660
C      00001670
C      00001680
C      00001690
C      00001700
C      00001710

```

11

11

ESTSET

AJG1324.GTDS.UPDATE.FORT

	KTBSFP =2	00001720
	KDRSFP =2	00001730
	KSRSPF =2	00001740
C		00001750
	IVSPNC(1) = 5	00001760
	IVSPNC(2) = 5	00001770
	IVSPNC(3) = 5	00001780
	IVSPNC(4) = 5	00001790
C		00001800
	KPRTB1 = 2	00001810
	KPRTB2 = 2	00001820
	KPRTB3 = 2	00001830
	KPRTB4 = 2	00001840
C		00001850
C		00001860
	APAR(1) = 1.00	00001870
	APAR(2) = 1.00	00001880
	APAR(3) = 6.00	00001890
	APAR(4) = 0.00	00001900
	APAR(5) = 0.00	00001910
C		00001920
	APARVR(1) = .33300	00001930
	APARVR(2) = .33300	00001940
	APARVR(2) = .33300	00001950
	APARVR(2) = .33300	00001960
	APARVR(2) = .33300	00001970
C		00001980
	CDRVAR = .33300	00001990
C		00002000
C		00002010
	RETURN	00002020
	END	00002030

***** END OF MEMBER ESTSET

203 RECORDS *****

GMAT

AJG1324.GTDS.UPDATE.FORT

```

SUBROUTINE GMAT(TEMPPK)                                00000010
C                                                       00000020
C VERSION OF 20 JULY 1979 IMPLEMENTED AT CSDL ON AN AMDAHL 470 V6. 00000030
C                                                       00000040
C PURPOSE                                               00000050
C EXECUTIVE PROGRAM FOR THE DETERMINATION OF THE G MATRIX - 00000060
C PARTIAL OF THE OSCULATING EQUINOCTIAL ELEMENTS WITH RESPECT 00000070
C TO THE SOLVE-FOR-PARAMETERS.                        00000080
C                                                       00000090
C PARAMETERS                                           00000100
C                                                       00000110
C TEMPPK      I   ARRAY OF THE PARTIAL OF THE MEAN EQUINOCTIAL 00000120
C               ELEMENTS WRT THE SOLVE-FOR-PARAMETERS.        00000130
C               0   ARRAY OF THE PARTIAL OF THE OSCULATING EQUI- 00000140
C                   NOCTIAL ELEMENTS WRT THE SOLVE-FOR-PARAMETERS. 00000150
C                                                       00000160
C /WORKER/                                           00000170
C                                                       00000180
C XLAMDA     I   MEAN FAST VARIABLE.                    00000190
C VPELMT     I   ARRAY OF MEAN ELEMENTS.                00000200
C                                                       00000210
C /VARMAT/                                           00000220
C                                                       00000230
C B1MAT      O   ARRAY OF THE PARTIAL OF THE SHORT PERIODICS 00000240
C               WRT THE MEAN EQUINOCTIAL ELEMENTS.          00000250
C B4MAT      O   ARRAY OF THE PARTIAL OF THE SHORT PERIODICS 00000260
C               WRT THE SOLVED-FOR-MODELLED PARAMETERS.      00000270
C                                                       00000280
C /ESTFLG/                                           00000290
C                                                       00000300
C KVRFLG     I   CONTROL SWITCH FOR THE SHORT PERIODIC PARTIAL 00000310
C               GENERATOR.                                  00000320
C KPRTB1     I   CONTROL SWITCH FOR PRINTING THE B1 MATRIX.  00000330
C KPRTB2     I   CONTROL SWITCH FOR PRINTING THE B2 MATRIX.  00000340
C KPRTB3     I   CONTROL SWITCH FOR PRINTING THE B3 MATRIX.  00000350
C KPRTB4     I   CONTROL SWITCH FOR PRINTING THE B4 MATRIX.  00000360
C                                                       00000370
C REFERENCES                                           00000380
C                                                       00000390
C "ORBIT DETERMINATION AND PREDICTION PROCESSES FOR LOW-    00000400
C ALTITUDE SATELLITES." BY A.J. GREEN                   00000410
C                                                       00000420
C ANALYSIS                                             00000430
C ANDREW J. GREEN, CPT, U.S. ARMY                       00000440
C                                                       00000450
C PROGRAMMER                                           00000460
C ANDREW J. GREEN, CPT, U.S. ARMY                     00000470
C                                                       00000480
C                                                       00000490
C IMPLICIT REAL*8(A-H,O-Z)                             00000500
C DIMENSION TEMPPK(6,20),TMAT(6,20),VPELMT(10)        00000510
C                                                       00000520
C COMMON/WORKER/ RWORK(3264) ,IWORK(13)                00000530
C EQUIVALENCE    (VPELMT(1) ,RWORK(2829) ) ,00000540
C 2              (XLAMDA ,RWORK(2851) ) ,00000550
C 3              (XMEAN ,RWORK(2814) ) 00000560
C EQUIVALENCE    (NOPARM ,IWORK(3) ) ,00000570

```

GMAT

AJG1324.GTDS.UPDATE.FORT

```
2          (NEQ          ,IWORK(5)          ),00000580
3          (NPERT        ,IWORK(9)          ) 00000590
C
COMMON/DCINT/ DPDCI(432), INDCI(26)
EQUIVALENCE   (TTO          ,DPDCI(127)      ) 00000600
C
COMMON/ESTFLG/ IANAL   ,IDIFF   ,IQDRT   ,ICBVAR   ,J22VAR   ,
1 ITBVAR   ,IDRVAR   ,ISRVAR   ,NVAR    ,LEVAR   , 00000640
2 KDRFLG   ,KPAR    ,KSTEP(20),KVRF LG ,KCPSP   , 00000650
3 KCSPP    ,KTSPP   ,KDRSPP   ,KSRSP   ,NVARSP  , 00000660
4 IVSFNC(4),KATMOS ,KPRTB1   ,KPRTB2   ,KPRTB3  , 00000670
5 KPRTB4
C
COMMON/VARMAT/ AMAT(6,6),DMAT(6,14),B1MAT(6,6),B4MAT(6,14) 00000680
C
SAVE THE FAST VARIABLE
C
XLAMDA=VPELMT(NOPARM)
C
PRINT THE B2 AND B3 MATRICIES
C
TIMOUT=TTO/86400.D0
IF(KPRTB2.NE.1) GO TO 3
WRITE(6,1000) TIMOUT
DO 2 I=1,6
WRITE(6,1001) (TEMPPK(I,J),J=1,6)
WRITE(6,1003)
2 CONTINUE
3 IF(KPRTB3.NE.1) GO TO 5
WRITE(6,1002) TIMOUT
DO 4 I=1,6
WRITE(6,1001) (TEMPPK(I,J),J=7,NEQ)
WRITE(6,1003)
4 CONTINUE
C
CALCULATE THE B1 AND B4 MATRICES.
C
5 CALL VARSP
C
PRINT THE B1 AND B4 MATRICES.
C
IF(KPRTB1.NE.1) GO TO 7
WRITE(6,1004) TIMOUT
DO 6 I=1,6
WRITE(6,1001) (B1MAT(I,J),J=1,6)
WRITE(6,1003)
6 CONTINUE
7 IF(KPRTB4.NE.1) GO TO 9
WRITE(6,1006) TIMOUT
NL=NEQ-6
DO 8 I=1,6
WRITE(6,1001) (B4MAT(I,J),J=1,NL)
WRITE(6,1003)
8 CONTINUE
C
FORM THE I+B1 MATRIX.
C
```

GMAT

AJG1324.GTDS.UPDATE.FORT

```
          9 DO 10 I=1,6                                00001150
            BIMAT(I,I)=BIMAT(I,I)+1.D0                00001160
          10 CONTINUE                                  00001170
C                                                  00001180
C          FORM THE (I+B1)(TEMPPK) MATRIX.            00001190
C                                                  00001200
C          CALL MATMUL(BIMAT,TEMPPK,TMAT,6,6,NEQ)     00001210
C                                                  00001220
C          ADD THE B4 MATRIX.                         00001230
C                                                  00001240
C          DO 30 I=1,6                                00001250
            DO 20 J=7,NEQ                              00001260
              N=J-6                                    00001270
              TMAT(I,J)=TMAT(I,J)+B4MAT(I,N)          00001280
          20 CONTINUE                                  00001290
          30 CONTINUE                                  00001300
C                                                  00001310
C          FORM THE OUTPUT MATRIX.                   00001320
C                                                  00001330
C          NN=NEQ+1                                    00001340
            DO 60 I=1,6                                00001350
              DO 40 J=1,NEQ                            00001360
                TEMPPK(I,J)=TMAT(I,J)                00001370
          40 CONTINUE                                  00001380
              DO 50 L=NN,20                            00001390
                TEMPPK(I,L)=0.D0                     00001400
          50 CONTINUE                                  00001410
          60 CONTINUE                                  00001420
C                                                  00001430
C          RETURN                                       00001440
          1000 FORMAT(////,41X,'THE B2 MATRIX AT TIME(DAYS) =',1P1D20.10,/) 00001450
          1001 FORMAT(1P6D22.12)                      00001460
          1002 FORMAT(////,41X,'THE B3 MATRIX AT TIME(DAYS) =',1P1D20.10,/) 00001470
          1003 FORMAT(/)                               00001480
          1004 FORMAT(////,41X,'THE B1 MATRIX AT TIME(DAYS) =',1P1D20.10,/) 00001490
          1006 FORMAT(////,41X,'THE B4 MATRIX AT TIME(DAYS) =',1P1D20.10,/) 00001500
          END                                           00001510
```

***** END OF MEMBER GMAT

151 RECORDS *****

```

C      SUBROUTINE HODRAG                                00000010
C      VERSION OF 19 MARCH 1979 IMPLEMENTED AT CSDL ON AMDAHL 470 V6 00000020
C      PURPOSE                                           00000030
C      TO CONTROL THE EVALUATION OF THE AVERAGED ELEMENT RATES 00000040
C      DUE TO DRAG, J2-DRAG, DRAG-J2 AND DRAG-DRAG EFFECTS. ALL 00000050
C      SHORT PERIODICS ARE EXPRESSED IN TERMS OF A FOURIER SERIES 00000060
C      IN THE MEAN-MEAN LONGITUDE.                       00000070
C      PARAMETERS                                         00000080
C      /ANAVIN/                                           00000090
C      ITHIRD      I   THIRD-BODY AVERAGING OPTION.       00000100
C      0=NO THIRD-BODY                                   00000110
C      1=TIME-DEPENDENT NUMERICAL AVERAGING              00000120
C      2=TIME-INDEPENDENT NUMERICAL AVERAGING           00000130
C      3=ANALYTICAL AVERAGING                           00000140
C      NQUAD       I   QUADRATURE ORDER(UNTIL THE AUTOMATIC QUADRATURE 00000150
C      ORDER SELECTION OPTION IS IMPLEMENTED IN 'SPGENN', 00000160
C      THIS SUBROUTINE ASSUMES THAT THE QUADRATURE ORDER 00000170
C      HAS BEEN DETERMINED BY A KEYWORD CARD OR BY A    00000180
C      PREVIOUS CALL TO 'VOQUAD'                        00000190
C      ICORR       I   CONTROL SWITCH FOR ISZAK'S J2 HEIGHT CORRECTION 00000200
C      IN THE DRAG QUADRATURE.                          00000210
C      IDRDR       I   CONTROL SWITCH FOR CONSIDERING 2ND ORDER 00000220
C      DRAG EFFECTS.                                    00000230
C      0=NO 2ND ORDER DRAG EFFECTS                      00000240
C      1=J2-DRAG EFFECTS                                00000250
C      2=J2-DRAG AND DRAG-DRAG EFFECTS                 00000260
C      3=J2-DRAG,DRAG-J2 AND DRAG-DRAG EFFECTS        00000270
C      DONE NUMERICALLY                                 00000280
C      4=J2-DRAG AND DRAG-DRAG EFFECT DONE            00000290
C      NUMERICALLY, DRAG-J2 EFFECTS DONE ANALYTICALLY 00000300
C      5=ISZAK'S J2 HEIGHT CORRECTION AND ANALYTIC    00000310
C      DRAG-J2 EFFECTS.                                00000320
C      NCHOJ2      I   NUMBER OF J2 SHORT PERIODIC COEFFICIENTS TO BE 00000330
C      CONSIDERED IN 'HODRAG'.                          00000340
C      NCHODR      I   NUMBER OF DRAG SHORT PERIODIC COEFFICIENTS TO BE 00000350
C      CONSIDERED IN 'HODRAG'.                          00000360
C      /FRC/                                              00000370
C      NMAX        O   MAXIMUM DEGREE FOR THE EARTH OR MOON FIELDS. 00000380
C      MMAX        O   MAXIMUM ORDER FOR THE EARTH OR MOON FIELDS. 00000390
C      /SWITCH/                                          00000400
C      IBURN       O   CONTROL SWITCH FOR POLYNOMIAL BURN MODEL. * 00000410
C      IRESON      O   CENTRAL BODY FIELD SWITCH.        00000420
C      1=NXM CENTRAL BODY FIELD PLUS HIGH ORDER        00000430
C      RESONANCE                                        00000440
C      2=NXM CENTRAL BODY FIELD ONLY                   00000450
C      3=HIGH ORDER RESONANCE ONLY                     00000460
C      4=NO CENTRAL BODY FIELD                         00000470
C      IBCDY       O   CENTRAL AND NON-CENTRAL BODY INDICATORS. 00000480

```

```

C
C
C   /WORKER/
C
C   OSCELM   O   ARRAY OF OSCULATING ELEMENTS.
C   ETA      O   ARRAY OF SHORT PERIODICS.
C   VPELMT   I   ARRAY OF MEAN ELEMENTS.
C   XLAMBA   I   MEAN FAST VARIABLE(MEAN MEAN LONGITUDE).
C   XMEAN    O   MEAN MOTION.
C   T        I   TIME FROM EPOCH.
C   NOPARM   I   NUMBER OF PARAMETERS.
C   NPERT    O   PERTURBATION INDICATOR.
C               1=CONTINUOUS TIME-DEPENDENT
C               2=CONTINUOUS TIME-INDEPENDENT
C               3=DRAG
C               4=SOLAR RADIATION PRESSURE
C
C   *   1=YES      2=NO
C
C   REFERENCES
C
C   "A FOURIER SERIES FORMULATION OF THE SHORT PERIODIC VARIATIONS
C   IN TERMS OF EQUINOCTIAL ELEMENTS." BY A.J. GREEN AND P.J. CEFOLA
C
C   ANALYSIS
C   ANDREW J. GREEN, CPT, U.S. ARMY, CSDL
C
C   PROGRAMMER
C   ANDREW J. GREEN, CPT, U.S. ARMY, CSDL
C
C *****START PROGRAM*****
C
C
C   IMPLICIT REAL*(A-H,O-Z)
C   DIMENSION   DPARRY(15,10)      ,VPELMT(10) ,AVRATE(10) ,
2             GM(11)      ,POSVEL(6,8),DUMMY(3)
C   DIMENSION   TEMPC(10,10),TEMPD(10,10)
C   DIMENSION   IBODY(9)      ,IBODYS(3)
C
C   COMMON/ANAVIN/  ISTESS      ,ITESSE      ,ITRESE      ,ISTHIR      ,
1             ITHRAR      ,ITHRE      ,ITESS      ,NEND      ,
2             MEND      ,LEND      ,ITRES      ,NRES(10) ,
3             MRES(10)   ,JRES(10)   ,NCSRES     ,LENDRS     ,
4             ITHIRD     ,NENDTH(8)  ,MENDTH(8)  ,JTWOSQ    ,
5             IQUAD(4)   ,NQUAD(4)   ,JPOS      ,JA      ,
6             JB      ,JC      ,JGHA      ,KPOS      ,
7             KA      ,KB      ,KC      ,KGHA      ,
8             ICORR     ,IPOS      ,IMOON     ,IMEAN     ,
9             IGHA      ,ISTRES     ,ITERM     ,ISHAD     ,
1            JTHDEP     ,JTMIND     ,JDRAG     ,JSOLAR    ,
2            J2SQSP     ,JSPCGB     ,JSPTHR     ,JSPPOS    ,
3            JSPA      ,JSFB      ,JSPC      ,JSFGHA    ,
4            KSPPOS     ,KSPA      ,KSF8      ,KSFC      ,
5            KSPGHA     ,KSPNC(4)  ,KSPRT(4)  ,NMAXSP   ,
6            MHAXSP     ,IDRDR     ,NCHOJ2    ,NCHODR   ,
EQUIVALENCE   (ITHDEP      ,IQUAD(1)      ),00001140

```

11

HODRAG

AJG1324.GTDS.UPDATE.FORT

	2	(ITMIND	,IQUAD(2)) ,00001150
	3	(IDRAG	,IQUAD(3)) ,00001160
	4	(ISOLAR	,IQUAD(4)) 00001170
C				00001180
		COMMON/CONST /	RCONST(51)	00001190
		EQUIVALENCE	(TWOPI	,RCONST(1)
C) 00001200
				00001210
		COMMON/FRC /	RFRC(1300) ,IFRC(50)	00001220
		EQUIVALENCE	(GM(1)	,RFRC(2)
	2	(POSVEL(1,1)	,RFRC(101)) ,00001230
	3	(NEODY	,IFRC(7)) ,00001240
	4	(ISUN	,IFRC(14)) 00001250
C				00001260
				00001270
		COMMON/SWITCH/	ISWIT(225)	00001280
		EQUIVALENCE	(IVOP	,ISWIT(3)
	2	(ITWOBD	,ISWIT(6)) ,00001290
	3	(IBURN	,ISWIT(12)) ,00001300
	4	(IRESON	,ISWIT(38)) ,00001310
	5	(IEODY(1)	,ISWIT(201)) ,00001320
	6	(ICENT	,IEODY(1)) ,00001330
C) 00001340
				00001350
		COMMON/WORKER/	RWORK(3264) ,IWORK(13)	00001360
		EQUIVALENCE	(DPARRY(1,1)	,RWORK(7)
	2	(TXMEAN	,RWORK(2671)) ,00001370
	3	(VPELMT(1)	,RWORK(2829)) ,00001380
	4	(AVRATE(1)	,RWORK(3068)) ,00001390
	5	(XLAMDA	,RWORK(2851)) ,00001400
	6	(XMEAN	,RWORK(2814)) ,00001410
	7	(T	,RWORK(3215)) ,00001420
	8	(TZERO	,RWORK(2850)) ,00001430
		EQUIVALENCE	(K	,IWORK(2)
	2	(NOPARM	,IWORK(3)) ,00001440
	3	(NPERT	,IWORK(9)) ,00001450
		COMMON/SPCOEF/	CQUAD(10,10),DQUAD(10,10)) 00001460
				00001470
C				00001480
				00001490
C		STORE THE MEAN MOTION AND SET THE VARIOUS SWITCHES.		00001500
C				00001510
		TXMEAN = XMEAN		00001520
		IREGNS = IRESN		00001530
		NMAXS = NMAX		00001540
		MMAXS = MMAX		00001550
		ITHRTE = ITHIRD		00001560
		ICORRT = ICORR		00001570
		ISURNT = IBURN		00001580
		KTENTI = KSFNC(2)		00001590
		KTENDR = KSPNC(3)		00001600
		IRESON = 2		00001610
		NMAX = 2		00001620
		MMAX = 0		00001630
		ITHIRD = 0		00001640
		ICORR = 2		00001650
		IBURN = 2		00001660
		KSPNC(2) = NCHOJ2		00001670
		KSFNC(3) = NCHODR		00001680
		KMAXNC = NCHOJ2		00001690
		IF(IDRDR.EQ.5) GO TO 100		00001700
C				00001710

11

HODRAG

AJG1324.GTDS.UPDATE.FORT

C	COMPUTE THE SHORT PERIODIC COEFFICIENTS DUE TO J2 USING	00001720
C	TIME-INDEPENDENT NUMERICAL AVERAGING.	00001730
C		00001740
	NPERT=2	00001750
	CALL LIMITS(FLOW,FHIGH,XLAMDA)	00001760
C		00001770
C	STORE THE J2 LIMITS.	00001780
C		00001790
	TFLOW=FLOW	00001800
	TFHIGH=FHIGH	00001810
C		00001820
	CALL EVAL(TZERO,2,KA,KB,KC,2,IBODY,POSVEL)	00001830
	CALL SPGENN(FCW,FHIGH)	00001840
	IF(IDRDR.EQ.1) GO TO 100	00001850
C		00001860
C	STORE THE J2 COEFFICIENTS.	00001870
C		00001880
	KMAXNC=MAX0(NCHOJ2,NCHODR)	00001890
	DO 40 I = 1,NOPARM	00001900
	DO 30 J = 1,KMAXNC	00001910
	TEMFC(I,J) = CQUAD(I,J)	00001920
	TEMPD(I,J) = DQUAD(I,J)	00001930
	30 CONTINUE	00001940
	40 CCNTINUE	00001950
C		00001960
C	COMPUTE THE ELEMENT RATES DUE TO DRAG, J2-DRAG AND	00001970
C	DRAG-DRAG EFFECTS.	00001980
C		00001990
	100 NPERT=3	00002000
	CALL LIMITS(FLOW,FHIGH,XLAMDA)	00002010
	IF(NPERT.EQ.0) GO TO 600	00002020
C		00002030
C	FIND THE POSITION OF THE SUN SO THAT THE DIURNAL	00002040
C	BULGE IN THE ATMOSPHERE CAN BE LOCATED.	00002050
C		00002060
	IBODYS(2) = IBODY(2)	00002070
	IBODYS(3) = IBODY(3)	00002080
	NBODYS = NBODY	00002090
C		00002100
	IBODY(2) = 3	00002110
	IBODY(3) = 0	00002120
	NBCDY = 2	00002130
C		00002140
	CALL EVAL(TZERO,1,2,2,2,2,IBODY,POSVEL)	00002150
	IF(IDRDR.EQ.1) GO TO 120	00002160
C		00002170
C	COMPUTE THE SHORT PERIODIC COEFFICIENTS DUE TO DRAG.	00002180
C		00002190
	CALL SPGENN(FLOW,FHIGH)	00002200
	IF(IDRDR.EQ.5) GO TO 160	00002210
C		00002220
C	ACCUMULATE THE SHORT PERIODIC COEFFICIENTS AND DETERMINE THE	00002230
C	CROSS COUPLING TERM IN THE FAST VARIABLE RATE.	00002240
C		00002250
	TK=2.00	00002260
	IF (IDRDR.EQ.2) TK=1.00	00002270
	DELLAN=0.00	00002280

HODRAG

AJG1324.GTDS.UPDATE.FORT

```
XFACT=(15.D0*XMEAN)/(16.D0*VPELMT(1)*VPELMT(1)) 00002290
DO 115 I=1,NOPARM 00002300
DO 110 J=1,KMAXNC 00002310
TEM1=CQUAD(I,J)*CQUAD(I,J)+DQUAD(I,J)*DQUAD(I,J) 00002320
TEM2=CQUAD(I,J)*TEMPC(I,J)+DQUAD(I,J)*TEMPC(I,J) 00002330
DELLAM=DELLAM+XFACT*(TEM1+TK*TEM2) 00002340
CQUAD(I,J)=CQUAD(I,J)+TEMPC(I,J) 00002350
DQUAD(I,J)=DQUAD(I,J)+TEMPC(I,J) 00002360
110 CONTINUE 00002370
115 CONTINUE 00002380
C 00002390
C ADD THE CROSS COUPLING TERM TO THE FAST VARIABLE RATE. 00002400
C 00002410
DPARRY(K,NOPARM) = DPARRY(K,NOPARM) + DELLAM 00002420
C 00002430
C COMPUTE THE VALUE OF THE ELEMENT RATES. 00002440
C 00002450
120 CALL RTQUAD(AVRATE,FLOW,FHIGH,NQUAD(NPERT),KMAXNC) 00002460
C 00002470
C ACCUMULATE THE ELEMENT RATES. 00002480
C 00002490
DO 125 I=1,NOPARM 00002500
DPARRY(K,I) = DPARRY(K,I) + AVRATE(I)/TWOPI 00002510
125 CONTINUE 00002520
C 00002530
C RESTORE THE THIRD BODIES. 00002540
C 00002550
IBODY(2) = IBODYS(2) 00002560
IBODY(3) = IBODYS(3) 00002570
NBODY = NBODYS 00002580
IF (IDRDR.LE.2) GO TO 600 00002590
C 00002600
C COMPUTE THE VALUE OF THE ELEMENT RATES DUE TO DRAG-J2 EFFECTS. 00002610
C 00002620
C 00002630
C THE DRAG SHORT PERIODIC COEFFICIENTS HAVE ALREADY BEEN DETERMINED. 00002640
C 00002650
KMAXNC=NCHODR 00002660
DO 135 I=1,NOPARM 00002670
DO 130 J=1,KMAXNC 00002680
CQUAD(I,J)=CQUAD(I,J) - TEMPC(I,J) 00002690
DQUAD(I,J)=DQUAD(I,J) - TEMPC(I,J) 00002700
130 CONTINUE 00002710
135 CONTINUE 00002720
IF (IDRDR.EQ.4) GO TO 160 00002730
C 00002740
C DETERMINE THE ELEMENT RATES NUMERICALLY. 00002750
C 00002760
NPERT=2 00002770
CALL EVAL(TZERO,2,KA,KB,KC,2,IBODY,POSVEL) 00002780
140 CALL RTQUAD(AVRATE,TFLOW,TFHIGH,NQUAD(NPERT),KMAXNC) 00002790
C 00002800
C ACCUMULATE THE ELEMENT RATES. 00002810
C 00002820
DO 145 I=1,NOPARM 00002830
DPARRY(K,I) = DPARRY(K,I) + AVRATE(I)/TWOPI 00002840
145 CONTINUE 00002850
```

11

HODRAG

AJG1324.GTDS.UPDATE.FORT

```
C
C SINCE THE J2 EFFECT HAS ALREADY BEEN INCLUDED PREVIOUSLY,
C IT MUST BE NOW BE REMOVED.
C
XMEAN = TXMEAN
CALL AUXPAR(VPELMT)
CALL VOQUAD(TFLOW,TFHIGH)
DO 150 I=1,NOPARM
    DPARRY(K,I) = DPARRY(K,I) - AVRATE(I)/TWOPI
150 CONTINUE
GO TO 601
C
C DETERMINE THE ELEMENT RATES ANALYTICALLY.
C
160 XMEAN=TXMEAN
CALL AUXPAR(VPELMT)
CALL DRAGJ2
C
C ACCUMULATE THE ELEMENT RATES.
C
DO 165 I=1,NOPARM
    DPARRY(K,I) = DPARRY(K,I) + AVRATE(I)
165 CONTINUE
GO TO 601
C
C RESTORE THE SWITCHES.
C
600 XMEAN = TXMEAN
CALL AUXPAR(VPELMT)
601 IRESON = IRESNS
NMAX = NMAXS
MMAX = MMAXS
ITHIRD = ITHRTE
ICORR = ICORRT
IBURN = IBURNT
KSFNC(2) = KTEMPI
KSFNC(3) = KTEMOR
C
RETURN
END
```

00002860
00002870
00002880
00002890
00002900
00002910
00002920
00002930
00002940
00002950
00002960
00002970
00002980
00002990
00003000
00003010
00003020
00003030
00003040
00003050
00003060
00003070
00003080
00003090
00003100
00003110
00003120
00003130
00003140
00003150
00003160
00003170
00003180
00003190
00003200
00003210
00003220
00003230
00003240
00003250

***** END OF MEMBER HODRAG 325 RECORDS *****

```

SUBROUTINE HWIRE
C
C
C PURPOSE
C FOR THE INITIAL DESIGN THIS SUBROUTINE SETS THE VALUES OF
C THE SHORT PERIODIC SWITCHES.
C
  IMPLICIT REAL*8(A-H,O-Z)
  COMMON/ANAVIN/  ISTE55      ,ITESSE      ,ITRESE      ,ISTHIR      ,
1                ITHRAR      ,ITHRE       ,ITESS        ,NEND        ,
2                MEND        ,LEND        ,ITRES        ,NRES(10)    ,
3                MRES(10)    ,JRES(10)    ,NCSRES       ,LENDRS      ,
4                ITHIRD     ,NENDTH(8)   ,NENDTH(8)   ,JTWOSQ    ,
5                IQUAD(4)   ,NQUAD(4)   ,JPOS         ,JA         ,
6                JB         ,JC         ,JGHA         ,KPOS         ,
7                KA         ,KB         ,KC         ,KGHA         ,
8                ICORR     ,IPOS        ,IMOON        ,IMEAN        ,
9                IGHA      ,ISTRES     ,ITERM        ,ISHAD        ,
1               JTMDEP     ,JTMIND     ,JDRAG        ,JSOLAR      ,
2               J2SQSP     ,JSPCGB     ,JSPTHR       ,JSFPOS      ,
3               JSPA       ,JSFB       ,JSPC         ,JSPGHA     ,
4               KSPFOS     ,KSPA       ,KSPB         ,KSPC         ,
5               KSPGHA     ,KSPNC(4)   ,KSPPRT(4)   ,NMAXSP    ,
6               MMAXSP     ,IORDR      ,NCHOJ2       ,NCHODR

C
COMMON/FRC / RFR(1300) ,IFRC(50)
EQUIVALENCE (NMAX ,IFRC(3) ) ,
1            (MMAX  ,IFRC(4) )

C
C JTMDEP CONTROL SWITCH FOR NUMERICAL SHORT PERIODICS DUE
C TO TIME-DEPENDENT CONTINUOUS PERTURBATIONS. *
C
C JTMIND CONTROL SWITCH FOR NUMERICAL SHORT PERIODICS DUE
C TO TIME-INDEPENDENT CONTINUOUS PERTURBATIONS. *
C
C JSPCGB CONTROL SWITCH FOR NUMERICAL SHORT PERIODICS DUE
C TO THE CENTRAL GRAVITATIONAL BODY.
C 0=NO CENTRAL BODY FIELD
C 1=TIME-DEPENDENT NUMERICAL SHORT PERIODICS
C 2=TIME-INDEPENDENT NUMERICAL SHORT PERIODICS
C 3=ANALYTICAL SHORT PERIODICS
C
C JSPTHR CONTROL SWITCH FOR THIRD-BODY NUMERICAL SHORT
C PERIODICS.
C 0=NO THIRD BODY
C 1=TIME-DEPENDENT NUMERICAL SHORT PERIODICS
C 2=TIME-INDEPENDENT NUMERICAL SHORT PERIODICS
C 3=ANALYTICAL SHORT PERIODICS
C
C JDRAG CONTROL SWITCH FOR DRAG SHORT PERIODICS. *
C
C JSOLAR CONTROL SWITCH FOR SOLAR RADIATION PRESSURE
C SHORT PERIODICS. *
C
C J2SQSP CONTROL SWITCH FOR J2 SQUARED SHORT PERIODICS.
C
C NMAXSP MAXIMUM DEGREE FOR THE CENTRAL BODY FIELD THAT
C WILL BE USED IN THE DETERMINATION OF THE SHORT
C PERIODICS.
C
C MMAXSP MAXIMUM ORDER FOR THE CENTRAL BODY FIELD THAT
C WILL BE USED IN THE DETERMINATION OF THE SHORT
C PERIODICS.
C
C KSPNC(NPERT) NUMBER OF SHORT PERIODIC COEFFICIENTS.
C
C KSPPRT(NPERT) CONTROL SWITCH FOR SHORT PERIODIC PRINT OPTION.*
C
C NPERT PERTURBATION INDICATOR

```

HWIRE

AJG1324.GTDS.UPDATE.FORT

C		1=TIME-DEPENDENT CONTINUOUS PERTURBATIONS	00000580
C		2=TIME-INDEPENDENT CONTINUOUS PERTURBATIONS	00000590
C		3=DRAG PERTURBATIONS	00000600
C		4=SOLAR RADIATION PRESSURE PERTURBATIONS	00000610
C	IDRDR	I CONTROL SWITCH FOR CONSIDERING 2ND ORDER	00000620
C		DRAG EFFECTS.	00000630
C		0=NO 2ND ORDER DRAG EFFECTS	00000640
C		1=J2-DRAG EFFECTS	00000650
C		2=J2-DRAG AND DRAG-DRAG EFFECTS	00000660
C		3=J2-DRAG,DRAG-J2 AND DRAG-DRAG EFFECTS	00000670
C		DONE NUMERICALLY	00000680
C		4=J2-DRAG AND DRAG-DRAG EFFECTS DONE	00000690
C		NUMERICALLY, DRAG-J2 DONE ANALYTICALLY	00000700
C		5=ISZAK'S J2 HEIGHT CORRECTION AND ANALYTIC	00000710
C		DRAG-J2 EFFECTS.	00000720
C	NCHOJ2	I NUMBER OF J2 SHORT PERIODIC COEFFICIENTS TO BE	00000730
C		CONSIDERED IN 'HODRAG'.	00000740
C	NCHODR	I NUMBER OF DRAG SHORT PERIODIC COEFFICIENTS TO BE	00000750
C		CONSIDERED IN 'HODRAG'.	00000760
C			00000770
C		* 1=YES 2=NO	00000780
C		HWIRE FLAGS	00000790
C			00000800
C	JTMDEP	= 2	00000810
C	JTHIND	= 1	00000820
C	JDRAG	= 1	00000830
C	JSOLAR	= 2	00000840
C	J2SQSP	= 1	00000850
C			00000860
C	JSPCGB	= 2	00000870
C	NMAXSP	= NMAX	00000880
C	MMAXSP	= MMAX	00000890
C			00000900
C	JSPTHR	= 0	00000910
C			00000920
C	JSPPOS	= 2	00000930
C	IF(JSPTHR.EQ.1)	JSPPOS=1	00000940
C	JSPA	= 2	00000950
C	JSPB	= 2	00000960
C	JSPC	= 2	00000970
C	JSPGHA	= 2	00000980
C			00000990
C	KSPFOS	= 2	00001000
C	IF(JSPTHR.EQ.2)	KSPPOS=1	00001010
C	KSPA	= 2	00001020
C	KSPB	= 2	00001030
C	KSPC	= 2	00001040
C	KSPGHA	= 2	00001050
C			00001060
C	KSPNC(1)	= 7	00001070
C	KSPNC(2)	= 7	00001080
C	KSPNC(3)	= 7	00001090
C	KSFNC(4)	= 7	00001100
C			00001110
C	KSPFRT(1)	= 2	00001120
C	KSPFRT(2)	= 2	00001130
C	KSPFRT(3)	= 2	00001140

11

HWIRE

AJG1324.GTDS.UPDATE.FORT

C	KSPRT(4)= 2	00001150
		00001160
	IDRDR = 5	00001170
	NCHOJ2 = 4	00001180
	NCHODR = 4	00001190
C		00001200
	RETURN	00001210
	END	00001220

***** END OF MEMBER HWIRE

122 RECORDS *****

-

=

11

	SUBROUTINE ORBITV(INTFLG,*)	00000100
C		00000200
C	VERSION 2.2	00000300
C		00000400
C	PURPOSE	00000500
C	TO INTEGRATE FOR POSITION AND VELOCITY AT THE REQUEST TIME	00000600
C	USING THE VARIATION-OF-PARAMETERS ORBIT GENERATOR	00000700
C		00000800
C	CALLING SEQUENCE	00000900
C	CALL ORBITV(INTFLG,*)	00001000
C	INTFLG=1 RETURN	00001100
C	INTFLG=2 PERFORM VOP INTEGRATION	00001200
C		00001300
C	COMMON BLOCK VARIABLES	00001400
C	INPUT	00001500
C	H STEPSIZE	00001600
C	IND ARRAY OF CONTROL SWITCHES	00001700
C	NPART NUMBER OF PARTIALS REQUIRED	00001800
C	NSTR NUMBER OF BACK POINTS RECOPIED	00001900
C	NOPARM NUMBER OF ORBITAL ELEMENTS INTEGRATED	00002000
C	NORDER NUMBER OF BACK POINTS USED IN INTEGRATOR	00002100
C	IORDER(1) ORDER OF INTERPOLATION OF EQS. OF MOTION	00002200
C	IORDER(2) ORDER OF INTERPOLATION OF VARIATIONAL EQS.	00002300
C	STREG VALUE OF INDEPENDENT VARIABLE AT T=T(K)	00002400
C	I2NDOR 2ND ORDER AVERAGING SWITCH FOR DRAG WHICH	00002410
C	IS USED IN 'RTQUAD'	00002420
C		00002500
C		00002600
C	INPUT-OUTPUT	00002700
C	NCOND SECTIONING CONDITION FLAG	00002800
C	XXSUM FIRST SUM VECTOR OF DERIVATIVES	00002900
C	TTO OUTPUT REQUEST TIME	00003000
C	DPARRAY DERIVATIVE ARRAY	00003100
C	PARARY ELEMENT VECTOR ARRAY	00003200
C	VEPARY PARTIAL DERIVATIVE ARRAY	00003300
C	VEVOPD PARTIAL DERIVATIVE RATES ARRAY	00003400
C		00003500
C	OUTPUT	00003600
C	K DERIVATIVE ARRAY INDICATOR OF VALUE AT T=T(K)	00003700
C	PXTXO VARIATIONAL PARTIAL DERIVATIVES	00003800
C	T TIME FROM EPOCH OF K TH DERIVATIVE	00003900
C	XDTO S/C VELOCITY VECTOR AT TIME TTO	00004000
C	XTO S/C POSITION VECTOR AT TIME TTO	00004100
C		00004200
C		00004300
C	EXTERNAL REFERENCES	00004400
C	CSTEPX	00004500
C	SECHK	00004600
C	CROSSV	00004700
C	HEMITR	00004800
C	HERMIT	00004900
C	INTPAR	00005000
C	DALLPV	00005100
C	EQUHPV	00005200
C	IDLVP	00005300
C	DPEL2X	00005400
C	ANPART	00005500

ORBITV

AJG1324.GTDS.UPDATE.FORT

```

C          CELEM                                00005600
C          RKINTG                                00005610
C          SPEXEC                                00005620
C          PROGRAMMER                            00005700
C          R. W. NELSON(PROGRAMMED ORIGINAL ORBIT SUBROUTINE) 00005800
C          PROGRAM MODIFICATIONS                 00005900
C          4/1/72 ORIGINAL SUBROUTINE ORBITV BY A. C. LONG    00006000
C          7/15/73 MODIFIED BY A. C. LONG TO INCLUDE MORE COMMENTS 00006100
C          6/15/74 BY R.PAJERSKI- ADDED NEW ELEMENT SET(KEPLERIAN) 00006200
C          1/10/75 BY R.PAJERSKI- DELETED ABS.VALUE TEST     00006300
C          7/20/79 BY A.J. GREEN,CSDL - INCLUDE THE DETERMINATION 00006400
C          OF THE PARTIALS FOR IVOP=12,(APG AND SPFG)         00006410
C          7/30/79 BY A. BOBICK ,C.S.DRAPER LAB - TO INCLUDE R-K INTEG. 00006420
C          AND HERMIT INTERPOLATION OPTIONS                00006500
C          IMPLICIT REAL*8(A-H,O-Z)                    00006600
C          COMMON      TEMPPK(6,20),      PKFC(6,6)          00006700
C          COMMON/DCINT/ DPDCI(432),      INDCI(26)          00006800
C          COMMON/ FRC / DPFRC(1300),     INTFRC(47)         00006900
C          COMMON/INTEG/ DPINT(149),      INT(9)             00007000
C          COMMON/SECTN/ DPSEC(675),      INSEC(325)         00007100
C          COMMON/SWITCH/ INSWI(200)      00007200
C          COMMON/TIMREG/ DTRG(94)        00007300
C          COMMON/VEPART/ VEPAR(1800)    00007400
C          COMMON/WORKER/ DFWOR(3264),    INWOR(13)          00007500
C          DIMENSION  VPELMT(10),        DPARRY(15,10),     XXSUM(10),    00007600
C          1          IND(100),           XTO(3),           XDTO(3),    00007700
C          2          PXTXO(6,20),        IORDER(2),        VEPARY(15,6,20), 00007800
C          3          OSCELM(10)          00007900
C          DIMENSION  TREG(40),          U(4),             US(4)       00008000
C          DIMENSION  GM(11)             00008100
C          EQUIVALENCE (DPDCI(1),XTO(1)) , (DPDCI(4),XDTO(1)), 00008200
C          1          (DPDCI(7),FXTXO(1,1)) , (DPDCI(127),TTO), 00008300
C          2          (INDCI(2),NPART)      00008400
C          EQUIVALENCE (DPWOR(7),DPARRY(1,1)) , (DPWOR(2819),XXSUM(1)), 00008500
C          1          (DPWOR(3215),T)      , (DPWOR(2653),OSCELM(1)), 00008600
C          2          (DPWOR(3216),H)      , (INWOR(2),K),      00008700
C          3          (INWOR(3),NOPARM)    , (INWOR(13),NSTR),   00008800
C          4          (INWOR(10), IORDER)  , (DPWOR(2829),VPELMT(1)) 00008900
C          EQUIVALENCE (VEPAR(1),VEPARY(1,1,1)) 00009000
C          EQUIVALENCE (INT(1),NORDER)      , (INT(8),IORDER(1)) 00009100
C          EQUIVALENCE (INSWI(1),IND(1))    00009200
C          EQUIVALENCE (INSEC(313),NCOND)   00009300
C          EQUIVALENCE (STREG,DTRG(92))    , (TREG(1),DTRG(1)) 00009400
C          DIMENSION  PARARY(15,10)        00009500
C          EQUIVALENCE (DPWOR(157),PARARY(1,1)) 00009600
C          EQUIVALENCE (DPFRC(2),GM(1))    , (INTFRC(1),ICENT) 00009700
C          DIMENSION  VEVOP(6,20)         ,VEVOPD(15,6,20) , 00009800
C          *          XVSUM(6,20)          00009900
C          EQUIVALENCE (DPWOR(307)         ,VEVOP(1,1)) , 00010000
C          *          (DPWOR(427)         ,VEVOPD(1,1,1)) , 00010100
C          *          (DPWOR(2383)        ,XVSUM(1,1)) , 00010200

```

ORBITV

AJG1324.GTDS.UPDATE.FORT

```

*          (INW(5)          ,NEQ)          00010700
EQUIVALENCE (INSWI(54),NSTATE) ,(INSEC(315) ,MANDON) 00010800
C          00010900
C          00011000
      NX=NORDER+1          00011100
      STIME=TTO          00011200
      IND3=IND(3)          00011300
      IF(INTFLG.EQ.1)GO TO 180 00011400
C          00011500
C          TEST FOR TERMINAL SECTION 00011600
C          00011700
      20 IF(NCONDT.GT.100) GO TO 999 00011800
C          00011900
C          TEST FOR SECTIONING WITH INTERVENING PRINT 00012000
C          00012100
      IF(NCONDT.LT.0) GO TO 150 00012200
C          00012300
C          IS REQUEST TIME LESS THEN CURRENT TIME, IF SO INTERPOLATE 00012400
C          00012500
      IF(IND3.EQ.7) T=TREG(K-2) 00012600
      40 IF(DABS(TTO).LE.DABS(T)) GO TO 168 00012700
C          00012800
C          SET PARAMETERS TO INTEGRATE ANOTHER STEP 00012900
C          00013000
C          *** UPDATE INDEPENDENT VARIABLE 00013100
C          00013200
      STREG = STREG + H 00013300
C          00013400
C          *** IF DOING R-K INTEGRATION SET K TO 15 AND INTEGRATE 00013500
C          00013600
      IF (IND(2) .NE. 4) GO TO 50 00013700
      K = 15 00013800
      CALL RKINTG(IERR) 00013900
      GO TO 150 00014000
C          00014100
C          *** CONTINUE HERE FOR STANDARD ADAMS METHOD (CSTEPX) 00014200
C          00014300
      50 K=K+1 00014400
C          00014500
C          IS THE DERIVATIVE ARRAY FULL, IF SO RECOPY THE LAST NSTR ROWS 00014600
C          00014700
      IF(K.LE.15) GO TO 110 00014800
      DO 100 I=1,NSTR 00014900
      NBACK = 15 - NSTR + I 00015000
      IF(IND3.NE.6.AND.IND3.NE.7) GO TO 90 00015100
      TREG(I)=TREG(NBACK) 00015200
      90 CONTINUE 00015300
      DO 100 J=1,NOPARM 00015400
      DPARRY(I,J)=DPARRY(NBACK,J) 00015500
      IF(IND3.EQ.7.AND.IND(26).NE.1) PARARY(I,J)=PARARY(NBACK,J) 00015600
C          00015700
C          00015800
      IF (NEQ.LE.0) GO TO 100 00015900
      DO 95 L=1,NEQ 00016000
      VEVOPD(I,J,L) = VEVOPD(15-NSTR+I,J,L) 00016100
      95 CONTINUE 00016200
      100 CONTINUE 00016300
      K=NSTR+1

```


C		00016400
C	INTEGRATE TO NEXT STEP	00016500
C		00016600
C	110 CALL CSTEPX(IERR)	00016700
C		00016800
C	CHECK FOR SECTIONING	00016900
C		00017000
C	150 CALL SECHK(&160,&168,&160)	00017100
C	GO TO 40	00017200
C		00017300
C	SECTIONING HAS OCCURRED	00017400
C		00017500
C	160 CALL CROSSV(MSGERR,&165)	00017600
C	GO TO 20	00017700
C		00017800
C	ERROR RETURN IF MAXIMUM CORRECTOR ITERATIONS WERE VIOLATED OR	00017900
C	ERROR FROM CROSSV	00018000
C		00018100
C	165 RETURN1	00018200
C		00018300
C	*** SKIP IF NOT USING R-K INTEGRATION AND HERMITE INTERPOLATION	00018400
C		00018500
C	168 IF (IND(2) .NE. 4) GO TO 169	00018600
C	CALL HERMIT(VPELMT,PARARY,DPARRY,NOPARM,STIME,H,STREG,IORDER(1))	00018700
C	GO TO 170	00018800
C		00018900
C	IS THIS A KS RUN, IF SO CALL THE TIME INTERPOLATOR	00019000
C		00019100
C	169 IF(IND3.EQ.6) CALL HEMITR(STIME,TTO,K,H,STREG,TREG)	00019200
C		00019300
C	IS THIS A DS RUN,IF SO CALL THE INTERPOLATOR	00019400
C		00019500
C	IF(IND3.EQ.7) CALL HEMIDS(STIME,TTO,K,H,STREG,TREG,NX,XTO,XDTO)	00019600
C	IF(IND3.EQ.7) GO TO 180	00019700
C		00019800
C	INTERPOLATE FOR ORBITAL ELEMENTS AT THE REQUEST TIME	00019900
C		00020000
C	CALL INTPAR(VPELMT,DPARRY,XXSUM,STREG,STIME,K,.FALSE.,NX,NOPARM,H)	00020100
C		00020200
C	BRANCH TO THE APPROPRIATE SUBROUTINE FOR COMPUTATION OF POSITION	00020300
C	AND VELOCITY FROM THE ORBITAL ELEMENTS	00020400
C		00020500
C	170 IF(IND3.GT.10) IND3=IND3-10	00020600
C	GO TO (171,172,172,173,173,174,171,176),IND3	00020700
C	171 CALL DALLPV(VPELMT,XTO,XDTO,JERROR)	00020800
C	GO TO 180	00020900
C		00020910
C	DETERMINE THE OSCULATING EQUINOCTIAL ORBITAL ELEMENTSPRIOR	00020920
C	TO DETERMINING POSITION AND VELOCITY	00020930
C		00020940
C	172 CALL SPEXEC	00020950
C	CALL EQUHPV(OSCELM,XTO,XDTO,JERROR,IND3)	00021000
C	GO TO 180	00021100
C	173 CALL IDLPV(VPELMT,XTO,XDTO,IND3)	00021200
C	GO TO 180	00021300
C	174 CALL DPEL2X(VPELMT,STIME,U,US,XTO,XDTO,SE2,CE2)	00021400
C	GO TO 180	00021500

ORBITV

AJG1324.GTDS.UPDATE.FORT

```

176 CALL CELEM(VPELMT,GM(1CENT),XTO,XDTO) 00021600
C 00021700
C ARE ANALYTIC PARTIALS REQUIRED 00021800
C 00021900
180 IF(NPART.NE.0) GO TO 999 00022000
IF (IND(4).EQ.1) GO TO 195 00022100
IF (NSTATE.EQ.0) GO TO 190 00022200
C 00022300
C CALCULATE ANALYTIC STATE PARTIALS 00022400
C 00022500
CALL ANPART(XTO,XDTO,TT0,2,PXTX0) 00022600
C 00022700
188 IF (NEQ.LE.0) GO TO 999 00022800
C 00022900
C SET UP TO COMPUTE DYNAMIC PARTIALS FOR NON-STATE PARAMETERS 00023000
C WHEN ANALYTIC OPTION IS ON. 00023100
C 00023200
190 N = NSTATE 00023300
GO TO 245 00023400
C 00023500
C TEST FOR MANEUVERS 00023600
C 00023700
195 N = 0 00023800
IF (MANDON.EQ.0) GO TO 245 00023900
C 00024000
C SET UP PARTIAL OUTPUT FOR NON-MANEUVER CASE 00024100
C 00024200
245 DO 250 I=1,NEQ 00024300
C *** IF DOING R-K CALL HERMIT INTERPOLATOR OTHERWISE INTPAR 00024400
IF (IND(2) .NE. 4) GO TO 247 00024500
CALL HERMIT(TEMPPK(1,N+I),VEPARY(1,1,I),VEVOPD(1,1,1), 00024600
* NOPARM,STIME,H,STREG,IORDER(2)) 00024700
GO TO 250 00024800
247 CALL INTPAR (TEMPPK(1,N+I),VEVOPD(1,1,I),XVSUM(1,I),STREG, 00024900
* STIME,K,.TRUE.,NX,NOPARM,H) 00025000
250 CONTINUE 00025100
C 00025200
C COMPUTE CARTESIAN VARIATIONAL PARTIALS FROM KEPLERIAN 00025300
C VOP VARIATIONSL PARTIALS. 00025400
C 00025500
IF (IND(3) .EQ. 8) GO TO 300 00025510
IF (IND(3) .NE. 12) GO TO 999 00025520
CALL GMAT(TEMPK) 00025530
CALL EPART(XTO,XDTO,PKPC) 00025540
GO TO 400 00025550
300 CALL KPART (XTO,PKPC) 00025600
CALL INV2 (6) 00025700
400 CALL MATHUL (PKPC,TEMPPK(1,N+1),PXTX0(1,N+1),6,6,20-N) 00025800
C 00025900
C 00026000
999 RETURN 00026100
END 00026200

```

***** END OF MEMBER ORBITV 280 RECORDS *****

RTQUAD

AJG1324.GTDS.UPDATE.FORT

```

SUBROUTINE RTQUAD(QUAD,AA,BB,NQUAD,ISPNC)                                00000010
C                                                                           00000020
C VERSION OF 19 MARCH 1979 IMPLEMENTED AT CSDL ON AMDAHL 470 V6        00000030
C                                                                           00000040
C PURPOSE                                                                 00000050
C EVALUATES A DEFINITE INTEGRAL WITH A GUASSIAN NUMERICAL QUAD-        00000060
C RATURE FORMULA WHEN FIRST ORDER SHORT PERIODICS ARE INCLUDED          00000070
C IN THE ORBITAL ELEMENTS.                                              00000080
C                                                                           00000090
C                                                                           00000100
C PARAMETERS                                                             00000110
C   QUAD   O   VALUE OF THE QUADRATURE.                                00000120
C   AA     I   LOWER LIMIT OF INTEGRATION.                             00000130
C   BB     I   UPPER LIMIT OF INTEGRATION.                             00000140
C   NQUAD  I   QUADRATURE ORDER PARAMETER.                            00000150
C   ISPNC  I   NUMBER OF COEFFICIENTS                                  00000160
C                                                                           00000170
C /WORKER/                                                                00000180
C   DPARDT I   PRECISION ELEMENT RATES COMPUTED IN *GQFUN*.           00000190
C   NOPARM I   NUMBER OF ORBITAL ELEMENTS.                             00000200
C   VPELMT I   MEAN ORBITAL ELEMENT VECTOR.                            00000210
C   I2NDOR I   2ND ORDER SWITCH WHICH IS USED IN EQINT.              00000220
C               1=2ND ORDER EFFECTS ARE BEING CONSIDERED IN           00000230
C               SUBROUTINE 'RTQUAD'.                                    00000240
C               2=2ND ORDER EFFECTS ARE NOT BEING CONSIDERED          00000250
C   ROA    O   THE MEAN R/A.                                           00000260
C   XML    O   THE MEAN-MEAN LONGITUDE.                                  00000270
C                                                                           00000280
C /SPCOEF/                                                                00000290
C   CQUAD  I   VALUE OF C COEFFICIENT                                  00000300
C   DQUAD  I   VALUE OF D COEFFICIENT                                  00000310
C                                                                           00000320
C                                                                           00000330
C EXTERNAL REFERENCES                                                    00000340
C   GQFUN   COMPUTES PRECISION ORBITAL ELEMENT RATES.                  00000350
C                                                                           00000360
C REFERENCES                                                              00000370
C   GTDS SUBROUTINE QUADRT                                              00000380
C                                                                           00000390
C   "A FOURIER SERIES FORMULATION OF THE SHORT PERIODIC VARIATIONS      00000400
C   IN TERMS OF EQUINOCTIAL ELEMENTS." BY A.J. GREEN AND P.J. CEFOLA 00000410
C                                                                           00000420
C ANALYSIS                                                                00000430
C   ANDREW J. GREEN, CPT, U.S. ARMY, CSDL                               00000440
C                                                                           00000450
C PROGRAMMER                                                              00000460
C   ANDREW J. GREEN, CPT, U.S. ARMY, CSDL                               00000470
C                                                                           00000480
C *****START PROGRAM*****00000490
C                                                                           00000500
C                                                                           00000510
C   IMPLICIT REAL*8(A-H,O-Z)                                           00000520
C   COMMON/WORKER/ RWORK(3264) ,IWORK(12)                               00000530
C   DIMENSION      QUAD(10) ,DPARDT(10),VPELMT(10),TEMELM(10)          00000540
C   DIMENSION      IXWBEG(7) ,IXWEND(7)                                 00000550
C   EQUIVALENCE    (ROA ,RWORK(2670) ),                                00000560
C   *              (XML ,RWORK(2672) ),                                00000570

```

RTQUAD

AJG1324.GTDS.UPDATE.FORT

```

*          (VPELMT(1)          ,RWORK(2829)          ),          00000580
*          (DPARDT(1)          ,RWORK(2840)          ),          00000590
*          (NOPARM             ,IWORK(3)           ),          00000600
*          (I2NDOR             ,IWORK(10)          ),          00000610
COMMON/SPCOEF/ CQUAD(10,10),DQUAD(10,10)          00000620

```

C

```

DIMENSION      XTAB(96) ,WTAB(96)          00000640
DIMENSION      XTAB1 ( 9) ,XTAB10 (10)     ,          00000650
*             XTAB20 (10) ,XTAB30 (10)     ,          00000660
*             XTAB40 (10) ,XTAB50 (10)     ,          00000670
*             XTAB60 (10) ,XTAB70 (10)     ,          00000680
*             XTAB80 (10) ,XTAB90 ( 7)     ,          00000690
DIMENSION      WTB1 ( 9) ,WTB10 (10)     ,          00000700
*             WTB20 (10) ,WTB30 (10)     ,          00000710
*             WTB40 (10) ,WTB50 (10)     ,          00000720
*             WTB60 (10) ,WTB70 (10)     ,          00000730
*             WTB80 (10) ,WTB90 ( 7)     ,          00000740

```

C

```

EQUIVALENCE   (XTB1 (1) ,XTAB( 1)      ),          00000760
*             (XTB10 (1) ,XTAB( 10)     ),          00000770
*             (XTB20 (1) ,XTAB( 20)     ),          00000780
*             (XTB30 (1) ,XTAB( 30)     ),          00000790
*             (XTB40 (1) ,XTAB( 40)     ),          00000800
*             (XTB50 (1) ,XTAB( 50)     ),          00000810
*             (XTB60 (1) ,XTAB( 60)     ),          00000820
*             (XTB70 (1) ,XTAB( 70)     ),          00000830
*             (XTB80 (1) ,XTAB( 80)     ),          00000840
*             (XTB90 (1) ,XTAB( 90)     ),          00000850
EQUIVALENCE   (WTB1 (1) ,WTAB( 1)      ),          00000860
*             (WTB10 (1) ,WTAB( 10)     ),          00000870
*             (WTB20 (1) ,WTAB( 20)     ),          00000880
*             (WTB30 (1) ,WTAB( 30)     ),          00000890
*             (WTB40 (1) ,WTAB( 40)     ),          00000900
*             (WTB50 (1) ,WTAB( 50)     ),          00000910
*             (WTB60 (1) ,WTAB( 60)     ),          00000920
*             (WTB70 (1) ,WTAB( 70)     ),          00000930
*             (WTB80 (1) ,WTAB( 80)     ),          00000940
*             (WTB90 (1) ,WTAB( 90)     ),          00000950

```

C
C
C

ABSCISSAE FOR ORDER 12 IN SEQUENCE 12.

```

DATA XTB 1    /.1252334085114689D+00      ,          00000980
2             .3678314989981802D+00      ,          00000990
3             .5873179542866174D+00      ,          00001000
4             .7699026741943047D+00      ,          00001010
5             .9041172563704749D+00      ,          00001020
6             .9815606342467192D+00      ,          00001030

```

C
C
C

ABSCISSAE FOR ORDER 16 IN SEQUENCE 16.

```

7             .9501250983763743D-01      ,          00001050
8             .2816035507792589D+00      ,          00001060
9             .4580167776572274D+00      /          00001070
DATA XTB 10   /.6178762444026437D+00      ,          00001080
1             .7554044083550030D+00      ,          00001090
2             .8656312023878317D+00      ,          00001100
3             .9445750230732326D+00      ,          00001110

```

I

I

I

11

RTQUAD

AJG1324.GTDS.UPDATE.FORT

	4	.9894009349916499D+00	,	00001150
C				00001160
C		ABSCISSAE FOR ORDER 20 IN SEQUENCE 20.		00001170
C				00001180
	5	.7652652113349732D-01	,	00001190
	6	.2277858511416451D+00	,	00001200
	7	.3737060887154195D+00	,	00001210
	8	.5108670019508271D+00	,	00001220
	9	.6360536807265150D+00	/	00001230
	DATA XTB 20	/ .7463319064601508D+00	,	00001240
	1	.8391169718222188D+00	,	00001250
	2	.9122344282513259D+00	,	00001260
	3	.9639719272779138D+00	,	00001270
	4	.9931285991850949D+00	,	00001280
C				00001290
C		ABSCISSAE FOR ORDER 24 IN SEQUENCE 24.		00001300
C				00001310
	5	.6405689286260562D-01	,	00001320
	6	.1911188674736163D+00	,	00001330
	7	.3150426796961634D+00	,	00001340
	8	.4337935076260451D+00	,	00001350
	9	.5454214713888395D+00	/	00001360
	DATA XTB 30	/ .6480936519369756D+00	,	00001370
	1	.7401241915785544D+00	,	00001380
	2	.8200019859739029D+00	,	00001390
	3	.8864155270044010D+00	,	00001400
	4	.9382745520027328D+00	,	00001410
	5	.9747285559713095D+00	,	00001420
	6	.9951872199970214D+00	,	00001430
C				00001440
C		ABSCISSAE FOR ORDER 32 IN SEQUENCE 32.		00001450
C				00001460
	7	.4830766568773832D-01	,	00001470
	8	.1444719615827965D+00	,	00001480
	9	.2392873622521371D+00	/	00001490
	DATA XTB 40	/ .3318686022821276D+00	,	00001500
	1	.4213512761306353D+00	,	00001510
	2	.5068999089322294D+00	,	00001520
	3	.5877157572407623D+00	,	00001530
	4	.6630442669302152D+00	,	00001540
	5	.7321821187402897D+00	,	00001550
	6	.7944837959679424D+00	,	00001560
	7	.8493676137325700D+00	,	00001570
	8	.8963211557660521D+00	,	00001580
	9	.9349060759377397D+00	/	00001590
	DATA XTB 50	/ .9647622555875064D+00	,	00001600
	1	.9856115115452683D+00	,	00001610
	2	.9972638618494816D+00	,	00001620
C				00001630
C		ABSCISSAE FOR ORDER 40 IN SEQUENCE 40.		00001640
C				00001650
	3	.3877241750605082D-01	,	00001660
	4	.1160840706752552D+00	,	00001670
	5	.1926975807013711D+00	,	00001680
	6	.2681521850072537D+00	,	00001690
	7	.3419940908257585D+00	,	00001700
	8	.4137792043716050D+00	,	00001710

11

11

RTQUAD

AJG1324.GTDS.UPDATE.FORT

9		.4830758016861787D+00	/	00001720
	DATA XTB 60	/.5494671250951282D+00	,	00001730
1		.6125538896679802D+00	,	00001740
2		.6719566846141795D+00	,	00001750
3		.7273182551899271D+00	,	00001760
4		.7783056514265194D+00	,	00001770
5		.8246122308333117D+00	,	00001780
6		.8659595032122595D+00	,	00001790
7		.9020988069688743D+00	,	00001800
8		.9328128082786765D+00	,	00001810
9		.9579168192137917D+00	/	00001820
	DATA XTB 70	/.9772599499837743D+00	,	00001830
1		.9907262386994570D+00	,	00001840
2		.9982377097105592D+00	,	00001850
				00001860
		ABSCISSAE FOR ORDER 48 IN SEQUENCE 48.		00001870
				00001880
3		.3239017096286936D-01	,	00001890
4		.9700469920946270D-01	,	00001900
5		.1612223560688917D+00	,	00001910
6		.2247637903946891D+00	,	00001920
7		.2873624873554556D+00	,	00001930
8		.3487558852921607D+00	,	00001940
9		.4086864819907167D+00	/	00001950
	DATA XTB 80	/.4669029047509584D+00	,	00001960
1		.5231609747222330D+00	,	00001970
2		.5772247260839727D+00	,	00001980
3		.6288673967765136D+00	,	00001990
4		.6778723796326639D+00	,	00002000
5		.7240341309238145D+00	,	00002010
6		.7671590325157403D+00	,	00002020
7		.8070662040294426D+00	,	00002030
8		.8435882616243935D+00	,	00002040
9		.8765720202742479D+00	/	00002050
	DATA XTB 90	/.9058791367155697D+00	,	00002060
1		.9313866907065543D+00	,	00002070
2		.9529877031604309D+00	,	00002080
3		.9705915925462472D+00	,	00002090
4		.9841245837228269D+00	,	00002100
5		.9935301722663509D+00	,	00002110
6		.9987710072524261D+00	/	00002120
				00002130
		WEIGHTS FOR ORDER 12 IN SEQUENCE 12.		00002140
				00002150
	DATA WTB 1	/.2491470458134026D+00	,	00002160
2		.2334925365383548D+00	,	00002170
3		.2031674267230659D+00	,	00002180
4		.1600783285433462D+00	,	00002190
5		.1069393259953184D+00	,	00002200
6		.4717533638651183D-01	,	00002210
				00002220
		WEIGHTS FOR ORDER 16 IN SEQUENCE 16.		00002230
				00002240
7		.1894506104550685D+00	,	00002250
8		.1826034150449236D+00	,	00002260
9		.1691565193950025D+00	/	00002270
	DATA WTB 10	/.1495959888165767D+00	,	00002280

C
C
C

C
C
C

C
C
C

11

11

RYQUAD

AJG1324.GTDS.UPDATE.FORT

1	.1246289712555339D+00	,	00002290
2	.9515851168249277D-01	,	00002300
3	.6225352393864789D-01	,	00002310
4	.2715245941175409D-01	,	00002320
C			00002330
C			00002340
C			00002350
	WEIGHTS FOR ORDER 20 IN SEQUENCE 20.		
5	.1527533871307258D+00	,	00002360
6	.1491729864726037D+00	,	00002370
7	.1420961093183920D+00	,	00002380
8	.1316886384491766D+00	,	00002390
9	.1181945319615184D+00	/	00002400
DATA WT B 20	/.1019301198172404D+00	,	00002410
1	.8327674157670474D-01	,	00002420
2	.6267204833410905D-01	,	00002430
3	.4060142980038694D-01	,	00002440
4	.1761400713915212D-01	,	00002450
C			00002460
C			00002470
C			00002480
	WEIGHTS FOR ORDER 24 IN SEQUENCE 24.		
5	.1279381953467521D+00	,	00002490
6	.1258374563468283D+00	,	00002500
7	.1216704729278034D+00	,	00002510
8	.1155056680537256D+00	,	00002520
9	.1074442701159656D+00	/	00002530
DATA WT B 30	/.9761865210411388D-01	,	00002540
1	.8619016153195327D-01	,	00002550
2	.7334648141108030D-01	,	00002560
3	.5929858491543678D-01	,	00002570
4	.4427743881741981D-01	,	00002580
5	.2853138862693366D-01	,	00002590
6	.1234122979998720D-01	,	00002600
C			00002610
C			00002620
C			00002630
	WEIGHTS FOR ORDER 32 IN SEQUENCE 32.		
7	.9654008851472780D-01	,	00002640
8	.9563872007927485D-01	,	00002650
9	.9384439908080455D-01	/	00002660
DATA WT B 40	/.9117387869576388D-01	,	00002670
1	.8765209300440391D-01	,	00002680
2	.8331192422694675D-01	,	00002690
3	.7819389578707030D-01	,	00002700
4	.7234579410884850D-01	,	00002710
5	.658222277636184D-01	,	00002720
6	.5868409347853555D-01	,	00002730
7	.5099805926237618D-01	,	00002740
8	.4283589802222668D-01	,	00002750
9	.3427386291302143D-01	/	00002760
DATA WT B 50	/.2539206530926206D-01	,	00002770
1	.1627439473090567D-01	,	00002780
2	.7018610009470096D-02	,	00002790
C			00002800
C			00002810
C			00002820
	WEIGHTS FOR ORDER 40 IN SEQUENCE 40.		
3	.7750594797842481D-01	,	00002830
4	.7703981816424796D-01	,	00002840
5	.7611036190062624D-01	,	00002850

-

C
C
C

11

RTQUAD

AJG1324.GTDS.UPDATE.FORT

6	.7472316905796826D-01	,	00002860
7	.7288658239580405D-01	,	00002870
8	.7061164739128677D-01	,	00002880
9	.6791204581523390D-01	/	00002890
DATA WTB 60	/.6480401345660103D-01	,	00002900
1	.6130624249292894D-01	,	00002910
2	.5743976909939155D-01	,	00002920
3	.5322784698393682D-01	,	00002930
4	.4869590763507223D-01	,	00002940
5	.4387090818567327D-01	,	00002950
6	.3878216797447202D-01	,	00002960
7	.3346019528254785D-01	,	00002970
8	.2793700693002340D-01	,	00002980
9	.2224584919416696D-01	/	00002990
DATA WTB 70	/.1642105838190789D-01	,	00003000
1	.1049828453115281D-01	,	00003010
2	.4521277098533191D-02	,	00003020

C
C
C

WEIGHTS FOR ORDER 48 IN SEQUENCE 48.

3	.6473769681268392D-01	,	00003030
4	.6446616443595007D-01	,	00003040
5	.6392423858464819D-01	,	00003050
6	.6311419228625402D-01	,	00003060
7	.6203942315989266D-01	,	00003070
8	.6070443916589389D-01	,	00003080
9	.5911483969839564D-01	/	00003090
DATA WTB 80	/.5727729210040321D-01	,	00003100
1	.5519950369998416D-01	,	00003110
2	.5289018948519367D-01	,	00003120
3	.5035903555385447D-01	,	00003130
4	.4761665849249047D-01	,	00003140
5	.4467456085669428D-01	,	00003150
6	.4154508294346475D-01	,	00003160
7	.3824135106583071D-01	,	00003170
8	.3477722256477044D-01	,	00003180
9	.3116722783279809D-01	/	00003190
DATA WTB 90	/.2742650970335695D-01	,	00003200
1	.2357076083932438D-01	,	00003210
2	.1961616045735553D-01	,	00003220
3	.1557931572294385D-01	,	00003230
4	.1147723457923454D-01	,	00003240
5	.7327553901276262D-02	,	00003250
6	.3153346052305839D-02	/	00003260

-C

DATA IXWBEG	/1	,7	,15	,25	,37	,00003300
*	53	,73	/			,00003310
DATA IXWEND	/6	,14	,24	,36	,52	,00003320
*	72	,96	/			,00003330

C
C
C

INITIALIZATION

I2NDOR=1	00003340
NOPAR=NOPARM-1	00003350
XX=(BB+AA)/2.DO	00003360
DD=(BB-AA)/2.DO	00003370
DO 1 I=1,NOPARM	00003380
	00003390
	00003400
	00003410
	00003420

||

RTQUAD

AJG1324.GTDS.UPDATE.FORT

```
      QUAD(I)=0.D0                                00003430
      TEMELM(I)=VPELMT(I)                        00003440
1 CONTINUE                                       00003450
C                                                00003460
      IBEG=IXWBEG(NQUAD)                          00003470
      IEND=IXWEND(NQUAD)                          00003480
      INDEX=IEND                                  00003490
C                                                00003500
C          ACCUMULATE THE QUADRATURE SUM OVER THE FIRST HALF OF 00003510
C          THE INTERVAL.                            00003520
3 CONTINUE                                       00003530
C                                                00003540
C          DETERMINE THE OSCULATING ELEMENTS TO 1ST ORDER.    00003550
C                                                00003560
C          DETERMINE MEAN ECCENTRIC LONGITUDE.                00003570
C                                                00003580
      EL=XX-DD*XTAB(INDEX)                         00003590
      XML=EL-TEMELM(3)*DSIN(EL)+TEMELM(2)*DCOS(EL) 00003600
C                                                00003610
C          INITIALIZE THE OSCULATING ELEMENTS.                00003620
C                                                00003630
      DO 4 I=1,NOPAR                               00003640
      VPELMT(I)=TEMELM(I)                          00003650
4 CONTINUE                                       00003660
      VPELMT(NOPARM)=XML                           00003670
C                                                00003680
      DO 6 J=1,ISFNC                               00003690
      TT=J                                          00003700
      TTML= TT*XML                                 00003710
      DSJ = DSIN(TTML)                            00003720
      DCJ = DCOS(TTML)                            00003730
      DO 5 I=1,NOPARM                              00003740
      VPELMT(I) = VPELMT(I) + CQUAD(I,J)*DSJ-DQUAD(I,J)*DCJ 00003750
5 CONTINUE                                       00003760
6 CONTINUE                                       00003770
C                                                00003780
C          COMPUTE THE R/A FACTOR.                            00003790
C                                                00003800
      ROA=1.D0-TEMELM(3)*DCOS(EL)-TEMELM(2)*DSIN(EL) 00003810
C                                                00003820
C          CALL GQFUN(EL)                                    00003830
C          WGHT=WTAB(INDEX)                                00003840
C          DO 7 I=1,NOPARM                                  00003850
C          QUAD(I)=QUAD(I)+WGHT*DPARDT(I)                00003860
7 CONTINUE                                       00003870
      INDEX=INDEX-1                                00003880
      IF (INDEX.GE.IBEG) GO TO 3                   00003890
C                                                00003900
C          IF (XTAB(IBEG).NE.0.D0) GO TO 8                00003910
C          INDEX=IBEG                                      00003920
C                                                00003930
C          ACCUMULATE THE QUADRATURE SUM OVER THE SECOND HALF OF 00003940
C          THE INTERVAL.                            00003950
C          00003960
8 CONTINUE                                       00003970
      INDEX=INDEX+1                                00003980
C                                                00003990
```

RTQUAD

AJG1324.GTDS.UPDATE.FORT

```

C      DETERMINE THE OSCULATING ELEMENTS TO 1ST ORDER.          00004000
C
C      DETERMINE MEAN ECCENTRIC LONGITUDE.                        00004010
C
C      EL=XX+DD*XTAB(INDEX)                                       00004020
C      XML=EL-TEMELM(3)*DSIN(EL)+TEMELM(2)*DCOS(EL)             00004030
C
C      INITIALIZE THE OSCULATING ELEMENTS.                        00004040
C
C      DO 9 I=1,NOPARM                                             00004050
C      VPFLMT(I)=TEMELM(I)                                        00004060
C      9 CONTINUE                                                 00004070
C      VPFLMT(NOPARM)=XML                                         00004080
C
C      DO 11 J=1,ISPNC                                             00004090
C      TT=J                                                        00004100
C      TTML= TT*XML                                               00004110
C      DSJ = DSIN(TTML)                                           00004120
C      DCJ = DCOS(TTML)                                           00004130
C      DO 10 I=1,NOPARM                                           00004140
C      VPFLMT(I) = VPFLMT(I) + CQUAD(I,J)*DSJ-DQUAD(I,J)*DCJ   00004150
C      10 CONTINUE                                               00004160
C      11 CONTINUE                                               00004170
C
C      COMPUTE THE R/A FACTOR.                                     00004180
C
C      ROA=1.D0-TEMELM(3)*DCOS(EL)-TEMELM(2)*DSIN(EL)           00004190
C
C      CALL GQFUN(EL)                                             00004200
C      WGHT=WTAB(INDEX)                                           00004210
C      DO 12 I=1,NOPARM                                           00004220
C      QUAD(I)=QUAD(I)+WGHT*DPARDT(I)                             00004230
C      12 CONTINUE                                               00004240
C      IF (INDEX.LT.IEND) GO TO 8                                  00004250
C
C      RETURN THE VALUE OF THE QUADRATURE AND MEAN ELEMENTS.    00004260
C
C      DO 13 I=1,NOPARM                                           00004270
C      QUAD(I)=DD*QUAD(I)                                         00004280
C      VPFLMT(I)=TEMELM(I)                                        00004290
C      13 CONTINUE                                               00004300
C      IENDCR=2                                                    00004310
C      RETURN                                                     00004320
C
C      END                                                         00004330
C
C      END                                                         00004340
C
C      END                                                         00004350
C
C      END                                                         00004360
C
C      END                                                         00004370
C
C      END                                                         00004380
C
C      END                                                         00004390
C
C      END                                                         00004400
C
C      END                                                         00004410
C
C      END                                                         00004420
C
C      END                                                         00004430
C
C      END                                                         00004440

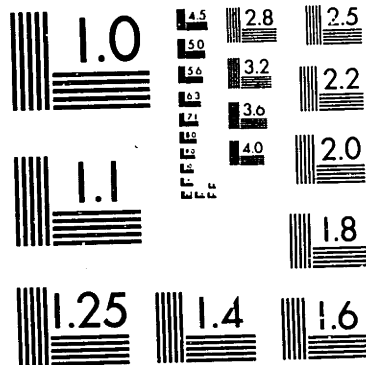
```

***** END OF MEMBER RTQUAD

444 RECORDS *****

=

C	SUBROUTINE SPCOTO		00000010
C			00000020
C	VERSION OF 20 JULY 1979 IMPLEMENTED AT CSDL ON AN AMDAHL 470 V6.		00000030
C			00000040
C	PURPOSE		00000050
C			00000060
C	TO DETERMINE THE TOTAL SHORT PERIODIC COEFFICIENTS.		00000070
C			00000080
C	PARAMETERS		00000090
C			00000100
C	/ESTFLG/		00000110
C			00000120
C	KCPSPP I CONTROL SWITCH FOR CONTINUOUS TIME-INDEPENDENT		00000130
C	PERTURBATIONS IN THE SHORT PERIODIC PARTIALS.*		00000140
C	KCBSPP I CONTROL SWITCH FOR CENTRAL BODY PERTURBATIONS		00000150
C	IN THE SHORT PERIODIC PARTIALS.*		00000160
C	KTBSPP I CONTROL SWITCH FOR THIRD-BODY PERTURBATIONS IN		00000170
C	THE SHORT PERIODIC PARTIALS.*		00000180
C	KDRSPP I CONTROL SWITCH FOR DRAG PERTURBATIONS IN THE		00000190
C	SHORT PERIODIC PARTIALS.*		00000200
C	KSRSP I CONTROL SWITCH FOR SOLAR RADIATION PRESSURE		00000210
C	PERTURBATIONS IN THE SHORT PERIODIC PARTIALS.*		00000220
C	NVARSP I MAXIMUM DEGREE OF THE CENTRAL BODY GRAVITATIONAL		00000230
C	FIELD TO BE CONSIDERED IN THE SHORT PERIODIC		00000240
C	GENERATOR.		00000250
C			00000260
C	/SFCOEF/		00000270
C			00000280
C	CQUAD O ARRAY OF C SHORT PERIODIC COEFFICIENT.		00000290
C	DQUAD O ARRAY OF D SHORT PERIODIC COEFFICIENT.		00000300
C			00000310
C	/FRC/		00000320
C			00000330
C	NBODY I NUMBER OF SOLAR SYSTEM BODIES CONSIDERED.		00000340
C	ISUN I SOLAR VECTOR INDICATOR.		00000350
C	GM I GRAVITATIONAL CONSTANT TIMES THE MASS OF THE		00000360
C	SOLAR SYSTEM BODY.		00000370
C	NMAX O MAXIMUM DEGREE OF THE CENTRAL BODY GRAVITATIONAL		00000380
C	FIELD.		00000390
C	MMAX O MAXIMUM ORDER OF THE CENTRAL BODY GRAVITATIONAL		00000400
C	FIELD.		00000410
C			00000420
C	/ANAVIN/		00000430
C			00000440
C	ITHIRD O THIRD-BODY AVERAGING OPTION.		00000450
C	POTENTIALS OF THE NONCENTRAL BODIES.		00000460
C	JTWOSQ O SECOND-ORDER J2 PERTURBATION CONTRL SWITCH.		00000470
C	IDRAG O QUADRATURE ORDER CONTROL SWITCH FOR DRAG.		00000480
C	ISOLAR O QUADRATURE ORDER CONTROL SWITCH FOR SOLAR		00000490
C	RADIATION PRESSURE.		00000500
C	ICORR O CONTROL SWITCH FOR SOLAR RADIATION PRESSURE.*		00000510
C	IDRDR O CONTROL SWITCH FOR 2ND ORDER DRAG EFFECTS.		00000520
C	KSPNC I ARRAY OF THE NUMBER OF SHORT PERIODIC		00000530
C	COEFFICIENTS.		00000540
C			00000550
C	/SWITCH/		00000560
C			00000570



MICROCOPY RESOLUTION TEST CHART
NATIONAL BUREAU OF STANDARDS-1963-A

20X

NOTICE THIS MATERIAL MAY BE PROTECTED BY
COPYRIGHT LAW (TITLE 17 U.S. CODE)

SFCOTO

AJG1324.GTDS.UPDATE.FORT

```

C      IRESON      0      CENTRAL BODY FIELD CONTROL SWITCH.      00000580
C      2=NXH FIELD      00000590
C      4=NO CENTRAL BODY FIELD      00000600
C      00000610
C      /WORKER/      00000620
C      00000630
C      VPELMT      I/O      ARRAY OF THE MEAN ELEMENTS.      00000640
C      XMEAN      0      MEAN MEAN MOTION.      00000650
C      XLAMDA      I      MEAN FAST VARIABLE.      00000650
C      NCPARM      I      NUMBER OF PARAMETERS.      00000670
C      NEQ      I      NUMBER OF VARIATIONAL EQUATIONS.      00000680
C      NPERT      0      PERTURBATION INDICATOR.      00000690
C      1=CONTINUOUS TIME-DEPENDENT      00000700
C      2=CONTINUOUS TIME-INDEPENDENT      00000710
C      3=DRAG      00000720
C      4=SOLAR RADIATION PRESSURE      00000730
C      00000740
C      REFERENCE      00000750
C      00000760
C      "ORBIT DETERMINATION AND PREDICTION PROCESSES FOR LOW
C      ALTITUDE SATELLITES." BY A.J. GREEN      00000770
C      00000780
C      ANALYSIS      00000790
C      ANDREW J. GREEN, CPT, U.S. ARMY, CSDL      00000800
C      00000810
C      PROGRAMMER      00000820
C      ANDREW J. GREEN, CPT, U.S. ARMY, CSDL      00000830
C      00000840
C      00000850
C      00000860
C      IMPLICIT REAL*8(A-H,O-Z)      00000870
C      DIMENSION      CTEMP(10,10),TEMP(10,10)      00000880
C      DIMENSION      ETA(10) ,OSCELN(10) ,VPELMT(10) ,
C      2      GM(11) ,PGSVEL(6,8),DUMMY(3)      00000890
C      DIMENSION      IBODY(9) ,IBODYS(3)      00000900
C      00000910
C      00000920
C      COMMON/ANAVIN/      ISTESS      ,ITESSE      ,ITRESE      ,ISTHIR      ,00000930
C      1      ITHRAR      ,ITHRE      ,ITRES      ,NEND      ,00000940
C      2      MEND      ,LEND      ,ITRES      ,NRES(10)      ,00000950
C      3      MRES(10)      ,JRES(10)      ,NCSRES      ,LENDRS      ,00000960
C      4      ITHIRD      ,NENDTH(8)      ,MENDTH(8)      ,JTWOSQ      ,00000970
C      5      IQUAD(4)      ,HQUAD(4)      ,JPOS      ,JA      ,00000980
C      6      JB      ,JC      ,JGHA      ,KPOS      ,00000990
C      7      KA      ,KB      ,KC      ,KGHA      ,0001000
C      8      ICORR      ,IFOS      ,IMOON      ,IMEAN      ,00001010
C      9      IGHA      ,ISTRES      ,ITERM      ,ISHAD      ,00001020
C      1      JTNDP      ,JTMIND      ,JDRAG      ,JSOLAR      ,00001030
C      2      J2SQSP      ,JSPCGB      ,JSPTHR      ,JSPPOS      ,00001040
C      3      JSPA      ,JSFB      ,JSFC      ,JSPGHA      ,00001050
C      4      KSPPOS      ,KSPA      ,KSPB      ,KSPC      ,00001060
C      5      KSPGHA      ,KSPHC(4)      ,KSPPRT(4)      ,NMAXSP      ,00001070
C      6      MMAXSP      ,IDRRD      00001080
C      00001090
C      COMMON/FRC /      RFRC(1300) ,IFRC(50)      00001100
C      EQUIVALENCE      (GM(1) ,RFRC(2)      ),00001110
C      2      (OSVEL(1,1) ,RFRC(101)      ),00001120
C      3      (NMAX ,IFRC(3)      ),00001130
C      4      (MMAX ,IFRC(4)      ),00001140

```

!!

SPCOTO

AJG1324.GTDS.UPDATE.FORT

```

5          (NBODY          ,IFRC(7)          ),00001150
6          (ISUN           ,IFRC(14)         ) 00001160
C
COMMON/SWITCH/ ISWIT(225)
EQUIVALENCE   (IVOP           ,ISWIT(3)          ),00001170
              (ITHOBD        ,ISWIT(6)          ),00001180
2              (IEURN         ,ISWIT(12)         ),00001190
3              (IRESN        ,ISWIT(38)         ),00001200
4              (IBODY(1)     ,ISWIT(201)        ),00001210
5              (ICENT       ,IBODY(1)          ),00001220
6
C
COMMON/WORKER/ RWORK(3264) ,IWORK(13)
EQUIVALENCE   (OSCELM(1)     ,RWORK(2653)       ),00001230
2              (ETA(1)       ,RWORK(2673)       ),00001240
3              (VPELMT(1)    ,RWORK(2829)       ),00001250
4              (XLAMDA       ,RWORK(2851)       ),00001260
5              (XMEAN        ,RWORK(2814)       ),00001270
6              (T            ,RWORK(3215)       ),00001280
7              (TZERO        ,RWORK(2850)       ) 00001290
EQUIVALENCE   (NOPARM       ,IWORK(3)           ),00001300
2              (NPRT        ,IWORK(9)           ) 00001310
C
COMMON/DCINT/  DPDCI(432), INDCI(26)
EQUIVALENCE   (TTO          ,DPDCI(127)        ) 00001320
C
COMMON/SPCOEF/ CQUAD(10,10),DQUAD(10,10)
C
COMMON/ESTFLG/ IANAL      ,IDIFF      ,IQDRT      ,ICBVAR      ,J22VAR      ,
1              ITBVAR     ,IDRVAR     ,ISRVAR     ,NVAR        ,LEVAR        ,
2              KDRFLG     ,KPAR       ,KSTEP(20) ,KVRFLG     ,KCPSPP       ,
3              KCBSPP     ,KTBSPP     ,KDRSPP     ,KRSRPP     ,NVARSP      ,
4              IVSFNC(4) ,KATHOS     ,KPRTB1     ,KPRTB2     ,KPRTB3      ,
5              KPRTB4
C
C          SAVE THE TIME AND INITIALIZE.
C
          TZERO=TTO
          DO 20 I=1,NOPARM
          DO 10 J=1,10
          CTEMP(I,J)=0.DO
          DTEMP(I,J)=0.DO
10 CONTINUE
20 CONTINUE
C
C          COMPUTE THE MEAN MOTION AND AUXILARY QUANTITIES.
C
          XMEAN = DSQRT(GH(ICENT)/(VPELMT(1)*VPELMT(1)*VPELMT(1)))
          CALL AUXPAR(VPELMT)
C
C          COMPUTE THE SHORT PERIODIC COEFFICIENTS DUE TO NUMERICAL
C          TIME-INDEPENDENT CONTINUOUS PERTURBATIONS.
C
200 IF(KCPSPP.EQ.2) GO TO 300
C
C          SET THE CENTRAL BODY SPHERICAL HARMONIC SWITCH.
C
          IRESNS=IRESON

```

!!

SPCOTO

AJG1324.GTDS.UPDATE.FORT

```

      NMAXS=NMAX                                00001720
      MMAXS=MMAX                                00001730
      IF(KCBSPP.NE.1) GO TO 210                  00001740
      NMAX=NVARSP                                00001750
      MMAX=0                                     00001760
      IRESO=2                                    00001770
      GO TO 220                                  00001780
210  NMAX=0                                     00001790
      MMAX=0                                     00001800
      IRESO=4                                    00001810
C                                          00001820
C      SET THE THIRD-BODY AND BURN SWITCH.      00001830
C                                          00001840
220  ITHRTE=ITHIRD                              00001850
      IF(KTBSPP.NE.1) GO TO 225                  00001860
      ITHIRD=2                                   00001870
      GO TO 226                                  00001880
225  ITHIRD=0                                    00001890
226  IBURNT=IBURN                               00001900
      IBURN=2                                    00001910
C                                          00001920
C      COMPUTE THE POSITIONS OF THE PERTURBING BODIES. 00001930
C                                          00001940
      CALL EVAL(TZERO,KSPPOS,KSPA,KSPB,KSPC,KSPGHA,IBODY,POSVEL) 00001950
C                                          00001960
C      COMPUTE THE LIMITS AND VALUE OF THE SHORT PERIODIC COEFFICIENTS. 00001970
C                                          00001980
      NPERT = 2                                  00001990
      CALL LIMITS(FLOW,FHIGH,XLAMDA)              00002000
      CALL SPGENN(FLOW,FHIGH)                    00002010
C                                          00002020
C      ACCUMULATE THE SHORT PERIODIC COEFFICIENTS.    00002030
C                                          00002040
      KNC=KSFNC(NPERT)                          00002050
      DO 240 I=1,NOPARM                          00002060
      DO 230 J=1,KNC                              00002070
      CTEMP(I,J)=CTEMP(I,J)+CQUAD(I,J)          00002080
      DTEMP(I,J)=DTEMP(I,J)+DQUAD(I,J)          00002090
230  CONTINUE                                    00002100
240  CONTINUE                                    00002110
C                                          00002120
C      RESTORE THE SWITCHES.                      00002130
C                                          00002140
      IRESO = IRESNS                             00002150
      ITHIRD = ITHRTE                            00002160
      IBURN = IBURNT                             00002170
      NMAX = NMAXS                               00002180
      MMAX = MMAXS                               00002190
C                                          00002200
C      COMPUTE THE SHORT PERIODIC COEFFICIENTS DUE TO DRAG PERTURBATIONS. 00002210
C                                          00002220
300  IF(KDRSPP.NE.1) GO TO 400                  00002230
C                                          00002240
C      COMPUTE THE LIMITS OF THE AVERAGING INTEGRAL. 00002250
C                                          00002260
      NPERT = 3                                  00002270
      CALL LIMITS(FLOW,FHIGH,XLAMDA)              00002280
```

11

SPCOTO

AJG1324,GTDS.UPDATE.FORT

```

      IF (NPERT.EQ.0) GO TO 400
C
C   FIND THE POSITION OF THE SUN SO THAT THE DIURNAL BULGE IN THE
C   ATMOSPHERE CAN BE LOCATED.
C
      IBODYS(2) = IBODY(2)
      IBODYS(3) = IBODY(3)
      NBOBYS = NBODY
C
      IBODY(2) = 3
      IBODY(3) = 0
      NBODY = 2
C
      CALL EVAL(TZERO,1,2,2,2,2,IBODY,POSVEL)
C
C   COMPUTE THE VALUE OF THE SHORT PERIODIC COEFFICIENTS.
C
      CALL SPGENN(FLOW,FHIGH)
C
C   ACCUMULATE THE SHORT PERIODIC COEFFICIENTS.
C
      KNC=KSPNC(NPERT)
      DO 340 I=1,NOPARM
      DO 330 J=1,KNC
      CTEMP(I,J)=CTEMP(I,J)+CQUAD(I,J)
      DTEMP(I,J)=DTEMP(I,J)+DQUAD(I,J)
330 CONTINUE
340 CONTINUE
C
C   RESTORE THE THIRD BODIES.
C
      IF (KSRSP.EQ.1) GO TO 410
      IBODY(2) = IBODYS(2)
      IBODY(3) = IBODYS(3)
      NBODY = NBOBYS
      GO TO 500
C
C   COMPUTE THE SHORT PERIODICS DUE TO SOLAR RADIATION PRESSURE.
C
400 IF (KSRSP.NE.1) GO TO 500
C
C   FIND AND STORE THE POSITION OF THE SUN.
C
      IBODYS(2) = IBODY(2)
      IBODYS(3) = IBODY(3)
      NBOBYS = NBODY
C
      IBODY(2) = 3
      IBODY(3) = 0
      NBODY = 2
C
      CALL EVAL(TZERO,1,2,2,2,2,IBODY,POSVEL)
C
410 ISUNS = ISUN
      ISUN = - 1
      CALL PHASS(IBODY,DUMMY,DUMMY,IERR)
      ISUN = 1

```

```

00002290
00002300
00002310
00002320
00002330
00002340
00002350
00002360
00002370
00002380
00002390
00002400
00002410
00002420
00002430
00002440
00002450
00002460
00002470
00002480
00002490
00002500
00002510
00002520
00002530
00002540
00002550
00002560
00002570
00002580
00002590
00002600
00002610
00002620
00002630
00002640
00002650
00002660
00002670
00002680
00002690
00002700
00002710
00002720
00002730
00002740
00002750
00002760
00002770
00002780
00002790
00002800
00002810
00002820
00002830
00002840
00002850

```

11

!!

SPCOTO

AJG1324.GTDS.UPDATE.FORT

```

C          00002860
C COMPUTE THE LIMITS AND VALUE OF THE SHORT PERIODIC COEFFICIENTS. 00002870
C          00002880
C          NPERT = 4 00002890
C          CALL LIMITS(FLOW,FHIGH,XLAMDA) 00002900
C          CALL SFGENN(FLOW,FHIGH) 00002910
C          00002920
C ACCUMULATE THE SHORT PERIODIC COEFFICIENTS. 00002930
C          00002940
C          KNC=KSFNC(NPERT) 00002950
C          DO 440 I=1,NOPARM 00002960
C          DO 430 J=1,KNC 00002970
C          CTEMP(I,J)=CTEMP(I,J)+CQUAD(I,J) 00002980
C          DTEMP(I,J)=DTEMP(I,J)+DQUAD(I,J) 00002990
C          430 CONTINUE 00003000
C          440 CONTINUE 00003010
C          00003020
C RESTORE THE THIRD BODIES. 00003030
C          00003040
C          IBODY(2) = IBODYS(2) 00003050
C          IBODY(3) = IBODYS(3) 00003060
C          NBODY = NBODYS 00003070
C          ISUN = ISUNS 00003080
C          00003090
C RESTORE THE FAST VARIABLE AND RETURN THE SHORT PERIODIC 00003100
C COEFFICIENTS. 00003110
C          00003120
C          500 VPELMT(NOPARM)=XLAMDA 00003130
C          DO 520 I=1,NOPARM 00003140
C          DO 510 J=1,10 00003150
C          CQUAD(I,J)=CTEMP(I,J) 00003160
C          DQUAD(I,J)=DTEMP(I,J) 00003170
C          510 CONTINUE 00003180
C          520 CONTINUE 00003190
C          00003200
C          RETURN 00003210
C          END 00003220

```

***** END OF MEMBER SPCOTO 322 RECORDS *****

-

-

!!

SPEXEC

AJG1324.GTDS.UPDATE.FORT

```

SUBROUTINE SPEXEC                                00000010
C                                                  00000020
C  VERSION OF 22 FEB 1979 IMPLEMENTED AT CSOL ON AMDAHL 470 V6. 00000030
C                                                  00000040
C  PURPOSE                                                    00000050
C    TO CONTROL THE EVALUATION OF THE OSCULATING ELEMENTS FOR 00000060
C    THE AVERAGED VOP ORBIT GENERATOR.                    00000070
C                                                  00000080
C  PARAMETERS                                                00000090
C                                                  00000100
C  /ANAVIN/                                                  00000110
C                                                  00000120
C    J2SPSQ   I  CONTROL SWITCH FOR J2 SHORT PERIODICS. *    00000130
C    JTMDEP   I  CONTROL SWITCH FOR NUMERICAL SHORT PERIODICS DUE 00000140
C               TO TIME-DEPENDENT CONTINUOUS PERTURBATIONS. * 00000150
C    JTMIND   I  CONTROL SWITCH FOR NUMERICAL SHORT PERIODICS DUE 00000160
C               TO TIME-INDEPENDENT CONTINUOUS PERTURBATIONS. * 00000170
C    JSPCGB   I  CONTROL SWITCH FOR NUMERICAL SHORT PERIODICS DUE 00000180
C               TO THE CENTRAL GRAVITATIONAL BODY.              00000190
C               0=NO CENTRAL BODY FIELD                        00000200
C               1=TIME-DEPENDENT NUMERICAL SHORT PERIODICS    00000210
C               2=TIME-INDEPENDENT NUMERICAL SHORT PERIODICS 00000220
C               3=ANALYTICAL SHORT PERIODICS                  00000230
C    ITHIRD   O  THIRD-BODY AVERAGING OPTION.                  00000240
C               0=NO THIRD-BODY                               00000250
C               1=TIME-DEPENDENT NUMERICAL AVERAGING          00000260
C               2=TIME-INDEPENDENT NUMERICAL AVERAGING        00000270
C               3=ANALYTICAL AVERAGING                        00000280
C    JSPTHR   I  CONTROL SWITCH FOR THIRD-BODY NUMERICAL SHORT 00000290
C               PERIODICS.                                    00000300
C               0=NO THIRD BODY                               00000310
C               1=TIME-DEPENDENT NUMERICAL SHORT PERIODICS    00000320
C               2=TIME-INDEPENDENT NUMERICAL SHORT PERIODICS 00000330
C               3=ANALYTICAL SHORT PERIODICS                  00000340
C    JDRAG    I  CONTROL SWITCH FOR DRAG SHORT PERIODICS. *    00000350
C    JSOLAR   I  CONTROL SWITCH FOR SOLAR RADIATION PRESSURE 00000360
C               SHORT PERIODICS. *                            00000370
C    NMAXSP   I  MAXIMUM DEGREE FOR THE CENTRAL BODY FIELD THAT 00000380
C               WILL BE USED IN THE DETERMINATION OF THE SHORT 00000390
C               PERIODICS.                                    00000400
C    MMAXSP   I  MAXIMUM ORDER FOR THE CENTRAL BODY FIELD THAT 00000410
C               WILL BE USED IN THE DETERMINATION OF THE SHORT 00000420
C               PERIODICS.                                    00000430
C               00000440
C  /FRC/                                                00000450
C                                                  00000460
C    NBODY    O  NUMBER OF SOLAR SYSTEM BODIES CONSIDERED.    00000470
C    ISUN     O  SOLAR VECTOR INDICATOR.                       00000480
C    GM       I  GRAVITATIONAL CONSTANT TIMES THE MASS OF THE 00000490
C               SOLAR SYSTEM BODY.                            00000500
C    NMAX     O  MAXIMUM DEGREE FOR THE EARTH OR MOON FIELDS. 00000510
C    MMAX     O  MAXIMUM ORDER FOR THE EARTH OR MOON FIELDS. 00000520
C               00000530
C  /SWITCH/                                             00000540
C                                                  00000550
C    IVOP     I  VOP TYPE.                                     00000560
C               12=AVERAGED EQUINOCTIAL ELEMENTS              00000570

```

```

C      ITWOBD   I   TWO-BODY MOTION. *                00000580
C      IBURN   O   CONTROL SWITCH FOR POLYNOMIAL BURN MODEL. * 00000590
C      IRESON  O   CENTRAL BODY FIELD SWITCH.          00000600
C                                     1=NXM CENTRAL BODY FIELD PLUS HIGH ORDER 00000610
C                                     RESONANCE                                00000620
C                                     2=NXM CENTRAL BODY FIELD ONLY            00000630
C                                     3=HIGH ORDER RESONANCE ONLY              00000640
C                                     4=NO CENTRAL BODY FIELD                  00000650
C      IBODY   O   CENTRAL AND NON-CENTRAL BODY INDICATORS. 00000660
C                                                     00000670
C      /WORKER/                                       00000680
C                                                     00000690
C      OSCELM  O   ARRAY OF OSCULATING ELEMENTS.         00000700
C      ETA     O   ARRAY OF SHORT PERIODICS.             00000710
C      VPELMT  I   ARRAY OF MEAN ELEMENTS.              00000720
C      XLAMBA  I   MEAN FAST VARIABLE(MEAN MEAN LONGITUDE). 00000730
C      XMEAN   O   MEAN MOTION.                         00000740
C      T       I   TIME FROM EPOCH OF KTH DERIVATIVE.    00000750
C      NOPARM  I   NUMBER OF PARAMETERS.                 00000760
C      NPERT   O   PERTURBATION INDICATOR.              00000770
C                                     1=CONTINUOUS TIME-DEPENDENT            00000780
C                                     2=CONTINUOUS TIME-INDEPENDENT          00000790
C                                     3=DRAG                                  00000800
C                                     4=SOLAR RADIATION PRESSURE              00000810
C                                                     00000820
C      /DCINT/                                       00000830
C                                                     00000840
C      TTO     I   OUTPUT TIME.                          00000850
C                                                     00000860
C                                                     00000870
C      *      1=YES          2=NO                        00000880
C                                                     00000890
C                                                     00000900
C      REFERENCES                                     00000910
C                                                     00000920
C      "A FOURIER SERIES FORMULATION OF THE SHORT PERIODIC VARIATIONS 00000930
C      IN TERMS OF EQUINOCTIAL ELEMENTS." BY A.J. GREEN AND P.J. CEFOLA 00000940
C                                                     00000950
C      ANALYSIS                                       00000960
C      ANDREW J. GREEN, CPT, U.S. ARMY, CSDL          00000970
C                                                     00000980
C      PROGRAMMER                                     00000990
C      ANDREW J. GREEN, CPT, U.S. ARMY, CSDL          00001000
C                                                     00001010
C *****START PROGRAM*****00001020
C                                                     00001030
C                                                     00001040
C      IMPLICIT REAL*8(A-H,O-Z)                       00001050
C      DIMENSION   ETA(10)   ,OSCELM(10) ,VPELMT(10) , 00001060
C      2           GM(11)    ,POSVEL(6,8),DUMMY(3)      00001070
C      DIMENSION   IBODY(9)  ,IBODYS(3)                00001080
C                                                     00001090
C      COMMON/ANAVIN/  ISTESS   ,ITESSE   ,ITRESE   ,ISTHIR   ,00001100
C      1              ITHRAR   ,ITHRE    ,ITRESS   ,NEND     ,00001110
C      2              MEND     ,LEND     ,ITRES    ,NRES(10) ,00001120
C      3              MRES(10) ,JRES(10) ,NCSRES   ,LENDRS   ,00001130
C      4              ITHIRD   ,NFENDTH(8) ,HENDTH(8) ,JTWSQ    ,00001140

```

SPEXEC

AJG1324.GTDS.UPDATE.FORT

```

5          IQUAD(4)      ,NQUAD(4)      ,JPOS      ,JA          ,00001150
6          JB           ,JC           ,JGHA      ,KPOS      ,00001160
7          KA           ,KB           ,KC         ,KGHA      ,00001170
8          ICORR        ,IFOS         ,IMOON     ,IMEAN     ,00001180
9          IGHA         ,ISTRES       ,ITERM     ,ISHAD     ,00001190
1         JTMDEP        ,JTMIND       ,JDRAG     ,JSOLAR    ,00001200
2         J2SQSP        ,JSPCGB       ,JSPTHR    ,JSPPOS    ,00001210
3         JSPA          ,JSPB         ,JSPC      ,JSPGHA    ,00001220
4         KSPPOS        ,KSPA         ,KSPB      ,KSFC      ,00001230
5         KSPGHA        ,KSPNC(4)    ,KSPPRT(4) ,NMAXSP    ,00001240
6         MMAXSP        ,IDRDR
C
COMMON/FRC / RFRC(1300) ,IFRC(50)
EQUIVALENCE (GM(1) ,RFRC(2) ) ,00001260
2 (POSVEL(1,1) ,RFRC(101) ) ,00001270
3 (NMAX ,IFRC(3) ) ,00001280
4 (MMAX ,IFRC(4) ) ,00001290
5 (NBODY ,IFRC(7) ) ,00001300
6 (ISUN ,IFRC(14) ) ,00001310
C
COMMON/SWITCH/ ISWIT(225)
EQUIVALENCE (IVOP ,ISWIT(3) ) ,00001320
2 (ITWOBD ,ISWIT(6) ) ,00001330
3 (IBURN ,ISWIT(12) ) ,00001340
4 (IRESCN ,ISWIT(38) ) ,00001350
5 (IBODY(1) ,ISWIT(201) ) ,00001360
6 (ICENT ,IBODY(1) ) ,00001370
C
COMMON/WORKER/ RWORK(3264) ,IWORK(13)
EQUIVALENCE (OSCELM(1) ,RWORK(2653) ) ,00001380
2 (ETA(1) ,RWORK(2673) ) ,00001390
3 (VPELMT(1) ,RWORK(2829) ) ,00001400
4 (XLAMDA ,RWORK(2851) ) ,00001410
5 (XMEAN ,RWORK(2814) ) ,00001420
6 (T ,RWORK(3215) ) ,00001430
7 (TZERO ,RWORK(2850) ) ,00001440
EQUIVALENCE (NOPARM ,IWORK(3) ) ,00001450
2 (NPRT ,IWORK(9) ) ,00001460
C
COMMON/DCINT/ DPDCI(432), INDCI(26)
EQUIVALENCE (TTO ,DPDCI(127) ) ,00001470
C
C SAVE THE TIME AND FAST VARIABLE. ,00001480
C ,00001490
C TZERO = TTO ,00001500
C XLAMDA = VPELMT(NOPARM) ,00001510
C ,00001520
C INITIALIZE THE OSCULATING ELEMENTS. ,00001530
C ,00001540
C DO 10 I=1,NOPARM ,00001550
C OSCELM(I) = VPELMT(I) ,00001560
C 10 CONTINUE ,00001570
C ,00001580
C COMPUTE THE MEAN MOTION AND TEST FOR TWO-BODY MOTION AND ,00001590
C AVERAGED EQUINOCTIAL ELEMENTS. ,00001600
C ,00001610
C XMEAN = DSQRT(GM(ICENT)/(VPELMT(1)*VPELMT(1)*VPELMT(1))) ,00001620
C ,00001630
C ,00001640
C ,00001650
C ,00001660
C ,00001670
C ,00001680
C ,00001690
C ,00001700
C ,00001710

```

```

IF (ITWOBD.EQ.1) GO TO 500                                00001720
IF (IVOP.NE.12) GO TO 500                                00001730
C                                                         00001740
C COMPUTE AUXILIARY QUANTITIES.                            00001750
C                                                         00001760
C CALL AUXPAR(VPELMT)                                     00001770
C                                                         00001780
C COMPUTE THE ANALYTICAL SHORT PERIODICS.                 00001790
C                                                         00001800
C CALL SPANAL                                             00001810
C                                                         00001820
C ACCUMULATE THE OSCULATING ELEMENTS.                    00001830
C                                                         00001840
C DO 11 I=1,NOPARM                                       00001850
C   OSCELM(I) = OSCELM(I) + ETA(I)                       00001860
11 CONTINUE                                              00001870
C                                                         00001880
C COMPUTE THE SHORT PERIODICS DUE TO THE J2 SQUARED PERTURBATIONS. 00001890
C                                                         00001900
C IF (J2SQSP.NE.1) GO TO 100                             00001910
C CALL SPJ2SQ                                           00001920
C                                                         00001930
C ACCUMULATE THE OSCULATING ELEMENTS.                    00001940
C                                                         00001950
C DO 12 I=1,NOPARM                                       00001960
C   OSCELM(I) = OSCELM(I) + ETA(I)                       00001970
12 CONTINUE                                              00001980
C                                                         00001990
C COMPUTE THE SHORT PERIODICS DUE TO NUMERICAL TIME-DEPENDENT 00002000
C CONTINUOUS PERTURBATIONS. REMEMBER THAT THIS FORMULATION IS 00002010
C NOT RIGOROUS.                                         00002020
C                                                         00002030
100 IF (JTMDEP.NE.1) GO TO 200                           00002040
C                                                         00002050
C SET THE CENTRAL BODY SPHERICAL HARMONIC SWITCHES AND THE SWITCHES 00002060
C TO BE USED IN SUBROUTINE 'EVAL'.                      00002070
C                                                         00002080
C IRESNS = IRESON                                       00002090
C NMAXS = NMAX                                           00002100
C MMAXS = MMAX                                           00002110
C JPOST = JPOS                                           00002120
C JAT = JA                                               00002130
C JBT = JB                                               00002140
C JCT = JC                                               00002150
C JGHAT = JGHA                                          00002160
C TSAVE = T                                              00002170
C                                                         00002180
C NMAX = NMAXSP                                         00002190
C MMAX = MMAXSP                                         00002200
C JPOS = JSPPOS                                         00002210
C JA = JSPA                                             00002220
C JB = JSPB                                             00002230
C JC = JSPC                                             00002240
C JGHA = JSPGHA                                         00002250
C                                                         00002260
C IF (JSPCGB.EQ.1) GO TO 110                             00002270
C IRESON = 4                                             00002280

```

II

SPEXEC

AJG1324.GTDS.UPDATE.FCRT

	GO TO 120	
	110 IRESON = 2	00002290
C		00002300
C	SET THE THIRD-BODY AND BURN SWITCH.	00002310
C		00002320
	120 ITHRTE = ITHIRD	00002330
	IF(JSPTHR.NE.1) GO TO 125	00002340
	ITHIRD = 1	00002350
	GO TO 126	00002360
	125 ITHIRD = 0	00002370
	126 IBURNT = IBURN	00002380
	IBURN = 2	00002390
C		00002400
C	COMPUTE THE LIMITS AND VALUE OF THE SHORT PERIODICS.	00002410
C		00002420
	NPERT = 1	00002430
	CALL LIMITS(FLOW,FHIGH,XLAMDA)	00002440
	CALL SPNUM(FLOW,FHIGH)	00002450
C		00002460
C	ACCUMULATE THE OSCULATING ELEMENTS.	00002470
C		00002480
	DO 130 I=1,NOPARM	00002490
	OSCELM(I) = OSCELM(I) + ETA(I)	00002500
	130 CONTINUE	00002510
C		00002520
C	RESTORE THE SWITCHES.	00002530
C		00002540
	IRESON = IRESNS	00002550
	ITHIRD = ITHRTE	00002560
	IBURN = IBURNT	00002570
	NMAX = NMAXS	00002580
	MMAX = MMAXS	00002590
	JFOS = JPOST	00002600
	JA = JAT	00002610
	JB = JBT	00002620
	JC = JCT	00002630
	JGHA = JGHAT	00002640
	T = TSAVE	00002650
C		00002660
C	COMPUTE THE SHORT PERIODICS DUE TO NUMERICAL TIME-INDEPENDENT	00002670
C	CONTINUOUS PERTURBATIONS.	00002680
C		00002690
	200 IF (JTMIND.NE.1) GO TO 300	00002700
C		00002710
C	SET THE CENTRAL BODY SPHERICAL HARMONIC SWITCH. FOR	00002720
C	SHORT PERIODICS M = 0.	00002730
C		00002740
	IRESNS = IRESON	00002750
	NMAXS = NMAX	00002760
	MMAXS = MMAX	00002770
	NMAX = NMAXSP	00002780
	MMAX = 0	00002790
C		00002800
C	IF (JSPCGB.EQ.2) GO TO 210	00002810
	IRESON = 4	00002820
	GO TO 220	00002830
	210 IRESON = 2	00002840
		00002850

II

SPEXEC

AJG1324.GTDS.UPDATE.FORT

```
C 00002860
C SET THE THIRD-BODY AND BURN SWITCH. 00002870
C 00002880
220 ITHRTE = ITHIRD 00002890
IF(JSPTHR.NE.2) GO TO 225 00002900
ITHIRD = 2 00002910
GO TO 226 00002920
225 ITHIRD = 0 00002930
226 IBURNT = IBURN 00002940
IBURN = 2 00002950
C 00002960
C COMPUTE THE POSITIONS OF THE PERTURBING BODIES. 00002970
C 00002980
CALL EVAL(TZERO,KSPPOS,KSPA,KSPB,KSPC,KSPGHA,IBODY,POSVEL) 00002990
C 00003000
C COMPUTE THE LIMITS AND VALUE OF THE SHORT PERIODICS. 00003010
C 00003020
NPERT = 2 00003030
CALL LIMITS(FLOW,FHIGH,XLAMDA) 00003040
CALL SPNUM(FLOW,FHIGH) 00003050
C 00003060
C ACCUMULATE THE OSCULATING ELEMENTS. 00003070
C 00003080
DO 230 I=1,NOPARM 00003090
OSCELM(I) = OSCELM(I) + ETA(I) 00003100
230 CONTINUE 00003110
C 00003120
C RESTORE THE SWITCHES. 00003130
C 00003140
IRESON = IRESNS 00003150
ITHIRD = ITHRTE 00003160
IBURN = IBURNT 00003170
NMAX = NMAXS 00003180
MMAX = MMAXS 00003190
C 00003200
C COMPUTE THE SHORT PERIODICS DUE TO DRAG. 00003210
C 00003220
300 IF (JDRAG.NE.1) GO TO 400 00003230
C 00003240
C COMPUTE THE LIMITS OF THE AVERAGING INTEGRAL. 00003250
C 00003260
NPERT = 3 00003270
CALL LIMITS(FLOW,FHIGH,XLAMDA) 00003280
IF (NPERT.EQ.0) GO TO 400 00003290
C 00003300
C FIND THE POSITION OF THE SUN SO THAT THE DIURNAL BULGE IN THE 00003310
C ATMOSPHERE CAN BE LOCATED. 00003320
C 00003330
IBODYS(2) = IBODY(2) 00003340
IBODYS(3) = IBODY(3) 00003350
NSODYS = NBODY 00003360
C 00003370
C 00003380
IBODY(2) = 3 00003390
IBODY(3) = 0 00003400
NBODY = 2 00003410
C 00003420
CALL EVAL(TZERO,1,2,2,2,2,IBODY,POSVEL)
```

11

SPEXEC

AJG1324.GTDS.UPDATE.FORT

C		00003430
C	COMPUTE THE VALUE OF THE SHORT PERIODICS.	00003440
C		00003450
C	CALL SPNUM(FLOW,FHIGH)	00003460
C		00003470
C	ACCUMULATE THE OSCULATING ELEMENTS.	00003480
C		00003490
C	DO 310 I=1,NOPARM	00003500
C	OSCELM(I) = OSCELM(I) + ETA(I)	00003510
C	310 CONTINUE	00003520
C		00003530
C	RESTORE THE THIRD BODIES.	00003540
C		00003550
C	IF (JSOLAR.EQ.1) GO TO 410	00003560
C	IBODY(2) = IBODYS(2)	00003570
C	IBODY(3) = IBODYS(3)	00003580
C	NBODY = NBODYS	00003590
C	GO TO 500	00003600
C		00003610
C	COMPUTE THE SHORT PERIODICS DUE TO SOLAR RADIATION PRESSURE.	00003620
C		00003630
C	400 IF (JSOLAR.NE.1) GO TO 500	00003640
C		00003650
C	FIND AND STORE THE POSITION OF THE SUN.	00003660
C		00003670
C	IBODYS(2) = IBODY(2)	00003680
C	IBODYS(3) = IBODY(3)	00003690
C	NBODYS = NBODY	00003700
C		00003710
C	IBODY(2) = 3	00003720
C	IBODY(3) = 0	00003730
C	NBODY = 2	00003740
C		00003750
C	CALL EVAL(TZERO,1,2,2,2,2,IBODY,POSVEL)	00003760
C		00003770
C	410 ISUNS = ISUN	00003780
C	ISUN = - 1	00003790
C	CALL PMASS(IBODY,DUMMY,DUMMY,IERR)	00003800
C	ISUN = 1	00003810
C		00003820
C	COMPUTE THE LIMITS AND VALUE OF THE SHORT PERIODICS.	00003830
C		00003840
C	NPL T = 4	00003850
C	CALL LIMITS(FLOW,FHIGH,XLAMDA)	00003860
C	CALL SPNUM(FLOW,FHIGH)	00003870
C		00003880
C	ACCUMULATE THE OSCULATING ELEMENTS.	00003890
C		00003900
C	DO 420 I=1,NOPARM	00003910
C	OSCELM(I) = OSCELM(I) + ETA(I)	00003920
C	420 CONTINUE	00003930
C		00003940
C	RESTORE THE THIRD BODIES.	00003950
C		00003960
C	IBODY(2) = IBODYS(2)	00003970
C	IBODY(3) = IBODYS(3)	00003980
C	NBODY = NBODYS	00003990

11

11

SPEXEC

AJG1324.GTDS.UPDATE.FORT

	ISUN = ISUNS	00004000
C		00004010
C	RESTORE THE FAST VARIABLE.	00004020
C		00004030
	500 VPELMT(NOPARM) = XIAMDA	00004040
	RETURN	00004050
C		00004060
	END	00004070

***** END OF MEMBER SPEXEC 407 RECORDS *****

-

=

11

```

SUBROUTINE SPGENN(FLOW,FHIGH)                                0000010
C                                                            0000020
C  VERSION OF 22 FEB 79 IMPLEMENTED AT CSDL ON AMDAHL 470 V6. 0000030
C                                                            0000040
C  PURPOSE                                                    0000050
C  CONTROLS THE NUMERICAL PROCEDURE FOR DETERMINING THE SHORT 0000060
C  PERIODIC COEFFICIENTS.                                    0000070
C                                                            0000080
C  PROGRAMMER                                                0000090
C  ANDREW J. GREEN, CPT, U.S. ARMY, CSDL                    0000100
C                                                            0000110
C *****START PROGRAM*****                                0000120
C                                                            0000130
C                                                            0000140
C  IMPLICIT REAL*8(A-H,O-Z)                                  0000150
C  DIMENSION  OSCELM(10),VPELMT(10),ETA(10)                 0000160
C  COMMON/ANAVIN/  ISTESS      ,ITESSE      ,ITRESE      ,ISTHIR      ,0000170
C  1 ITHRAR      ,ITHRE      ,ITRESS      ,NEND      ,0000180
C  2 MEND      ,LEND      ,ITRES      ,NRES(10)   ,0000190
C  3 MRES(10)   ,JRES(10)   ,NCSRES      ,LENDRS      ,0000200
C  4 ITHIRD      ,NENDTH(8) ,MENDTH(8) ,JTWOSQ      ,0000210
C  5 IQUAD(4)   ,NQUAD(4)   ,JPOS      ,JA      ,0000220
C  6 JB      ,JC      ,JGHA      ,KPOS      ,0000230
C  7 KA      ,KB      ,KC      ,KGHA      ,0000240
C  8 ICORR      ,IPOS      ,IMOON      ,IMEAN      ,0000250
C  9 IGHA      ,ISTRES      ,ITERM      ,ISHAD      ,0000260
C  1 JTHDEP      ,JTHIND      ,JDRAG      ,JSOLAR      ,0000270
C  2 J2SQSP      ,JSFCGB      ,JSPTHR      ,JSPPOS      ,0000280
C  3 JSPA      ,JSPB      ,JSPC      ,JSPGHA      ,0000290
C  4 KSPPOS      ,KSPA      ,KSPB      ,KSPC      ,0000300
C  5 KSPGHA      ,KSPNC(4)   ,KSPPR(4)   ,NMAXSP      ,0000310
C  6 MMAXSP      ,IDRDR      ,NCHOJ2      ,NCHODR      0000320
C                                                            0000330
C  COMMON/WORKER/  RWORK(3264) ,IWORK(13)                 0000340
C  EQUIVALENCE      (OSCELM(1)      ,RWORK(2653)      ,0000350
C  2 (ETA(1)      ,RWORK(2673)      ),0000360
C  3 (VPELMT(1)   ,RWORK(2829)      ),0000370
C  4 (XLAMDA      ,RWORK(2851)      ),0000380
C  5 (XMEAN      ,RWORK(2814)      ),0000390
C  6 (T      ,RWORK(3215)      ),0000400
C  7 (TZERO      ,RWORK(2850)      ) 0000410
C  EQUIVALENCE      (NOPARM      ,IWORK(3)      ),0000420
C  2 (NPERT      ,IWORK(9)      ) 0000430
C                                                            0000440
C  IF THE NUMBER OF SHORT PERIODIC COEFFICIENTS IS GIVEN, SIMPLY 0000450
C  CALCULATE THE COEFFICIENTS. THE QUADRATURE ORDER FOR THE 0000460
C  DETERMINATION OF THE COEFFICIENTS IS THE SAME AS USED IN THE 0000470
C  DETERMINATION OF THE MEAN ELEMENT RATES.                    0000480
C                                                            0000490
C  IF(KSPNC(NPERT).LE.0) GO TO 100                            0000500
C  CALL SPQUAD(FLOW,FHIGH,NQUAD(NPERT),KSPNC(NPERT))          0000510
C  RETURN                                                       0000520
C                                                            0000530
C  DETERMINE THE NUMBER OF COEFFICIENTS TO BE USED. THE CRITERION 0000540
C  WILL BE DETERMINED. FOR THE PRESENT TIME THE MAXIMUM ALLOWABLE 0000550
C  NUMBER OF COEFFICIENTS WILL BE SET.                          0000560
C                                                            0000570

```

!!

SPGENN

AJG1324.GTDS.UPDATE.FORT

100 KSPNC(NPERT) = 10
RETURN

C

END

00000580
00000590
00000600
00000610

***** END OF MEMBER SPGENN 61 RECORDS *****

-

=

!!

SPNUM

AJG1324.GTDS.UPDATE.FORT

```

SUBROUTINE SPNUM(FLOW,FHIGH)                                00000010
C                                                           00000020
C   VERSION OF FEB 1979 IMPLEMENTED AT CSDL ON AMDAHL 470 V6. 00000030
C                                                           00000040
C   PURPOSE                                                    00000050
C     TO COMPUTE THE NUMERICAL SHORT PERIODICS.              00000060
C                                                           00000070
C   PARAMETERS                                                00000080
C                                                           00000090
C     ETA      O   ARRAY OF SHORT PERIODICS                  00000100
C     CQUAD    O   ARRAY OF C COEFFICIENTS                  00000110
C     DQUAD    O   ARRAY OF D COEFFICIENTS                  00000120
C     KSPNC    I   NUMBER OF NUMERICAL SHORT PERIODIC      00000130
C                   COEFFICIENTS. MAX ALLOWABLE IS 10.     00000140
C                   (.LE.0)=PROGRAM WILL DETERMINE NUMBER  00000150
C                   (.GT.0)=PROGRAM WILL USE THE NUMBER GIVEN 00000160
C     KSPPR    I   CONTROL SWITCH FOR THE PRINT OPTION.    00000170
C                   1=YES                                    00000180
C                   2=NO                                    00000190
C     FLOW     I   LOWER LIMIT OF INTEGRATION.              00000200
C     FHIGH    I   UPPER LIMIT OF INTEGRATION.             00000210
C                                                           00000220
C     SEE SUBROUTINE SPEXEC FOR DEFINITION OF OTHER PARAMETERS 00000230
C                                                           00000240
C   ANALYSIS                                                  00000250
C     ANDREW J. GREEN, CPT, U.S. ARMY, CSDL                 00000260
C                                                           00000270
C   PROGRAMMER                                               00000280
C     ANDREW J. GREEN, CPT, U.S. ARMY, CSDL                 00000290
C                                                           00000300
C *****START PROGRAM*****                                00000310
C                                                           00000320
C                                                           00000330
C                                                           00000340
C   IMPLICIT REAL*8(A-H,O-Z)                                00000350
C   DIMENSION OSCELM(10),ETA(10),VPELMT(10)                00000360
C   COMMON/ANAVIN/  ISTESS      ,ITESSE      ,ITRESE      ,ISTHIR      ,00000370
C                   ITHRAR      ,ITHRE       ,ITESS       ,NEND        ,00000380
C                   MEND        ,LEND        ,ITRES       ,NRES(10)   ,00000390
C                   MRES(10)    ,JRES(10)    ,NCSRES      ,LENDORS    ,00000400
C                   ITHIRD     ,NENDTH(8)   ,MENDTH(8)   ,JTWOSQ    ,00000410
C                   IQUAD(4)    ,NQAD(4)    ,JPOS        ,JA         ,00000420
C                   JB         ,JC         ,JGHA        ,KPOS      ,00000430
C                   KA         ,KB         ,KC         ,KGHA     ,00000440
C                   ICORR      ,IPOS       ,IMOON      ,IMEAN    ,00000450
C                   IGHA      ,ISTRES     ,ITERM      ,ISHAD    ,00000460
C                   JTMDEP     ,JTMIND     ,JDRAG      ,JSOLAR   ,00000470
C                   J2SQSP     ,JSFCGB     ,JSPTHR     ,JSPPOS   ,00000480
C                   JSPA       ,JSFB      ,JSPC       ,JSPGHA   ,00000490
C                   KSPPOS     ,KSPA       ,KSPB       ,KSPC     ,00000500
C                   KSPGHA     ,KSPNC(4)   ,KSPPR(4)   ,NMAXSP   ,00000510
C                   MMAXSP     ,IDRDR     ,00000520
C                                                           00000530
C   COMMON/WORKER/  RWORK(3264) ,IWORK(13)                  00000540
C   EQUIVALENCE    (OSCELM(1) ,RWORK(2653)                ),00000550
C                   (ETA(1)   ,RWORK(2673)                ),00000560
C                   (VPELMT(1),RWORK(2829)                ),00000570
C                   (XLAMDA   ,RWORK(2851)                ),00000570

```

SPNUM

AJG1324.GTDS.UPDATE.FORT

```

5          (XMEAN          ,RWORK(2814)          ),00000580
6          (T              ,RWCRK(3215)          ),00000590
7          (TZERO         ,RWORK(2850)          ) 00000600
EQUIVALENCE (NOPARM      ,IWORK(3)           ),00000610
2          (NFERT        ,IWORK(9)           ) 00000620
C
COMMON/SPCOEF/  CQUAD(10,10), DQUAD(10,10)          00000630
C
C INITIALIZE THE SHORT PERIODIC FUNCTIONS.          00000650
C
C DO 100 I=1,NOPARM                                  00000670
  ETA(I) = 0.00                                      00000680
100 CONTINUE                                         00000700
C
C COMPUTE THE SHORT PERIODIC COEFFICIENTS.          00000710
C
C CALL SPGENN(FLOW,FHIGH)                            00000720
C
C COMPUTE THE SHORT PERIODIC FUNCTIONS.              00000730
C
C CALL SPGENN(FLOW,FHIGH)                            00000740
C
C COMPUTE THE SHORT PERIODIC FUNCTIONS.              00000750
C
C COMPUTE THE SHORT PERIODIC FUNCTIONS.              00000760
C
C KTI = KSPNC(NPERT)                                 00000770
DO 110 J=1,KTI                                       00000780
  TT=J                                                 00000790
  TLJ = TT*XLAMDA                                     00000800
  DSJ = DSIN(TLJ)                                    00000810
  DCJ = DCOS(TLJ)                                    00000820
DO 105 I=1,NOPARM                                     00000830
  TEMPER = CQUAD(I,J)*DSJ-DQUAD(I,J)*DCJ            00000840
  ETA(I) = ETA(I) + TEMPER                           00000850
105 CONTINUE                                         00000870
110 CONTINUE                                         00000880
C
C PRINT THE SHORT PERIODIC COEFFICIENTS.            00000890
C
C IF(KSPRRT(NPERT).EQ.1) CALL SPFRRT                 00000910
RETURN                                               00000920
C
C END                                                 00000930
C
C END                                                 00000940
C
C END                                                 00000950

```

***** END OF MEMBER SPNUM 95 RECORDS *****

SPPRT

AJG1324.GTDS.UPDATE.FORT

```

SUBROUTINE SPPRT                                00000010
C                                                00000020
C VERSION OF FEB 1979 IMPLEMENTED AT CSDL ON AMDAHL 470 V6. 00000030
C                                                00000040
C PURPOSE                                           00000050
C TO PRINT THE NUMERICAL SHORT PERIODIC FUNCTIONS AND COEFFICIENTS.00000060
C                                                00000070
C PARAMETERS                                         00000080
C /DCINT/                                           00000090
C TTO      I   OUTPUT REQUEST TIME IN SECONDS.      00000100
C                                                00000110
C TTO      I   OUTPUT REQUEST TIME IN SECONDS.      00000120
C SEE SUBROUTINES SPEXEC AND SPNUM FOR ADDITIONAL DEFINITIONS. 00000130
C                                                00000140
C PROGRAMMER                                         00000150
C ANDREW J. GREEN, CPT, U.S. ARMY, CSDL            00000160
C ANDREW J. GREEN, CPT, U.S. ARMY, CSDL            00000170
C ANDREW J. GREEN, CPT, U.S. ARMY, CSDL            00000180
C *****START PROGRAM*****00000190
C                                                00000200
C                                                00000210
C                                                00000220
C IMPLICIT REAL*8(A-H,O-Z)                          00000230
C DIMENSION  OSCELM(10),VPELMT(10),ETA(10)          00000240
C COMMON/ANAVIN/  ISTESS      ,ITESSE      ,ITRESE      ,ISTHIR      ,00000250
1 ITHRAR      ,ITHRE      ,ITESS      ,NEND      ,00000260
2 MEND      ,LEND      ,ITRES      ,NRES(10)  ,00000270
3 MRES(10)   ,JRES(10)   ,NCSRES      ,LENDRS      ,00000280
4 ITHIRD     ,NENDTH(8)  ,MENDTH(8)  ,JTWOSQ      ,00000290
5 IQUAD(4)   ,NQUAD(4)   ,JPOS      ,JA      ,00000300
6 JB      ,JC      ,JGHA      ,KPOS      ,00000310
7 KA      ,KB      ,KC      ,KGHA      ,00000320
8 ICORR     ,IPOS      ,IMOON     ,IMEAN      ,00000330
9 IGHA      ,ISTRES     ,ITERM      ,ISHAD      ,00000340
1 JTHDEP     ,JTMIND     ,JDRAG      ,JSOLAR      ,00000350
2 J2SQSP     ,JSPCGB     ,JSPTHR     ,JSPPOS     ,00000360
3 JSPA      ,JSPB      ,JSPC      ,JSPGHA     ,00000370
4 KSPPOS     ,KSPA      ,KSPB      ,KSPC      ,00000380
5 KSPFGHA    ,KSPNC(4)   ,KSPPRT(4)  ,NMAXSP     ,00000390
6 MMAXSP     ,IDRDR      ,00000400
C COMMON/WORKER/  RWORK(3264) ,IWORK(13)            00000410
EQUIVALENCE      (OSCELM(1) ,RWORK(2653)          ),00000420
2 (ETA(1) ,RWORK(2673)          ),00000430
3 (VPELMT(1) ,RWORK(2829)         ),00000440
4 (XLAMDA ,RWORK(2851)          ),00000450
5 (XMEAN ,RWORK(2814)          ),00000460
6 (T ,RWORK(3215)          ),00000470
7 (TZERO ,RWORK(2850)          ) 00000480
EQUIVALENCE      (NOPARM ,IWORK(3)          ),00000490
2 (NPERT ,IWORK(9)          ) 00000500
C COMMON/SPCOEF/  CQUAD(10,10), DQUAD(10,10)        00000510
C                                                00000520
C COMMON/DCINT/  DPDCI(432), INDCI(26)              00000530
EQUIVALENCE      (TTO ,DPDCI(127)          ) 00000540
C KTI = KSPNC(NPERT)                                00000550
C                                                00000560
C                                                00000570

```

SPRRT

AJG1324.GTDS.UPDATE.FORT

```

TIMOUT=TTO/86400.000                                00000580
WRITE(6,1000)                                        00000590
WRITE(6,1001)NPERT,NQUAD(NPERT),TIMOUT              00000600
WRITE(6,1002)                                        00000610
WRITE(6,1006)(VPELMT(I),I=1,5),XLAMDA              00000620
WRITE(6,1003)                                        00000630
WRITE(6,1006)(ETA(I),I=1,NOPARM)                   00000640
WRITE(6,1004)                                        00000650
DO 10 K=1,KTI                                       00000660
WRITE(6,1006)(CQUAD(I,K),I=1,NOPARM)               00000670
10 CONTINUE                                         00000680
WRITE(6,1005)                                        00000690
DO 20 K=1,KTI                                       00000700
WRITE(6,1006)(DQUAD(I,K),I=1,NOPARM)               00000710
20 CONTINUE                                         00000720
RETURN                                              00000730
1000 FORMAT(' ++++++SHORT PERIOD+++++',10000740
*CDICS+++++',10000750
*+++++')                                           00000760
1001 FORMAT(/,' NPERT = ',I4,6X,'QUADRATURE PARAMETER = ',I4,
*6X,'TIME(DAYS) = ',1P1020.10)                    00000770
1002 FORMAT(/,9X,'VPELMT(1)',13X,'VPELMT(2)',13X,'VPELMT(3)',13X,
*'VPELMT(4)',13X,'VPELMT(5)',13X,'VPELMT(6)')    00000790
1003 FORMAT(/,10X,'ETA(1)',16X,'ETA(2)',16X,'ETA(3)',16X,'ETA(4)',
*16X,'ETA(5)',16X,'ETA(6)')                       00000810
1004 FORMAT(/,8X,'CQUAD(1,K)',12X,'CQUAD(2,K)',12X,'CQUAD(3,K)',12X,
*'CQUAD(4,K)',12X,'CQUAD(5,K)',12X,'CQUAD(6,K)') 00000830
1005 FORMAT(/,8X,'DQUAD(1,K)',12X,'DQUAD(2,K)',12X,'DQUAD(3,K)',12X,
*'DQUAD(4,K)',12X,'DQUAD(5,K)',12X,'DQUAD(6,K)') 00000850
1006 FORMAT(1P6D22.12)                              00000870
END                                                  00000880

```

***** END OF MEMBER SPRRT

88 RECORDS *****

SPQUAD

AJG1324.GTDS.UPDATE.FORT

```

SUBROUTINE SPQUAD(AA,BB,ISPQO,ISPNC)                                00000010
C                                                                    00000020
C VERSION OF FEB 1979 IMPLEMENTED AT CSDL ON AMDAHL 470 V6.      00000030
C                                                                    00000040
C PURPOSE                                                           00000050
C   EVALUATES THE COEFFICIENTS OF THE SHORT PERIODICS WITH A     00000060
C   GAUSSIAN NUMERICAL QUADRATURE FORMULA.                        00000070
C                                                                    00000080
C PARAMETERS                                                         00000090
C   AA      I   LOWER LIMIT OF INTEGRATION.                       00000100
C   BB      I   UPPER LIMIT OF INTEGRATION.                       00000110
C   ISPQO   I   QUADRATURE ORDER PARAMETER.                      00000120
C   ISPNC   I   NUMBER OF COEFFICIENTS.                          00000130
C                                                                    00000140
C /WORKER/                                                            00000150
C   DPARDT  I   PRECISION ELEMENT RATES COMPUTED IN *GQFUN*.    00000160
C   NOPARM  I   NUMBER OF ORBITAL ELEMENTS.                      00000170
C   VPELMT  I   ORBITAL ELEMENT VECTOR.                          00000180
C                                                                    00000190
C /SPCOEF/                                                            00000200
C   CQUAD   O   VALUE OF THE C COEFFICIENTS QUADRATURE.         00000210
C   DQUAD   O   VALUE OF THE D COEFFICIENTS QUADRATURE.         00000220
C                                                                    00000230
C EXTERNAL REFERENCES                                                00000240
C   GQFUN    COMPUTES PRECISION ORBITAL ELEMENT RATES.          00000250
C                                                                    00000260
C REFERENCES                                                           00000270
C   SUBROUTINE QUADRT                                             00000280
C                                                                    00000290
C ANALYSIS                                                            00000300
C   ANDREW J. GREEN, CPT, U.S. ARMY, CSDL                        00000310
C                                                                    00000320
C PROGRAMMER                                                           00000330
C   ANDREW J. GREEN, CPT, U.S. ARMY, CSDL                        00000340
C                                                                    00000350
C IMPLICIT REAL*8(A-H,O-Z)                                          00000360
C COMMON/WORKER/ RWCRK(3264) ,IWORK(12)                          00000370
C DIMENSION      VPELMT(10),DPARDT(10)                          00000380
C DIMENSION      IXWBEG(7) ,IXWEND(7)                          00000390
C EQUIVALENCE    (XMEAN ,RWORK(2814) ),                        00000400
C *              (VPELMT(1) ,RWORK(2829) ),                    00000410
C *              (DPARDT(1) ,RWORK(2840) ),                    00000420
C *              (NOPARM ,IWORK(3) )                            00000430
C COMMON/CONST/  TWOPI,PI                                        00000440
C COMMON/SPCOEF/ CQUAD(10,10),DQUAD(10,10)                    00000450
C                                                                    00000460
C DIMENSION      XTAB(96) ,WTAB(96)                             00000470
C DIMENSION      XTB1 ( 9) ,XTB10 (10) ,                       00000480
C *              XTB20 (10) ,XTB30 (10) ,                       00000490
C *              XTB40 (10) ,XTB50 (10) ,                       00000500
C *              XTB60 (10) ,XTB70 (10) ,                       00000510
C *              XTB80 (10) ,XTB90 ( 7) ,                       00000520
C DIMENSION      WTB1 ( 9) ,WTB10 (10) ,                       00000530
C *              WTB20 (10) ,WTB30 (10) ,                       00000540
C *              WTB40 (10) ,WTB50 (10) ,                       00000550
C *              WTB60 (10) ,WTB70 (10) ,                       00000560
C *              WTB80 (10) ,WTB90 ( 7) ,                       00000570

```


SPQUAD

AJG1324.GTDS.UPDATE.FORT

C					00000580
	EQUIVALENCE	(XTB1 (1)	,XTAB(1)),	00000590
*		(XTB10 (1)	,XTAB(10)),	00000600
*		(XTB20 (1)	,XTAB(20)),	00000610
*		(XTB30 (1)	,XTAB(30)),	00000620
*		(XTB40 (1)	,XTAB(40)),	00000630
*		(XTB50 (1)	,XTAB(50)),	00000640
*		(XTB60 (1)	,XTAB(60)),	00000650
*		(XTB70 (1)	,XTAB(70)),	00000660
*		(XTB80 (1)	,XTAB(80)),	00000670
*		(XTB90 (1)	,XTAB(90))	00000680
	EQUIVALENCE	(WTB1 (1)	,WTAB(1)),	00000690
*		(WTB10 (1)	,WTAB(10)),	00000700
*		(WTB20 (1)	,WTAB(20)),	00000710
*		(WTB30 (1)	,WTAB(30)),	00000720
*		(WTB40 (1)	,WTAB(40)),	00000730
*		(WTB50 (1)	,WTAB(50)),	00000740
*		(WTB60 (1)	,WTAB(60)),	00000750
*		(WTB70 (1)	,WTAB(70)),	00000760
*		(WTB80 (1)	,WTAB(80)),	00000770
*		(WTB90 (1)	,WTAB(90))	00000780
C					00000790
C					00000800
C					00000810
	DATA XTB 1	/ .1252334085114689D+00	,		00000820
	2	.3678314989981802D+00	,		00000830
	3	.5873179542866174D+00	,		00000840
	4	.7699026741943047D+00	,		00000850
	5	.9041172563704749D+00	,		00000860
	6	.9815606342467192D+00	,		00000870
					00000880
C					00000890
C					00000900
C					00000910
					00000920
					00000930
	DATA XTB 10	/ .6178762444026437D+00	,		00000940
	1	.7554044083550030D+00	,		00000950
	2	.8656312023878317D+00	,		00000960
	3	.9445750230732326D+00	,		00000970
	4	.9894009349916499D+00	,		00000980
					00000990
C					00001000
C					00001010
C					00001020
					00001030
					00001040
					00001050
					00001060
	DATA XTB 20	/ .7463319064601508D+00	,		00001070
	1	.8391169718222189D+00	,		00001080
	2	.9122344282513259D+00	,		00001090
	3	.9639719272779138D+00	,		00001100
	4	.9931285991850949D+00	,		00001110
					00001120
C					00001130
C					00001140
C					

11

||

SPQUAD

AJG1324.GTDS.UPDATE.FORT

5	.6405689286260562D-01	,	00001150
6	.1911188674736163D+00	,	00001160
7	.3150426796961634D+00	,	00001170
8	.4337935076260451D+00	,	00001180
9	.5454214713988395D+00	/	00001190
DATA XTB 30	/ .6480936519369756D+00	,	00001200
1	.7401241915785544D+00	,	00001210
2	.8200019259739029D+00	,	00001220
3	.8864155270044010D+00	,	00001230
4	.9382745520027328D+00	,	00001240
5	.9747285559713095D+00	,	00001250
6	.9951872199970214D+00	,	00001260

C
C
C

ABSCISSAE FOR ORDER 32 IN SEQUENCE 32.

7	.4830766568773832D-01	,	00001300
8	.1444719615827965D+00	,	00001310
9	.2392873622521371D+00	/	00001320
DATA XTB 40	/ .3318686022821276D+00	,	00001330
1	.4213512761306353D+00	,	00001340
2	.5068999089322294D+00	,	00001350
3	.5877157572407623D+00	,	00001360
4	.6630442669302152D+00	,	00001370
5	.7321821187402897D+00	,	00001380
6	.7944837959679424D+00	,	00001390
7	.8493676137325700D+00	,	00001400
8	.8963211557660521D+00	,	00001410
9	.9349060759377397D+00	/	00001420
DATA XTB 50	/ .9647622555875064D+00	,	00001430
1	.9856115115452683D+00	,	00001440
2	.9972638618494816D+00	,	00001450

C
C
C

ABSCISSAE FOR ORDER 40 IN SEQUENCE 40.

3	.3877241750605082D-01	,	00001490
4	.1160840706752552D+00	,	00001500
5	.1926975807013711D+00	,	00001510
6	.2681521850072537D+00	,	00001520
7	.3419940908257585D+00	,	00001530
8	.4137792043716050D+00	,	00001540
9	.4830758916861787D+00	/	00001550
DATA XTB 60	/ .5494671250951282D+00	,	00001560
1	.6125538396679802D+00	,	00001570
2	.6719566846141795D+00	,	00001580
3	.7273182551899271D+00	,	00001590
4	.7783056514265194D+00	,	00001600
5	.8246122308333117D+00	,	00001610
6	.8659595032122595D+00	,	00001620
7	.9020988069688743D+00	,	00001630
8	.9328128082786765D+00	,	00001640
9	.9579168192137917D+00	/	00001650
DATA XTB 70	/ .9772599499837743D+00	,	00001660
1	.9907262386994570D+00	,	00001670
2	.9982377097105592D+00	,	00001680

-

C
C
C

ABSCISSAE FOR ORDER 48 IN SEQUENCE 48.

00001690
00001700
00001710

||

11

SPQUAD

AJG1324.GTDS.UPDATE.FORT

3	.3238017096286936D-01	,	00001720
4	.9700469920946270D-01	,	00001730
5	.1612223560688917D+00	,	00001740
6	.2247637903946891D+00	,	00001750
7	.2873624873554556D+00	,	00001760
8	.3487558852921607D+00	,	00001770
9	.4086864819907167D+00	/	00001780
DATA XTB 80	/ .4669029047509584D+00	,	00001790
1	.5231609747222330D+00	,	00001800
2	.5772247260839727D+00	,	00001810
3	.6288673967765136D+00	,	00001820
4	.6778723796326639D+00	,	00001830
5	.7240341309238146D+00	,	00001840
6	.7671590325157403D+00	,	00001850
7	.8070662040294426D+00	,	00001860
8	.8435882616243935D+00	,	00001870
9	.8765720202742479D+00	/	00001880
DATA XTB 90	/ .9058791367155697D+00	,	00001890
1	.9313866907065543D+00	,	00001900
2	.9529877031604309D+00	,	00001910
3	.9705915925462472D+00	,	00001920
4	.9841245837228269D+00	,	00001930
5	.9935301722663508D+00	,	00001940
6	.9987710072524261D+00	/	00001950

C
C
C

WEIGHTS FOR ORDER 12 IN SEQUENCE 12.

DATA WTB 1	/ .2491470458134028D+00	,	00001960
2	.2334925365383548D+00	,	00001970
3	.2031674267230659D+00	,	00001980
4	.1600783265433462D+00	,	00001990
5	.1069393259953184D+00	,	00002000
6	.4717533638651183D-01	,	00002010

C
C
C

WEIGHTS FOR ORDER 16 IN SEQUENCE 16.

7	.1894506104550685D+00	,	00002020
8	.1826034150449235D+00	,	00002030
9	.1691565193950025D+00	/	00002040
DATA WTB 10	/ .1495959888165767D+00	,	00002050
1	.1246289712555339D+00	,	00002060
2	.9515851169249277D-01	,	00002070
3	.6225352393864789D-01	,	00002080
4	.2715245941175409D-01	,	00002090

C
C
C

WEIGHTS FOR ORDER 20 IN SEQUENCE 20.

5	.1527533871307258D+00	,	00002100
6	.1491729864726037D+00	,	00002110
7	.1420961093183820D+00	,	00002120
8	.1316886384491766D+00	,	00002130
9	.1181945319615184D+00	/	00002140
DATA WTB 20	/ .1019301198172404D+00	,	00002150
1	.8327674157670474D-01	,	00002160
2	.6267204833410905D-01	,	00002170
3	.4060142980039694D-01	,	00002180
4	.1761400713915212D-01	,	00002190

-

11

11

SPQUAD

AJG1324.GTDS.UPDATE.FORT

C
C
C

WEIGHTS FOR ORDER 24 IN SEQUENCE 24.

5	.1279381953467521D+00	,	00002290
6	.1258374563468283D+00	,	00002300
7	.12167047292780340+00	,	00002310
8	.1155056680537256D+00	,	00002320
9	.1074442701159656D+00	/	00002330
DATA WTB 30	/.9761855210411338D-01	,	00002340
1	.8619016153195327D-01	,	00002350
2	.7334648141108030D-01	,	00002360
3	.5929858491543678D-01	,	00002370
4	.4427743881741981D-01	,	00002380
5	.2853138862893366D-01	,	00002390
6	.1234122979998720D-01	,	00002400

C
C
C

WEIGHTS FOR ORDER 32 IN SEQUENCE 32.

7	.9654008851472780D-01	,	00002440
8	.9563872007927485D-01	,	00002450
9	.9384439908080455D-01	/	00002460
DATA WTB 40	/.9117387869576388D-01	,	00002470
1	.8765209300440381D-01	,	00002480
2	.8331192422694675D-01	,	00002490
3	.7819389578707030D-01	,	00002500
4	.7234579410884850D-01	,	00002510
5	.6582222277636184D-01	,	00002520
6	.5868409347853555D-01	,	00002530
7	.5099805926237618D-01	,	00002540
8	.4283589802222669D-01	,	00002550
9	.3427386291302143D-01	/	00002560
DATA WTB 50	/.2539206530926206D-01	,	00002570
1	.1627439473090567D-01	,	00002580
2	.7018610009470096D-02	,	00002590

C
C
C

WEIGHTS FOR ORDER 40 IN SEQUENCE 40.

3	.7750594797842481D-01	,	00002630
4	.7703981816424796D-01	,	00002640
5	.7611036190062624D-01	,	00002650
6	.7472316905796826D-01	,	00002660
7	.7288658239580405D-01	,	00002670
8	.7061164739128677D-01	,	00002680
9	.6791204581523390D-01	/	00002690
DATA WTB 60	/.6480401345660103D-01	,	00002700
1	.6130624249292894D-01	,	00002710
2	.5743976909939155D-01	,	00002720
3	.5322784698393682D-01	,	00002730
4	.4869580763507223D-01	,	00002740
5	.4387090818567327D-01	,	00002750
6	.3878216797447202D-01	,	00002760
7	.3346019528254785D-01	,	00002770
8	.2793700698002340D-01	,	00002780
9	.2224584919416696D-01	/	00002790
DATA WTB 70	/.1642105838190789D-01	,	00002800
1	.1049828453115281D-01	,	00002810
2	.4521277098533191D-02	,	00002820

11

11

SPQUAD

AJG1324.GTDS.UPDATE.FORT

```

C                                     00003430
C   COMPUTE THE MEAN MEAN LONGITUDE.  00003440
C                                     00003450
C   XML=EL-VPELMT(3)*DSIN(EL)+VPELMT(2)*DCOS(EL) 00003460
C                                     00003470
C   COMPUTE THE SHORT PERIODIC COEFFICIENTS OVER THE FIRST HALF. 00003480
C                                     00003490
C   DO 5 K=1,ISPNC 00003500
C     TT=K 00003510
C     DCK = DCOS(TT*XML) 00003520
C     DSK = DSIN(TT*XML) 00003530
C     DO 4 I=1,NOPARM 00003540
C       WGDP = WGHT*DPARDT(I) 00003550
C       CQUAD(I,K)=CQUAD(I,K)+WGDP*DCK 00003560
C       DQUAD(I,K)=DQUAD(I,K)+WGDP*DSK 00003570
C     4 CONTINUE 00003580
C     5 CONTINUE 00003590
C     INDEX=INDEX-1 00003600
C     IF (INDEX.GE.IBEG) GO TO 3 00003610
C   C                                     00003620
C     IF (XTAB(IBEG).NE.0.D0) GO TO 6 00003630
C     INDEX=IBEG 00003640
C   C                                     00003650
C   C ACCUMULATE THE QUADRATURE SUM OVER THE SECOND HALF OF THE INTERVAL. 00003660
C   C                                     00003670
C   C                                     00003680
C     6 CONTINUE 00003690
C   C                                     00003700
C   C   COMPUTE THE ELEMENT RATES. 00003710
C   C                                     00003720
C   C   INDEX=INDEX+1 00003730
C   C   EL = XX+DD*XTAB(INDEX) 00003740
C   C   CALL GQFUN(EL) 00003750
C   C   WGHT=WTAB(INDEX) 00003760
C   C   C                                     00003770
C   C   COMPUTE THE MEAN MEAN LONGITUDE. 00003780
C   C   C                                     00003790
C   C   XML=EL-VPELMT(3)*DSIN(EL)+VPELMT(2)*DCOS(EL) 00003800
C   C   C                                     00003810
C   C   COMPUTE THE SHORT PERIODIC COEFFICIENTS OVER THE SECOND HALF. 00003820
C   C   C                                     00003830
C   C   DO 8 K=1,ISPNC 00003840
C   C     TT=K 00003850
C   C     DCK=DCOS(TT*XML) 00003860
C   C     DSK=DSIN(TT*XML) 00003870
C   C     DO 7 I=1,NOPARM 00003880
C   C       WGDP=WGHT*DPARDT(I) 00003890
C   C       CQUAD(I,K)=CQUAD(I,K)+WGDP*DCK 00003900
C   C       DQUAD(I,K)=DQUAD(I,K)+WGDP*DSK 00003910
C   C     7 CONTINUE 00003920
C   C     8 CONTINUE 00003930
C   C     IF (INDEX.LT.IEND) GO TO 6 00003940
C   C   C                                     00003950
C   C   C RETURN THE VALUE OF THE COEFFICIENTS AND DIVIDE BY THE MEAN 00003960
C   C   C MOTION AND THE COEFFICIENT NUMBER. 00003970
C   C   C                                     00003980
C   C   C   DDPI = DD/(PI*XMEAN) 00003990

```

11

SPQUAD

AJG1324.GTDS.UPDATE.FORT

```
DO 10 K=1,ISPNC                                00004000
  TT=K                                           00004010
DO 9 I=1,NOFARM                                 00004020
  CQUAD(I,K)=(DDPI*CQUAD(I,K))/TT              00004030
  DQUAD(I,K)=(DDPI*DQUAD(I,K))/TT              00004040
9 CONTINUE                                       00004050
10 CONTINUE                                      00004060
C                                                 00004070
C   ACCOUNT FOR THE COUPLING BETWEEN THE FIRST AND SIXTH MEAN 00004080
C   ELEMENTS IN THE SHORT PERIODICS.              00004090
C                                                 00004100
C   A15=1.5D0/VPELMT(1)                            00004110
DO 11 K=1,ISPNC                                 00004120
  TT=K                                           00004130
  AK15=A15/TT                                     00004140
  CQUAD(6,K)=CQUAD(6,K)+AK15*DQUAD(1,K)         00004150
  DQUAD(6,K)=DQUAD(6,K)-AK15*CQUAD(1,K)         00004160
11 CONTINUE                                      00004170
C                                                 00004180
C   RETURN                                          00004190
C                                                 00004200
C   END                                            00004210

***** END OF MEMBER SPQUAD      421 RECORDS *****
```

```

SUBROUTINE VARDIF                                00000010
C                                                  00000020
C VERSION OF 20 JULY 1979 IMPLEMENTED AT CSDL ON AN AMDAHL 470 V6. 00000030
C                                                  00000040
C PURPOSE                                         00000050
C   TO COMPUTE THE A AND/OR D MATRICES WITH A FINITE-DIFFERENCING 00000060
C   TECHNIQUE.                                   00000070
C                                                  00000080
C PARAMETERS                                     00000090
C   /FRC/                                         00000100
C                                                  00000110
C   CDRAG    I/O  DRAG COEFFICIENT.              00000120
C                                                  00000130
C   /NEWPAR/                                     00000140
C                                                  00000150
C   APAR     I/O  ARRAY OF DENSITY PARAMETERS.   00000160
C   XS       I    ARRAY OF STEPSIZE USED TO COMPUTE PARTIALS. 00000170
C                                                  00000180
C   /ESTFLG/                                     00000190
C                                                  00000200
C   IDIFF    I    CONTROL SWITCH FOR FINITE-DIFFERENCING.      00000210
C               0=APPROACH NOT USED                          00000220
C               1=A MATRIX ONLY                              00000230
C               2=D MATRIX ONLY                              00000240
C               3=BOTH A AND D MATRICES                       00000250
C   KPAR     I    PARAMETER ESTIMATION OPTION.                00000260
C               0=NONE                                        00000270
C               1=SOLVE FOR CDRAG ONLY                        00000280
C               2=SOLVE FOR THE 5 PARAMETERS IN THE ADAPTIVE  00000290
C                 HARRIS-PRIESTER ATMOSPHERE.                00000300
C               3=SOLVE FOR THE 3 PARAMETERS IN THE ADAPTIVE  00000310
C                 HARRIS-FRIESTER ATMOSPHERE.                 00000320
C   KSTEP    I    ARRAY OF CONTROL SWITCHES FOR THE PERTURBING 00000330
C                 STEPSIZE.                                    00000340
C               1=STEPSIZE IS GIVEN IN XS                     00000350
C               2=STEPSIZE IS XS*PARAMETER                    00000360
C                                                  00000370
C   /VARMAT/                                     00000380
C                                                  00000390
C   AMAT     O    THE A MATRIX.                            00000400
C   DMAT     O    THE D MATRIX.                            00000410
C                                                  00000420
C   /WORKER/                                     00000430
C                                                  00000440
C   VPELMT   I    ARRAY OF MEAN ELEMENTS.                  00000450
C   NOPARM   I    NUMBER OF PARAMETERS.                    00000460
C   NPRT     O    PERTURBATION INDICATOR.                  00000470
C               1=CONTINUOUS TIME-DEPENDENT                  00000480
C               2=CONTINUOUS TIME-INDEPENDENT                00000490
C               3=DRAG                                        00000500
C               4=SOLAR RADIATION PRESSURE                   00000510
C   DPARRY   I    ARRAY OF ELEMENT DERIVATIVES.            00000520
C                                                  00000530
C   REFERENCES                                     00000540
C   "ORBIT DETERMINATION AND PREDICTION PROCESSES FOR LOW-ALTITUDE 00000550
C   SATELLITES." BY A.J. GREEN                           00000560
C                                                  00000570

```



```

C      00000580
C      ANALYSIS      00000590
C      ANDREW J. GREEN, CPT, U.S. ARMY      00000600
C      00000610
C      PROGRAMMER      00000620
C      ANDREW J. GREEN, CPT, U.S. ARMY      00000630
C      00000640
C      00000650
C      00000660
C      IMPLICIT REAL*8(A-H,O-Z)      00000670
C      DIMENSION TEHSAV(10),TEMRAT(10),DPARRY(15,10),VPELMT(10),
2      SAE(3),TSAE(3)      00000680
C      00000690
C      00000700
C      COMMON/THRUST/ DPTH(150), INTHR(50)      00000710
C      EQUIVALENCE (DPTH(61) ,SAE(1) )00000720
C      00000730
C      COMMON/ANAVIN/ YSTESS ,ITESSE ,ITRESE ,ISTHIR ,00000740
1      ITHRAR ,ITHRE ,ITESS ,ITRES ,NEND ,00000750
2      MEND ,LEND ,ITRES ,NRES(10) ,00000760
3      MRES(10) ,JRES(10) ,NCSRES ,LENDRS ,00000770
4      ITHIRD ,NENDTH(8) ,MENDTH(8) ,JTWOSQ ,00000780
5      IQUAD(4) ,NQAD(4) ,JPOS ,JA ,00000790
6      JB ,JC ,JGHA ,KPOS ,00000800
7      KA ,KB ,KC ,KGHA ,00000810
8      ICORR ,IPOS ,IMOON ,IMEAN ,00000820
9      IGHA ,ISTRES ,ITERM ,ISHAD ,00000830
1     JTMDEP ,JTMIND ,JDRAG ,JSOLAR ,00000840
2     J2SQSP ,JSPCGB ,JSPTHR ,JSPPOS ,00000850
3     JSPA ,JSFB ,JSPC ,JSPGHA ,00000860
4     KSPPOS ,KSPA ,KSPB ,KSPC ,00000870
5     KSPGHA ,KSPNC(4) ,KSPPR(4) ,NMAXSP ,00000880
6     MMAXSP ,IDRCR ,NCHQJ2 ,NCHODR
C      00000890
C      00000900
C      COMMON/FRC / RFRC(1300) ,IFRC(50)      00000910
C      EQUIVALENCE (CDRAG ,RFRC(154) ) ,00000920
1     (NMAX ,IFRC(3) ) ,00000930
2     (MMAX ,IFRC(4) ) 00000940
C      00000950
C      COMMON/WORKER/ RWORK(3264) ,IWORK(13)      00000960
C      EQUIVALENCE (DPARRY(1,1) ,RWORK(7) ) ,00000970
2     (VPELMT(1) ,RWORK(2829) ) 00000980
C      EQUIVALENCE (K ,IWORK(2) ) ,00000990
2     (NOPARM ,IWORK(3) ) ,00001000
3     (NEQ ,IWORK(5) ) ,00001010
4     (NPRT ,IWORK(9) ) 00001020
C      00001030
C      COMMON/ESTFLG/ IANAL ,IDIFF ,IQDRT ,ICBVAR ,J22VAR , 00001040
1     ITBVAR ,IDRVAR ,ISRVAR ,NVAR ,LEVAR , 00001050
2     KDRFLG ,KPAR ,KSTEP(20) ,KVRFLG ,KCPSP , 00001060
3     KCBSP ,KTBSPP ,KDRSPP ,KRSPP ,NVARSP , 00001070
4     IVSPNC(4) ,KATMOS ,KPRTB1 ,KPRTB2 ,KPRTB3 , 00001080
5     KPRTB4 00001090
C      00001100
C      COMMON/VARMAT/ AMAT(6,6) ,DMAT(6,14) ,B1MAT(6,6) ,B4MAT(6,14) 00001110
C      00001120
C      COMMON/NEWPAR/ XS(20) ,APAR(5) ,APARVR(5) ,CDRVAR 00001130
C      00001140

```

VARDIF

AJG1324.GTDS.UPDATE.FORT

```
C      SAVE THE DERIVATIVE ARRAY AND INITIALIZE THE A AND D MATRICES.      00001150
C
  DO 10 I=1,NOPARM
  TEMSAV(I)=DPARRY(K,I)
10 CONTINUE
  DO 40 I=1,6
  DO 20 J=1,6
  AMAT(I,J)=0.D0
20 CONTINUE
  DO 30 L=1,14
  DMAT(I,L)=0.D0
30 CONTINUE
40 CONTINUE
C
C      COMPUTE THE A MATRIX.
C
  IF(IDIFF.EQ.2) GO TO 300
  DO 100 J=1,5
  TEMP=VPELMT(J)
  STEP=XS(J)*DABS(VPELMT(J))
  IF((DABS(VPELMT(J)).LT.1.D-10).OR.(KSTEP(J).EQ.1)) STEP=XS(J)
  VPELMT(J)=VPELMT(J)+STEP
  CALL AVRAGE
  DO 50 I=1,6
  TEMRAT(I)=DPARRY(K,I)
50 CONTINUE
  VPELMT(J)=VPELMT(J)-2.D0*STEP
  CALL AVRAGE
  DO 75 I=1,6
  AMAT(I,J)=(TEMRAT(I)-DPARRY(K,I))/(2.D0*STEP)
75 CONTINUE
  VPELMT(J)=TEMP
100 CONTINUE
C
C      COMPUTE THE D MATRIX.
C
300 IF((IDIFF.EQ.1).OR.(KPAR.EQ.0)) GO TO 900
C
C      CHECK FOR THE PARAMETER ESTIMATION OPTION. FOR OPTIONS 1,2, AND 3
C      ONLY THE DRAG FORCE MODEL NEEDS TO BE CONSIDERED.
C
  IF(KPAR.GT.3) GO TO 500
C
  KNMAX=NMAX
  KMMAX=MMAX
  KRES=IRESON
  KTESS=ITESS
  KNCRS=NCSRES
  KTHIRD=ITHIRD
  KTWOSQ=JTWOSQ
  KTHDEP=ITHDEP
  KTHIND=ITHIND
  KSOLAR=ISOLAR
C
  NMAX=0
  MMAX=0
  IRESON=4
C
```

VARDIF

AJG1324.GTDS.UPDATE.FORT

```
ITESS=0 00001720
NCSRES=0 00001730
ITHIRD=0 00001740
JTWOSQ=2 00001750
ITHDEP=2 00001760
ITHIND=2 00001770
ISOLAR=2 00001780
C 00001790
KKPAR=KPAR 00001800
GO TO (310,400,401), KKPAP 00001810
C 00001820
C DETERMINE THE D MATRIX WHEN CDRAG IS A SOLVE-FOR PARAMETER. 00001830
C 00001840
310 TEMP=CDRAG 00001850
DO 320 I=1,3 00001860
TSAE(I)=SAE(I) 00001870
320 CONTINUE 00001880
STEP=XS(7)*CDRAG 00001890
IF((CDRAG.LT.1.D-10).OR.(KSTEP(7).EQ.1)) STEP=XS(7) 00001900
CDRAG=CDRAG+STEP 00001910
RHO=CDRAG/TEMP 00001920
DO 330 I=1,3 00001930
SAE(I)=TSAE(I)*RHO 00001940
330 CONTINUE 00001950
CALL AVRAGE 00001960
DO 350 I=1,6 00001970
TEMRAT(I)=DPARRY(K,I) 00001980
350 CONTINUE 00001990
CDRAG=CDRAG-2.D0*STEP 00002000
RHO=CDRAG/TEMP 00002010
DO 360 I=1,3 00002020
SAE(I)=TSAE(I)*RHO 00002030
360 CONTINUE 00002040
CALL AVRAGE 00002050
DO 375 I=1,6 00002060
DMAT(I,1)=(TEMRAT(I)-DPARRY(K,I))/(2.D0*STEP) 00002070
375 CONTINUE 00002080
CDRAG=TEMP 00002090
DO 380 I=1,3 00002100
SAE(I)=TSAE(I) 00002110
380 CONTINUE 00002120
GO TO 490 00002130
C 00002140
C DETERMINE THE D MATRIX WHEN PARAMETERS WITHIN THE ADAPTIVE 00002150
C MODIFIED HARRIS-PRIESTER ATMOSPHERE ARE THE SOLVE-FOR-PARAMETERS. 00002160
C 00002170
400 N=5 00002180
GO TO 403 00002190
401 N=3 00002200
403 DO 430 J=1,N 00002210
L=6+J 00002220
TEMP=APAR(J) 00002230
STEP=XS(L)*DABS(APAR(J) ) 00002240
IF((DABS(APAR(J))).LT.1.D-10).OR.(KSTEP(L).EQ.1)) STEP=XS(L) 00002250
APAR(J)=APAR(J)+STEP 00002260
CALL AVRAGE 00002270
DO 410 I=1,6 00002280
```

VARDIF

AJG1324.GTDS.UPDATE.FORT

```
      TEMRAT(I)=DPARRY(K,I)                                00002290
410 CONTINUE                                              00002300
      APAR(J)=APAR(J)-2.D0*STEP                            00002310
      CALL AVRAGE                                          00002320
      DO 420 I=1,6                                         00002330
      DMAT(I,J)=(TEMRAT(I)-DPARRY(K,I))/(2.D0*STEP)      00002340
420 CONTINUE                                              00002350
      APAR(J)=TEMP                                         00002360
430 CONTINUE                                              00002370
C                                                         00002380
C   RESET THE SWITCHES.                                    00002390
C                                                         00002400
490 NMAX=KNMAX                                           00002410
      NMAX=KNMAX                                           00002420
      ITESS=KTESS                                          00002430
      NCSRES=KNCRESES                                     00002440
      ITHIRD=KTHIRD                                        00002450
      JTWOSQ=KTWOSQ                                       00002460
      ITHDEP=KTMDEP                                       00002470
      ITHIND=KTMIND                                       00002480
      ISOLAR=KSOLAR                                       00002490
      GO TO 900                                           00002500
C                                                         00002510
C   ADDITIONAL ESTIMATION OPTIONS WOULD BE INCLUDED HERE. 00002520
C                                                         00002530
500 CONTINUE                                              00002540
C                                                         00002550
C   RESET THE DERIVATIVE ARRAY.                           00002560
C                                                         00002570
900 DO 910 I=1,6                                         00002580
      DPARRY(K,I)=TEMSAV(I)                               00002590
910 CONTINUE                                              00002600
C                                                         00002610
      RETURN                                              00002620
      END                                                  00002630
```

***** END OF MEMBER VARDIF 263 RECORDS *****

VARSP

AJG1324.GTDS.UPDATE.FORT

```
C SUBROUTINE VARSP 00000010
C 00000020
C VERSION OF 13 JULY 1979 IMPLEMENTED AT CSDL ON AN AMDAHL 470 V6. 00000030
C 00000040
C PURPOSE 00000050
C 00000060
C EXECUTIVE PROGRAM FOR THE DETERMINATION OF THE B1 AND B4 00000070
C MATRICES. 00000080
C 00000090
C PARAMETERS 00000100
C 00000110
C /ESTFLG/ 00000120
C 00000130
C KVTFLG I CONTROL SWITCH FOR THE SHORT PERIODIC PARTIALS 00000140
C 0=NEGLECT THE B1 AND B4 MATRICES 00000150
C 1=B1 MATRIX ONLY,DONE ANALYTICALLY 00000160
C 2=B1 MATRIX ONLY,DONE BY FINITE-DIFFERENCING 00000170
C 3=B4 MATRIX ONLY,DONE BY FINITE-DIFFERENCING 00000180
C 4=BOTH B1 AND B4 MATRICES,DONE BY FINITE- 00000190
C DIFFERENCING 00000200
C 00000210
C REFERENCE 00000220
C 00000230
C "ORBIT DETERMINATION AND PREDICTION PROCESSES FOR LOW- 00000240
C ALTITUDE SATELLITES." BY A.J. GREEN 00000250
C 00000260
C ANALYSIS 00000270
C ANDREW J. GREEN, CPT,U.S. ARMY, CSDL 00000280
C 00000290
C PROGRAMMER 00000300
C ANDREW J. GREEN, CPT, U.S. ARMY, CSDL 00000310
C 00000320
C IMPLICIT REAL*8(A-H,O-Z) 00000330
C 00000340
C COMMON/ESTFLG/ IANAL ,IDIFF ,IQDRT ,ICBVAR ,J22VAR , 00000350
1 ITBVAR ,IDRVAR ,ISRVAR ,NVAR ,LEVAR , 00000360
2 KDRFLG ,KPAR ,KSTEP(20),KVRFLG ,KCPSPP , 00000370
3 KCBSPP ,KTBSPP ,KDRSPP ,KRSPP ,NVARSP , 00000380
4 IVSFNC(4),KATMOS ,KPRTB1 ,KPRTB2 ,KPRTB3 , 00000390
5 KFRTB4 00000400
C 00000410
C COMMON/VARMAT/ AMAT(6,6),DMAT(6,14),B1MAT(6,6),B4MAT(6,14) 00000420
C 00000430
C 00000440
C CHECK FOR TYPE OF SHORT PERIODIC PARTIALS. 00000450
C 00000460
C IF(KVRFLG.EQ.0) GO TO 300 00000470
C IF(KVRFLG.NE.1) GO TO 200 00000480
C 00000490
C ANALYTICAL SHORT PERIODIC PARTIALS. 00000500
C 00000510
C 100 CALL VRSPAN 00000520
C GO TO 400 00000530
C 00000540
C SHORT PERIODIC PARTIALS VIA FINITE-DIFFERENCEING. 00000550
C 00000560
C 200 CALL VRSPFD 00000570
```

11

VARSP

AJG1324.6TDS.UPDATE.FORT

	GO TO 400	00000580
C		00000590
C	INITIALIZE THE B1 AND B4 MATRICES AND RETURN IF KVRFLG=0.	00000600
C		00000610
	300 DO 330 I=1,6	00000620
	DO 310 J=1,6	00000630
	B1MAT(I,J)=0.D0	00000640
	310 CONTINUE	00000650
	DO 320 L=1,14	00000660
	B4MAT(I,L)=0.D0	00000670
	320 CONTINUE	00000680
	330 CONTINUE	00000690
C		00000700
	400 RETURN	00000710
	END	00000720

***** END OF MEMBER VARSP

72 RECORDS *****

-

=

11

```

SUBROUTINE VRSPFD                                00000010
C                                                  00000020
C VERSION OF 13 JULY 1979 IMPLEMENTED AT CSOL ON AN AMDAHL 470 V6. 00000030
C                                                  00000040
C PURPOSE                                         00000050
C                                                  00000060
C   TO DETERMINE THE B1 AND/OR B4 MATRICES BY A FINITE-DIFFERENCING 00000070
C   TECHNIQUE.                                   00000080
C                                                  00000090
C PARAMETERS                                     00000100
C                                                  00000110
C   /ANAVIN/                                     00000120
C                                                  00000130
C   ITHIRD   0   CONTROL SWITCH FOR 3RD BODIES.   00000140
C   KSPNC    0   ARRAY OF THE NUMBER OF SHORT PERIODIC COEF- 00000150
C               FICIENTS FOR EACH PERTURBATIONS.   00000160
C                                                  00000170
C   /ESTFLG/                                     00000180
C                                                  00000190
C   KPAR     I   PARAMETER ESTIMATION OPTION.     00000200
C               0=NONE                             00000210
C               1=SOLVE FOR CDAG                   00000220
C               2=SOLVE FOR THE 5 PARAMETERS,A1 - A5, IN THE 00000230
C                 ADAPTIVE MODIFIED HARRIS-PRIESTER ATMOSPHERE. 00000240
C               3=SOLVE FOR THE 3 PARAMETERS,A1 - A3, IN THE 00000250
C                 ADAPTIVE MODIFIED HARRIS-PRIESTER ATMOSPHERE. 00000260
C   KSTEP    I   ARRAY OF CONTROL SWITCHES FOR THE PERTURBING 00000270
C               STEPSIZE.                           00000280
C               1=STEPSIZE IS GIVEN IN XS           00000290
C               2=STEPSIZE IS XS*PARAMETER         00000300
C   KVRFLG   I   CONTROL SWITCH FORT HE SHORT PERIODIC PARTIALS. 00000310
C               0=NONE                             00000320
C               1=B1 MATRIX - ANALYTICALLY         00000330
C               2=B1 MATRIX ONLY - FINITE DIFFERENCING 00000340
C               3=B4 MATRIX ONLY - FINITE DIFFERENCING 00000350
C               4=BOTH B1 AND B4 MATRICES - FINITE DIFFERENCING 00000360
C                                                  00000370
C   /NEWPAR/                                     00000380
C                                                  00000390
C   APAR     I/O  ARRAY OF DENSITY PARAMETERS.    00000400
C   XS       I   ARRAY OF STEPSIZE USED TO COMPUTE PARTIALS. 00000410
C                                                  00000420
C   /SPCOEF/                                     00000430
C                                                  00000440
C   CQUAD    I   ARRAY OF THE C SHORT PERIODIC COEFFICIENT. 00000450
C   DQUAD    I   ARRAY OF THE D SHORT PERIODIC COEFFICIENT. 00000460
C                                                  00000470
C   /WORKER/                                     00000480
C                                                  00000490
C   VPELMT   I/O  ARRAY OF THE MEAN ELEMENTS.     00000500
C   XLAMDA   I   MEAN FAST VARIABLE.              00000510
C   NOPARM   I   NUMBER OF PARAMETERS.            00000520
C   NEQ      I   NUMBER OF VARIATIONAL EQUATIONS. 00000530
C                                                  00000540
C REFERENCES                                     00000550
C                                                  00000560
C   "ORBIT DETERMINATION AND PREDICTION PROCESSES FOR LOW- 00000570

```

```

C      ALTITUDE SATELLITES." BY A.J. GREEN                                00000580
C                                                                 00000590
C      ANALYSIS                                                            00000600
C      ANDREW J. GREEN, CPT, U.S. ARMY                                    00000610
C                                                                 00000620
C      PROGRAMMER                                                            00000630
C      ANDREW J. GREEN, CPT, U.S. ARMY                                    00000640
C                                                                 00000650
C                                                                 00000660
C      IMPLICIT REAL*8(A-H,O-Z)                                           00000670
C      DIMENSION XMMAT(6,5),XMMAT(6,5),XCQUAD(6,10),XDQUAD(6,10),      00000680
C      2      XKMAT(6,14),XLMAT(6,14),VPELMT(10),SAE(3),TSAE(3)         00000690
C      DIMENSION INC(4)                                                    00000700
C                                                                 00000710
C      COMMON/THRUST/ DPTH(150), INT(50)                                    00000720
C      EQUIVALENCE (DPTH(61) ,SAE(1) )00000730
C                                                                 00000740
C      COMMON/ANAVIN/  ISTESE ,ITRESE ,ISTHIR ,00000750
C      1      ITHRAR ,ITHRE ,ITRES ,NEND ,00000760
C      2      MEND ,LEND ,ITRES ,NRES(10) ,00000770
C      3      MRES(10) ,JRES(10) ,NCSRES ,LENDRES ,00000780
C      4      ITHIRD ,NENDTH(8) ,MENDTH(8) ,JTWOSQ ,00000790
C      5      IQUAD(4) ,NQUAD(4) ,JPOS ,JA ,00000800
C      6      JB ,JC ,JGHA ,KPOS ,00000810
C      7      KA ,KB ,KC ,KGHA ,00000820
C      8      ICORR ,IPOS ,IMOON ,IMEAN ,00000830
C      9      IGHA ,ISTRES ,ITERM ,ISHAD ,00000840
C      1      JTMDEP ,JTMIND ,JDRAG ,JSOLAR ,00000850
C      2      J2SQSP ,JSFCGB ,JSPTHR ,JSPPOS ,00000860
C      3      JSPA ,JSPB ,JSPC ,JSPGHA ,00000870
C      4      KSPPOS ,KSPA ,KSPB ,KSPC ,00000880
C      5      KSPGHA ,KSPNC(4) ,KSPPR(4) ,NMAXSP ,00000890
C      6      MMAXSP ,IDRDR ,NCHOJ2 ,NCHODR 00000900
C                                                                 00000910
C      COMMON/FRC / RFRC(1300) ,IFRC(50)                                    00000920
C      EQUIVALENCE (CDRAG ,RFRC(154) ) 00000930
C                                                                 00000940
C      COMMON/WORKER/ RWORK(3264) ,IWORK(13)                               00000950
C      EQUIVALENCE (VPELMT(1) ,RWORK(2829) ) ,00000960
C      2      (XLAMDA ,RWORK(2851) ) 00000970
C      EQUIVALENCE (NOPARM ,IWORK(3) ) ,00000980
C      2      (NEQ ,IWORK(5) ) ,00000990
C      3      (NPRT ,IWORK(9) ) 00001000
C                                                                 00001010
C      COMMON/ESTFLG/ IANAL ,IDIFF ,IQDRT ,ICBVAR ,J22VAR , 00001020
C      1      ITBVAR ,IDRVAR ,ISRVAR ,NVAR ,LEVAR , 00001030
C      2      KDRFLG ,KPAR ,KSTEP(20),KVRFLG ,KCFSP , 00001040
C      3      KCBSP ,KTBSPP ,KDRSPP ,KRSPP ,NVARSP , 00001050
C      4      IVSFNC(4),KATMOS ,KPRTB1 ,KPRTB2 ,KPRTB3 , 00001060
C      5      KPRTB4 00001070
C                                                                 00001080
C      COMMON/VARMAT/ AMAT(6,6),DMAT(6,14),BIMAT(6,6),B4MAT(6,14)      00001090
C                                                                 00001100
C      COMMON/NEWPAR/ XS(20) ,APAR(5) ,APARVR(5),CDRVAR 00001110
C                                                                 00001120
C      COMMON/SPCOEF/ EQUAD(10,10),DQUAD(10,10) 00001130
C                                                                 00001140

```


VRSPFD

AJG1324.GTDS.UPDATE.FORT

```

C   SET THE NUMBER OF SHORT PERIODIC COEFFICIENTS AND INITIALIZE.      00001150
C   DO 1 I=1,4                                                            00001160
C   INC(I)=KSPNC(I)                                                       00001170
C   KSPNC(I)=IVSPNC(I)                                                    00001180
C   1 CONTINUE                                                             00001190
C   KMAX=MAX0(KSPNC(1),KSPNC(2),KSPNC(3),KSPNC(4))                      00001200
C   DO 7 I=1,6                                                            00001210
C   DO 5 J=1,6                                                            00001220
C   BIMAT(I,J)=0.00                                                       00001230
C   5 CONTINUE                                                             00001240
C   DO 6 L=1,14                                                           00001250
C   B4MAT(I,L)=0.00                                                       00001260
C   6 CONTINUE                                                             00001270
C   7 CONTINUE                                                             00001280
C   COMPUTE THE B1 MATRIX                                                 00001290
C   IF(KVRFLG.EQ.3) GO TO 300                                             00001300
C   DO 250 J=1,5                                                           00001310
C   TEMP=VPELMT(J)                                                         00001320
C   STEP=XS(J)*DABS(VPELMT(J))                                             00001330
C   IF((DABS(VPELMT(J)).LT.1.D-10).OR.(KSTEP(J).EQ.1)) STEP=XS(J)       00001340
C   VPELMT(J)=VPELMT(J)+STEP                                              00001350
C   CALL SPCOTO                                                            00001360
C   DO 220 I=1,6                                                           00001370
C   DO 210 L=1,KMAX                                                        00001380
C   XCQUAD(I,L)=CQUAD(I,L)                                                00001390
C   XDQUAD(I,L)=DQUAD(I,L)                                               00001400
C   210 CONTINUE                                                           00001410
C   220 CONTINUE                                                           00001420
C   VPELMT(J)=VPELMT(J)-2.00*STEP                                         00001430
C   CALL SPCOTO                                                            00001440
C   DO 240 L=1,KMAX                                                        00001450
C   XL=L                                                                    00001460
C   DO 230 I=1,6                                                           00001470
C   XMMAT(I,J)=(XCQUAD(I,L)-CQUAD(I,L))/(2.00*STEP)                    00001480
C   XNMAT(I,J)=(XDQUAD(I,L)-DQUAD(I,L))/(2.00*STEP)                    00001490
C   BIMAT(I,J)=BIMAT(I,J)+XMMAT(I,J)*DSIN(XL*XLAMDA)-                  00001500
C   * XNMAT(I,J)*DCOS(XL*XLAMDA)                                         00001510
C   230 CONTINUE                                                           00001520
C   240 CONTINUE                                                           00001530
C   VPELMT(J)=TEMP                                                         00001540
C   250 CONTINUE                                                           00001550
C   DO THE 6TH COLUMN OF THE B1 MATRIX                                    00001560
C   CALL SPCOTO                                                            00001570
C   DO 270 L=1,KMAX                                                        00001580
C   XL=L                                                                    00001590
C   DO 260 I=1,6                                                           00001600
C   BIMAT(I,6)=BIMAT(I,6)+CQUAD(I,L)*XL*DCOS(XL*XLAMDA)+              00001610
C   * DQUAD(I,L)*XL*DSIN(XL*XLAMDA)                                       00001620
C   260 CONTINUE                                                           00001630
C   270 CONTINUE                                                           00001640
C   00001650
C   00001660
C   00001670
C   00001680
C   00001690
C   00001700
C   00001710

```

C	COMPUTE THE B4 MATRIX.	00001720
C		00001730
C	300 IF((KVRFLG.LE.2).OR.(KPAR.EQ.0)) GO TO 900	00001740
C		00001750
C	CHECK FOR THE PARAMETER ESTIMATION OPTION. FOR OPTIONS 1,2 AND 3,	00001760
C	ONLY THE DRAG FORCE MODEL NEEDS TO BE CONSIDERED.	00001770
C		00001780
C	N=NEQ-6	00001790
C	IF(KPAR.GT.3) GO TO 900	00001800
C		00001810
C	MCPSPP=KCPSP	00001820
C	MSRSPP=KSRSP	00001830
C	KCFSP=2	00001840
C	KSRSP=2	00001850
C		00001860
C	KKPAR=KPAR	00001870
C	GO TO (303,400,400), KKPAR	00001880
C		00001890
C	DETERMINE THE B4 MATRIX WHEN CDRAG IS A SOLVE-FOR-PARAMETER.	00001900
C		00001910
C	303 TEMP=CDRAG	00001920
C	DO 304 I=1,3	00001930
C	TSAE(I)=SAF(I)	00001940
C	304 CONTINUE	00001950
C	STEP=XS(7)*CDRAG	00001960
C	IF((CDRAG.LT.1.D-10).OR.(KSTEP(7).EQ.1)) STEP=XS(7)	00001970
C	CDRAG=CDRAG+STEP	00001980
C	RHO=CDRAG/TEMP	00001990
C	DO 305 I=1,3	00002000
C	SAE(I)=TSAE(I)*RHO	00002010
C	305 CONTINUE	00002020
C	CALL SPCOTO	00002030
C	DO 320 I=1,6	00002040
C	DO 310 L=1,KMAX	00002050
C	XCQUAD(I,L)=CQUAD(I,L)	00002060
C	XDQUAD(I,L)=DQUAD(I,L)	00002070
C	310 CONTINUE	00002080
C	320 CONTINUE	00002090
C	CDRAG=CDRAG-2.D0*STEP	00002100
C	RHO=CDRAG/TEMP	00002110
C	DO 325 I=1,3	00002120
C	SAE(I)=TSAE(I)*RHO	00002130
C	325 CONTINUE	00002140
C	CALL SPCOTO	00002150
C	DO 340 L=1,KMAX	00002160
C	XL=L	00002170
C	DO 330 I=1,6	00002180
C	XKMAT(I,1)=(XCQUAD(I,L)-CQUAD(I,L))/(2.D0*STEP)	00002190
C	XLMAT(I,1)=(XDQUAD(I,L)-DQUAD(I,L))/(2.D0*STEP)	00002200
C	B4MAT(I,1)=B4MAT(I,1)+XKMAT(I,1)*DSIN(XL*XLAMDA)-	00002210
C	* XLMAT(I,1)*DCOS(XL*XLAMDA)	00002220
C	330 CONTINUE	00002230
C	340 CONTINUE	00002240
C	CDRAG=TEMP	00002250
C	DO 345 I=1,3	00002260
C	SAE(I)=TSAE(I)	00002270
C	345 CONTINUE	00002280

```

          GO TO 490
C
C   DETERMINE THE B4 MATRIX WHEN THE APAR'S ARE THE SOLVE-FOR-
C   PARAMETERS.
C
400 DO 450 J=1,N
      JLL=6+J
      TEMP=APAR(J)
      STEP=XS(JLL)*DABS(APAR(J))
      IF((DASS(APAR(J)).LT.1.D-10).OR.(KSTEP(JLL).EQ.1)) STEP=XS(JLL)
      APAR(J)=APAR(J)+STEP
      CALL SFCOTO
      DO 420 I=1,6
      DO 410 L=1,KMAX
      XCQUAD(I,L)=CQUAD(I,L)
      XDQUAD(I,L)=DQUAD(I,L)
410 CONTINUE
420 CONTINUE
      APAR(J)=APAR(J)-2.D0*STEP
      CALL SPCOTO
      DO 440 L=1,KMAX
      XL=L
      DO 430 I=1,6
      XKMAT(I,J)=(XCQUAD(I,L)-CQUAD(I,L))/(2.D0*STEP)
      XLMAT(I,J)=(XDQUAD(I,L)-DQUAD(I,L))/(2.D0*STEP)
      B4MAT(I,J)=B4MAT(I,J)+XKMAT(I,J)*DSIN(XL*XLAMDA)-
      *      XLMAT(I,J)*DCOS(XL*XLAMDA)
430 CONTINUE
440 CONTINUE
      APAR(J)=TEMP
450 CONTINUE
C
C   RESET THE FLAGS.
C
490 KCPSPP=MCPSPP
      KRSPP=MSRSP
C
C   ADDITIONAL ESTIMATION OPTIONS WOULD BE INCLUDED HERE.
C
500 CONTINUE
C
C   RESET THE NUMBER OF SHORT PERIODIC COEFFICIENTS.
C
900 DO 910 I=1,4
      KSPNC(I)=INC(I)
- 910 CONTINUE
C
      RETURN
      END

```

```

00002290
00002300
00002310
00002320
00002330
00002340
00002350
00002360
00002370
00002380
00002390
00002400
00002410
00002420
00002430
00002440
00002450
00002460
00002470
00002480
00002490
00002500
00002510
00002520
00002530
00002540
00002550
00002560
00002570
00002580
00002590
00002600
00002610
00002620
00002630
00002640
00002650
00002660
00002670
00002680
00002690
00002700
00002710
00002720
00002730
00002740
00002750
00002760
00002770

```

***** END OF MEMBER VRSPFD 277 RECORDS *****

Appendix G

MEASUREMENT EQUATIONS AND PARTIAL DERIVATIVES

This appendix is taken from Section 7.2.3 of Reference 67. Range, range rate and the gimbal angle (X_{30} , Y_{30} , X_{85} , Y_{85}) measurements used in VHF and USB (Unified S-Band) tracking stations are presented in this appendix. A more detailed discussion is given in Reference 67.

Range Observations for USB

The expected value of $\rho(t_R)$ is computed from ephemeris information and station coordinates using the following equation

$$\rho(t_R) = \frac{1}{2} \{ |\bar{r}_V(t_V) - \bar{r}_T(t_T)| + |\bar{r}_V(t_V) - \bar{r}_R(t_R)| \}$$

(G-1)

For simplicity, this equation is presented in an inertial reference frame, where

- \bar{r}_V ~ spacecraft inertial position vector
- \bar{r}_T ~ transmitting site inertial position vector
- \bar{r}_R ~ receiving site inertial position vector
- t_T ~ time at which the measured signal left the ground transmitter

t_v \sim time at which the measured signal was received and retransmitted by the spacecraft. The assumption of instantaneous turnaround is used; the constant bias in the observed range caused by the spacecraft electronic delay is accounted for as a measurement error elsewhere in GTDS.

t_r \sim time tag of the reduced observed range (that is, the time at which the measured signal arrived at the ground receiver).

The algorithm used in GTDS to compute $\rho(t_R)$ proceeds as follows:

1. Calculate $\bar{r}_R(t_R)$
2. Calculate iteratively the downlink propagation distance $\rho_d(t_R)$ using the following equations:

$$(a) \quad \rho_d(t_R) = |\bar{r}_v(t_v) - \bar{r}_R(t_R)|$$

$$(b) \quad \delta_d(t_R) = \rho_d(t_R)/c \quad (G-2)$$

$$(c) \quad t_v = t_R - \delta_d(t_R)$$

The iteration process is initiated by assuming that $t_v = t_R$, and is terminated when successive values of $\delta_d(t_R)$ agree to within 10^{-8} seconds.

3. Calculate iteratively the uplink propagation distance $\rho_u(t_R)$ using the following equations:

$$(a) \quad \rho_u(t_R) = |\bar{r}(t_v) - \bar{r}_T(t_T)|$$

$$(b) \quad \delta_u(t_R) = \rho_u(t_R)/c \quad (G-3)$$

$$(c) \quad t_T = t_v - \delta_u(t_R)$$

The iteration is initiated by assuming that

$\delta_u(t_R) = \delta_d(t_R)$, and is terminated when successive values of $\delta_u(t_R)$ agree to within 10^{-8} seconds.

4. The following geometrically exact equation is used to compute the expected value of the range $\rho(t_R)$ for the USB system

$$\rho(t_R) = [\rho_u(t_R) + \rho_d(t_R)]/2 \quad (G-4)$$

The partial derivatives of the expected range [Equation (G-1)] in inertial coordinates (USB system) are

$$\begin{aligned} \frac{\partial \rho(t_R)}{\partial \bar{r}_V(t_V)} &= \frac{1}{2\rho_u\rho_d} \{ \rho_d [\bar{r}_V^T(t_V) - \bar{r}_T^T(t_T)] \\ &+ \rho_u [\bar{r}_V^T(t_V) - \bar{r}_R^T(t_R)] \} \end{aligned} \quad (G-5)$$

$$\frac{\partial \rho(t_R)}{\partial \dot{\bar{r}}_V(t_V)} = 0 \quad (G-6)$$

If it is assumed that $\rho_u = \rho_d = \rho(t_R)$, Equation (G-5) reduces to

$$\frac{\partial \rho(t_R)}{\partial \bar{r}_V(t_V)} = \frac{1}{2\rho(t_R)} \{ 2\bar{r}_V^T(t_V) - [\bar{r}_T^T(t_T) + \bar{r}_R^T(t_R)] \} \quad (G-7)$$

Range Observations for VHF

Range data produced by the VHF system is less accurate than that produced by the USB tracking system; therefore, it does not warrant the application of the iterative solution described above. Instead, the following more efficient algorithm is used to determine an instantaneous approximation for $\rho(t_R)$ using VHF range data

$$\begin{aligned}\rho(t_R) &= |\bar{r}_V(t_V) - \bar{r}_T(t_V)| = |\bar{r}_{1t}(t_V)| \\ &= \sqrt{x_{1t}^2 + y_{1t}^2 + z_{1t}^2}\end{aligned}\tag{G-8}$$

where

$$t_V = t_R - \rho(t_R)/c$$

and \bar{r}_{1t} is the spacecraft position vector in local tangent plane coordinates.

The partial derivatives of the expected range in local tangent plane coordinates are

$$\frac{\partial \rho(t_R)}{\partial \bar{r}_{1t}(t_V)} = \frac{\bar{r}_{1t}^T(t_V)}{\rho(t_R)}\tag{G-9}$$

$$\frac{\partial \rho(t_R)}{\partial \dot{r}_{1t}(t_v)} = 0 \quad (G-10)$$

Range Rate Observations for USB

The modeling of the expected value of the range rate which is most precise is to difference the average range at the beginning and end of the count interval as shown below

$$\dot{\rho}(t_R) = \frac{[\rho_u(t_R) + \rho_d(t_R)] - [\rho_u(t_R - \Delta t_{RR}) + \rho_d(t_R - \Delta t_{RR})]}{2\Delta t_{RR}} \quad (G-11)$$

where

- $\rho_u(t_R) \sim$ uplink propagation path of a signal arriving at the receiver at t_R
- $\rho_d(t_R) \sim$ downlink propagation path of a signal arriving at the receiver at t_R
- $\Delta t_{RR} \sim$ Doppler count time interval

The calculations for these uplink and downlink ranges are iteratively corrected for the light time delay in exactly the same manner as the USB range observations. This method is used for USB measurements where the time tag on the observed data is t_R (corresponding to the end of the count interval) and the count interval Δt_{RR} corresponds to the sample interval. This method is accurate for both two-way and three-way Doppler measurements

using the USB system. Two-way Doppler measurements are obtained when the transmitting and receiving antennas are the same, while three-way Doppler measurements are obtained when the transmitting and receiving antennas are different.

The range-rate partial derivatives with respect to the epoch state elements \bar{R} and $\dot{\bar{R}}$ are computed most efficiently by using the algorithms for the range partial derivatives

$$\frac{\dot{\partial \rho(t_R)}}{\partial \bar{R}} = \frac{\frac{\partial \rho(t_R)}{\partial \bar{R}} - \frac{\partial \rho(t_R - \Delta t_{RR})}{\partial \bar{R}}}{\Delta t_{RR}} \quad (G-12)$$

$$\frac{\dot{\partial \rho(t_R)}}{\partial \dot{\bar{R}}} = \frac{\frac{\partial \rho(t_R)}{\partial \dot{\bar{R}}} - \frac{\partial \rho(t_R - \Delta t_{RR})}{\partial \dot{\bar{R}}}}{\Delta t_{RR}} \quad (G-13)$$

Range Rate Observations for VHF

The VHF range rate, which is the least accurate but most efficient, calculates the instantaneous range rate at the mid-point of the Doppler count interval as seen at the spacecraft. This value is used to approximate the average range rate over the uplink and downlink paths, and is therefore denoted $\dot{\rho}_{avg}$. It is computed as

$$\dot{\rho}_{\text{avg}} = \frac{\bar{r}_{1t}(t_v) \cdot \dot{\bar{r}}_{1t}(t_v)}{|\bar{r}_{1t}(t_v)|} \quad (\text{G-14})$$

The position and velocity vectors are expressed in station-centered local tangent plane coordinates evaluated at the vehicle turnaround time t_v . When this method is used the processor modifies the time tag on the VHF data according to the relationship

$$t_v = t_R + \frac{\Delta t_{RR}}{2} - \frac{|\bar{r}_{1t}(t_v)|}{c} \quad (\text{G-15})$$

The partial derivatives of $\dot{\rho}_{\text{avg}}$ with respect to local tangent plane coordinates are

$$\frac{\partial \dot{\rho}_{\text{avg}}}{\partial \bar{r}_{1t}} = \frac{1}{\rho(t_R)} \left[\begin{matrix} \dot{\bar{r}}_{1t}^T \\ \rho_{\text{avg}} \\ \bar{r}_{1t}^T \end{matrix} \right] \quad (\text{G-16})$$

$$\frac{\partial \dot{\rho}_{\text{avg}}}{\partial \dot{\bar{r}}_{1t}} = \frac{\bar{r}_{1t}^T}{\rho(t_R)} \quad (\text{G-17})$$

Gimbal Angles X_{30} and Y_{30}

The gimbal angles for the 30-foot antennas in the VHF and USB systems are denoted X_{30} and Y_{30} . The X_{30} -axis is aligned north-south in the local horizon (tangent) plane at the tracking

station. The reference plane for the angular measurements is the vertical plane which is aligned east-west and includes the tracking station zenith. The angle X_{30} is measured from the vertical axis (zenith) to the projection of the station-to-spacecraft vector onto the reference plane. This angle is positive when the spacecraft is east of the station, i.e.

$$X_{30} = \tan^{-1} \left(\frac{x_{1t}}{z_{1t}} \right) \quad -\frac{\pi}{2} \leq X_{30} \leq \frac{\pi}{2} \quad (G-18)$$

The angle Y_{30} is measured from the projection of the station-to-spacecraft vector onto the reference plane to the vector itself. This angle is positive when the spacecraft is north of the station, i.e.

$$Y_{30} = \tan^{-1} \left(\frac{y_{1t}}{\sqrt{x_{1t}^2 + z_{1t}^2}} \right) \quad -\frac{\pi}{2} \leq Y_{30} \leq \frac{\pi}{2} \quad (G-19)$$

The partial derivatives of X_{30} and Y_{30} with respect to the local tangent plane coordinates are

$$\frac{\partial X_{30}}{\partial \bar{r}_{1t}} = \frac{1}{(x_{1t}^2 + z_{1t}^2)} [z_{1t}, 0, -x_{1t}] \quad (G-20)$$

$$\frac{\partial X_{30}}{\partial \dot{\bar{r}}_{1t}} = 0$$

and

$$\frac{\partial Y_{30}}{\partial \bar{r}_{1t}} = \frac{1}{\rho^2} \left[\frac{-x_{1t}y_{1t}}{\sqrt{x_{1t}^2 + z_{1t}^2}}, \sqrt{x_{1t}^2 + z_{1t}^2}, \frac{-y_{1t}z_{1t}}{\sqrt{x_{1t}^2 + z_{1t}^2}} \right] \quad (G-21)$$

$$\frac{\partial Y_{30}}{\partial \dot{\bar{r}}_{1t}} = 0$$

where

$$\rho = \sqrt{x_{1t}^2 + y_{1t}^2 + z_{1t}^2}$$

Gimbal Angles X_{85} and Y_{85}

The gimbal angles associated with the USB 85-foot antennas are denoted X_{85} and Y_{85} . The X_{85} -axis is aligned east-west in the local horizon (tangent) plane at the tracking station. The reference plane for the angular measurements is the vertical plane which is aligned north-south and includes the tracking station zenith. The angle X_{85} is measured from the vertical axis (zenith) to the projection of the station-to-spacecraft vector onto the reference plane. This angle is positive when the spacecraft is south of the station, i.e.

$$X_{85} = \tan^{-1} \left(-\frac{y_{1t}}{z_{1t}} \right) \quad -\frac{\pi}{2} \leq X_{85} \leq \frac{\pi}{2} \quad (\text{G-22})$$

The angle Y_{85} is measured from the projection of the station-to-spacecraft vector onto the reference plane to the vector itself. This angle is positive when the spacecraft is east of the station, i.e.,

$$Y_{85} = \tan^{-1} \left(\frac{x_{LT}}{\sqrt{y_{1t}^2 + z_{1t}^2}} \right) \quad -\frac{\pi}{2} \leq Y_{85} \leq \frac{\pi}{2} \quad (\text{G-23})$$

The partial derivatives of X_{85} and Y_{85} with respect to the local tangent plane coordinates are

$$\frac{\partial X_{85}}{\partial \bar{r}_{1t}} = \frac{1}{(y_{1t}^2 + z_{1t}^2)} [0, -z_{1t}, y_{1t}] \quad (\text{G-24})$$

$$\frac{\partial X_{85}}{\partial \dot{\bar{r}}_{1t}} = 0$$

and

$$\frac{\partial Y_{85}}{\partial \bar{r}_{1t}} = \frac{1}{\rho^2} \left[\frac{1}{\sqrt{y_{1t}^2 + z_{1t}^2}}, \frac{-x_{1t}y_{1t}}{\sqrt{y_{1t}^2 + z_{1t}^2}}, \frac{-x_{1t}z_{1t}}{\sqrt{y_{1t}^2 + z_{1t}^2}} \right] \quad (\text{G-25})$$

$$\frac{\partial Y_{85}}{\partial \dot{\bar{r}}_{1t}} = 0$$

REFERENCES

1. Shaver, Jeffrey S., "Formulation and Evaluation of Parallel Algorithms for the Orbit Determination Problem," Ph.D. Dissertation, Massachusetts Institute of Technology, Cambridge, MA, January 1980.
2. Drutz, A., "427M: A Contractor's View of Lessons Learned," Proceedings of the IEEE 1978 National Aerospace and Electronics Conference, New York: IEEE, 1978, pp. 1327-1532.
3. McClain, W. D., A Recursively Formulated First-Order Semi-analytic Artificial Satellite Theory Based on the Generalized Method of Averaging, Vol. 1, November 1977, CSC/TR-77/6010, Computer Sciences Corporation, Silver Spring, Maryland, NASA-CR-156782, N78-28147, 1978.
4. McClain, W. D., A Recursively Formulated First-Order Semi-analytic Artificial Satellite Theory Based on the Generalized Method of Averaging, Vol. 2, May 1978, CSC/TR-78/6001, Computer Sciences Corporation, Silver Spring, Maryland, NASA-CR-156783, N78-28148, 1978.
5. Cefola, P. J., and W. D. McClain, "A Recursive Formulation of the Short-Periodic Perturbations in Equinoctial Variables," 78-1383, AIAA/AAS Astrodynamics Conference, Palo Alto, California, August 1978.
6. Zeis, E. G., "A Computerized Algebraic Utility for the Construction of Nonsingular Satellite Theories," M.S. Thesis, Massachusetts Institute of Technology, September 1978.
7. Zeis, E., and P. Cefola, "Computerized Algebraic Utilities for the Construction of Nonsingular Satellite Theories," 78-1381, AIAA/AAS Astrodynamics Conference, Palo Alto, Calif., August 1978.
8. Cefola, P., "On the Development of a Recursive Semianalytical Orbit Prediction Method," presented at the NASA/GSFC Flight Mechanics Conference, Greenbelt, Maryland, May 1976.
9. McClain, W. D., et al., "Development and Evaluation of a Hybrid Averaged Orbit Generator," No. 78-1382, AIAA/AAS Astrodynamics Conference, Palo Alto, Calif., August 1978.
10. Cefola, P., A. Long, and G. Holloway, "The Long-Term Prediction of Artificial Satellite Orbits," No. 74-170, AIAA Aerospace Sciences Meeting, Washington, D.C., February 1974.

11. Cefola, P., and R. Broucke, "On the Formulation of the Gravitational Potential in Terms of Equinoctial Variables," No. 75-9, AIAA Aerospace Sciences Meeting, Pasadena, Calif., January 1975.
12. Long, A. C., and W. D. McClain, "Optimal Perturbation Models for Averaged Orbit Generation," No. 76-815, AIAA/AAS Astrodynamics Conference, San Diego, Calif., August 1976.
13. Cefola, P. J., "A Recursive Formulation for the Tesseral Disturbing Function in Equinoctial Variables," No. 76-839, AIAA/AAS Astrodynamics Conference, San Diego, Calif., August 1976.
14. Cefola, P., "Application of Semianalytical Satellite Theories to Precision Orbit Determination," Proceedings of the NASA/GSFC Flight Mechanics Conference, Greenbelt, Maryland, October 1977.
15. Broucke, R., and P. Cefola, "On the Equinoctial Orbital Elements," Celestial Mechanics, Vol. 5, No. 3, pp. 303-310, 1972.
16. Morrison, J. A., "Generalized Method of Averaging and the Von Zeipel Method," Progress in Astronautics and Aeronautics, Volume 17: Methods in Astrodynamics and Celestial Mechanics, (R. L. Duncombe and V. G. Szebeheley, editors), New York: Academic Press, 1966, pp. 117-138.
17. Dowd, Douglas, L., "Adaptive Estimation of Atmospheric Drag on Near Earth Satellites," Ph.D. Dissertation, The University of Texas at Austin, Austin, Texas, December 1977.
18. King-Hele, D. G., "Measurements of Upper Atmosphere Rotational Speed from Changes in Satellite Orbits," R.A.E. Technical Report 71171, August 1971.
19. Uphoff, C., "Numerical Averaging in Orbit Prediction," AIAA Journal, Vol. 11, No. 11, November 1973, pp. 1513-1516.
20. Lutzky, D., and C. Uphoff, "Short Periodic Variations and Second-Order Numerical Averaging," No. 75-11, AIAA Aerospace Sciences Meeting, Pasadena, Calif., January 1975.
21. Kaula, W. M., Theory of Satellite Geodesy, Blaisdell Publishing Co., Waltham, MA, 1966.
22. Boyer, R. A., ed., MACSYMA Reference Manual, Project MAC - MIT, AD-774767, Massachusetts Institute of Technology, Cambridge, MA, 1977.

23. Bruce, R. W., A Survey of Model Atmospheres Used in the Analysis of Satellite Orbits, Aerospace Corporation, under Contract No. AF.04(695)-469, 10 April 1965.
24. Jacchia, L. G., J. W. Slowey and I. G. Campbell, "An Analysis of the Solar Activity Effects in the Upper Atmosphere," Planetary and Space Science, Vol. 21, 1973, pp. 1835-1847.
25. King-Hele, D. G., "The Upper Atmosphere and its Influence on Satellite Orbits," Dynamics of Satellites, ed. Bruno Morando, Springer-Verlag, New York, 1970.
26. King-Hele, D. G., "Upper Atmosphere Studies by Ranging to Satellites," Proc. Roy. Soc. Lond. A, Vol. 284, pp. 555-563, 1977.
27. Elyasberg, P. E., et al., "The Estimation of Accuracy of Short-Term Atmospheric Density Prediction," Astronautical Research, eds. L. G. Napolitano, et al., 1972, pp. 31-42.
28. Kameko, V. F., et al., "Prediction of the Density of the Upper Atmosphere for the Duration of Artificial Earth Satellites," Translated from Kosmicheskie Issledovaniya, Vol. 10, No. 3, pp. 450-453, May-June 1972, Plenum Publishing Corporation, New York.
29. Elyasberg, P. E., and B. V. Kugaenko, "Effects of Upper Atmosphere Density Variations on Artificial Earth Satellite Orbits," Space Research XVI, Akademie-Verlag, Berlin, 1976.
30. Lane, M. H., P. M. Fitzpatrick, and J. J. Murphy, On the Representation of Air Density in Satellite Deceleration Equations by Power Functions with Integral Exponents, Technical Documentary Report No. APGC-TRD-62-1S, Air Proving Ground Center, Eglin AFB, March 1962.
31. Cook, G. E., and D. G. King-Hele, "The Contraction of Satellite Orbits Under the Influence of Air Drag, V. with Day-Night Variations in Air Density," Vol. 259A, 1965 (Phil. Trans. of the Royal Society).
32. Chen, Sean C. H., Ephemeris Generation for Earth Satellites Considering Earth Oblateness and Atmospheric Drag, May 1974, M-240-1239, Northrop Services, Inc., Huntsville, Alabama, NASA Contract NAS8-21810.
33. Fominov, A. M., "A New Atmospheric Model and Earth-Satellite Motion," NASA Technical Translations TT-F-17108, July 1976, Conference on Scientific Research by Artificial Satellite Observations, Budapest, Hungary, October 21-24, 1974.

34. Jacchia, L. G., Revised Static Model of the Thermosphere and Exosphere with Empirical Temperature Profiles, Smithsonian Astrophysical Observatory Special Report No. 332, May 1971.
35. Roberts, C. E., Jr., "An Analytical Model for Upper Atmosphere Densities Based upon Jacchia's 1970 Models," Celestial Mechanics, Vol. 4, No. 3/4, pp. 368-377, 1971.
36. Elyasberg, P. E., B. V. Kugaenko, V. M. Synitsyn, and M. I. Voiskovsky, "Upper Atmosphere Density Determination from the Cosmos Satellite Deceleration Results," Space Research XII, Akademie-Verlag, Berlin, 1972.
37. Mueller, Alan C., Atmospheric Density Models, June 1977, ACM-TR-106, Analytical and Computational Mathematics, Inc., Houston, Texas, NASA Contract NAS9-15171.
38. Hedin, A. E., et al., "A Global Thermospheric Model Based on Mass Spectrometer and Incoherent Scatter Data, MSIS 1. N₂ Density and Temperature," Journal of Geophysical Research, Vol. 82, No. 16, June 1, 1977.
39. Cook, G. E., D. G. King-Hele and M. C. Walker, "The Contraction of Satellite Orbits Under the Influence of Air Drag, Part I," Proceedings of the Royal Society, Vol. 257A, 1960.
40. Cook, G. E., D. G. King-Hele, and M. C. Walker, "The Contraction of Satellite Orbits Under the Influence of Air Drag, II. with Oblate Atmosphere," Proceedings of the Royal Society, Vol 264A, 1961.
41. King-Hele, D. G., "The Contraction of Satellite Orbits Under the Influence of Air Drag, III. High Eccentricity Orbits ($.2 < e < 1$)," Proceedings of the Royal Society, Vol. 267A, 1962.
42. Cook, G. E., and D. G. King-Hele, "The Contraction of Satellite Orbits Under Influence of Air Drag, V. With Scale Height Dependent on Altitude," Proceedings of the Royal Society, Vol. 275A, 1963.
43. Cook, G. E., and D. G. King-Hele, "The Contraction of Satellite Orbits Under the Influence of Air Drag, VI. Near Circular Orbits with Day to Night Variation in Air Density," Proceedings of the Royal Society, Vol. 303A, 1968.
44. Santora, F. A., "Satellite Drag Perturbations in an Oblate Atmosphere with Day-to-Night Density Variation," AIAA Mechanics and Control of Flight Conference, Anaheim, CA, August 1974.

45. Zee, C. H., "Trajectories of Satellites Under the Combined Influence of Earth Oblateness and Drag," Celestial Mechanics, Vol. 3, No. 2, pp. 148-168, 1971.
46. Barry, B. F., and C. K. Rowe, "Long-Term Orbit Prediction Using Two-Variable Asymptotic Expansions and the Automated Manipulation Capabilities of the FORMAC Language," No. 72-938, AIAA/AAS Astrodynamics Conference, Palo Alto, Calif., September 1972.
47. Vinh, N. X., and J. M. Longuski, "Analytic Theory of Orbit Contraction due to Atmospheric Drag," Acta. Astronautica, Vol. 6, 1979, pp. 697-723.
48. Brouwer, D., and G. Hori, "Theoretical Evaluation of Atmospheric Drag Effects in the Motion of an Artificial Satellite," The Astronomical Journal, Vol. 66, No. 5, June 1961.
49. Brouwer, D., "Solution of the Problem of Artificial Satellite Theory Without Drag," The Astronomical Journal, Vol. 64, No. 1274, November 1959.
50. Lane, M. H., "The Development of an Artificial Satellite Theory Using a Power-Law Atmospheric Density Representation," AIAA Paper No. 65-35, AIAA Aerospace Sciences Meeting, N.Y., 1965.
51. Willey, R. E., and V. L. Pisacane, The Motion of an Artificial Satellite in a Nonspherical Gravitational Field and an Atmosphere with a Quadratic Scale Height, Johns Hopkins Applied Physics Lab, Technical Memorandum TG1236, January 1974 (also J. Astronomical Sciences, March-June 1974).
52. Vinti, John P., "New Method of Solution for Unretarded Satellite Orbits," Journal of Research of the National Bureau of Standards, Vol. 63B, No. 2, October-December 1959.
53. Sherrill, T. J., "Development of a Satellite Drag Theory Based on the Vinti Formulation," Ph.D. Dissertation, University of California, Berkeley, Calif., 1966.
54. Watson, J. S., G. D. Mistretta, and N. L. Bonavito, "An Analytic Method to Account for Drag in the Vinti Satellite Theory," Celestial Mechanics, Vol. 11, No. 2, pp. 145-178, 1975.
55. Scheifele, G., A. Mueller, and S. Starke, A Singularity Free Analytical Solution of Artificial Satellite Motion with Drag, Analytical and Computational Mathematics, Inc., Technical Report ACM-TR-103, Houston, Texas, March 1977.

56. Scheifele, G., and O. Graf, "Analytical Satellite Theories Based on a New Set of Canonical Elements," No. 74-838, AIAA Mechanics and Control of Flight Conference, Anaheim, Calif., August 1974.
57. Pimm, R. S., "Long-Term Orbital Trajectory Determination by Superposition of Gravity and Drag Perturbations," No. 71-376, AAS/AIAA Astrodynamics Specialists Conference, Ft. Lauderdale, Florida, August 1971.
58. Wagner, C. A., B. C. Douglas, and R. G. Williamson, The Road Program, January 1974, X-921-74-144, Goddard Space Flight Center, Greenbelt, Maryland.
59. Izsak, I. G., "A Note on Perturbation Theory," The Astronomical Journal, October 1963, Vol. 68, No. 8, pp. 559-561.
60. Liu, J. J., "A Semi-Analytic Theory for the Motion of a Close-Earth Artificial Satellite with Drag," No. 79-D123, AIAA Aerospace Sciences Meeting, New Orleans, La., January 1979.
61. Alford, R. L., and J. J. Liu, The Orbital Decay and Lifetime (LIFTIM) Prediction Program, May 1974, M-240-1278, Northrop Services, Inc., Huntsville, Alabama.
62. Rauch, H. E., "Optimum Estimation of Satellite Trajectories Including Random Fluctuations in Drag," AIAA Journal, Vol. 3, No. 4, 1965.
63. Rios Neto, Atair, "The Estimation of the State and the Unmodeled Atmospheric Drag for Near Earth Satellites," Ph.D. Dissertation, The University of Texas at Austin, March 1973.
64. Tapley, B. D., "Statistical Orbit Determination Theory," Recent Advances in Dynamical Astronomy, eds. B. D. Tapley and V. Szebehely, pp. 396-425, D. Reidel Publishing Co., Dordrecht-Holland, 1973.
65. Tapley, B., A. R. Neto and B. E. Schutz, "Orbit Determination in the Presence of Atmospheric Errors," COSPAR IAU-IUTAM Symposium, Sao Paulo, Brazil, Satellite Dynamics, Springer-Verlag, 1975.
66. Argentiero, P., "An Adaptive Technique for Estimating the Atmospheric Density Profile During the A.E. Mission," NASA TM X-66202, February 1973.
67. Cappellari, J.O., C. E. Velez, and A. J. Fuchs (eds.), Mathematical Theory of the Goddard Trajectory Determination System, Goddard Space Flight Center, X-582-76-77, April 1976.

68. Collins, Sean K., "Long Term Prediction of Super-Synchronous Orbits Over Very Long Time Spans," pending Ph.D. Thesis, Massachusetts Institute of Technology, Cambridge, MA.
69. Kaniecki, J. P., "Short Periodic Variations in the First-Order Semianalytical Satellite Theory," M.S. Thesis, Massachusetts Institute of Technology, Cambridge, MA, August 1979.
70. Mathews, J., and R. L. Walker, Mathematical Methods of Physics, 2nd ed., W. A. Benjamin, Inc., Menlo Park, Calif., 1970.
71. Early, L. W., unpublished work, CSDL, Cambridge, MA, August 1979.
72. Gelb, A., editor, Applied Optimal Estimation, Cambridge, MA, MIT Press, 1974.
73. Research and Development Goddard Trajectory Determination System (R&D GTDS) User's Guide, Edited jointly by Computer Sciences Corporation and Systems Development and Analysis Branch (GSFC), draft version, July 1978.
74. Long, A., W. D. McClain, and P. J. Cefola, Mathematical Specifications for the Earth Satellite Mission Analysis Program (ESMAP), June 1975, CSC/SD-75/6025, Computer Sciences Corporation, Silver Spring, Maryland, NASA Contract NAS5-11999.
75. Bobick, Aaron, "VOP Single Step Integration," CSDL Internal Memo, POP-016-79-AB, August 1979.
76. Mueller, A., G. Scheifele, and S. Starke, "An Analytical Orbit Predictor for Near-Earth Satellites," 79-0122, AIAA Aerospace Sciences Meeting, New Orleans, LA, January 1979.
77. Broucke, R. A., "On the Matrizant of the Two-Body Problem," Astronomy and Astrophysics, Vol. 6, pp. 173-182, 1970.
78. Broucke, R. A., Unpublished lecture notes on Advanced Dynamics and Celestial Mechanics, August 1971.
79. Vinti, John P., "Gaussian Variational Equations for Osculating Elements of an Arbitrary Separable Reference Orbit," Celestial Mechanics, Vol. 7, pp. 367-375, 1973.
80. Battin, R. H., Astronautical Guidance, New York, New York, McGraw-Hill, 1964.

BIOGRAPHY

Andrew Joseph Green was born on 2 February 1950 in Utica, New York, the son of Kathleen and Hugh Green. He attended Waterville Central High School in Waterville, New York from 1964 to 1968. In May 1970 he received an Applied Science degree from Mohawk Valley Community College in Utica, New York. From 1970 to 1974 he attended the United States Military Academy. Upon graduation from the Military Academy, he was commissioned a Second Lieutenant in the Armor Branch of the United States Army. He married Theresa Belfield on 5 June 1974. He has successfully completed the following Army schools: Ranger, Airborne, Armor Officer Basic, Motor Officer. He served 17 months with the 3rd Armor Cavalry Regiment in Fort Bliss, Texas. In September 1976 he entered Massachusetts Institute of Technology. He received a Master of Science from MIT in September 1977. He is a Fannie and John Hertz Foundation Fellow and is currently a Captain in the U. S. Army. He has two children, Christopher and Andrea.